



Image Compression based on Machine Learning Methods- Survey on Recent Advancements

Ezhilan R¹, Baskar D² and Vinod Kumar D^{3*}

¹Assistant Professor – Biomedical Engineering, Vinayaka Mission's Kirupananda Variyar Engineering College, Vinayaka Mission's Research Foundation (Deemed to be University), Salem, Tamil Nadu, India.

²Assistant Professor - Electrical and Electronics Engineering, Annai Teresa College of Engineering, Viluppuram, Tamil Nadu, India.

³Professor and Head - Biomedical Engineering, Vinayaka Mission's Kirupananda Variyar Engineering College, Vinayaka Mission's Research Foundation (Deemed to be University), Salem, Tamil Nadu, India.

Received: 16 Jan 2021

Revised: 01 Feb 2021

Accepted: 16 Mar 2021

*Address for Correspondence

Vinod Kumar D

Professor and Head - Biomedical Engineering,
Vinayaka Mission's Kirupananda Variyar Engineering College,
Vinayaka Mission's Research Foundation (Deemed to be University),
Salem, Tamil Nadu, India.



This is an Open Access Journal / article distributed under the terms of the **Creative Commons Attribution License** (CC BY-NC-ND 3.0) which permits unrestricted use, distribution, and reproduction in any medium, provided the original work is properly cited. All rights reserved.

ABSTRACT

Image compression play significant role in the data transfer and storage. Recently Machine learning has achieved tremendous success in various domain of image processing. Further due to large increase in image data, the research activities in image compression continue to preserve bandwidth or storage resources. This paper focuses on research on the combination of traditional compression algorithms and machine learning techniques. Both compression and learning algorithms are discussed, providing background and reasoning for their combination. This help to understand the current trends and future scope in image compression using machine learning.

Keywords: Image compression, Machine Learning, PCA, SVM, CNN

INTRODUCTION

Natural images tend to contain a high number of redundant information; neighbouring pixels tend to exhibit a correlation [1]. Most image compression algorithms tend to take advantage of this correlation to reduce the size of images stored. Image compression is one of the vast and highly explored area of research. Here, compression doesn't mean only reducing the image size. Along with reduction in data it also leads to the position to reconstruct the original data. During the last few years, due to improved computational power as well as improved and diversified



**Ezhilan et al.,**

machine learning and deep learning techniques, they have been explored and applied in many high level image processing applications such as object detection, pattern recognition, optical character recognition, classification, speech recognition, face recognition, computer vision, super resolution, image in painting, image generation, image enhancement, machine translation etc. However, it is limitedly used in image compression kind of low-level image processing during recent years only. Various survey articles on image compression or data compression is found in literature. But in this article a survey of machine learning or deep learning-based image compression methods during almost around last decade is carried out.

Need for Image Compression Techniques

Data takes up lesser storage when compressed. As a result, this allows more data to be stored with less disk space. This is especially useful in healthcare, where medical images need to be archived, and dataset volume is massive. Some image compression techniques involving extracting the most useful components of the image (PCA), which can be used for feature summarization or extraction and data analysis. Federal government or security agencies need to maintain records of people in a pre-determined, standard, and uniform manners. Thus, images from all sources need to be compressed to be of one uniform shape, size, and resolution.

Types of Image Compression

Image compression can be categorized by their ability to re-create the original image from its compressed form.

Lossy Compression

Lossy compression, as its name suggests, is a form of data compression that retains useful image details while discarding a few bits in order to reduce its size or to extract important components. Thus, in lossy compression, data is irreversibly lost, and the original image cannot be completely re-created.

Lossless Compression

Lossless compression is a form of data or image compression under which any sort of data loss is avoided, and thus, compressed images are larger in size. However, the original image can be re-constructed using this kind of image compression.

Traditional Image Compression Algorithms

Discrete Cosine Transforms are the base algorithm for JPEG compression, one of the most widely used image compression algorithms [2]. It works by dividing an image into squares and applying a discrete cosine function to the resulting matrix of values, hence representing the image as a superposition of wavelets rather than pixel values [3]. The DCT itself does not compress the image but provides crucial information about the nature of it. The compression process takes place after the DCT. This process, quantisation, will ignore higher frequency patterns, that are less likely to be perceived as quality loss to the human eye. For a real image, this process would be repeated for all the 8x8, or other size, squares within the entire picture. By reducing the data stored by the amount desired, the process provides compression whilst limiting the impact of lost data on human perception of the image. An alternative transformation is the Discrete Cosine Transform (DCT) [4] which is often used in lossy image and video compression algorithms such as JPEG[5], MPEG[6], H264[7], H265[8] due to its energy compaction property and low blocking artifacts. Unlike DFT, DCT contains only real coefficients. DCT of a signal is the DFT of a signal with mirrored padding, so that the DFT input becomes even and the results are real. Due to this mirroring, abrupt changes in high-frequency terms of consecutive blocks are prevented. Better Portable Graphics (BPG) is a wrapper around High Efficiency Video Coding (HEVC) providing much better compression efficiency compared to JPEG. HEVC [8], also known as H265, is the latest video coding standard by ITU-T Video Coding Experts Group, providing up to 50% better compression rate at the same quality compared to its earlier version H264 [7]. BPG uses the intra-coding [9] of HEVC, which is mainly designed to compress a video frame using only the information content in the current frame of interest. Hence, the performance of BPG is directly linked to the HEVC.



**Ezhilan et al.,****Machine Learning Based Image Compression**

Machine Learning is a subset of Artificial Intelligence concerned with “teaching” computers how to act without being explicitly programmed for every possible scenario. The central concept in Machine Learning is developing algorithms that can self-learn by training on a massive number of inputs. In machine learning handcrafted features are used so specific features are to be specified, while in deep learning features are taken care by the network such as recurrent neural network or convolutional neural network. Machine learning has been explored for improving image compression in different ways such as for removing the JPEG compression artifacts, for determining the quantization coefficients, image retrieval with image compression, color image compression etc. In many cases it has been used to improve JPEG standard or comparative analysis has been made with JPEG standard [10].

Feature extraction can be thought as a special case of reducing the dimensionality. Scale Invariant Feature Transform (SIFT) features are exploited [11] to achieve image compression in multi-view application. It is a two step image compression. In case of three images C1, C2, C3 are acquired from three different cameras, in proposed method, from the input images SIFT features are extracted and matched after outlier removal using RANSAC and correlation based methods are used to compress the middle image C2, while C1 and C3 having standard compression method. Machine learning approach is not used for image compression, but it is used to detect JPEG compression for image forensics [12]. The approach uses a joint feature vector of 24-length, which consist of Harris-Stephens corner, Hough line and Hough peaks, for the basis of classification. SVM is used for classification. Compression of colored biomedical images using machine learning based vector quantization and orthogonal transforms is presented [13]. Calculation of centers of clusters is obtained based on machine learning and accordingly codebook is also generated which is used for vector quantization on transformed image for compression of biomedical images.

Content based image retrieval (CBIR) using local features, most of the part of image is not useful for local feature extraction, so instead of compression of feature descriptors directly, compression of image patches centered around the SIFT key points is considered [14]. It is only concerned with matching the descriptors but not concerned with the visual quality of image. The pixel intensity near the border are predicted using feed forward neural network, which results in reduction in blocking artifacts and improved PSNR. Instead it improves JPEG by addressing its problem of quantization noise and blocking artifacts [15]. The approach of combined SVM with DCT for image compression [16]. Due to the support vector concept of SVM, it is used to approximate the DCT coefficients. The approach is for specific accuracy, but it can be extended for different accuracy also. Color image compression is proposed using supervised learning [17]. It minimizes the total prediction error that occurs in traditional approach and it also avoids the computation burden due to use of kernel principal component analysis. Image features are required to be stored in binary form in CBIR. Unified and simultaneous coding is performed on images and image features. It used two different deep networks for image compression and for image features and then combined the two networks for the task of CBIR [18].

Multiple semantic regions are detected using new CNN architecture [19]; this leads to content aware JPEG also. For adaptive bit rate in image compression, deep neural network is used. The architecture can be easily modified for different categories of images such as natural images, cartoons, selfies, sketches, presentations etc. A framework for image compression with variable rate and an architecture based on convolutional and deconvolutional LSTM recurrent networks is proposed [20]. The proposed network is needed to be trained once and it is progressive. It provides better performance than JPEG, JPEG 2000 and WebP. Image modeling is improved using recurrent variational auto encoder [21]. The approach transforms an image gradually from global conceptual aspects to low level details. The global information allows to achieve high quality conceptual compression. A 12-layer deep convolution is proposed [22, 23] to address the image compression artifacts which improves the PSNR by 1.79 dB compared to JPEG. The motivation was from the use of ConvNets for image super resolution which can be thought as a special case of artifacts removal.





Ezhilan et al.,

Two CNNs: compact convolutional neural network (Com CNN) and reconstruction neural network (Rec CNN), are integrated into compression framework [24]. This improves the image compression quality for low bit rate. The design is compatible with some other standards also. A framework named Deep N-JPEG is presented [25] for image compression. It presents semi-analytical model to represent the processing mechanism differences between human visual system and deep neural network at frequency domain. Image compression architecture is proposed. It utilizes advantages of convolutional auto encoder (CAE) to achieve high coding efficiency [26]. In this conventional transform are replaced by CAE, and principal component analysis is also utilized. For compression artifacts, in which a compact and efficient network is formulated for reduction of compression artifacts. A four-layer convolutional network ARCNN is proposed [27].

Machine learning approach used for image and video compression is found where grayscale image and color labels of a few representative pixels are used, based on which a model is learned [28]. Then the model predicts the color of other pixels. Using training of single recurrent neural network better compression was achieved [21] for specified quality irrespective of the input image but limited to 32x32 images. However, it was improved for images of arbitrary size [29]. It was achieved by designing a stronger patch based residual encoder and design of entropy encoder that can capture long term dependencies between patches in the image. Neural network principal part analysis: Principal part Analysis (PCA) is ready to extract the principal info of the information. It's been proven that natural image may be diagrammatic as principal components. Neural network approach PCA to compress the color image. The obtained of Principal part Analysis are quaternion matrix may be break up into 8x8 sub - blocks and vector quantization to form of a replacement sample set. The sample set then is employed to coach the quaternion neural network adopting figure Generalized Hebbian algorithmic program (QGHA), effort a quaternion weight constant that may get the principal components (PCs), the load may be accustomed compress and reconstructed the image [30, 42].

Image compressions exploitation PCA and Improved technique with MLP neural network: In this paper data compression, the researcher's main focuses on the principal part analysis with the neural network approaches is termed statistical procedure. Transform n-dimensional mathematical space to m - dimensional mathematical space. To compress these pictures PCA based mostly neural network model is used and based on the resolution technique that is generally employed in arithmetic. PCA technique takes the collection of information and transforms it to the new knowledge which has a similar applied math property [31, 44]. The transform knowledge from n- dimensional house to m - dimensional house that is that the knowledge reduction techniques.

Performance Evaluation Metrics

There are eight parameters to evaluate the performance of the Image Compression algorithms are Mean Square Error (MSE), Maximum Absolute Error (MAE), Peak Signal to Noise Ratio (PSNR), Mean Structural Similarity (MSSIM) Index, Universal Image Quality (UIQ) Index, the Compression Rate (CR), the compression time (CT) and decompression time (DT).

The MSE and PSNR are defined [32,33] in eq. (1).

$$MSE = \frac{1}{M * N} \sum_{i=0}^{M-1} \sum_{j=0}^{N-1} (I_0(i, j) - I_r(i, j))^2 \tag{1}$$

With I_0 the image to compress and I_r the reconstructed image and (M, N) the size of the image. The PSNR is given in eq. (2).

$$PSNR = 10 \log_{10} \left(\frac{255^2}{MSE} \right) \tag{2}$$





Ezhilan et al.,

The MSE represents the mean error into energy. It shows the energy of the difference between the original image and the reconstructed image. PSNR gives an objective measure of the distortion introduced by the compression. It is expressed in decibels (dB). Maximum Absolute Error (MAE) defined by (3) shows the worst-case error occurring in the compressed image [34].

$$MAE = \max |I_0(i, j) - I_r(i, j)| \tag{3}$$

Usually, in practice, MSSIM index allows evaluating the overall image quality. MSSIM is defined [35,36] in eq. (4).

$$MSSIM(I_0, I_r) = \frac{1}{M} \sum_{j=1}^M SSIM(X_j, Y_j) \tag{4}$$

Where x_j and y_j are the image contents at the j -th local window; and M is the number of local windows in the image and $SSIM(x, y) = [1(x, y)]^\alpha \cdot [c(x, y)]^\beta \cdot [s(x, y)]^\gamma$ with $\alpha > 0$, $\beta > 0$ and $\gamma > 0$ are parameters used to adjust the relative importance of the three components. The UIQ Index models any distortion as a combination of three different factors: loss of correlation, luminance distortion, and contrast distortion [37]. It is defined by in eq. (5).

$$Q = \frac{4\sigma_{I_0, I_r} \overline{I_0 I_r}}{(\sigma_{I_0}^2 + \sigma_{I_r}^2) \left[(\overline{I_0})^2 + (\overline{I_r})^2 \right]} \tag{5}$$

In equation (4) and (5) the best value 1 is achieved if and only $I_0 = I_r$.

The MSSIM, SSIM and UIQ as define above, are the practical index use to evaluate the overall image quality.

The Compression rate (CR) is defined as the ratio between the uncompressed size and compressed size. The CR is given by Sayood K and Salomon D et al., [38,39,41] in (6) and (7).

$$CR = \frac{\text{size of compressed image}}{\text{size of original image}} \tag{6}$$

In percentage form, the CR is given by (16).

$$CR(100\%) = 100 - \frac{\text{size of compressed image}}{\text{size of original image}} \times 100 \tag{7}$$

The compression time and decompression time are evaluated when we start the program in MATLAB. CT and DT depending on the computer used to simulate the program. For the medical image, the goal of the introduced method in this paper is to maintain the diagnostic-related information at a high compression ratio. The medical applications require saving many images taken by different devices for patients in large numbers and for a long time [40, 43].

CONCLUSION

In this paper, various image compression techniques based on Machine Learning are discussed. Image compression may be lossy or lossless. Lossless compression is preferred for archival purposes and often for medical imaging, technical drawings etc. Lossy compression methods are suitable for natural images such as photographs where minor loss of fidelity is acceptable. The Performance Evaluation Metrics for image compression algorithm such as Mean Square Error (MSE), Maximum Absolute Error (MAE), Peak Signal to Noise Ratio (PSNR) and the Compression rate (CR) are discussed. This will help to understand the current trends and future scope in image compression using machine learning.





Ezhilan et al.,

REFERENCES

1. Kinsner, W. (2002). Compression and its metrics for multimedia. Cognitive Informatics, 2002. Proceedings. First IEEE International Conference, pp. 107 - 12
2. Luo, Weiqi & Huang, Jiwu & Qiu, Guoping. (2010). JPEG Error Analysis and Its Applications to Digital Image Forensics. Information Forensics and Security, IEEE Transactions on. 5. 480 - 491.
3. Caroline, Elizabeth & Sheeba, G. & Jeyaseelan, Jeyarani & Mary, F.S.R.. (2012). A reconfigurable DCT/IDCT architecture for video codec: A Review. 2012 3rd International Conference on Computing, Communication and Networking Technologies, ICCCNT 2012. 1-5.
4. N. Ahmed, T. Natarajan, and K. R. Rao, "Discrete cosine transform," IEEE transactions on Computers, vol. 100, no. 1, pp. 90–93, 1974.
5. G. K. Wallace, "The jpeg still picture compression standard," IEEE transactions on consumer electronics, vol. 38, no. 1, pp. xviii–xxxiv, 1992
6. D. Le Gall, "Mpeg: A video compression standard for multimedia applications," Communications of the ACM, vol. 34, no. 4, pp. 46–59, 1991.
7. T. Wiegand, G. J. Sullivan, G. Bjontegaard, and A. Luthra, "Overview of the h.264/avc video coding standard," IEEE Transactions on Circuits and Systems for Video Technology, vol. 13, pp. 560–576, July 2003.
8. G. J. Sullivan, J. Ohm, W. Han, and T. Wiegand, "Overview of the high efficiency video coding (hevc) standard," IEEE Transactions on Circuits and Systems for Video Technology, vol. 22, pp. 1649–1668, Dec 2012.
9. J. Lainema, F. Bossen, W. Han, J. Min, and K. Ugur, "Intra coding of the hevc standard," IEEE Transactions on Circuits and Systems for Video Technology, vol. 22, pp. 1792–1801, Dec 2012.
10. M. I. Patel, S. Suthar and J. Thakar, "Survey on Image Compression using Machine Learning and Deep Learning," 2019 International Conference on Intelligent Computing and Control Systems (ICCS), Madurai, India, 2019, pp. 1103-1105
11. H. Bai, M. Zhang, M. Liu, A. Wang and Y. Zhao, "Two-Stage Multiview Image Compression Using Interview SIFT Matching," 2014 Data Compression Conference, Snowbird, UT, 2014
12. Yongsoo choi, et al. , "JPEG Compression Detection based on Edge-Corner Features Using SVM", International Conference on Machine learning and Data Science, 2017
13. Aurelle Tchagna Kouanou, Daniel Tchiotso, René Tchinda, Christian Tchito Tchapg, Adelaide Nicole Kengnou Telem, Romanic Kengne, "A Machine Learning Algorithm for Biomedical Images Compression Using Orthogonal Transforms", International Journal of Image, Graphics and Signal Processing(IJIGSP), Vol.10, No.11, pp. 38-53,2018
14. A Makar, Mina et al. "Compression of image patches for local feature extraction", IEEE International Conference on Acoustics, Speech and Signal Processing, 2009
15. J. Quijas and O. Fuentes, "Removing JPEG blocking artifacts using machine learning," Southwest Symposium on Image Analysis and Interpretation, San Diego, CA, 2014, pp. 77-80
16. J. Robinson, Vojislav Kecman, "Combining Support Vector Machine Learning with the Discrete Cosine Transform in Image Compression", IEEE Transactions on Neural Networks, Volume 14, Issue 4, July 2003
17. Xuedong Liu et al., "Fast and high efficient color image compression using machine learning", 2nd IEEE Advanced Information Management, Communicates, Electronic and Automation Control Conference, 2018
18. A, Qingyu Zhang, " Deep network based image coding for simultaneous compression and retrieval", IEEE ICIP, 2017
19. Prakash, Aaditya et al. "Semantic Perceptual Image Compression Using Deep Convolution Networks" Data Compression Conference (DCC),2017, pp 250-259.
20. Minnen, David & Toderici, George & Covell, Michele & Chinen, Troy & Johnston, Nick & Shor, Joel & Jin Hwang, Sung & Vincent, Damien & Singh, Saurabh, "Spatially adaptive image compression using a tiled deep network", 2018
21. George Toderici, "Variable Rate Image Compression with Recurrent Neural Networks", ICLR, 2016





Ezhilan et al.,

22. Karol Gregor, "Towards Conceptual compression", arXiv, 2016
23. Lukas Caviglli, "CAS-CNN: A Deep Convolutional Neural Network for Image Compression Artifact Suppression", arXiv, 2017
24. Feng Jiang, "An End-to-End Compression Framework Based on Convolutional Neural Networks", arXiv, 2017
25. Zihau liu, "DeepN-JPEG: A Deep Neural Network favourable JPEG based Image Compression Framework" arXiv, 2018
26. Zhengxue Cheng, Heming Sun, Masaru Takeuchi, and JiroKatto, "Deep Convolution Auto Encoder- based Lossy Image Compression" 2018
27. Chao, "Compression Artifacts Reduction by Deep Convolution Network", *IEEE Conference on Computer Vision*, 2015
28. Li Cheng, S. V. N. Vishwanathan, "Learning to Compress Images and Videos", *24th International Conference on Machine Learning*, 2007
29. G. Toderici et al., "Full Resolution Image Compression with Recurrent Neural Networks," *2017 IEEE Conference on Computer Vision and Pattern Recognition (CVPR)*, Honolulu, HI, 2017, pp. 5435-5443.
30. Gaidhane, Vilas H., Vijander Singh and M. Kumar. "Image Compression Using PCA and Improved Technique with MLP Neural Network." *2010 International Conference on Advances in Recent Technologies in Communication and Computing* (2010): 106-110.
31. Sonal and D. Kumar. "A Study of Various Image Compression Techniques." (2007).
32. Kartheeswaran S, Dharmaraj D, Durairaj C (2017) A data-parallelism approach for pso-ann based medical image reconstruction on amulti-core system. *IMU* 8: 21-31.
33. Ayoobkhan MUA, Chikkannan E, Ramakrishnan K (2017) Lossy image compression based on prediction error and vector quantisation. *EURASIP J Image Video Process* 35: 1-13.
34. Ananthi VP, Balasubramaniam P (2016) A new image denoising method using interval-valued intuitionistic fuzzy sets for the removalof impulse noise. *Sig Pro* 121: 81-93.
35. Wang Z, Bovik CA, Sheikh HR, Simoncelli EP (2004) Image quality assessment: from error visibility to structural similarity. *IEEE TIP* 13:600-612.
36. Hore A, Ziou D (2010) Image quality metrics: psnr vs. ssim. *IEEE International Conference on Pattern Recognition* 2366-2369.
37. Wang Z, Bovik CA (2002) A universal image quality index. *IEEE Sig Pro Letters* 9: 81-84.
38. Sayood K (2006) Introduction to data compression. Morgan Kaufmann, San Francisco.
39. Salomon D, Concise A (2008) Introduction to data compression. Verlag, London.
40. Hussein Abouali A (2015) Object-based vq for image compression. *Ain Shams Eng J* 6: 211-216.
41. Muthukrishnan, A.; Charles Rajesh Kumar, J.; Vinod Kumar, D.; Kanagaraj, M. Internet of image things-discrete wavelet transform and Gabor wavelet transform based image enhancement resolution technique for IoT satellite applications. *Cogn. Syst. Res.* 2019, 57, 46–53.
42. Charles Rajesh Kumar. J , Vinod Kumar. D, Baskar. D, Mary Arunsi. B, Jenova. R, M.A.Majid." VLSI design and implementation of High-performance Binary-weighted convolutional artificial neural networks for embedded vision based Internet of Things (IoT)".16th International Learning & Technology Conference (L&T), Procedia Computer science (Elsevier), Jeddah,2018.
43. Charles Rajesh Kumar, J., Vinod Kumar, D., Majid, M.A. "Wind energy programme in India: Emerging energy alternatives for sustainable growth" *Energy and Environment*, 2019, 30(7), pp. 1135–1189
44. Baskar. D, Selvam. P, "Machine Learning framework for Power System Fault Detection and Classification," *International Journal of Scientific & Technology Research*, vol. 9, no. 2, pp. 2002-2008, Feb. 2020.





A Comprehensive Review on Medicinal Plants in Western Ghats with Antitubercular Activity

Jayalakshmi P M^{1*}, Manu Jose² and Prasanth Francis²

¹College of Pharmaceutical Sciences, Government Medical College, Thiruvananthapuram, Kerala, India.

²Nirmala College of Pharmacy, Muvattupuzha, Kerala, India.

Received: 27 Feb 2021

Revised: 01 Mar 2021

Accepted: 06 Mar 2021

*Address for Correspondence

Jayalakshmi P M

College of Pharmaceutical Sciences,

Government Medical College,

Thiruvananthapuram, Kerala.

E-mail: pmjayalakshmi94@gmail.com



This is an Open Access Journal / article distributed under the terms of the **Creative Commons Attribution License** (CC BY-NC-ND 3.0) which permits unrestricted use, distribution, and reproduction in any medium, provided the original work is properly cited. All rights reserved.

ABSTRACT

Treatment of TB has become a challenge in recent times due to development of multi drug resistant forms. This has been further complicated by co infection with HIV and diabetes. TB infection is forecasted to rise by 20% in the next 20 years. The western slop of southern Western Ghats is a repository of medicinal plants with high content of active constituents. This review summarise plants abundant in Western Ghats with proven anti TB activity along with their active constituents. Also, various methods to identify anti TB activity is elaborated. The study identified various active chemical moieties which can be further modified to optimise anti TB activity. Studies to identify the usefulness of using these plants extracts along with regular drug treatment can be initiated to combat multi drug resistant TB forms.

Keywords: Tuberculosis, Medicinal Plants, Western Ghats, *In-vitro* Screening Methods

INTRODUCTION

Tuberculosis (TB) is chronic infectious disease. Infection was affected through the lung with acid-fast bacillus *Mycobacterium tuberculosis*, was first identified as a pathogen by Robert Koch in 1882 [1]. With over 9 million cases and 1.5 million deaths annually, tuberculosis is the deadliest known infectious disease. Worldwide tuberculosis (TB) is one of the leading cause of mortality from a single infectious agent and the leading cause of death for persons suffering from HIV infection. This account for about 40% of death in world population. India is one among the top 20 high tuberculosis burden countries with increasing burden of multidrug resistant tuberculosis and coinfection with Diabetes mellitus and HIV infection. The prevalence of tuberculosis varied based on the sex and distribution of population in urban and rural areas. The prevalence was higher in male population in urban areas and female population in rural areas. Some epidemiologist forecast a rise of 20% incidence in the next 20 years. There will be a cumulative rise in TB cases largely due to HIV pandemic. As a result of emergence of resistance by mycobacterium

30396



**Jayalakshmi et al.,**

tuberculosis against first line anti TB drugs, there occur an increased control efforts on tuberculosis. Drug resistant tuberculosis management is very critical. There should be a clear understanding of drug resistance to ensure accurate diagnosis and an early arbitration of appropriate treatment. Worldwide only 50% of patients with Multi drug resistant TB achieve successful completion of treatment. This is partially due to the high death rates (2,50,000 estimated death from MDR-TB/XDR-TB) and due to poor follow up. In India, only 46% of resistant TB cases achieved successful completion of treatment. Further outcome of extensively drug resistant tuberculosis (XDR-TB; resistant to at least one fluoroquinolone and injectable aminoglycoside in addition to MDR-TB), has been reported in 9.5 % MDR-TB patients in 2015. India, one of the six countries with huge MDR-TB burden. Also they failed to implement a nationwide drug resistance surveillance. Interruption in tuberculosis treatments are the strongest reason for acquired mono drug resistance. It also promote a high risk of bacterial mutations that eventually results in recurrence and in Multi drug resistant tuberculosis. Regional analysis of India such as in east, west, north, south and central India for estimate of drug resistance showed that the burden of drug resistant and multi drug resistant tuberculosis were increased for past 20 years. West India is the region with highest number of Drug resistant tuberculosis cases in the decade from 2006 to 2015. In this region prevalence of MDR-TB is high. There occur a rapid emergence of drug resistant and multidrug resistant tuberculosis in over populated urban areas of India including the metropolitan cities such as Mumbai, Pune and major cities such as Gujarat. Increased risk of infection spreading is mainly due to overcrowding, inadequacy in community TB control programmes and the high variability in the anti TB treatment regimens. Irregularities in the usage of second line drugs results in inadequate treatment for MDR-TB which in turn results in emergence of resistance. There is an imminent need to check the indiscriminate use of second line drugs and should recommend judicious use of newer drugs to gain better outcomes in patient with multidrug resistant tuberculosis. The high prevalence of MDR-TB reported shows the significance of need of critical gap between treatment regimen and the need of better formulations comprising of newer drugs that have distinct mode of action [2].

Many pharmaceutical companies have been indifferent to serious development of new antituberculosis medicines because they estimate their profits based solely on comparative expenses. However, recently, international organizations such as the Global Alliance for TB Drug Development (TB Alliance) and Stop TB Partnership (WHO) have taken a leading role in initiating efforts to end the tuberculosis epidemic. The main challenges for new antituberculosis drugs are (1) shortening treatment time, (2) simplifying the treatment method, (3) treating MDR/XDR-TB, (4) treating tuberculosis/HIV simultaneously, and (5) ensuring superior safety. The new antituberculosis drugs that display low toxicity, excellent antituberculosis activity, and efficacy against resting-phase bacteria are beneficial for short-course therapy and prevent secondary infections from those already infected. Although long-term combination therapy is currently the basis of tuberculosis treatment, the development of short-term tuberculosis treatments can be safer for children and help prevent MDR/XDR-TB. TB treatment is generally comprised of 2 months with isoniazid, rifampicin, ethambutol and pyrazinamide (the intensive phase), followed by four additional months of isoniazid and rifampicin therapy (the continuation phase). Unfortunately, lack of adherence to prescribed treatment procedures and inefficient healthcare structures have contributed to the development of multidrug-resistant TB (MDR-TB, defined as resistance to at least isoniazid and rifampicin, two front-line drugs used for the treatment of TB) that requires at least 20 months of treatment with second-line drugs comprised of capreomycin, kanamycin, amikacin and fluoroquinolones; these are more toxic and less efficient, with cure rates in the range of 60–75%. In patients affected by XDR-TB, the chances of successful treatment are quite low, underpinning the need for urgent discovery of novel compounds with activity against MTB strains resistant to second-line drugs.

Recently, a few reports have claimed the emergence of a 'totally drug-resistant TB' strain with a limited chance of successful therapy. Moreover, there is an urgent need to come to an agreement on the definition of these strains of MTB, mainly in terms of their severity. Hence, the search for new antitubercular drugs is a priority so as to overcome the problem of drug resistance and to finally eradicate TB. Natural products long have been recognized as an important source of therapeutically effective medicines. Traditional herbal medicines have demonstrated significant activities in antitumor, antiinflammatory, analgesic, immunomodulation, antimicrobial, allergy, antiviral and





Jayalakshmi et al.,

antitubercular assays. The chemical novelty associated with natural products is higher than that of any other source: 40% of the chemical scaffolds in the published database of natural products, Dictionary of Natural Products, Chapman & Hall, are absent from synthetic chemistry.

METHODOLOGY

Related Scientific studies published in journals, books, and reports were reviewed. Relevant literatures were searched in Google Scholar and various electronic databases including Science Direct, IEEE Xplore, Scopus, SciFinder, and MEDLINE using a specific search terms including "TB", "kerala medicinal plants", "anti-TB".

In Vitro Anti-Tb Screening Method

Biological assays, then, must be carried out in order to identify promising plant extracts, to guide the separation and isolation, and to evaluate lead compounds. Bioactive compounds are the chemical weapons of self-defense in very competitive environments. They are important in treatment of many diseases, such as the deadly forms of cancer, and the emergence of bacterial resistance, is essentially based on active chemical principals such as antibiotics, antifungals, anticancer, antimalarial and anti-inflammatory agents. The screening of bioactive compounds involves a large number of analysis that allow assessing the potential of biological extracts or molecules. The assays can be performed at the whole animal, cell-based or molecular levels [4]. Using preliminary functional assays for naturally occurring pure compounds as well as extracts from higher and lower forms of plants, microorganisms and marine organisms, it has been noted that inhibitory activity against *M. tuberculosis* is widespread in Nature [6]. The different *In vitro* methods for discover antitubercular agents in natural products research are briefly described.

MABA-Microplate Alamar Blue Assay

Most common method used for doing anti tubercular drug screening. The dye Alamar blue used for screening of antitubercular activity. Alamar Blue (oxidised form) which is blue in colour turns pink in colour(reduced form) upon reduction within live bacteria. Since Mycobacterium is an aerobic organism, presence of growth turns alamar blue dye to pink colour. This principle has been used to predict the presence or absence of growth of *Mycobacterium tuberculosis* for testing antitubercular agents [7]. It may also indicate the cellular growth and metabolism of any bacteria based on the colour conversion. Visual inspection was used to determine the colors of the contents of each well, with blue interpreted as no growth, pink as growth, and MIC as the last concentration in which blue color were observed. The growth of the bacteria can be monitored using a flourimeter or spectrophotometer (610nm) or a visual colour change [8]. The minimum inhibitory concentration (MIC) is defined as the minimum concentration of tested compound to which there was not higher shift from resazurin (blue) to resorufin (pink) than that generated by control of a 1:100 dilution of the bacterial inoculums.

Agar diffusion: Disk methods comprise the placing of filter paper disks containing test compounds on agar plate surfaces previously inoculated with the test organism. The test molecules or plant extracts then diffuse into the agar and inhibit growth of the test microorganisms [9]. After incubation, mean diameters of growth inhibition zones are recorded. Diffusion assays are generally recommended for polar molecules than non-polar molecules or mixture of compounds such as essential oils [10].

Agar dilution: In the 1950s, Canetti *et al.* described the first Drug Susceptibility Testing (DST) method for *M. tuberculosis*, involving the preparation of a concentration series of drugs against *M. tuberculosis* complex in Lowenstein-Jensen medium, inoculation of the bacterial cultures on the slants, and reading of the inhibition of growth by drugs at different concentrations. The agar dilution tests permit to determine the MIC [11,12]. The major disadvantage of such assays are the time required to visibly detect the growth of microbial colonies.

Radiometric: BACTEC 460® instrument is a semi-automated radiometric drug susceptibility testing (RAD) method that measures the [14] CO₂ produced by metabolic breakdown of (1-¹⁴C) palmitic acid in a liquid Middlebrook 7H12





Jayalakshmi et al.,

medium [13,14,15]. With this method, multiple concentrations can be tested and an MIC calculated. However, although results are generally available in 5 days, the tests performed on the BACTEC system are costly and are not suited to the evaluation of large numbers of compounds. Other radiometric assay system, which can be employed to screen for inhibitors of mycobacterial growth uses a strain of the rapidly growing saprophyte *Mycobacterium aurum* is used as the test organism. Inhibition of its growth is highly predictive of activity against *M. tuberculosis*, which cannot itself be used in screening because of its growth characteristics and highly infectious nature. The viability of *M. aurum* in the presence of a test sample is monitored by measuring the uptake of radiolabelled uracil into the cells. In a microtiter plate format, the screen has the potential for testing several thousand samples per day [16].

Flow cytometry: Flow cytometry was used to study the effects of antimicrobial agents in prokaryotes. Fluorescein diacetate (FDA), a non fluorescent diacetyl fluorescein ester that becomes fluorescent upon hydrolysis by cytoplasmic esterases [17] and are used for the susceptibility testing of *M. tuberculosis*. Pina-Vaz et al. stained *M. tuberculosis* in the absence or presence of antimycobacterial drugs with SYTO 16 (a nucleic acid fluorescent stain that only penetrates into cells with severe lesion of the membrane). The time needed to obtain susceptibility results of *M. tuberculosis* using classical methodologies is still too long, and flow cytometry is a promising technique in the setting of the clinical laboratory, giving fast results. However, the higher cost of equipment is a limitation of this methodology [18].

Reporter gene assays: Genes encoding luciferase enzymes have been cloned from several species of firefly, beetle, crustacean, bacteria and the sea pansy. Other fluorescent proteins such as the red fluorescent protein (RFP) and green fluorescent protein (GFP) has been used. They were introduced into the mycobacteria by using plasmids. This method permits the rapid determination of bacterial viability by measuring the expression of an introduced fluorescent or luminescent protein [19,20]. Application of these proteins permits to work in multi-well formats with more convenient high throughput detection. The use of reporter gene assay for commercial applications is often limited by patent restrictions. The number of laboratories reported to be using this technology for primary screens of natural products is fairly small [21].

The table which shows the different medicinal plants available in western ghats that possess antitubercular potential. The table which include the botanical source, the chief chemical constituents present in the plants that might be responsible for the antitubercular activity, different plant parts in which activity studies were performed, the plant extracts on which activity has been studied and established, different methods used for extraction of phytochemicals and common method used for antitubercular screening.

CONCLUSION

This survey identified 34 medicinal plants from western ghats with potential effects on TB. Among them 8 plants whose active constituents responsible for anti TB activity has been identified. However, two among them, Aloverose and Annonacin are bulky high molecular weight structures than others. Moieties such as Abuquinoneb, Allicin, 1-acetoxy chavicol, Andrographolide, piperacin, and with a ferin A possess molecular weight less than 470.6gm/mol. Based on Lipinski rule of 5, these molecules can be modified and expanded for optimised activity. Chemical groups as methoxy, quinone, amides acetates, hydroxy and sulphoxide groups present in these molecules indicate the importance of these groups for activity. Also these groups act as a possible link for further expansion of these molecules. The presence of sulphoxide group in Allicin and the similarity of the structure with anti TB drug Dapsone shows the possibility of modified Allicin with aromatic groups on both sides as a probable anti TB molecule. The remaining 26 plants identified in this study are partially explored. Mixture of chemical constituents are identified with anti TB properties rather than a single moiety. Further studies can be designed in these plants to separate these constituents and evaluate their anti TB potential. Due to lack of interest in pharmaceutical industry to develop new molecules against multi drug resistant TB, studies can be initiated in the direction of concurrent usage of these plant extracts with current drug regime. This may improve patient compliance, reduce side-effects and improve the efficiency to combat multi drug resistant TB strains.





REFERENCES

1. Balkis A Talip, Roy D Sleator, Colm J Lowery, James S G Dooley, William J Snelling. An update on Global Tuberculosis. *Infectious diseases. Research and Treatment*.2013; 6:39-50.
2. Vishal Goyal, Vijay Kadam, PrashantNarang, Vikram Singh. Prevalence of drug resistant tuberculosis in India: systematic review and Meta Analysis. *BMC Public Health*. 2017; 17:817-837.
3. Setzer, W.; Vogler, B. (2006). Bioassays for Activity. In: Cseke, L.;Kirakosyan, A.; Kaufman, B.; Warber, S.; Duke, J.; Briemann, H.(eds). *Natural Products from Plants*. CRC Press, Boca Raton, USA, p. 390-413.
4. Olga Maria Lage, María C. Ramos, Rita Calisto, Eduarda Almeida, VitorVasconcelos Francisca Vicente. Current Screening Methodologies in Drug Discovery for Selected Human Diseases. *Marine drugs*. 2018;16(279):1-31.
5. Copp, B.R.; Pearce, A.N. (2007). Natural product growth inhibitors of *M. tuberculosis*. *Nat. Prod. Rep.* 24(2), 278-297.
6. Okunade, A.L.; Elvin-Lewis, M.P.; Lewis, W.H. (2004). Natural antimycobacterial metabolites: current status. *Phytochemistry*. 65(8), 1017-1032.
7. Montoro E, Lemus D, Eschemendia Martin A, Portaels F, Palomino J C,. Comparative evaluation of the nitrate reduction assay, the MTT assay and the resazurin micro titre assay for drug susceptibility testing of clinical isolates of *Mycobacterium tuberculosis*. 2005; 55:500-515.
8. Martin A, Camacho M, Portaels F, Palomino JC. Resazurinmicrotiter assay plate testing of *Mycobacterium tuberculosis* susceptibilities to second-line drugs: rapid, simple, and inexpensive method. *Antimicrobial agents and chemotherapy*. 2003;47(11):3616-3619.
9. Hadacek, F.; Greger, H. (2000). Testing of Antifungal Natural Products: Methodologies, Comparability of Results and Assay Choice. *Phytochem. Anal.* 11, 137-147
10. Lahlou, M. (2004). Methods to study the phytochemistry and bioactivity of essential oils. *Phytother. Res.* 18(6), 435-448
11. Canetti, G.; Froman, S.; Grosset, J.; Hauduroy, P.; Langerova, M.;Mahler, H.T.; Meissner, G.; Mitchinson, D. A.; Sula, L. (1963). Mycobacteria: Laboratory Methods for Testing Drug Sensitivity and Resistance. *Bull. World. Health. Organ.* 29, 565-578
12. Van-Klengeren, B.; Dessens-Kroon, M.; Van-der-Laan, T.; Kremer, K.; Van- Soolingen, D. (2007). Drug susceptibility testing of *M. tuberculosis* complex by use of a high-throughput, reproducible, absolute concentration method. *J. Clin. Microbiol.* 45(8), 2662-2668
13. Ashtekar, D.R.; Fernandes, F.; Khadse, B.G.; Shirodkar, M.V. (1987). A rapid method for the evaluation of new antituberculous agents. *Chemotherapy*. 33(1), 22-27
14. Collins, L.; Franzblau, S.G. (1997). Microplatealamar blue assay versus BACTEC 460 system for high-throughput screening of compounds against *M. tuberculosis* and *M. avium*. *Antimicrob. Agents. Chemother.* 41(5), 1004-1009
15. Laszlo, A.; Gill, P.; Handzel, V.; Hodgkin, M.M.; Helbecque, D.M. (1983). Conventional and radiometric drug susceptibility testing of *M. tuberculosis* complex. *J. Clin. Microbiol.* 18(6), 1335-1339.
16. Chung, G.A.; Aktar, Z.; Jackson, S.; Duncan, K. (1995). High-throughput screen for detecting antimycobacterial agents. *Antimicrob. Agents. Chemother.* 39(10), 2235-2238
17. Norden, M.A.; Kurzynski, T.A.; Bownds, S.E.; Callister, S.M.; Schell,R.F. (1995). Rapid susceptibility testing of *M. tuberculosis* (H37Ra) byflow cytometry. *J. Clin. Microbiol.* 33(5), 1231-1237.
18. Pina-Vaz, C.; Costa-de-Oliveira, S.; Rodrigues, A.G. (2005). Safesusceptibility testing of *M. tuberculosis* by flow cytometry with thefluorescent nucleic acid stain SYTO 16. *J. Med. Microbiol.* 54(Pt 1), 77-81.
19. Pauli, G.F.; Case, R.J.; Inui, T.; Wang, Y.; Cho, S.; Fischer, N.H Franzblau, S.G. (2005). New perspectives on natural products in TB drug research. *Life. Sci.* 78(5), 485-494.
20. Arain, T.M.; Resconi, A.E.; Singh, D.C.; Stover, C.K. (1996). Reporter gene technology to assess activity of antimycobacterial agents in macrophages. *Antimicrob. Agents. Chemother.* 40(6), 1542-1544
21. New, D.C.; Miller-Martini, D.M.; Wong, Y.H. (2003). Reporter gene assays and their applications to bioassays of natural products. *Phytother. Res.* 17(5), 439-448





Jayalakshmi et al.,

22. Chutima Linmat Vapirat, Sinenartsirisopaporn, Prasat Kittakoop. Antitubercular and Antiplasmodial constituents of *Abrusprecatorius*. *Planta Medica*.2004;70(3):276-278.
23. Balungile Madikizela, Ashwell Rungano Ndhala, Jeffrey Franklin Finnie et al. In vitro antimicrobial activity of extracts from plants used traditionally in South Africa to treat tuberculosis and related symptoms. Evidence based complementary and Alternative medicine.2013;2013:1-8.
24. Rajasekhar Saha, Azhar Ahmed. Phytochemical constituents and Pharmacological activities of *Acalypha indica* Linn: A review. International journal of Pharmacaceutical sciences and research.2011;2(8):1900-1904.
25. Tanmoy Sinha, Abhijith Bandyopadhyay. Ehnopharmacological importance and valuable phytochemicals of *Acalypha indica* (L.) A review. *Int.J.Res.Pharm.Sci*.2012;3(3):360-368
26. Vikranth Arya. A Review on Anti-Tubercular Plants. International Journal Of Pharm Tech Research.2011;3(2):572-880.
27. Renu Gupta, Bandana Takur, Pushpendra Singh et al. Anti tuberculosis activity of selected medicinal plants against multi drug resistant Mycobacterium tuberculosis isolates. *Indian J Med Res*.2010;131:809-813.
28. Ignacimuthu S, Shanmugam N. Antimycobacterial activity of two natural alkaloids, Vasicine acetate and 2-acetylbenzyl amine, isolated from Indian shrub *Adhatoda Vasica* Ness. Leaves. *Journal of biosciences*.2010;35(4):565-570.
29. Suja K P, Leny Jose, Divya Lakshmanan et al. Isolation and characterisation of Antimycobacterial compounds from fruits of *Aeglemarmelos* (L) correa. *Journal of Communicable Diseases*.2017;49(4):32-38.
30. S. Phongpaichit, V. Vuddhakul, S. Subhadhirasakul et al Evaluation of the antimycobacterial activity of extracts from plants used as self medication by AIDS patients in Thailand. *Pharmaceutical biology*.2006;44(1):71-75.
31. R Pratap Chandran, Dipu Divakaran, OSSD Consortium. Isolation and characterisation of antimycobacterial compounds from the leaf of *Aloe vera* (L.) Burm.f.*Journal of Applied Pharmaceutical Sciences*.2017;7(2):217-222.
32. Allan Patrick G Macabeo, Karsten Krohn, Dietmar Gehelet al. Indole alkaloids from the leaves of Philippine *Alstoniascholaris*. *Phytochemistry*. 2005;66:1158-1162.
33. Maksun Radji, Marita Kunniati, Ariyani Kiranasari. Comparative antimycobacterial activity of some Indonesian medicinal plants against multi drug resistant Mycobacterium tuberculosis. *Journal of Applied Pharmaceutical sciences*.2015;5(1):19-22.
34. Amudha Prabu, Sameer Hassan, Prabuseenivasan et al Andrographolide: A potent Antituberculosis compound that targets Aminoglycoside 2'-N-acetyltransferase in Mycobacterium tuberculosis.*J.Mol.Graph Model*.2015;61:133-140.
35. Ana V, Coria Tellez, Efigenia Montalvo Gonzalez et al *Annonamuricata*: A comprehensive review on its traditional medicinal uses, Phytochemicals, Pharmacological activities, mechanism of action and toxicity. *Arabian Journal of Chemistry* 2016
36. Shuaibu Babaji Sanusi, Mohd Fadzelly Abu Baker, Maryati Mohammed et al. South east Asian Medicinal plants as a potential Source of Antituberculosis agent. Evidence based complementary and Alternative Medicine.2017;2017:1-39.
37. Sara E Gomaa, Maizatulkamal Yahayu, Mukhtiningdh Nurjayadi et al Antimicrobial compounds from *Catharanthus roseus*. A review. International Journal of Scientific and technology.2019;8(10):113-121.
38. M.Suresh, P K Rath, A Panneerselvam et al. Antimycobacterial effect of Leaf extract of *Centellaasiatica* (Mackinlayaceae).*Research journal of Pharmacy and technology*.2010;3(3):872-876.
39. Suriyati Mohamad, Nur Najihah Ismail, Thaigarajan Parumasivam. Antituberculosis activity, Phytochemical identification of *Costusspeciosus* (J Koenig)sm, *Cymbopogancitratus* (DC-Ex.Nees) stapf and *Tabernae Montana coronaria* (L) wild and their effect on growth Kinetics and cellular integrity of Mycobacterium tuberculosis H37RV *BMC complementary and Alternative medicine*.2018;18(1):5
40. Benjamin U Ogudo, TemitopeO Lawal, Bolanle A Adeniyi. Extracts of *Zingiberofficinale* Rosc. (ginger) and *Curcuma longa* Linn (turmeric) Rhizomes inhibited non tuberculous Mycobacterium in vitro. *Journal of Biology, Agriculture and Health care*.2014;4(12):95-103.
41. Ramaiah Maddi, Cevilal K, Satish Babu et al. Invitro MABA antituberculosis assay of *Eclipta alba* (L) Hask Whole plant. *The Pharma Innovation journal*.2017;6(5):103-105.





Jayalakshmi et al.,

42. Mohammed Yousif Ibrahim, Najihah Mohd Hashim, Abdalbasit Adam Mariod et al. alpha mangostin from *Garcinia mangostana* Linn. An updated review of its pharmacological properties. *Arabian journal of Chemistry*.2016;9:317-329.
43. Anupama Roy. Pharmacological activities of Indian Heliotrope (*Heliotropium indicum* L): A review. *Journal of Pharmacognosy and Phytochemistry*.2015;4(3):101-104.
44. Rajandeeep Kaur and Harpeetkaur. Antitubercular activity and phytochemical screening of selected medicinal plants. *Oriental journal of chemistry*.2015;31(1):597-600.
45. Gangandeeep Chaudhary, Sandeep Goyal, Priyanka Ponnina. Lawsonia inermis Linnaeus. A Phytopharmacological review. *International Journal of Pharmaceutical sciences and drug research*.2010;2(2):91-98.
46. Khushboo Dhirajlal Jethva, Dhara Rajendrakumar Bhatt, Maitreyi N Zaveri. Antimycobacterial screening of selected medicinal plants against *Mycobacterium tuberculosis* H37RV using Agar Dilution method and the Microplate Resazurin assay. *International journal of Mycobacteriology*.2020;9:150-155.
47. Jonel P Saludes, Mary J Garson, Scott G Franzblau et al. Antitubercular constituents from the hexane fractions of *Morindacitrifolia* Linn.(Rubiaceae). *Phytother.Res*.2002;16:683-685.
48. Rasik Bihari Vyas, Dr. Purnima Shrivastava, Dr. Geeta Parihar. Evaluation of Anti-Mycobacterial Activity of *Ocimum sanctum* and *Lantana camara* Against *M. Tuberculosis* standard strain.2018;2(10):1-6.
49. Chandan Singh, Santosh K Singh, Gopal Nath et al. Anti-mycobacterial activity of *Piper longum* L. Fruit extracts against multi drug resistant *Mycobacterium* spp. *International journal of Phytomedicine*.2011;3:353-361.
50. Noviany Hasan, Hasnah Osman, suriyati Mohammed et al The chemical components of *Sesbania grandiflora* root and their Antituberculosis activity. *Pharmaceuticals*.2012;5(8):882-889.
51. Joseph M Nguta, Regina Appiahpong, Alexander K Nyarko et al. Antimycobacterial and Cytotoxic activity of selected medicinal plant extracts. *Journal of ethnopharmacology*.2016;182:10-15.
52. L B N Putra Dwija, Mita Anggraoni, Ni Putu Ariantari. Antituberculosis activity of Forest Kedondong (*Spondia spinnata*) stem bark extract against multiple drug resistant (MDR) strain of *Mycobacterium tuberculosis*. *Bali medical journal*.2016;5(1):27-30.
53. Gaber El Saber Baliha, Luay M Alkazni, Lamiaa G Wasef et al. *Syzygium aromaticum* L (Myrtaceae). Traditional uses, Bioactive chemical constituents, pharmacological and toxicological activities. *Biomolecules*.2020;10(2):202-218.
54. Mohamed F Alajmi, Ramzi A Mothana, Adnan J Al-Rehaily, Jamal M Khalid. Antimycobacterial activity and safety profile assessment of *Alpinia galangal* and *Tinospora cordifolia*. Evidence based complementary and alternative medicine. 2018;2:1-12.
55. Neerja Tiwari. Jayaprakash Thakur, Dharmendra Saika. Antitubercular diterpenoids from *Vitex trifolia*. *Phytomedicine*.2013;20(7):605-610.
56. Periyakaruppan Adakappan, Manickavasagan K annapiran, Arulandhuanthonisamy. Antimycobacterial activity of *Withania somnifera* and *Pueraria tuberosa* against *Mycobacterium tuberculosis* H₃₇RV. *J Acad Indus Res*.2012;1(14):153-156.
57. Panomwan Panseela, Kanlaya Lomchoey, Samran Pratsai et al. Antiplasmodial and antimycobacterial cyclopeptide alkaloids from the root of *Ziziphus mauritiana*. *Phytochemistry*.2011;72:909-915.
58. Assam Jean Paul, Yumsu Tcham Mare Flaubert, Moni Ndedi Esther Del Florence. Phytochemical screening, Antimycobacterial activity of three medicinal Cameroonians plants and acute toxicity of hydroethanolic extract of *Vitellaria paradoxa*. *Journal of Drug Delivery and Therapeutics*.2020;10(1):96-104..
59. Mehdi Sharif Rad, Elena Maria Varoni, Bahare Saheli et al. Plants of the Genus *Zingiber* as a source of Bioactive Phytochemicals from tradition to pharmacy. *Molecules*. 2017; 22(12):2145.
60. N.J.Yob, S.Mohd Joffry, M M R Meor Mohd Affandi et al. *Zingiber zerumbet* (L) smith. A review of its ethnomedicinal, chemical and pharmacological uses. Evidence based complementary and alternative medicine.2011;2011:1-12.





Jayalakshmi et al.,

Medicinal Plants of Western Ghats with Antitubercular Activity

Sl No.	Botanical name	Common name Regional name	Chemical constituent	Plant parts used	Type of solvents used for extraction	Method of extraction	Method of anti TB assay
1	<i>Abrus precatorius</i> ^{22, 23} Family: Fabaceae	Bead Vine Black eyed susan Bhudhist rosary bead Crab's Eye Indian liquorice Rosary pea Wild liquorice <i>Chuvannakunni</i> <i>Kunnikuru</i> <i>Kunni</i> <i>Kakani</i> <i>Gunj</i>	Abruquinone B (flavonoid Isoflavoquinone)	Leaves Stem	Petroleum ether Dichloromethane Ethanol Water	maceration	MABA
2	<i>Acalypha indica</i> ^{24, 25, 26, 27} Family: Euphorbaceae	Indian copper leaf Indian acalypha Indian nettle Three seeded mercury <i>Kuppumani</i>	Kaempferol (flavonoid Tetrahydroflavone) acalyphamide and other amides, quinone, sterols, cyanogenic glycoside	Leaves Whole plant	Aqueous Ethyl acetate fraction of methanolic extract Aqueous fraction of methanolic extract	soxhlet extraction	Microbroth dilution method Colorimetric Bact/Alert 3D system
3	<i>Adhatoda vasaka</i> ^{26, 27, 28} Family: Acanthaceae	Adosa <i>Adalodakam</i>	quinazoline alkaloids (vasicoline, vasicolinone, vasicinone, vasicine, triterpenes and anisotine) Bromhexine Ambroxol Vasicine acetate 2-acetyl benzyl amine	Leaves	Hexane Ethyl acetate Methanol Aqueous	sequential extraction	conventional method of Grange and Snell Broth microdilution method
4	<i>Aegle marmelos</i> ²⁹ Family: Rutaceae	Bael tree Bengal quince Holy fruit tree Indian Bael	Imperatorin(pso ralen) β-sitosterol(phyto	Whole fruit	Hexane Chloroform methanol	Pressurised sequential extraction	Rezazurinmi crotitre assay





Jayalakshmi et al.,

		Stone apple Wood apple <i>Koolakam,</i> <i>Koovalam,</i> <i>Vilvam,</i> <i>Mavilavu</i>	sterols)stigmast erol(phytosterol)plumbagin(nap hthaquinone)ma rmesinmarmin(coumarin)				
5	<i>Allium cepa</i> ²⁷ Family: Alliaceae	Bulb onion Common onion <i>Ulli</i>	Volatile oil with sulphurous constituent including allylpropyl disul phide, sulphur containing compounds including allicin, alliin, flavonoids; phenolic acids and sterols	Bulb	Aqueous Aqueous Ethanolic	soxhlet extraction	Broth microdilutio n method MABA
6	<i>Allium sativum</i> ²⁷ Family: Alliaceae	Garlic <i>Velluli</i>	Allicin Sulphur containi ng amino acids known as alliin	Clove	Aqueous Aqueous Ethanolic	soxhlet extraction	Broth microdilutio n method MABA
7	<i>Alpinia galanga</i> ³⁰ Family: Zingiberaceae	Java galangal Siamese ginger Greater galang <i>Aratha</i> <i>Kolaratha</i> <i>Kolinji</i> <i>Pararatha</i>	1' - acetoxychavicol acetate	Rhizom e	Chlorofom Methanol Water	maceration	MABA
8	<i>Aloe vera</i> ³¹ Family: Asphodelaceae	Medicinal Aloe Burnt Aloe <i>Kattarvazha</i>	Aloverose (polysaccharide)	Leaves Leaves Leaves	Pure gel Chloroform Methanol Hydroethanolic extracts	hot and cold extraction cold maceration.	Broth microdilutio n method Agar well diffusion method MABA
9	<i>Alstonia scholaris</i> ³² Family: Apocynaceae	Devil tree Shaitan wood <i>Daivappala</i> <i>Ezhilampala</i>	seco-uleine alkaloids, manilamine N4 -methyl	leaves	methanol	Methanolic extraction	MABA





Jayalakshmi et al.,

		<i>Mangalappala</i> <i>Pala</i> <i>Yekshippala</i>	angustilobine B 20- (E)- vallesamineang ustilobine B N4 -oxide 20(S)- tubotaiwine 6,7-seco- angustilobine				
10	<i>Andrographis paniculata</i> ^{33,34} Family: Acanthaceae	Andrographis Green chiretta Kalmegh <i>Kakaanjiram</i> <i>Kiriyathu</i> <i>Nilavepu</i> <i>Nilamkanjiram</i>	Andrographolid e(diterpenoid)	herbs	aqueous	maceration	Broth microdilutio n method
11	<i>Annona muricata</i> ^{33,35} Family: Annonaceae	Soursop Guanabana Graviola Prickly custard apple <i>Cancer chakka</i> <i>Mullanjakka</i> <i>Mulluathi</i> <i>Mullathi</i>	Annonacin(acet ogenins)	leaves	aqueous	maceration	Broth microdilutio n method
12	<i>Catharanthus roseus</i> ³⁷ Family: Apocynaceae	Periwinkle Rose periwinkle Madagascar periwinkle Vinca <i>Aadam-Howa chedi</i> <i>Anchithalthetti</i> <i>Banappovu</i> <i>Kasithetti</i> <i>Kuppavela</i> <i>Nithyakalyani</i> <i>Savakottapacha</i> <i>Savamnaripoovu</i> <i>Sadapushpi</i> <i>Simitherichedi</i> <i>Smasanapochedi</i> <i>Ushamalari</i> <i>Vishanarayani</i>	Perivine Ursolic acid(terpene) Oleanolic acid(pentacyclic triterpenoids)	leaves	80% methanol	Methanolic extraction	Agar diffusion Microbroth dilution
13	<i>Centella asiatica</i> ^{33,36,38} Family: Apiaceae/ Umbelliferae	Indian penny— wort Spadeleaf Pohekula Gotu kola <i>Kodangal</i> <i>Kodakan</i>	Octadectrienoic acid (poly unsaturated fattyacid)n- hexadecanoicaci d(saturated	leaves	Ethanollic extract	Ethanollic extraction	Broth microdilutio n method





Jayalakshmi et al.,

		<i>Kuthirakulambuchedi</i> <i>Mutthil</i> <i>Vellara</i>	fattyacid)				
14	<i>Costus speciosus</i> ³⁹ Family: Costaceae	Costus Cane reed Crepe ginger Spiral ginger <i>Aanakoova</i> <i>Aanappoo</i> <i>Channa</i> <i>Channakoova</i> <i>Malavayambu</i> <i>Narumchanna</i> <i>Nuchanna</i>	7-Ergosterol Pentadecanoic acid or Pentadecylic acid Stigmast-4-en-3-one Lanost-8-en-3-ol, (3 β) Octadecanoic acid, methyl ester or Stearic acid, methyl ester or Methyl stearate Hexadecanoic acid, methyl ester or Methyl palmitate or Palmitic acid, methyl ester 9,12-Octadecadienoic acid (Z,Z), methyl ester or Linoleic acid, methyl ester or Methyl linoleate Hexadecanoic acid or n-Hexadecanoic acid or Palmitic acid or Palmitinic acid(fattyacids)	Stems flowers	80% methanol n-hexane chloroform ethyl acetate n-butanol	Exhaustive maceration with 80% alcohol The methanol extracts were sequentially partitioned using five solvents of different polarities: n-hexane, chloroform, ethyl acetate, and n butanol	MIC method
15	<i>Curcuma longa</i> ⁴⁰ Family: Zingiberaceae	Turmeric <i>Manjal</i>	Curcuminoids	Rhizome	Methanol Dichloromethane n-hexane	Soxhlet extraction	MIC method MBC method
16	<i>Cymbopogon citratus</i> ³⁹ Family: Poaceae/Graminae	Oil grass Lemon grass Melissa grass West Indian lemon grass <i>Chayapullu</i> <i>Chenganampullu</i> <i>Chonakapullu</i>	9,12-Octadecadienoic acid (Z,Z) or Linoleic acid(fattyacid) Stigmasterol or Sigmasta-5,22-dien3-	rhizomes	80% methanol n-hexane chloroform ethyl acetate n-butanol	Exhaustive maceration with 80% alcohol The methanol extracts were sequentially	MIC method





		<i>Inchipullu</i> <i>Kavattapullu</i> <i>Kothipullu</i> <i>Padarpullu</i> <i>Sambarapullu</i> <i>Thannakkapullu</i> <i>Theruvapullu</i> <i>Thyilapullu</i> <i>Vasanapullu</i>	ol(phytosterols), (3 β , 22E) 7,10- Octadecadienoic acid, methyl ester γ -Sitosterol or Clionasterol or Stigmast5-en-3- ol, (3 β) Selina-6-en-4-ol 5-Cholestene-3- ol, 24-methyl Hexadecanoic acid, methyl ester or Methyl palmitate or Palmitic acid, methyl ester Cyclooctacosane			partitioned using five solvents of different polarities: n- hexane, chloroform, ethyl acetate, and n butanol	
17	<i>Eclipta prostrata</i> ⁴¹ Family: Asteraceae/composi tae	False daisy Trailing eclipta Bhringaraj Thistle <i>Kaithoni</i> <i>Kaiyan-takara</i> <i>Kanjunni</i> <i>Kayyonni</i>	EcliptalEcliptine Ecliptalbine α - Terthienylmeth anol β -amyrin, Sigmasterol(phy tosterol) Polypeptides	Whole plant	Ethanolic extract Aqueous extract	maceration	MABA
18	<i>Garcinia mangostana</i> ⁴² Family: Clusiaceae/Guttifer ae	<i>mangostana</i> Mangosta Mangustan Mangosteen <i>Mangosta</i> <i>Mangustan</i>	α -mangostin , β - mangostin , γ - mangostin(xant hones), garcinone D(xanthones), mangostenol, garcinone B, mangostanin, mangostanol, mangostenone A, tovophyllin B , demethylcalaba xanthone trapezifolixanth one mangostinone	Fruits	chloroform methanol extract	Freeze drying	Microbroth dilution
19	<i>Heliotropium indicum</i> ^{36,43} Family:	Indian turnsole <i>Thekkada</i> <i>Therkkada</i>	1-dodecanol Beta linalool	Aerial parts	Volatile oil	hydrodistilla tion	MABA





Jayalakshmi et al.,

	Boraginaceae	<i>Thekkida</i>					
20	<i>Lawsonia inermis</i> ⁴⁵ Family: Lythraceae	Henna plant Camphire Egyptian privet Cypress shrub Samphire <i>Mailanchi</i> <i>Pontalasi</i>	Luteolin- 7 α - glycoside Luteolin- 3' α - glycoside Cosmosiin Stigmasterol Acacetin Fraxetin Scopoletin Esculetin p-coumaric acid Betulinic acid Botulin Lupeol Apigenin Apiin Lawsoniaside Lalioside 1,2-dihydroxy- 4-o-glucosyloxy naphthalene 2-methoxy-3- methyl-1,4- naphthoquinon e	Leaves	Hexane Acetone methanol	Soxhlet extraction	MABA
21	<i>Leptadenia reticulata</i> ⁴⁶ Family: Asclepiaceae	<i>Kurunivalli</i> <i>Karkodavalli</i> <i>Palachedi</i>	Leptadenol Leptidin beta sitosterol, Beta amyrrin acetate	Roots	Alcoholic extract Hydroalcoholic extract Aqueous extract	Alcoholic extraction Hydroalcohol ic extraction Aqueous extraction	Agar dilution method Microplatere sazurin assay method ¹⁸
22	<i>Morinda citrifolia</i> ^{46,47} Family: Rubiaceae	Indian Mulberry Beach Mulberry Cheese Friut <i>Noni</i>	Anthraquinones alizarin and its glycosides, nordamnacanth ol. Ursolic acid and β sitosterol. asperuloside and caproic acid ⁵	Unripe fruits	Crude extract	Ethanollic extract.	Broth microdilutio n method
23	<i>Ocimum sanctum</i> ^{46,48} Family: Lamiaceae	Holy basil <i>Tulsi</i>	Ursolic acid, apigenin, orientinluteolin, apigenin-7- Oglucuronide,	leaves	Aqueous methanolic	Hot water extraction Methanolic extraction	MABA





Jayalakshmi et al.,

			luteolin-7-Oglucuronide				
24	<i>Piper longum</i> ⁴⁹ Family: Piperaceae	Indian long pepper <i>Tippili</i>	Piperine (alkaloid)	Fruits	methanol	maceration	Broth microdilution method
25	<i>Sesbania grandiflora</i> ^{36,50} Family: Fabaceae/Leguminosae	Basna Humming bird tree Sesban <i>Agathicheera</i> <i>Agathi</i> <i>Agathi</i> <i>Argathi</i> <i>Basna</i> <i>Rudramaram</i>	Medicarpin(flavanoid) Sativan(flavanoid) Betulinic acid(Pentacyclic triterpenoids)	Roots	Aqueous methanol	maceration	Tetrazolium microplate assay
26	<i>Solanum torvum</i> ^{36,51} Family: Solanaceae	Turkeyberry Devil's Fig <i>Anachunda</i> <i>Chunda</i> <i>Cheriyamodumuttika</i> <i>Chithramchunda</i> <i>Malamchunda</i> <i>Parachunda</i>	Tannins, Flavanoids- Torvanol A	leaves	Hydroethanolic extract	maceration	MABA
27	<i>Spondias pinnata</i> ⁵² Family: Anacardiaceae	Hog plum Indian hog plum Wild mango <i>Ambazham</i> <i>Kattambazham</i> <i>Mampulli</i> <i>Pithanam</i>	Flavonoids Polyphenols Steroids Alkaloids saponins	bark	Ethanol Chloroform	maceration	MABA
28	<i>Syzygium aromaticum</i> ^{44,53} Family: Myrtaceae	Clove trees Clove <i>Grambu</i> <i>Karayambu</i>	Eugenol Thymol Carvarcol (terpenes)	buds	Hexane Acetone methanol	Soxhlet extraction	MABA
29	<i>Tinospora cordifolia</i> ⁵⁴ Family: Menispermaceae	Moon creeper Bile Killer Heart leaved moonseed <i>Amruthu</i> <i>Amruthavalli</i> <i>Chitamruthu</i> <i>Siddamrith</i>	Furanolactones, clerodine derivatives Tinosporides	leaves	Dichloromethane Phenol	percolation	Broth microdilution method
30	<i>Vitex trifolia</i> ^{36,55} Family: Verbenaceae	Arabian lilac Hand of Mary Indian Privet Indian three leaf Vitex <i>Nochi</i> <i>Vellonochi</i>	Halimanediterpenoid (9-hydroxy-13(14)-labden-15, 16-olide)	leaves	methanol	Extraction under reduced pressure	MABA





Jayalakshmi et al.,

31	<i>Withania somnifera</i> ⁵⁶ Family: Solanaceae	Winter cherry <i>Amukkuram</i>	Withaferin A(steroidal lactone)	Leaves roots	aqueous	Maceration	MABA
32	<i>Ziziphus mauritiana</i> ^{56,57} Family: Rhamnaceae	Jujube tree Common Jujube Indian Jujube Chinese date <i>Badari</i> <i>Badaram</i> <i>Cherumali</i> <i>Elentha</i> <i>Jujube</i> <i>Ilantha</i> <i>Kolam</i> <i>Lanthapazham</i> <i>Parinthudar</i> <i>Perimthudali</i>	Mauritine (cyclic peptides) Nummularine(c yclopeptide alkaloids)	root	Methanol Ethanol	maceration	MABA
33	<i>Zingiber officinae</i> ^{36,40,58,59} Family: Zingiberaceae	Canton ginger Ginger Halia Spice ginger <i>Andrakam</i> <i>Chukku</i> <i>Erukizhangu</i> <i>Inchi</i>	Gingerol Shogaol Paradol (Alkaloid)	Rhizom e	Methanol Dichloromethane n-hexane Hydroethanol (70/30) Distilled water	Soxhlet extraction Maceration Decoction	MABA
34	<i>Zingiber zerumbet</i> ^{36,60} Family: Zingiberaceae	Bitter Ginger Broad leaved Ginger Pine cone ginger Shampoo ginger Wild ginger Zerumbet ginger <i>Kattinchi</i> <i>Kollinchi</i> <i>Kattukolinchi</i>	Zerumbone(ses quiterpenoids) Alpha humulene Humulene epoxide II (epoxides) Caryophyllene oxide (terpenes) Camphene (terpenes)	Rhizom e	Chloroform methanol	maceration	MABA





Groundwater Quality Characteristics at Aravakurichi Taluk in Karur District Tamilnadu, India

Veerakumar D¹, Ilavarasan N^{2*} and Muthulingam M³

¹Ph.D Research Scholar, Department of Zoology, Annamalai University, Annamalainagar, Tamil Nadu, India.

²Assistant Professor, Department of Zoology, Government Arts College, Karur, Tamil Nadu, India.

³Associate Professor, Department of Zoology, Annamalai University, Annamalainagar, Tamil Nadu, India.

Received: 12 Mar 2021

Revised: 13 Mar 2021

Accepted: 15 Mar 2021

*Address for Correspondence

Ilavarasan N

Assistant Professor,

Department of Zoology,

Government Arts College,

Karur, Tamil Nadu, India.

Email: veerakumarduraisamy1992@gmail.com



This is an Open Access Journal / article distributed under the terms of the **Creative Commons Attribution License** (CC BY-NC-ND 3.0) which permits unrestricted use, distribution, and reproduction in any medium, provided the original work is properly cited. All rights reserved.

ABSTRACT

Water is an important part to human life. The real points of the present work are to survey the nature of the ground water and its effect in Around Aravakurichi Taluk, Karur District of Tamilnadu, India. The present examination center to bring a mindfulness among the general population about the nature of ground water by taking water tests from different areas for Physico – Chemical investigation of the ground water. This examination result was compared and the WHO, ICMR, USPH and European standards of drinking water quality parameters with the accompanying water quality parameters to be specific pH, Electrical conductivity, Cl, Na, K, Ca, Mg, Total dissolved solids, Total hardness, Fluoride and so on. Different chemical strategies have been utilized to research the degree level of contamination in ground water.

Keywords: Ground Water characteristics, Aravakurichi Taluk, Karur, Tamil Nadu, India.

INTRODUCTION

This paper attempts to center around the drinking water nature of Aravakurichi Taluk Karur. Karur is an industrial town situated on the banks of the waterway Amaravathi. It is situated at 10.95° N, 78.08° E and 396 km from Chennai on southwest course. Amaravathi stream is a tributary to the waterway Kavery. It is conversions with stream Kavery

30411



**Veerakumar et al.,**

at around 12 km downstream of Karur. During the most recent four decades, the town emerged as a noteworthy material focus with its 1000 odd power loom and handloom color units creating bedspreads, towels and furnishing. There are around 1000 units along a 17 km extend on the banks of river Amaravathi, which attempt bleaching, dyeing, weaving, tailoring, knitting, knotting, packing, transporting and trading. There are 487 textile units in capacity and discharge around 14,610 kilo liters for each day of treated emanating into the stream, Amaravathy. The drinking water quality in the Karur town is contaminated because of ceaseless release of effluents (Shanmugapriya *et al.*, 2017). Karur is limited by Namakkal region in the north, Dindigul area in the south, Tiruchirapalli district on the east and Erode region on the west. It has a zone of 2896 sq.km. Populace is 1076588 according to 2011 census (Salahudeen *et al.*, 2013). Water likely is the most imperative natural resource on the world, life can't exist and industries can't work without water. Not at all like numerous other raw materials there is not a viable alternative for water in a significant number of its employments. Water assets are the most misused of the nature. Contamination of water bodies is expanding relentlessly because of fast industrialization and urbanization, and changing ways of life. Water contamination may mean adjustment in physical, substance and natural qualities of water. Contaminations from modern, horticultural, urban, residential, radioactive and mining sources, and these poisons sullied the water that end up unfit for living communities. Addition of abundance of unfortunate substances to water that makes it destructive to man, creature and oceanic life. Water quality can be surveyed with the accompanying TDS parameters (American Public Health Association, 2005) (Table 1). World Health Organization (WHO) (1984, 1996) has given the rules to survey the drinking water quality (World Health Organization (WHO), 1984) (Table 2) (Udhayakumar *et al.*, 2016). A basic scrutiny of the accessible writing has uncovered that no logical examination was completed concerning the nature of ground water in and around Aravakurichi Taluk. Along these lines, an endeavor has been made to survey the quality of ground water in and around Aravakurichi Taluk at Karur District.

MATERIALS AND METHODS

Ground water samples were collected from 5 bore wells in and around Aravakurichi Taluk. The sampling stations are represented as T. Pasupathipalayam, T. Sivan Colony, T. Sengalapuram, Vengadapuram, Chinnadharapuram. The water samples were collected in one liter polythene bottles. All samples were refrigerated at 4°C till the completion of analysis. The samples were subjected to physico-chemical analysis. The Ph was determined immediately at the place of collection with the help of pH pen. Total dissolved solids and Electrical conductivity of the water analysis kit (Elico). Carbonate, bicarbonate, calcium, magnesium, total hardness and chloride were estimated by titrimetric method. BOD, COD and dissolved oxygen were estimated by reflux method. Nitrate and sulphate were estimated by using spectrophotometric method using standard procedure. (APHA 1995; Zahir Hussain and Rajadurai, 2013).

RESULTS AND DISCUSSION

Electrical conductivity

The EC values for samples range between 910 and 3142 (μ mho/ cm). The EC value is directly proportional to the Total dissolved matter. Our samples show higher EC values than the permissible limit. The electrical conductivity of all the Five places is not in the permissible limits. Among all the five places, Chinnadharapuram shows very high value (electrical conductivity) due to this wage of effluents. When EC value exists at 3000 μ mho/cm, the generation of almost all the crops would be affected and it may result in much reduced yield (Srinivas *et al.*, 2000) (Table3). Electrical conductivity is the measure of the ability of water to conduct electrical current. This capacity depends upon the grouping of ions, ionic mobility, and temperature. The electrical conductivity of water straightforwardly related with its total dissolved solids content is expressed as Micro Siemens/cm at 250 C (Shrinivasa Rao and Venkateswaralu, 2000).



**Veerakumar et al.,****Total hardness (TH)**

The total hardness in ground water samples collected from the study area ranged from 200 to 400 mg/L. The total hardness of all water samples are within the limit (600 mg/lit). Hardness of water is caused by carbonates, bicarbonates, sulphates and chlorides of calcium and magnesium. It prevents the lather formation with soap and increases the boiling point of water. The maximum permissible limit of total hardness for drinking purpose is 600 mg/L. Hardness more than 300 mg/L may cause heart and kidney problems. A commonly used parameter for water quality is hardness due to the presence of Ca and Mg with anion like Sulphate, Chloride and Bicarbonate. For these, Manivasakam (2005) has suggested some standards (Table 4). Maximum permissible limit of calcium and magnesium in drinking water is 100 mg/L and 50 mg/L as suggested by and WHO. The pH value of water source is a measure of the hydrogen ion concentration in water and indicates whether the water is acidic or alkaline (Kotaiah and Kumaraswamy, 1994). Most of the bio-logical and chemical reactions are influenced by the pH of water system. All the sampling locations were found to have water pH within these permissible limits, which lies in the range prescribed by WHO (World Health Organization, 1996). Basically, the pH was determined by the amount of dissolved carbon di oxide which forms carbonic acid in water. The pH values of all water samples are within the range of 7.22 and 7.87 and it falls in the acceptable limits. The value of alkalinity is within the limit in all places.

Total dissolved solids

The total dissolved solids in water are due to presence of all inorganic and organic substances. High values of TDS in cause's gastrointestinal irritation to the human and prolonged use of such water may result in the formation of kidney stones and also cause heart attack. The high percentage of TDS also imparts alkalinity nature to water. TDS indicate the salinity behavior of groundwater. Water containing more than 500 mg/L of TDS is not considered desirable for drinking water. The most desirable limit of TDS is 500 mg/L and maximum allowable limit is 1500 mg/L. The total dissolved solids present in the water sample ranges from 637 to 2179 which exceeds the permissible limit of 500 mg/lit.

Calcium: The calcium values are found to be in the range of 50-96 within permissible limit of WHO (200 ppm). It is directly related to hardness. It is common in natural waters and essential for all organisms. Calcium plays an important role for proper bone growth. The rock, lime stone and industrial waste are the rich sources of calcium from where it is leached in the ground water. The magnesium values are found to be in the range 18-38 ppm. The magnesium values exceed the permissible limit of WHO (150 ppm) in most of the ground water samples.

Chloride: In the present analysis, the chloride content varies from 220 to 760 mg/L. Most of the ground water samples show chloride concentration within the permissible limit (250 mg/L). Except Chinnadharapuram (760 mg/L). High concentration of chloride is considered to be an indicator of pollution by organic waste of animals and industrial origin (Yadav, 2011).

Fluoride: In the present case, the value of fluoride concentration in ground water samples lie between 0.4 and 1.0 mg/L. All water samples have fluoride concentration within permissible limit (1.0mg/L) of WHO. Groundwater contamination due to fluoride may be due to geological factors such as weathering of minerals, and decomposition of certain minerals in earth. High fluoride content in ground water causes serious damage to the teeth and bones of human system leads to dental fluorosis and skeletal fluorosis. Hence excess fluoride should be removed from water and this process is called defluoridation.

Nitrate: The nitrate in water is responsible for the growth of blue green algae (Abdul Jameel, 2002). The nitrate values are found to be in the range 22 - 40 ppm for the ground water samples. Most of the values of ground water samples are within the permissible limit of WHO (45 ppm).



**Veerakumar et al.,**

Sulphate: High concentrations of sulphate are due to the effluent from industries and the run-off agricultural land (Zahir Hussain and Rajadurai, 2013). The sulphate values are recorded within the range 28 - 164 ppm. The values of sulphates are exceeded the permissible limit of WHO (250 ppm) in most of the ground water samples.

CONCLUSION

The examination of water quality in and around Aravakurichi Taluk, Karur District of Tamilnadu has been done. The information is contrasted and standard parameters recommended by WHO, ICMR, UPSH and European standards. The pH, Total hardness the whole water test are well inside allowable permissible points. The TDS of all the water tests isn't inside allowable breaking points. The investigation of water quality parameters of the Chinnadharapuram territory plainly shows that the examples of stations are exceptionally contaminated. Consequently it is proposed that essential careful steps to be embraced before use, else it might prompts numerous general medical problems. It requires starter treatment to decrease the hardness and disintegrated solids. So, it is reasoned that According to this report, the ground water in and around Aravakurichi Taluk, Karur is appropriate for drinking purposes, agricultural utilization, industrial purposes and generally it is not harmful to human beings whereas some sample needs preliminary treatments before usage.

REFERENCES

1. American Public Health Association. (2005). APHA (2005) Standard methods for the examination of water and wastewater. *APHA Washington DC, USA*.
2. APHA, Standard method for the examination of the water and waste water 16th edition APHA. Washington DC. (1985)
3. CH. Srinivas, RS. Piska, Chinna Venkateswar, MSS. Rao, et al. (2000). Studies on ground water quality of Hyderabad. *Pollution Research*, **19**, 2
4. Jameel, A. A. (2002). Evaluation of drinking water quality in Tiruchirapalli, Tamil Nadu. *Indian journal of environmental health*, *44*(2), 108-112.
5. Kotaiah, B and Kumara Swamy, N., 1994, Environmental Engineering Laboratory manual, 1st ed., Charotar Publishing House, Anand, Gujarat, 49-55.
6. Manivasakam, N. (2005). Physico-chemical examination of water sewage and industrial effluents. *Physico-chemical examination of water sewage and industrial effluents.*, (Ed. 5).
7. Salahudeen, M., Saranya, E., Gunasekaran, C., & Vadivalagan, C. (2013). Studies on the abundance and distribution of birds in three different habitats of Karur District, South India. *Journal of Entomology and Zoology Studies*, *1*(3), 57-63.
8. Shanmugapriya, J., Senthil, J., Anand, PH., and Indhira, K. (2017). Impact of dyeing industrial effluents on the groundwater quality in karur town India. *International Journal of Development Research*, *7*, (07), 14199-14203
9. Srinivasa Rao, C. H., Subba Rao, A., & Rupa, T. R. (2000). Plant mobilization of soil reserve potassium from fifteen smectitic soils in relation to soil test potassium and mineralogy. *Soil science*, *165*(7), 578-586.
10. Udhayakumar, R., Manivannan, P., Raghu, K., & Vaideki, S. (2016). Assessment of physico-chemical characteristics of water in Tamilnadu. *Ecotoxicology and environmental safety*, *134*, 474-477.
11. World Health Organization (WHO), 1984; 1996. Has Given the Guidelines to Assess the Drinking Water Quality)
12. World Health Organization, 1984 and 1996. Guidelines for Drinking Water Quality, Recommendations of WHO. Geneva 1, pp. 1-130.





Veerakumar et al.,

13. Yadav, S. S., & Kumar, R. (2011). Monitoring water quality of Kosi River in Rampur district, Uttar Pradesh, India. *Advances in Applied Science Research*, 2(2), 197-201.
14. Zahir, H., & Rajadurai, D. (2013). Study on groundwater pollution at Sukkaliyur in Karur District, Tamil Nadu. *Advances in Applied Science Research*, 4(4), 461-464.

Table 1: TDS parameters (Udhayakumar et al., 2016)

S.No	TDS	Water quality
1	Less than 1000 ppm	Fresh
2	1000–3000 ppm	Slightly saline
3	3000–10,000	Moderately saline
4	10,000–35,000	Very saline
5	Greater than 35,000	Briny

Table 2: Water quality parameters (Udhayakumar et al., 2016)

Constituent	Unit	Guideline value
Chloride	Mg/lit	250
Copper	Mg/lit	1
Hardness	Mg/lit	500 (as CaCO ₃)
Hydrogen sulphide		Odour not to be detected at all
Iron	Mg/lit	0.3
Manganese	Mg/lit	0.1
pH		6.5–8.5
Sodium	Mg/lit	200
Sulphate	Mg/lit	400

Table 3: Water quality vs electrical conductivity (Udhayakumar et al., 2016)

Water quality	Electrical conductivity
Excellent	<250
Good	250–750
Permissible	750–2000
Needs treatment	2000–3000
Unsuitable for most purposes	>3000

Table 4: Water quality vs hardness (Udhayakumar et al., 2016)

Types of water	Hardness in mg/ lit of CaCO ₃
Soft water	0–50
Moderately soft	50–100
Neither hard nor soft	100–150
Moderately hard	150–200
Hard water	200–300
Very hard	>300





Veerakumar et al.,

Table 5: Physico-Chemical Characteristics of groundwater samples

	T. Pasupathipalayam	T. Sivan Colony	T. Sengalapuram	Vengadapuram	Chinnadharapuram
Physical Examination					
Turbidity NT Units	1	2	1	3	2
Total Dissolved Solids mg/l	777	637	918	762	2179
Electrical Conductivity	1110	910	1314	1098	3142
Chemical Examination					
pH	7.42	7.87	7.22	7.56	7.42
Phe, Alkalinity	0	0	0	0	0
Alkalinity	240	72	260	184	232
Total Hardness	245	200	328	248	400
Calcium	94	50	74	62	96
Magnesium	23	18	35	22	38
Iron	0.28	0.3	0.27	0.24	0.26
Manganese as Mn	0	0	0	0	0
Free Ammonia	0.01	0.01	0.01	0.01	0.01
Nitrate	0.03	0.03	0.03	0.03	0.03
Nitrate	24	24	27	22	40
Chloride	226	240	270	220	760
Fluoride	1.0	0.4	1.0	1.0	1.0
Sulphate	28	32	34	47	164
Phosphate	0.02	0.02	0.03	0.03	0.03

Table 6: Comparison of groundwater quality with drinking water standards

Parameter	Unit	WHO	ICMR	USPH	European Standards	Present sample study
Electrical Conductivity	(μ S/cm)	300	-	300	400	910-3142
Total Hardness	mg/L	200-600	300	500	-	200-400
pH		6.5-9.2	6.5-8.5	6.0-88.5	6.5-8.5	7.22-7.87
Total Dissolved Solids	mg/L	500	500-1500	500	500	637-2179
Calcium	mg/L	75	75	100	100	50-96
Magnesium	mg/L	50	50	30	-	18-38
Chloride	mg/L	250	250	250	250	220-760
Fluride	mg/L	1.0-1.5	-	-	-	0.4-1.0

USPH – United States Public Health.

WHO – World Health Organization.

ICMR – Indian Council of Medical Research





Veerakumar et al.,

<p style="text-align: center;">Figure 1: Turbidity NT Units</p>	<p style="text-align: center;">Total Dissolved Solids</p>
<p style="text-align: center;">Figure 1: Turbidity NT Units</p> <p>S 1= T. Pasupathipalayam, S 2= T. Sivan Colony, S 3= T. Sengalapuram, S 4= Vengadapuram, S 5= Chinnadharapuram.</p>	<p style="text-align: center;">Figure 2: Total Dissolved Solids</p> <p>S 1= T. Pasupathipalayam, S 2= T. Sivan Colony, S 3= T. Sengalapuram, S 4= Vengadapuram, S 5= Chinnadharapuram</p>
<p style="text-align: center;">Electrical Conductivity</p>	<p style="text-align: center;">Chemical Examination</p>
<p style="text-align: center;">Figure 3: Electrical Conductivity</p> <p>S 1= T. Pasupathipalayam, S 2= T. Sivan Colony, S 3= T. Sengalapuram, S 4= Vengadapuram, S 5= Chinnadharapuram.</p>	<p style="text-align: center;">Figure 4: Chemical Examination of Water</p> <p>S 1= T. Pasupathipalayam, S 2= T. Sivan Colony, S 3= T. Sengalapuram, S 4= Vengadapuram, S 5= Chinnadharapuram.</p>





RESEARCH ARTICLE

BROD: A Novel Reliable Opinion Based Optimized Deep Learning Prediction Algorithm of Different Financial Frauds in Cloud Environment

N.Valliammal¹ and G.Padmavathi²

¹Assistant Professor (SS), Department of Computer Science, Avinashilingam Institute for Home science and Higher Education for Women, Coimbatore, Tamil Nadu, India.

²Professor, Department of Computer Science, Avinashilingam Institute for Home science and Higher Education for Women, Coimbatore, Tamil Nadu, India.

Received: 15 Mar 2021

Revised: 22 Mar 2021

Accepted: 27 Mar 2021

*Address for Correspondence

N.Valliammal

Assistant Professor (SS),

Department of Computer Science,

Avinashilingam Institute for Home science and Higher Education for Women,

Coimbatore, Tamil Nadu, India.

Email: vallinarayanambe@gmail.com



This is an Open Access Journal / article distributed under the terms of the **Creative Commons Attribution License** (CC BY-NC-ND 3.0) which permits unrestricted use, distribution, and reproduction in any medium, provided the original work is properly cited. All rights reserved.

ABSTRACT

Financial Fraud is the biggest threat in today's digital era. Financial Frauds are increasing day by day which leads to the several criminal activities even to bankrupts This kind of illegal activities involves the complex network of trade and financial transactions, which is then difficult for the extraction of fraud features and which also leads to fatal end of the common man. India losses 228 crores in 52,000 cases in financial fraud in between March and December 2019. Financial fraud bring huge loss in the assets. Financial fraud effects the victim's mental health and may also lead to trauma. However, the intelligent system is required for an efficient detection and prediction of the frauds which can overcome the above-mentioned problems. In this proposed system the dataset is collected from different kinds of sources like Twitter, web-based interface Naver, paxet and so on. Earlier Prediction of fraud patterns of opinion mining is important because it is used to prevent the financial fraud. Prediction of fraud works based on the best optimized features extracted from BAT. Unlike in an existing system, the proposed system works on the principle of fusing the network and fraud features, in order to predict the different frauds. Hence the paper proposes the integration of the BAT optimized ORM-(Opinion based Rule Methodology) and Hybrid LSTM (Long Short-Term Memory) for an effective financial fraud's prediction. Also, the paper explores the usage of the deep learning networks for an efficient classification and prediction. The proposed algorithm has been tested with the different datasets and found to be an efficient in terms of prediction of different frauds such as Money laundering, Phishing and even credit card fault payments.



**Valliammal and Padmavathi**

In today's digital world cloud storage has become a vital role in storage environment, but there is no proper security in cloud storage for financial fraud, so the novel algorithm will predict the financial fraud in cloud storage hence it is proved as novel reliable method. The model is developed with other existing algorithms, the proposed model outperforms best in terms of Accuracy and also it predicts the fraud. Also, the proposed algorithm has better prediction ratio of 85%-92%, which is then reliable than other existing machine learning algorithms.

Keywords: Deep learning networks, financial frauds, Phishing, Money Laundering.

INTRODUCTION

Financial fraud is act of deceiving someone's money, investment with help of a computer. This leads to huge loss of money and also leads the victim to depression, anxiety and also suicidal thoughts. Because of the fast increment in versatile business and the development of the cloud environment, budgetary extortion in portable installment has emerged and turns out to be progressively normal. In excess of 87 levels of vendors bolster either versatile application or a portable webpage for internet shopping or both. There are different types of financial fraud like identity theft, Phishing and credit card fraud. According to Consumer Sentinel Network Federal Trade Commission of USA tracked a report in 2019 about financial fraud 1.7 million were fraud related 651,000 were identity theft complaints and 23 percent reported money was lost. The credit card fraud ranks first in top losses of financial fraud 246,763 cases with 45%. Financial fraud can disrupts any business whether small or big. It threatens the survival of the business by reducing the partners or clients whose is associated with. Financial Fraud spoils the good will of the organization. Financial fraud can also affect the common man. It leads them to mental depression, anxiety and even leads to suicidal thoughts. Therefore, to overcome all the problem an effective reliable financial fraud detection and prediction is necessary.

Optimal features are extracted from BAT optimized opinion-based rule (ORM). For predefined prediction analysis effective feature extraction methods is needed. News information is extracted from different sources Twitter, Naver and Paxnet. The total amount of data collected from web-based interface like Cosmo is 1,920, KODI is 3,967. After optimized BAT Evaluation the best features from Cosmo is 1257, KODI is 2684. 70% of data were utilized for training, and 30% of data were utilized for testing. Further Predicting analysis is done using LSTM network. In LSTM, training phase is generally done by back propagation algorithm. Early prediction of financial fraud is important because it can reduce the losses and prevent from destructions. Financial fraud like Phishing, money laundering and credit cards are predicted with highest accuracy using BROD algorithm. BROD algorithm is predicting accurately comparing with BAT and LSTM network. Comparative analysis is done with optimization of different existing LSTM algorithm. Various algorithm is applied in order to validate the proposed algorithm. Proposed algorithm is better at Experimental results like Accuracy, sensitivity and specificity. Also, the proposed algorithm has better prediction ratio of 85%-92%, which is then reliable than other existing machine learning algorithms.

Our Contribution in This Paper

Our contribution is to design the hybrid algorithm which works on LSTM to predict the financial frauds. The proposed algorithm works on the met heuristic algorithm which works on the principle of BAT algorithm for the feature selection which is then fed to LSTM for the prediction of time series data forecasting. The organization of the paper is described as: Section-I illustrates related works by more than one authors. Section-II deals with the proposed architecture. Dataset description, experimentation and results were presented in Section-III. Section-IV deals with the conclusion.



**Valliammal and Padmavathi****Section-I - Related Works**

There are numerous review articles that emphasize on financial fraudulent analysis detection due to its emerging need in this digital world. There are many categories in fraud analysis such as money laundering, smart phones, telecommunication sectors, credit or debit card dealings and so on causes a severe issue on both administration and business side. In general, scam identification and rectification are carried out either by statistical or machine learning model. Initially, we reviewed on traditional statistical methods to detect the financial frauds and its limitations. Richard *et.al* analyzed the diverse statistical solutions for fraud recognition and refinement. They focused on computer intrusion, financial debit card transactions, communiqué sector etc., [11]. Then we proceeded with the machine learning modules for prediction of fraudulent data's in the financial sectors. The detail description of the existing modules is given below. Roger *et.al* [12] developed a pictorial technique for identifying the scam data in financial sectors and also noted the other common problems in fraud analysis are given. The limitations are also declared such as

Dongxu Huang *et.al* [13] proposed a graphical approach for fraud analysis. The proposed "Codetect" method is focused only on feature extraction from complex patterns for detection of fraudulent data's which includes both network contents and transaction details information. Directed graph structures are adopted to visualize the fraud network in terms of nodes and its relationship as edges and also it utilizes the sparse medium, feature medium in parallel condition. This increases the understandability of the anomaly features form the network and enhances the detection accuracy. The challenges on implementing this technique are statistical analysis for each network which is not efficient for large financial networks and not developed any detection techniques in this work. Prabin *et.al* [14] deliberated about the internal corruption in financial business sectors. The significant objective of the proposed module is to make simple crafted by accountants in identifying the interior fraud. KDIFD is referred as "knowledge-driven internal fraud detection" explores the forensic information and combined with the data mining predictive algorithms such as OLAP [15] and neural network analysis for detection process. Auditors are benefited with the proposed structure which discovers about the backgrounds, data structures in terms of the employer's transaction details and freedom to himself in arranging the data's in his own acquiescent formats as per his convenience to detect the data fraud or not. The limitation of the proposed technique is focused only for the internal corruption detection and limited source. Weiyu Si *et.al* [16] developed the multi-objective detection reinforcement module which incorporates two phases of the neural network. The first part is made out of four layers of completely associated systems for taking in highlights from the financial information and decreasing the vulnerability of the input data. The subsequent part is a layer of Long Short-Term Memory (LSTM) and a layer of completely associated system to execute self-educated fortification exchanging to adjust the profit and hazards. The drawback of the proposed technique is not discussed about any real-time data's and only focused feature extraction.

Andrea *et.al* [17] explored the diverse machine learning techniques for identification of the credit card scam. Initially, they analyzed the impacts of frauds in smart cards usage and followed by the description of supervised learning modules for classification and prediction problems. Linear regression and decision tree algorithms are trained based on the real-data observed from the bank sectors to detect the frauds and also to enable the alarms based on the feedback data received from the end user. The limitations of the proposed model are less sufficient in fraud rectification solutions instead it alerts the users in prior using the feedback alert system. To overcome these existing modules, we developed a hybrid technique named as BAT Optimized Reliable Opinion Based Deep Learning (BROD) which combines the LSTM neural network and opinion based ruling algorithm with its BAT optimized feature selectors under cloud environment.

Section-II - Proposed Architecture

Figure 1 demonstrates the proposed architecture. The proposed architecture consists of data collection unit based on opinion rule logics, optimized data selector using the BAT algorithm and predictor using LSTM mechanism.





Valliammal and Padmavathi

Data Collection Methods

News information was collected from a web-based interface 'Naver' provided by South Korea also tweets posted on Twitter. The data is extracted and cleaned for further processing. It contains. Thus, 1,920 reports identified with Cosmo Chem. were collected and 3,967 reports applicable to KODI Corp. Above all else, money related information identified with stock venture should be gathered, which includes a wide range of information depicting the budgetary state or pattern of speculation. Most speculators used to allude to differing kinds of information, for example, news and reports just as clients' suppositions. Specifically, choices for stock speculation are profoundly influenced by financial specialists' conduct, and along these lines, conclusions referenced by speculators are important to evaluate chance. To ensure this, our investigation classifies and gathers two kinds of information (news and social information). They have various highlights; for instance, news is moderately objective since it depends on realities, while social information is very emotional on the grounds that it might be founded on truth or bits of gossip created by different speculators. In like manner, thinking about various highlights of information, news as well as social information are gathered. News is gathered from administrations gave by online interfaces through web creeping. On account of social information, there are an assortment of databases, for example, Twitter as well as articles posted on notices, and they are likewise gathered in a similar way.

Feature Extraction

To integrate the Opinion mining techniques, we have used the word2vec will convert the words into vectors to calculate the frequency of words, repeated words in the database are extracted with different attributes, features and data sentences etc. in which opinions are used as the basic inputs. Word2vec gives the best optimized features for further data processing.

Optimized Feature Selector

Feature selection is an important phase in Machine Learning that play a vital role in performance of the model. Irrelevant feature selection will affect the model. It will select only most important features to predict the target variable. The system has adopted the meta heuristic algorithms which is based on BAT algorithm for feature selection. The bat algorithm is chosen because of its following reasons:

1. Low Complexity and High Flexible
2. Low Computational mechanism
3. Better Accuracy.

Bat Algorithm as Feature Selector

The standard bat method depended on the vocalizations or bio-sonar attributes of micro paddles. The main concepts of the "BAT Algorithm" is to pre-process and optimize the features based on the vocalization's sound, pulsation rates and intensity. Yang *et.al* initiated this technique within three steps [4 -7].

Step 1: The wings observe the natural vocalizations sound to detect the distance of its neighbours during the prey search and also identifies the type of prey without the barriers.

Step 2: Major parameters used in the algorithm is Velocity (V_i), bats position (x_i), search space denoted by its frequency (Q), wavelength(λ) and Echo sound intensity (S_o), parameters are described briefly in table II.

Step 3: The loudness or echo sound are deviated from $\{Q_{min}, Q_{max}\}$.

Automatic adjustments of the pulse rates and its intensity level denoted by 'u' which varies between $\{0,1\}$ based on the proximity of the target. The echo sound metric is deviated between $\{S_o - S_{min}\}$

Mathematical Model of this BAT calculations are

- Initially identified the 'Q' range and denoted as Equ.1

$$Q_i = Q_{min} + (Q_{max} - Q_{min})\omega \quad (1)$$





Valliammal and Padmavathi

- Velocity is updated based on Equ.2

$$L_i = L_i^{g-1} + (P_i^{g-1} - P_i) \tag{2}$$

- Distance is calculated based on Equ.3

$$P_i^g = P_i^{g-1} + L_i^g \tag{3}$$

- Loudness range is updated based on Equ.4

$$S_i^{g+1} = \rho S_i^g \tag{4}$$

Where $\omega \in (0, 1)$ and ‘Qmin’ is the minimum frequency =0 and ‘Qmax’ is the maximum frequency that primarily based on the problem statement. The wings are primarily denoted between the ranges of ‘Q’. Subsequently bat figuring can be consisted as a repetition tuning computation to provide a functional fusion of inspection and abuse. The discharge ratios fundamentally contribute a mechanism to customize regulate then auto-zooming into the location with promising preparations. To illustrate signs of enhancement preparation, it is key for the group of the bat and the exhausted discharge. As the commotion typically reduces when a bat has originated its quarry, whereas the step of heartbeat release extends, the uproar can be chosen as any valuation of settlement, between Smin and Smax, tolerating Smin = 0 concludes which a bat has as of late found the quarry and rapidly leave transmitting any stable. The working mechanism for BAT algorithm is as follows

- Step1:** Initialize the initial BAT populations.
- Step2:** Initialize the Loudness, velocity, frequencies
- Step3:** Calculate the fitness function for the threshold feature selection in terms of velocity, frequency and Loudness
- Step4:** Iterate the above-mentioned values until it reaches the fitness function
- Step5:** Stop the process

The specification of bat algorithms used in the proposed algorithm for the better feature selector is depicted in the table III.

LSTM Network

A long short-term memory (LSTM) network is the combination of RNN with LSTM units [8]. The LSTM network has been demonstrated in fig.2. This network includes four stages (i) Cell (ii) Incoming state (iii) Outcome state (iv) forget state. Cell are known to be LSTM memories to recollect the values completed the time intervals. Gate is known to be LSTM special structure with input vectors (range between 0 & 1). The gates pass the information if the output gate value is “1”, it does not allow the information when the output value is “0” [8-10].

- Z_c cell state’s weight matrix
- B_c cell state’s bias vector.
- I_t input gate
- f_t overlook gate (utilized to aid the network to overlook the past input data and return the memory cells).

Cell states are used to record the present state. It is known as fundamental of the calculation node and it given as follows

$$C_t = f_t \cdot C_{t-1} + i_t \cdot \tanh(Z_c \cdot [P_{t-1}, P_t + b_c]) \tag{5}$$





Valliammal and Padmavathi

Where,

The control of the contribution and overlook gate can be correspondingly directed as:

$$i_t = \sigma(Z_i \cdot [P_{t-1}, P_t] + b_i) \tag{6}$$

$$f_t = \sigma(Z_f \cdot [P_{t-1}, P_t] + b_f) \tag{7}$$

Where,

Z_i → Input gate weight matrix

Z_f → forget gate weight matrix

b_i → input gate bias vector

b_f → forget gate bias vector

The LSTM output gate can control the data in the cell state of the present time to flow into the present output. The yield D can be conveyed as:

$$D_t = \sigma(Z_o \cdot [O_{t-1}, P_t] + b_o) \tag{8}$$

Where

Z_o → output gate weight matrix

b_o → output gate bias vector

LSTM final output can be expressed as

$$O_t = D_t \cdot \tanh(c_t) \tag{9}$$

In LSTM network, training phase generally adopts the back-propagation algorithm.

The overall working algorithm and pseudo code for the proposed architecture are given as follows

1. Extraction of Attributes using the two categories such as Opinion Mining mechanisms using Word2vec format
2. Selection of Features using met heuristic BAT algorithm.
3. Prediction using the LSTM Mechanism.

Pseudo-Code for the BROD-PREIDCT

1. Input F= {F₁, F₂,F₃,F₄,F₅.....F_n}
2. Outputs O= Predicted Outputs for different Frauds.
Feature selection using BAT algorithms
3. Initialize the initial Population with features
4. F= {F₁, F₂,F₃,F₄,F₅.....F_n}
5. Initialize the loudness and pulse rate A
6. Define the Pulse rate and loudness
7. If(F is not equal to F_n)
8. While(t<maximum iteration)
9. Produce new results by modifying the frequency and modernizing velocities and position points by equations (1), (2)and (3)
10. If (rand>t)
11. Choose the solutions between the finest solutions arbitrarily
12. Make the Best solutions from the above step
13. End
14. If (rand <A &&f(x)<f(f_n^{best}))
15. Select the best results and accept the results
16. Update the loudness, positions
17. End
18. End while
19. End





Valliammal and Padmavathi

20. For each feature construct the M Sequences from the selected features using BAT optimizers
21. Initialize the various θ_1 θ_2 θ_3 in LSTM
22. While $j < \text{Epoch}$ do
23. Construct the M sequence LSTM networks by using calculating the Output gates, Input gates and Forget gates using equations (6),(7) and (8)
24. End while
25. End

Section-III

Dataset Description

Our procedure utilizes web slithering for investigating the information. News information was collected from a web-based interface 'Naver' provided by South Korea (<http://news.naver.com>), also tweets posted on Twitter also articles posted on 3 online networks – DC inside [21] Finance administration in Naver [22] and Paxnet [23] - were gathered for 2 firms KODI Corp. furthermore, Cosmo Chem. for 1 year as appeared in Table 4.

Thus, 1,920 reports identified with Cosmo Chem. were collected, and 3,967 reports applicable to KODI Corp. were gathered (Table IV). Between them, the vast majority of conclusions happened in Finance administration upheld by Naver (1,552 assessments identified with Cosmo Chem. also, 3,218 sentiments identified with KODI Corp.), that is the most dynamic sites to split individual opinion on explicit stocks.

Performance Evaluation

The features which are extracted from the different financial datasets are used for the training and testing process. For evaluation, 70% of data were utilized for training, and 30% of data were utilized for testing. The assessment is carried out for the different BAT optimized datasets with the following parameters.

Accuracy

This function computes subset accuracy the set of labels predicted for a sample must exactly match the corresponding set of labels predicted. Accuracy is the most useful performance measure and just a ratio of correctly predicted observations with the total number of observations.

$$\text{Accuracy} = \frac{DR}{TNI} \times 100 \quad (10)$$

Sensitivity

It is also known as TRUE POSITIVE RATE. It is proportion of the samples which are exactly positive which gives a positive prediction. Sensitivity is expressed as probability of true positive samples from total number of samples.

$$\text{Sensitivity} = \frac{TP}{TP+TN} \times 100 \quad (11)$$

Specificity

It is also known as TRUE NEGATIVE RATE. It is proportion of the samples which are exactly negative which gives a wrong prediction. Specificity is expressed as probability of true negative samples from total number of samples.

$$\text{Specificity} = \frac{TN}{TP+TN} \times 100 \quad (12)$$



**Valliammal and Padmavathi**

TP and TN denotes 'True Positive' and 'True Negative' values and DR& TNI Denotes Number of Detected Outcomes and Whole number of Iterations. The performance of the proposed hybrid LSTM algorithms has been evaluated by different cases which are as follows]

Accuracy Prediction

For accuracy of prediction, the proposed algorithms were analyzed for the different neurons which are considered to be ROC (region of convergence) and compared with the other existing LSTM based learned algorithms. The best features are extracted from BAT and fed into LSTM Model with different number of neurons and its accurate prediction. From the above tables, it is very clear that the optimized feature selector based LSTM has better accuracy of prediction when compared with existing LSTM algorithm. Moreover to analyze and strengthen its performance, more parameters such as sensitivity and specificity were calculated and compared with the existing algorithms. Hence to prove the efficiency of the bat optimized LSTM, we have compared the other optimization algorithm such as Particle Swarm Optimization and Genetic Algorithms which was demonstrated in table VIII. From the above tables, it is clear that the proposed algorithms with BAT optimizer has much more sensitivity and selectivity when compared with the traditional LSTM mechanism. To validate the proposed algorithm, we have taken the different frauds in the data and compared with the other learning-based fraud systems. From the above figure, proposed BROD algorithm outperforms the other learning algorithms in terms of selectivity, specificity and accuracy of prediction. Moreover, the proposed algorithm has been validated for the different frauds in which the algorithm proposed has superior performance when compared with the other existing algorithms.

Section-IV**CONCLUSION**

Financial fraud is an important problem in today's world. Prevention of financial fraud is important to reduce the economic losses. Financial fraud it is dangerous for industries and also for common people. It causes mental depression and even suicidal thoughts. To solve this problem the novel BROD helps to prevent the financial fraud before happening In this paper, explored the most recent financial fraud detection by Novel BROD which works on the principle of Bat optimized LSTM which has Opinions as the major inputs. The experimental data were collected from web-based interface and various methodologies were analyzed for validating the proposed algorithm. Nearly 15 attributes were collected and analyzed by using the proposed algorithm to detect the various kinds of financial frauds. Optimization algorithm PSO and GA is used to optimize the BROD model, for optimizing prediction model. Experimental outcomes demonstrate that the proposed algorithm has better performance in terms of accuracy, sensitivity and specificity when compared with the other deep learning algorithms without optimization. Proposed algorithm predicts 82-90% accurately. It works better than SVM method used for detecting bank fraud. In future work, we aim to advance the performance of the algorithm by integrating machine learning in deep learning algorithms.

REFERENCES

1. Kount(2016). "Mobile payments fraud survey report. Technical report" "Javelin strategy and research," 2016.
2. S. Panigrahi, A. Kundu, S. Sural, and A. K. Majumdar(2009), "Credit card fraud detection: a fusion approach using Dempstershafer theory and bayesian learning" ,Article in Information Fusion, Vol. 10, no. 4,pp.354–363.
3. Xie yang(2013). "Bat Algorithm: Literature Review and Applications." Int. J. Bio-Inspired Computation, Vol. 5, No. 3,pp 141-149.
4. NesrineTalb(2019). "Design of Fuzzy Controller rule base using Bat Algorithm.Special Issue on Emerging and Renewable Energy" Generation and Automation,Energy Procedia 162 241–250





Valliammal and Padmavathi

- IztokFister Jr. and IztokFister(2014).“Bat algorithm: Recent advances”. CINTI 2014 • 15th IEEE International Symposium on Computational Intelligence and Informatics. 19–21 November.
5. SwetaSrivastava and Sudip Kumar Sahana(2019).“Application of Bat Algorithm for Transport Network Design Problem”Hindawi Applied Computational Intelligence and Soft Computing Article ID 9864090, Vol.2019.
 6. Alex Sherstinsky(2020). “Fundamentals of Recurrent Neural Network (RNN) and Long Short-Term Memory (LSTM) Network. Elsevier journal “Physica D: Nonlinear Phenomena”, Volume 404, Special Issue on Machine Learning and Dynamical Systems
 7. Has,imSak, Andrew Senior, Franc,oise Beaufays(2014). Long “Short-Term Memory Recurrent Neural Network Architectures for Large Scale Acoustic Modeling” Google, USA.
 8. [10] Xingjian Shi Zhourong Chen Hao Wang Dit-Yan Yeung(2015).“Convolutional LSTM Network: A Machine Learning Approach for Precipitation Nowcasting”, Proceedings of 28th International Conference on neural information processing system, Vol. 1,pp-802-810.
 9. [11] D.J.H. Richard J. Bolton(2002.). “Statistical fraud detection: A review” Statistical Science, Vol.17 No 3,pp:235–249.
 10. [12] Roger A. Leite, Theresia Gschwandtner, Silvia Miksch, Simone .Kriglstein, Margit Pohl, Erich Gstrein, and Johannes Kuntner(2018), “EVA: Visual Analytics to Identify Fraudulent Events” IEEE TRANSACTIONS ON VISUALIZATION AND COMPUTER GRAPHICS, Vol. 24, NO. 1.
 11. Dongxu Huang, Dejun Mu, Libin Yang, Xiaoyan Cai. Co Detect(2018),“Financial Fraud Detection with Anomaly Feature Detection” IEEE Access, DOI 10.1109/ACCESS.2018.2816564,pp-19161-19174.
 12. Prabin Kumar Panigrahi(2011),“A Framework for Discovering Internal Financial Fraud using Analytics”2011 International Conference on Communication Systems and Network Technologies, DOI 10.1109/CSNT.2011.74.
 13. Qian L., Tong L., Wei X., (2009). “A subjective and objective integrated method for fraud detection in financial systems” Proceedings of the Eighth International Conference on Machine Learning and Cybernetics, Baoding ,DOI: 10.1109/ICMLC.2009.521230.
 14. Weiyu Si, Jinke Li, Ruonan Rao, Peng Ding(2017).“A Multi-Objective Deep Reinforcement Learning Approach for Stock Index Futures intraday Trading”, 10th International Symposium on Computational Intelligence and Design.DOI 10.1109/ISCID.2017.210.
 15. Andrea Dal Pozzolo(2018).“Adaptive Machine Learning for Credit Card Fraud Detection” A thesis. Université Libre de Bruxelles,
 16. Dahee Choi, Kyungho Lee(2018).“An Artificial Intelligence Approach to Financial Fraud Detection under IoT Environment: A Survey and Implementation. Security and Communication Networks” Security and Communication Networks.
 17. Lin Chen, Zhilin Qiao, Minggang Wang, Chao Wang, Ruijin Du, H. Eugene Stanley (2015).“Which artificial intelligence algorithm better predicts the Chinese stock market?” IEEE Access,Vol.14, No 8.
 18. YujinJeong, Sunhye Kim, Byungun Yoo.(2018),“An Algorithm for Supporting Decision Making in Stock Investment through Opinion Mining and Machine Learning”. Proceedings of PICMET '18: Technology Management for Interconnected World.
 19. Nana Kwame Gyamfi ,Jamal-Deen Abdulai(2018),“Bank Fraud Detection Using Support Vector Machine”,2018 IEEE 9th Annual Information Technology, Electronics and Mobile Communication Conference.





Valliammal and Padmavathi

Table 1: Literature Survey

S. No	Author	Title	Journal & Year	Methods	Advantages	Limitation
1	Dahee Cho, Kyungho Lee	An Artificial Intelligence Approach to Financial Fraud Detection under IoT Environment: A Survey and Implementation.	Hindawi Security and Communication Networks Volume 2018.	It is implemented in both ML and DL methods to compare the efficiency of the problem.	It discovers hidden patterns of financial fraud using supervised and unsupervised learning algorithm.	ANN process takes longer than machine learning process.
2	Weiyu Si, Jinke Li, Ruonan Rao, Peng Ding	A Multi-Objective Deep Reinforcement Learning Approach for Stock Index Futures intraday Trading.	10th International Symposium on Computational Intelligence and Design, 2017	Reinforcement learning methods and deep neural learning methods	Recurrent networks uses older actions as the feedback in order to make continuous actions for balancing the trade and profit.	The proposed technique is not discussed about any real-time data's and only focused feature extraction
3	Dongxu Huang, Dejun Mu, Libin Yang, Xiaoyan Cai. CoDetect:	"Financial Fraud Detection with Anomaly Feature Detection"	Journal of IEEE Access, 2018	Novel fraud detection method codetect detects anomaly features in financial transactions.	Increases the understandability of the anomaly features from the network and enhances the detection accuracy	Analysis for each network which is not efficient for large financial networks.
4	Sahil Dhankhad, Emad A. Mohammed, Behrouz Far	Supervised Machine Learning Algorithms for Credit Card Fraudulent Transaction Detection: A Comparative Study	IEEE International Conference on Information Reuse and Integration for Data Science, 2018	SVM, Random Forest, Logistic Regression, Gradient Boosting, MLP Classifier, DTree, KNN and Naive Bayes.	The best features will lead to get higher accuracy for credit card fraud detection. Results of all models is superior in its performance.	Limited size of training and test dataset.
5	Andrea Dal Pozzolo..	Adaptive Machine	A thesis. Université Libre	Classification and detection using Linear	Models are trained based	It is not sufficient





Valliammal and Padmavathi

		Learning for Credit Card Fraud Detection	de Bruxelles,2018	Regression and decision tree algorithm.	on the real-data which is observed from the bank sectors to detect the frauds trigger alarm based on the feedback data received from the end user	in rectifying the solution but it instead it just send alarm and alerts the user.
6	<u>Nana Kwame Gyamfi, Jamal-DeenAbdulai</u>	Bank Fraud Detection Using Support	2018 IEEE 9th Annual Information Technology, Electronics and Mobile Communication Conference (IEMCON),2018	SVM to detect bank fraud	Fraud has been detected well using SVM method.	Takes more time.

Table 2: Symbols and notations of the parameters

S.No	Symbol	Description
1	Velocity (L _i)	Each virtual bat flies randomly with its velocity. As higher the velocity faster, it moves through search space.
2	Position (xi)	Each individual has its position(solution)
3	frequency (Q)	Each bat is assigned a frequency randomly to draw a uniform form [Q _{min} , Q _{max}].
4	Wavelength (lambda)	Wavelength varies depending on the prey.
5	Echo sound intensity (S _o)	Loudness to search the prey

Table 3: Represents the Feature Selector Mechanism using the BAT algorithm

Sl.no	Description of features	Feature Description
01	No of Input Features (initial population)	15
02	No of feature selected	06
03	Initial Velocity	20%
04	No of Iterations	BAT optimized
05	Initial Loudness	0.9

Table 4: Total Number of Datasets for Evaluation

Data Set Details	News	DC Inside	Finance in Naver	Twitter	Paxnet	Total
Cosmo	187	25	1552	44	112	1920
KODI	341	359	3218	49	0	3967





Valliammal and Padmavathi

Table 5: Total Number of Datasets for Evaluation after BAT optimizer

Data Set Details	News	DC Inside	Finance in Naver	Twitter	Paxnet	Total
Cosmo	135	25	1023	24	50	1257
KODI	200	250	2209	25	0	2684

Table 6: Accuracy of Prediction with the different number of neurons For the Proposed Algorithm

Sl.no	Number of Neurons	Accuracy of Prediction (%)
01	N=50	95%
02	N=100	94.5%
03	N=150	95%
04	N=200	96%
05	N=250	95.5%
06	N=300	95%

Table 7: Comparative Analysis between the proposed algorithms with the Existing Algorithms in terms of accuracy of Prediction

Sl.no	Number of Neurons	Accuracy of Prediction (%) For Proposed Algorithms	Accuracy of Prediction for LSTM (without optimizer)[16]
01	N=50	95%	90%
02	N=100	94.5%	91%
03	N=150	95%	91%
04	N=200	96%	92%
05	N=250	95.5%	90%
06	N=300	95%	90%

Table 8: demonstrates that BAT optimized LSTM has outperformed other optimization algorithm in terms of predicting the different categories of attacks.

Sl.no	Number of Neurons	Accuracy of Prediction (%) For Proposed Algorithms	Accuracy of prediction using PSO	Accuracy of prediction using GA
01	N=50	95%	92%	89%
02	N=100	94.5%	91.5%	85%
03	N=150	95%	91%	85%
04	N=200	96%	91%	84%
05	N=250	95.5%	90%	83%
06	N=300	95%	89%	83%

Table 9: Comparative Analysis between the proposed algorithms with the Existing Algorithms in terms of Sensitivity

Factor Sl.no	Number of Neurons	Sensitivity for Proposed Algorithms	Sensitivity for LSTM (without optimizer)[16]
01	N=50	90%	84%
02	N=100	90%	83.5%
03	N=150	91.5%	81%
04	N=200	91%	82.5%
05	N=250	90%	82%
06	N=300	90.5%	81.5%





Valliammal and Padmavathi

Table 10: Comparative Analysis between the proposed algorithms with the Existing Algorithms in terms of Selectivity

Sl.no	Number of Neurons	Selectivity For Proposed Algorithms	Sensitivity for LSTM(without optimizer)[16]
01	N=50	88%	83%
02	N=100	90%	82.5%
03	N=150	90.5%	80%
04	N=200	91%	80.5%
05	N=250	89%	82%
06	N=300	89.5%	82.5%

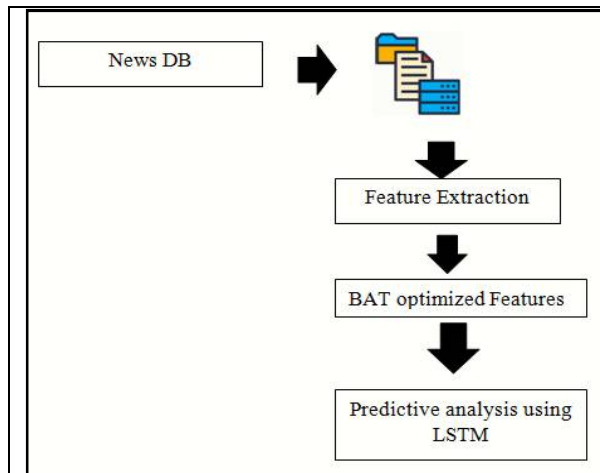


Figure 1 Proposed Architecture

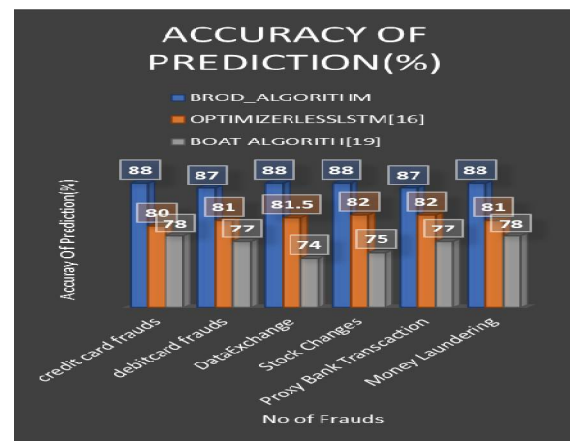


Figure2 Performance Evaluation for the Proposed BROD Algorithm for the different frauds and compared with the existing algorithms in terms of accuracy of prediction

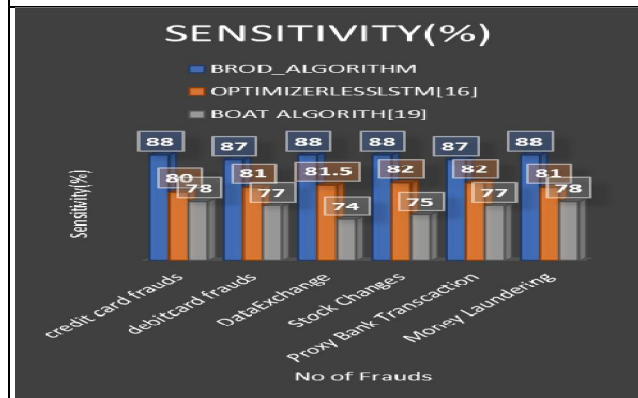


Figure 3 Performance Evaluation for the Proposed BROD Algorithm for the different frauds and compared with the existing algorithms in terms of Sensitivity.

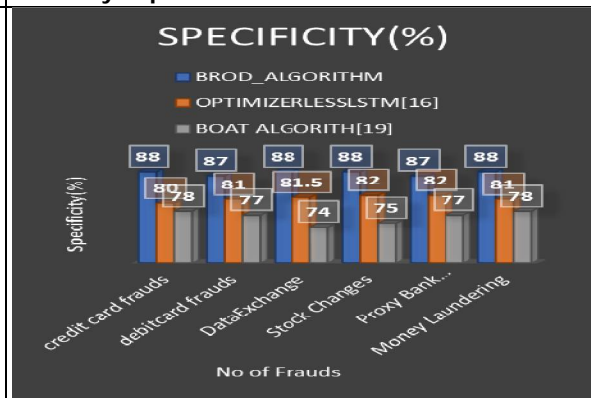


Figure5 Performance Evaluation for the Proposed BROD Algorithm for the different frauds and compared with the existing algorithms in terms of Specificity.





RESEARCH ARTICLE

An Efficient Framework for Opinion Analysis of Twitter Data on Diabetic Drugs Using Machine Learning Techniques

S. Radha Priya* and M. Devapriya

Department of Computer Science, Government Arts College(A), Coimbatore, Tamil Nadu, India.

Received: 15 Mar 2021

Revised: 22 Mar 2021

Accepted: 27 Mar 2021

*Address for Correspondence

S. Radha Priya

Department of Computer Science,
Government Arts College(A),
Coimbatore, Tamil Nadu, India.
Email: arjaideep2002@yahoo.co.in



This is an Open Access Journal / article distributed under the terms of the **Creative Commons Attribution License** (CC BY-NC-ND 3.0) which permits unrestricted use, distribution, and reproduction in any medium, provided the original work is properly cited. All rights reserved.

ABSTRACT

Wide clinical testings are essential before a medicine is accommodated in the market. But this is very challenging to determine all the Adverse Drug Reactions (ADR) for any approved drugs due to limited number of clinical trials. Twitter is a social media space where opinions of the public are communicated in day to day life. So advancements in science have resulted in the flourishing of enormous public data and the attainability of the vast datasets present excess research chances. The tweets provide data containing valuable information about drugs and their effects. An endeavour is made in this paper to comprehend opinion of the public on the antidiabetic drugs (Generic and Branded) to identify the level of ADR by examining the content of tweets using sentiment analysis (opinion mining) and Machine Learning(ML) methods. Opinion of people regarding diabetic drugs is taken from twitter from 2017 to 2019 for analysis. Initially preprocessing is done to remove noise from the data making it useful for further analysis. After data cleaning, feature extraction and selection techniques are carried out for improving the classification accuracy. Machine learning techniques are used to analyse finally the optimized dataset and comparison of results are done.

Keywords: Diabetic drugs, Twitter data, Preprocessing, Feature selection, Classification

INTRODUCTION

Due to great success of the social media, a large number of people are now utilizing social network services in order to gain active interaction with other users [20]. Social media site such as twitter is a very potent communication device and about 360 million messages are created daily. News about life events, sharing of opinions and discussions are communicated through this media. The data collected and gathered from twitter can be utilized for surveying opinion of people [1]. In twitter, users send brief messages called tweets. In this research twitter Application



**Radha Priya and Devapriya**

Programming Interface (API) is used for data collection. Opinion mining has numerous uses in wide variety of domains. In particular, it plays a major role in the field of healthcare through the analysis of drugs related opinions. In this research opinion analysis of tweets regarding metformin (drug which is used for diabetes) is done. Metformin is a molecule used for treatment of type-II diabetes (Maturity Onset Diabetes). Diabetes is a condition where there is insufficient insulin in the human body or the insulin that is secreted is ineffective causing high blood sugar levels. International Diabetes Federation states that the top three countries with massive number of diabetes are China, India and United States [2]. 60% of physicians are of the opinion that lucidity and genuineness of social media helps to enhance the quality of care provided to the patients [13]. To enhance health care standard through social media analytics evolving efficacious methods of collecting, surveying and envisioning data to transfer different data into knowledge and business intelligence is urgently needed. Twitter social networking platform is a valuable source for recognizing ADR due to its effective and real time nature [14][15]. Research using twitter analysis to investigate ADRs has progressively grown in recent years [16][17]. ADR monitoring profits from social media analytics in a number of ways adding merit to the current practice of pharmacovigilance[18]. Metformin is a commonly used drug and is a safe and effective treatment for type-2 diabetes. It reduces the amount of glucose made by liver and it increases the effect of insulin on human body. Metformin are available as generic and as brand name drugs. This work analyses people's opinion in twitter towards metformin and their related branded medicine by using opinion mining and machine learning approaches [3]. The objective of this paper is to predict the adverse effects of the antidiabetic drug metformin there by providing feedback to the physicians. The rest of the paper is modelled as follows: the section II deals with related work, section III deals with proposed scheme, section IV deals with methodology, section V deals with Results and Discussion, Section VI deals with Conclusion and Future Scope.

Related Works

Different sentiment analysis techniques are utilized to analysing the twitter dataset for various purposes. Some of the existing system is described in this section. M. bouazizi, T. ohtsuki [4] have made a study on tweets which contained more than one sentiments instead of an overall single sentiment. This is called as multiclass sentiment. For this study the SENTA tool was used. In their approach the authors determine all the sentiments in a particular tweet and provide a score for each sentiment depending on their weightage. This process is called Quantification. Pulkit et al. [5] made a study on reach of a tweet and survival of the tweet using the Sep 18, 2016 post uri terrorist attack, Indian public tweets from twitter. They had gathered 59,988 tweets over a period of one month from Sep 18, 2016. Using last retweet, number of retweets, number of favourites it is possible to determine information flow of data on twitter. They have used Naïve Bayes and SVM algorithm to classify the data after preprocessing. Also the trend of positive and negative tweets were also studied. Sudarshan Sirsat et al. [6] has done a study in sentiment analysis on opinion from twitter regarding a product using Textblob in python and Naïve Bayes algorithm. Attributes such as likes and retweets were also measured. Hetu et al. [7] Proposed sentiment analysis model for data from twitter based on anaconda python. Data set is extracted from kaggle in which they clarify the opinions based on positive and negative reviews. The proposed method gives great accuracy on huge data set. Ali hasan et al. [8] proposed a model using a combination of lexicon based sentiment analysis and supervised machine learning algorithm. This hybrid approach was used to analyse twitter data containing public views about political parties and elections. This model basically converts tweets in urdu language to English and does further processing. In this research. Naïve Bayes and SVM classifier and Sentiment Lexicons: W-WSD, Senti Word Net and Text Blob have been used. Asha S Manek et al [21] made a sentiment analysis study on a large movie review data set from the web using Gini Index based feature selection method with support vector machine classifier. The Gini Index method is more competent in classification enforcement in terms of decreased error rate and accuracy. Achin jain and vanita jain [20] have made a study on sentiment analysis about twitter data regarding the opinion of the public about government policies on renewable energy. Feature selection was done using Cfs subset evaluation and information gain methods and accuracy was compared. Five different machine learning algorithms were used, SVM proved best accuracy on combination with PUK kernel and Cfs subset evaluation.



**Radha Priya and Devapriya****Proposed Scheme**

In the proposed opinion mining system, terminologies which are used are listed below.

Medication Selection

To analyse the twitter data specific drug names are needed. In this research the drug Metformin is selected to view related effects on twitter data. Criteria for choosing Metformin are since metformin is in the market for 50 years sufficient tweets would exist for the effects to be reported. This drug most probably will not be taken by patients whose condition prevented them from posting tweets frequently. The generic drug name Metformin, the equal brand names: Baymet, Diamet, Emfor, Formin, Glumet, Glyciphage and Gluformin are the drugs chosen for data retrieval. The given medicines are prescribed for treating type-2 diabetes mellitus. Metformin is on the World Health Organization's (WHO) list of essential medicines and is the safest and most efficacious medicine necessary in the health care system [9].

Twitter

Jack Dorsey, Noah Glass, Biz Stone, and Evan Williams launched twitter in July 2006. At present there are 330 million twitter users actively using it. The number of adults who use twitter media increased from year 2010 to 2019 is illustrated in the below figure. Twitter is one of the biggest communal networking sites. Twitter is used as a universal platform for opinion sharing, news distribution, discussion and socialization. Consequently, such a tremendous amount and high pace flow of twitter data created at each moment have the ability of being used for important analytical and interpretation purposes [10].

Opinion Mining (OM)/Sentiment analysis (SA)

Opinion Mining (OM) is a process of surveying the public opinion about a given product, service or topic. It is also named as Sentiment Analysis which involves creating a system to collate and survey the emotions, opinions and other messages made in site posts, notes, reports or tweets. Opinion mining software facilitates automatic extraction of opinions in text and also tracks attitudes and opinions. There are two main goals of opinion mining. To collect opinions from raw and disorganized text using algorithmic or statistical techniques or a mixture of both. To recognize and extort object visages that have been noticed and commented by an opinion holder. To determine the polarity of opinions with respect to the given target. Opinion mining and sentiment analysis are used as a sub-component technology in recommendation systems. It is used for identifying people's opinion about any product(e.g. Metformin) and then used to analyse about their level of satisfaction[11].

Machine Learning (ML) approach

Machine learning examines the ability of computers to learn based on data. To make decisions in highly complex areas the computer programs are synthesized to automatically learn to identify complex patterns and make intelligent decisions based on optimized data. ML algorithms are used to determine the opinion mining as a typical text analysis issue that makes use of objective features. A set of training data are taken where each data is labelled to a class. The classification model is associated to the features in the testing data to one of the class labels. Then for a particular feature of unidentified class the model is used to envision a class label for it. The supervised learning methods depend on the existence of training data which are labeled [12]. There are plentiful supervised classifiers available. The above Figure. 2 illustrates the functioning of supervised binary classification. The proposed system utilises three supervised machine learning algorithms to classify the ADR of Metformin with the twitter data. The supervised machine learning materializes from the labelled cases in the training data set. It helps the learning models to be trained efficaciously, so that they can yield great classification accuracy. Therefore a judicious selection of the machine learning algorithms with organized and methodical pathway is mandatory [11].



**Radha Priya and Devapriya****Proposed Methodology**

Figure 3 shows the schema for the proposed research. The proposed architecture consists of Dataset Collection and Preprocessing, Feature Extraction, Feature Selection and classifier models. The research work has been approached in five different phases:

Data Collection

Having a complete and solid dataset is the fundamental step to execute opinion mining. The required material knowledge could be possessed from twitter media. Twitter opinions regarding ADR of Metformin and relevant branded drugs were used in this study to construct the classification model. In order to collate real time data by the users twitter offers Application Programming Interface (API). Twitter API keys are important to accessorize the twitter streaming API. Twitter API keys are API key, API secret, Access token and Access token secret. Tweepy are library files that are used to capture the twitter data. Tweepy is a tool which organizes the connection among computer programs and web services. In this research R-tool is used for collection of tweets posted in recent past by the users to retrieve metformin related tweets. The gathered data is stored into the .csv file.

Data Pre-Processing

In order to achieve good results it is very important to exercise text preprocessing steps before examining the tweets [22]. Each twitter text contains characters not above 140. A variety of colloquial languages can be used for tweeting. Tweets contain unwanted data such as URL, hashtag, punctuations, stop words, white spaces etc., These need to be removed to give rise to a meaningful message. Steps involved in the preprocessing of tweets are as follows:

Uniform Resource Locator (URL): URL does not play any role in opinion analysis. So URL markings with HTTP:// or HTTPS:// can be eliminated for efficacious analysis.

Conversion to Lower Case: While creating tweets the text contains a mixture of both upper and lower case characters which makes it difficult for analysis. Hence the text is uniformly converted into lowercase characters [6].

User name Removal: Twitter texts contain user names. Their presence does not help in opinion analysis so it should be removed.

Removing the Punctuations (#, @, etc.): Punctuation are to be removed to make analysis easy.

Remove Blank spaces: This step is used to remove the unwanted blank space which helps for the tokenization of the tweets.

Tokenization: Tokenization means breaking the sentence into words.

Removing stop words: English stop words enlisted and gathered in python programming language are removed to reduce the computational load.

Lemmatization: Lemmatization is the process of grouping inflected forms together as a single base form known as lemma. Ex: reducing "treatment", "treating", or "treats" to the lemma "treat".

Table 1 depicts the examples of preprocessed tweets. After preprocessing is done, the analysis goes to the next step called feature extraction. Retrieval of valuable words from the tweet body is called feature extraction.

Feature Extraction

In feature extraction the words which denote the ADR of metformin are made available in the dataset. These words are present in the list of ADR declared by WHO. For twitter data analysis the following attributes were taken as the inputs.

Favourite: Refers to the messages from individuals which are liked by the other users.

Favourite count: Returns the number of times this 'tweet' has been liked by other users.

Truncated: It will allow for matching on the included entities even if they are not visible in the tweet body.

Re-tweet: TRUE if this status has been retweeted.

isRetweet: Whether or not the tweet that we are looking at is an original tweet or that is a retweet of what someone else has tweeted.



**Radha Priya and Devapriya**

Retweet count: Returns the number of times that particular tweet has been retweeted.

The above attributes are the primary necessity of the twitter media which is appropriated for the research and it resonates the essence of message sharing logic. These attributes echos the treatment with medicine metformin through the twitter messages [19]. The final features are extracted in the model, if the tweet message is favourite, favourite count and retweet count is one or more than one then tweet is labelled as 1 else 0. The python coding is used to retrieve the twitter messages with side effects specified in WHO list. The individuals whose favourite count and retweet count is more than one indicates echoing of liking and sharing of the same side effects. The feature engineering methodology is applied for fruitful recognition and classification of ADR.

Feature Selection

In the present era with vast developments in Science and Engineering large datasets are increasingly the norm for which feature selection is widely used. Several features are routinely present in social media data sets. For efficacious opinion analysis many feature selection techniques have been developed that has a important part for recognizing compatible features and enhancing classification accuracy. In this proposed system Glowworm Swarm Optimization (GSO) technique is applied to refine the extracted features for opinion classification. It is important to monitor that the execution of the proposed optimization algorithm is dependent on the classification results. This research tests the features on different optimization algorithms with Support Vector Machine (SVM) classifier to select the best one. The other feature selection techniques used are Genetic Algorithm (GA) and Particle Swarm Optimization (PSO) used along with SVM. The GA is used to imitate the natural selection of survival of the fittest theories expressed in genetic engineering. PSO refines a target function by operating a population based search. Even though the GA and PSO prove to be efficient in feature selection the major disadvantage of GA is it requires repeated fitness function evaluation for complex problems and for PSO it is the non-optimal tuning of input features. To overcome the drawbacks, a GSO algorithm is proposed to optimize the input features to produce the high accuracy of classification.

Classification models

The Supervised Machine learning algorithms Naïve Bayes(NB), K-Nearest Neighbour(KNN) and Support Vector Machine(SVM) are proposed in this research. The data is labelled and from the training data the algorithms are trained to predict the output. Each supervised machine learning algorithm has its own advantages and disadvantages. NB algorithm is constructed from the Bayes theorem which is founded from the independence theory. It utilises independence among its features. The disadvantage of NB is, it is difficult to gather data that have purely independent features. KNN algorithm segregates the co-ordinates into clusters which are identified by a specific character. This classifier is able to function well with low level of input features but as the features increase to high levels it finds it difficult to predict the output of new data point. It is necessary to determine the distance of every point occurrence to all training data. SVM classifies the data based on the concept of decision planes. SVM predicts with the highest accuracy than NB and KNN [23].

RESULTS AND DISCUSSION

The intended system is executed in the python 3.6 with Anaconda 3.vb distribution with Sci-kit machine learning packages. The intended technique has been tested with the datasets after pre-processing which are gathered from the twitter media using twitter API. Initially, 1047 metformin related twitter messages were taken for analysis. After preprocessing, feature extraction technique is applied to extract 176 appropriate messages from twitter data. Totally twitter data have 14 attributes, but 6 attributes are appropriate for identifying the ADR of the diabetic drugs(Metformin and equal branded medicine). Various evaluation process is considered to be most important phase, since the proposed algorithm has selected the minimum feature vectors from the extracted features and performance of classification models calculated. The feature selection and ML algorithm provided by the python machine learning toolbox is utilized for assessing the effort of the proposed methodology and calculates the level of



**Radha Priya and Devapriya**

side effects present in the extracted dataset. The results proved that SVM has low misclassification rate than the other algorithms. Considering the results achieved by all the employed classifiers, experimental results proved the GSO optimization with SVM classification algorithm has increased the performance of the algorithms. Figure 4 shows the graphical representation of accuracy of various feature selection algorithms with SVM. Figure 5 shows the graphical representation of accuracy of various Machine learning algorithms with GSO.

CONCLUSION AND FUTURE SCOPE

Opinion mining attributes to the utilization of natural language processing and text analysis. It is widely applied to the data from the social media regarding opinions of the customers about the product and health care materials. In this research proposed approach have been applied on healthcare and pharmacovigilance spheres, regarding ADR of antidiabetic drugs using twitter data. For accurate prediction of ADR of metformin related drugs various feature selection algorithms and machine learning algorithms are used. Results following the experiments show the efficacy of the proposed approach and GSO with SVM functioned undoubtedly better than the other machine learning algorithms. The proposed work can be compared with other classification algorithms to know the performance level. The number of patients with each ADR can be explored. Other Social Media web sites can be analysed and compared.

REFERENCES

1. N. M. DHANYA, U. C. HARISH " Sentiment Analysis of Twitter Data on Demonetization Using Machine Learning Techniques" Springer International Publishing Aug 2018.
2. International Diabetes Federation (IDF), IDF Diabetes Atlas, International Diabetes Federation (IDF), Brussels, Belgium, 2019.
3. "Metformin Hydrochloride". The American Society of Health-System Pharmacists. Archived from the original on 24 December 2016. Retrieved 2 January 2017.
4. BOUAZIZI, M., OHTSUKI, T.: "Multi-Class Sentiment Analysis in Twitter: What if Classification is Not the Answer". IEEE Access. 6, 64486-64502 (2018).
5. PULKITGARG, HIMANSHUGARG, VIRENDERRANGA "Sentiment Analysis of the Uri Terror Attack Using Twitter" International Conference on Computing, Communication and Automation (ICCCA2017).
6. PROF. SUDARSHANSIRSAT, DR.SUJATARAO, DR.BHARTIWUKKADADA "Sentiment Analysis on Twitter Data for product evaluation" IOSR Journal of Engineering (IOSRJEN) ISSN (e): 2250-3021, ISSN (p): 2278-8719PP 22-25.(2019)
7. HETUBHAVSAR, RICHAMANGLANI, "Sentiment Analysis of Twitter Data using Python" International Research Journal of Engineering and Technology (IRJET) Mar 2019e-ISSN: 2395-0056 p-ISSN: 2395-0072.
8. ALI HASAN, SANA MOIN, AHMAD KARIM Machine Learning-Based Sentiment Analysis for Twitter Accounts" 2018 by the authors. Licensee MDPI, Basel, Switzerland.
9. KAZANO, "Alogliptin and metformin hydrochloride tablet, film coated". Daily Med. 14 June 2019. Retrieved 15 May 2020.
10. SUN, S., LUO, C., CHEN, J.: A review of natural language processing techniques for opinion mining systems". Inf. Fusion 36, 10–25 (2017)
11. BIFET, A., FRANK, E.: "Sentiment Knowledge Discovery in Twitter Streaming Data. In: Pfahringer, B., Holmes, G., Hoffmann, A. (eds.) DS 2010. LNCS, vol. 6332, pp. 1–15. Springer, Heidelberg.
12. M.R. SMITH AND T. MARTINEZ, "Improving Classification Accuracy by Identifying and Removing Instances that Should Be Misclassified". Proceedings of International Joint Conference on Neural Networks (IJCNN 2011). pp. 2690–2697.
13. A.AKAY, A.DRAGOMIR, BJORN-ERIK ERLANDSSON "Network-Based Modeling and Intelligent Data Mining of Social Media for Improving Care", IEEE Journal of Biomedical and Health Informatics, 2015.





Radha Priya and Devapriya

14. XIAO LIU, HSINCHUN CHEN "Identifying Adverse Drug Events from Patient Social Media: A Case Study for Diabetes", IEEE Intelligent Systems, 2015.
15. THIN NGUYEN, MARK E.LARSEN, BRIDIANNE O'DEA, DINH PHUNG, SVETHA VENKATESH, HELEN CHRISTENSEN "Estimation of the prevalence of Adverse Drug Reactions from Social Media", International Journal of Medical Information, 2017, 130-137.
16. ABEED SARKER, RACHEL GINN, AZADEH NIKFARJAM, SMITH, SWETHA JAYARAMAN, TEJASWI UPADHAYA, GRACIELA GONZALEZ "Utilizing Social Media Data for Pharmacovigilance: A review", Journal of Biomedical Informatics 54(2015)202-212.
17. MING YANG, MELODY KIANG, WEI SHANG "Filtering big data from social media-Building an early warning system for adverse drug reactions", Journal of Biomedical Informatics,2015.
18. YICHUAN WANG, NICK HAJLI, "Exploring the path to big data analytics success in healthcare", Journal of Business Research,2017.
19. SI LI, CHIA-HUI YU, YICHUAN WANG, YEDURAG BABU," Exploring Adverse Drug reactions of diabetes medicine using social media analytstics and interactive visualizations", International Journal of Information Management. Dec 2018.
20. ACHIN JAIN AND VANITA JAIN "Sentiment Classification of twitter data belonging to renewable energy using machine learning", Journal of Information and Optimization Sciences, Vol. 40 (2019).
21. ASHA S.MANEK, P.DEEPA SHENOY,M.CHANDRA MOHAN, VENUGOPAL.K.R, "Aspect term extraction for sentiment analysis in large movie reviews using Gini Index feature selection method", Springer, Dec 2015.
22. NEETU ANAND, DHRUVI GOYAL AND TAPAS KUMAR "Analyzing and Preprocessing the Twitter Data for Opinion Mining" Springer Nature Singapore Pte Ltd. 2018 B. Tiwari et al. (eds.), Proceedings of International Conference on Recent Advancement on Computer and Communication, Lecture Notes in Networks and Systems 34.
23. S.RADHA PRIYA, DR.M.DEVAPRIYA "Twitter Sentiment Analysis with Diabetic Drugs Using Machine Learning Techniques with Glowworm Swarm Optimization Algorithm", International Journal of Engineering Research and Technology, Volume 9, Issue 07, ISSN 2278-0181, July 2020.

Table 1. Examples of preprocessed data

Original	Pre-processed
RT @medivizor: Does metformin treatment improve heart enlargement in coronary artery disease? https://t.co/0KBbD7OqLG via @medivizor #Heart...	['merformin', 'treat', 'improve', 'heart', 'enlarge', 'coronary', 'artery', 'disease']
@JayMo_215 Good! Hypoglycemia is not fun and can be very serious. Several things can cause it.	['hypoglycemia', 'fun', 'very', 'serious', 'several', 'things', 'cause']





Radha Priya and Devapriya

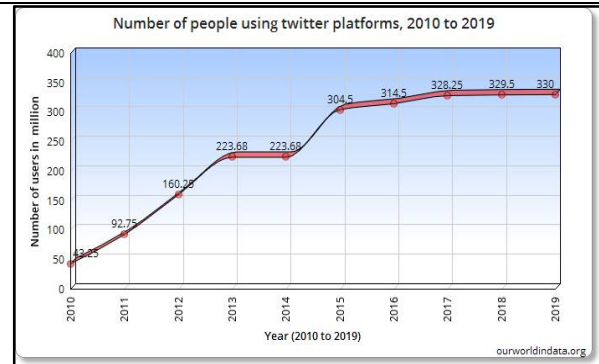


Figure 1. Number of users in twitter social media (2010 – 2019)

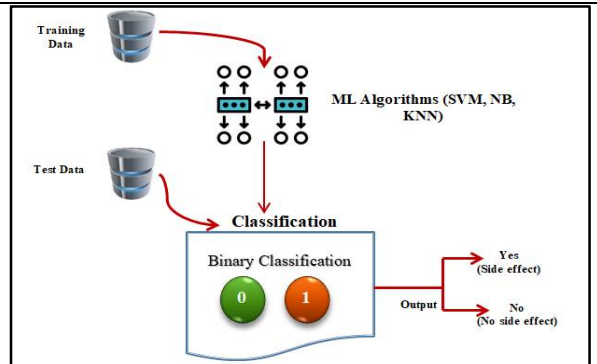


Figure 2. Functioning of supervised binary classification

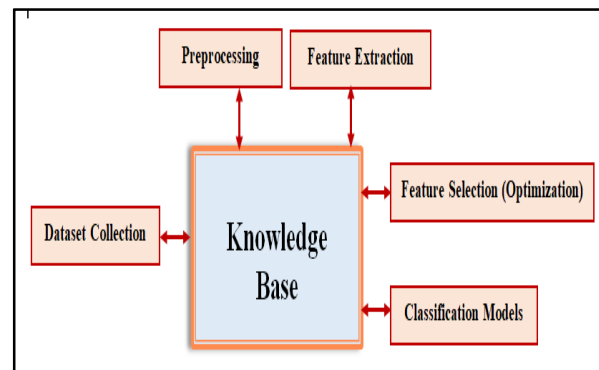


Figure.3. Block diagram for the proposed system

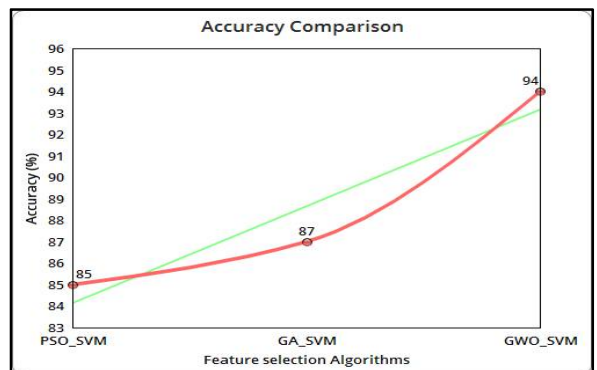


Figure .4 Accuracy of Various Feature Optimization Algorithms with SVM

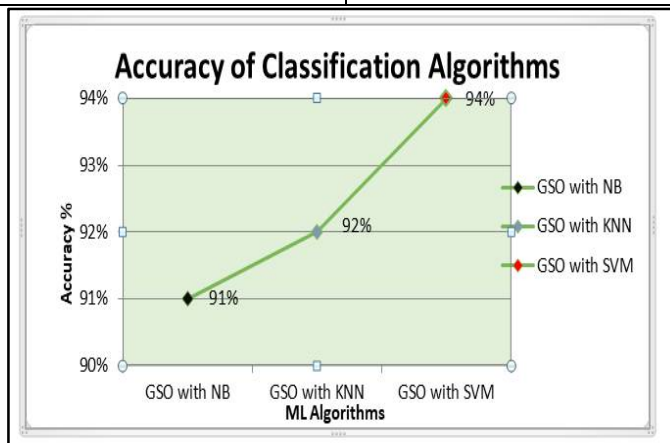


Figure .5 Accuracy measure of Various Classification Algorithms





RESEARCH ARTICLE

An Effective Behaviour-Based Fraud Detection Using CNN with Fine-Grained Attribute-Level Co-Occurrences in Online Payment Services

Valliammal N* and Sudhamathy G*

Assistant Professor, Department of Computer Science, Avinashilingam Institute for Home Science and Higher Education for Women, Coimbatore, Tamil Nadu, India.

Received: 15 Mar 2021

Revised: 22 Mar 2021

Accepted: 27 Mar 2021

*Address for Correspondence

Valliammal N

Assistant Professor,
Department of Computer Science,
Avinashilingam Institute for Home Science and Higher Education for Women,
Coimbatore, Tamil Nadu, India.
Email : vallinarayanbce@gmail.com



This is an Open Access Journal / article distributed under the terms of the **Creative Commons Attribution License** (CC BY-NC-ND 3.0) which permits unrestricted use, distribution, and reproduction in any medium, provided the original work is properly cited. All rights reserved.

ABSTRACT

In Today's Internet World, Fraud risk on intentional deception is made for financial gain. The usage of credit and debit card fraud has been a growing issue in recent years, not because of the increased prevalence of card payments in e-commerce. Each Year billions of dollars are lost in the revenue. The preventative measures for fraud still show room for improvement. Recently An additional fraud detection method is suggested based on the co-occurrence-based fraud detection system that works based on customer buying behaviour. In case of an individual there exists many transactions, the correlation of co-occurrence connects the graphs generated through various transactions. This graph is prepared by the personal details. Fraudsters assume the actions of customers on a daily basis, and fraud trends are rapidly evolving. So, fraud detection systems need to monitor online transactions efficiently with the use of unsupervised learning, because some fraudsters commit frauds once through the online medium and then switch to other techniques. This proposed system uses deep learning method Convolutional Neural Network (CNN) to learn from co-occurrence relationship with behavior model (BM) called as BM-CNN. The learned behavior model is utilized to predict the fraudulent transactions. The output of the approach is validated by a real-time database acquired from a commercial bank. It is useful for optimizing the effectiveness of detecting the fraudulent online payments.

Keywords: Online Payment Services; Fraud Detection; Network Embedding; User Behavioural Modelling; deep learning; CNN





INTRODUCTION

In 2016, recorded that the quantity of bogus e-commerce card transactions (chargebacks) in Latin America is equivalent to 1.4% of the cumulative net of the economy [1]. There are several key issues for accurately detecting these payments. The large number of transactions which have to be analysed in real-time, and the assumption that scams may not happen regularly but it generates extremely unbalanced databases. In addition to it, there is a huge price difference between the scam understood a valid payment as a scam, because in the today's situation, By generating chargeback the merchant's financial losses were very larger Card-based payment solutions are a simple way of promoting purchases for the extremely hectic lives of the people of developed and emerging countries. Conversely, the extensive use of credit and debit cards has contributed to a stable industry for scammers. With huge amounts of money to be traded annually, it'd be advisable to remember that the requisite measures are taken to protect the system. Payment card theft is the abuse of a card to allow payments without permission or forgery[2]. It might take place in different ways and with various methods. The utilization of a stolen credit card to enable illicit transactions through the internet or at an area is a money robbery also known as digital and physical fraud[3]. In another side, forgery requires modifying physical cards by techniques which include cut and insert and de-emboss/re-emboss [4]. Payment theft has a range of effects. Direct cash effects are noticeable and this disturbs especially traders, since they're the participant that many of the damages must have [5].

The management of financial crime by all banking sector is becoming a major concern of online payment fraud. The development and availability of innovative card payment forgery, like data theft, cyber-attack, and zombie blogs, are extremely problematic, and leading to magnitude of the risk. Cost effective identification of forgery in the online is seen by all banking sector as a big problem and a lead for growing attention. Scams generally vary from the everyday life of the victim to obtain the funds of the victim [6]. This may be the core principle of the viability of behavior-based scam identification. Based on the idea, the academic group is dedicated to create behavioral frameworks to appropriately recognize the difference in terms of behavioral structures. The key task is to develop a successful behavioral framework with low-quality conduct details [7]. Two additional strategies are used for detecting fraud. The differential analysis monitors and compares transaction usage patterns to usage history, which represents a recipient's regular conduct. Any major difference from regular behavior shows that there is a possible scam. The robustness of the agencies allows further dividing behavioral frameworks into the unified framework [8] as well as the population-level framework [9]. In this research, the purpose is to design the relevant data improvement strategies for the most advanced behavioral framework that operate too known framework improvement methods. In particular, dataset enhancement can be successfully carried out for behavioral modelling. Interactions between every person and its identifier, for instance, the payment amount, would be founded for every payment. In order to indicate whether the payment is illegitimate or ordinary, every address will also be connected. The collection of payments which be separated into a couple of disjointed subgroups as per the nature of the payments, i.e. natural and illegitimate collections of payments. Because a business will occur in large exchanges, the co-occurrence interaction binds the graphs created by various payments. The principle is that every system used for internet transactions has a standard detection, as is supposed to be three main phases. It is presumed that the likelihood of a payment being a scam is raised with the amount of transactions reached from a certain origin as the particular session. The main supposition is that the only way to identify that a crime is committed by revealing it to the consumer. This study employs a deep learning approach to train about the interaction of co-occurrence. The trained behavior framework is applied for detecting the illegitimate payments.

The major contributions are summarized as follows:

1. A new effectual data augmentation scheme and a single interface between network embedding schemes and behavioral frameworks are designed via modifying the conserved correlation systems based on deep learning-based classification of behavioral frameworks.



**Valliammal and Sudhamathy**

2. The designed algorithms tested on a real-time online card transaction service case. It is confirmed that the designed algorithm considerably better than the standard classifiers depending on classification performance evaluation metrics.
3. The remaining part of this article is prepared as follows: Section 2 gives the review of literature. Section 3 presents the methodology of proposed deep learning-based scam identification and Section 4 illustrates its performance. Section 5 summarizes this paper and suggests the future scope.

LITERATURE REVIEW

In [11] developed a Fraud-BNC, a modified Bayesian Network Classifier (BNC) for an online card scam identification issue. The process of designing Fraud-BNC was executed via a Hyper-Heuristic Evolutionary Algorithm (HHEA) which delivers data about the BNC into a categorization and checks for the most appropriate mixture of these elements for a certain database. The scammers also generate novel trends or susceptibilities to check payments with the consideration of novel authentication functions in card payments. In [12], several critical matters emerging during the session were highlighted, particularly on the subject of digital frauds and card payment theft. The existing legal system is provided by Greek judges which have addressed the most core concepts of digital banking offences involving financial crimes, distribution of false facts and the theft on credit and debit cards. In [14] a new method was suggested, based on theoretical and computer-precious development of classical banking. Large-scale information and a reply back analysis by more than 100,000 policy clients suggest that mobile payments cause clients theft. Primarily, consumers with interest amount deadlines will eventually make more denied complaints, and clients with monthly installment plans will be more dishonest, with increased client contact over period. Many current data mining methods, like the Hidden Markov model, fugitive logic, nearest K neighbour, genetic algorithms, the Bayesian network, the artificial immune system, the neural network, decision tree, support vector machine, a modified approach and the ensemble classification have been employed to identify theft. that's the case in all industries. The aim of [15] was to combine different methods to data mining that are needed to identify payment scams and provide a regular financial field view. Data disparity also poses substantial challenges in the fraud prevention. The efficacy of the current method of detecting fraud is in doubt only if the suspicious activity was accomplished after detecting malicious practice.

Proposed Methodology

This model aimed at developing the corresponding data augmentation methods for the standard behavior frameworks which serve as the well-identified approaches of system development [18]. There out, as illustrated in Fig. 1, the entire workflow of the information-driven fraudulent identification method encompasses the following major processes: data interpretation, augmentation and classification using CNN. In data interpretation, the information are interpreted suitably via regenerating the lossless payment file details. In data augmentation, the information is realized for behavioral modeling through creating the correlation graph and heterogeneous transfer embedding schemes for defining and extracting greatly fine-grained co-occurrences among payment features. After, according to the augmented information, the respected behavioral frameworks are introduced for achieving the identification of fraudulent activities. Lastly, in classification process, this fraudulent detection model is executed according to the amount of accesses through the client and a likelihood that differs over period. In this work, CNN is used in the training process for acquiring resultant distrust value of scam.

Data Interpretation

Card transaction details are commonly personal information which has several identities denoting the features in payments. This work uses a correlation graph which represents the information properly in card transaction facilities for regenerating the payment details such as B2C and C2C payments [19]. Each feature of a payment T is concerned as the person and its identity. Also, every identity has a class for defining whether this payment is scam or regular



**Valliammal and Sudhamathy**

represented by T_0 and T_1 . Because a person can serve different payments, the co-occurrence correlation is used for linking the graphs created via various payments.

Data Augmentation

To achieve the data augmentation for behavioral modeling, network embedding schemes [20] are employed. It is excellent to solve graphical challenges and deep interactions efficiently. After that, until this process is begun, the system architecture to be maintained must be established. This process will not explicitly contribute to predict patterns for detecting fraud in payments electronically.

Derived Networks

During the information gathering, there are B2C and C2C payments. The fraction of scams in C2C payments is not limited than the scams in B2C payments [21]. Also, the strategy used for identifying the C2C scam payments is significantly varied from that of B2C payments. The certain architecture of derived networks is based on the information demands of particular behavioral frameworks. By using the entire graph to the least-connected graph, it takes only the pair of nodes related to the account details as edges. The findings are significantly weaker than the entire structure of the graph and examine the unique features, such as account details, may not have a definitive role. Thus, a full graph structure of random pair of nodes is adopted in the derived network and the correlation of each pair of nodes is determined.

Heterogeneous Network Embedding

The heterogeneous network embedding schemes are used for learning the particular vector spaces related to the derived networks [22]. For the behavioral frameworks, the mapping operations of such vector spaces is obtained as $\phi(\cdot)$. The variable $sim(\vec{X}, \vec{Y})$ where the vectors \vec{X}, \vec{Y} split from $\phi(\cdot)$ is determined in order to deduce further possible correlations.

Proposed Classification Framework for Online Payment Fraud Identification

This proposed framework categorizes customer behavioural frameworks into demographic- and user-level frameworks based on the granularity of behavioural agents. Also, these two frameworks are constructed using the derived network and serve as the 2 convolution layers of CNN. Every scam payment has several payment attributes. The collection of such payment attributes is influencing the offline payment, however various attribute collections can comprise a many influence on the framework after processing the convolution. Every payment attribute has the likelihood to happen anywhere for guaranteeing that each collection of attributes is acquired, thus the nodes between the primary and final input layer are fully connected (Fig.2), however the linking weight modifies in every iteration.

Demographic-Level Frameworks

It detects scams via identifying the demographic-level behavioural misuses. Behavioral data-based classifiers can be used as such frameworks. Information debugging for classification algorithms is only appropriate for data augmentation by maintaining the co-occurrence level of behavioural features. For that end, construct a network of derived transactions where the vertices represent the characteristics of the payment and the edges with the weights reflect the level of co-occurrence, without considering the payments tags. In the training process, payment tags also come into place. To obtain the mapping correlation $\phi P(\cdot)$ via embedding the class-free network. After the attributes are fed to the CNN training according to the $\phi P(\cdot)$.

User-Level Frameworks

It detects the scam via recognizing the single behavioural misuses. They are viewed as a clear example of how forgery is recognized. The sufficiency of behavioural details depends strongly on reliability. The consistency and linearity of payment behavioural details should be understood to create standard behavioural frameworks on an





Valliammal and Sudhamathy

individual basis. While creating the derived network, the tag will then be taken into consideration. Here, positive and negative correlations created from T_0 and T_1 , respectively are extracted. The positive correlation is increased with the agent involved, when the negative correlation weakens between agents. In this step, the mapping relationship $\phi I(\cdot)$ is obtained via integrating the network embedding scheme into the label-aware network. In addition, the likelihood of user-level framework is obtained as $\phi I(\cdot)$.

Complex Behavioural Frameworks

Training from different facets of the framework can contribute to improved outcomes. In this case, a unified scheme is applied to combine choices from multiple frameworks to improve performance. Using the intersection to merge choices at demographic and user levels. On the other hand, crime can only be determined if each framework judgments are dishonest. Two categories of frameworks are used in identifying the scam. The succeeding B2C payment are being converted into a high-class operation focused on knowledgeable vectors with the utilization of complex behavioural frameworks and also projected as either scam or regular.

Proposed CNN Framework

In this framework, Data attribute vector is considered and a convolution layer is operated with 1D convolution kernel attribute vector. The findings are specifically influenced by the single-layer convolution. But, the CNN has 2 convolutional layers for identifying the card payment scams by learning a huge amount of data. This CNN framework is adapted to transform the attributes into the desired format. The card payment attributes are split into demographic and user-level frameworks. Every framework consists of various attributes depending on behaviour.

In this CNN framework, the major layer is a convolutional layer which has the maximum computation cost and difficulty. Conversely, every neuron of node in a single layer takes the attributes which are linked to nodes in preceding and subsequent layer which considerably decreases the amount of variables for CNN. The convolution of attribute maps in preceding layer is determined via the convolution kernel and the resultant attribute map is determined using the activation functions. The convolutional layer is defined as:

$$x_j^l = f \left(\sum_{i \in M_j} x_j^{l-1} * k_j^l + b_j^l \right) \quad (1)$$

In Eq. (1), x_j^l is j^{th} attribute map in l^{th} convolution layer, $*$ is the convolution process, M_j is the group of each input attribute maps, k_j^l is the weight of the convolution kernel j in l , b_j^l is the bias, $f(\cdot)$ is the activation function. Also, pooling layer consists of max-pooling and average-pooling operations to reduce the feature dimensionality. The pooling process is given as:

$$P_j = \frac{1}{|PR_j|} \sum_{i \in PR_j} a_i \quad (2)$$

In Eq. (2), P_j is the pooling range of j^{th} pooling area PR_j , a_i is the range in the pooling area acquired from i^{th} activation function. For a group of input attributes, the activation function is utilized for representing the resultant neuron and enhancing the CNN's nonlinear functioning capability. Subsequently, the activation function is used for nonlinear conversion of the convolutional layer's outputs as:

$$Y_i^{(l)} = Y \left(C_i^{(l)} \right) \quad (3)$$

In Eq. (3), $Y_i^{(l)}$ is the activation function's output and $C_i^{(l)}$ denotes the input which it accepts.

Here, Rectified Linear Units (ReLUs) represented as $Y_i^{(l)} = \max(0, Y_i^{(l)})$ are employed. It transforms the findings to 0 when it accepts a negative input whereas it gives similar input when it is positive. The last layer is a classical feed-forward network with one or more hidden layers. Moreover, the softmax is used in the output layer:

$$y_i^{(l)} = f \left(z_i^{(l)} \right), z_i^{(l)} = \sum_{i=1}^{m_i^{(l-1)}} w_i^{(l-1)} y_i^{(l-1)} \quad (4)$$





Valliammal and Sudhamathy

In Eq. (4), $w_i^{(l-1)}$ is the weights which must be adjusted using the fully-connected layer for defining every label and f stands for the nonlinear transfer function. Then, the CNN is learning by the stochastic gradient descent mechanism [19]. It measures the gradients using the random instance from the training database. As a result, CNN is trained. The payment scam identification challenge is defined in user-level behavioural frameworks as: For a considered payment, its scam value scored via its respected likelihood in the single-agent behavioural framework measures whether the payment is scam or regular. It may consider 2 different cases:

1. The payment offers entire details;
2. The payment loss data in few features.

Earlier, its likelihood in behavioural frameworks is determined. Because each feature is needed for computing the scam value of the payment in the behaviour framework, it is complex to analyse the payment with lost data. Therefore, the mean likelihood of each payment is determined which corresponds to prior features of the payment with identity i , the likelihood $p_{g_u^a}(i)$ and the group of such payment identities is denoted as I_i' . After, the behavioural framework $p_{g_u^a}$ related to the agent $p_{g_u^a}(i)$ is described and the domain of $p_{g_u^a}$ is denoted as $\mathcal{P}_{g_u^a}$. For a payment identity i , a novel distribution $p'_{g_u^a}$ is obtained via eliminating I_i' from $p_{g_u^a}$ and the domain of $p'_{g_u^a}$ is represented as $\mathcal{P}'_{g_u^a}$. Moreover, its score $score_{g_u^a}(i)$ is determined as:

$$score_{g_u^a}(i) = \frac{p_{g_u^a}(i) \times \exp(-H_{g_u^a})}{N_0 + \frac{1}{|\mathcal{P}'_{g_u^a}|} \times \sum_{i' \in \mathcal{P}'_{g_u^a}} p_{g_u^a}(i')} \tag{5}$$

Where $H_{g_u^a} = -\sum_{i \in \mathcal{P}_{g_u^a}} p_{g_u^a}(i) \times \log_2 p_{g_u^a}(i)$ (6)

Here, $|\mathcal{P}'_{g_u^a}|$ stands for the cardinality of $\mathcal{P}'_{g_u^a}$ to fine-tune the effect of payments compared to the payment t_i in the behavioural framework. The higher N_0 reduces the effect of other payments on the score. Consider $N_0 = 0$, notice that there is a strong distinction between scam and regular payment scores. For a feature category $a \in A$, consider a period Ω^a and the decision is obtained by,

$$r^a(i) = \begin{cases} 1 & score_{g_u^a}(i) \in \Omega^a \\ 0 & score_{g_u^a}(i) \notin \Omega^a \end{cases} \tag{7}$$

In Eq. (7), scam payments are denoted by class 1 and regular payments are denoted by class 0. The higher and lower bounds of Ω^a are based on the scores distribution of training data. The procedure of online payment scam identification is presented in algorithm 1

Algorithm 1: The procedure of identifying the online payment fraud using BM-CNN

```

Input: The group of feature/attribute categories taken as neurons  $A$ , The group of payment identities  $I$ , input convolution layer
Output: The group of decision  $R$ 
Initialize  $R = \emptyset$ ;
For each  $i \in I$  do
 $r(i) := 0$ ;
For each  $a \in A$  do
Determine scam score of the payment using Eq.(5)
Obtain  $r^a(i)$  by Eq. (7);
 $r(i) := r(i) \vee r^a(i)$ ;
End For
Apply  $r^a(i)'$  as convolution layer 1 of CNN;
Apply  $r^a(i)''$  as convolution layer 2 of CNN;
 $r(i) := r(i) \wedge r^a(i)'$ ;
 $r(i) := r(i) \wedge r^a(i)''$ ;
Include  $r(i)$  into  $R$ ;
End For
Return decision  $R$  as regular or scam
    
```





EXPERIMENTAL RESULTS AND DISCUSSION

To analyze the efficiency of BM-CNN, this model is executed on a real-time online banking payment transaction database acquired from the biggest commercial bank in India, the card payments details is issued by the Reserve Bank of India on a monthly basis available in <https://www.kaggle.com/karvalo/indian-card-payment-data-set>. The data comprises the payment done in retail and ATM transactions in India from April 2011 to August 2019. It establishes payments through debit & credit cards, ATMs, etc. It is utilized for verifying the card payment development in India. The data contains monthly statistics of the following information from Apr'2011 to Aug'2019. The proposed BM-CNN, Fraud-BNC [11], KNN [17] and Naïve Bayes [17] approaches are implemented in MATLAB (Version 2018a) with the provided toolbox and comparison among them is done with the parameters such as Precision, Recall, F-measure and Accuracy.

Precision: It represents the fraction of fake payments which were accurately predicted at True Positive (TP) cases

$$Precision = \frac{TP}{FP + TP}$$

Recall: It represents the accurately predicted fake payments to the total number of fake payments in database.

$$Recall = \frac{TP}{TP + FN}$$

F-measure: It is the harmonic average of precision and recall.

$$F - measure = \frac{2 * (Recall * Precision)}{(Recall + Precision)}$$

Accuracy: It is the fraction of accurately predicted fake payments and the overall amount of payments as:

$$Accuracy = \frac{TP + TN}{TP + TN + FP + FN}$$

Precision Rate comparison

From Fig.3, it indicates that the precision of proposed and existing models for the amount of attributes in given databases. While amount of attributes is increasing, the corresponding precision is also maximized. For e.g., the BM-CNN provides a precision of 94% compared to the Naïve bayes, KNN and Fraud-BNC. This is because the BM-CNN needs neither high-dimensional attributes nor derived factors and may discover a comparatively better sorted collection of input within a specified amount of interval

Recall Rate comparison

From Fig.4, it indicates the recall of proposed and existing models for the amount of attributes in a given database. As increasing the amount of attributes, the recall is also maximized. For e.g., the BM-CNN attains a recall of 92% compared to the Naïve bayes, KNN and Fraud-BNC. This is because the BM-CNN saves computation time of the derived factors which provides the easiest fine-tuning of BM-CNN.

F-Measure Rate Comparison

From Fig.5, it indicates that the f-measure of proposed and existing models for the amount of attributes in a given databases. While maximizing the amount of attributes, the f-measure is also maximized. For e.g., the BM-CNN provides an f-measure of 96% compared to the all other models. Since it considers the fine grained co-occurrences of transaction details and thus the real-world online payment transactions are achieved.

Accuracy Comparison

From Fig.6, it gives the accuracy of proposed and existing models for the amount of attributes in a given databases. The BM-CNN increases the accuracy while reducing the processing time. The BM-CNN attains the accuracy of 95.65% compared to all other models since it does not require a huge number of derived factors during pre-processing.





CONCLUSION

In this paper, an effective fraud detection model is proposed for behavioural models in online payment fraud detection via modelling co-occurrence correlations of transactional features. The improved CNN algorithm is built for enhancing the performance and stability of the model. It requires neither high-dimensional features nor derived factors to determine the comparatively better arranged collection of input within a specified amount of interval and online transactions need quick reply and precise recognition. The computation time is reduced. With the usage of the real-time dataset, this model is implemented and tested against existing models. From the analysis, the BM-CNN can achieve a better efficiency compared to the other classification algorithms. The future work will be focused on finding the sequence features of transactions. Further, LSTM will consider for handling the storage of trader's behaviour for finding the malicious transactions precisely.

REFERENCES

1. Cyber Source.: Online fraud report (Latin America edition). Tech. rep., Cyber Source Corporation, a Visa Company, 2016
2. L. Balan and M. Popescu.: Credit card fraud. *The USV Annals of Economics and Public Administration*, 11(1):81–85, 2011.
3. K. Chaudhary, J. Yadav, and B. Mallick.: A review of fraud detection techniques: Credit card. *International Journal of Computer Applications*, 45(1):39–44, 2012.
4. Y. Kou, C.-T. Lu, S. Sirwongwattana, and Y.-P. Huang.: Survey of fraud detection techniques. In *Networking, sensing and control, 2004 IEEE international conference on*, volume 2, pages 749–754. IEEE, 2004.
5. J. T. Quah and M. Sriganesh .: Real-time credit card fraud detection using computational intelligence. *Expert systems with applications*, 35(4):1721–1732, 2008.
6. B. Cao, M. Mao, S. Viidu, and P. S. Yu, "Hitfraud.: A broad learning approach for collective fraud detection in heterogeneous information networks," in *Proc. IEEE ICDM 2017, New Orleans, LA, USA, November 18-21, 2017*, pp. 769–774.
7. M. A. Ali, B. Arief, M. Emms, and A. P. A. van Moorsel.: Does the online card payment landscape unwittingly facilitate fraud?" *IEEE Security & Privacy*, vol. 15, no. 2, pp. 78–86, 2017.
8. Khodadadi, S. A. Hosseini, E. Tavakoli, and H. R. Rabiee.: Continuous-time user modeling in presence of badges: A probabilistic approach *ACM Trans. Knowledge Discovery from Data*, vol. 12, no. 3, pp. 37:1–37:30, 2018.
9. Q. Cao, X. Yang, J. Yu, and C. Palow.: Uncovering large groups of active malicious accounts in online social networks, in *Proc. ACM SIGSAC 2014*, pp. 477–488, 2014.
10. Wei, W., Li, J., Cao, L., Ou, Y., & Chen, J.: Effective detection of sophisticated online banking fraud on extremely imbalanced data. *World Wide Web*, 16(4), 449-475, 2013.
11. deSá, A. G., Pereira, A. C., & Pappa, G. L.: A customized classification algorithm for credit card fraud detection. *Engineering Applications of Artificial Intelligence*, 72, 21-29, 2018.
12. Rachavelias, M. G.: Online financial crimes and fraud committed with electronic means of payment—a general approach and case studies in Greece, In *Era Forum*, Vol. 19, 3, 339-355, 2020.
13. Zhou, H., Chai, H. F., & Qiu, M. L.: Fraud detection within bankcard enrollment on mobile device based payment using machine learning. *Frontiers of Information Technology & Electronic Engineering*, 19(12), 1537-1545, 2018
14. Garnefeld, I., Eggert, A., Husemann- Kopetzky, M., & Böhm, E.: Exploring the link between payment schemes and customer fraud: a mental accounting perspective, *Journal of the Academy of Marketing Science*, 47(4), 595-616, 2016.





Valliammal and Sudhamathy

15. Mishra, S. P., & Kumari, P.: Analysis of Techniques for Credit Card Fraud Detection: A Data Mining Perspective. In *New Paradigm in Decision Science and Management* Springer, Singapore, pp. 89-98, 2020
16. Darwish, S. M.: A bio-inspired credit card fraud detection model based on user behavior analysis suitable for business management in electronic banking". *Journal of Ambient Intelligence and Humanized Computing*, 1-15, 2020.
17. Itoo, F., & Singh, S.: Comparison and analysis of logistic regression, Naïve Bayes and KNN machine learning algorithms for credit card fraud detection. *International Journal of Information Technology*, 1-9, 2020.
18. T. Chen and C. Guestrin. :Xgboost A scalable tree boosting system, in Proc. ACM SIGKDD 2016, CA, USA, August 13-17, pp. 785–794, 2016.
19. Wang, C., & Zhu, H.: Representing Fine-Grained Co-Occurrences for Behavior-Based Fraud Detection in Online Payment Services. *IEEE Transactions on Dependable and Secure Computing*, 2020.
20. P. Cui, X. Wang, J. Pei, and W. Zhu.: A survey on network embedding IEEE Trans. Knowledge and Data Engineering, vol. 31, no. 5, pp. 833–852, 2019.
21. C. Shi, B. Hu, W. X. Zhao, and P. S. Yu.: Heterogeneous information network embedding for recommendation IEEE Trans. Knowledge Data Engineering, vol. 31, no. 2, pp. 357–370, 2019.
22. Y. LeCun, Y. Bengio, and G. Hinton.: Deep learning Nature, vol. 521, no. 7553, pp. 436–444, 2015.
23. R. G. J. Wijnhoven and P. H. N. de With.: Fast training of object detection using stochastic gradient descent in Proceedings of International Conference on Pattern Recognition (ICPR), pp. 424–427, Tsukuba, Japan, 2010.

Table 1: The Literature Review

S. No	Author	Title	Journal & Year	Methods	Advantages	Limitation
1	Zhou, H., Chai, H. F., & Qiu, M. L.	Fraud detection within bankcard enrollment on mobile device based payment using machine learning.	<i>Frontiers of Information Technology & Electronic Engineering</i> , 2018	Logistic Regression, Random Forest and Gradient Boost Decision Tree	ML performs better than expert rules, particularly in differentiating high and low risks	No optimization algorithms are performed
2	Itoo, F., & Singh, S,	Comparison and analysis of logistic regression, Naïve Bayes and KNN machine learning algorithms for credit card fraud detection.	<i>International Journal of Information Technology</i> , 2020	Regression Model, Naïve Bayes and k-nearest neighbour	Here, the fine-grained interplay of payment features is derived using a knowledge diagram	The challenge was typically the identification of specific forms of natural or deceptive structures in such classifiers
3	Darwish, S. M	A bio-inspired credit card fraud detection model based on user behavior analysis suitable for business management in electronic banking.	<i>Journal of Ambient Intelligence and Humanized Computing</i> , 2020	K-Means and Artificial Bee Colony	The development was made in the two-level paradigm to detect malware.	Only one algorithm is implemented.





Valliammal and Sudhamathy

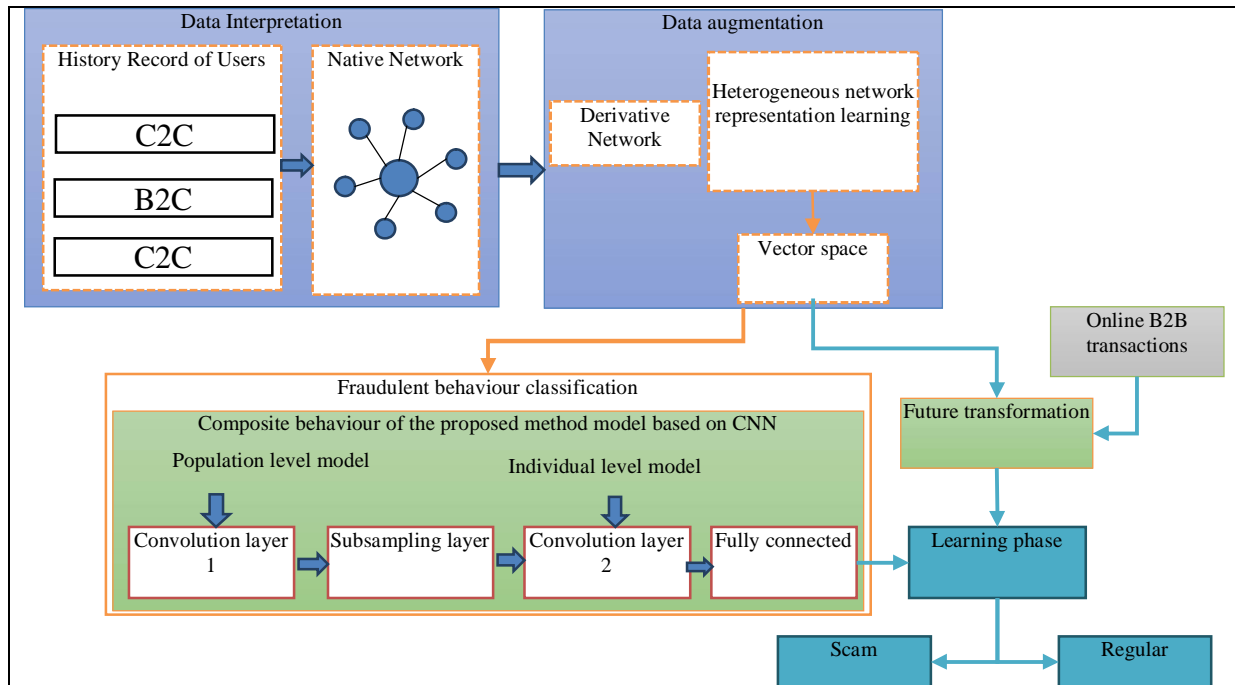


Fig.1. Workflow of BM-CNN based Payment Fraudulent Identification Framework

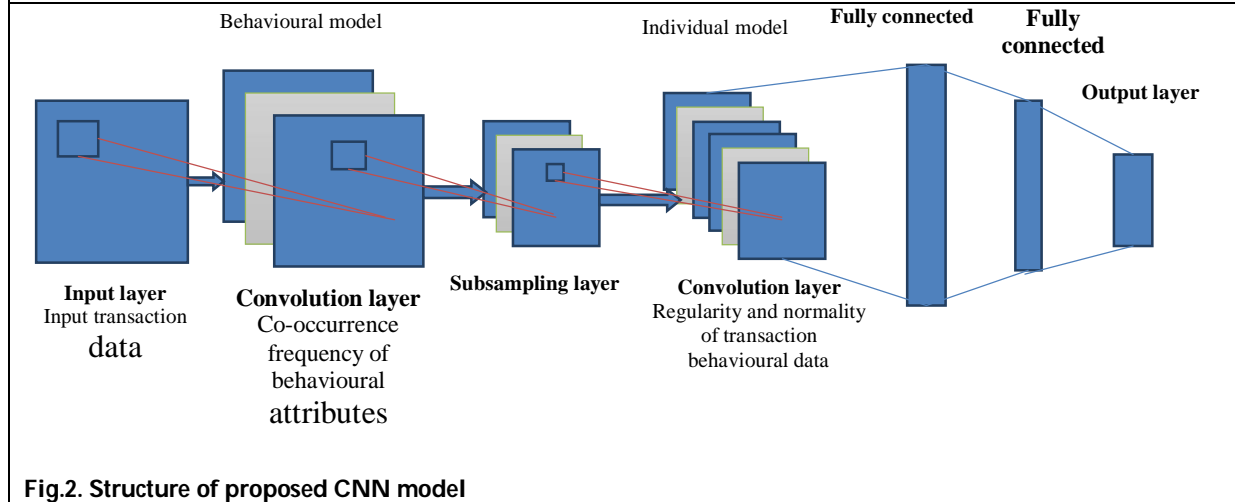


Fig.2. Structure of proposed CNN model





Valliammal and Sudhamathy

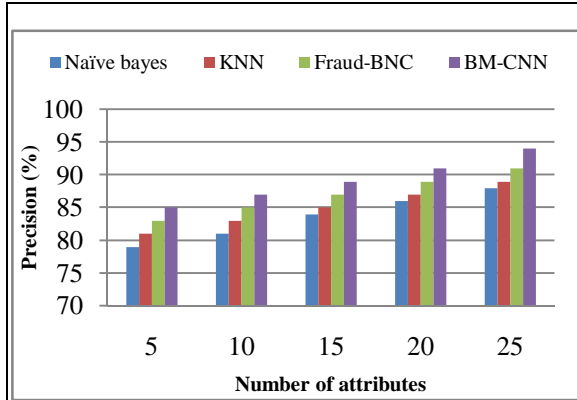


Fig.3. Result of Precision

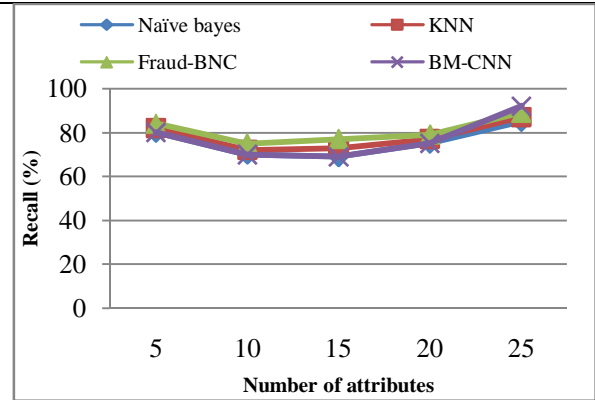


Fig.4. Result of Recall

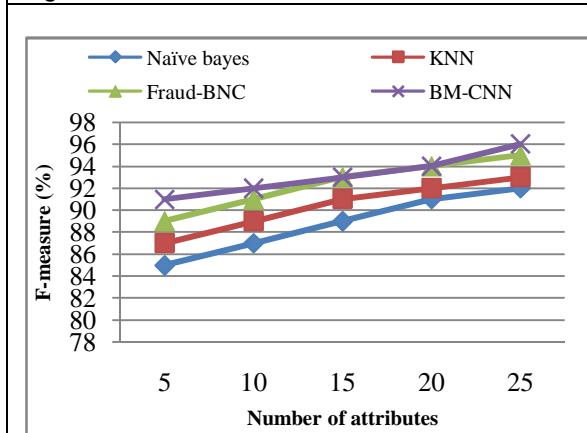


Fig.5. Result of F-measure

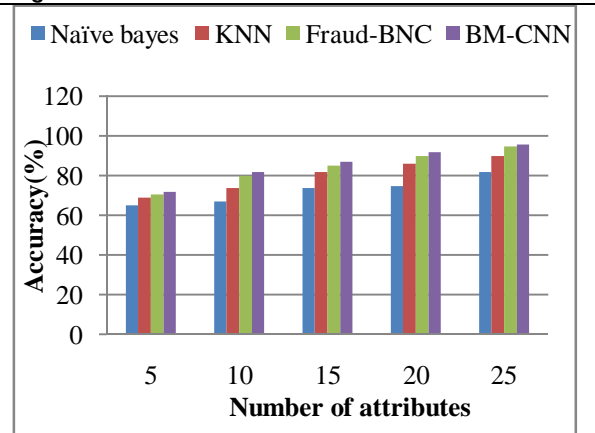


Fig.6. Result of Accuracy





RESEARCH ARTICLE

Comparative Evaluation of Anti-Inflammatory Activity of Vatsanabha Purified by Two Different Methods

Deepa jose¹, Teresa Cyriac², Rajarajeswari L. A^{2*} and Sahilat. S²

¹Vice Principal, Nirmala College of Pharmacy, Muvattupuzha, Ernakulum, Kerala, India.

²B. Pharm Graduates, Nirmala College of Pharmacy, Muvattupuzha, Ernakulum, Kerala, India.

Received: 03 Mar 2021

Revised: 05 Mar 2021

Accepted: 06 Mar 2021

*Address for Correspondence

Rajarajeswari L. A

B. Pharm Graduates,

Nirmala College of Pharmacy,

Muvattupuzha,

Ernakulum, Kerala, India.

Email: rajarajeswarianil308@gmail.com



This is an Open Access Journal / article distributed under the terms of the **Creative Commons Attribution License** (CC BY-NC-ND 3.0) which permits unrestricted use, distribution, and reproduction in any medium, provided the original work is properly cited. All rights reserved.

ABSTRACT

Nowadays ancient system of medicine is gaining importance due to increasing side effects of modern medicines. Medicinal scriptures of Ayurveda are major source of knowledge about the drugs for various emerging diseases. Inflammation is a chronic disease condition. Many inflammatory diseases are cured by ayurvedic medicines. These medicines must gain acceptance in present world. Vatsanabha is a drug which is found in Himalayan region in India. Vatsanabha when subjected to Shodhana process act as a potent drug to treat various diseases which is practiced by Ayurvedic physicians since ancient period. Shodhana processed Vatsanabha is the chief constituent in formulation swasanantharam tablets which is used for respiratory disease like asthma. Ayurvedic literature reveals Vatsanabha as 'mahavisha' (poisonous drug) which cause toxicity to body when consumed in pure form. The crude drug is processed or purified using cow's urine or cow's milk. On treatment with cow's urine or cow's milk, aconitine is converted into aconine which is nontoxic. The drug shows anti-inflammatory activity as well as anti-asthmatic activity. It is also known for its antipyretic activity. The present investigation is to compare the anti-inflammatory activity of Vatsanabha purified by two different methods such as treatment with Cow's milk and Cow's urine. The anti-inflammatory studies include Human RBC Stabilization method and albumin denaturation method. The absorbance is determined at 560nm and 660 nm respectively. By using the absorbance value, percentage inhibition values are calculated and compared.

Keywords: Vatsanabha, Anti-inflammatory activity, Aconite, Albumin denaturation, Shodhana.





Deepa jose et al.,

INTRODUCTION

Aconitum ferox known as Vatsanabha or Mahavisha, is a species of monk's hood from the family of Ranunculaceae. The roots of Vatsanabha are therapeutically potent in Ayurveda and are used extensively in different classical formulation. Severe and potentially fatal toxic effect can result by the administration of aconitum plant extract [2]. The purification of aconite root reduces the toxic effect of the drug without compromising its pharmacological properties. Ingestion of unpurified drug causes burning in entire body, senselessness, inhibition of heart rate and finally death [7]. The diterpene alkaloids such as hypoaconitine, aconitine and mesaconitine are the poisonous components present in the root tubers, which is converted in to less toxic alkaloids such as aconine, benzoyl aconine and pyroaconine by alkaline treatment, heating or through deacylation and oxidation reaction [7,9,18]. Shodhana or purification can be defined as the removal of unwanted part of drug and eradication of highly toxic ingredients. In addition to detoxification properties, the efficacy and potency of the drug can be increased by sodhana process. Cow's urine or cow's milk is used as the classical medium of sodhana [11]. Sodhana by both cow's urine and cow's milk reduces cardiac and neuromuscular toxic effects of aconite without affecting activity. Soaking of roots in cow's urine and boiling of roots in cow's milk hydrolyzes aconite alkaloids in to less toxic and nontoxic derivatives [7]. The tuberous roots are commonly employed for various diseases and used in herbal medicine only after processing. Vatsanabha can be used in the treatment of neuromuscular anomalies, digestive impairment, fever cough, inflammation, diabetes and various respiratory disorders. It is also used as analgesic, antirheumatic, cardiotoxic and antidote for poisoning due to rats, rodents and snake bites [4,18].

MATERIALS AND METHODS

Materials

Earthen pot, cow's urine, cow's milk, glass container, stick, muslin cloth.

Chemicals

Alsever (2% dextrose, 0.8% sodium citrate, 0.5% citric acid and 0.42% NaCl), phosphate buffer, iso saline, hypo saline, bovine albumin, Hydrochloric acid, Dragondroff's reagent, Wagner's reagent, Molisch's reagent, sodium nitroprusside, pyridine, sodium hydroxide, Bontrager's reagent, ferric chloride, gelatin, concentrated HCl, magnesium turnings, concentrated sulphuric acid, Salkowski's reagent, acetic anhydride.

METHODOLOGY

Purification Methods

Two traditional methods for purification of *Aconitum ferox* are described in Ayurveda [7,11].

Purification of Vatsanabha using cow's urine [1]

100 g of Vatsanabha tuber was cleaned and dried which was then cut into small pieces and dipped in a stone or earthen vessel containing one liter of cow urine for three consecutive days. Each day the cow's urine was replaced with the fresh one. On the fourth day, the roots were washed with water; the outer cortical layers were peeled off and the product was again washed with warm water and the sundried pieces were pulverized and kept in an air tight glass container [12].

Purification of Vatsanabha using cow's milk [1]

100 g of Vatsanabha was tied in a muslin cloth into a poultice which was suspended in the centre of a pot with the help of a stick. Cow's milk was poured in the vessel to completely immerse the bundle. It was then heated on a stove for six hrs at 100°C. Then the pieces of Vatsanabha tubers were taken out and washed with water. The outer layers of



**Deepa jose et al.,**

the roots were peeled off. After proper drying the Vatsanabha pieces were then made into powder and kept in an air tight glass container [12]. (Fig: 1)

Extraction of Purified Vatsanabha

The Ayurvedic Shodhana treated drug material was treated with petroleum ether and then subjected to Soxhlet extraction to complete 20 cycles with alcohol. The alcoholic extract obtained was filtered and concentrated on a water bath to obtain a thick paste. [15,21] (Fig: 2)

Invitro Anti-Inflammatory Tests

Human Red Blood Cell Membrane Stabilization [5,13, 19]

The Blood was collected from healthy human who has not taken any NSAIDs for 2 weeks before the experiment and mixed with equal volume of a seiver (2% dextrose, 0.8% sodium citrate, 0.5% citric acid and 0.42% Sodium Chloride) solution. Blood was centrifuged (3000 rpm) for 10 minutes and the packed cells were washed with iso saline. (Fig: 6) To 2ml of extract, 1ml of phosphate buffer adjusted to pH 6.3 using pH meter (Fig: 4), 2ml of hypo saline and 0.5ml of HRBC suspension, was added. Instead of extract 2ml of water was used in the control. All the assay mixtures were incubated at 37°C for 30 minutes in BOD incubator (Fig: 5) and centrifuged. Hemoglobin content in the supernatant solution is estimated using UV at 560nm [10]. The % hemolysis is calculated by assuming hemolysis produced in water as 100%. The % of HRBC membrane stabilization is calculated using the formula. (Fig: 3)

$$\text{Percentage protection} = 100 - (\text{Optical Density of sample} / \text{optical Density of control} \times 100)$$

Inhibition of Albumin Denaturation [5,13, 19]

The reaction mixture consists of test extracts and 1% aqueous solution of bovine albumin fraction. The pH of the reaction mixture was adjusted using small amount of 1N Hydrochloric acid. The sample extracts were incubated at 37°C for 20 min in BOD incubator (Fig: 5) and the heated to 51°C for 20 min, after cooling the samples, the turbidity was measured at 660 nm. The experiment was performed in triplicate. (Fig: 3)

The percentage inhibition of albumin denaturation was calculated as follows:

$$\text{Percentage inhibition} = (\text{absorbance Control} - \text{Absorbance Sample}) \times 100 / \text{Absorbance control}$$

RESULTS

Phytochemical analysis

Phytochemical analysis showed the presence of alkaloids, carbohydrates, glycosides, tannins, flavonoids and steroids [21].

Inhibition of Albumin Denaturation

The percentage inhibition of albumin denaturation by Vatsanabha purified using milk and urine are shown in the Table 2 and Table 3 respectively. The graphical representations of the results are shown in Graph 1 and Graph 2 respectively.

The result of comparative evaluation of albumin denaturation inhibition by Vatsanabha purified by Milk and Urine is represented as a bar chart in graph 4. The result of comparative evaluation of albumin denaturation inhibition by Vatsanabha purified by Milk, Urine and the standard drug Aspirin is represented as a bar chart in graph 5.

Human Red Blood Cell Membrane Stabilization

The result of anti-inflammatory activity assay by human RBC Membrane Stabilization method is tabulated in Table 3 and 4. The graphical representation of the HRBC Membrane Stabilization by the Vatsanabha treated with Milk and Urine are depicted in the graphs 6 and 7 respectively. HRBC Membrane Stabilization by Vatsanabha purified by Milk

30452





Deepa jose et al.,

and Urine was compared and graphical representation is shown in graph 9. HRBC Membrane Stabilization by Vatsanabha purified by Milk, Urine and the standard drug Aspirin was compared and graphical representation is shown in graph 10.

STATISTICAL ANALYSIS

Two Way Analysis of Variance

The method used for statistical analysis is 2-way analysis of variance. The anti-inflammatory activity of Vatsanabha purified by cow's urine and cow's milk were compared using this method.

DISCUSSION

Albumin Denaturation Inhibition Method

Inflammation is a body response to injury, infection or destruction characterized by heat, redness, pain, swelling and disturbed physiological functions. It is triggered by the release of chemical mediators from injured tissue and migrating cells [14,5]. Inflammation is a complex process, associated with pain and involves the increase of vascular permeability, increase of protein denaturation and membrane alteration. By the application of elevated temperature or pH, strong acid or base, organic solvents or other chemical agents, proteins lose their secondary and tertiary structure which is known as protein denaturation. Inflammation occurs as a result of denaturation of proteins. [13,17] Anti-inflammatory activity of *Aconitum ferox* was evaluated by albumin denaturation inhibition method. *Aconitum ferox* is purified by Ayurvedic Shodhana using two different media such as cow's urine and cow's milk. A comparative evaluation of anti-inflammatory activity was carried out. At the concentration of 200 µg/ml the highest anti-inflammatory activity was observed with the ethanolic extract of root purified by cow's urine. At 200 µg/ml ethanolic root extract of *Aconitum* purified by cow's urine exhibited the albumin denaturation inhibition of 64.28 % while for Aspirin it was 85.92 % at 200 µg/ml.

Human Red Blood Cell Membrane Stabilization

Cellular infiltration is an important aspect of an inflammatory response. During inflammation leukocytes release their lysosomal enzymes, including proteases, causing further tissue damage and subsequent inflammation. At the time of inflammation leukocytes are found in tissues. The first step of phagocytosis is the chemotactic movement of leukocytes towards the foreign body which induces inflammation.[4] Damage to cell membranes will further make the cell more susceptible to secondary damage by means of free radical-induced lipid peroxidation. As the red blood cell membrane is similar to that of lysosomal membrane, inhibition of red blood cell hemolysis may provide insights into the inflammatory process. Stabilization of these cell membranes may retard or inhibit the lysis and subsequent release of the cytoplasmic contents which, in turn, minimize the tissue damage and, hence, the inflammatory response. Most of the non-steroidal drugs as well as anti-inflammatory drugs act by inhibiting or stabilizing the membrane of lysosomal enzyme [16, 20, 12].

Aconitum ferox was subjected to anti-inflammatory studies using Human RBC Stabilization method. After the purification process of *Aconitum ferox* by using cow's urine and cow's milk separately, the percentage protection was calculated from the absorbance values obtained at 560 nm [10]. . The percentage protection obtained for drug purified by cow's urine and cow's milk were compared. At concentration 200 µg/ml, the root extract of drug purified by urine was found to show maximum percentage protection of 65.55%. The percentage stabilization for ethanolic root extract of *Aconitum* purified by cow's milk was found to be 57.15% at a concentration of 200 µg/ml. The percentage protection of HRBC Membrane was found to be higher for urine treated *Aconitum* when compared to that of milk treated *Aconitum* at same concentration. Vatsanabha purified by urine treatment, exhibited highest stabilization of HRBC Membrane, revealing the anti-inflammatory activity of *Aconitum ferox*.





Deepa jose et al.,

CONCLUSION

Aconitum ferox, belonging to the family *Ranunculaceae* was selected for the study; which is a therapeutically potent plant in Ayurveda. The unpurified *Aconitum ferox* is toxic. The aim of the study was to purify the *Aconitum* by two different detoxification methods using cow's milk and cow's urine and to compare the anti-inflammatory activity. The root of *Aconitum ferox* was purified by treatment with cow's milk and cow's urine. The purified *Aconitum ferox* was extracted with ethanol and was subjected to preliminary phytochemical screening. The extract showed the presence of alkaloids, steroids, carbohydrates, glycosides, tannins and flavonoids. The total ethanolic extracts of purified *Aconitum ferox* were evaluated for *in vitro* anti-inflammatory using albumin denaturation inhibition method of Human red blood cell stabilization method. Aspirin was used as the standard drug. The results were compared between each other and with the anti-inflammatory activity exhibited by the standard drug aspirin; by the above two methods in three different concentrations. Ethanolic root extract of *Aconitum ferox* purified by cow's urine exhibited higher inhibition of albumin denaturation compared to ethanolic root extract of *Aconitum ferox* purified by cow's milk. In Human Red Blood Cell Membrane Stabilization method, the percentage protection was found to be higher for urine treated drug when compared to that of milk treated drug in all concentrations tested. The study concluded that the *Aconitum ferox* purified with both cow's urine and cow's milk possessed anti-inflammatory activity. But the *Aconitum ferox* purified with cow's urine showed higher anti-inflammatory activity than the *Aconitum ferox* purified with cow's milk. However further studies are recommended to ensure that treatment with cow's urine and cow's milk removed all toxic compounds from *Aconitum ferox*.

REFERENCES

1. Pandey A et al. Therapeutic potential of vatsanabha. *International Journal of Ayurveda Pharmaceutical Chemistry*. 2017; 2(6):271-277.
2. Marija Povsnar et al. Rare tradition of the folk medicinal use of *Aconitum* spp. is kept alive in Solčavsko, Slovenia. *Journal of Ethnobiology and Ethnomedicine*. 2017; 13(45): 1-14.
3. Ashok Kumar Panda, Saroj Kumar Debnath, Overdose effect of Aconite containing Ayurvedic Medicine ('Mahashankha Vati'). *International Journal of Ayurveda Research*. 2010 Jul-Sep; 1(3): 183–186.
4. Chioma A Anosikeet.al. Membrane stabilization as a mechanism of the anti-inflammatory activity of methanol extract of garden egg (*Solanum aethiopicum*). *DARU Journal of Pharmaceutical Sciences*. 2012; 20(1): 76
5. Ghumrey S et al. Assessment of invitro anti-inflammatory activity of *Cynodon Dactylon* and Acyclovir showing synergistic effect by albumin denaturation and membrane stabilization assay. *Modern Approaches in Drug Designing*. 2017.
6. Nidhi Srivastava, Vikas Sharma, Barkha Kamal, Vikash S. Jadon, *Aconitum*: Need for sustainable exploitation. *International Journal of Green Pharmacy*. 2010: 220228.
7. Dr Amala Jyothi Et Al, Vatsanabha: An Agada Perspective. *International Ayurvedic Medical Journal*. 2016; 4(7): 1235-1247.
8. Jampani Bhogi Hanuman and Alfred Katz, New Lipo Norditerpenoid Alkaloids from Root Tubers of *Aconitum ferox*. *Journal of Natural Products*. 1994; 57(1): 105-115.
9. So Young Lee et al, Norditerpenoid and Dianthramide Glucoside Alkaloids from Cultivated *Aconitum* Species from Korea. *Archives of Pharmacal Research*. 2007; 30(6): 691-694.
10. Arya N, Kumar H. Comparitive physico-chemical profile of 'Vatsanabha' (*Aconitum ferox*, *Ranunculaceae*) mula processed through cow's urine and cow's milk.. *International Journal of Research in Ayurveda & Pharmacy*. 2017; 8(5):217-222.
11. Raman S. Belge , Archana R. Belge, Ayurvedic Shodhana Treatments and Their Applied Aspect with Special Reference to Loha. *IOSR Journal of Pharmacy and Biological Sciences*. 2012; 2(1): 45-49.
12. Parvesh Kumar, Rajeev Ranjan, Rudramani Deepak, Naresh Kumar, Shodhana Procedure of Various Visha & amp; Upvisha in Ayurveda. *World Journal of Pharmaceutical Research*. 2018; 7(4): 472-479.





Deepa jose et al.,

13. Godhandaraman Sangeetha *et.al.* In vitro anti-inflammatory activity of different parts of *Pedaliium murex* (L.). *International Journal of Herbal Medicine*. 2016; 4(3): 31-36.
14. Panda A, Debnath S. Overdose effect of aconite containing ayurvedic medicine ('Mahashankha Vati'). *International Journal of Ayurveda Research*. 2010; 1(3):183.
15. Deore S, Moon K, Khadabadi S, Deokate U, Baviskar B. Evaluation of toxicity of 'Vatsanabha' (*Aconitum ferox*, Ranunculaceae) Before and After Shodhana. *Journal of Young Pharmacists*. 2013; 5(1):3-6.
16. Anosike C, Obidao.O.Membrane stabilization as mechanism of the anti-inflammatory of methanol extract of garden egg(*Solanumaethiopicum*). *DARU Journal of Pharmaceutical Science*.2012.
17. Nurul Izzati Osman *et.al.* In vitro xanthine oxidase and albumin denaturation inhibition assay of *Barringtonia racemosa* L. and total phenolic content analysis for potential anti-inflammatory use in gouty arthritis. *Journal of intercultural ethnopharmacology*. 2013; 5(4): 343–349.
18. J B Hanuman *et.al.* Isolation and identification of four non diterpenoid alkaloids from processed and unprocessed root tubers of *Aconitum ferox*. *Journal of natural products*. 1993; 56(6): 801-809.
19. Xiao K, Wang L, Liu Y, *et al.* Study of a conitine toxicity in rat embryos in vitro. *Birth Defects Research Part B Developmental and Reproductive Toxicology*. June 2007; 8 (3): 208–212.
20. Amita Misra *et al.* AFLP Markers for Identification of *Aconitum* Species. Medicinal and Aromatic Plant Science and Biotechnology, *Global Science Books*. 2010; 4(1): 15-19.
21. Umorya H *et al.* Qualitative phytochemical screening of *Aconitum ferox* roots.2018; 1(7): 9529-9531.

Table 1: Percentage Inhibition of Albumin Denaturation of Vatsanabha purified by Milk

CONCENTRATION	ABSORBANCE	PERCENTAGE INHIBITION
100 µg/ml	0.142	44.89 %
150 µg/ml	0.148	51.02 %
200 µg/ml	0.153	56.12 %

Table 2: Percentage Inhibition of Albumin Denaturation of Vatsanabha purified by Urine.

CONCENTRATION	ABSORBANCE	PERCENTAGE INHIBITION
100 µg/ml	0.152	55.10%
150 µg/ml	0.157	60.20%
200 µg/ml	0.161	64.28%

Table 3: Human Red Blood Cell Membrane Stabilization by Milk Treated Vatsanabha

CONCENTRATION	ABSORBANCE (560nm)	PERCENTAGE HAEMOLYSIS	PERCENTAGE PROTECTION
100 µg/ml	0.068	57.14%	42.86%
150 µg/ml	0.059	49.57%	50.43%
200 µg/ml	0.051	42.85%	57.15%

Table 4: Human Red Blood Cell Membrane Stabilization by Urine Treated Vatsanabha

CONCENTRATION	ABSORBANCE (560nm)	PERCENTAGE HAEMOLYSIS	PERCENTAGE PROTECTION
100 µg/ml	0.052	48.69%	56.31%
150 µg/ml	0.048	40.33%	59.67%
200 µg/ml	0.041	34.45%	65.55%





Deepa jose et al.,

<p>Graph 1:Albumin Denaturation inhibition by Milk Treated Vatsanabha</p>	<p>Graph 2: Albumin Denaturation inhibition by Urine Treated Vatsanabha</p>
<p>Graph 3: Albumin Denaturation inhibition by Standard Aspirin.</p>	<p>Graph 4: Comparison of Albumin Denaturation inhibition by Vatsanabha purified using Milk and Urine.</p>
<p>Graph 5: Comparison of Albumin Denaturation inhibition by Milk, Urine treated Vatsanabha and Aspirin</p>	<p>Graph 6: Human Red Blood Cell Membrane Stabilization by Milk Treated Vatsanabha</p>





Deepa jose et al.,

<p style="text-align: center;">HUMAN RED BLOOD CELL MEMBRANE STABILIZATION BY URINE TREATED VATSANABHA</p> <table border="1"> <caption>Data for Graph 7</caption> <thead> <tr> <th>Concentration (µg/ml)</th> <th>% Protection</th> </tr> </thead> <tbody> <tr> <td>100</td> <td>56.81</td> </tr> <tr> <td>150</td> <td>59.67</td> </tr> <tr> <td>200</td> <td>68.55</td> </tr> </tbody> </table>	Concentration (µg/ml)	% Protection	100	56.81	150	59.67	200	68.55	<table border="1"> <caption>Data for Graph 8</caption> <thead> <tr> <th>Concentration (µg/ml)</th> <th>% Protection</th> </tr> </thead> <tbody> <tr> <td>100</td> <td>~65</td> </tr> <tr> <td>150</td> <td>~70</td> </tr> <tr> <td>200</td> <td>~75</td> </tr> </tbody> </table>	Concentration (µg/ml)	% Protection	100	~65	150	~70	200	~75												
Concentration (µg/ml)	% Protection																												
100	56.81																												
150	59.67																												
200	68.55																												
Concentration (µg/ml)	% Protection																												
100	~65																												
150	~70																												
200	~75																												
<p>Graph 7: Human Red Blood Cell Membrane Stabilization by Urine Treated Vatsanabha</p>	<p>Graph 8: HRBC Membrane Stabilization by Standard Aspirin.</p>																												
<table border="1"> <caption>Data for Graph 9</caption> <thead> <tr> <th>Concentration (µg/ml)</th> <th>Milk (% Protection)</th> <th>Urine (% Protection)</th> </tr> </thead> <tbody> <tr> <td>100</td> <td>~42</td> <td>~55</td> </tr> <tr> <td>150</td> <td>~50</td> <td>~58</td> </tr> <tr> <td>200</td> <td>~55</td> <td>~65</td> </tr> </tbody> </table>	Concentration (µg/ml)	Milk (% Protection)	Urine (% Protection)	100	~42	~55	150	~50	~58	200	~55	~65	<table border="1"> <caption>Data for Graph 10</caption> <thead> <tr> <th>Concentration (µg/ml)</th> <th>Milk (% Protection)</th> <th>Urine (% Protection)</th> <th>Aspirin (% Protection)</th> </tr> </thead> <tbody> <tr> <td>100</td> <td>~42</td> <td>~55</td> <td>~70</td> </tr> <tr> <td>150</td> <td>~50</td> <td>~58</td> <td>~75</td> </tr> <tr> <td>200</td> <td>~55</td> <td>~65</td> <td>~80</td> </tr> </tbody> </table>	Concentration (µg/ml)	Milk (% Protection)	Urine (% Protection)	Aspirin (% Protection)	100	~42	~55	~70	150	~50	~58	~75	200	~55	~65	~80
Concentration (µg/ml)	Milk (% Protection)	Urine (% Protection)																											
100	~42	~55																											
150	~50	~58																											
200	~55	~65																											
Concentration (µg/ml)	Milk (% Protection)	Urine (% Protection)	Aspirin (% Protection)																										
100	~42	~55	~70																										
150	~50	~58	~75																										
200	~55	~65	~80																										
<p>Graph 9: Comparison of Human Red Blood Cell Membrane Stabilization by Vatsanabha purified by Milk and Urine.</p>	<p>Graph 10: Comparison of Human Red Blood Cell Membrane Stabilization by Vatsanabha purified by Milk, Urine and standard drug Aspirin.</p>																												





Strongly (Properly) Set Colorable Graphs

Nisha Reena Nazareth*, Bhagalaxmi Navada and Lolita Priya Castelino

Department of Mathematics, Shri Madhwa Vadiraja Institute of Technology and Management, Bantakal Udipi-574115. Affiliated to Visvesvaraya Technological University, Belagavi, India.

Received: 05 Mar 2021

Revised: 10 Mar 2021

Accepted: 18 Mar 2021

*Address for Correspondence

Nisha Reena Nazareth

Department of Mathematics,

Shri Madhwa Vadiraja Institute of Technology and Management,

Bantakal Udupi-574115.

Affiliated to Visvesvaraya Technological University, Belagavi, India.

Email: nisha.maths@sode-edu.in



This is an Open Access Journal / article distributed under the terms of the **Creative Commons Attribution License** (CC BY-NC-ND 3.0) which permits unrestricted use, distribution, and reproduction in any medium, provided the original work is properly cited. All rights reserved.

ABSTRACT

In this article we discuss about the set coloring number of star graph and it is seen that it is strongly and properly set colorable. Also, its splitting and line graphs are not found to be strongly and properly set colorable. In addition to these, we have proved that fan and wheel graphs are not strongly (properly) set colorable.

Mathematics Subject Classification 2020: 05C15

Keywords: Set coloring, set coloring number, strongly (properly) set coloring graph, splitting graph, line graph.

INTRODUCTION

In certain mathematical fields that use graph theory, it has been found that allotting colors to the vertices and to the edges of a graph is very effective. For all the notations and terminology we follow Harary [2] and West [4] and all graphs considered in our study are simple. In the year 2009, Hegde [3] introduced set coloring of a graph, motivated by the work of Acharya [1] on labelling the vertices and edges of a graph.

Definition 1.1. [3] A graph G is set colorable if the process of assigning colors to the vertices by the elements of the power set of a non empty set X subject to the condition that colors on vertices and edges are distinct. A graph G is strongly set colorable if the sets on the edges and vertices of that graph G collectively form $2^X - \{\phi\}$ subsets of X .

Also, the graph is properly set colorable if $2^X - \{\phi\}$ subsets of X are received on edges. In [3], he has also given a prerequisite, for any graph G to be a strongly set colourable is $n + m + 1 = 2k$, where $n = |V|$, $m = |E|$ and $k = |X|$. Similarly, to be properly set colorable, $m + 1 = 2^k$ is a required prerequisite for any graph G .





Nisha Reena Nazareth et al.,

Set Coloring Number

Set coloring number of a graph G is symbolized by $\sigma(G)$, which is the minimum cardinality of a set X such that G has a set coloring.

Theorem 2.1. Every imaginable graph G can be set colourable.

Proof. Proof of this theorem follows from definition of set coloring in [3].

From the above theorem it is clear that any given graph G we can find a set coloring number $\sigma(G)$. In [3], Hegde has given the bound $\lceil \log_2(m+1) \rceil \leq \sigma(G) \leq n-1$ using this we have obtained the theorem as follows.

Theorem 2.2. For any $a \geq 1$, $\sigma(S_{2^a}) = a$.

Proof. Consider a star graph S_{2^a} with 2^a vertices and $2^a - 1$ edges. We clearly know that $\sigma(S_{2^a}) \geq a$.

On the assumption that the existence of a set coloring (f, f') of S_{2^a} with regards to a set X with a colors, both f and f' are one-one and the colors on the edges are dissimilar.

$$\text{Then we have } f'(v, v_1) \oplus f'(v, v_2) \oplus f'(v, v_3) \oplus \dots \oplus f'(v, v_{2^a}) = \phi$$

Consider the vertex at the center of S_{2^a} as v_1 and $v_2, v_3, v_4, \dots, v_{2^a}$ are the vertices adjacent to v_1 . Assign full set to v_1 and remaining sets to $v_2, v_3, v_4, \dots, v_{2^a}$. Let $X_1, X_2, X_3, \dots, X_{2^a}$ be the subsets of X . Assign v_1 with the set $X_1 = X$ and the vertices $v_2, v_3, v_4, \dots, v_{2^a}$ are assigned by $X_1, X_2, X_3, \dots, X_{2^a}$ such that sets on edges are non empty subsets of X .

Properly and Strongly Set Colorable Graphs

Theorem 3.1. A star graph S_n is strongly set colored if and only if $n = 2^{k-1}$, $k \geq 1$.

Proof. Consider a star S_n having n number of vertices and $n - 1$ number of edges. Let us assume that S_n is strongly set colorable with regards to a set X with $|X| = k$, where $k \geq 0$.

Then we have $p + q + 1 = 2^k \Rightarrow n = 2^{k-1}$. Conversely, assume that $n = 2^{k-1}$, $k \geq 0$.

Consider the vertex at the center of S_n as v_1 and $v_2, v_3, v_4, \dots, v_n$ are the vertices adjacent to v_1 . Assign full set to v_1 and remaining sets to $v_2, v_3, v_4, \dots, v_n$. Applying symmetric difference to the adjacent vertices, we obtain $2^X - \{\phi\}$ distinct subsets of X , which proves the theorem.

Theorem 3.2. A star graph S_n is properly set colorable definitely and only if $n = 2^k$, $k \geq 0$.

Proof. Let S_n be a star graph with n number of vertices and $n - 1$ number of edges.

Assume that S_n is properly set colorable with regards to a set X with $|X| = k$, where $k \geq 0$.

Then we have $q + 1 = 2^k \Rightarrow (n - 1) + 1 = 2^k \Rightarrow n = 2^k$. Conversely, assume that $n = 2^k$, $k \geq 0$.

Consider the vertex at the center of S_n as v_1 and $v_2, v_3, v_4, \dots, v_n$ are the vertices adjacent to v_1 . Assign full set to v_1 and remaining sets to $v_2, v_3, v_4, \dots, v_n$. Applying symmetric difference to the adjacent vertices, we obtain $2^X - \{\phi\}$ distinct subsets of X .

Thus, S_n is properly set colorable.

Theorem 3.3. The splitting graph $S'(S_{2^a})$ of a properly and strongly set colorable graph S_{2^a} is not properly and strongly set colorable.

Proof. Consider a star S_{2^a} with 2^a vertices and $2^a - 1$ edges for some $a = 1, 2, 3, \dots$. Its splitting graph is denoted by $S'(S_{2^a})$ has 2^{a+1} vertices and $3(2^a - 1)$ edges.

Case(i): Let $S'(S_{2^a})$ is properly set colorable. Then there exists, $k = 1, 2, 3, \dots$ such that $q + 1 = 2^k$. That is, $3(2^a - 1) + 1 = 3(2^a) - 2 = 2(3(2^{a-1}) - 1) \neq 2^k$, which is an inconsistency. Hence, $S'(S_{2^a})$ is not properly set colorable.





Nisha Reena Nazareth et al.,

Case(ii): Let $S'(S_{2^a})$ is strongly set colorable. Then there exists, $k = 1, 2, 3, \dots$ such that $p+q + 1 = 2^k$. That is, $2^{2^{a+1}} + 3(2^a - 1) + 1 = 2^{2^{a+1}} + 3(2^a) - 2 = 2(2^a + 3(2^{a-1}) - 1) \neq 2^k$, which is an inconsistency. Hence, $S'(S_{2^a})$ cannot be strongly set colorable. In addition to the Theorem 11 of Hegde [3], we have found that, the complete bipartite graph $K_{r,s}$ is strongly set colorable if $r = s = 2^n - 1$.

Theorem 3.4. The splitting graph $S'(K_{r,s})$ of a strongly set colorable complete bipartite graph $K_{r,s}$ is not strongly set colorable.

Proof. Let $K_{r,s}$ be any complete bipartite graph with rs vertices and $(r^2s+rs^2-2rs)/2$ edges. Assume that $K_{r,s}$ is strongly set colorable.

Then there exists, $k = 1, 2, 3, \dots$ such that $|V(K_{r,s})| + |E(K_{r,s})| + 1 = 2^k$. That is, $rs + [(r^2s+rs^2-2rs)/2] + 1 \neq 2^k$, which is an inconsistency. Hence, $K_{r,s}$ is not strongly set colorable.

Theorem 3.5. Let S_{2^a} is a strongly and properly set colorable graph. Then the line graph $L(S_{2^a})$ is not strongly and properly set colorable.

Proof. Consider a star S_{2^a} having 2^a vertices and 2^{a-1} edges for some $a = 1, 2, 3, \dots$.

Its line graph is denoted by $L(S_{2^a})$ has $2^a - 1$ vertices and $(2^a - 1)(2^a - 2)/2$ edges.

Case(i): Let $L(S_{2^a})$ is strongly set colorable. Then there exists, $k = 1, 2, 3, \dots$ such that $|V(L(S_{2^a}))| + |E(L(S_{2^a}))| + 1 = 2^k$. That is, $2^a - 1 + [(2^a - 1)(2^a - 2)/2] + 1 = (2^a - 1)2^{a-1} + 1 \neq 2^k$, which is an inconsistency. Hence, $L(S_{2^a})$ is not strongly set colorable.

Case(ii): Let $L(S_{2^a})$ is properly set colorable.

Then there exists, $k = 1, 2, 3, \dots$ such that $|E(L(S_{2^a}))| + 1 = 2^k$. That is, $(2^a - 1)(2^a - 2)/2 + 1 = (2^a - 1)(2^{a-1} - 1) + 1 \neq 2^k$, which is an inconsistency. Hence, $L(S_{2^a})$ is not properly set colorable.

Theorem 3.6. An uniform binary tree T_l having one edge with degree one added to the root vertex having 2^l vertices and $2^l - 1$ edges, for $l \geq 2$ is strongly set colorable if

$$l = k - 1$$

Proof. Let T_l be an uniform binary tree having one edge with degree one added to the root vertex having 2^l vertices and $2^l - 1$ edges. Let us assume that T_l is a graph that is strongly set colorable.

Then $|V(T_l)| + |E(T_l)| + 1 = 2^k$

$$2^l + 2^l - 1 + 1 = 2^k$$

$$2^{l+1} = 2^k$$

$$l = k - 1 \text{ for } l \geq 2.$$

Theorem 3.7. A fan graph $F(1, n)$ is acquired by joining each vertex of P_n with K_1 is not strongly and properly set colorable.

Proof. Consider a fan graph $F(1, n)$ having $n + 1$ vertices and $2n - 1$ edges.

Let us assume that $F(1, n)$ is strongly set colorable. Then there exists, $k = 1, 2, 3, \dots$ such that $|V(F(1, n))| + |E(F(1, n))| + 1 = 2^k$. That is, $n + 1 + 2n - 1 + 1 = 3n + 1 \neq 2^k$, which is an inconsistency. Hence, $F(1, n)$ is not strongly set colorable.

Theorem 3.8. A wheel graph W_n is acquired by joining each vertex of C_n with K_1 is not strongly and properly set colorable.

Proof. Consider a wheel graph W_n having n number of vertices and $2(n-1)$ number of edges.

Case(i): Let W_n is a strongly set colorable graph.

Then there exists, $k = 1, 2, 3, \dots$ such that $|V(W_n)| + |E(W_n)| + 1 = 2^k$. That is, $n + 2(n - 1) + 1 = 3n - 1 \neq 2^k$, which is an inconsistency. Hence, W_n is not strongly set colorable.

Case(ii): Let W_n is properly set colorable. Then there exists, $k = 1, 2, 3, \dots$ such that $q + 1 = 2^k$. That is, $2(n - 1) + 1 = 2n - 1 \neq 2^k$, which is an inconsistency. Hence, W_n is not properly set colorable.

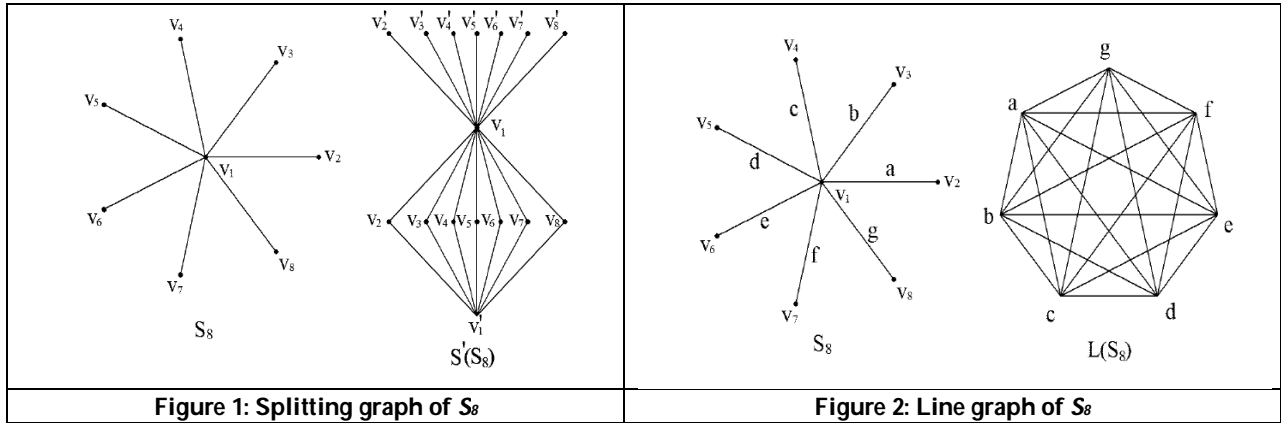




Nisha Reena Nazareth et al.,

REFERENCES

1. B. D. Acharya. Set-valuations and their applications. *MRI Lecture Notes in Applied Mathematics*, 2, 1983.
2. F. Harary. Graph theory. *Addison Wesley, Academic Press*, 1972.
3. S. M. Hegde. Set colorings of graphs. *European Journal of Combinatorics*, 30 pp. 986-995, 2009.
4. D. B. West. Introduction to graph theory. *Practice Hall of India, New Delhi*, 2003.





J-Continuous Functions in Topological Spaces

PL.Meenakshi* and K.Sivakamasundari

Assistant Professor, Department of Mathematics, Avinashilingam Institute for Home Science and Higher Education for Women, Coimbatore, Tamil Nadu, India.

Received: 03 Mar 2021

Revised: 08 Mar 2021

Accepted: 18 Mar 2021

*Address for Correspondence

PL. Meenakshi

Assistant Professor,

Department of Mathematics,

Avinashilingam Institute for Home Science and Higher Education for Women,

Coimbatore, Tamil Nadu, India.

Email: plmeenakshi22@gmail.com



This is an Open Access Journal / article distributed under the terms of the **Creative Commons Attribution License** (CC BY-NC-ND 3.0) which permits unrestricted use, distribution, and reproduction in any medium, provided the original work is properly cited. All rights reserved.

ABSTRACT

The notion of J-continuous functions is initiated here. Dependence and independence of J-continuous functions with many existing continuous functions are analysed. Moreover using some separation axioms, it is proved that composition of J-continuous functions is preserved and properties of J-continuous functions are obtained in this article.

Keywords: J-closed, J-continuous, JTC-space, continuous, g-continuous.

INTRODUCTION

The intention of regular open sets were introduced by Stone [32] and using the hypothesis semi-regularization of a topological space is formulated. In 1968, Velicko [35] propounded an idea in particular δ -open sets stronger than openness. Levine [15] has generated generalized closed sets in 1970. Dunham [8] has established Cl^* utilizing the view of g-closed sets. Regular*-openness using Cl^* has introduced by Pious Missier [29] in 2016. In 2019, the authors have introduced η^* -open sets [17] which lies between δ -Open sets and open sets. Its fundamental properties are studied and the persuasions of η^* -cluster points, η^* -adherent points and η^* -derived sets are initiated and studied in the same article. Moreover, the authors have instituted J-closed sets with the help of η^* -open sets [18] and observed their features. Functions are important tool for studying properties of spaces and for constructing new spaces from the existing spaces. An important theme in general topology concerns the differently altered types of continuity by using generalized closed sets. In 1970, Norman Levine [15] instituted the concept of continuous functions. δ -continuity initiated by Noiri [25]. Munshi [22] defined super continuous functions. Further numerous authors have devoted their research towards continuity. The concept of J-continuous functions is initiated here. Dependence and independence of J-continuous functions with many existing continuous functions are analysed. Moreover using some separation axioms, it is proved that composition of J-continuous functions is preserved and properties of J-





Meenakshi and Sivakamasundari

continuous functions are obtained in this article. For this article some essential definitions and results in topological spaces are required which are given in section 2. Throughout this article, a topological space is denoted by (Y, ζ) .

Preliminaries

Definition 2.1. Let (Y, ζ) be a topological space. If D is a non-empty subset of (Y, ζ) then the intersection of all closed sets having D is called **closure of D** and is denoted by $Cl(D)$. The union of all open sets contained in D is called **interior of D** and is denoted by $int(D)$.

Definition 2.2. A subset A of a topological space (Y, ζ) is called **generalized closed** (briefly **g -closed**) [15] if $Cl(D) \subseteq M$ whenever $D \subseteq M$ and M is open in (Y, ζ) .

Definition 2.3. [8] If $D \subseteq Y$, then

- (i) $Cl^*(D)$ is the intersection of all generalized closed sets in Y having D which is said to be **generalized closure** of D .
- (ii) $int^*(D)$ is the unification of all generalized open sets in Y contained in D which is said to be **generalized interior** of D .

Definition 2.4. A subset D of (Y, ζ) is called a

- 1) **regular closed set** [32] if $D = Cl(int(D))$
- 2) **semi-closed set** [14] if $int(Cl(D)) \subseteq D$
- 3) **α -closed set** [26] if $Cl(int(Cl(D))) \subseteq D$
- 4) **pre-closed set** [16] if $Cl(int(D)) \subseteq D$
- 5) **semi pre-closed set** [1] if $int(Cl(int(D))) \subseteq D$
- 6) **π -closed set** [36] if it is the finite intersection of regular closed sets.

The corresponding complements are their corresponding open sets. The corresponding closures are defined as the intersection of corresponding sets having D . A subset D of (Y, ζ) is called **clopen** if it is both open and closed in (Y, ζ) .

Definition 2.5. [35] A set D is called **δ -open** when D can be represented as the union of regular open sets. The δ -closure and δ -interior are defined as usual using δ -closedness and δ -openness.

Definition 2.6. A set D is called **regular*-open (or r^* -open)** [29] if $D = int(Cl^*(D))$. The corresponding complement, closure, interior are defined in the usual manner.

Definition 2.7. [17] A subset D is known as **η^* -open** [17] if it is a union of regular*-open sets (r^* -opensets). The corresponding complement of a η^* -open set is called a **η^* -closed set**. (i) $\eta^*-Cl^*(D)$ is the intersection of all η^* -closed sets in Y having D which is said to be **η^* -closure** of D . (ii) $\eta^*-int^*(D)$ is the unification of all η^* -open sets in Y contained in D which is said to be **η^* -interior** of D .

Definition 2.8. Let $D \subseteq Y$. A subset D in Y is known as **J-closed set** [18] if $Cl(D) \subseteq M$ whenever $D \subseteq M$, M is η^* -open in Y . We represent the collection of all J-closed sets of (Y, ζ) by $JC(Y, \zeta)$. The complement of J-closed is said to be J-open in (Y, ζ) .

Definition 2.9. [19] The **J-closure of D** (briefly **JCl(D)**) of a topological space (Y, ζ) is defined as follows. $JCl(D) = \cap \{F \subseteq Y : D \subseteq F \text{ and } F \in JC(Y, \zeta)\}$.

Definition 2.10. Let $D \subseteq Y$. A subset D in Y is known as

- 1) **gs -closed** [2] if $sCl(D) \subseteq M$ whenever $D \subseteq M$ and M is open in (Y, ζ) .
- 2) **gpr -closed** [10] if $pCl(D) \subseteq M$ whenever $D \subseteq M$ and M is regular open in (Y, ζ) .
- 3) **πg -closed** [9] if $Cl(D) \subseteq M$ whenever $D \subseteq M$ and M is π -open in (Y, ζ) .
- 4) **$g\delta$ -closed** [6] if $Cl(D) \subseteq M$ whenever $D \subseteq M$ and M is δ -open in (Y, ζ) .





Meenakshi and Sivakamasundari

- 5) π gs-closed [3] if $sCl(D) \subseteq M$ whenever $D \subseteq M$ and M is π -open in (Y, ζ) .
- 6) π gp-closed[28] if $pCl(D) \subseteq M$ whenever $D \subseteq M$ and M is π -open in (Y, ζ) .
- 7) rwg -closed [23] if $Cl(int(D)) \subseteq M$ whenever $D \subseteq M$ and M is regular open in (Y, ζ) .
- 8) $\pi g\alpha$ -closed [12] if $\alpha Cl(D) \subseteq M$ whenever $D \subseteq M$ and M is π -open in (Y, ζ) .
- 9) πgsp -closed [31] if $spCl(D) \subseteq M$ whenever $D \subseteq M$ and M is π -open in (Y, ζ) .
- 10) $gspr$ -closed [24] if $spCl(D) \subseteq M$ whenever $D \subseteq M$ and M is regular open in (Y, ζ) .
- 11) g^*s -closed [30] if $sCl(D) \subseteq M$ whenever $D \subseteq M$ and M is g s-open in (Y, ζ) .
- 12) δg^* -closed [33] if $\delta Cl(D) \subseteq M$ whenever $D \subseteq M$ and M is g -open in (Y, ζ) .
- 13) δg -closed [7] if $\delta Cl(D) \subseteq M$ whenever $D \subseteq M$ and M is open in (Y, ζ) .
- 14) **regular generalized closed** (briefly **rg-closed**) [27] if $Cl(D) \subseteq M$ whenever $D \subseteq M$ and M is regular open in (Y, ζ) .

The corresponding complements are their corresponding open sets.

Definition 2.11. A function $f : (Y, \zeta) \rightarrow (Z, \sigma)$ is said to be

1. **continuous** [15] if $f^{-1}(U)$ is a closed set in (Y, ζ) for every closed set U in (Z, σ) .
2. **Super continuous** [22] if $f^{-1}(U)$ is a δ -closed set of (Y, ζ) for every closed set U of (Z, σ) .
3. **g-continuous** [4] if $f^{-1}(U)$ is a g -closed set in (Y, ζ) for every closed set U in (Z, σ) .
4. **gs-continuous** [5] if $f^{-1}(U)$ is a gs -closed set in (Y, ζ) for every closed set U in (Z, σ) .
5. **π gs-continuous** [3] if $f^{-1}(U)$ is a π gs-closed set in (Y, ζ) for every closed set U in (Z, σ) .
6. **π gsp-continuous** [31] if $f^{-1}(U)$ is a π gsp-closed set in (Y, ζ) for every closed set U in (Z, σ) .
7. **gspr-continuous** [24] if $f^{-1}(U)$ is a $gspr$ -closed set in (Y, ζ) for every closed set U in (Z, σ) .
8. **g^*s -continuous** [30] if $f^{-1}(U)$ is a g^*s -closed set in (Y, ζ) for every closed set U in (Z, σ) .
9. **δg^* -continuous** [34] if $f^{-1}(U)$ is a δg^* -closed set in (Y, ζ) for every closed set U in (Z, σ) .
10. **Strongly continuous** [13] if the inverse image of every subset of (Z, σ) is clopen in (Y, ζ) .
11. **Totally continuous** [11] if the inverse image of every open set of (Z, σ) is clopen in (Y, ζ) .
12. **δ -continuous** [25] if $f^{-1}(U)$ is a δ -closed set of (Y, ζ) for every δ -closed set U of (Y, σ) .
13. **δg -continuous** [7] if $f^{-1}(U)$ is a δg -closed set in (Y, ζ) for every closed set U in (Y, σ) .
14. **$g\delta$ -continuous** [6] if $f^{-1}(U)$ is a $g\delta$ -closed set in (Y, ζ) for every closed set U in (Y, σ) .
15. **gpr-continuous** [10] if $f^{-1}(U)$ is a gpr -closed set in (Y, ζ) for every closed set V in (Z, σ) .
16. **π gp-continuous** [28] if $f^{-1}(U)$ is a π gp-closed set in (Y, ζ) for every closed set U in (Z, σ) .
17. **$\pi g\alpha$ -continuous** [9] if $f^{-1}(U)$ is a $\pi g\alpha$ -closed set in (Y, ζ) for every closed set U in (Z, σ) .
18. **πg -continuous** [9] if $f^{-1}(U)$ is a πg -closed set in (Y, ζ) for every closed set U in (Z, σ) .

Definition 2.12. [21] Let $D \subseteq Y$. A subset D of (Y, ζ) is known as

1. **JT δ -space** when each J -closed subset D is δ -closed.
2. **JTC-space** when each J -closed subset D is closed.
3. **JT δg^* -space** when each J -closed subset D is δg^* -closed.
4. **JT δg -space** when each J -closed subset D is δg -closed.
5. **JTg-space** when each J -closed subset D is g -closed.
6. **$g\delta$ TJ-space** when each $g\delta$ -closed subset D is J -closed.

Definition 2.13. (i) Let $D \subseteq Y$. A subset D of (Y, ζ) is known as (i) **T_δ -space** [6] if every $g\delta$ -closed subset of (Y, ζ) is δ -closed in (Y, ζ) . (ii) **Semi-regular space** [7] if every closed subset of (Y, ζ) is δ -closed in (Y, ζ) .

Remark 2.14.[19] For each $y \in Y$, $y \in Cl(D)$ if and only if $U \cap D \neq \emptyset$ for every J -open set U in (Y, ζ) containing y .

Note 2.15. In diagrams, $X \rightarrow Z$ represents X implies Z not satisfying the condition for reversible. $X \rightleftarrows Z$ represents X and Z are not equivalent.





Meenakshi and Sivakamasundari

Remark 2.16.[18] A (i) δ -closed set; (ii) δg^* -closed set; (iii) δg -closed set; (iv) g -closed set; (v) closed set ; is a J -closed set but not conversely.

Remark 2.17.[18] A J -closed is (i) $g\delta$ -closed; (ii) rg -closed;(iii) gpr -closed; (iv) rwg -closed; (v) $gspr$ -closed; (vi) πg -closed; (vii) πgp -closed; (viii) πgsp -closed;(ix) πgs -closed; (x) $\pi g\alpha$ -closed; but not conversely.

Remark 2.18.[20] Every clopen is J -open.

J-Continuous Functions

This section contains perception of J -continuous functions along with the analysis of this new concept with existing other g -continuous functions and their related features.

Definition 3.1. A function $v: (Y, \zeta) \rightarrow (Z, \sigma)$ is known as **J-continuous** if for every closed set E in (Z, σ) , $v^{-1}(E)$ is a J -closed set in (Y, ζ) .

Example 3.2. Consider $v: (Y, \zeta) \rightarrow (Z, \sigma)$ is many-one into function defined by $v(p) = s$, $v(t) = t$, $v(s) = s$. Consider $Y = Z = \{z, t, s\}$ with $\zeta = \{Y, \varphi, \{z\}\}$ and $\sigma = \{Z, \varphi, \{z\}, \{t\}, \{z, t\}\}$, $\sigma^c = \{Z, \varphi, \{s\}, \{t, s\}, \{z, s\}\}$. Then v is J -continuous as $JC(Y, \zeta) = P(Y) - \{z\}$.

Proposition 3.3. A continuous function $v: (Y, \zeta) \rightarrow (Z, \sigma)$ becomes a J -continuous function but the converse part is not true.

Proof Assume U is any closed set in (Z, σ) . By the hypothesis, v is continuous. Therefore $v^{-1}(U)$ is a closed set in (Y, ζ) . By Remark 2.16.(v), $v^{-1}(U)$ is a J -closed set in (Y, ζ) . Hence v is a J -continuous function.

Counter Example 3.4. Consider $v: (Y, \zeta) \rightarrow (Z, \sigma)$ is an identity function. Take $Y = Z = \{z, t, s\}$ with $\zeta = \{Y, \varphi, \{z, t\}\}$ and $\sigma = \{Z, \varphi, \{z\}, \{t\}, \{z, t\}\}$. Here $\sigma^c = \{Z, \varphi, \{s\}, \{t, s\}, \{z, s\}\}$ and $\zeta^c = \{Y, \varphi, \{s\}\}$. Then v is J -continuous as $JC(Y, \zeta) = P(Y)$ but not continuous. Because for the closed sets $\{t, s\}$ and $\{z, s\}$ in (Z, σ) , the inverse images are not closed in (Y, ζ) .

Proposition 3.5. A δg^* -continuous function $v: (Y, \zeta) \rightarrow (Z, \sigma)$ becomes a J -continuous function but the converse part is not true.

Proof Assume U is any closed set in (Z, σ) . By the given condition that v is δg^* -continuous, $v^{-1}(U)$ is δg^* -closed in (Y, ζ) . By Remark 2.16.(ii), $v^{-1}(U)$ represents J -closed in (Y, ζ) . Hence v is J -continuous.

Counter Example 3.6. Let $v: (Y, \zeta) \rightarrow (Z, \sigma)$ be the many-one into function defined by $v(z) = t$, $v(t) = t$, $v(s) = s$. Consider $Y = Z = \{z, t, s\}$ with $\zeta = \{Y, \varphi, \{z\}\}$ and $\sigma = \{Z, \varphi, \{z, t\}\}$. Here $\sigma^c = \{Z, \varphi, \{s\}\}$ and $\delta g^*C(Y, \zeta) = \{Y, \varphi, \{t, s\}\}$. Then v is J -continuous as $JC(Y, \zeta) = P(Y) - \{z\}$ but not a δg^* -continuous function. Because for the closed set $\{s\}$ in (Z, σ) , $v^{-1}(\{s\}) = \{s\}$ represents not a δg^* -closed set in (Y, ζ) .

Proposition 3.7. A δg -continuous function $v: (Y, \zeta) \rightarrow (Z, \sigma)$ becomes a J -continuous function but the converse part is not true.

Proof Consider U is any closed set in (Z, σ) . By the hypothesis, v is δg -continuous. This gives that $v^{-1}(U)$ is δg -closed in (Y, ζ) . By Remark 2.16.(iii), $v^{-1}(U)$ represents J -closed in (Y, ζ) . Hence v is J -continuous.

Counter Example 3.8. Let $v: (Y, \zeta) \rightarrow (Z, \sigma)$ be the bijective function defined by $v(z) = z$, $v(t) = s$, $v(s) = t$. Consider $Y = Z = \{z, t, s\}$ with $\zeta = \{Y, \varphi, \{z\}, \{z, t\}\}$ and $\sigma = \{Z, \varphi, \{z, t\}\}$. Here $\sigma^c = \{Z, \varphi, \{s\}\}$ and $\delta gC(Y, \zeta) = \{Y, \varphi, \{s\}, \{z, s\}, \{t, s\}\}$. Then v is J -continuous as $JC(Y, \zeta) = P(Y) - \{z\}$ but v isn't δg -continuous. Because for $\{s\}$ in (Z, σ) , $v^{-1}(\{s\}) = \{t\}$ is not a δg -closed in (Y, ζ) .

Proposition 3.9. A g -continuous function $v: (Y, \zeta) \rightarrow (Z, \sigma)$ becomes a J -continuous function but the converse is not true.





Meenakshi and Sivakamasundari

Proof Assume U is any closed set in (Z, σ) . By the given condition, v is g -continuous, $v^{-1}(U)$ is g -closed in (Y, ζ) . By **Remark 2.16.(iv)**, $v^{-1}(U)$ represents J -closed in (Y, ζ) . Hence v is J -continuous.

Counter Example 3.10. Let $v : (Y, \zeta) \rightarrow (Z, \sigma)$ be the many-one into function defined by $v(z) = t$, $v(t) = s$, $v(s) = t$. Consider $Y = Z = \{z, t, s\}$ with $\zeta = \{Y, \varphi, \{z\}, \{z, t\}\}$ and $\sigma = \{Z, \varphi, \{z, t\}\}$. Here $\sigma^c = \{Z, \varphi, \{s\}\}$ and $gC(Y, \zeta) = \{Y, \varphi, \{s\}, \{z, s\}, \{t, s\}\}$. Then v is J -continuous as $JC(Y, \zeta) = P(Y) - \{z\}$ but v isn't g -continuous. Because for the closed set $\{s\}$ in (Z, σ) , $v^{-1}(\{s\}) = \{t\}$ is not g -closed in (Y, ζ) .

Proposition 3.11. A \hat{g} -continuous function $v : (Y, \zeta) \rightarrow (Z, \sigma)$ becomes a J -continuous function but the converse is not true.

Proof Given $v : (Y, \zeta) \rightarrow (Z, \sigma)$ is a \hat{g} -continuous function. Consider U is any closed set in (Z, σ) . Since v is \hat{g} -continuous, $v^{-1}(U)$ is \hat{g} -closed in (Y, ζ) . By **Remark 2.16.(vi)**, $v^{-1}(U)$ is J -closed in (Y, ζ) . Hence v is J -continuous.

Counter Example 3.12. Let $v : (Y, \zeta) \rightarrow (Z, \sigma)$ be the many-one into function defined by $v(z) = t$, $v(t) = s$, $v(s) = t$. Consider $Y = Z = \{z, t, s\}$ with $\zeta = \{Y, \varphi, \{z\}, \{z, t\}\}$ and $\sigma = \{Z, \varphi, \{z, t\}\}$. Here $\sigma^c = \{Z, \varphi, \{s\}\}$ and $\hat{g}C(Y, \zeta) = \{Y, \varphi, \{s\}, \{t, s\}\}$. Then v is J -continuous as $JC(Y, \zeta) = P(Y) - \{z\}$ but v is not \hat{g} -continuous. Because for the closed set $\{s\}$ in (Z, σ) , $v^{-1}(\{s\}) = \{t\}$ is not a \hat{g} -closed set in (Y, ζ) .

Proposition 3.13. A J -continuous function $v : (Y, \zeta) \rightarrow (Z, \sigma)$ becomes a $g\delta$ -continuous function but the converse part is not true.

Proof Assume U represents any closed set in (Z, σ) . Since v is J -continuous, $v^{-1}(U)$ is J -closed in (Y, ζ) . By **Remark 2.17.(i)**, $v^{-1}(U)$ is $g\delta$ -closed in (Y, ζ) . Hence v is $g\delta$ -continuous.

Counter Example 3.14. Let $v : (Y, \zeta) \rightarrow (Z, \sigma)$ be the bijective function defined by $v(z) = s$, $v(t) = t$, $v(s) = z$. Consider $Y = Z = \{z, t, s\}$ with $\zeta = \{Y, \varphi, \{z\}, \{z, t\}\}$ and $\sigma = \{Z, \varphi, \{z, t\}\}$. Here $JC(Y, \zeta) = P(Y) - \{z\}$, $\sigma^c = \{Z, \varphi, \{s\}\}$. Then v is $g\delta$ -continuous as $g\delta C(Y, \zeta) = P(Y)$ but not J -continuous. Because for the closed set $\{s\}$ in (Z, σ) , $v^{-1}(\{s\}) = \{z\}$ isn't J -closed in (Y, ζ) .

Theorem 3.15. A J -continuous function $v : (Y, \zeta) \rightarrow (Z, \sigma)$ is a (i) rg -continuous function (ii) gpr -continuous function (iii) rwg -continuous function (iv) $gspr$ -continuous function (v) πg -continuous function (vi) πgp -continuous function (vii) πgs -continuous function (viii) πgsp -continuous function (ix) $\pi g\alpha$ -continuous function.

Proof Clear.

Remark 3.16. The other part of Theorem 3.15. is not true. This can be seen from the upcoming Counter Examples.

Counter Example 3.17. In the above **Counter Example 3.14**, $rgC(Y, \zeta) = gprC(Y, \zeta) = rwgC(Y, \zeta) = gsprC(Y, \zeta) = \pi gC(Y, \zeta) = \pi gpC(Y, \zeta) = \pi gsC(Y, \zeta) = \pi gspC(Y, \zeta) = \pi g\alpha C(Y, \zeta) = P(Y)$. Then v is rg -continuous, gpr -continuous, rwg -continuous, $gspr$ -continuous, πg -continuous and πgp -continuous, πgs -continuous, πgsp -continuous, $\pi g\alpha$ -continuous respectively but not J -continuous. Because for the closed set $\{s\}$ in (Z, σ) , $v^{-1}(\{s\}) = \{z\}$ is not J -closed in (Y, ζ) .

Theorem 3.18. A function $v : (Y, \zeta) \rightarrow (Z, \sigma)$ is J -continuous \Leftrightarrow if for every open set E in (Z, σ) , $v^{-1}(E)$ is a J -open set in (Y, ζ) .

Proof Necessity Let $v : (Y, \zeta) \rightarrow (Z, \sigma)$ be J -continuous and E be an open set in (Z, σ) . Then $Z - E$ is closed in (Z, σ) . Since v is J -continuous, $v^{-1}(Z - E) = Z - v^{-1}(E)$ is J -closed in (Y, ζ) and hence $v^{-1}(E)$ is J -open in (Y, ζ) .

Sufficiency Assume that $v^{-1}(F)$ is J -open in (Y, ζ) for each open set F in (Z, σ) . Let F be a closed set in (Z, σ) . Then $Z - F$ is open in (Z, σ) . By assumption, $v^{-1}(Z - F) = Z - v^{-1}(F)$ is J -open in (Y, ζ) which implies that $v^{-1}(F)$ is J -closed in (Y, ζ) . Hence v is J -continuous.





Meenakshi and Sivakamasundari

Remark 3.19. The upcoming Counter Examples explain that J-continuous function is not equivalent of gs-continuous, g^* s-continuous and δ -continuous.

Counter Example 3.20. Let $v : (Y, \zeta) \rightarrow (Z, \sigma)$ be the bijective function defined by $v(z) = s$, $v(t) = t$, $v(s) = z$. Consider $Y = Z = \{z, t, s\}$ with $\zeta = \{Y, \varphi, \{z, t\}\}$ and $\sigma = \{Z, \varphi, \{z\}\}$. Here $gsO(Y, \zeta) = g^*sO(Y, \zeta) = \{Y, \varphi, \{z\}, \{t\}, \{z, t\}\}$. Then v is J-continuous as $JO(Y, \zeta) = P(Y)$ but not gs-continuous and g^* s-continuous respectively. Because for the open set $\{z\}$ in (Z, σ) , $v^{-1}(\{z\}) = \{s\}$ is not gs-open and g^* s-open in (Y, ζ) .

Counter Example 3.21. Let $v : (Y, \zeta) \rightarrow (Z, \sigma)$ be the function defined by $v(z) = s$, $v(t) = t$, $v(s) = z$. Consider $Y = Z = \{z, t, s\}$ with $\zeta = \{Y, \varphi, \{z\}, \{t\}, \{z, t\}\}$ and $\sigma = \{Z, \varphi, \{z, t\}\}$. Here $gsO(Y, \zeta) = g^*sO(Y, \zeta) = \{Y, \varphi, \{z\}, \{t\}, \{z, t\}, \{z, s\}, \{t, s\}\}$. Then v is gs-continuous and g^* s-continuous respectively but not J-continuous as $JO(Y, \zeta) = \zeta$. Because for the open set $\{z, t\}$ in (Z, σ) , $v^{-1}(\{z, t\}) = \{t, s\}$ need not be J-open in (Y, ζ) .

Counter Example 3.22. Consider $v : (Y, \zeta) \rightarrow (Z, \sigma)$ is the function defined by $v(z) = t$, $v(t) = s$, $v(s) = z$. Consider $Y = \{z, t, s\}$, $Z = \{z, t, s, i\}$ with $\zeta = \{Y, \varphi, \{z\}, \{t\}, \{z, t\}\}$ and $\sigma = \{Z, \varphi, \{z\}\}$. Here $\sigma^c = \{Z, \varphi, \{t, s, i\}\}$ and $\delta C(Y, \zeta) = \{Y, \varphi, \{s\}, \{z, s\}, \{t, s\}\}$. Then v is not J-continuous as $JC(Y, \zeta) = \{Y, \varphi, \{s\}, \{z, s\}, \{t, s\}\}$ but it is δ -continuous because $\delta C(Z, \sigma) = \{Z, \varphi\}$ only.

Counter Example 3.23. Let $v : (Y, \zeta) \rightarrow (Z, \sigma)$ be an identity function. Consider $Y = Z = \{z, t, s\}$ with $\zeta = \{Y, \varphi, \{z\}\}$ and $\sigma = \{Z, \varphi, \{z\}, \{t\}, \{z, t\}\} = \delta C(Z, \sigma)$. Here $\sigma^c = \{Z, \varphi, \{s\}, \{t, s\}, \{z, r\}\}$ and $\delta C(Y, \zeta) = \{Y, \varphi\}$. Then v is J-continuous as $JC(Y, \zeta) = P(Y) - \{z\}$ but v isn't δ -continuous. Because for $\{t, s\}$, the δ -closed set in (Z, σ) , the inverse image is $\{t, s\}$ not a δ -closed set in (Y, ζ) .

Proposition 3.24. A super continuous function $v : (Y, \zeta) \rightarrow (Z, \sigma)$ becomes a J-continuous function but the converse need not be true.

Proof Given $v : (Y, \zeta) \rightarrow (Z, \sigma)$ represents a super continuous function. Assume U is any closed set in (Z, σ) . We get $v^{-1}(U)$ is δ -closed in (Y, ζ) (since v is a super continuous function). By **Remark 2.16.(i)**, $v^{-1}(U)$ is a J-closed set in (Y, ζ) . Hence v is J-continuous.

Remark 3.25. The other part of the above Proposition is disproved from the upcoming Counter Example.

Counter Example 3.26. Let $v : (Y, \zeta) \rightarrow (Z, \sigma)$ be the bijective function defined by $v(z) = t$, $v(t) = z$, $v(s) = r$. Consider $Y = Z = \{z, t, s\}$ with $\zeta = \{Y, \varphi, \{z, t\}\}$ and $\sigma = \{Z, \varphi, \{z\}\}$. Here $\sigma^c = \{Z, \varphi, \{t, s\}\}$ and $\delta C(Y, \zeta) = \{Y, \varphi\}$. Then v is J-continuous as $JC(Y, \zeta) = P(Y)$ but not super continuous. Because for the closed set $\{t, s\}$ in (Z, σ) , $v^{-1}(\{t, s\}) = \{z, s\}$ is not δ -closed in (Y, ζ) .

Remark 3.27. From the abovementioned Propositions, we have the accompanying pictorial diagram.

Proposition 3.28. A totally continuous function $v : (Y, \zeta) \rightarrow (Z, \sigma)$ is a J-continuous function but the converse is not true.

Proof Consider U is any open set in (Z, σ) . Since v is a totally continuous function, $v^{-1}(U)$ is clopen in (Y, ζ) . By **Remark 2.18.**, $v^{-1}(U)$ is J-open in (Y, ζ) . Hence v is J-continuous.

Proposition 3.29. A strongly continuous function $v : (Y, \zeta) \rightarrow (Z, \sigma)$ represents a J-continuous function but the converse part not true.

Proof Let U be any closed subset in (Z, σ) . Since v is a strongly continuous function, $v^{-1}(U)$ is clopen in (Y, ζ) . By **Remark 2.18.**, $v^{-1}(U)$ is J-open in (Y, ζ) . Hence v is J-continuous.

Remark 3.30. The reverse of the above Propositions can be seen to be untrue from the upcoming Counter Examples.





Meenakshi and Sivakamasundari

Counter Example 3.31. Let $v : (Y, \zeta) \rightarrow (Z, \sigma)$ be the identity function. Consider $Y = Z = \{z, t, s\}$ with $\zeta = \{Y, \varphi, \{z, t\}\}$ and $\sigma = \{Z, \varphi, \{z\}, \{t\}, \{z, t\}\}$. Here $\sigma^c = \{Z, \varphi, \{s\}, \{t, s\}, \{z, s\}\}$ and $\zeta^c = \{Y, \varphi, \{s\}\}$. Then v is J-continuous as $JC(Y, \zeta) = P(Y)$ but not strongly continuous and is not totally continuous. Because for the subset $\{z, s\}$ in (Z, σ) , the inverse image is not clopen in (Y, ζ) and for $\{z\}$ in (Z, σ) , no set is clopen in (Y, ζ) respectively.

Proposition 3.32. $v : (Y, \zeta) \rightarrow (Z, \sigma)$ is continuous when v is a J-continuous function and (Y, ζ) is a JTC-space.

Proof Let U be any closed set in (Z, σ) . Since v is J-continuous, $v^{-1}(U)$ is J-closed in (Y, ζ) and (Y, ζ) is a JTC-space. Therefore $v^{-1}(U)$ is closed in (Y, ζ) implies v is continuous.

Result 3.33.

- (a) v is super continuous when $v : (Y, \zeta) \rightarrow (Z, \sigma)$ represents a J-continuous function and (Y, ζ) is a JT δ -space.
- (b) f is δg^* -continuous when $v : (Y, \zeta) \rightarrow (Z, \sigma)$ represents a J-continuous function and (Y, ζ) is a JT δg^* -space.
- (c) v is δg -continuous when $v : (Y, \zeta) \rightarrow (Z, \sigma)$ represents a J-continuous function and (Y, ζ) is a JT δg -space.
- (d) v is g -continuous when $v : (Y, \zeta) \rightarrow (Z, \sigma)$ represents a J-continuous function and (Y, ζ) is a JT g -space.

Proof Similar to Proposition 3.32.

Proposition 3.34. If (Y, ζ) represents a $g\delta TJ$ -space and $v : (Y, \zeta) \rightarrow (Z, \sigma)$, a $g\delta$ -continuous function. Then v is J-continuous.

Proof Let U be a closed set in (Z, σ) . v is $g\delta$ -continuous, $v^{-1}(U)$ is $g\delta$ -closed in (Y, ζ) and (Y, ζ) is a $g\delta TJ$ -space. Hence $v^{-1}(U)$ is J-closed in (Y, ζ) which gives $v : (Y, \zeta) \rightarrow (Z, \sigma)$ is J-continuous.

Theorem 3.35. If $v : (Y, \zeta) \rightarrow (Z, \sigma)$ is a J-continuous function, then \forall subset D of (Y, ζ) , $v(JCl(D)) \subseteq Cl(v(D))$.

Proof Consider D is a subset of (Y, ζ) . Then $Cl(v(D))$ is a closed set in (Z, σ) . We get $v^{-1}(Cl(v(D)))$ is a J-closed set in (Y, ζ) (1) (since v is a J-continuous function). We know $v(D) \subseteq Cl(v(D))$, $D \subseteq v^{-1}(Cl(v(D)))$. From (1), $v^{-1}(Cl(v(D)))$ is a J-closed set containing D . By Definition 3.2.1., we have $JCl(D) \subseteq v^{-1}(Cl(v(D))) \Rightarrow v(JCl(D)) \subseteq Cl(v(D))$.

Corollary 3.36. (a) If $v : (Y, \zeta) \rightarrow (Z, \sigma)$ is a super continuous function, then \forall subset D of (Y, ζ) , $JCl(D) \subseteq Cl(v(D))$

(b) If $v : (Y, \zeta) \rightarrow (Z, \sigma)$ is a totally continuous function, then \forall subset D of (Y, ζ) , $v(JCl(D)) \subseteq Cl(v(D))$.

Proof (a) and (b) We know that a super continuous function $v : (Y, \zeta) \rightarrow (Z, \sigma)$ is a J-continuous function (by Proposition 3.24.) and a totally continuous function $v : (Y, \zeta) \rightarrow (Z, \sigma)$ is a J-continuous function (by Proposition 3.28.) and also it follows from the previous Theorem 3.35.

Proposition 3.37. Consider $v : (Y, \zeta) \rightarrow (Z, \sigma)$ is a function. If \forall point $x \in Y$ and \forall open set T in (Z, σ) containing $v(x)$, \exists a J-open set U in (Y, ζ) containing x such that $v(U) \subseteq T$, then \forall subset E of (Y, ζ) , $v(JCl(E)) \subseteq Cl(v(E))$.

Proof Consider E is any subset of (Y, ζ) and $y \in v(JCl(E))$. Therefore $y = v(x)$ for some $x \in JCl(E) \subseteq Y$. Let T be any open set in (Z, σ) such that $v(x) \in T$. Then by hypothesis, \exists a J-open set U in (Y, ζ) containing x with $v(U) \subseteq T$. By

Remark 2.14., $U \cap E \neq \varphi$, then $v(U \cap E) \neq \varphi$ which implies that $T \cap v(E) \neq \varphi$. Hence $y \in Cl(v(E))$. Thus $v(JCl(E)) \subseteq Cl(v(E))$.

COMPOSITION OF FUNCTIONS

Remark 3.38. The upcoming Counter Example explains that the composition of two J-continuous functions need not be J-continuous.

Counter Example 3.39. Let $v : (Y, \zeta) \rightarrow (Z, \sigma)$ be the bijective function defined by $v(z) = t, v(t) = s, v(s) = z$. Consider $Y = Z = P = \{z, t, s\}$ with $\zeta = \{Y, \varphi, \{z\}\}$ and $\sigma = \{Z, \varphi, \{s\}\}$, $\mu = \{P, \varphi, \{z, t\}\}$. Then f is J-continuous as $JC(Y, \zeta) = P(Y) - \{z\}$. Let $w : (Z, \sigma) \rightarrow (P, \mu)$ be the one-one onto function defined by $w(z) = z, w(t) = s, w(s) = t$. Then w is J-continuous as $JC(Z, \sigma) = P(Z) - \{s\}$. Consider the composition function $w \circ v : (Y, \zeta) \rightarrow (P, \mu)$ such that $(w \circ v)(z) = w(v(z)) = s, (w \circ v)(t) = w(v(t)) = t$





Meenakshi and Sivakamasundari

and $(w \circ v)(s) = w(v(s)) = z$. But their composition $w \circ v$ is not J-continuous. Because for the closed set $\{s\}$ in (P, μ) , $v^{-1}(w^{-1}(\{z\})) = \{s\}$ is not J-closed in (Y, ζ) .

Proposition 3.40. If $v : (Y, \zeta) \rightarrow (Z, \sigma)$, a J-continuous function and $w : (Z, \sigma) \rightarrow (P, \mu)$, a J-continuous function, then $w \circ v : (Y, \zeta) \rightarrow (P, \mu)$ is a J-continuous function when (Z, σ) is a JTC-space.

Proof Consider U is any closed set in (P, μ) . Hence $w^{-1}(U)$ is J-closed in (Z, σ) (since $w : (Z, \sigma) \rightarrow (P, \mu)$ is a J-continuous function). Consider (Z, σ) is a JTC-space. Therefore $w^{-1}(U)$ is closed in (Z, σ) . So $(w \circ v)^{-1}(U) = v^{-1}(w^{-1}(U))$ is J-closed in (Y, ζ) (since $v : (Y, \zeta) \rightarrow (Z, \sigma)$ represents a J-continuous function). Hence $w \circ v$ is J-continuous function.

Remark 3.41. The composition of J-continuous function becomes a J-continuous function when (Z, σ) is a T_δ -space can be seen by the accompanying Proposition.

Proposition 3.42. If $v : (Y, \zeta) \rightarrow (Z, \sigma)$, a J-continuous function and $w : (Z, \sigma) \rightarrow (P, \mu)$, a J-continuous function, then $w \circ v : (Y, \zeta) \rightarrow (P, \mu)$ is a J-continuous function when (Z, σ) is a T_δ -space.

Proof Consider U is any closed set in (P, μ) . Hence $w^{-1}(U)$ is J-closed in (Z, σ) (since $w : (Z, \sigma) \rightarrow (P, \mu)$ is a J-continuous function). By Remark 2.17.(i), $w^{-1}(U)$ is $g\delta$ -closed. Consider (Z, σ) is a T_δ -space. Therefore $w^{-1}(U)$ is δ -closed in (Z, σ) . Hence $w^{-1}(U)$ is closed in (Z, σ) . So $(w \circ v)^{-1}(U) = v^{-1}(w^{-1}(U))$ is J-closed in (Y, ζ) (since $v : (Y, \zeta) \rightarrow (Z, \sigma)$ is a J-continuous function). Hence $w \circ v$ is a J-continuous function.

Proposition 3.43. If $v : (Y, \zeta) \rightarrow (Z, \sigma)$, a J-continuous function and $w : (Z, \sigma) \rightarrow (P, \mu)$, a super continuous function, then $w \circ v : (Y, \zeta) \rightarrow (P, \mu)$ is a J-continuous function.

Proof Consider U is any closed set in (P, μ) . Hence $w^{-1}(U)$ is δ -closed in (Z, σ) (since $w : (Z, \sigma) \rightarrow (P, \mu)$ is a super continuous function). This implies $w^{-1}(U)$ is closed in (Z, σ) . So $(w \circ v)^{-1}(U) = v^{-1}(w^{-1}(U))$ is J-closed in (Y, ζ) (since $v : (Y, \zeta) \rightarrow (Z, \sigma)$ is a J-continuous function). Hence $w \circ v$ is a J-continuous function.

Proposition 3.44. If $v : (Y, \zeta) \rightarrow (Z, \sigma)$, a super continuous function and $w : (Z, \sigma) \rightarrow (P, \mu)$, a super continuous function, then $w \circ v : (Y, \zeta) \rightarrow (P, \mu)$ is a J-continuous function.

Proof Let U be any closed set in (P, μ) . Hence $w^{-1}(U)$ is δ -closed in (Z, σ) (since $w : (Z, \sigma) \rightarrow (P, \mu)$ is a super continuous function). This implies $w^{-1}(U)$ is closed in (Z, σ) . So $(w \circ v)^{-1}(U) = v^{-1}(w^{-1}(U))$ is δ -closed in (Y, ζ) (since $v : (Y, \zeta) \rightarrow (Z, \sigma)$ is a super continuous function). By Remark 2.16.(i), $v^{-1}(w^{-1}(U))$ is J-closed in (Y, ζ) . Hence $w \circ v$ is a J-continuous function.

Proposition 3.45. If $v : (Y, \zeta) \rightarrow (Z, \sigma)$, a J-continuous function and $w : (Z, \sigma) \rightarrow (P, \mu)$, a continuous function, then $w \circ v : (Y, \zeta) \rightarrow (P, \mu)$ is a J-continuous function.

Proof Consider U is any closed set in (P, μ) . Hence $w^{-1}(U)$ is closed in (Z, σ) (since $w : (Z, \sigma) \rightarrow (P, \mu)$ is a continuous function). Given $v : (Y, \zeta) \rightarrow (Z, \sigma)$ is a J-continuous function. So $(w \circ v)^{-1}(U) = v^{-1}(w^{-1}(U))$ is J-closed in (Y, ζ) . Hence $w \circ v$ is a J-continuous function.

REFERENCES

1. Andrijevic, D., Semi pre open sets, Math. Vesnik, 38 (1), pp.24-32, 1986.
2. Arya, S.P. and Nour, T.M., Characterization of s-normal space, Indian. J. Pure. Appl. Math., 21(8), pp.717-719, 1990.
3. Aslim, G., Caksu Guler, A. and Noiri, T., On πg_s -closed sets in topological spaces, Acta. Math. Hungar., 112 (4), pp.275-283, 2006.





Meenakshi and Sivakamasundari

4. Balachandran, K., Sundaram, P. and Maki, H. On generalized continuous maps in topological spaces, Mem.Fac.Sci.Kochi.Univ.Ser.A.Math., 12 ,pp. 5-13,1991.
5. Devi, R., Balachandran, K. and Maki, H. Semi-generalized homeomorphisms and generalized semi-homeomorphisms in topological spaces, Indian J. Pure Appl. Math., 26 , pp.271-284,1995.
6. Dontchev,J,Arokiarani,I and Balachandran,K., On generalized δ -closed sets and almost weakly Hausdorff spaces,Q&A in General Topology,18 , pp.17-30,2004.
7. Dontchev,J. and Ganster,M.,On δ -generalized closed sets and $T_{3/4}$ spaces, Mem. Fac. Sci. Kochi. Univ.math.,17,pp.15-31,1996.
8. Dunham.W., A New Closure Operator for Non- T_1 Topologies, Kyungpook Math.J.,22,pp. 55-60,1982.
9. Ekici, E. and Baker, C. W., On πg -closed sets and continuity, Kochi. J. of Mathematics,2 , pp.35-42,2007.
10. Gnanambal, Y. Studies on generalized pre-regular closed sets and generalizations of locally closed sets, Ph.D., Thesis, Bharathiar University, Coimbatore, TamilNadu,1998.
11. Jain, R.C., Role of regular open sets in general topology, Ph.D. Thesis, Meerut University, India,1980.
12. Janaki, C. Studies on $\pi g\alpha$ -closed sets in topology, Ph.D. Thesis, Bharathiar University, Coimbatore, India,2009.
13. Levine, N. Strong continuity in topological spaces, Amer. Math. Monthly, 67,pp. 269-275,1960.
14. Levine,N., Semi open sets and semi continuity in topological spaces, Amer. Math. Monthly, 70 ,pp.36-41,1963.
15. Levine,N., Generalized closed in set in topology, Rend. Circ. Math. Paleremo, vol.19 , pp.89-96,1970.
16. Mashour,A.S., On pre continuous and weak pre continuous functions, Pro.Math. Phys.Soc. Egypt, vol. 53 ,pp.47-53,1982.
17. Meenakshi,PL. and Sivakamasundari.K., Unification of regular star open sets,IJRAR,Special issue,pp.20-23,2019.
18. Meenakshi,PL.and Sivakamasundari.K.,J-closed sets in topological spaces,JETIR,Vol 6(5),pp.193-201,2019.
19. Meenakshi,PL.and Sivakamasundari.K., Analytical Exertions of J-closed sets,ADV MATH SCI JOURNAL ,Special Issue,no 3,pp.100-110,2019.
20. Meenakshi,PL. and Sivakamasundari, K. J-open Sets in topological spaces, Research Highlights,JADU,Vol.30,No.1,pp.41, 2020.
21. Meenakshi,PL.and Sivakamasundari.K., J-separation axioms in topological spaces, AIP Conference Proceedings 2261,pp.030075-1-030075-15.,2020.
22. Munshi, B. M. and Bassan, D. S. Super-Continuous Mappings, Indian J. Pure Appl. Math., 13(2) , pp.229-236,1982.
23. Nagaveni,N., Studies on generalizations of homeomorphisms in topological spaces,Ph.D Thesis ,Bharathiar University,Coimbatore,1999.
24. Navalagi, G., Chandrashekhara, A. S. and Gurushantanavar, S. V. On gspr-closed sets in topological spaces, International Journal of Mathematics and Computer Applications, 2(1-2), pp.51-58,2010.
25. Noiri, T., On δ -continuous functions, J .Korean Math. Soc.,16, pp.161-166,1980.
26. Njastad,O., On some classes of nearly open sets,Pacific J.Math.,15,pp.961-970,1965.
27. Palaniappan, N. and Rao, K.C., Regular generalised closed sets, Kyungpook Math. Journal,33, pp.211-219,1993.
28. Park,J. H. On πgp -closed sets in topological spaces, Indian J. Pure Appl. Math., 112(4),pp.257-283,2006.
29. Pious Missier,S, Annalakshmi,M., Between Regular Open Sets and Open Sets , IJMA- 7(5),pp.128-133,2016.
30. Pushpalatha, A. and Anitha, K. g's-closed sets in topological spaces, Int. J. Contemp. Math. Sciences, 6(19), pp.917-929,2011.
31. Sarsak, M.S. and Rajesh, N. π -generalized semi-pre-closed sets,International Mathematical Forum, 5(12) ,pp.573-578,2010.





Meenakshi and Sivakamasundari

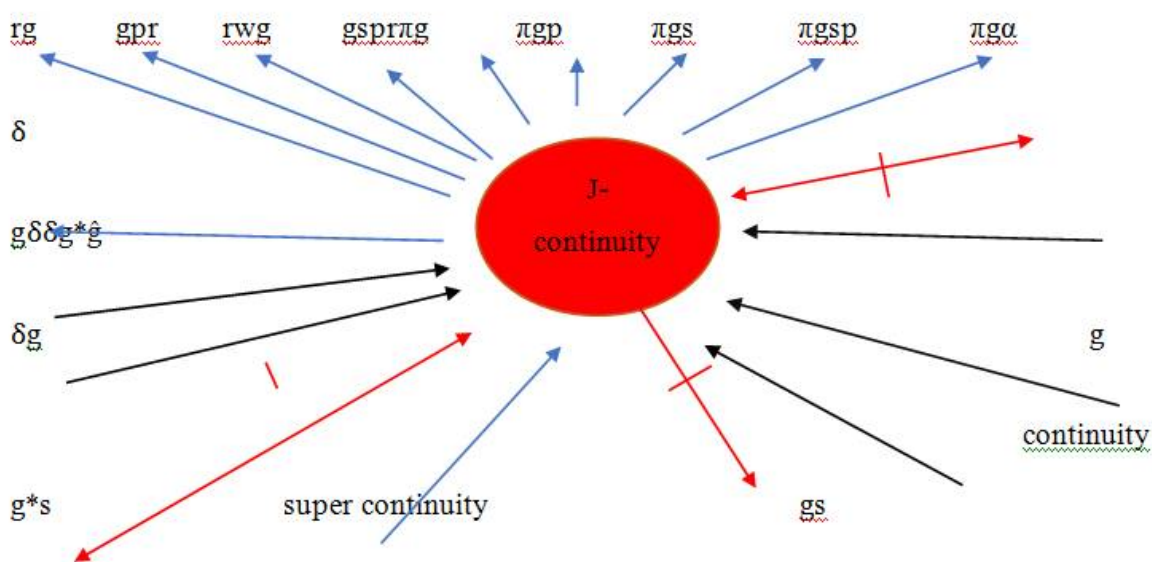
32. Stone, M., Application at the theory on Boolean rings to general topology, Transl. Amer. Math. Soc., 41 ,pp.374-481,1937.

33. Sudha, R. and Sivakamasundari, K. δg^* -closed sets in topological spaces, International Journal of Mathematical Archive, 3(3), pp.1222-1230,2012.

34. Sudha, R. and Sivakamasundari, K., δg^* -continuous functions in topological spaces, International Journal of Computer Applications, 74(18), pp.21-24,2013.

35. Velicko, N.V., H-closed sets. Topological spaces, Amer. Math. Soc. Transl., 78, pp.103-118,1968.

36. Zaitsav, V., On certain classes of topological spaces and their bicomactification, Dokl. Akad. Nauk. SSSR, 178, pp.778-779,1968.



Remark 3.27. From the abovementioned Propositions, we have the accompanying pictorial diagram.





Impact of Cross-Diffusion on Cu -water and Al_2O_3 -Water Nanofluid Flow over a Rotating Cone

Padmaja K and B. Rushi Kumar*

Department of Mathematics, School of Advanced Sciences, VIT, Vellore, Tamil Nadu, India.

Received: 03 Mar 2021

Revised: 08 Mar 2021

Accepted: 18 Mar 2021

*Address for Correspondence

B. Rushi Kumar

Department of Mathematics,
School of Advanced Sciences,
VIT, Vellore, Tamil Nadu, India.
Email: rushikumar@vit.ac.in



This is an Open Access Journal / article distributed under the terms of the **Creative Commons Attribution License** (CC BY-NC-ND 3.0) which permits unrestricted use, distribution, and reproduction in any medium, provided the original work is properly cited. All rights reserved.

ABSTRACT

In this paper, we investigate numerically the nanofluid flow about a vertical rotating cone with Dufour and Soret effects along with the impacts of thermal radiation, magnetic field, and chemical reaction. A steady, laminar, and incompressible nanofluid flow is considered. A uniform suction/injection of the fluid is present on the surface of the cone. The cone is symmetric about the axis of rotation and is rotating with an angular rotating velocity. The governing equations pertinent to the fluid flow are nonlinear partial differential equations (PDEs). Using similarity transformation variables, these partial differential equations are converted into ordinary differential equations (ODEs). MATLAB bvp4c solver is used to solve the converted system of ODEs. To achieve a clear understanding about the physical insights of the problem, the two nanofluids - Cu -water and Al_2O_3 -water are analysed. The graphical representations of tangential, normal, circumferential velocity profiles, temperature profiles and concentration profiles with respect to various fluid flow parameters are investigated.

Keywords: Nanofluids, Dufour and Soret effects, Rotating cone, Cu -water, Al_2O_3 -water

INTRODUCTION

In many industries like turbo machine manufacturing, polymer production, food processing, chemical, water treatment, and metallurgical industries the process of transfer of heat and mass play a vital role. Most of the heat transfer processes involve the usage of fluids such as water or ethylene glycol as coolants. To get better cooling without wastage of energy, the efficiency of the coolants have to be improved. Choi and Eastman [1] created colloidal suspensions of nanoparticles and base fluid called nanofluids. It is a very compatible fluid that can be used to reduce or induce the level of heat transfer in a bigger range of real life applications [2]. Heat and mass transfer in a rotating cone has been extensively studied by many researchers in the past. Much information about this subject can





Padmaja and Rushi Kumar

be studied in the papers by Tien *et al.* [3], Himasekhar *et al.* [4], Rehan Ali Shah *et al.* [5], Sambath *et al.* [6], Shahzad Ahmad *et al.* [7], Chamkha *et al.* [8]. C. N. Guled and B. B. Singh [9] investigated the transfer of heat and mass of a steady, electrically conducting, MHD fluid on a cone along with the magnetic field impacts, uniform suction/injection, as well as radiation effects. Dulal Pal *et al.* [10] studied the flow of the fluid over a plate. The plate considered is flat and in an inclined position. The effects of a heat source/sink which is non-uniform and impacts of thermophoresis is analysed. Rushi Kumar *et al.* [11] investigated the transfer of heat and mass in a moving cone as well as in a flat plate along with the impacts of chemical reaction and magnetic effects.

Yeping Peng *et al.* [12] analysed the impacts of the magnetic effects and the thermal radiation effects on rate of heat transfer on the nanofluid in two coaxial tubes. Zahir Shah *et al.* [13] investigated the Casson nanofluid flow which is considered as radiative and electrically conducting over a stretching sheet which is non linear. The impacts of radiation effects, heat flux, and chemical reaction effects are analysed numerically. Ramreddy *et al.* [14] investigated the nanofluid flow in a flat, vertical semi-infinite plate subject to the Soret effects. Sudarsana Reddy *et al.* [15] investigated the heat and mass transfer in two nanofluids Al_2O_3 water and TiO_2 water along with the effects of heat generation/absorption over a sheet which is stretchable embedded in a permeable medium. Reddy *et al.* [16] analysed the transfer of heat and mass in two nano fluids-Cu-water and Ag-water in two different volume fractions. Dzulkifli *et al.* [17] studied the flow of a nanofluid in the boundary layer and heat transfer analysis through a sheet which is stretchable along with the effects of thermophoresis and Brownian motion parameter. Saleem *et al.* [18] investigated the Nano Walter's B fluid flow over a rotating cone along with a magnetic regime. The impacts of Brownian motion effects and thermophoresis on the rates of heat transfer as well as mass transfer are presented. Raju *et al.* [19] made a comparative study on the influence of thermophoresis and Brownian motion effects along with magnetic field parameters in three different nanofluids- Maxwell, Jeffrey and Oldroyd-B nanofluids past a cone.

Sravanthi [20] analysed the impacts of velocity slip effects, thermal radiation effects on the transfer of heat of nanofluid flow over a vertical cone. The velocity slip is of second order and the thermal radiation is nonlinear and the effects of a non uniform heat source or sink are considered. Copper with water is taken to be the nanofluid under the analysis. Abbas *et al.* [21] investigated the rotating nanofluids- Cu-water, Al_2O_3 -water, TiO_2 -water in a moving rotating plate and the rates of heat transfers based on the shapes of the nanoparticles. Based on such an in-depth literature review, we analysed that the study of nanofluid with the inclusion of transfer of heat and mass along with magnetic, thermal radiation effects in a rotating cone has not been investigated yet. In this regard, we consider, a rotating cone with two nano fluids-Cu-water and Al_2O_3 -water. The thermodynamical properties of the nanoparticles- Cu and Al_2O_3 and base fluid- H_2O are considered to the heat transfer and magnetic effects. The influence and impacts of various parameters involved in the tangential, normal and circumferential velocities, temperature and concentration profiles are presented through graphs.

Mathematical Modelling

Consider an upward directed, rotating cone, rotating around the x-axis with a rotational velocity Ω along with magnetic field B_0 in the z-axis as shown in the flow diagram. A steady-state, laminar, incompressible nanofluid flow is considered. A uniform suction/ injection of the nanofluid of velocity w_0 is present at the surface of the cone. Within the sights of Soret and Dufour impacts, along with the consideration of mass concentration, the governing fluid flow equations of the boundary layer are analysed. By incorporating the above assumptions and Boussinesq's approximation into the basic governing equations, we get

$$\frac{\partial u}{\partial x} + \frac{\partial w}{\partial z} + \frac{u}{x} = 0 \quad (1)$$

$$\rho_{nf} \left(u \frac{\partial u}{\partial x} + w \frac{\partial u}{\partial z} + \frac{u^2}{x} \right) = \mu_{nf} \left(\frac{\partial^2 u}{\partial z^2} \right) - \sigma_{nf} B_0^2 u + (\rho\beta)_{nf} g (T - T_\infty) \cos\beta + (\rho\beta)_{nf} g (C - C_\infty) \cos\beta \quad (2)$$

$$\rho_{nf} \left(u \frac{\partial v}{\partial x} + w \frac{\partial v}{\partial z} + \frac{uv}{x} \right) = \mu_{nf} \left(\frac{\partial^2 v}{\partial z^2} \right) - \sigma_{nf} B_0^2 v \quad (3)$$





Padmaja and Rushi Kumar

$$u \frac{\partial T}{\partial x} + w \frac{\partial T}{\partial z} = \frac{\kappa_{nf}}{(\rho C_p)_{nf}} \frac{\partial^2 T}{\partial z^2} + \frac{D_m K_T}{C_s C_p} \frac{\partial^2 C}{\partial z^2} + \frac{Q_0(T-T_\infty)}{(\rho C_p)_{nf}} - \frac{1}{(\rho C_p)_{nf}} \frac{\partial q_r}{\partial z} \quad (4)$$

$$u \frac{\partial C}{\partial x} + w \frac{\partial C}{\partial z} = D_m \frac{\partial^2 C}{\partial z^2} + \frac{D_m K_T}{T_m} \frac{\partial^2 T}{\partial z^2} - k_r (C - C_\infty) \quad (5)$$

The resultant boundary conditions are

$$u = 0, v = x\Omega \sin\beta, w = w_0, T = T_w(x), C = C_w(x) \text{ at } z = 0$$

$$u \rightarrow 0, v \rightarrow 0, T \rightarrow T_\infty, C \rightarrow C_\infty \text{ at } z \rightarrow \infty \quad (6)$$

In the above equations, u, v, w are velocities in x, y and z directions respectively. T is fluid's local temperature and C is fluid's local concentration. ρ_{nf} is nanofluid's density, μ_{nf} is nanofluid's dynamic viscosity, κ_{nf} is nanofluid's conductivity, C_p is specific heat.

The radiation heat flux (Beg *et al.* [22]) is given by

$$\frac{\partial q_r}{\partial z} = -4a\sigma^*(T_\infty^4 - T^4) \quad (7)$$

$$T^4 \text{ can be expanded using Taylor's series about } T_\infty \text{ as } T^4 = 4T_\infty^3 - 3T_\infty^4 \quad (8)$$

The thermodynamical properties of the nano fluids are

$$\mu_{nf} = \frac{\mu_f}{(1 - \phi_{nf})^{2.5}}, \quad \nu_{nf} = \frac{\mu_{nf}}{\rho_{nf}}, \quad \rho_{nf} = (1 - \phi_{nf})\rho_f + \phi_{nf}\rho_s + \phi_{nf}\rho_s, \quad (\rho\beta)_{nf} = (1 - \phi_{nf})(\rho\beta)_f + \phi_{nf}(\rho\beta)_s,$$

$$(\rho C_p)_{nf} = (1 - \phi_{nf})(\rho C_p)_f + \phi_{nf}(\rho C_p)_s, \quad K_{nf} = \frac{(K_s + 2K_f) - 2\phi_{nf}(K_f - K_s)}{(K_s + K_f) + 2\phi_{nf}(K_f + K_s)} \quad (9)$$

Buckingham's π theorem is used to obtain the non-dimensional transformations (10). These transformations are employed to simplify the equations (1-5) along with the equation (6).

$$\eta = \left(\frac{\Omega \sin\beta}{v}\right)^{1/2} z, \quad u = -\frac{1}{2} x \Omega \sin\beta f'(\eta), \quad v = x \Omega \sin\beta h(\eta), \quad w = (v \Omega \sin\beta)^{1/2} f(\eta),$$

$$\theta = \frac{T - T_\infty}{T_w - T_\infty}, \quad \phi = \frac{C - C_\infty}{C_w - C_\infty}, \quad T_w - T_\infty = \frac{(T_L - T_\infty)x}{L}, \quad C_w - C_\infty = \frac{(C_L - C_\infty)x}{L}$$

$$M = \frac{\sigma_{nf} B_0^2}{\rho_f \Omega \sin\beta}, \quad \gamma = \frac{k_r}{\Omega \sin\beta}, \quad Gr = \frac{g \beta_f \cos\beta (T_w - T_\infty) L^3}{\nu^2}, \quad Re = \frac{\Omega L^2 \sin\beta}{\nu_f}, \quad Ri = \frac{Gr}{Re^2}, \quad Sr = \frac{D_m K_t C_w - C_\infty}{\nu T_m (T_w - T_\infty)}$$

$$Pr = \frac{(\mu C_p)_f}{K_f}, \quad Sc = \frac{\nu}{D_m}, \quad Du = \frac{D_m K_t C_w - C_\infty}{C_s C_p \nu (T_w - T_\infty)}, \quad \delta = \frac{Q_0}{(\rho C_p)_f \Omega \sin\beta}, \quad N = \frac{C_w - C_\infty}{T_w - T_\infty}, \quad Rd = \frac{16\nu a^* T_\infty^3}{K_f \Omega \sin\beta} \quad (10)$$

In the above quantities, L is cone's slant height, T_L denotes cone shallow's temperature and C_L is cone shallow's concentration;

By substituting (9) and (10) in equations (1-5),

$$f''' = \frac{1}{a_1} \left[\frac{Mf'}{a_2} - f'^2 - f''f + 2 \frac{a_3}{a_2} Ri(\theta + N\phi) \right] \quad (11)$$

$$h'' = \frac{1}{a_1} \left[h'f - f'h - \frac{Mh}{a_2} \right] \quad (12)$$

$$\theta'' = \frac{1}{a_4} \left[Rd\theta - \delta Pr\theta - Du Pr \phi'' + a_5 Pr f \theta' - \frac{1}{2} Pr a_5 f' \theta \right] \quad (13)$$

$$\phi'' = Sc f \phi' - \frac{1}{2} Sc f' \phi - Sr Sc \theta'' + \delta Sc \quad (14)$$

The associated boundary conditions are





Padmaja and Rushi Kumar

$$f = 0.1, f' = 0, h = 1, \theta = 1, \phi = 1 \text{ at } \eta = 0$$

$$f = 0, h = 0, \theta = 0, \phi = 0 \text{ at } \eta \rightarrow \infty \text{ (15)}$$

here primes refer derivatives about η

$$a_1 = \frac{1}{(1 - \phi_{nf})^{2.5}} \frac{1}{(1 - \phi_{nf}) + \phi_{nf} \left(\frac{\rho_s}{\rho_f} \right)}, \quad a_2 = (1 - \phi_{nf}) + \phi_{nf} \left(\frac{\rho_s}{\rho_f} \right),$$

$$a_3 = (1 - \phi_{nf}) + \phi_{nf} \left(\frac{(\rho\beta)_s}{(\rho\beta)_f} \right), \quad a_4 = \frac{(K_s + 2K_f) - 2\phi(K_f - K_s)}{(K_s + K_f) + 2\phi(K_f + K_f)}$$

$$a_5 = \left((1 - \phi_{nf})(\rho C_p)_f + \phi_{nf}(\rho C_p)_s \right), \quad a_6 = \frac{1}{a_4}$$

Method of Solution

Runge-Kutta method along with shooting technique is implemented to solve equations (10-14) with the related boundary condition (15). To solve this problem with bvp4c package in MATLAB, we provide functions that evaluate the differential equations subject to their residuals in the boundary. Consider

$$f = F(1); f' = F(2); f'' = F(3); h = F(4); h' = F(5); \theta = F(6); \theta' = F(7); \phi = F(8); \phi' = F(9);$$

The non-linear differential equations (9-13) are converted into the following first order differential equations

$$\begin{bmatrix} f' \\ f'' \\ f''' \\ h' \\ h'' \\ \theta' \\ \theta'' \\ \phi' \\ \phi'' \end{bmatrix} = \begin{bmatrix} F(2) \\ F(3) \\ \frac{1}{a_1} \left[\frac{MF(2)}{a_2} - F(2)^2 - F(3)F(1) + 2 \frac{a_3}{a_2} Ri(F(6) + NF(8)) \right] \\ F(5) \\ \frac{1}{a_1} \left[F(1)F(5) - F(2)F(4) + \frac{MF(2)}{a_2} \right] \\ F(7) \\ \frac{1}{SrScDuPr-a_4} \left[F(1)[ScDuPrF(9) - a_5PrF(7)] - \frac{F(2)}{2} [ScDuPrF(8) - Pra_5F(6)] - F(6)[Rd - \delta Pr] + \delta ScDuPrF(8) \right] \\ F(9) \\ \frac{1}{SrScDuPr-a_4} \left[F(1)[Sca_4F(9) + a_5PrSrScF(7)] - \frac{F(2)}{2} [Pra_5SrScF(6) - Sca_4F(8)] - \delta Sca_4F(8) + F(6)[RdSrSc - \delta PrSrSc] \right] \end{bmatrix}$$

This problem is solved numerically by considering it as an initial value problem and is solved using bvp4c package in MATLAB.

RESULTS AND DISCUSSIONS

The nanofluids are formed by considering the Copper nanoparticles and Alumina nanoparticles in the base fluid water with a volumetric fraction of 0.15. The thermodynamical properties of the nano particles and the base fluid are taken into account while solving the problem. The thermodynamical properties- C_p, ρ, K, β of Cu, Al_2O_3 and H_2O are given in table-1. We have done a numerical investigation of the considered problem and have presented the graphs for tangential, normal and circumferential velocities and temperature, concentration profiles using various numerical values for the fluid flow parameters. The graphs obtained are for various values of Dufour number (Du), Soret number (Sr), Magnetic parameter (M) and radiation and parameter (Rd) are presented here, in figures (2-13).

Figures (2-4) depict the tangential velocity, temperature and concentration profiles plotted against η for various values of Du . It can be observed that the velocity in tangential direction increases as Du increases. There is a rise in temperature with a rise in Du . This is because the increase in Du increases the rate at which the heat transfer takes place which in turn increases the temperature. As Du relates the concentration gradient and energy flux, an increase in Du , increments the concentration gradient which reduces the concentration. Alumina has higher specific heat than copper. As we know specific heat is the quantity of energy (heat) per unit mass that is required to increase the





Padmaja and Rushi Kumar

temperature by one-degree Celsius. The nanofluid alumina with water has higher temperatures in a lower Dufour number than copper with water because of its higher specific heat.

Figures (5-9) depicts the velocity, temperature and concentration profiles for various values of Sr . In Alumina-water it can be observed that for higher values of Sr there is an increase in the tangential velocity and circumferential velocity curves while a same trend is observed in copper-water. In Alumina-water in can observed that for higher values of Sr there is a decrease in the tangential velocity curves while a reverse trend is observed in Copper-water. There is an increase in temperature curves with an increase in Sr . A same trend is observed in copper water. With an increase in Sr there is a decrease in concentration. A same trend is observed in copper-water. Soret number is the ratio of temperature difference to concentration. As the Sr increases the temperature curves increases and concentration curves decreases.

Figures (10-11) show the tangential and circumferential velocity profile for various values of M . With an increase in M , the velocity profiles decreases. When the magnetic parameter increases, a Lorentz force sets in, which reduces the velocity. Both the nanofluids depict the same trend. Figure (12-13) depict tangential velocity, temperature profile for distinct values of Rd . With an increase in Rd there is an increase in velocity and temperature curves. As Rd increases, the intensity of heat generation increases which in turn breaks the bond between the molecules and rises the velocity. As Rd increases, there is an increase in surface heat flux which leads to an increase in the temperature curves.

CONCLUSION

A detailed investigation is done by analysing the impacts of the magnetic parameter, radiation parameter, and chemical reaction parameter along with Dufour and Soret effects in two nanofluids-Cu-water and Al_2O_3 -water over a vertical rotating cone. Based on this present investigation, the following conclusions are derived. The heat transfer rate of Cu-water is better compared than that of Al_2O_3 -water as copper has high thermal conductivity. The mass transfer capacity of Al_2O_3 -water is comparatively better because of the higher specific heat of alumina. The greater values of M lower the velocity profiles. The increase in Sr and Du increases the temperature profile and decreases the concentration profile. With an increase in the Rd , the velocity in tangential direction and temperature increases.

REFERENCES

1. S.U.S. Choi and Jeffrey Eastman. Enhancing thermal conductivity of fluids with nanoparticles. volume 66, 1995.
2. Kaufui V Wong and Omar De Leon. Applications of nanofluids: current and future. *Advances in mechanical engineering*, 2:519659, 2010.
3. CL Tien and IJ Tsuji. A theoretical analysis of laminar forced flow and heat transfer about a rotating cone. *Journal of Heat Transfer*, 1965.
4. K Himasekhar, PKj Sarma, and K Janardhan. Laminar mixed convection from a vertical rotating cone. *International communications in heat and mass transfer*, 16(1):99–106, 1989.
5. Rehan Ali Shah, Muhammad Shuaib, and Aamir Khan. Dufour and soret effect on heat and mass transfer with radiative heat flux in a viscous liquid over a rotating disk. *The European Physical Journal Plus*, 132(8):342, 2017.
6. P Sambath, DS Sankar, and KK Viswanathan. A numerical study of dissipative chemically reactive radiative mhd flow past a vertical cone with nonuniform mass flux. *International Journal of Applied Mechanics and Engineering*, 25(1):159–176, 2020.
7. Shahzad Ahmad, Kashif Ali, Rabia Saleem, and Hina Bashir. Thermal analysis of nanofluid flow due to rotating cone/plate—a numerical study. *AIP Advances*, 10(7):075024, 2020.




Padmaja and Rushi Kumar

8. Ali J Chamkha and SMM El-Kabeir. Unsteady heat and mass transfer by mhd mixed convection flow over an impulsively stretched vertical surface with chemical reaction and solet and dufour effects. *Chemical Engineering Communications*, 200(9):1220–1236, 2013.
9. CN Guled and BB Singh. Homotopy analysis of the radiation effect on mhd flow with heat and mass transfer due to a point sink. *Advances in Mathematical Physics*, 2016, 2016.
10. Dulal Pal and Hiranmoy Mondal. Influence of solet-dufour and thermophoresis on hydromagnetic mixed convection heat and mass transfer over an inclined flat plate with nonuniform heat source/sink and chemical reaction. *International Journal for Computational Methods in Engineering Science and Mechanics*, 19(2):49–60, 2018.
11. B Rushi Kumar and R Sivaraj. Heat and mass transfer in mhd viscoelastic fluid flow over a vertical cone and flat plate with variable viscosity. *International Journal of Heat and Mass Transfer*, 56(1-2):370–379, 2013.
12. Yeping Peng, Ali Sulaiman Alsagri, Masoud Afrand, and R Moradi. A numerical simulation for magnetohydrodynamic nanofluid flow and heat transfer in rotating horizontal annulus with thermal radiation. *RSC advances*, 9(39):22185–22197, 2019.
13. Zahir Shah, Poom Kumam, and Wejdan Deebani. Radiative mhd casson nanofluid flow with activation energy and chemical reaction over past nonlinearly stretching surface through entropy generation. *Scientific Reports*, 10(1):1–14, 2020.
14. Ch RamReddy, PVSN Murthy, Ali J Chamkha, and AM Rashad. Solet effect on mixed convection flow in a nanofluid under convective boundary condition. *International Journal of Heat and Mass Transfer*, 64:384–392, 2013.
15. P Sudarsana Reddy and Ali J Chamkha. Solet and dufour effects on mhd convective flow of al_2o_3 –water and tio_2 –water nanofluids past a stretching sheet in porous media with heat generation/absorption. *Advanced Powder Technology*, 27(4):1207–1218, 2016.
16. S Veera Reddy, GSS Raju, and AG Vijaya Kumar. A numerical investigation on mhd couple heat and mass transfer past a rotating vertical cone embedded in a porous medium. *International Journal of Engineering & Technology*, 7(4.10):956–962, 2018.
17. NF Dzulkifli, N Bachok, I Pop, NA Yacob, NM Arifin, and H Rosali. Solet and dufour effects on unsteady boundary layer flow and heat transfer of nanofluid over a stretching/shrinking sheet: A stability analysis. *Journal of Chemical Engineering & Process Technology*, 8(3):1000336, 2017.
18. S Saleem, Hina Firdous, S Nadeem, and AU Khan. Convective heat and mass transfer in magneto walter's b nanofluid flow induced by a rotating cone. *Arabian Journal for Science and Engineering*, 44(2):1515–1523, 2019.
19. CSK Raju, N Sandeep, and A Malvandi. Free convective heat and mass transfer of mhd nonnewtonian nanofluids over a cone in the presence of non-uniform heat source/sink. *Journal of Molecular Liquids*, 221:108–115, 2016.
20. CS Sravanthi. Second order velocity slip and thermal jump of cu –water nanofluid over a cone in the presence of nonlinear radiation and nonuniform heat source/sink using homotopy analysis method. *Heat Transfer—Asian Research*, 49(1):86–102, 2020.
21. W Abbas and MM Magdy. Heat and mass transfer analysis of nanofluid flow based on cu , al_2o_3 , and tio_2 over a moving rotating plate and impact of various nanoparticle shapes. *Mathematical Problems in Engineering*, 2020, 2020.
22. Anwar Beg and SK Ghosh. Analytical study of magnetohydrodynamic radiation convection with surface temperature oscillation and secondary flow effects. *Int. J. Applied Mathematics and Mechanics*, 6:1–22, 2010.

Nomenclature

a	Absorption parameter
B_o	Magnetic field strength
C_p	Specific heat at constant pressure
C_s	Concentration susceptibility
C	Local concentration of nanofluid
C_w	Concentration of nanofluid on the wall





Padmaja and Rushi Kumar

C_∞	Concentration of nanofluid in free stream
D_m	Molecular Diffusivity
Du	Dufour number
f_w	Dimensionless suction/injection parameter
g	Acceleration due to gravity
K_f	Base fluid's thermal conductivity
K_{nf}	Nanofluid's thermal conductivity
K_s	Nanoparticle's thermal conductivity
K_T	Ratio of thermal diffusivity
k_r	Chemical reaction parameter
M	Dimensionless magnetic field parameter
N	Buoyancy parameter
Pr	Prandtl number
Q_0	Heat generation parameter
q_r	Radiative heat flux
Ri	Richardson number
Rd	Dimensionless radiation parameter
Sr	Soret number
Sc	Schmidt number
T	Local temperature of nanofluid
T_w	Temperature of nanofluid on the wall
T_∞	Temperature of nanofluid in free stream
β_f	Base fluid's thermal expansion coefficient
β_{nf}	Nanofluid's thermal expansion coefficient
β_s	Nanoparticle's thermal expansion coefficient
δ	Dimensionless heat generation parameter
γ	Dimensionless chemical reaction parameter
ρ_f	Base fluid's density
ρ_s	Nanoparticle's density
ρ_{nf}	Nanofluid's density
$(\rho C_p)_{nf}$	Heat capacitance of nanofluid
μ_f	Base fluid's dynamic viscosity
μ_s	Nanoparticle's dynamic viscosity
μ_{nf}	Nanofluid's dynamic viscosity
ν_f	Base fluid's kinematic viscosity
ν_s	Nanoparticle's kinematic viscosity
ν_{nf}	Nanofluid's kinematic viscosity
σ_{nf}	Nanofluid's electrical conductivity
θ	Dimensionless temperature
ϕ	Dimensionless concentration
ϕ_{nf}	Volume fraction of nanofluid

Subscripts used	nf	Nanofluid
	s	Base fluid
		Nanoparticles
	∞	Condition in free stream
	w	Condition on the wall





Padmaja and Rushi Kumar

Table 1: Thermodynamical Properties

Thermodynamical properties	Water	Copper	Alumina
$C_p(J/(kgK))$	4179	385	765
$\rho(kg/m^3)$	997.1	8933	3970
$K(W/m K)$	0.613	400	40
$\beta * 10^{-5}(K^{-1})$	21	1.67	0.85

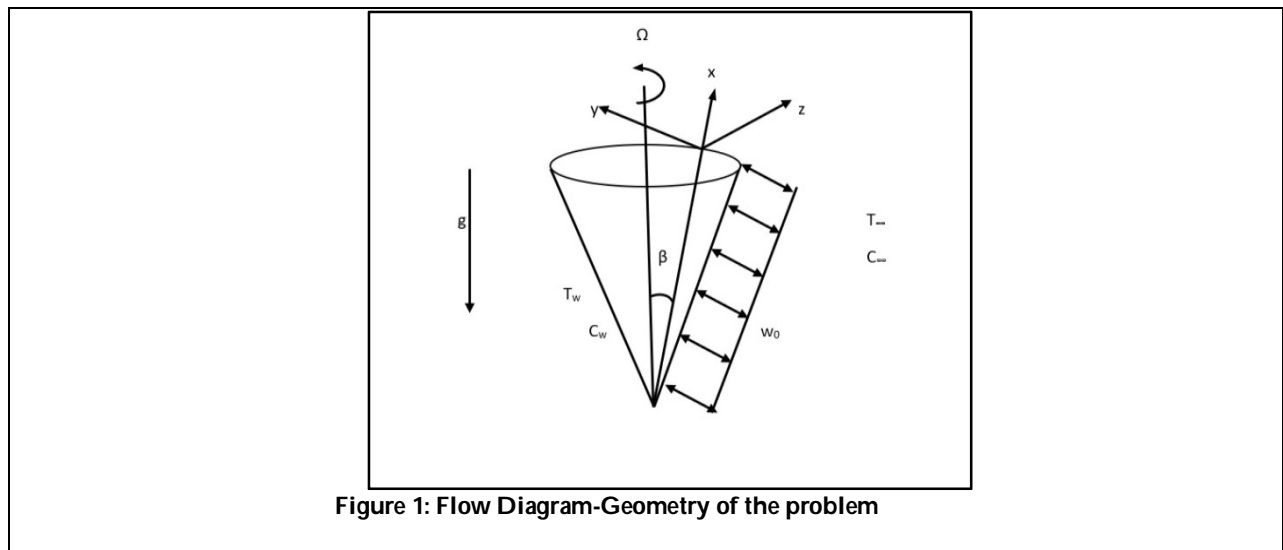


Figure 1: Flow Diagram-Geometry of the problem

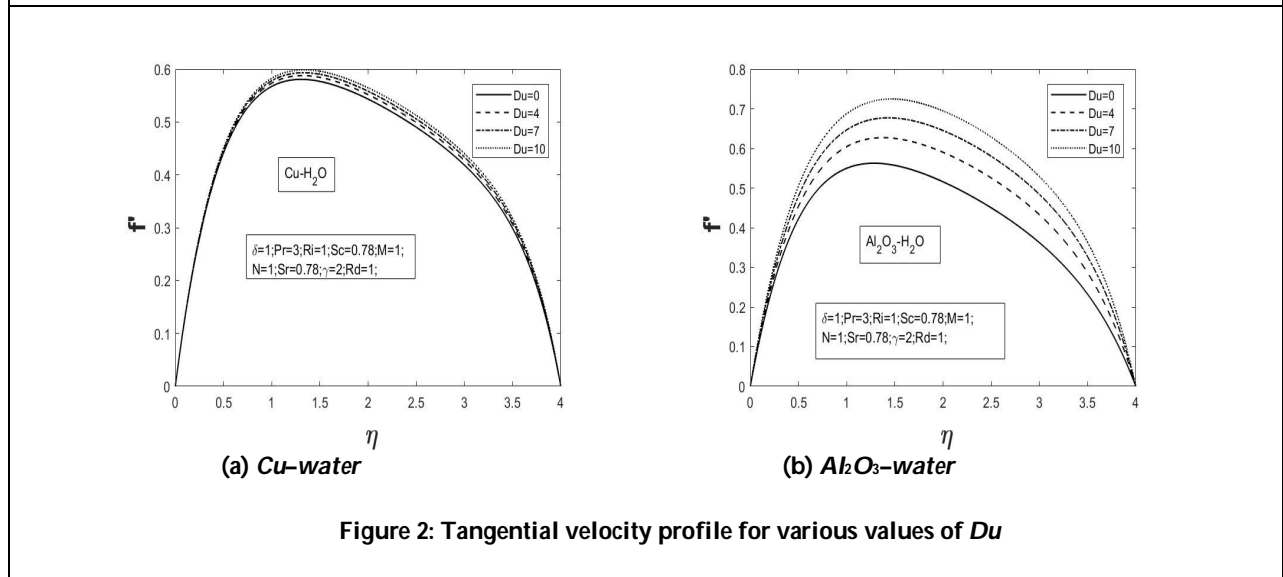


Figure 2: Tangential velocity profile for various values of Du





Padmaja and Rushi Kumar

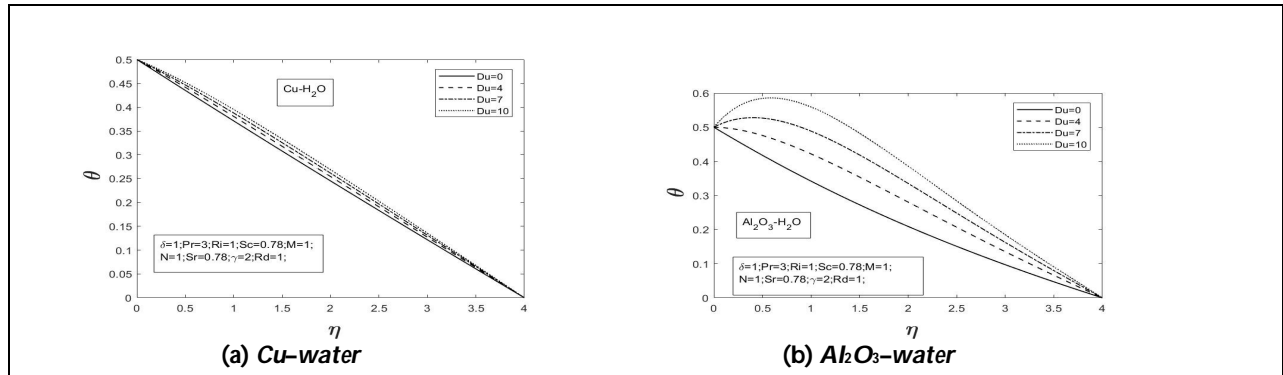


Figure 3: Temperature profile for various values of Du

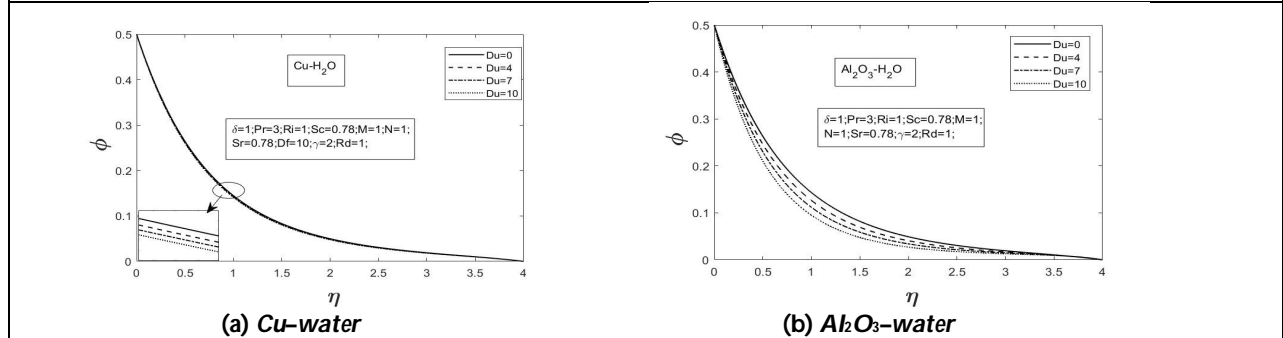


Figure 4: Concentration profile for various values of Du

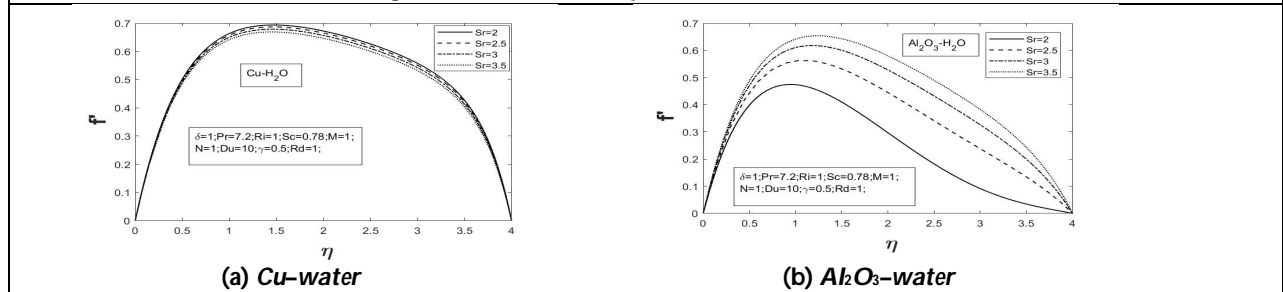


Figure 5: Tangential velocity profile for various values of Sr

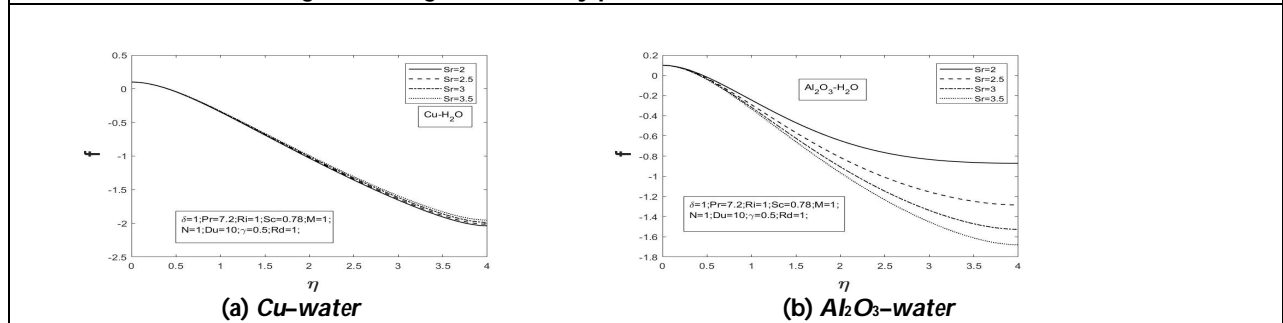
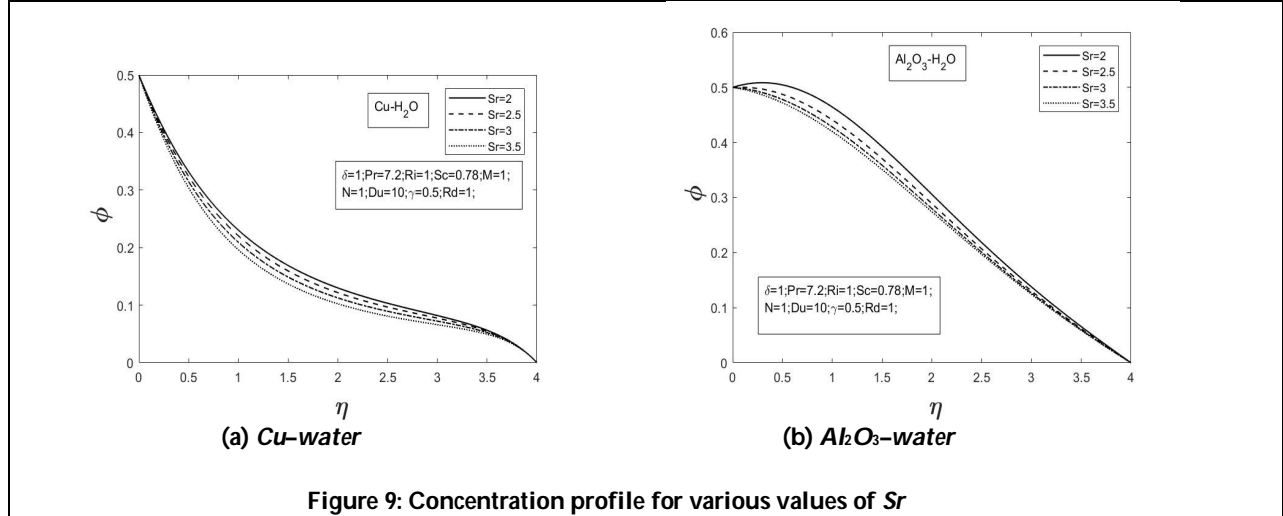
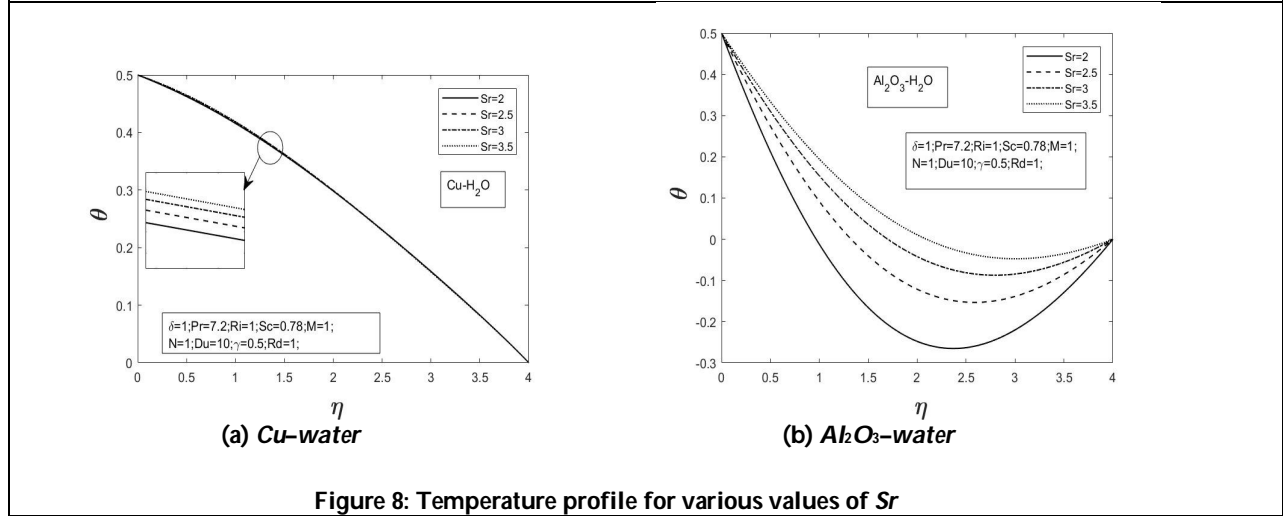
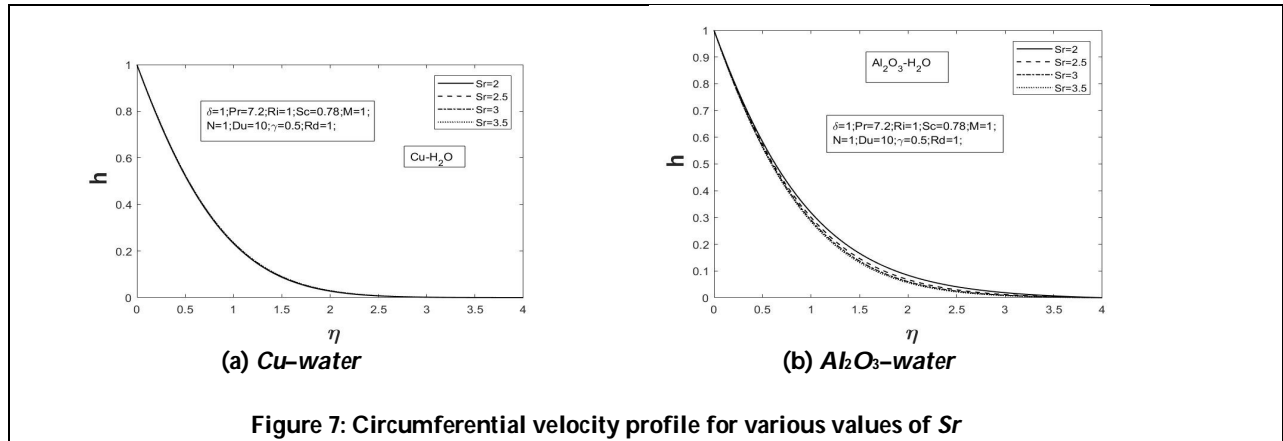


Figure 6: Normal velocity profile for various values of Sr



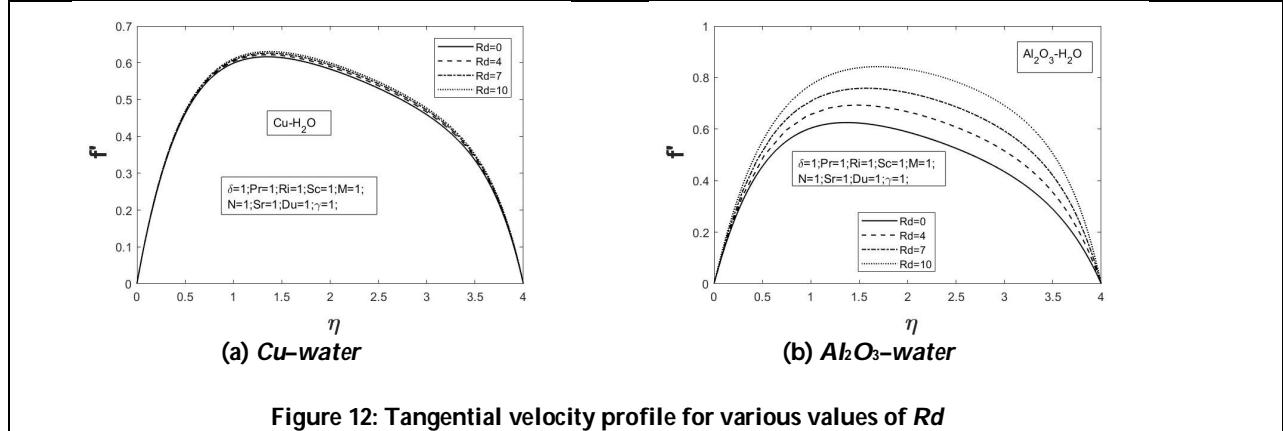
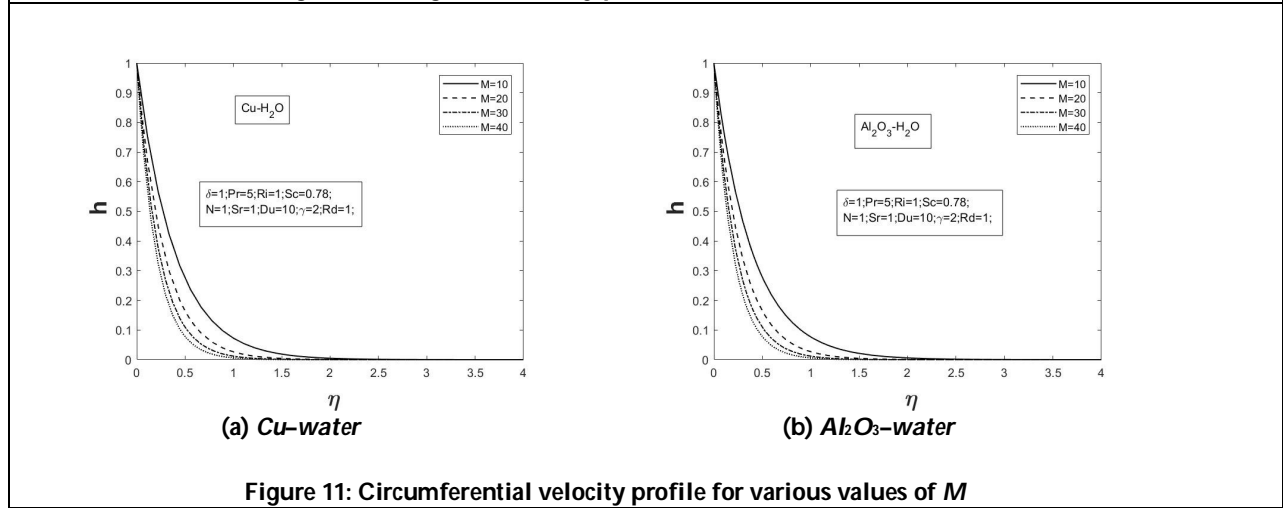
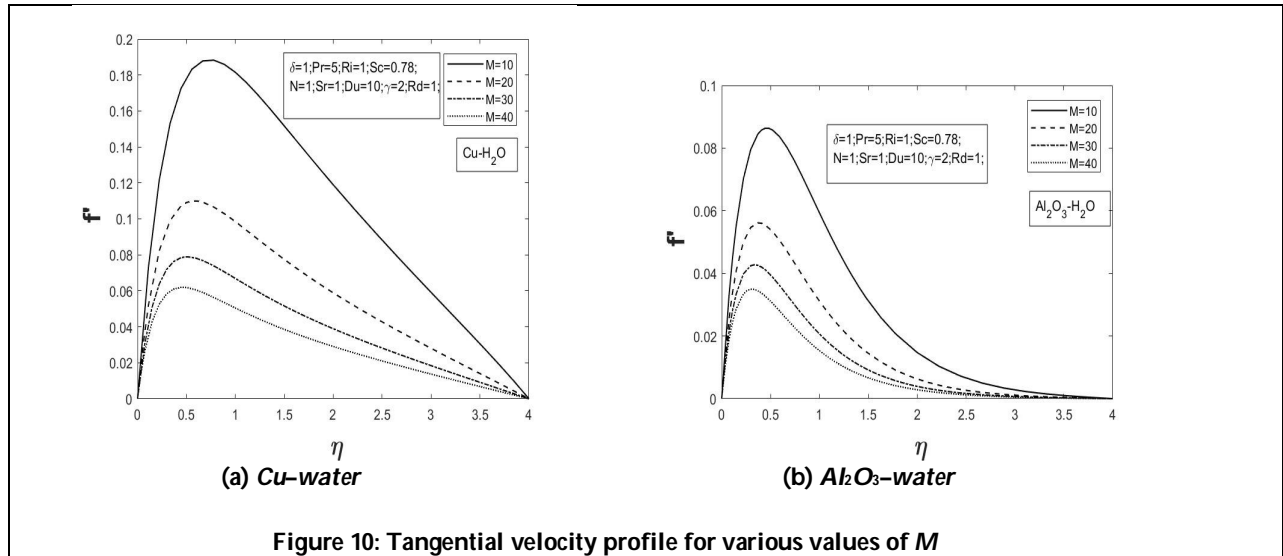


Padmaja and Rushi Kumar





Padmaja and Rushi Kumar





Padmaja and Rushi Kumar

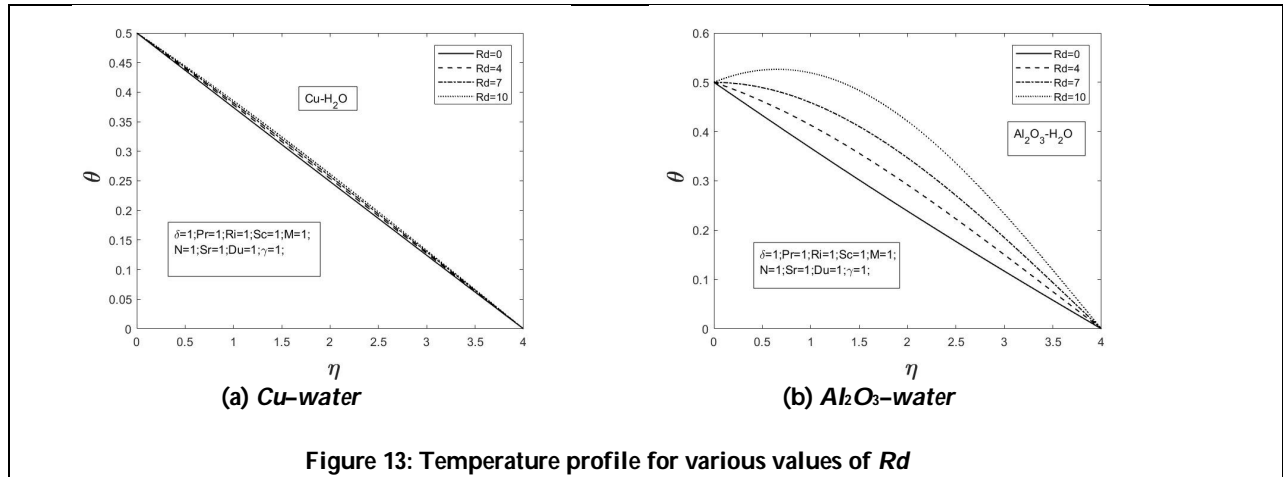


Figure 13: Temperature profile for various values of Rd





δP_s - Continuity and Decomposition of Perfect Continuity and Complete Continuity

Vidhyapriya P^{1*} Shanmugapriya H¹ and Sivakamasundari K²

¹Research Scholar, Department of Mathematics, Avinashilingam Institute for Home Science and Higher Education for Women, Coimbatore, Tamil Nadu, India.

²Professor, Department of Mathematics, Avinashilingam Institute for Home Science and Higher Education for Women, Coimbatore, Tamil Nadu, India.

Received: 24 Feb 2021

Revised: 04 Mar 2021

Accepted: 10 Mar 2021

*Address for Correspondence

Vidhyapriya P

Research Scholar,

Department of Mathematics,

Avinashilingam Institute for Home Science and Higher Education for Women,

Coimbatore, Tamil Nadu, India.

Email: pvidhyapriya19@gmail.com



This is an Open Access Journal / article distributed under the terms of the **Creative Commons Attribution License** (CC BY-NC-ND 3.0) which permits unrestricted use, distribution, and reproduction in any medium, provided the original work is properly cited. All rights reserved.

ABSTRACT

The purpose of this paper is to introduce a new concept of functions called δP_s - continuous functions. This class of functions is defined using new class of sets called δP_s - open sets in topological spaces and to obtain some important decomposition of perfect continuity and complete continuity.

Keywords: Continuous, P_s -Continuous, α -Continuous, Closed Sets

INTRODUCTION

In 1968 [33], the class of δ -open subsets of a topological space was first introduced by Velicko. This class of sets plays an important role in the study of various properties in topological spaces. Since then many authors used this class to define new classes of sets in topological spaces. In 1993, Raychaudhuri and Mukherjee [29] introduced and investigated a class of sets called δ -preopen.

Khalaf and Asaad [4] introduced a concept called P_s -open sets in topological spaces. This class of sets lies strictly between the classes of δ -open and preopen sets. Combining the concepts of δ -preopen and P_s -open sets, a new class of sets called δP_s -open sets [34] is introduced by the authors. This class of sets lies between the classes of P_s -open and δ -preopen sets. The behaviour of δP_s -open sets in various spaces such as locally indiscrete, hyperconnected, extremely disconnected, semi- T_1 , s -regular spaces are discussed and various interesting results are obtained. In this paper δP_s - continuous functions are defined and properties are studied. These are used to obtain new decompositions of perfect continuity and complete continuity in this article.





Preliminaries

Definition 2.1. A subset A of a space X is said to be

- (i) Preopen [21] if $A \subseteq \text{Int}(Cl(A))$
- (ii) Semi-open [20] if $A \subseteq Cl(\text{Int}(A))$
- (iii) Regular open [32] if $A = \text{Int}(Cl(A))$
- (iv) Clopen if A is both open and closed
- (v) δ -open[33] if for each $x \in A$, there exists an open set G such that $x \in G \subseteq \text{Int}ClG \subseteq A$
- (vi) θ -open [33] if for each $x \in A$ there exists an open set G such that $x \in G \subseteq ClG \subseteq A$
- (vii) δ -preopen [29] if $C \subseteq \text{Int}(\delta Cl(A))$
- (viii) θ -semi-open [16] if for each $x \in A$, there exists a semi-open set G such that $x \in G \subseteq ClG \subseteq A$
- (ix) semi- θ -open [7] if for each $x \in A$, there exists a semi-open set G such that $x \in G \subseteq sClG \subseteq A$
- (x) β -open [1] if $A \subseteq Cl(\text{Int}(Cl(A)))$
- (xi) e^* -open [11] if $A \subseteq Cl(\text{Int}(\delta - Cl(A)))$
- (xii) δ -semi-open [28] if $A \subseteq Cl(\delta - \text{Int}(A))$
- (xiii) α -open [22] if $A \subseteq \text{Int}(Cl(\text{Int}(A)))$
- (xiv) δ -semi- θ -open [36] if for each $x \in A$, there exists a δ -semiopen such that $x \in U \subseteq \delta - scl(U) \subseteq A$
- (xv) δ -semiregular [36] if $A = \delta - scl(\delta - sCl(A))$

- The closure and interior of A with respect to X are denoted by $Cl(A)$ and $\text{Int}(A)$ respectively.
- The intersection of particular class of closed sets of X containing A is called the corresponding closure of A.
- The union of particular class of open sets of X contained in A is called the corresponding interior of A.
- The family of all preopen (resp. Semi-open, regular open, δ -open, θ -open, δ -preopen, θ -semiopen, β -open, regular semi-open, e^* -open, δ -semiopen, α -open, δ -semi- θ -open, δ -semiregular open) subsets of X is denoted by $PO(X)$ (resp. $SO(X)$, $RO(X)$, $\delta O(X)$, $\theta O(X)$, $\delta PO(X)$, $\theta SO(X)$, $S\theta O(X)$, $\beta O(X)$, $RSO(X)$, $e^*O(X)$, $\delta SO(X)$, $\alpha O(X)$, $\delta S\theta O(X)$, $\delta SRO(X)$).
- The complement of a preopen (resp. resp. Semi-open, regular open, δ -open, θ -open, δ -preopen, θ -semiopen, semi- θ -open, β -open, regular semiopen, e^* -open, δ -semiopen, α -open, δ -semi- θ -open, δ -semiregular open) is said to be preclosed [10] (resp. resp. Semi-closed, regular closed, δ -closed, θ -closed, δ -preclosed, θ -semiclosed, semi- θ -closed, β -closed, regular semiclosed, e^* -closed, δ -semiclosed, α -closed, δ -semi- θ -closed, δ -semiregular closed).
- The family of all preclosed [10] (resp. resp. Semi-closed, regular closed, δ -closed, θ -closed, δ -preclosed, θ -semiclosed, semi- θ -closed, β -closed, regular semiclosed, e^* -closed, δ -semiclosed, α -closed, δ -semi- θ -closed, δ -semiregular closed) subsets of X is denoted by $PC(X)$ (resp. $SC(X)$, $RC(X)$, $\delta C(X)$, $\theta C(X)$, $\delta PC(X)$, $\theta SC(X)$, $S\theta C(X)$, $\beta C(X)$, $RSO(X)$, $e^*C(X)$, $\delta SC(X)$, $\alpha C(X)$, $\delta S\theta C(X)$, $\delta SRC(X)$).
- A subset A of a space X is called clopen, if A is both open and closed, while it is called regular open, $\text{Int}(Cl(A)) = A$.

Definition 2.2 [25]. A subset A of a space X is said to be preregular if A is both preopen and preclosed.

Definition 2.3 [3]. A space X is s-regular if for each $x \in X$ and each open set G containing x, there exists a semi-open set H such that $x \in H \subseteq sClH \subseteq G$.

Definition 2.4 [20]. A space X is called semi- T_1 if for each pair of distinct points x, y in X, there exists a pair of semi-open sets, one containing x but not y and the other containing y but not x.

Proposition 2.5 [20]. A space X is semi- T_1 if for any point $x \in X$, the singleton set {x} is semi-closed.

Definition 2.6 [7]. A space (X, τ) is said to be extremely disconnected if $ClU \in \tau$ for every $U \in \tau$.

Theorem 2.7 [35]. A space X is extremely disconnected if and only if $\delta O(X) = \theta SO(X)$.

Definition 2.8 [10]. A space X is said to be hyperconnected if every nonempty open subset of X is dense.

Definition 2.9 [10]. A space X is called locally indiscrete if every open subset of X is closed.

Lemma 2.10. If X is locally indiscrete space, then

- (i) Each semi-open subset of X is closed and
- (ii) Each semi-closed subset of X is open.





Vidhyapriya et al.,

Proposition 2.11 [3]. Let (Y, τ_Y) be a subspace of a space (X, τ) . Then, the following statements are true:

- (i) If $A \in PO(X, \tau)$ and $A \subseteq Y$, then $A \in PO(Y, \tau_Y)$.
- (ii) If $F \in SC(X, \tau)$ and $F \subseteq Y$, then $F \in SC(Y, \tau_Y)$.
- (iii) If $F \in SC(Y, \tau_Y)$ and $Y \in SC(X, \tau)$, then $F \in SC(X, \tau)$.

Proposition 2.12 [29]. Let A, Y be subsets of topological space (X, τ) such that $A \subseteq Y \in \delta O(X)$. If $A \in \delta PO(Y)$, then $A \in \delta PO(X)$

Proposition 2.13 [29]. In a topological space (X, τ) , if $A \in \delta PO(X)$, $B \in \delta O(X)$ then $A \cap B \in \delta PO(X)$

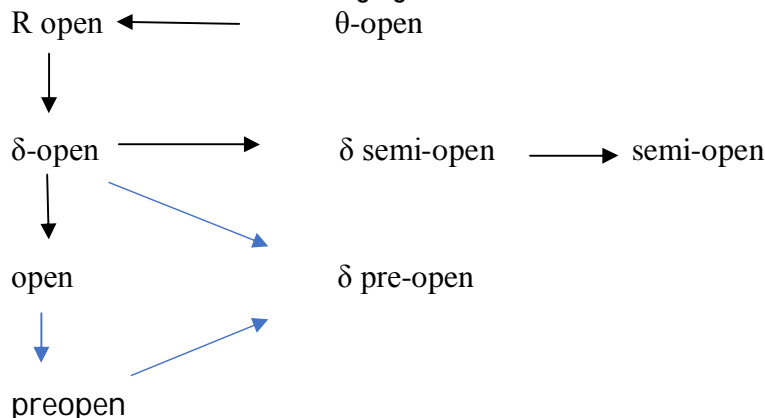
Theorem 2.14. Let A be a subset of a topological space (X, τ) . Then, we have:

- (i) If $A \in SO(X)$, then $pCIA = CIA$ [10].
- (ii) If $A \in \beta O(X)$, then $Cl_b A = CIA$ [20].
- (iii) If $A \in \beta O(X)$, then $\alpha ClX = ClX$ [3].

Definition 2.15[4]. A subset A of a space X is called P_s -open if for each $x \in A \in PO(X)$, there exists a semi-closed set F such that $x \in F \subseteq Z$. The family of all P_s -open sets of a topological space (X, τ) is denoted by $P_sO(X, \tau)$ or $P_sO(X)$.

Lemma 2.16[6]. Let A be a subset of a topological space (X, τ) . Then if A is preopen in (X, τ) , then it is δ -preopen in (X, τ) .

Remark 2.17. From the following figure we have



Lemma 2.18[32]. Union of δ -preopen sets is δ -preopen.

Definition 2.19. A function $f: X \rightarrow Y$ is said to be precontinuous [21] (resp. α -continuous [30], θ_s -continuous [17], perfectly continuous [27], complete continuous [5] and super continuous [23]) if the inverse image of each open subset of Y is preopen (resp. α -open, θ -semi-open, clopen, regular open and δ -open) in X .

Definition 2.20. A function $f: X \rightarrow Y$ is said to be almost precontinuous [24] (resp. almost continuous in the sense of Singal and Singal [31] and almost θ_s -continuous [18]) if the inverse image of each regular open subset of Y is preopen (resp. open and θ -semi-open) in X .

Definition 2.21. A function $f: X \rightarrow Y$ is called contra-continuous [8] (resp. contra-semi-continuous [9]) if the inverse image of every open subset of Y is closed (resp. semiclosed) in X .

Definition 2.22. A function $f: X \rightarrow Y$ is said to be δ -continuous [26] (resp. θ -continuous [13]) if for each $x \in X$ and each open set V of Y containing $f(x)$, there exists an open set U of X containing x such that $f(IntClU) \subseteq IntC(V)$ (resp. $f(IntCl(U)) \subseteq Int(Cl(V))$ and $f(Cl(U)) \subseteq Cl(V)$).

Definition 2.23. A function $f: (X, \tau) \rightarrow (Y, \sigma)$ is said to be

1. δ -precontinuous if for each $x \in X$ and each δ -preopen set V containing $f(x)$, there is a δ -preopen set U in X containing x such that $f(U) \subseteq V$
2. δ^* -almost-continuous [9] if $f^{-1}(V) \in \delta PO(X, \tau)$ for each $V \in \delta PO(Y, \tau)$

Definition 2.24[4]. A function $f: X \rightarrow Y$ is called P_s -continuous at a point $x \in X$ if for each $x \in X$ and each open set V of Y containing $f(x)$, there exists a P_s -open set U of X containing x such that $f(U) \subseteq V$. If f is P_s -continuous at every point of X , then it is called P_s -continuous.

Proposition 2.25[4]. If $f: X \rightarrow Y$ is a continuous and open function and V is a preopen set of Y ,





then $f^{-1}(V)$ is a preopen set of X .

Proposition 2.26[4]. If $f: X \rightarrow Y$ is a continuous and open function and F is a semi-closed set of Y , then $f^{-1}(F)$ is a semi-closed set of X .

3. δP_s -Open Sets in Topological Spaces

Definition 3.1. A δ -preopen subset A of a space X is called a δP_s -open set if for each $x \in A$, there exists a semi-closed set F such that $x \in F \subseteq A$.

Proposition 3.2. A subset A of a space X is δP_s -open if and only if A is a δ -preopen set and A is a union of semi-closed sets.

Proposition 3.3. Any union of δP_s -open sets is a δP_s -open set.

Proof: Let $\{A_\alpha\}$ be a collection of δP_s -open sets. Consider $A = \cup A_\alpha$.

A is a δ -preopen set from the lemma 2.18.

• For every $x \in A, x \in A_\alpha$, for some α and since A_α is a δP_s -open set, there exists a semi-closed set F_x such that $x \in A_\alpha \subseteq F_x \subseteq A_\alpha = A \therefore x \in F_x \subseteq A$

Thus, A is a δP_s -open set.

Proposition 3.4. If a space X is semi- T_1 , then $\delta P_s O(X) = \delta PO(X)$.

Proof: Let $A \subseteq X$ and $A \in \delta PO(X)$. If $A = \phi$, then $A \in \delta P_s O(X)$. If $A \neq \phi$, then for each $x \in A$, by theorem 2.5. $\{x\}$ is semi-closed set, since X is semi- T_1

Now $x \in \{x\} \subseteq A$. Therefore $A \in \delta P_s O(X)$ by proposition 3.2. Hence $\delta PO(X) \subseteq \delta P_s O(X)$.

But $\delta P_s O(X) \subseteq \delta PO(X)$ in general, by proposition 3.2. Therefore, $\delta P_s O(X) = \delta PO(X)$.

Proposition 3.5. Every regular open set is δP_s -open set (ie) $RO(X) \subseteq \delta P_s O(X)$.

Proof: Let A be regular open by a Theorem 3.2[12], A is semiclosed and preopen.

Now A is preopen $\Rightarrow A$ is δ -preopen [By Remark 2.16]

A is semiclosed \Rightarrow for each $x \in A$ there exists the semiclosed set A itself, such that $x \in A \subseteq A$

Hence A is in $\delta P_s O(X)$. $\therefore RO(X) \subseteq \delta P_s O(X)$

Proposition 3.6. Every P_s -open set is a δP_s -open set.

Proof: Let A be a P_s -open set, By Lemma-2.16, A is preopen. (1)

Moreover since A is P_s -open, we get, for each $x \in A$ there exists a semi-closed set F such that $x \in F \subseteq A$ (2)

From (1) & (2) we get, A is δP_s -open.

Proposition 3.7: A δ -open set is a δP_s -open set.

Proof: From theorem 2.8[4], A δ -open set is P_s -open set.

Now by above property, a P_s -open set is a δP_s -open set. Now by Proposition 3.6, a P_s -open set is δP_s -open set.

Hence a δ -open set is δP_s -open set.

Lemma 3.8. In a hyperconnected space,

(i) $\delta O(X) = \{X, \phi\}$

(ii) $\delta PO(X) = \mathcal{P}(X)$

Proof: (i) Let (X, τ) be hyperconnected. Then for $G \in \tau, \text{Cl}G = X$ (1)

If $A \neq \phi$ and $A \in \delta O(X)$, for all $x \in A$, there exists an open set G such that $x \in G \subseteq \text{Int Cl}G = \text{Int}X = X \subseteq A \Rightarrow A = X$.

$\therefore \delta O(X) = \{X, \phi\}$

(ii) For any subset $A, A \subseteq X = \text{Int}X = \text{Int}(\delta \text{Cl}A) [\because \delta \text{Cl}(A) = \{X, \phi\}]$

• A is δ -preopen. • $\delta PO(X) = \mathcal{P}(X)$, the power set of X

Proposition 3.9. In a locally indiscrete space, $SC(X) \subseteq \delta P_s O(X)$.

Proof: The proof is similar to that of proposition 3.8.

Proposition 3.10. If a topological space (X, τ) is s -regular, then $\tau \subseteq \delta P_s O(X)$.

Proof: Let $A \subseteq X$ and $A \in \tau$.

If $A = \phi$, then $A \in \delta P_s O(X)$





Vidhyapriya et al.,

If $A \neq \emptyset$, since X is s -regular, then by definition 2.3 for each $x \in A$, there exists $U \in SO(X)$ such that $x \in U \subseteq sCl U \subseteq A$. Thus, we have $x \in sCl U \subseteq A$. Since $A \in \tau$, we get $A \in PO(X)$ which implies $A \in \delta PO(X)$. Moreover for all $x \in A$ there exist a s -closed set $sclU$ such that $x \in scl U \subseteq A$. Hence $A \in \delta PsO(X)$. Thus $\tau \subseteq \delta PsO(X)$

Corollary 3.11. For any subset $A \subseteq X$. The following conditions are equivalent:

- (i) A is clopen.
- (ii) A is δ -open and δ -closed
- (iii) A is P_s -open and δ -closed.
- (iv) A is α -open and δ -closed.
- (v) A is δP_s -open and δ -closed.
- (vi) A is δ -preopen and δ -closed

Proof. (i) \Rightarrow (ii) By Lemma 2.7[5]

(ii) \Rightarrow (iii) By Proposition 2.8[4]

(iii) \Rightarrow (iv) From (iii) we get A is P_s -open and δ -closed. Now by Corollary 2.16[4]

A is α -open

\therefore (iii) \Rightarrow (iv)

(iv) \Rightarrow (v) From (iv) A is α -open $\Rightarrow A$ is δ -preopen (1)

A is δ -closed $\Rightarrow A$ is semi-closed. (2)

(1) & (2) $\Rightarrow A$ is δP_s -open.

\therefore (iv) \Rightarrow (v)

(v) \Rightarrow (vi) A is δP_s -open $\Rightarrow \delta$ -preopen by definition 3.1

\therefore (v) \Rightarrow (vi)

(vi) \Rightarrow (i) Now A is δ -preopen $\Rightarrow A \subseteq int(\delta cl A)$

But A is δ -closed also $\therefore A \subseteq int A \Rightarrow A$ is open and

Moreover A is δ closed $\Rightarrow A$ is closed

Hence A is clopen.

\therefore (vi) \Rightarrow (i)

Corollary 3.12. For a semi-regular space the following conditions are equivalent:

- (i) A is regular open.
- (ii) A is P_s -open and semi-closed.
- (iii) A is open and semi-closed.
- (iv) A is α -open and semi-closed.
- (v) A is δP_s -open and s -closed
- (vi) A is δ -preopen and s -closed.

Proof. In a semi-regular space, δ -closed sets coincide with closed sets. So $\delta PO(X)=PO(X)$.

And $\delta PsO(X)= PsO(X)$.

Hence the result follows from Corollary 2.17[4] and Proposition 3.5.

Corollary 3.13. For any topological space, the following statements are equivalent:

- (i) A is regular open.
- (ii) A is δ -open and δ -semiregular.
- (iii) A is δ -open and δ -semi- θ -closed.
- (iv) A is δ -open and δ -semiclosed.
- (v) A is α -open and δ -semiclosed
- (vi) A is δP_s -open and δ -semiclosed.
- (vii) A is δ -preopen and δ -semiclosed.
- (viii) A is α -preopen and e^* -closed.





Vidhyapriya et al.,

Proof. The proof follow from Theorem 7.15[34] and from Corollary 3.12

Proposition 3.14. For any topological space, if $A \in \delta PO(X)$ and either $A \in \eta O(X) \cup S\theta O(X)$, then $A \in \delta P_s O(X)$.

Proof: Let $A \in \eta O(X)$ and $A \in \delta PO(X)$. If $A = \phi$, then $A \in \delta P_s O(X)$. If $A \neq \phi$, Since $A \in \eta O(X)$, then $A = \cup F_\alpha$, where $F_\alpha \in \delta C(X)$, for each α . Since $\delta C(X) \subseteq SC(X)$, then $F_\alpha \in SC(X)$, for each α . Since $A \in \delta PO(X)$. Then by Proposition 3.2, $A \in \delta P_s O(X)$. Suppose that $A \in S\theta O(X)$ and $A \in \delta PO(X)$. If $X = \phi$, then $A \in \delta P_s O(X)$. If $A \neq \phi$, Since $A \in S\theta O(X)$, then for each $x \in A$, there exists $U \in SO(X)$ such that $x \in U \subseteq sCIU \subseteq A$ implies that $x \in sCIU \subseteq A$ and $A \in \delta PO(X)$. Therefore, by Definition 3.1, $A \in \delta P_s O(X)$.

Corollary 3.15. For any subset A of a space X . If $A \in \theta SO(X) \cap \delta PO(X)$, then $A \in \delta P_s O(X)$.

Proof. Follows from the Proposition 3.14, and the fact that $\theta SO(X) \subset S\theta O(X)$ or $\theta SO(X) \subset \eta O(X)$ [10].

Proposition 3.16. Let (X, τ) be any extremally disconnected space. If $A \in \theta SO(X)$, then $A \in \delta P_s O(X)$.

Proof. Let $A \in \theta SO(X)$. If $A = \phi$, then $A \in \delta P_s O(X)$. If $A \neq \phi$. Since X is extremally disconnected, then by Theorem 2.8, $\theta SO(X) = \delta O(X)$. Hence $A \in \delta O(X)$. But $\delta O(X) \subseteq \delta P_s O(X)$ by proposition 3.7. Therefore, $A \in \delta P_s O(X)$.

Proposition 3.17. Let (Y, τ_Y) be a subspace of a space (X, τ) . If $A \in \delta P_s O(Y, \tau_Y)$ and $Y \in RO(X, \tau)$, then $A \in \delta P_s O(X, \tau)$.

Proof. Let $A \in \delta P_s O(Y, \tau_Y)$, then $A \in \delta PO(Y, \tau_Y)$ and for each $x \in A$, there exists $F \in SC(Y, \tau_Y)$ such that $x \in F \subseteq A$. Since $Y \in RO(X, \tau)$, then $Y \in \delta PO(X, \tau)$ and since $A \in \delta PO(Y, \tau_Y)$, then by Theorem 2.14, $A \in \delta PO(X, \tau)$. Again since $Y \in RO(X, \tau)$, then $Y \in SC(X, \tau)$ and since $F \in SC(Y, \tau_Y)$, by Theorem 2.13(iii), $F \in SC(X, \tau)$. Hence, $A \in \delta P_s O(X, \tau)$.

Proposition 3.18. Let A and B be any subsets of a space X . If $A \in \delta P_s O(X)$ and $B \in RSO(X)$, then $A \cap B \in \delta P_s O(B)$.

Proof. Let $A \in \delta P_s O(X)$, then $A \in \delta PO(X)$ and $A = \cup F_\alpha$ where $F_\alpha \in SC(X)$ for each α by Proposition 3.2. Then $A \cap B = (\cup F_\alpha) \cap B = \cup (F_\alpha \cap B)$. Since $B \in RSO(X)$, then $B \in \delta SO(X)$ and by theorem 3.5[34], $A \cap B \in \delta PO(B)$. Again since $B \in RSO(X)$, then $B \in SC(X)$ and hence $F_\alpha \cap B \in SC(X)$ for each α . Since $F_\alpha \cap B \subseteq B$ and $F_\alpha \cap B \in SC(X)$ for each α . Then by Theorem 2.11 (ii), $F_\alpha \cap B \in SC(B)$. Therefore, by Proposition 3.2, $A \cap B \in \delta P_s O(B)$.

Proposition 3.19. If $A \in \delta P_s O(X)$ and B is an δ -open subspace of a space X , then $A \cap B \in \delta P_s O(B)$.

Proof. Let $A \in \delta P_s O(X)$, then $A \in \delta PO(X)$ and $A = \cup F_\alpha$ where $F_\alpha \in SC(X)$ for each α by Proposition 3.2. Then $A \cap B = \cup F_\alpha \cap B = \cup (F_\alpha \cap B)$. Since B is an δ -open subspace of X , and by lemma 2.13, $A \cap B \in \delta PO(X)$. Again since B is δ -open then B is open. Then by Lemma 2.12, $F_\alpha \cap B \in SC(B)$ for each α . Then by Proposition 3.2, $A \cap B \in \delta P_s O(B)$.

Corollary 3.20. If either $B \in RSO(X)$ or B is an δ -open subspace of a space X and $A \in \delta P_s O(X)$, then $A \cap B \in \delta P_s O(B)$.

Proof. Follows directly from proposition 3.18 and proposition 3.19

Definition 3.21. A point $x \in X$ is said to be δP_s -interior point of A if there exists a δP_s -open set U containing x such that $U \subseteq A$. The set of all δP_s -interior points of A is said to be δP_s -interior of A and is denoted by δP_s -Int A .

Definition 3.22. Let A be a set in a space X . A point $x \in X$ is in the δP_s -Closure of A if and only if $A \cap U \neq \phi$ for every $U \in \delta P_s O(X)$ containing x and is denoted by δP_s -Cl(A).

4. δP_s -Continuous Functions

Definition 4.1. A function $f: X \rightarrow Y$ is called δP_s -continuous at a point $x \in X$ if for each $x \in X$ and each open set V of Y containing $f(x)$, there exists a δP_s -open set U of X containing x such that $f(U) \subseteq V$. If f is δP_s -continuous at every point of X , then it is called δP_s -continuous.

Lemma 4.2. Every complete continuous function is δP_s -continuous.

Proof. Let $f: X \rightarrow Y$ be a complete continuous function. Let $x \in X$ and V be an open set containing $f(x)$. Then $f^{-1}(V)$ is





Vidhyapriya et al.,

regular open in X , since f is complete continuous. Choosing $U = f^{-1}(V)$ will give $f(U) \subseteq V$ and $x \in f(U)$.
 Moreover $f^{-1}(V)$ is δP_S -open from Proposition 3.5.
 Hence f is δP_S -continuous at x . Since x is arbitrary, f is a δP_S -continuous function.

Proposition 4.3. Every super continuous function is δP_S -continuous function.

Proof. The proof follows as in the above proposition and from the Proposition 3.7.

Proposition 4.4. Every P_S -continuous function is δP_S -continuous function.

Proof. The proof follows as in the above proposition and from the Proposition 3.6

Proposition 4.5. Every δP_S -continuous function is δ -precontinuous function.

Proof. The proof follows as in the Proposition 4.2 and from the Definition 3.21.

Note 4.6. From the above results we obtain the following implication diagram.

Complete continuous

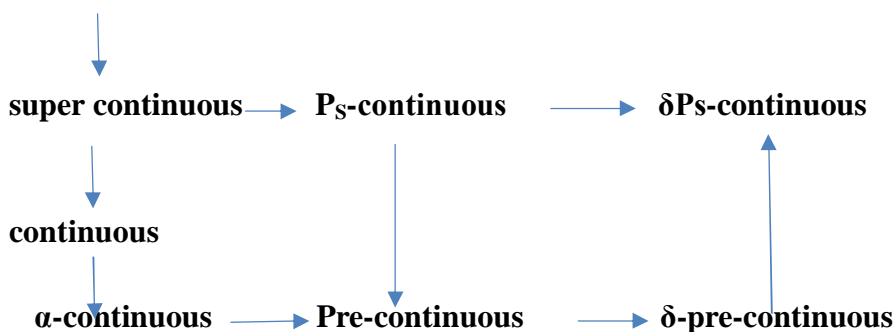


Diagram 4.1

Proposition 4.7. For a function $f: X \rightarrow Y$, the following statements are equivalent:

1. f is δP_S -continuous.
2. $f^{-1}(V)$ is δP_S -open set in X , for each open set V in Y .
3. $f^{-1}(F)$ is δP_S -closed set in X , for each closed set F in Y .
4. $f(\delta P_S Cl A) \subseteq Cl f(A)$, for each $A \subseteq X$.
5. $\delta P_S Cl f^{-1}(B) \subseteq f^{-1}(Cl B)$, for each $B \subseteq Y$.
6. $f^{-1}(Int B) \subseteq \delta P_S Int f^{-1}(B)$, for each $B \subseteq Y$.
7. $Int f(A) \subseteq f(P_S Int A)$, for each $A \subseteq X$.

Proof. (1) \Rightarrow (2)

Let $f: X \rightarrow Y$ be δP_S -continuous function.

To Prove. $f^{-1}(V)$ is δP_S open in $X \forall$ open set V in Y

Let V be open in Y . Let $x \in f^{-1}(V)$. Then $f(x) \in V$

By definition 4.1, $\exists \delta P_S$ -open set U of X containing $x \ni f(U) \subseteq V \Rightarrow x \in U \subseteq f^{-1}(V)$.

By definition 3.21 x is an δP_S int point of $f^{-1}(V)$. Since x is arbitrary, $f^{-1}(V)$ is δP_S -open.

(2) \Rightarrow (3) Obvious

(3) \Rightarrow (4)

For $A \subseteq X$, $Cl f(A)$ is closed in Y .

$$\therefore Cl(Cl f(A)) = Cl(f(A))$$

Then by (3) $f^{-1}(\delta P_S Cl A) \subseteq Cl(f(A))$.





Vidhyapriya et al.,

(4) \Rightarrow (5)

Let $B \subseteq Y$ and $f^{-1}(B) = A \Rightarrow B$

Then by (4) $f(\delta P_S Cl(f^{-1}(B))) = f(\delta P_S Cl A) \subseteq Cl f(A)$

$= Cl f(f^{-1}(B)) \subseteq Cl B$

$\therefore \delta P_S Cl(f^{-1}(B)) \subseteq f^{-1}(Cl B)$

(5) \Rightarrow (6)

As lemma prove $\delta P_S int A = (\delta P_S Cl A)^c$

\therefore From (5) $(\delta P_S Cl(f^{-1}(B)))^c \supseteq (f^{-1}(Cl B))^c$

$\Rightarrow \delta P_S int B \supseteq f^{-1}(Cl B)^c = f^{-1}(int B)$

$\therefore f^{-1}(int B) \subseteq \delta P_S int B$

(6) \Rightarrow (7)

Let $A \subseteq X$. Let $B \subseteq Y$ such that $A = f^{-1}(B)$

$\Rightarrow f(A) \subseteq B$

$\Rightarrow Int f(A) \subseteq Int(B)$

$\Rightarrow f^{-1}(Int f(A)) \subseteq f^{-1}(Int B) \subseteq \delta P_S Int f^{-1}(B) = \delta P_S Int A$

$\therefore Int f(A) \subseteq f(\delta P_S Int A)$

Proposition 4.8. A function $f: X \rightarrow Y$ is δP_S -continuous if and only if f is pre-continuous and for each $x \in X$ and each open set V of Y containing $f(x)$, there exists a semi-closed set F in X containing x such that $f(F) \subseteq V$.

Proof. Let $f: X \rightarrow Y$ be δP_S -continuous, since every δP_S -open set is δ -preopen, f is δ -precontinuous also. Let $x \in X$ and V be any set containing $f(x)$. From the definition of δP_S -continuity, there exists a δP_S -open set U of X containing x , such that $f(U) \subseteq V$. From the definition of δP_S -open set, for all $x \in U$, there exists a closed set F of X such that $x \in F \subseteq U$.

$\therefore f(F) \subseteq f(U) \subseteq V$

\Leftrightarrow Let the criteria be true. To prove f is δP_S -continuous. From the criteria, f is δ -precontinuous which implies $f^{-1}(V)$ is δ -preopen set.

Let $x \in f^{-1}(V)$ then $f(x) \in V$ and by hypothesis there exists a semi-closed set F in X such that $x \in F$ and $f(F) \subseteq V \Rightarrow x \in F \subseteq f^{-1}(V)$.

$\therefore f^{-1}(V)$ is δP_S -open $\Rightarrow f$ is δP_S -continuous.

Proposition 4.9. If $f: X \rightarrow Y$ is a continuous and an open function and V is a δP_S -open set of Y , then $f^{-1}(V)$ is a δP_S -open set of X .

Proof. Let V be a δP_S -open set of Y , then by Proposition 3.2, V is a δ -preopen set of Y and $V = \cup F_\alpha$, where F_α is a semi-closed set of Y for each α . Then $f^{-1}(V) = f^{-1}(\cup F_\alpha) = \cup f^{-1}(F_\alpha)$, where F_α is semi-closed set of Y for each α . Since f is a continuous and open function. Then by Proposition 2.25, $f^{-1}(V)$ is a preopen set of X and thereby $f^{-1}(V)$ is δ -preopen and by Proposition 2.26, $f^{-1}(F_\alpha)$ is a semi-closed set of X for each α . Hence by 3.2, $f^{-1}(V)$ is a δP_S -open set of X .

Corollary 4.10. If $f: X \rightarrow Y$ is a continuous and open function and F is a δP_S -closed set of Y , then $f^{-1}(F)$ is a δP_S -closed set of X .

Proposition 4.11. The following statements are equivalent for a function $f: X \rightarrow Y$:

1. f is perfectly continuous.
2. f is super continuous and δ -contra continuous
3. f is P_S -continuous and δ -contra-continuous.
4. f is α -continuous and δ -contra-continuous.
5. f is δP_S -continuous and δ -contra continuous
6. f is δ -pre-continuous and δ -contra-continuous.

Proof. This is an immediate consequence of Corollary 3.11.

Proposition 4.12. The following statements are equivalent for a function $f: X \rightarrow Y$, in a semi-regular space:

1. f is complete continuous.





Vidhyapriya et al.,

2. f is δP_S -continuous and contra-semicontinuous.
3. f is δP_S continuous and contra-semicontinuous.
4. f is α -continuous and contra-semicontinuous.
5. f is δP_S -continuous and contra semicontinuous.
6. f is precontinuous and contra-semicontinuous.

Proof. This is an immediate consequence of Corollary 3.12.

Proposition 4.13. The following statements are equivalent for a function $f: X \rightarrow Y$:

f is complete continuous

f is super continuous and δ -semicomplete continuous

f is super continuous and contra- δ -semi θ complete continuous

f is super continuous and contra - δ semicontinuous

f is α -continuous and contra- δ -semicontinuous

f is δP_S -continuous and contra - δ -semicontinuous

f is δP -continuous and contra - δ -semicontinuous

A is α -precontinuous and contra- e^* continuous

Proof: This is an immediate consequence of Corollary 3.13.

Proposition 4.14. If $f: X \rightarrow Y$ be θ_S -continuous and precontinuous, then f is δP_S -continuous.

Proof. Let $f: X \rightarrow Y$ be θ_S -continuous and precontinuous. Let V be an open set in Y . Since f is θ_S continuous and precontinuous function $f^{-1}(V)$ is θ -semiopen and preopen in X . This implies $f^{-1}(V)$ is θ -semiopen and δ -preopen. By Corollary 3.15, $f^{-1}(V)$ is $\delta P_S O(X)$. Then by Proposition 4.5[2], f is δP_S -continuous.

Corollary 4.15. If a function $f: (X, \tau) \rightarrow (Y, \sigma)$ is almost θ_S -continuous and almost precontinuous, then $f: (X, \tau) \rightarrow (Y, \sigma)$ is δP_S -continuous.

Proof. Let $f: X \rightarrow Y$ be almost θ_S -continuous and almost precontinuous function. Let V be open in Y , then by definition almost θ_S -continuous and almost precontinuous function, $f^{-1}(V)$ is semiopen and preopen. From Corollary 2.20[3], $f^{-1}(V)$ is P_S -open which implies $f^{-1}(V)$ is δP_S open [Since Each clopen set is δP_S -open]. Hence by Proposition 4.5[2], f is δP_S -continuous.

Corollary 4.16. Let X be a locally indiscrete space. Then the function $f: (X, \tau) \rightarrow (Y, \sigma)$ is almost continuous if and only if $f: (X, \tau) \rightarrow (Y, \sigma)$ is δP_S -continuous.

Proof. Follows from Proposition 3.9.

Corollary 4.17. Let $f: X \rightarrow Y$ be a function and X is locally indiscrete space. Then f is δP_S -continuous if and only if f is continuous.

Proof. Follows from Proposition 3.9.

Corollary 4.18. Let $f: X \rightarrow Y$ be a function and X is s -regular space. If f is continuous, then f is δP_S -continuous.

Proof. Follows from Proposition 3.10.

Corollary 4.19. Let $f: X \rightarrow Y$ be a function and X is semi- T_1 space. Then f is δP_S -continuous if and only if f is δ -precontinuous.

Proof. Follows from Proposition 3.4.

Proposition 4.20. Let X be an extremally disconnected space. If the function $f: (X, \tau) \rightarrow (Y, \sigma)$ is almost θ_S -continuous, then $f: (X, \tau) \rightarrow (Y, \sigma)$ is δP_S -continuous.

Proof. Let $H \in \sigma$, then H is regular open set in (Y, σ) . Since $f: (X, \tau) \rightarrow (Y, \sigma)$ is almost θ_S -continuous. Then $f^{-1}(H)$ is θ -semi-open set in X . Since X is extremally disconnected space. Then by Proposition 3.16, $f^{-1}(H)$ is δP_S -open set in X .





Vidhyapriya et al.,

Therefore, by Proposition 4.5[2], $f:(X,\tau) \rightarrow (Y,\sigma)$ is δP_S -continuous.

Proposition 4.21. Let $f : X \rightarrow Y$ be a function. Let B be any basis for τ in Y . Then f is δP_S - continuous if and only if for each $B \in \mathcal{B}$, $f^{-1}(B)$ is a δP_S -open subset of X .

Proof. Necessity. Suppose that f is δP_S - continuous. Then since each $B \in \mathcal{B}$ is an open subset of Y and f is δP_S -continuous, $f^{-1}(B)$ is a δP_S -open subset of X by Proposition 4.5[2]

Sufficiency. Let V be any open subset of Y . Then $V = \cup\{B_i : i \in I\}$ where every B_i is a member of \mathcal{B} for a suitable index set I , it follows that $f^{-1}(V) = f^{-1}(\cup\{B_i : i \in I\}) = \cup f^{-1}(\{B_i : i \in I\})$. Since $f^{-1}(B_i)$ is a δP_S -open subset of X for each $i \in I$, by hypothesis $f^{-1}(V)$ is the union of a family of δP_S -open sets of X and hence is δP_S -open set of X , by Proposition 3.3. Therefore, by Proposition 4.5[2], f is δP_S - continuous.

Proposition 4.22. Let $f:X \rightarrow Y$ be δP_S -continuous function. If A is either open or regular semi-open subset of X , then $f|_A:A \rightarrow Y$ is δP_S -continuous in the subspace A .

Proof. Let V be any open set of Y . Since f is δP_S - continuous, $f^{-1}(V)$ is δP_S - open set in X , then by Proposition 4.5[2]. Since A is either open or regular semi-open subset of X . $(f|_A)^{-1}(V) = f^{-1}(V) \cap A$ is a δP_S -open subspace of A by Proposition 3.19. This shows that $f|_A:A \rightarrow Y$ is δP_S -continuous.

From Proposition 4.22, we obtain the following corollary

Corollary 4.23. Let $f:X \rightarrow Y$ be δP_S -continuous function. If A is regular open subset of X , then $f|_A:A \rightarrow Y$ is δP_S -continuous in the subspace A .

Proof: If A is regular open then it is open. Hence from Proposition 4.21, the proof follows.

Proposition 4.24. A function $f:X \rightarrow Y$ is δP_S - continuous. If for each $x \in X$, there exists a regular open set A of X containing x such that $f|_A:A \rightarrow Y$ is δP_S -continuous.

Proof. Let $x \in X$, then by hypothesis, there exists a regular open set A containing x such that $f|_A:A \rightarrow Y$ is δP_S -continuous. Let V be any open set of Y containing $f(x)$, there exists a δP_S -open set U in A containing x such that $(f|_A)(U) \subseteq V$. Since A is regular open set. By Proposition 3.17, U is δP_S -open set in X and hence $f(U) \subseteq V$. This shows that f is δP_S -continuous.

Corollary 4.25. Let $\{U_\alpha : \alpha \in \Delta\}$ be a regular open cover of a topological space X . A function $f:X \rightarrow Y$ is δP_S -continuous if and only if $f|_{U_\alpha}:U_\alpha \rightarrow Y$ is δP_S -continuous for each $\alpha \in \Delta$.

Proof. Let $\{U_\alpha/\alpha \in \Delta\}$ be a regular open cover of a topological space X . Let $F:X \rightarrow Y$ be a regular open cover of a topological space X . Let $F:X \rightarrow Y$ be δP_S -continuous. By Corollary 4.22 $f|_{U_\alpha} : U_\alpha \rightarrow Y$ is δP_S -continuous $\forall \alpha \in \Delta$.

Conversely, let $f|_{U_\alpha} : U_\alpha \rightarrow Y$ be δP_S -continuous, $\forall \alpha \in \Delta$

Now, $\forall x \in X$, there exists $U_\alpha \in \{U_\alpha/\alpha \in \Delta\}$ containing x , since $\{U_\alpha\}$ is a cover for X . Then by Proposition 4.23 $f|_{U_\alpha} : U_\alpha \rightarrow Y$ is δP_S -continuous.

Proposition 4.26. If $X = R \cup S$, where R and S are regular open sets and $f:X \rightarrow Y$ is a function such that both $f|_R$ and $f|_S$ are δP_S -continuous, then f is δP_S -continuous.

Proof. Let V be any open set of Y . Then $f^{-1}(V) = (f|_R)^{-1}(V) \cup (f|_S)^{-1}(V)$. Since $f|_R$ and $f|_S$ are δP_S - continuous. Then by Proposition 4.5[2], $(f|_R)^{-1}(V)$ and $(f|_S)^{-1}(V)$ are δP_S -open sets in R and S , respectively. Since R and S are regular open sets in X , then by Proposition 3.17, $(f|_R)^{-1}(V)$ and $(f|_S)^{-1}(V)$ are δP_S -open sets in X . Since union of two δP_S -open sets is δP_S -open. Hence $f^{-1}(V)$ is δP_S - open set in X . Therefore, by Proposition 4.5[2], f is δP_S -continuous.

The following is the pasting lemma for δP_S -continuity.

Proposition 4.27. Let $X = R_1 \cup R_2$, where R_1 and R_2 are regular open sets in X . Let $f:R_1 \rightarrow Y$ and $g:R_2 \rightarrow Y$ be P_S -continuous. If $f(x) = g(x)$ for each $x \in R_1 \cap R_2$. Then $h:R_1 \cup R_2 \rightarrow Y$ such that





Vidhyapriya et al.,

$$h(x) = \begin{cases} f(x) & \text{if } x \in R_1 \\ g(x) & \text{if } x \in R_2 \end{cases} \text{ is } \delta P_S\text{-continuous.}$$

Proof. Let O be an open set of Y . Now $h^{-1}(O) = f^{-1}(O) \cup g^{-1}(O)$. Since f is δP_S -continuous, then by Proposition 4.5[2], $f^{-1}(O)$ is δP_S -open set in R_1 . But R_1 is regular open set in X . Then by Proposition 3.17, $f^{-1}(O)$ is δP_S -open set in X . Similarly, $g^{-1}(O)$ is δP_S -open set in R_2 and hence, δP_S -open set in X . Since union of two δP_S -open sets is δP_S -open. Therefore, $h^{-1}(O) = f^{-1}(O) \cup g^{-1}(O)$ is a δP_S -open set in X . Hence by Proposition 4.5[2], h is δP_S -continuous.

Proposition 4.28. Let $f: X \rightarrow Y$ be δP_S -continuous surjection and A be either δ -open or regular semi-open subset of X . If f is an δ -open function, then the function $g: A \rightarrow f(A)$, defined by $g(x) = f(x)$ for each $x \in A$, is δP_S -continuous.

Proof. Putting $H = f(A)$. Let $x \in A$ and let V be any open set in H containing $g(x)$. Since H is open in Y and V is open in H , then V is open in Y . Since f is δP_S -continuous, there exists a δP_S -open set U in X containing x such that $f(U) \subseteq V$. Taking $W = U \cap A$, since A is either δ -open or regular semi-open subset of X . Then by Proposition 3.20, W is a δP_S -open set in A containing x and $g(W) \subseteq V \cap H = V_H$. Then $g(W) \subseteq V_H$. This shows that g is δP_S -continuous.

Proposition 4.29. Let $f: X \rightarrow Y$ be a δP_S -continuous. If Y is an open subset of a topological space Z , then $f: X \rightarrow Z$ is δP_S -continuous.

Proof. Let V be an open set in Z . Then $V \cap Y$ is open in Y . Since f is δP_S -continuous, by Proposition 4.5[2], $f^{-1}(V \cap Y)$ is δP_S -open set in X . But $f(x) \in Y$ for each $x \in X$, and thus $f^{-1}(V) = f^{-1}(V \cap Y)$ is a δP_S -open subset of X . Therefore, by Proposition 4.5[2], $f: X \rightarrow Z$ is δP_S -continuous.

Example 4.31. Let $X = Y = Z = \{a, b, c\}$, $\tau = \{X, \phi, \{a\}, \{b\}, \{a, b\}\}$, $\sigma = \{X, \phi, \{a, b\}\}$ and $\eta = \{X, \phi, \{c\}\}$. Define $f: (X, \tau) \rightarrow (Y, \sigma)$ and $g: (Y, \sigma) \rightarrow (Z, \eta)$ as identity functions. Then f and g are δP_S -continuous functions but $g \circ f$ is not δP_S -continuous as $f^{-1}(g^{-1}\{a, b\}) = \{a, b\}$ is not δP_S -closed in (X, τ) .

Proposition 4.32. Let $f: X \rightarrow Y$ and $g: Y \rightarrow Z$ be functions. Then the composition function $g \circ f: X \rightarrow Z$ is δP_S -continuous if f and g satisfy one of the following conditions:

f is δP_S -continuous and g is continuous.

f is continuous and open and g is δP_S -continuous.

Proof. 1. Let W be any open subset of Z . Since g is continuous, $g^{-1}(W)$ is open subset of Y . Since f is δP_S -continuous, then by Proposition 4.5[2], $(g \circ f)^{-1}(W) = f^{-1}(g^{-1}(W))$ is δP_S -open subset in X . Therefore, by Proposition 4.5[2], $g \circ f$ is δP_S -continuous.

2. Let W be any open subset of Z . Since g is δP_S -continuous, by Proposition 4.5[2], $g^{-1}(W)$ is δP_S -open subset of Y . Since f is continuous and open, then by Proposition 4.7, $f^{-1}(g^{-1}(W)) = (g \circ f)^{-1}(W)$ is a δP_S -open set in X . Hence by Proposition 4.5[2], $g \circ f$ is δP_S -continuous.

REFERENCES

1. Abd El-Monsef M. E., El-Deeb S. N. and Mahmood R.A., "β-open sets and β-continuous mappings", Bull. Fac. Sci. Assuit Univ., 12(1)(1983), 1-18.
2. Abdulla A. S., "On some applications of special subsets in topology", Ph.D. Thesis, Tanta Univ., 1986.
3. Ahmed N. K., "On Some Types of Separation Axioms", M.Sc., Thesis, College of Science, Salahaddin Univ., 1990.
4. Alias B. Khalaf, and Baravan A. Asaad, "P_s-open sets and P_s-Continuity in Topological spaces", J. Duhok Univ., 12(2) (2009), 183-192.
5. Arya S.P. and Gupta R, "On Strongly Continuous Mappings", Kyungpook Math. J., 14(1974), 131-143.
6. Caldas M., Fukutake T., Jafari S. and Noiri T., "Some Applications of δ-preopen Sets in Topological Spaces", Bulletin of the Institute of Mathematics Academia Sinica 33(3) (2005), 261-276.





Vidhyapriya et al.,

7. Di Maio G. And Noiri T., Di Maio G. and Noiri T., "On s-closed spaces", Indian J. Pure Appl. Math., 18 (3) (1987), 226-233.
8. Dontchev J., "Contra-continuous functions and strongly S-closed spaces", Internat. J. Math. and Math. Sci., 19 (2) (1996), 303-310.
9. Dontchev J. and Noiri T., "Contra-semicontinuous functions", Math. Pannonica, 10 (1999), 159-168.
10. Dontchev J., "Survey on preopen sets", The Proceedings of the Yatsushiro Topological Conference, (1998), 1-18.
11. E. Ekici, "One* -open sets and (D, S) * -sets", Mathematica Moravica, 13 (2009), 29-36
12. El-Deeb S. N. Hasanein I. A, Mashhour A.S. and Noiri T., "On P-regular spaces", Bull. Math. Soc. Sci. Math. R.S. Roum, 27(4) (1983), 311-315.
13. Fomin S., "Extensions of topological spaces", Ann. of Math., 44 (3) (1943), 471-480.
14. Guo T. Y., "A characterization of extremally disconnected spaces", J. Central China Normal Univ. Natur. Sci., 21(2) (1981),169-170.
15. Jankovic D. S., "A note on mappings of externally disconnected spaces", Acta math. Hungar., 46(1-2) (1985),83-92.
16. Joseph J. E. and Kwack M. H., "On S-closed spaces", Proc. Amer. Math. Soc., 80(2) (1980),341-348.
17. Khalaf A. B. and Easif F. H., "θs-continuous functions", J. Dohuk Univ., (special issue) 2 (1) (1999), 1-7.
18. Khalaf A. B. and Abdul-Jabbar A. M., "Almost θs-continuity and weak θs-continuity in topological spaces", J. Dohuk Univ., 4 (2) (2001), 171-177.
19. Levine N., "Semi-open sets and semi-continuity in topological spaces", Amer. Math. Monthly, 70(1) (1963), 36-41.
20. Maheshwari S. N. and Prasad R., "Some new separation axioms", Ann. Soc. Sci. Bruxelles, Ser. I., 89(1975), 395-402.
21. Masshour A. S., El-Monsef M. E. A.,and El-Deeb S.N., "On precontinuous and weak precontinuous mappings", Proc. Math. Phys. Soc., Egypt, 53(1982), 47-53.
22. Mashhour A.S., Hasanein A and S. N. El-Deeb S.N., "α-Continuous and α -Open Mappings", Acta Math. Hung. 41 (34) (1983), 213--218.
23. Munshi B.M., and Bassan D.S., "Super Continuous Mappings", Indian J.Pure and Applied Mathematics, 13(2), 229-236 (1982).
24. Nasef A. A. and Noiri T., "Some weak forms of almost continuity", Acta Math. Hungar., 74 (3) (1997), 211- 219.
25. Navalalagi G. B., "Pre-neighbourhoods", The Mathematics Education, 32(4) (1998), 201-206.
26. Noiri T., "On δ-continuous functions", J. Korean Math. Soc., 16 (2) (1980), 161-166.
27. Noiri T., "Supercontinuity and some strong forms of continuity", Indian J. Pure Appl. Math., 15 (3) (1984), 241-250.
28. Park J.H., Lee B.Y. and Son M.J., "On δ-semiopen sets in topological spaces", J. Indian Acad. Math., 19, No 1 (1997), 59-67
29. Raychaudhuri S. and Mukherjee M. N., "On δ-almost continuity and δ-preopen sets", Bull. Inst. Math. Acad. Sinica, 21 (1993), 357-366.
30. Reilly I. L. and Vamanmurthy M. K., "On α-continuity in topological spaces", Acta Math. Hungar., 45 (1-2) (1985), 27-32
31. Singal M. K. and Singal A. R., "Almost continuous mappings", Yokohama Math. J., 16 (1968), 63-73.
32. Stone M. H., "Applications of the theory of Boolean rings to topology", Trans. Amer. Math. Soc., 41(1937), 375-481.
33. Velicko N. V., "H-closed Topological spaces", Amer. Math. Soc. Transl., 78(2) (1968),103-118.
34. Vidhyapriya P, Shanmugapriya H and Sivakamasundari K, "δPs-Open Sets in Topological Spaces", AIP Conference Proceedings 2261, 030103 (2020).
35. Yunis R. H., "Properties of θ-semi-open sets", Zanco J. Of Pure and Applied Sciences, 19(1) (2001), 116-122.
36. Zanyar A. Ameen, Baravan A. Asaad and Ramadhan A. Muhammed, "On superclasses of δ-open sets in topological spaces", Int. J. of Applied Mathematics, 32(2), (2019) 259-277.





k- Regular Interval Valued Fuzzy Soft Matrices

P. Poongodi^{1*} and C.Vinitha²

¹Associate Professor, Department of Mathematics, KG College of Arts and Science, Coimbatore, Tamil Nadu, India

²II M.Sc Mathematics, Department of Mathematics, KG College of Arts and Science, Coimbatore, Tamil Nadu, India

Received: 27 Feb 2021

Revised: 15 Mar 2021

Accepted: 18 Mar 2021

*Address for Correspondence

P. Poongodi

Associate Professor,
Department of Mathematics,
KG College of Arts and Science,
Coimbatore, Tamil Nadu, India
Email: poongodi_happi@rediffmail.com



This is an Open Access Journal / article distributed under the terms of the **Creative Commons Attribution License** (CC BY-NC-ND 3.0) which permits unrestricted use, distribution, and reproduction in any medium, provided the original work is properly cited. All rights reserved.

ABSTRACT

In this paper, we proposed Interval valued fuzzy soft matrices and defined some operations on Interval valued fuzzy soft matrices. Finally we extend our approach in to develop the concept of k-regularity on Interval Valued Fuzzy Soft Matrix (IVFSM) as a generalization of regular Fuzzy Matrices and as an extension of k – regular fuzzy matrices. Also some basic properties of a k – regular IVFSM are derived.

Keywords: Soft set, Fuzzy soft set, Interval valued fuzzy soft set, Fuzzy soft matrices, Interval Valued Fuzzy Soft Matrices(IVFSM), k-regularity.

AMS Subject Classification: 15B15, 15A09.

INTRODUCTION

The concept of soft sets was first formulated by Molodtsov [1999] as a completely new mathematical tool for solving problems dealing with uncertainties in [7]. Later on Maji *et al* [2] have studied the theory of fuzzy soft set. Majumdar *et al*[3] have further generalized the concept of fuzzy soft sets. Maji *et al* [4] extended soft sets to intuitionistic fuzzy soft sets. Yong *et al* introduced a matrix representation of a fuzzy soft set and applied it in certain decision making problems. In [5] Manash Jyoti Borah *et al* extended fuzzy soft matrix theory and its application.

We deal with Interval Valued Fuzzy Soft Matrices (IVFSM) that is, matrices whose entries are intervals and all the intervals are subintervals of the interval [0,1]. Thomason introduced fuzzy matrices and discussed about the convergence of powers of a fuzzy matrix [11]. Recently the concept of k regularity of an IVFM a generalization of regularity of fuzzy matrix was developed by Meenakshi and Poongodi [10]. In [8, 9], Poongodi have studied the





Poongodi and Vinitha

concept of k – regular interval valued fuzzy matrix as a generalization of a regular fuzzy matrix and discussed about various inverses and orderings on interval valued fuzzy matrices. A matrix $A \in F_n$, the set of all $n \times n$ fuzzy matrices is said to be right(left) k - regular if there exists $X (Y) \in F_n$, such that $A^k X A = A^k (A Y A^k = A^k)$, $X(Y)$ is called a right (left) k -g inverse of A , where k is a positive integer.

In this paper, we proposed Interval valued fuzzy soft matrices and defined some operations on Interval valued fuzzy soft matrices. Finally we extend our approach in to develop the concept of k -regularity on Interval Valued Fuzzy Soft Matrix (IVFSM) as a generalization of regular Fuzzy Matrices and as an extension of k – regular fuzzy matrices. Also some basic properties of a k – regular IVFSM are derived.

Preliminaries

In this section, we present some basic notion of fuzzy soft set theory and fuzzy soft matrices.

Definition 2.1

Suppose that the initial universe set is denoted by U and the set of parameters by E , let $P(U)$ denotes the power set of U . A pair (F,E) is called a **soft set** over U where F is a mapping given by $F: E \rightarrow P(U)$. Clearly, a soft set is a mapping from parameters to $P(U)$, and it is not a set, but a parameterized family of subsets of the Universe.

Example 2.2

Suppose that $U = \{a_1, a_2, a_3, a_4\}$ is a set of students and $E = \{p_1, p_2, p_3\}$ is a set of parameters, which stand for result, conduct and sports performances respectively. Consider $(F,E) = \{ \{result = a_1, a_3, a_4\} \{conduct = a_1, a_2\} \{sports performances = a_2, a_3, a_4\} \}$ We can represent a soft set in the form of Table1

Definition 2.3

Let the initial Universe set is U and the set of parameters be E . Let $A \subseteq E$. A pair (F, A) is called **fuzzy soft set** over U where F is a mapping given by $F: A \rightarrow I^U$, where I^U denotes the collection of all fuzzy subsets of U .

Example 2.4

Consider the example 2.2, in soft set (F, E) , if s_1 is medium in studies, we cannot expressed with only the two numbers 0 and 1, we can characterize it by a membership function instead of the crisp number 0 and 1, which associates with each element a real number in the interval $[0,1]$. Then fuzzy soft set can describe as where $A = \{e_1, e_2\}$ $(F, A) = \{F(e_1) = \{(s_1, 0.9), (s_2, 0.3), (s_3, 0.8), (s_4, 0.9)\}, F(e_2) = \{(s_1, 0.8), (s_2, 0.9), (s_3, 0.4), (s_4, 0.3)\}\}$ We can represent a fuzzy soft set in the form of table2

Definition 2.5

Let U be an initial universe, E be a set of parameters and $A \subseteq E$. Then a pair (\underline{F}_A, E) is called an interval-valued fuzzy soft set over $P(U)$ where \underline{F}_A is a mapping given by $\underline{F}_A: A \rightarrow P(U)$.

An interval-valued fuzzy soft set is a parameterized family of interval-valued fuzzy subsets of U . An interval-valued fuzzy soft set is also a special case of a soft set because it is still a mapping from parameters to $P(U)$. $\forall e \in A, \underline{F}_A(e)$ is referred as an interval-valued fuzzy set of U . It can be written as: $\underline{F}_A(e) = \{(x, \mu_{\underline{F}_A}^-(x)) : x \in U\}$ where $\mu_{\underline{F}_A}^-(x)$ is the interval-valued fuzzy membership degree that object x holds on parameter e . If $\forall e \in E, \forall x \in U, \mu_{\underline{F}_A}^-(x) = \mu_{\underline{F}_A}^+(x)$, then \underline{F}_A will degenerated to be a standard fuzzy set and then (\underline{F}_A, E) will be degenerated to be a traditional fuzzy soft set.

Definition 2.6

Let $U = \{c_1, c_2, c_3, \dots, c_m\}$ be the Universal set and E be the set of parameters given by $E = \{e_1, e_2, e_3, \dots, e_n\}$. Let $A \subseteq E$ and (F, A) be a Interval Valued Fuzzy Soft set in the fuzzy soft class (U, E) . Then Interval Valued fuzzy soft set (F, A)





Poongodi and Vinitha

in a matrix form as $A_{m \times n} = [a_{ij}]_{m \times n}$ or $A = [a_{ij}]$, $i = 1, 2, \dots, m, j = 1, 2, \dots, n$,

$$\text{Where } a_{ij} = \begin{cases} ([\mu_{jL}(c_i), \mu_{jU}(c_i)]) & \text{if } e_j \in A \\ (0,1) & \text{if } e_j \notin A \end{cases}$$

$\mu_{jL}(c_i)$ represents the lower bound membership of c_i in the Interval valued fuzzy set $F(e_j)$ and $\mu_{jU}(c_i)$ represents the upper bound membership of c_i in the Interval valued fuzzy set $F(e_j)$. Also $\mu_{jL}(c_i) \leq \mu_{jU}(c_i)$

Example 2.7

Suppose that there are four houses under consideration, namely the universes $U = \{h_1, h_2, h_3, h_4\}$, and the parameter set $E = \{e_1, e_2, e_3\}$ where e_i stands for “beautiful”, “large”, and “in green surroundings” respectively. Consider the mapping F from parameter set $A = \{e_1, e_2\} \subseteq E$ to all interval valued fuzzy subsets of power set U . Consider an interval valued fuzzy soft set (F, A) which describes the “attractiveness of houses” that is considering for purchase. Then interval valued fuzzy soft set (F, A) is $F(e_1) = \{(h_1, [0.4, 0.7]), (h_2, [0.6, 0.9]), (h_3, [0.4, 0.9]), (h_4, [0.5, 0.6])\}$

$F(e_2) = \{(h_1, [0.1, 0.8]), (h_2, [0.3, 0.7]), (h_3, [0.5, 0.7]), (h_4, [0.4, 0.6])\}$

The interval valued fuzzy soft set in matrix form is represented as

$$\begin{pmatrix} [0.4, 0.7] & [0.1, 0.8] & [0.0, 0.0] \\ [0.6, 0.9] & [0.3, 0.7] & [0.0, 0.0] \\ [0.4, 0.9] & [0.5, 0.7] & [0.0, 0.0] \\ [0.5, 0.6] & [0.4, 0.6] & [0.0, 0.0] \end{pmatrix}$$

Definition 2.8

If $A = [a_{ij}] \in \text{IVFSM}_{m \times n}$, $B = [b_{ij}] \in \text{IVFSM}_{m \times n}$, then the addition and subtraction of Interval Valued Fuzzy Soft Matrices (IVFSM) of A and B is defined as

$$A + B = \{ \max[\mu_{AL}(a_{ij}), \mu_{BL}(b_{ij})], \max[\mu_{AU}(a_{ij}), \mu_{BU}(b_{ij})] \} \forall i, j$$

$$A - B = \{ \min[\mu_{AL}(a_{ij}), \mu_{BL}(b_{ij})], \min[\mu_{AU}(a_{ij}), \mu_{BU}(b_{ij})] \} \forall i, j$$

Definition 2.9

If $A = [a_{ij}] \in \text{IVFSM}_{m \times n}$, $B = [b_{jk}] \in \text{IVFSM}_{n \times p}$, then the product of interval valued fuzzy soft matrix relation of A and B is defined as

$$A * B = [c_{ik}]_{m \times p}, = \{ \text{Max}\{\text{Min}[\mu_{AL}(a_{ij}), \mu_{BL}(b_{ij})]\}, \text{Max}\{\text{Min}[\mu_{AU}(a_{ij}), \mu_{BU}(b_{ij})]\} \}$$

Definition 2.10

A matrix $A \in (\text{IVFM})_n$ is said to be right k -regular if there exist a matrix $X \in (\text{IVFM})_n$, such that $A^k X A = A^k$, for some positive integer k . X is called a right k -g inverse of A . Let $A \{1^k\} = \{ X / A^k X A = A^k \}$.

Definition 2.11

A matrix $A \in (\text{IVFM})_n$ is said to be left k -regular if there exist a matrix $Y \in (\text{IVFM})_n$, such that $A Y A^k = A^k$, for some positive integer k . Y is called a left k -g inverse of A . Let $A \{1^k\} = \{ Y / A Y A^k = A^k \}$.

Lemma 2.12

For $A = [A_L, A_U] \in (\text{IVFM})_{mn}$ and $B = [B_L, B_U] \in (\text{IVFM})_{np}$, the following hold.

(i) $A^T = [A_L^T, A_U^T]$

(ii) $AB = [A_L B_L, A_U B_U]$

Lemma 2.13

For $A, B \in (\text{IVFM})_{mn}$

(i) $R(B) \subseteq R(A) \Leftrightarrow B = XA$ for some $X \in (\text{IVFM})_m$

(ii) $C(B) \subseteq C(A) \Leftrightarrow B = AY$ for some $Y \in (\text{IVFM})_n$





Poongodi and Vinita

Theorem 2.14

Let $A = [A_L, A_U] \in (IVFM)_{mn}$.
Then A is regular IVFM $\Leftrightarrow A_L$ and $A_U \in F_{mn}$ are regular.

Theorem 2.15

Let $A = [A_L, A_U]$ be an $(IVFM)_{mn}$
Then, (i) $R(A) = [R(A_L), R(A_U)] \in (IVFM)_{1n}$
(ii) $C(A) = [C(A_L), C(A_U)] \in (IVFM)_{1m}$

k - Regular Interval Valued Fuzzy Soft Matrices

In this section, we introduce the concept of k – regular IVFSM. Let F_n denotes the set of all fuzzy soft matrices. The row and column ranks of a k – regular IVFSM are determined.

Definition 3.1

A matrix $A \in (IVFSM)_n$ is said to be right k – regular if there exist a matrix $X \in (IVFSM)_n$, such that $A^k X A = A^k$, for some positive integer k . X is called a right k – g inverse of A . Let $A \{1^k\} = \{X / A^k X A = A^k\}$.

Definition 3.2

A matrix $A \in (IVFSM)_n$ is said to be left k – regular if there exist a matrix $Y \in (IVFSM)_n$, such that $A Y A^k = A^k$, for some positive integer k . Y is called a left k – g inverse of A . Let $A \{1^k\} = \{Y / A Y A^k = A^k\}$.
In general, right k – regular IVFSM is different from left k – regular IVFSM. Hence a right k – g inverse need not be a left k – g inverse. This is illustrated in the following example.

Example 3.3

Let us consider $A = \begin{bmatrix} [0,0] & [0.2,0.5] & [0,0] \\ [0,0] & [0.5,1] & [0.3,0.5] \\ [0.1,0.5] & [0,0] & [0,0] \end{bmatrix} \in (IVFSM)_{3 \times 3}$

For this $A, A^2 = \begin{bmatrix} [0,0] & [0.2,0.5] & [0.2,0.5] \\ [0.1,0.5] & [0.5,1] & [0.3,0.5] \\ [0,0] & [0.1,0.5] & [0,0] \end{bmatrix}$

$A^3 = \begin{bmatrix} [0.1,0.5] & [0.2,0.5] & [0.2,0.5] \\ [0.1,0.5] & [0.5,1] & [0.3,0.5] \\ [0,0] & [0.1,0.5] & [0.1,0.5] \end{bmatrix}$

For $X = \begin{bmatrix} [0.4,0.5] & [0,0] & [0.3,0.5] \\ [0.2,0.5] & [0.5,1] & [0,0] \\ [0,0] & [0.4,0.5] & [0,0] \end{bmatrix}$

$A^3 X A = A^3$. Hence A is 3 – regular. For $k = 3, A^3 X A = A^3$ but $A X A^3 \neq A^3$
Hence X is a right 3 – g inverse but not a left 3 – g inverse.

Remark 3.4

In particular for $k=1$, Definitions (3.1) and (3.2) reduce to regular IVFSM, and in the case $A_L = A_U$, Definitions (3.1) and (3.2) reduce to right k – regular and left k – regular fuzzy soft matrix.





Poongodi and Vinitha

Theorem 3.5

Let $A = [A_L, A_U] \in (IVFSM)_n$. Then A is right k – regular IVFSM $\Leftrightarrow A_L$ and $A_U \in F_n$ are right k – regular.

Proof:

Let $A = [A_L, A_U] \in (IVFSM)_n$.

Since A is right k – regular IVFSM, there exists $X \in (IVFSM)_n$, such that $A^k X A = A^k$

Let $X = [X_L, X_U]$ with $X_L, X_U \in F_n$

Then by Lemma (2.3) (ii),

$$\begin{aligned} A^k X A = A^k &\Rightarrow [A_L, A_U]^k [X_L, X_U] [A_L, A_U] = [A_L, A_U]^k \\ &\Rightarrow [A_L^k, A_U^k] [X_L, X_U] [A_L, A_U] = [A_L^k, A_U^k] \\ &\Rightarrow [A_L^k X_L A_L, A_U^k X_U A_U] = [A_L^k, A_U^k] \\ &\Rightarrow A_L^k X_L A_L = A_L^k \text{ and } A_U^k X_U A_U = A_U^k \end{aligned}$$

Therefore A_L is right k – regular and A_U is right k – regular $\in F_n$. Thus A is right k – Regular IVFSM $\Rightarrow A_L$ and $A_U \in F_n$ are right k – regular.

Conversely, Suppose A_L and $A_U \in F_n$ are right k – regular, then $A_L^k X_L A_L = A_L^k$ and

$A_U^k X_U A_U = A_U^k$ for some X_L and $X_U \in F_n$. $X_L \in (A_L)_r(1^k)$, $X_U \in (A_U)_r(1^k)$.

Since $A_L \leq A_U$, it is possible to choose at least one $V \in (A_L)_r(1^k)$ and $W \in (A_U)_r(1^k)$ such that $V \leq W$.

Let us define the interval valued fuzzy matrix $Z = [V, W]$. Then by Lemma(2.12)(ii),

$$\begin{aligned} A^k Z A &= [A_L^k, A_U^k] [V, W] [A_L, A_U] \\ &= [A_L^k V A_L, A_U^k W A_U] \\ &= [A_L^k, A_U^k] \\ &= A^k. \end{aligned}$$

Thus A is right k – regular IVFSM. Hence the theorem.

Theorem 3.6

Let $A = [A_L, A_U] \in (IVFSM)_n$. Then A is left k – regular IVFSM $\Leftrightarrow A_L$ and $A_U \in F_n$ are left k – regular.

Proof:

This can be proved along the same lines as that of Theorem (3.5).

Lemma 3.7

For $A, B \in (IVFSM)_n$, and a positive integer k , the following hold.

(i) If A is right k – regular and $R(B) \in R(A^k)$ then, $B = BXA$ for each right k – g inverse X of A .

(ii) If A is left k – regular and $C(B) \in C(A^k)$ then, $B = AYB$ for each left k – g inverse Y of A .

Proof:

(i) Since $R(B) \in R(A^k)$, by Lemma (2.13), there exists Z such that $B = ZA^k$. Since A is right k – regular, by Definition (3.1), $A^k X A = A^k$ for some $X \in A_r(1^k)$

Hence $B = ZA^k = ZA^k X A = BXA$. Thus (i) holds.

(ii) Since $C(B) \in C(A^k)$, by Lemma (2.13), there exists U such that $B = A^k U$. Since A is left k – regular, by Definition (3.2), $A Y A^k = A^k$ for some $Y \in A_l(1^k)$

Hence $B = A^k U = A Y A^k U = AYB$. Thus (ii) holds.

Theorem 3.8

For $A, B \in (IVFSM)_n$, with $R(A) = R(B)$ and $R(A^k) = R(B^k)$ then A is right k – regular IVFSM $\Leftrightarrow B$ is right k – regular IVFSM.

Proof:

Let A be a right k – regular IVFSM satisfying $R(B^k) \in R(A^k)$ and $R(A) \in R(B)$. Since $R(B^k) \in R(A^k)$, by Lemma (3.7), $B^k = B^k X A$ for each k – g inverse X of A . Since $R(A) \in R(B)$, by Lemma (2.13), $A = Y B$ for some $Y \in (IVFSM)_n$.

Substituting for A in $B^k = B^k X A$, we get,

$$B^k = B^k X A = B^k X Y B = B^k Z B \text{ where } XY = Z.$$





Poongodi and Vinitha

Hence B is a right k – regular IVFSM.

Conversely, if B is a right k – regular IVFSM satisfying $R(A^k) \in R(B^k)$ and $R(B) \in R(A)$, then A is right k – regular IVFSM can be proved in the same manner. Hence the theorem.

Theorem 3.9

For $A, B \in (IVFSM)_n$, with $C(A) = C(B)$ and $C(A^k) = C(B^k)$ then A is left k – regular IVFSM $\Leftrightarrow B$ is left k – regular IVFSM.

Proof:

This is similar to Theorem (3.8) and hence omitted.

Theorem 3.10

For $A = [A_L, A_U]$ and $B = [B_L, B_U] \in (IVFSM)_n$, with $R(A) = R(B)$ and $R(A^k) = R(B^k)$ then the following are equivalent:

- (i) A is right k – regular IVFSM
- (ii) A_L and A_U are right k – regular fuzzy matrices
- (iii) B is right k – regular IVFSM
- (iv) B_L and B_U are right k – regular fuzzy matrices

Proof:

- (i) \Leftrightarrow (ii) and (iii) \Leftrightarrow (iv) are precisely Theorem (3.5).
- (i) \Leftrightarrow (iii) This follows from Theorem (3.8).

Theorem 3.11

For $A = [A_L, A_U]$ and $B = [B_L, B_U] \in (IVFSM)_n$, with $C(A) = C(B)$ and $C(A^k) = C(B^k)$ then the following are equivalent:

- (i) A is left k – regular IVFSM
- (ii) A_L and A_U are left k – regular fuzzy soft matrices
- (iii) B is left k – regular IVFSM
- (iv) B_L and B_U are left k – regular fuzzy soft matrices

Proof:

- (i) \Leftrightarrow (ii) and (iii) \Leftrightarrow (iv) are precisely Theorem (3.6).
- (i) \Leftrightarrow (iii) This follows from Theorem (3.9).

Theorem 3.12

Let $A = [A_L, A_U] \in (IVFSM)_n$, and k be a positive integer, then the following hold.

- (i) if $X = [X_L, X_U] \in A_{r\{1^k\}}$ then $q_c(A_L^k) = q_c(A_L^k X_L)$, $q_c(A_U^k) = q_c(A_U^k X_U)$
and $q_r(A_L^k) \leq q_r(X_L A_L) \leq q_r(A_L)$, $q_r(A_U^k) \leq q_r(X_U A_U) \leq q_r(A_U)$
- (ii) if $X \in A_{r\{1^k\}}$ then $q_c(A^k) = q_c(A^k X)$ and $q_r(A^k) \leq q_r(XA) \leq q_r(A)$
- (iii) if $X = [X_L, X_U] \in A_{l\{1^k\}}$ then $q_r(A_L^k) = q_r(X_L A_L^k)$, $q_r(A_U^k) = q_r(X_U A_U^k)$
and $q_c(A_L^k) \leq q_c(A_L X_L) \leq q_c(A_L)$, $q_c(A_U^k) \leq q_c(A_U X_U) \leq q_c(A_U)$
- (iv) if $X \in A_{l\{1^k\}}$ then $q_r(A^k) = q_r(XA^k)$ and $q_c(A^k) \leq q_c(A X) \leq q_c(A)$

Proof:

Let $A = [A_L, A_U]$

- (i) since $X = [X_L, X_U] \in A_{r\{1^k\}}$, By Definition(3.1) and Lemma (2.12)(ii), $A_L^k X_L A_L = A_L^k$ and $A_U^k X_U A_U = A_U^k$

By Lemma (2.13),

$$C(A_L^k) = C(A_L^k X_L A_L) \subseteq C(A_L^k X_L) \subseteq C(A_L^k) \text{ -----(3.1)}$$

$$\text{and } C(A_U^k) = C(A_U^k X_U A_U) \subseteq C(A_U^k X_U) \subseteq C(A_U^k) \text{ -----(3.2)}$$

$$\Rightarrow q_c(A_L^k) = q_c(A_L^k X_L) \text{ and } q_c(A_U^k) = q_c(A_U^k X_U)$$

Since $A_L^k X_L A_L = A_L^k$ and $A_U^k X_U A_U = A_U^k$ we have,

$$A_L^k = A_L^k X_L A_L = A_L^k (X_L A_L)^2 = \dots = A_L^k (X_L A_L)^k$$





Poongodi and Vinitha

$A_U^k = A_U^k X_U A_U = A_U^k (X_U A_U)^2 = \dots = A_U^k (X_U A_U)^k$
 Therefore, $A_L^k = A_L^k (X_L A_L)^k$, Hence by Lemma (2.13),
 $R(A_L^k) = R(A_L^k (X_L A_L)^k) \subseteq R((X_L A_L)^k) \subseteq R(X_L A_L) \subseteq R(A_L)$
 Therefore $R(A_L^k) \in R(X_L A_L) \in R(A_L)$ -----(3.3)

$Q_r(A_L^k) \leq Q_r(X_L A_L) \leq Q_r(A_L)$
 Similarly, $A_U^k = A_U^k (X_U A_U)^k$, Hence by Lemma (2.13),
 $R(A_U^k) = R(A_U^k (X_U A_U)^k) \subseteq R((X_U A_U)^k) \subseteq R(X_U A_U) \subseteq R(A_U)$
 Therefore $R(A_U^k) \subseteq R(X_U A_U) \subseteq R(A_U)$ -----(3.4)

$Q_r(A_U^k) \leq Q_r(X_U A_U) \leq Q_r(A_U)$ Thus (i) holds.
 since $A = [A_L, A_U] \in (IVFSM)_n$. From (3.1) and (3.2)
 $C(A^k) = C([A_L^k, A_U^k])$

$$= [C(A_L^k), C(A_U^k)] \quad [\text{By Theorem (2.15)}]$$

$$= [C(A_L^k X_L), C(A_U^k X_U)] = C(A^k X)$$

And $Q_c(A^k) = Q_c(A^k X)$

Similarly From (3.3) and (3.4)
 $R(A^k) = R([A_L^k, A_U^k])$
 $= [R(A_L^k), R(A_U^k)] \quad [\text{By Theorem (2.15)}]$
 $\subseteq [R(X_L A_L), R(X_U A_U)]$
 $\subseteq [R(A_L), R(A_U)] = R(A)$

Therefore, $R(A^k) \subseteq R(XA) \subseteq R(A)$.
 $\Rightarrow Q_r(A^k) \leq Q_r(XA) \leq Q_r(A)$. Thus (ii) holds.
 Proof is similar to that of (i) and hence omitted.
 Proof is similar to that of (ii) and hence omitted.

CONCLUSION

In this paper, we proposed Interval valued fuzzy soft matrices and defined some operations on Interval valued fuzzy soft matrices. Finally we extend our approach in to develop the concept of k-regularity on Interval Valued Fuzzy Soft Matrix (IVFSM) as a generalization of regular Fuzzy Matrices and as an extension of k – regular fuzzy matrices. Also some basic properties of a k – regular IVFSM are derived.

REFERENCES

1. Kim, K.H., and Roush, F.N.,(1980), Generalized fuzzy matrices, Fuzzy sets and systems, 4, 293 – 315.
2. Maji P.K., Biswas R. and Roy A.R. 2001. "Fuzzy Soft Set". The Journal of Fuzzy Mathematics, 9(3):pp 589- 602.
3. Majumdar, P., Samantha, S.K. 2010. "Generalised fuzzy soft sets" Computers and mathematics with applications 59, pp:1425-1432.
4. Maji, P.K., Biswas, R., Roy, A.R., 2004. "Intuitionistic Fuzzy soft sets", Journal of fuzzy mathematics, 12, pp:669-683.
5. Manash Jyoti Borah, Tridiv Jyoti Neog, Dushmantha Kumar Sut. 2012. " Fuzzy soft matrix theory and its Decision making" IJMER VOL2, pp:121-127.
6. Meenakshi, AR., (2008), Fuzzy Matrix, Theory and Applications, MJP Publishers, Chennai.
7. Molodtsov D. 1999. "Soft set theory-first result", Computers and Mathematics with Applications, 37: pp 19-31
8. Poongodi. P., (2013) "Inverses of k-Regular Interval-Valued Fuzzy Matrices", Intern. J. Fuzzy Mathematical Archive Vol. 1, 56-61
9. Poongodi. P., (2020) "Orderings on Generalized Regular Interval Valued Fuzzy Matrices", International Journal of Engineering and Advanced Technology (IJEAT), Volume-10, Issue-1, October 2020.
10. Shyamal. A.K., and Pal. M., (2006), Interval Valued Fuzzy Matrices, Journal of Fuzzy Mathematics, Vol 14, No 3, 582 – 592.





Pongodi and Vinitha

11. Thomason, M.G.,(1977), Convergence of powers of fuzzy matrix, J.Math Anal. Appl. 57, 476 – 480.
 12. Yong Yang and Chenli Ji., 2011."Fuzzy soft matrices and their applications "part I, LNAI 7002,pp:618-627

Table 1

U	Result(p ₁)	Conduct(p ₂)	Sports(p ₃)
a ₁	1	1	0
a ₂	0	1	1
a ₃	1	0	1
a ₄	1	0	1

Table 2

U	Result(e ₁)	Conduct(e ₂)
S ₁	0.9	0.8
S ₂	0.3	0.9
S ₃	0.8	0.4
S ₄	0.9	0.3





RESEARCH ARTICLE

Optimization of Process Parameters during Electrical Discharge Machining of Hastelloy C276

K. Jayakumar^{1*}, P.K. Mohinish Kumar², R. Ramakrishnan² and P. Naveenraj²

¹Associate Professor, Department of Mechanical Engineering, Sri Sivasubramaniya Nadar College of Engineering, Kalavakkam - 603110, Tamil Nadu, India.

²UG Student, Department of Mechanical Engineering, Sri Sivasubramaniya Nadar College of Engineering, Kalavakkam - 603110, Tamil Nadu, India.

Received: 26 Feb 2021

Revised: 12 Mar 2021

Accepted: 15 Mar 2021

*Address for Correspondence

K. Jayakumar

Associate Professor,
Department of Mechanical Engineering,
Sri Sivasubramaniya Nadar College of Engineering,
Kalavakkam - 603110, Tamil Nadu, India.
Email: kjayakumar@ssn.edu.in



This is an Open Access Journal / article distributed under the terms of the **Creative Commons Attribution License** (CC BY-NC-ND 3.0) which permits unrestricted use, distribution, and reproduction in any medium, provided the original work is properly cited. All rights reserved.

ABSTRACT

The alloy C-276 alloy is a Ni – Mo - Cr based high temperature resistant super alloy which has excellent resistance to stress corrosion cracking, pitting and oxidizing atmospheres. Hastelloy is widely used in Chemical, Petrochemical, Oil and pump, Gas, Pharmaceutical, Nuclear Power, Solar Power, Pulp and paper production industries. But, during traditional machining of this alloy for making components in different applications creates rapid work harden effect, high heat in machining which raises the weld of the work piece material to the cutting tool surface and later creates notching effect. From different nontraditional machining processes, the Electrical discharge machining (EDM) is the most versatile process and is apt for machining this kind of difficult to machine materials irrespective of its hardness and strength. In the present work, EDM experiments were carried out on the Hastelloy C276 using copper electrode by varying process parameters like current, voltage, pulse on time and electrode diameter as per Taguchi's L9 array. To evaluate the machine ability of the material during EDM, the surface roughness and material removal rate (MRR) were considered as the output responses. The results showed that, average surface roughness (Ra) value increased from 2.246 μm to 3.872 μm for the variation of selected four process parameter. Also, the MRR varied from 0.022 g/min to 0.131 g/min when increase in all four parameters. It is critical to set the process parameters that control the outputs in an optimized condition to obtain the maximum MRR and minimum surface roughness value. Hence, optimum process parameter combination was also identified to get high MRR and low Ra value during machining of the Hastelloy C-276.



Jayakumar *et al.*,**Keywords:** Hastelloy, EDM parameter, Surface roughness, MRR, Taguchi's L9 array, Optimization.

INTRODUCTION

Although there are several variations of the Hastelloy of nickel-based alloy, Hastelloy C-276 is the most widely used in different application. Hastelloy C276 is a Nickel (57 wt%)-chromium (15.5 wt%) -molybdenum (16 wt%) wrought alloy which is considered the most adaptable corrosion resistant alloy existing [1]. This alloy is resistant to the creation of grain boundary precipitates in the weld heat-affected zone, thus making it suitable for most chemical process applications in an as welded condition. Hastelloy C-276 also has outstanding resistance to pitting, stress-corrosion cracking and corroding atmospheres up to 1035 °C and also has excellent resistance to a wide spread variation of chemical atmospheres [2]. EDM is a machining process in which desired profile is obtained by using electrical spark discharges. Material is removed from the work piece by a sequence of current liberations between work piece and tool electrode, disconnected by a dielectric fluid and subject to an applied voltage. When the voltage between the work piece and tool electrode is increased, the intensity of the electric field in the space between the electrodes becomes higher, causing dielectric breakdown of the liquid, and produces an electric spark and it can be controlled as per the shape of the tool electrode [3]. As a result, material is melted, vaporized and removed from the work piece. EDM process is used to machine different difficult to machine materials like super alloys and composites. Few research works have been started in EDM of Hastelloy C276. Maurya and Porwal found that pulse on time (Ton), pulse off time (Toff) and current are the key factors affecting the qualitative measures like surface finish, MRR and TWR during EDM of any materials [4].

Rajesh Choudhary *et al.* [5] identified that current was the significant factor for surface finish followed by Ton time, tool electrode and Toff time during EDM of Hastelloy C-4. They found that the lowest roughness was found at 4A, 100µs Ton time, 47µs Toff time by copper electrode. Baburaja *et al.* [6] tried to machine Hastelloy C276 using Wire EDM process by varying Ton, Toff, wire tension and wire feed speed and measured the surface roughness as the response variable. Wire EDM of Hastelloy C276 was tried to optimize the MRR and Kerf by varying current, voltage, Ton and Toff time [7]. They used Taguchi-Grey analysis for optimization and identified current and voltage were the most significant factors for both responses. From the literature, it was identified that the study on effect of EDM parameter on Hastelloy C276 is in preliminary stage and it can be further analyzed in detail to improve the machinability of this material. Hence, the aim of the present investigation is to examine the effect of EDM parameter along with electrode of different diameter on surface roughness and MRR on Haste alloy C276. Also, the present study suggests the optimum process parameter combination to improve the selected two machinability responses.

MATERIALS AND METHODS

Electrical Discharge Machining (EDM) was used do the drilling of Hastelloy C276 plate of ¼ inch (6.3 mm) thickness with size of work piece of size 30 x 30 mm and is shown in Fig. 1.a. The EDM machine (Make: Electronica Machine Tools Ltd and Model: ZNC) has table size of 500 X 350 mm with electric motor of 1.5 HP was used to drill the work piece and is shown in Fig. 1.b. The copper electrode of varying diameter 6, 8 and 10 mm was used for the drilling and depth of hole was maintained as 4 mm as common for all work pieces with varying current, voltage and pulse on time (Ton). The copper electrode is having more thermal and electrical conductivity and produces smooth finish on the steel work piece compared to other electrode materials [8] and hence it was chosen as tool electrode material in the present study. The Toff time was maintained as fixed value as 30 µs in all experiments and deionized water is used as dielectric fluid. The close view of copper electrode and work piece is shown in Fig. 1.c. The EDM parameters were selected as per the available literature for EDM of the selected work piece material and facility available in the machine and are listed in table 1. Taguchi's L9 orthogonal array experimental design was used to carry out the experiments since it reduces the total number of experiments for the 3 levels 4 factors experiments with 81 full factorial experiments. The experimental runs and the results are listed in table 2. Fig. 1.d shows the nine work pieces





after EDM process. To examine the machinability responses of the HastelloyC276, average surface roughness (Ra) value and MRR were selected as the machinability responses. Ra values were measured using Mitutoyo Surfptest SJ210 model having stylus diameter of 5 μm using cut off length $\lambda_c = 0.8$ mm and number of samples $n = 5$. Average roughness value was measured on the circumference of the inner side of the hole at three different orientations and average of these 3 readings were reported in the result. MRR of the machined material was calculated by using the following formula and the results are given in the table 2. Fig. 2 shows the arrangement for measurement of surface roughness.

Material Removal Rate (MRR) = (Final Weight - Initial Weight) / Time taken during machining

$$\text{MRR} = \text{Weight loss} / \text{Time (gram/min)}$$

RESULTS AND DISCUSSION

Effect of EDM parameters on MRR

Minitab 17 software was used to plot the main effect plots using the experimental results to analyze the effect of EDM parameter on MRR and Surface roughness and are shown in Fig. 3 and 4. From the graph shown in Fig. 3.a, it was inferred that, the MRR increases with the increase in peak current. This is because of the increase of the energy per pulse causing temperature rises suddenly that leads to fast melting of work piece material at sparking zones. The increase in voltage decreased the MRR initially, due to decrease in gap current and after that MRR was increased with increase in gap between electrode and work piece which enhanced the easy removal of machined debris (Fig. 3.b). From Fig. 3. c, the increase in Ton time, increased the MRR due to the increase in discharge energy and spark intensity, as the electrode has more time to remove the material [9]. Increase in electrode diameter initially increased the MRR because larger electrode diameter increases the electrode area, which increases the spark energy and intensity. Further increase in electrode diameter decreased the MRR due to the difficulty in removal of melted debris from the gap between electrode and work piece (Fig. 3.d).

Effect of EDM Parameters on Surface Roughness

From Fig. 4.a, the increase in current increased the powerful sparks with high energy density discharge with increase in size and depth of crater on the work surface which in turn increased the surface roughness of the material [10].As power (Current with Ton time and Voltage) of the EDM electric pulses increased, sparks become more energetic, origins more melting and affects the surface over a longer duration, leading to non-uniform erosion and deeper craters which amplified the value of Ra (Fig. 4.b and 4. c). From Fig. 4.d, the surface roughness decreased as increase in electrode diameter at the beginning. Since small-diameter tool electrode produces a relatively large discharge gap which loses more energy to the dielectric and allows less energy to be transferred to the work piece which forms shallow craters with less roughness value. After that, if the diameter of the electrode increases, the flushing efficiency of dielectric fluid is reduced since the gap between work piece and electrode get decreases thus increased the surface roughness.

Optimization of Process Parameters to Improve MRR and Surface Roughness

From the main effect plot shown in Fig.5, optimum process parameter combination for getting maximum MRR was identified for the levels of Current (Level 3), Voltage (Level 3), Ton (Level 2) and Electrode diameter (Level 2). For getting smooth surface on the inner surface of machined hole, the optimum EDM parameter condition was identified from the Fig. 6 as Current (L2), Voltage (L1), Ton (L2) and Electrode diameter (L2).





CONCLUSIONS

In this experimental study, the effect of EDM process parameter with varying electrode diameter on variation of surface roughness and MRR on nickel-based super alloy-Hastelloy C276 plate was analyzed and the following major inferences were drawn.

- For getting high MRR, high current and voltage with medium Ton time and electrode diameter combinations were suggested. The electrode with 8 mm diameter gave optimum responses for both surface finish and MRR.
- The Surface roughness value is low for medium current, Ton time and Electrode diameter with low voltage.
- From the analysis of variance and slope of the graphs from Fig. 5 and 6, it was found that Ton time and electrode diameter have more significant effect on MRR. Same way, current and voltage were identified as the most significant factors which affect the surface roughness.

REFERENCES

- Khadar Basha SK, Murahari Kolli, Jagannadha Raju MV. Parametric optimization of EDM on Hastelloy C-276 Using Taguchi L18 Technique. International Journal of Engineering & Technology. 2018; 7(2): 714-716.
- Alay shah, Prof. Bindu Pillai. Development of fuzzy model for microslots using EDM. IOSR Journal of Engineering. 2012; 2(5): 1255-1258.
- Jayakumar K. Optimization of Process Parameters During EDM on Inconel Alloy 625. Lecture Notes in Mechanical Engineering. 2021; 897-904.
- Ranu Maurya, Rajesh Kumar Porwal. EDM of Hastelloy - An Overview. Materials Today: Proceedings. 2020; 26(2): 311-315.
- Rajesh Choudhary, Himanshu Garg. Effect of Cryogenic Treatment of Tool Electrode on the Machining Performance and Surface Finish during Electrical Discharge Machining of Hastelloy C-4. Materials Today: Proceedings. 2017; 4(2): 1158-1166.
- Baburaja K, Venkata Subbaiah K, Vanaja T, Ramesh N N. Resultant Surface Roughness Aluminium and Hastelloy C-276 using Wire Electro Discharge Machining. Materials Today: Proceedings. 2017; 4(2): 1013-1018.
- Karim Baig Md, Venkaiah N. Parametric optimization of WEDM for HastelloyC276 using GRA method. International Journal of Engineering Development and Research. 2014; 1(2): 1-7.
- Kaitao XU, ZOU Bin, HUANG Chuanzhen, YAO Yang, ZHOU Huijun, LIU Zhanqiang. Machinability of Hastelloy C-276 Using Hot-pressed Sintered Ti(C7N3)-based Cermet Cutting Tools. 2015; 28(3): 599-606.
- Yadav AK. A parametric optimization and experimental analysis of Wire-EDM on hastelloy-C22 by taguchi method.2017; 1-10.
- Ramesh S, Jenarathanan MP. Investigation of Powder Mixed EDM of Nickel-Based Superalloy Using Cobalt, Zinc and Molybdenum Powders. Transactions of the Indian Institute of Metals. 2021; 1-14.

Table 1. Process parameters and levels

Factors and Levels	Level 1	Level 2	Level 3
Current (A)	15	20	25
Voltage (V)	50	65	80
Ton (μ s)	20	30	40
Electrode diameter (mm)	6	8	10





Jayakumar et al.,

Table 2. Experimental run and results

Sl No	Current (A)-I	Voltage (V)	Ton (μ s)	Electrode Dia.	MRR (g/min)	Surface roughness (μ m)-Ra
1	15	50	20	6	0.022	2.758
2	15	65	30	8	0.065	2.246
3	15	80	40	10	0.061	3.455
4	20	50	40	10	0.094	2.422
5	20	65	20	6	0.066	2.348
6	20	80	30	8	0.100	2.677
7	25	50	30	8	0.131	2.715
8	25	65	40	10	0.048	3.872
9	25	80	20	6	0.105	3.648

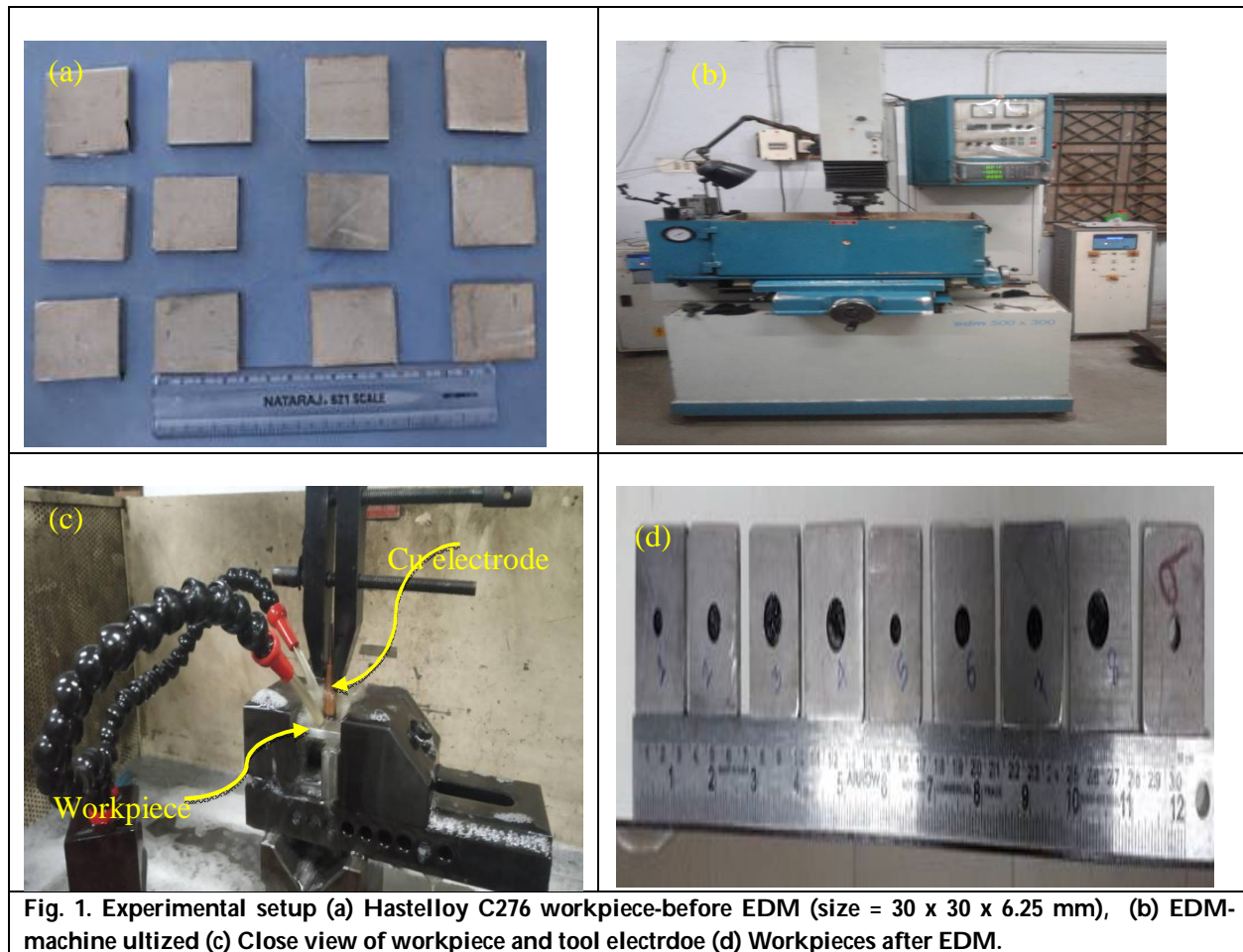


Fig. 1. Experimental setup (a) Hastelloy C276 workpiece-before EDM (size = 30 x 30 x 6.25 mm), (b) EDM-machine utilized (c) Close view of workpiece and tool electrode (d) Workpieces after EDM.



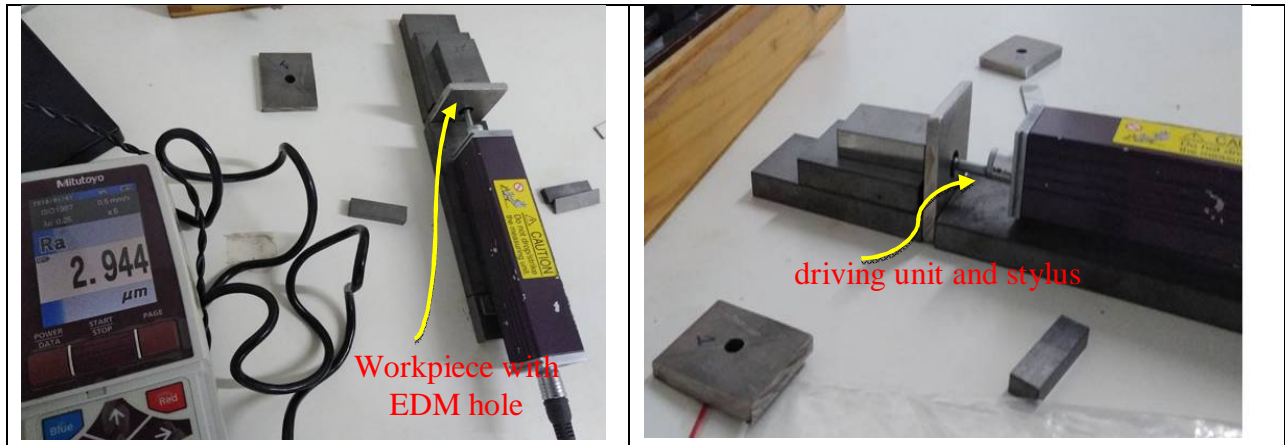


Fig. 2. Arrangement for surface roughness measurement

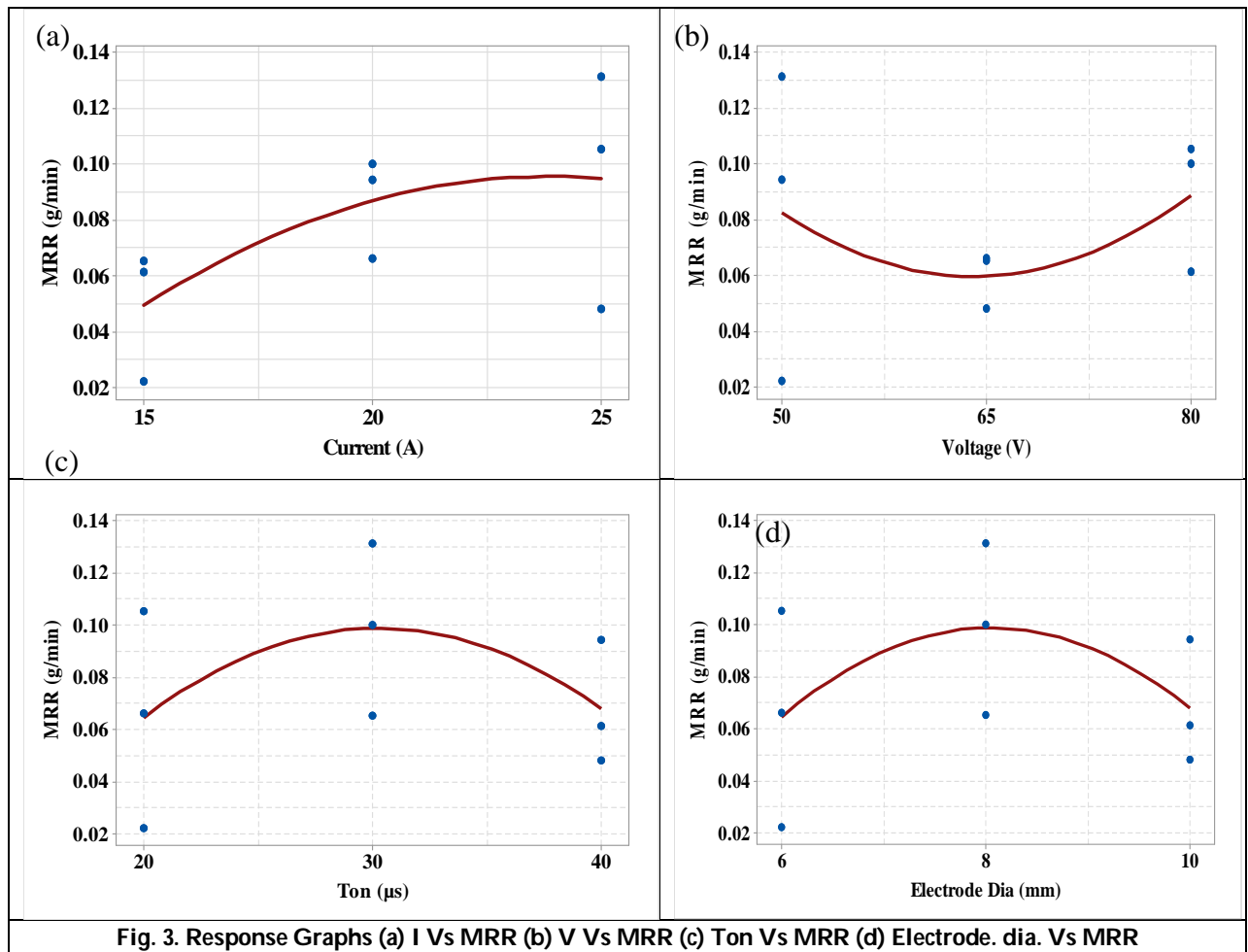


Fig. 3. Response Graphs (a) I Vs MRR (b) V Vs MRR (c) Ton Vs MRR (d) Electrode. dia. Vs MRR





Jayakumar et al.,

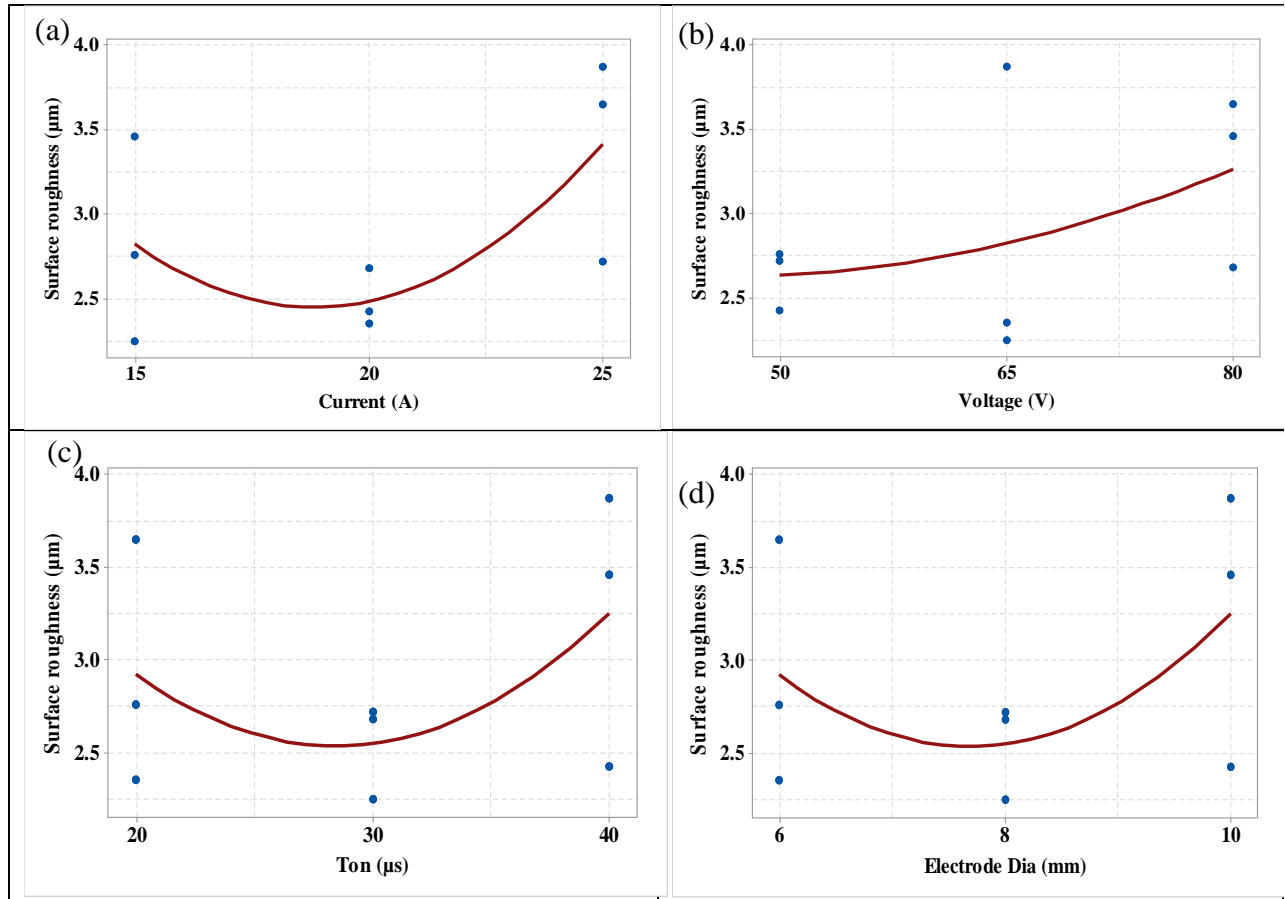


Fig. 4. Response graphs: (a) I Vs Ra (b) V Vs Ra (c) Ton Vs Ra (d) Electrode dia. Vs Ra

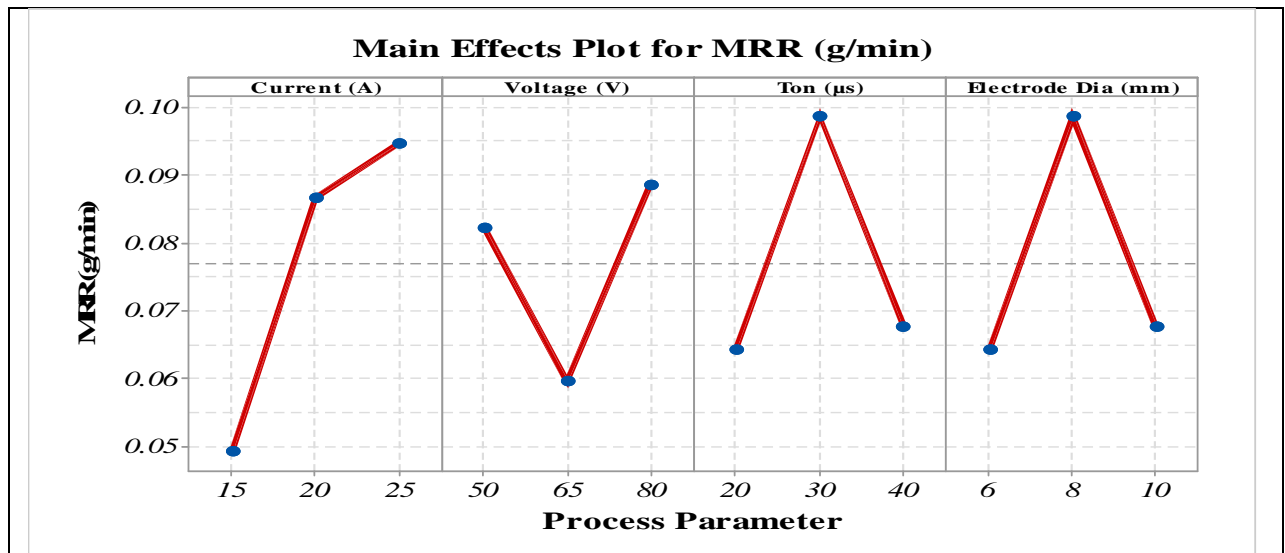
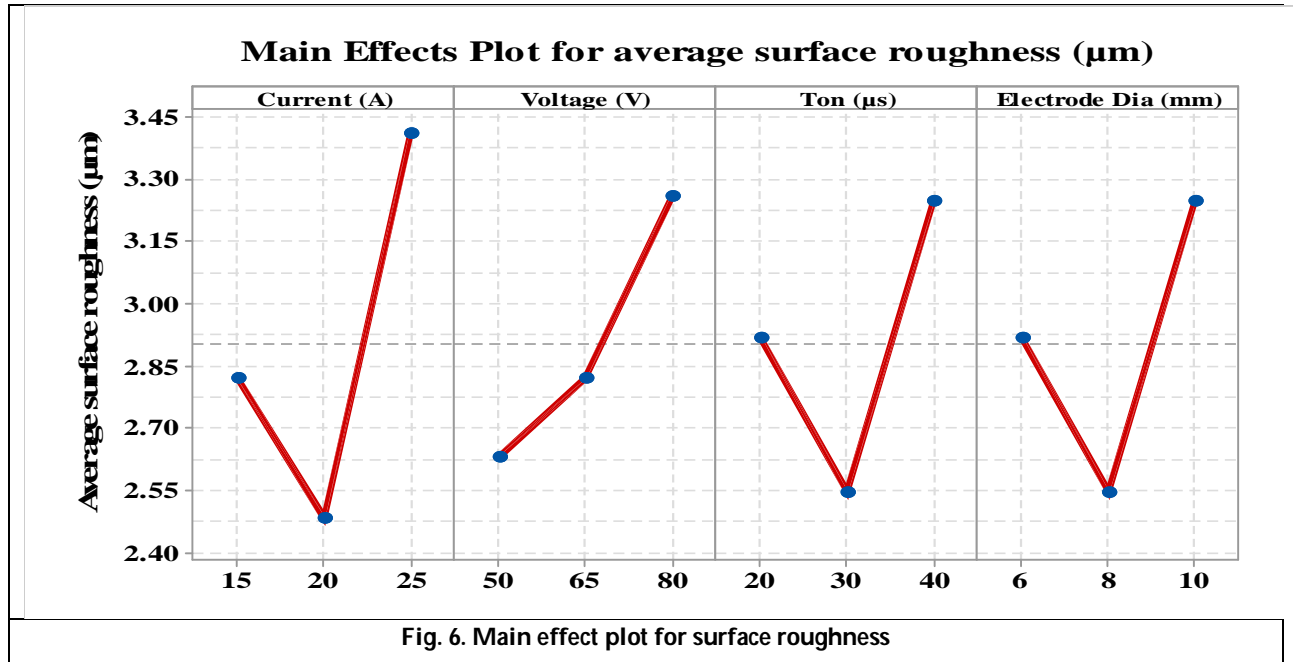


Fig. 5. Main effect plot for MRR







Performance Evaluation of RC Frames with Strong Masonry Infill

Jonathan T Mark and I. Yamini Sreevalli*

School of Civil Engineering, VIT Chennai, Chennai – 600127, Tamil Nadu, India.

Received: 23 Feb 2021

Revised: 06 Mar 2021

Accepted: 12 Mar 2021

*Address for Correspondence

I. Yamini Sreevalli

Associate Professor,
School of Civil Engineering,
VIT Chennai, Chennai – 600127, Tamil Nadu, India.
Email: yaminisreevalli.i@vit.ac.in



This is an Open Access Journal / article distributed under the terms of the **Creative Commons Attribution License** (CC BY-NC-ND 3.0) which permits unrestricted use, distribution, and reproduction in any medium, provided the original work is properly cited. All rights reserved.

ABSTRACT

Prior to the use of design codes for structures masonry infill which had been used as load bearing structures are now used as partition walls in buildings. Though the masonry infill does not take part in the load transfer mechanism, it plays a major role in affecting the behaviour of frame when subjected to seismic loading. The main parameters influencing such behaviour are the relative strength and relative stiffness of infill and frame. This paper aims in understanding the various failure phases in RC infilled frame specimens with different relative strength and relative stiffness when subjected to monotonic loading, through numerical simulation. The software adopted for the simulation of specimens is ABAQUS. Sensitivity analysis is done in order to bring out the appropriate mesh size for more accuracy in simulation results. The validation of the numerical specimens is done by comparing with the numerical and experimental results that have been published. Performance and failure of the infilled frames is expressed in terms of drift percentage. Predominant flexural failure is observed in specimen with relative stiffness of 2.44 and relative strength of 0.34 whereas shear failure is initiated in specimens with relative stiffness of 3.59 and relative strength of 2.47.

Keywords: Relative Strength, Relative Stiffness, Strong masonry infill, One Bay, ABAQUS

INTRODUCTION

The construction of RC frames in contact with the masonry infills have a beneficial effect of increasing the in-plane stiffness which helps in limiting the drift of the structure. On the contrary, many experimental results show that shear failure was dominant in masonry infilled RC frames with ductile design. This observation has led to study the interaction of infill on RC frames experimentally and numerically. Mehrabi *et. al.* [11] conducted an experimental study on the influence of parameters such as strength of infill and frame, number of bays, aspect ratio, and the loading type on the masonry infilled frame's performance. The conclusion from the experimental observation was



**Jonathan T Mark and Yamini Sreevalli**

that brittle shear failure was dominant in strong frame with strong infill and weak frame with strong infill. The failure patterns were classified into five major types.

Experiments were conducted on varying percentage of reinforcement by Murthy and Jain [14]. A total of 12 specimens reduced to a scale of 1:2.7 were tested. All the specimens were single bay single storey with varying sizes of bricks. The specimens were subjected to cyclic loading. It was concluded the presence of infill increased the stiffness and strength thereby improving the energy dissipation capacity. Experimental and numerical studies were carried out by Al-Chaar *et. al.* [1] on infilled RC specimens. All specimens were half-scaled. The parameters varied for the study were type of masonry and the number of bays. The initial stiffness was found to be increased by the infill's presence and the failure pattern was found to be influence by number of bays. Experimental observations of Colangelo [5], Kakaletsis and Karayannis [10], Zovkic *et. al.* [21] also concluded that infill plays a major role in increasing the stiffness and determining the failure pattern of the frame irrespective of the openings, type of frame, openings and infill's strength. The seismic behaviour of RC framed building with infill which was affected due to L'Aquila earthquake was investigated by Michele *et. al.* [13]. It was observed that the behaviour of buildings in terms of stiffness, strength and global ductility were greatly influenced by the presence of infill.

Stavridis [18], Tempestti and Stavridis [20] did numerical studies on the behaviour of infilled RC frames by varying several parameters. It was concluded that the behavior and failure patterns were majorly influenced by relative stiffness and relative strength of frame to infill. Simple classification and prediction methods were proposed to identify the failure mechanisms in infilled RC frames. Micro, meso and macro modelling are the types of modelling approaches used to capture and predict the non-linear behaviour of a material or structure. Tarque *et. al.* [19] reviewed the above modelling techniques and concluded that though macro modelling techniques consume less time and are cost effective, they might not be able to effectively capture the frame-infill interaction when compared to micro modelling techniques. Hakan *et. al.* [8] investigated numerically the effect of infill walls on RC residential buildings when subjected to seismic loading, considering the Turkish Earthquake Code (TEC). The analysis results displayed the beneficial effects of infill in rigidity, roof displacement and the seismic performance of the building.

Finite element modelling technique that can be used as an alternative to experimental tests under seismic loading was introduced by Hossameldeen and Xavier [9]. The analysis included cyclic loading on various infill configuration of RC infilled frames. Comparison between numerical and experimental results revealed that non-linear behavior was captured with accurate prediction of strength, stiffness and failure patterns. Allouzi and Irfanoglu [3] studied numerically, the infilled specimens using ABAQUS software. All specimens were single bay-single storey with infilled masonry. Parameters mainly used for the identification of failure mode of specimens were relative strength and relative stiffness. The shear and flexural failure patterns have been identified using a new hysteretic model. Earlier studies reveal that parameters such as strength of infill, number of bays affect the behavior and failure pattern in infilled RC frames. An attempt has been made to understand and classify the behavior and failure patterns of RC infilled frame by considering the relative strength and relative stiffness parameters in relation with the global drift. Ductile frame having relative stiffness of 2.44 and relative strength of 0.34 and non-ductile frame with relative stiffness of 3.59 and relative strength of 2.47 subjected to monotonic loading are considered in the study. Strong masonry infill is considered in all the specimens. ABAQUS software was used for numerical simulation.

Details of the Specimens

The frame for analysis is adapted from a six storey, three bay, reinforced concrete moment-resisting frame with height to length ratio of 1:1.5. Ground storey middle bay frame, as shown in Fig.1 is taken for analysis. The frame specimen was half scaled with dimension 60.5in x 90in. The frames were adopted from Mehrabi *et. al.* [11] which were designed based on ACI 318-89. Two types of frames considered for the study were, ductile frame (DF) – seismic load design and the non-ductile frame (NDF) – gravity load design. The DF differed from the NDF in the spacing of stirrups in columns and beams, where the stirrups were placed closely at the ends of members in DF and the stirrups were spaced equally throughout the members in NDF. The compressive strength of concrete was 4.5 ksi.



**Jonathan T Mark and Yamini Sreevalli**

Yield stress of main bars and stirrups was 60 ksi and 53 ksi respectively. A spacing of 1.5 inch was provided for the stirrups towards the beam column joints and the ends in the DF specimen. Concrete masonry unit (CMU) with dimensions 3.625 in x 3.625 in x 7.625 in (100 mm x 100 mm x 200 mm) was selected as infill for the frame. The compressive strength of CMU was 2.4 ksi (16.5 MPa) and was categorised as strong infill. The mortar used in the masonry had an average compressive strength of 2.15 ksi (13.5 MPa). Fig.2 shows the dimensions and detailing of non-ductile bare frame specimen. The specimens considered for this study are non-ductile bare frame (NDBF-1), ductile bare frame (DBF-1), non-ductile frame infilled with strong masonry (NDFSM-1) and ductile frame infilled with strong masonry (DFSM-1). All specimens considered are of single bay and single storey. The dimensions, aspect ratio and the reinforcement details of the specimen are given in Table 1.

Finite Element Modelling

The finite element analysis software, ABAQUS 6.14 was used for simulation of the specimens. The material model of various materials used, the interface between the surfaces, boundary conditions and meshing that are required for accurate prediction of the behaviour is described in the following sections.

Material Model

The linear (elastic) and non-linear (plastic) properties of concrete and masonry are the main requirements to capture the cracking, crushing and the failure patterns in the specimen. Young's modulus, density and Poisson's ratio are the main parameters for defining the elastic properties. The elastic properties of concrete, masonry and reinforcing steel used in the specimens are shown in Table 2. Various models such as concrete smeared cracking, Drucker Prager and concrete damage plasticity are available in ABAQUS library through which non-linear simulation can be done effectively. The CDP model has been used by many researches in recent time and is found to effectively capture the failure patterns in reinforced concrete specimens. Material characterization in CDP is defined by plasticity, tensile and compressive behaviour of the material. The stress and strain values obtained from the curves and the corresponding damage values in tension and compression are used to define the tensile and compression behaviour. The parametric values such as K , f_b/f_c , dilation angle and eccentricity obtained from Nasiri and Liu [15] are used to define the plasticity of a material. The values are tabulated in Table 3.

Interface

Interface in this study represents the surface area of contact between the masonry. Failure patterns can be well defined well when the masonry is modelled with mortar enclosing it. The interaction property assigned to the interface was 'Surface to Surface' provide by ABAQUS. The surface between the frame and the brick were assigned the same property of interaction. The interaction property was based on cohesive, tangential and damage behaviour of the bricks. In tangential behaviour the co-efficient of friction was given as 0.87. The cohesive behavior was defined by interaction separation of nodes on the onset of failure. Damage parameters were obtained from Al Louzi, 2015 providing the traction behaviour. The constraint property 'embedded region' was assigned for the reinforcement to be constrained with the frame. The interface details are given in Fig. 3. The assignment of master and slave surfaces in the interface is shown in Fig. 4.

Meshing

Many types of meshing elements are available in ABAQUS library. For concrete and mortar material 3D hexahedral stress element was adopted. For reinforcement in the specimen, truss element (T3D2H) was adopted. The mesh size adopted based on sensitivity analysis was 2.5. The average computational time required for the completion of analysis of bare frame and infilled frames were 12 hours and 36 hours respectively.

Boundary Conditions and Loading

All specimens had a foundation of size 18 in x 18 in x 122 in which was assigned to act as a fixed support (Encastre). The load was displacement controlled type. The surface on the left side of the beam projection was exerted with a





Jonathan T Mark and Yamini Sreevalli

displacement of 2 inch (3.33%). The yield in the longitudinal reinforcement and stirrups was attained before the maximum displacement of the specimen. The yield of either longitudinal bars or the stirrups defined the failure of the specimen. The failure was defined as shear when the stirrups yielded and the failure was defined as flexure when the longitudinal bar yielded.

Mesh Sensitivity Analysis

Mesh sensitivity analysis was carried out in order to select suitable mesh size which can simulate the behaviour of the bare and infilled frame with minimum deviation from the actual behaviour. The simulated results were validated with the results of Mehrabi's [11] specimens 1 & 2. The results of the mesh sensitivity analysis are shown in table 4 & 5. It can be seen from the above table that specimens with mesh size 2.5 and 1.5 have less error when compared to the specimens with mesh size 2 and 1. As the mesh size increased from 1 to 2.5 computational time decreased. Hence a mesh size of 2.5 was adopted for the numerical analysis. Similarly mesh sensitivity analysis has also been carried out for one bay infilled non ductile frame. The various mesh size adopted for the sensitivity analysis were 2.5, 2 and 1.5. The results of the analysis can be found in table 5. From the table it can be observed that the specimen with mesh size 2 performs better than the other specimens as compared with the experimental results. But due to the limitations in computational time mesh size 2.5 has been considered for further analysis.

Relative Stiffness

Relative stiffness can be stated as the ratio of stiffness of infill to the stiffness of the frame. In this study the relative stiffness relation given by Smith [17] is taken as one of the main parameters which defines the failure pattern of the specimen.

$$\lambda h = \sqrt[4]{\frac{E_w t_w \sin(2\theta)}{4E_c I_c h_w}} h \quad (1)$$

Where,

E_w - Elastic Modulus of the wall panel

t_w - Thickness of the wall panel

h_w - Height of the wall panel

E_c - Elastic modulus of the column

I_c - Moment of inertia of the column

h - height of the frame

θ – angle between the diagonal of the frame and the horizontal

The relative stiffness for non-ductile frame was 3.6 and for ductile frame was 2.44.

Relative Strength of the Specimen

Relative strength is defined as the ratio of peak strength developed due to the lateral resistance of the wall to the shear strength provided by the two columns Al Louzi, [2]. Relative strength is given as,

$$\text{RelativeStrength} = \frac{V_{peak}}{V_{sh}} \quad (2)$$

Where,

$$V_{peak} = C A_w + \mu_0 N_w$$

$$V_{sh} = 2(V_s + V_c)$$

C is the shear strength with zero normal stress; A_w is the area of the wall, μ_0 is the coefficient of friction of masonry, N_w is the vertical load applied on the wall, V_s is the shear capacity provided by the stirrups and V_c is the shear capacity provided by the concrete.

The relative strength of the ductile and non-ductile frames is calculated to be 0.34 and 2.47 respectively.





NUMERICAL RESULTS AND DISCUSSIONS

General Observations

The axial stress in reinforcement and tensile damage of RC ductile and non-ductile bare frames, subjected to lateral loading from the simulation are represented in Fig. 5 and Fig.6. The increase in tensile damage with cracking strain can be used to relate the failure patterns at each element and node of the specimen. The degree of damage can be observed from the figures. It can be observed from Fig.5 and Fig. 6 that major cracks prevail in both the specimens. In NDBF-1 specimen the column stirrups have yielded and the longitudinal reinforcement has reached the yield stress. Whereas in DBF-1, the longitudinal reinforcement alone has yielded. The diagonal strut formation in the masonry can be observed from Fig. 7 and Fig.8. The damage in beam and columns can also be observed. Though the failure pattern in frame of both the specimens is observed to be similar the yield of stirrups occurred at different phases. From the axial results the stirrup yield in specimens can be observed to occur at the bottom of left column. In all the specimens the beam column joints had flexural cracks but did not form any hinges rather hinges were formed in the columns of ductile frames.

Load Drift Curves

Fig. 9 represents the load vs displacement curves for the all the specimens considered in this study. The figure above depicts clearly that the increase in stiffness was contributed in major by the infill as the load attained for any particular drift is higher in case of infilled frames when compared to bare frames. An increase in load carrying capacity of 57.7% and 14.5% was observed in infilled non-ductile and ductile specimens respectively when compared to the corresponding bare frames.

Structural Performance- Damage State

Performance limits are given for structural elements by various standards in terms of the drift percentage. The three main performance level are Immediate Occupancy (IO), Life Safety (LS) and Collapse Prevention (CP). The drift percentage suggested by FEMA-273 [6] for the performance levels of unreinforced masonry walls are 0.1%, 0.5% and 0.6% respectively. The drift percentage for concrete frames are 1%, 2% and 4% respectively. Many researchers like Mehrabi and Shing [12], Calvi and Bolognini [4] and Hak *et. al.* [7] have given limit states for infilled RC frames based on various parameters like failure pattern and damage states. In this study, damage in infill RC specimens are classified under seven stages. The stages involve the damage in concrete, masonry and reinforcement and the maximum load attained by the specimens. The details of the seven stages are explained in Table 6. From the results it can be observed that the longitudinal reinforcement in NDBF-1 yielded at a drift of 1.2% (24.69 kips) with the stirrups yielding at 1.8% (27.61 kips). In DBF-1 the yielding of longitudinal bars occurred at a drift of 1.09% (28.09 kips) without any yield of stirrups. The maximum load attained by the NDBF-1 and DBF-1 were 28.4 kips and 31.73 kips respectively.

The first crack in NDFSM-1 was observed at the left column-foundation joint, affecting the brick adjacent to it with a slight damage. In beam crack was observed near the top right at 0.31% drift, at which the masonry also had the initial crack at the surface of interaction of masonry and column towards the left side. The major diagonal crack occurred at a drift of 0.64% and the spalling of CMU was observed at a drift of 0.9%. The yield of stirrups was at 0.8% drift (44.35 kips) where as the yield of longitudinal reinforcement was at 1.1% drift (43.53 kips). It can be seen that the yielding of stirrups occurred earlier than the yielding of longitudinal bars indicating that the specimen had failed by shear. A maximum load of 44.35 kips was attained by the specimen. In DFSM-1 the yield of longitudinal bars occurred at 1.2% (44.92%) drift as similar to NDFMS-1, but the stirrups yielded at 1.5% drift (49.4 kips). The ductility provided in DFSM-1 can be sited as the reason for variation in behaviour in the yielding of longitudinal bars and the stirrups. A maximum load of 52.27 kips was attained by the specimen.





Jonathan T Mark and Yamini Sreevalli

CONCLUSIONS

In this study, two single bay specimens were studied numerically. Masonry infilled ductile frame had a relative stiffness of 2.44 and relative strength of 0.34. The masonry infilled non-ductile frame had a relative stiffness of 3.6 and a relative strength of 2.47. The results can be summarised as follows:

- 1) Predominant flexural failure was observed in ductile bare frame where as shear failure was observed in non-ductile bare frame.
- 2) The specimen with relative stiffness and relative strength of 0.34 and 2.44 had a predominant flexural failure. The specimen with relative stiffness and relative strength of 3.6 and 2.47 failed by shear.
- 3) The initial stiffness of the frame is influenced by the presence of infill and is independent of the ductility conditions.
- 4) Various stages of failure have been proposed along with the load attained and the corresponding drift percentage..
- 5) The yielding of longitudinal reinforcement occurred prior to the yielding of stirrups in DFSM-1 specimen where as in NDFSMS-1 specimen the shear stirrups yielded prior to the longitudinal reinforcement.
- 6) In comparison with the bare frame, the peak load was 57.7% and 14.5% more for non-ductile and ductile specimens respectively.

REFERENCES

1. Al-Chaar, G., Issa, M. and Sweeney, S. (2002), "Behavior of masonry-infilled nonductile reinforced concrete frames", *Journal of Structural Engineering*, **128**(8), 1055-1063.
2. Al Louzi (2015), "Seismic in-plane response of reinforced concrete frames with masonry infill walls", Ph.D. Dissertation, Purdue University, West Lafayette, Indiana.
3. Al Louzi and Ayhan Irfanoglu (2018), "Development of new non-linear dynamic response model of reinforced concrete frames with infill walls", *Advances in Structural Engineering*, **21**(14), 2154-2168.
4. Calvi, G.M. and Bolognini (2001), "Seismic response of reinforced concrete frames infilled with masonry panels weakly reinforced", *Journal of Earthquake Engineering*, **5**(2), 153-185.
5. Colangelo, F. (2005), "Pseudo-dynamic seismic response of reinforced concrete frames infilled with non-structural brick masonry", *Earthquake engineering & structural dynamics*, **34**(10), 1219-1241.
6. FEMA 273 (1993), "NEHRP guidelines for the seismic rehabilitation of buildings", Federal Emergency Management Agency, U.S. Department of Homeland Security, Washington DC, USA.
7. Hak, S., Morandi, P., Magnes, G. and Sullivan, T.J. (2012), "Damage control for clay masonry infills in the design of RC frame structures", *Journal of Earthquake Engineering*, **16**(1), 35.
8. Hakan Dilmac, Hakan Ulutas, Hamide Tekeli and Fuat Demir (2018), "The investigation of seismic performance of existing RC buildings with and without infill walls", *Computers and Concrete*, **22**(5), 439-447.
9. Hossameldeen M. Mohamed and Xavier Romao, "Performance analysis of a detailed FE modelling strategy to simulate the behaviour of masonry-infilled RC frames under cyclic loading" *Earthquakes and Structures*, **14** (6), 551-565.
10. Kakaletsis, D.J. and Karayannis, C.G. (2008), "Influence of masonry strength and openings on infilled R/C frames under cycling loading", *Journal of Earthquake Engineering*, **12**(2), 197-221.
11. Mehrabi, A.B., Benson Shing, P., Schuller, M.P. and Noland, J.L. (1996), "Experimental evaluation of masonry-infilled RC frames", *Journal of Structural engineering*, **122**(3), 228-237.
12. Mehrabi, A.B. and Shing, P.B. (2003), "Seismic analysis of Masonry-infilled reinforced concrete frames", *TMS Journal*.
13. Michele Palermo, Ricardo Rafael Hernandez, Silvia Mazzoni and Tomaso Trombetti, "On the seismic behavior of a reinforced concrete building with masonry infills collapsed during the 2009 L'Aquila earthquake", *Earthquakes and Structures*, **6**(1), 045-069.





Jonathan T Mark and Yamini Sreevalli

14. Murthy, C.V.R. and Jain, S.K. (2000), "Beneficial influence of masonry infill walls on seismic performance of RC frame buildings", *12th World conference On Earthquake Engineering*, Auckland, New Zealand, January.
15. Nasiri, E. and Liu, Y. (2017), "Development of a detailed 3D FE model for analysis of the in-plane behaviour of masonry infilled concrete frames", *Engineering Structures*, **143**, 603-616.
16. Qunxian Huang, Zixiong Guo and Kuang, J.S. (2016), "Designing infilled reinforced concrete frames with the 'strong frame-weak infill' principle", *Engineering Structures*, **123**, 341-353.
17. Smith, B.S. (1967), "Methods for predicting the lateral stiffness and strength of multi-storey infilled frames", *Building Sciences*, **2**, 247-257.
18. Stavridis, A. (2009), "Analytical and experimental study of seismic performance of reinforced concrete frames infilled with masonry walls", Ph.D. Dissertation, UC San Diego.
19. Tarque Nicola, Candido Leandro, Camata Guido and Spacone Enrico (2015), "Masonry infilled frame structures: state-of-the-art review of numerical modelling", *Earthquakes and Structures*, **8**, 225-251.
20. Tempestti, J.M. and Stavridis, A. (2017), "Simplified method to assess lateral resistance of infilled reinforced concrete frames", *16th World Conference in Earthquake Engineering*, Santiago, Chile, January.
21. Zovkic, J., Sigmund, V. and Guljas, I. (2013), "Cyclic testing of a single bay reinforced concrete frames with various types of masonry infill", *Earthquake engineering & structural dynamics*, **42**(8), 1131-1149.

Table 1 Specimen Details

S.No.	Specimen ID	Panel Dimension (c/c distance) (h x l) (in)	Aspect Ratio	Member Details		Reinfor cement (%)	Shear reinforcement
				Column (in)	Beam (in)		
01	NDBF -1	60.5 x 90	0.67	7 x 7	7 x 9	3.2	#2 @ 3' c/c
02	DBF - 1	60.5 x 90	0.67	8x 8	8x 9	3.2	#2 @ 3' c/c and #3 @ 1.5' at the ends of beam and columns
03	NDFSM- 1	60.5 x 90	0.67	7 x 7	7 x 9	3.2	#2 @ 3' c/c
04	DFSM - 1	60.5 x 90	0.67	8 x 8	8x 9	3.2	#2 @ 3' c/c and #3 @ 1.5' at the ends of beam and columns

Table 2 Elastic Properties

Material	Density (kip/in ³)	Modulus of Elasticity (ksi)	Poisson Ratio
Concrete	2.23 E-06	3180	0.2
Steel	7.2636 E-06	29000	0.3
Masonry	2.15547 E-06	1965	0.2

Table3 Model parameters for CDP

Dilation Angle	Eccentricity	fb0/fc0	K	Viscosity Parameter
18	0.1	1.16	0.667	0.001

Table 4 Mesh Sensitivity Analysis of Bare Frame

Mesh Size (in)	No. of Elements	Maximum Load (kips)			Error (%)	Computational time (hours)	Initial Stiffness, k _i (kips/in)
		Experimental (Mehrabi)	Numerical (Mehrabi)	Numerical			
2.5	9,422	23.88	27.5	26.91	-2	4	67.66
2	13,474			32.2	17	6	35
1.5	21386			26.8	-2	11	56.02
1	50243			20.96	-23	103	54.8





Jonathan T Mark and Yamini Sreevalli

Table 5 Mesh Sensitivity Analysis of Infilled frame

Mesh Size (in)	No. of Elements	Maximum Load (kips)		Error (%)	Computational time (hours)	Secant Stiffness, k_s (kips/in)
		Experimental (Mehrabi)	Numerical (NDF)			
2.5	29,655	33.85	37.61	11	48	117.33
2	33,974		35.93	6.1	168	91.43
1.5	60,578		44.68	32	192	131.2

Table 6 Drift ratio and corresponding load at various phases of failure of specimens

Specimen	I		II		III		IV		V		VI		VII	
	Drift (%)	Load (kips)												
NDBF	0.127	8.702	0.27	14.31	-	-	-	-	-	-	1.2	24.69	1.8	27.61
DBF	0.127	8.702	0.27	27	-	-	-	-	-	-	1.09	28.09		
NDFSM-1	0.07	31.84	0.31	38.36	0.31	38.36	0.64	42.54	0.9	44.35	1.1	43.53	0.8	44.35
DFSM-1	0.05	30.93	0.31	38.04	0.31	38.04	0.7	42.45	0.9	44.76	1.2	44.92	1.5	49.4

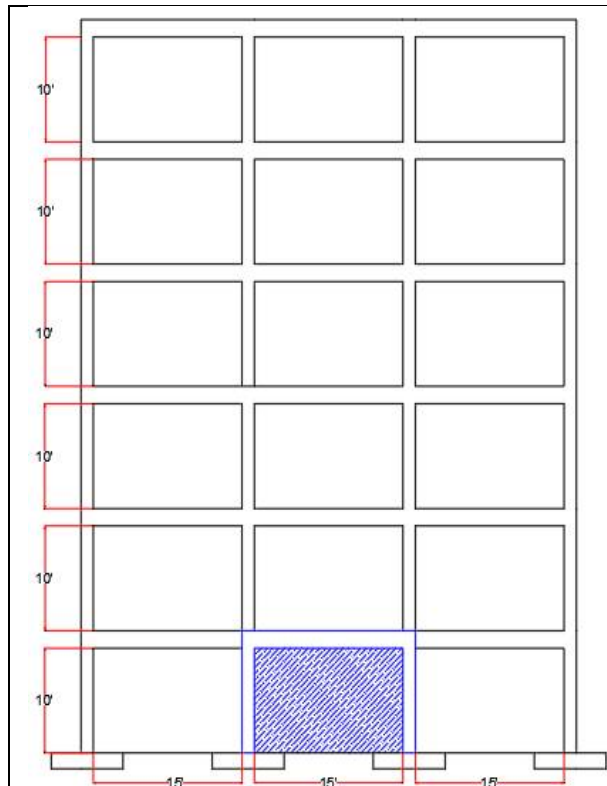
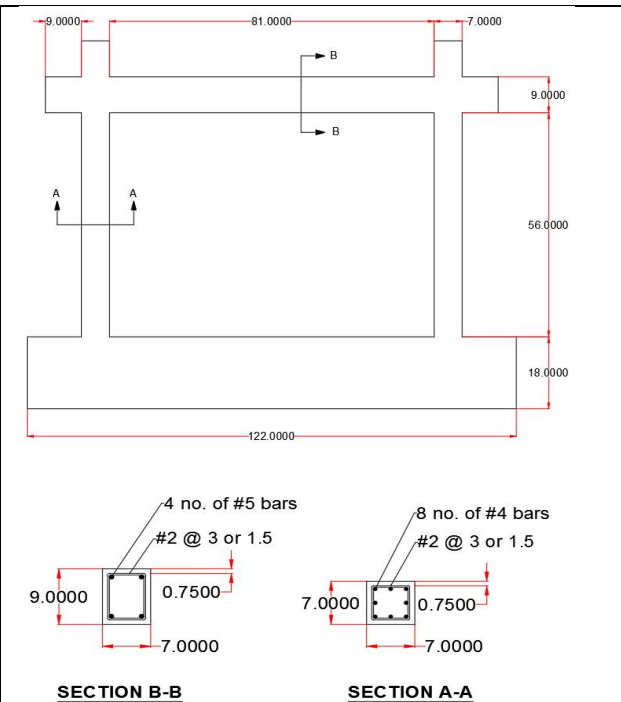


Fig. 1 Prototype with the selected frame



ALL DIMENSIONS ARE IN INCHES

Fig. 2 Dimension of one bay NDBF specimen and Detailing





Jonathan T Mark and Yamini Sreevalli

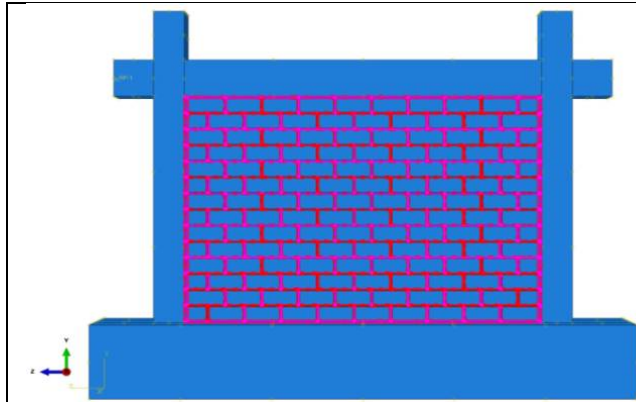


Fig.3 – Brick and mortar model

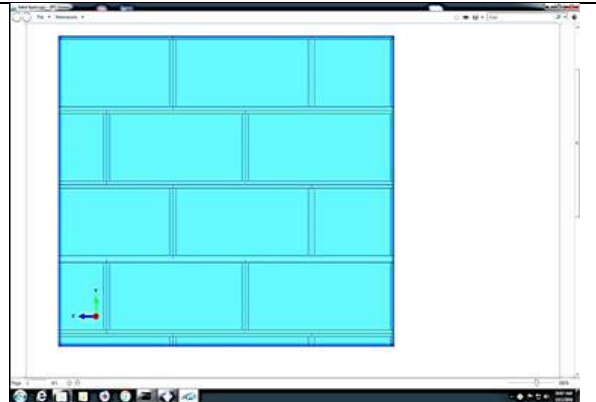


Fig.3A – Half mortar Masonry

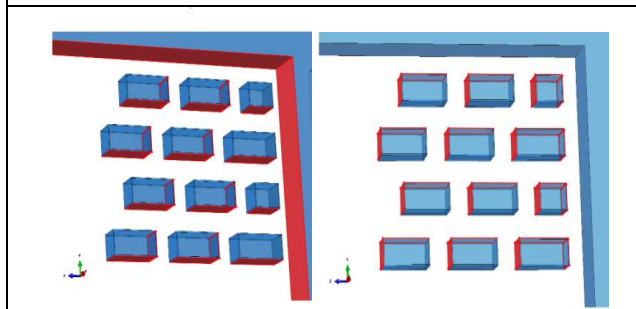


Fig. 4 Assignment of interface property



Fig. 5 Axial stress and tensile damage in NDBF - 1



Fig. 6 Axial stress and tensile damage in DBF - 1

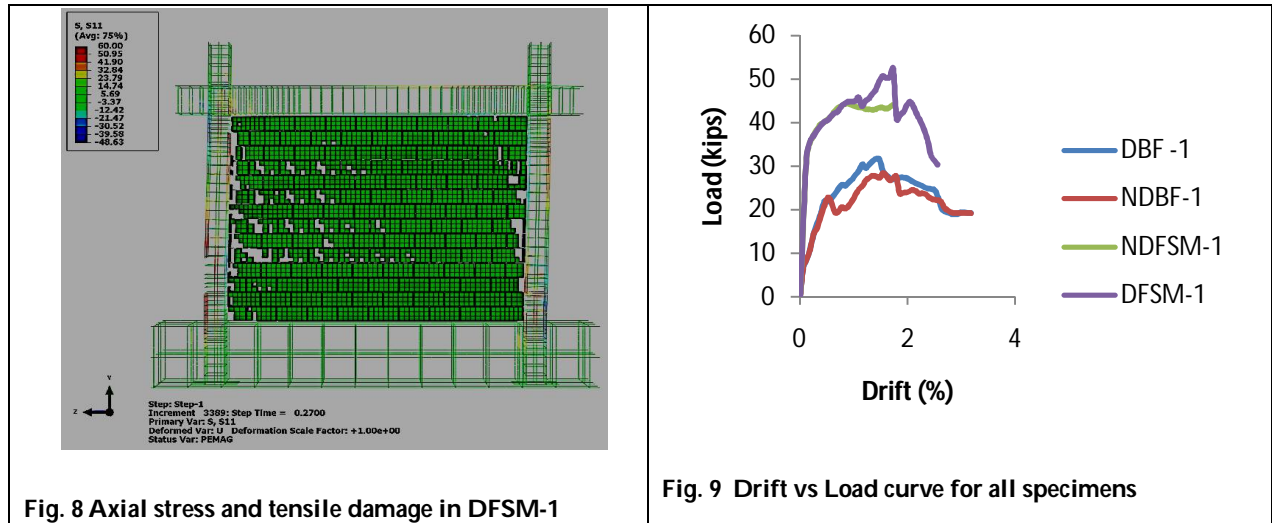


Fig. 7 Axial stress and tensile damage in NDFSMS - 1





Jonathan T Mark and Yamini Sreevalli





RESEARCH ARTICLE

Isolation and Purification of Antimicrobial Protein from *Cocos nucifera* and its Efficacy on Human Pathogens

Subashini R*, Anitha R, Kiruthika N, Kowsalya G, Sivadharshini J

Department of Biomedical Engineering, Sri Sivasubramaniya Nadar College of Engineering, Kalavakkam, Tamil Nadu, India.

Received: 25 Feb 2021

Revised: 10 Mar 2021

Accepted: 15 Mar 2021

*Address for Correspondence

Subashini R

Department of Biomedical Engineering,
Sri Sivasubramaniya Nadar College of Engineering,
Kalavakkam, Tamil Nadu, India.
Email: subashinir@ssn.edu.in



This is an Open Access Journal / article distributed under the terms of the **Creative Commons Attribution License** (CC BY-NC-ND 3.0) which permits unrestricted use, distribution, and reproduction in any medium, provided the original work is properly cited. All rights reserved.

ABSTRACT

A different class of naturally occurring molecules such as antimicrobial peptides and proteins (AMPs), which are produced as a first line of defense by all multicellular organisms. They have the ability to directly kill bacteria, yeasts, fungi, viruses and even cancer cells. An expressive negative impact on human health was initiated by infectious pathogenic bacteria. Currently, microbes acquire a significant enhance in resistance to the commercially available antibiotics that has been observed in all kinds of pathogenic conditions and such common infections are prevented by finding novel approaches. A wide number of defense proteins with bactericidal properties have been characterized and in the present study, a novel AMP was isolated and partially purified from the milk of *Cocos nucifera* through ammonium sulfate precipitation method followed by dialysis. The antimicrobial property of the partially purified protein was tested against various human pathogens like *Streptococcus sp.*, *Staphylococcus spp.*, *Pseudomonas aeruginosa*, *Bacillus sp.*, *Salmonella typhi*. and *Escherichia coli*. The isolated AMP showed antimicrobial activity against all the tested microbial strains except *Bacillus sp.* The activity of the isolated protein was comparatively higher with the partially purified fraction than that of the crude protein. Currently, there is a need for alternative against synthetic chemicals used for antimicrobial therapy due to the quick upsurge in the resistant development among the microbes which is a great challenge to conventional therapies. Hence, the bioactive protein isolated in the present study might fulfill this role since, it displayed antibacterial and antifungal activities and it can be exploited in the development of novel therapeutic agents with further characterization studies.

Keywords: *Cocos nucifera*, SDS-PAGE, AMPs, Human pathogens, bioactive peptide.





Subashini et al.,

INTRODUCTION

Plants are considered as one of the worthy resources of naturally occurring bioactive compounds with antimicrobial activity, as well as proteins. The antimicrobial proteins (AMPs) of plant origin signify one of the main hurdles of plant innate immunity to environmental stress factors which are attracting considerable research interest presently. These class of small molecules are of molecular weight ranging from 2 to 10 kDa with amphiphilic properties and are usually cationic proteins [1]. There are evidences that these cationic charged peptides are appropriate for antibacterial and antiviral activities. AMPs possess a key variation in their structures, but it is reported that most of the plant AMPs comprised of a solid/dense three-dimensional structure which might be due to the presence of intramolecular disulfide bonds [2, 3]. There are several sub-divisions in the plant AMPs leading to several families based upon the resemblance of amino acid sequence, position of disulfide bonds including the presence of cysteine motifs and finally the structure of secondary elements [2, 4]. These are mainly produced by the plants in response to any abiotic or biotic stress factors hence, it takes part as a vital role in innate immunity also, it is reported to have a wide spread range of properties such as antiviral, antibacterial, anti-fungal, insecticidal and anti-proliferative actions. Such kind of activities can be exploited for the progress of novel drugs in the health care industry.

When compared to other plant resources, coconut (*Cocos nucifera* L.) contains a significant source of proteins and a comparatively a well-balanced amino acid profile. Since the milk of coconut possess a major amount of natural minerals, vitamin C and a high quality of proteins, it is measured as a loved food for people with nutritive deficits. But the main focus of research on *Cocos nucifera* is towards its high oil content and there are very few research studies are evidenced towards coconut proteins [5]. A high molecular weight cocosin have been isolated from the endosperm of *Cocos nucifera* by Sjogren and Spsychalski [6]. In an earlier study conducted by Kwon et al [7], have isolated and fractionated five protein fractions from the flour of coconut. Globulins from the endosperm of mature coconut was isolated and characterized by Garcia et al [8]. Wang and Ng [9], isolated an anti-fungal peptide from coconut that showed activity against *Physalospora pircola*, *Mycosphaerella spp.* and *Fusarium oxysporum*. In an additional research work done by Mandal et al [10], discovered three antibacterial peptides from coconut (green) water against *Bacillus subtilis*, *Psuedomonas aeruginosa*, *E. coli* and *S. aureus*. The present work aims to provide insights to the isolation and partial purification of a novel AMP from the endosperm of *Cocos nucifera* and to test its efficiency against human pathogens.

MATERIALS AND METHODS

Test Sample Preparation

Coconut Milk Extraction

AMP'S are present in various sources while, in the present study, coconut is chosen as the source material because they offer a worthy source of proteins with good nutritive value and comparatively well proportionate amino acid profile. Mature coconut was purchased in the resident store of Thiruporur, Chennai. The endosperm of the mature coconut was grated and enveloped in a muslin cloth and squeezed to collect the milk. The collected coconut milk was filtered again using the muslin cloth and stored at -20°C for further use.

Lyophilization

The prepared coconut milk was subjected to lyophilization with frozen condition. The basic principle of lyophilization involves sublimation where dense particle changes right to a vapor devoid of a liquid phase. Frozen sample was then positioned under a profound vacuum, underneath the tripartite point of water and heat energy was applied on the sample triggering the ice to sublime. 5 g of freeze dried sample was obtained as a result of lyophilization of 30ml of coconut milk. It is then placed in a sealed container and stored at -20°C for further use.





Subashini et al.,

Defatting

The dried coconut milk was then defatted using *n*-hexane. The sample was mixed through *n*-hexane at a ratio of 1:10w/v. and was allowed to defat for one hour at room temperature (RT) and then the same process was repeated once again for complete defatting. Then the sample was kept in fume-hood for evaporation of the residual solvent. After defatting, the powdered coconut milk was stored in a sealed container at -20°C.

Protein Extraction

The defatted sample was mixed with the extraction buffer (35 mM potassium phosphate buffer pH 7.6 with 10 mM β-mercaptoethanol, 0.4 M NaCl, 0.1 M PMSF, 0.02 % sodium azide and 1 mM EDTA). The above mixture was then shaken for 3hrs. and centrifuged at 3000 rpm for 30 min., in a refrigerated centrifuge and the supernatant was collected which served as a protein source for further experiments. The supernatant was added with 22.7 g of ammonium sulfate until 80% saturation was attained. It was placed in a shaker for an hour for complete dissolution of ammonium sulphate and then spun at 3000rpm for 30 min. The pellet was recovered and dissolved in phosphate buffer and dialyzed for 24 hrs. in an iced bath with four changes of buffer. The resultant solution was spun to isolate the soluble, insoluble fractions and stored at -20°C for further use. Protein content was determined for both the fractions by Bradford's assay and SDS-PAGE to know the protein profile and to fix the fraction in which low molecular proteins are concentrated.

Determination of Total Protein Concentration

The total protein concentration was evaluated spectrophotometrically using Bradford's assay method with stock solution of BSA (2 mg/ml) as a reference standard and the OD was measured at 295 nm [11].

SDS-PAGE

By adopting Laemmli method [12], the sodium dodecyl sulphate-polyacrylamide was carried out for the isolated protein to check the protein profile using 12 % acrylamide. The protein sample was mixed with sample buffer (0.125M Tris (pH 6.8), 2.5% SDS, 20% glycerol, 0.002% bromophenol blue and 10% β-mercapto ethanol) and boiled for 5 min. Then the sample (40 µg) was loaded onto the gel consisting of 10 % each resolving and stacking gel within the electrophoresis unit (Bio-Rad) in order to separate the protein. Electrophoresis was performed with 100 V power until the sample touched bottom of resolving gel. Coomassie-Blue R-250 was used for staining and de-staining was done using 40 % methanol and 10 % glacial acetic acid. The mass of the antimicrobial peptide was determined using the known molecular weight marker (Bench Mark™ Protein Ladder).

Determination of Antimicrobial Activity

Microbes and Culture Conditions: Microorganisms namely, *Streptococcus spp.*, *Staphylococcus aureus*, *Pseudomonas aeruginosa*, *Bacillus subtilis*, *Salmonella typhi*. and *Escherichia coli* were used in the present study. The microorganisms were cultured and preserved on Muller-Hinton Agar (MHA) plates and stored at 4°C.

Antimicrobial Susceptibility Test

Antimicrobial activity was tested using agar disc diffusion method. The prepared inoculum was seeded with MHA plates and a hole with a width of 6 mm was punched using a sterilized cork borer. Various concentrations of protein samples such as 5, 10, 20 µg/ml were employed on to each well. The reference standard ciprofloxacin (5 µg/ml) disc was used as positive control and 10 % DMSO was used as negative control. Then it was incubated at 37°C for 24hours. The antimicrobial activity was indicated by the presence of clearing zone around the wells (zone of inhibition (ZOI)). The experiments were done in triplicates.

Statistical Analysis

Data in the present study were obtained with mean ± standard deviations of three parallel measurements. The differences among the groups in all studied parameters were analyzed by one-way analysis of variance (ANOVA).



**Subashini et al.,**

The statistical analysis was done by SPSS software (San Diego, USA). *P* values < 0.05 was measured statistically significant [13].

RESULTS AND DISCUSSION

The extraction and purification of AMPs was the primary step in isolating AMPs from the source plant material. However, several AMPs were effectively separated from crude plant extracts and these methods require efficient and sophisticated techniques [2]. Isolation and purification of significant novel AMPs with subsequent sequencing and examining for parallel AMPs in databases is an operative way of identifying new AMPs [14] and many number of AMPs were isolated and recognized using the above techniques. Moreira *et al* [15] reported isolation and functional characterization of an AMP from the crude plant extract of *Lippia sidoides* Cham. (Rosemary pepper) flowers by Octyl-Sepharose hydrophobic column partitioning. Likewise Camargo Filho *et al* [16] reported an antiviral peptide (2kDa) from sorghum (*Sorghum bicolor*) seeds through gel filtration, ion exchange and high-performance liquid chromatography, which displayed significant inhibitory effect on type I herpes simplex virus and herpes bovine virus. Accordingly in the present study, a novel AMP was separated from the endosperm of *Cocos nucifera* which showed potential inhibitory effect towards certain human disease causing microbes and that can be utilized in future for antimicrobial therapy without any side effects. We found that the isolated protein exerted strong antibacterial activity against various gram positive and gram negative bacterial strains as indicated by the zone of inhibition.

Many groups of plant-based AMPs are since been identified with an antimicrobial activity and are purified and characterized which includes hevein-type proteins, glycine-rich proteins, defensins, snakins, puroindolines, lipid transfer proteins and cyclotides [17]. These are considered currently as a significant candidate for developing novel techniques towards monitoring crop loss including new drugs for the treatment of numerous pathogenic conditions in humans and also the recurrent rise of antibiotic-resistant microbes and the disappointment of some conventional antibiotics have all lead to a serious search of new antimicrobial means. In a previously reported study, Vieira *et al* [18] isolated and characterized a novel antimicrobial peptide from the plant *Lecythis pisonis* seeds, which is reported to have inhibitory action against *Candida albicans*. In another study, a novel AMP called Tu-AMP 1 and Tu-AMP 2 was isolated from the bulbs of *Tulipa gesneriana* L. [19].

From the Bradford's assay, it was shown that the insoluble portion exhibited higher protein content of 20.47 µg/ml and the soluble fraction revealed 8.75 µg/ml. The protein profile of both the portions indicated that the portion with insoluble fraction comprises the high molecular weight proteins (45 kDa to 119 kDa) and the fractions with soluble portion contains the low molecular proteins (ranging from 17 kDa to 100 kDa). The molecular mass data acquired for both soluble and insoluble fractions were within the range of already reported molecular weight data of coconut milk proteins in an earlier research work done by Algar and Mabesa [5]. The molecular weight of the isolated AMP was predicted to be 20 kDa through electrophoretic studies.

Antimicrobial activity of both the fractions were tested against various human pathogens and it was observed after the incubation period that the low molecular weight protein was effective against *Streptococcus spp.*, *Staphylococcus aureus*, *Pseudomonas aeruginosa*, *Salmonella typhi*. and *Escherichia coli* as indicated by a larger zone of inhibition (ZOI) (Table 1). The AMP was less active against *Bacillus subtilis*. The crude protein extract exhibited a maximum of antimicrobial effect against *Pseudomonas aeruginosa* with the ZOI value of 32.7±0.94 at a concentration of 20 µg/ml followed by *Salmonella typhi*. (31.3±1.24) whereas that of the reference standard Ciprofloxacin produced ZOI value of 36.3±1.24 (Table 1).

The antimicrobial activity of the partially purified fraction was relatively higher while compared with the crude extract (Fig. 1). The same strain of *Pseudomonas aeruginosa* exhibited susceptibility to the partially purified AMP as indicated by the ZOI value of 33.8±0.83 and the APM has minimal effectively on *Streptococcus spp.* (26.8 ± 1.02) (Table



**Subashini et al.,**

1). The partially purified low molecular weight AMP showed intermediate effect on *Staphylococcus aureus* and *E. coli* while the *Bacillus subtilis* was resistant. Similar results were obtained for a previously conducted study by Sun *et al* [20] where an antibacterial peptide was isolated from protein source of *Spirulina platensis* and it showed antibacterial effect towards *Pseudomonas sp.* and *E. coli* with a ZOI values of 16 and 12 µg/ml respectively. Hence, from the study, it is inferred that the extract of coconut AMP has increased efficiency as compared with the reported algal AMP. These AMPs might act upon bacteria by its ability to cause membrane collapse by interaction with membrane lipids on the bacterial cell surface leading to cell [21-23]. Further purification and characterization of the isolated AMP is under progress.

The World Health Organization (WHO) described that the plants are the rich source to get variety of bioactive compounds and drug molecules and hence, it has to be investigated further to know their activities, efficiency and safety. Therefore an effort was made to explore the probable antimicrobial peptides of medicinal plant. In an earlier reported study, A 7.8 kDa of antimicrobial protein was isolated from the seeds of motherwort [24], likewise in the present study we identified a 20 kDa protein of *Cocos nucifera* subject to further purification and characterization of the isolated AMP is under progress.

CONCLUSION

It is possible to make the plant AMPs as a promising antimicrobial agents by the development of peptide libraries and modern proteomics tools. A negatively charged partially purified protein was extracted from *Cocos nucifera* milk sample with a molecular weight of 20 kDa and exhibited antimicrobial activity against *Pseudomonas aeruginosa*, *Salmonella typhi*. and *E. coli*. The results of the present study directs that apart from the nutritive aids of *Cocos nucifera* milk proteins, it revealed additional useful stuffs and played a key role in preventing the human pathogens and hence, with further characterization studies the isolated AMP can be exploited in the health industry for its probable antimicrobial property.

CONFLICT OF INTEREST

We declare that we have no conflict of interest.

REFERENCES

1. Barashkova AS, Rogozhin EA. Isolation of antimicrobial peptides from different plant sources: Does a general extraction method exist? *Plant Methods* 2020;16(143):1-10.
2. Tang SS, Prodhan ZH, Biswas SK, Le CF, Sekaran SD. Antimicrobial peptides from different plant sources: isolation, characterization, and purification. *Phytochemistry* 2018;154:94–105.
3. Campos ML, De Souza CM, De Oliveira KBS, Dias SC, Franco OL. The role of antimicrobial peptides in plant immunity. *J Exp Bot* 2018;69:4997–5011.
4. Tam JP, Wang S, Wong KH, Tan WL. Antimicrobial peptides from plants. *Pharmaceuticals* 2015;8:711–57.
5. Algar AFC, Mabesa LB. Isolation and partial characterization of a low molecular weight antimicrobial protein from coconut (*Cocos nucifera* L.) milk. *Int Food Res J* 2015;22(5):1813-1816.
6. Sjogren B, Szychalski R. The molecular weight of cocosin. *JACS* 1930;52:4400-4.
7. Kwon K, Kwan HP, Rhee KH. Fractionation and characterization of proteins from Coconut (*Cocos nucifera* L.). *J AgrilFood Chem* 1996;44:1741-45.
8. Garcia RN, Arocena RV, Laurena AC, Tecson Mendoza EM. 11S and 7S globulins of coconut (*Cocos nucifera* L.): purification and characterization. *J AgrilFood Chem* 2005;53:1734-39.
9. Wang H, Ng TB. An anti-fungal peptide from the coconut. *Peptides* 2005;26:2392-96.





Subashini et al.,

10. Mandal SM, Dey S, Mandal M, Sarkar S, Maria-Neto S, Franco OL. Identification and structural insights of three antimicrobial peptides isolated from green coconut water. *Peptides* 2009;30(4):633-37.
11. Bradford MM. A rapid sensitive method for the quantification of microgram quantities of protein utilizing the principle of protein-Dye Binding. *Anal Biochem* 1976;72:248-254.
12. Laemmli UK. Cleavage of structural proteins during the assembly of the head of bacteriophage T4. *Nature* 1970;227:680-685.
13. Anitha R, Subashini R, Senthil Kumar R. In silico and in vitro approaches to evaluate the bioactivity of *Cassia auriculata* L extracts. *IET Nanobiotechnol* 2020;14(3):210-216.
14. Odintsova TI, Vassilevski AA, Slavokhotova AA, Musolyamov AK, Finkina AI, Khadeeva NV et al. A novel antifungal heveintype peptide from *Triticum kiharae* seeds with a unique 10-cysteine motif. *FEBS J* 2009;276:4266-4275.
15. Moreira JS, Almeida RG, Tavares LS, Santos MO, Viccini LF, Vasconcelos IM et al. Identification of botryticidal proteins with similarity to NBS-LRR proteins in rosemary pepper (*Lippia sidoides* Cham.) flowers. *The Prot J* 2011;30:32-8.
16. Camargo Filho I, Cortez D, Ueda-Nakamura T, Nakamura C, Dias Filho B. Antiviral activity and mode of action of a peptide isolated from *Sorghum bicolor*. *Phytomed* 2008;15:202-8.
17. Noonan J, Williams WP, Shan X. Investigation of antimicrobial peptide genes associated with fungus and insect resistance in maize. *Int J Mol Sci* 2017;18(9):1938.
18. Vieira MEB, Vasconcelos IM, Machado OLT, Gomes VM, André de Carvalho O. Isolation, characterization and mechanism of action of an antimicrobial peptide from *Lecythis pisonis* seeds with inhibitory activity against *Candida albicans*. *Acta Biochimica Biophysica Sinica* 2015;47(9):716–29.
19. Fujimura M, Ideguchi M, Minami Y, Watanabe, Tadera K. Purification, characterization, and sequencing of novel antimicrobial peptides, Tu-AMP 1 and Tu-AMP 2, from bulbs of tulip (*Tulipa gesneriana* L.). *Biosci Biotechnol Biochem* 2004;68(3):571–7.
20. Sun Y, Chang R, Li Q. Isolation and characterization of an antibacterial peptide from protein hydrolysates of *Spirulina platensis*. *Eur Food Res Technol* 2016;242:685–92.
21. Epanand RM, Vogel HJ. Diversity of antimicrobial peptides and their mechanisms of action. *Biochimica et Biophysica Acta* 1999;1462(1-2):11–28.
22. Sitaram N, Nagaraj R. Interaction of antimicrobial peptides with biological and model membranes: structural and charge requirements for activity. *Biochimica et Biophysica Acta* 1999;1462(1-2):29–54.
23. Yeaman MR, Yount NY. Mechanisms of antimicrobial peptide action and resistance. *Pharmacol Rev* 2003;55:27–55.
24. Yang X, Xiao Y, Wang X, Pei Y. Expression of a novel small antimicrobial protein from the seeds of motherwort (*Leonurus japonicus*) confers disease resistance in tobacco. *Appl Environ Microbiol* 2007;73(3):939-46.

Table 1. Zone of Inhibition Values of Crude Protein and Partially Purified Protein.

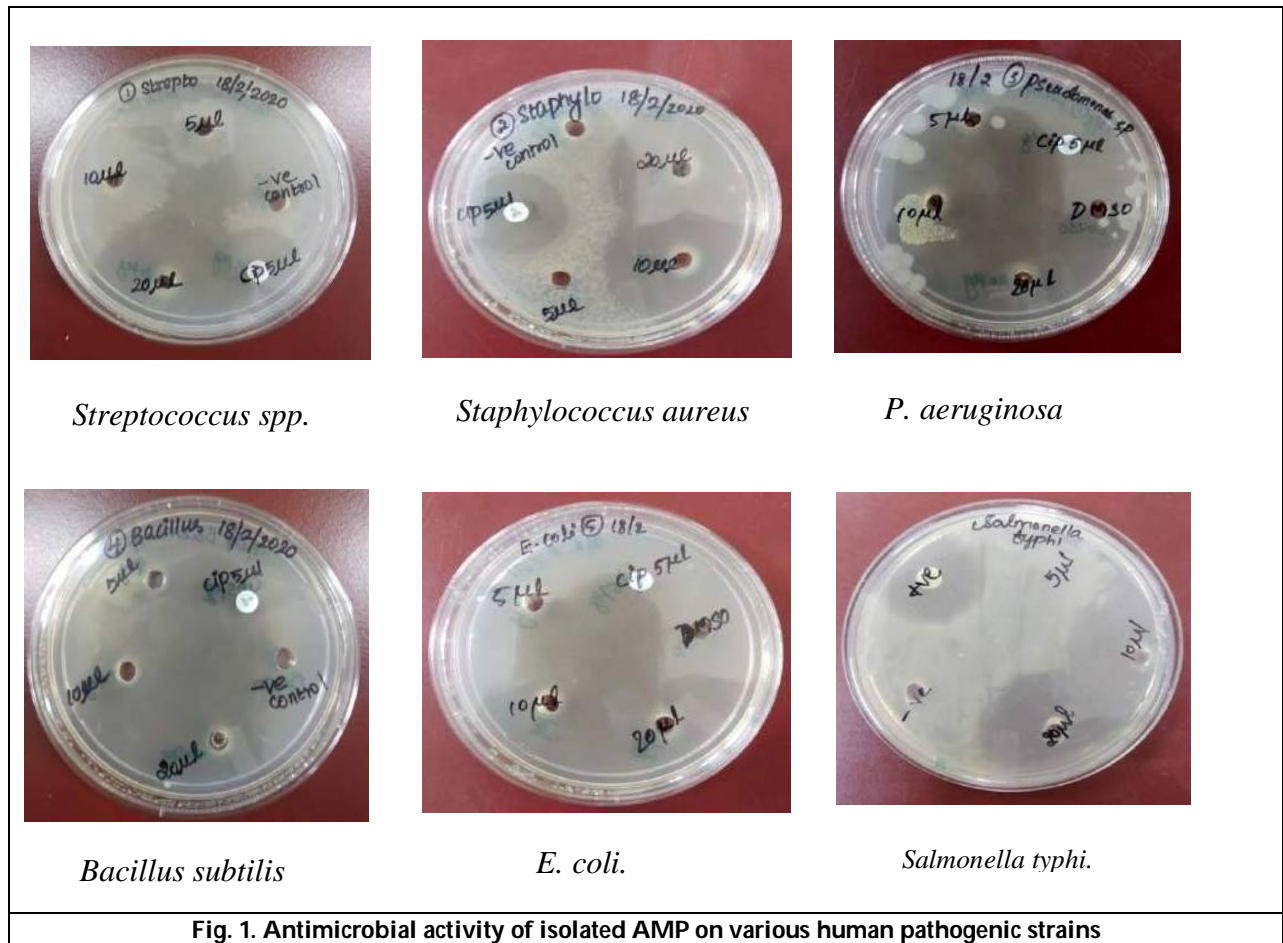
Strains	ZOI (mm) of Crude protein			ZOI (mm) of partially purified protein				
	5 µg/ml	10 µg/ml	20 µg/ml	5 µg/ml	10 µg/ml	20 µg/ml	+ve control	10 % DMSO
<i>Streptococcus spp.</i>	5±0.09	10.3±0.32	24.7±1.24	10±0.4	13.1±0.52	26.8±1.02	28.2±1.22	--
<i>Staphylococcus aureus</i>	20±0.57	27.3±0.94	29.6±0.54	25±0.6	29.9±0.81	30.3±1.26	34.4±0.83	--
<i>Pseudomonas aeruginosa</i>	19±0.5	27±0.81	32.7±0.94	25±0.5	27.5±0.69	33.8±0.83	36.8±1.22	--
<i>Salmonella typhi.</i>	20±0.3	23.3±0.46	31.3±1.24	23±0.6	24.2±0.73	32.2±0.92	38.4±0.66	--
<i>Bacillus subtilis</i>	0	0	0	0	0	0	0	--
<i>Escherichia coli</i>	21±1.0	25±1.3	30.2±0.67	25±1.0	26.6±1.05	32±0.67	34.5±1.38	--

Values are the means ± SD, n = 3, P < 0.05. ZOI: Zone of inhibition, +ve control: Ciprofloxacin, -: No ZOI.





Subashini et al.,





A New Operation Approach in Topological Spaces

Shanmugapriya H^{1*}, Vidhyapriya P¹ and Sivakamasundari K²

¹Research Scholars, Department of Mathematics, Avinashilingam Institute for Home Science and Higher Education for Women, Coimbatore, Tamil Nadu, India.

²Professor, Department of Mathematics, Avinashilingam Institute for Home Science and Higher Education for Women, Coimbatore, Tamil Nadu, India.

Received: 23 Feb 2021

Revised: 03 Mar 2021

Accepted: 06 Mar 2021

*Address for Correspondence

Shanmugapriya H

Research Scholars,

Department of Mathematics,

Avinashilingam Institute for Home Science and Higher Education for Women,

Coimbatore, Tamil Nadu, India.

Email: shanmugapriyahs@gmail.com



This is an Open Access Journal / article distributed under the terms of the **Creative Commons Attribution License** (CC BY-NC-ND 3.0) which permits unrestricted use, distribution, and reproduction in any medium, provided the original work is properly cited. All rights reserved.

ABSTRACT

The main aim of this paper is to introduce the concept of an operation on a new class of δ P_s-open subsets in topological spaces. Moreover the concepts of q -open sets, q -regular sets are defined using the newly introduced operation here. Some concepts namely q -limit points, q -closure, cl_q of a subset S [$qCl(S)$ and $Cl_q(S)$ respectively] are defined and studied.

Keywords: q -open sets, q -regular spaces, q -limit points, q -closure and Cl_q .

INTRODUCTION

"The idea of semi-open sets was initiated by Levine in 1963[9]. In 1968 [14], the class of δ -open subsets of a topological space was first initiated by Velicko. This class of sets plays an important role in the study of various properties in topological spaces. Since then many authors used this class to define new classes of sets in topological spaces. The idea of pre open sets was initiated by Mashhour, Abd El-Monsef and El-Deeb in 1982[11]. On the other hand, Kasaharain 1979 [8] defined the idea of an operation on τ and initiated the concept of α -closed graphs of functions. The operation α had will be renamed as γ operation on τ by Ogata in 1991[6]. In 1993, Raychaudhuri and Mukherjee [12] initiated and investigated a class of sets ceached δ -pre open. Cuong and Maki in 2008[2] explained and analysed the idea of the mapping γ_p on the collection of each pre open subsets of (X, τ) , and initiated the notion of pre γ_p -open sets and studied some of their properties.

Khalaf and Asaad in 2009 [1] initiated a new concept ceached P_s-open sets in topological spaces. Operation approaches on P_s-open sets and its separation axioms was initiated by Assad in 2016[3]. Combining the concepts of

30529





Shanmugapriya et al.,

δ -pre open and P_s -open sets, a new class of sets called δP_s -open sets is initiated by Vidhyapriya, Shanmugapriya and Sivakamsundari in 2020 [13]. The main purpose of this paper is to initiate the concept of an operation ϱ on δP_s -open subsets in topological spaces using this operation we define the idea of ϱ -open sets and obtain some topological properties of ϱ -open sets."

Preliminaries

"The closure and interior of S with respect to W are meant by $Cl(S)$ and $Int(S)$ respectively".

Definition 2.1: "A subset S of a space W is called

1. δ -pre open [12] if $S \subseteq Int(\delta Cl(S))$

2. Semi-open [9] if $S \subseteq Cl(Int(S))$

The complement of a semi-open set is called a semi-closed set."

Definition 2.2[13] : "A δ -pre open subset S of a space W is called as **δP_s -open** set if for each $p \in S$, there will be a semi closed set F satisfying that $p \in F \subseteq S$."

Definition 2.3[6]: "An operation γ on topology τ on W is a mapping $\gamma: \tau \rightarrow P(W)$ satisfying that $U \subseteq U^\gamma$ for each $U \in \tau$ where U^γ denotes the value of U under γ . A nonempty set S of W is called **γ -open** if for each $p \in S$, there will be an open set U satisfying that $p \in U$ and $U^\gamma \subseteq S$.

Definition 2.4[2]: An operation γ_p on $PO(W)$ is a mapping $\gamma_p: PO(W) \rightarrow P(W)$ satisfying that $U \subseteq U^{\gamma_p}$ for each $U \in PO(W)$, where U^{γ_p} denotes the value of U under γ_p . A nonempty set S of W is called **pre γ_p -open** if for each $p \in S$, there will be a pre open set U satisfying that $p \in U$ and $U^{\gamma_p} \subseteq S$."

Definition 2.5[10]: "A space W is called **semi- T_1** if for each pair of distinct points p, q in W , there will be a pair of semi-open sets, one having p but not q and the other having q not p .

Proposition 2.6[13]: Every regular open set is a δP_s -open set."

Definition 2.7[5]: "A space W is called **locally indiscrete** if each open subset of W is closed.

Theorem 2.8[13] (i). In a locally indiscrete space, $\delta P_s O(W) =$ (ii). If a space W is semi- T_1 , then $\delta P_s O(W) = \delta PO(W)$."

Proposition 2.9[13]: "Every P_s -open set is a δP_s -open set.

Proposition 2.10[3]: Every P_s^γ -open set is a P_s -open set."

Proposition 2.11[13]: "Any union of δP_s -open sets is a δP_s -open set."

Definition 2.12[13]: "A point p in W is said to be **δP_s -closure** of S if $f S \cap U \neq \varphi$, for each δP_s -open set U having p , it is meant by $\delta P_s Cl(S)$."

Operation Approaches on δP_s -Open Sets in Topological Spaces

Definition 3.1: An operation ϱ on $\delta P_s O(W)$ is a mapping $\varrho: \delta P_s O(W) \rightarrow P(W)$ satisfying that, $H \subseteq H^\varrho$ for each $H \in \delta P_s O(W)$, where $P(W)$ is the power set of W and H^ϱ is the value of H under ϱ .





Shanmugapriya et al.,

Exemplar 3.2: Let $W = \{p, q, r\}$ and $\tau = \{\phi, W, \{p\}\}$ $\delta P_s O(W) = \{\phi, W, \{q\}, \{r\}, \{q, r\}\}$. An operation $q : \delta P_s O(W) \rightarrow P(W)$ is defined as follows, for each $H \in \delta P_s O(W)$

$$H^q = \begin{cases} clH, & \text{if } r \in H \\ H, & \text{if } r \notin H \end{cases}$$

Then, $H^q(\{q\}) = \{q\}$, $H^q(\{r\}) = \{q, r\}$, $H^q(\{q, r\}) = \{q, r\}$

Definition 3.3: Let (W, τ) be a topological space and $q : \delta P_s O(W) \rightarrow P(W)$ be an operation on $\delta P_s O(W)$. A nonempty set S of W is called **q-open set** if for each $p \in S$, there will be a δP_s -open set H satisfying that $p \in H$ and $H^q \subseteq S$.

“The complement of a q-open set of W is called a q-closed set.

The collection of each q-open subsets of a space (W, τ) is meant by $qO(W)$.

For each $p \in W$, the collection of each q-open sets of (W, τ) having a point p is meant by $qO(W, p)$.

Proposition 3.4: Every q-open set is a δP_s -open set.

Proof: Consider a q-open set S . Then by definition 3.3 for each $p \in S$, there will be a δP_s -open set H with $p \in H_p$ and $H_p^q \subseteq S$. But by definition 3.1, each $H_p \subseteq H_p^q$.

Hence, $S = \cup_{p \in S} \{p\} \subseteq \cup H_p \subseteq \cup H_p^q \subseteq S$.

In turn which implies, $S = \cup H_p$ which is a δP_s -open set, since any union of δP_s -open sets is a δP_s -open set, by proposition 2.11.

Exemplar 3.5 Let $W = \{p, q, r\}$ and $\tau = \{\phi, W, \{p\}, \{q\}, \{p, q\}\} = \delta P_s O(W)$. An operation $q : \delta P_s O(W) \rightarrow P(W)$ is defined as follows, for each $H \in \delta P_s O(W)$

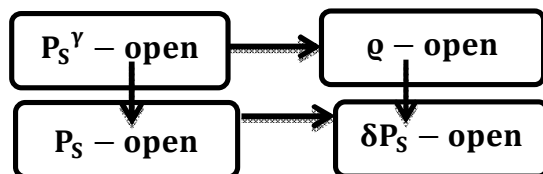
$$H^q = \begin{cases} clH, & \text{if } p \in H \\ H, & \text{if } p \notin H \end{cases}$$

Therefore, $qO(W) = \{\phi, W, \{q\}\}$

Clearly the above example gives that every q-open set is δP_s -open set.

(i.e) $qO(W) \subseteq \delta P_s O(W)$ but the converse is not true” since $\{p\}$ and $\{p, q\}$ are in $\delta P_s O(W)$ but not in $qO(W)$.

Remark 3.6:



Remark 3.7

In general we cannot compare P_s^γ -open sets and q-open sets. But if q is the restricted map, $P_s^\gamma | \delta P_s O(W)$, then P_s^γ -open sets are q-open sets, Since each P_s -open set is a δP_s -open set.

Definition 3.8: The identity mapping id on $\delta P_s O(W)$ is a mapping $q^{id} : \delta P_s O(W) \rightarrow P(W)$ satisfying that $q^{id}(H) = H$ for every $H \in \delta P_s O(W)$.

Remark 3.9: A subset S is q^{id} -open of W iff S is δP_s -open in W . Then $\delta P_s O(W) = q^{id}O(W)$.

Proposition 3.10: Let (W, τ) be a topological space and $q : \delta P_s O(W) \rightarrow P(W)$ be an operation on $\delta P_s O(W)$. “Then the results below are true:

(a) The union of any collection of q-open sets in W is also a q-open.

(b) The intersection of any collection of q-closed sets in W is also a q-closed.

Proof: (a) Consider a collection $\{S_\lambda\}_{\lambda \in \Delta}$ of q-open sets in W . Then for each $p \in S_\lambda$, by definition 3.3, there will be a δP_s -open set H with $p \in H$ and $H^q \subseteq S_\lambda \subseteq \cup \{S_\lambda\}$.





Shanmugapriya et al.,

Thus $\cup\{S_\lambda\}$ is a q -open set.

(b) Consider a collection $\{T_\lambda\}_{\lambda \in \Delta}$ of q -closed sets in W . Then $\{T_\lambda^c\}_{\lambda \in \Delta}$ is the q -open sets which implies $\cup\{T_\lambda^c\}$ is a q -open set from part (a). But $\cup\{T_\lambda^c\} = (\cap\{T_\lambda\})^c$. Hence $\cap\{T_\lambda\}$ is a q -closed set.

Generally, the intersection (resp. the union) of any two q -open (resp. q -closed) sets in (W, τ) will not be a q -open (resp. q -closed) sets as given in the exemplar below.

Exemplar 3.11: Consider the space $W = \{p, q, r, s\}$ and $\tau = \{ \phi, W, \{p\}, \{p, q\} \}$

$\delta P_s O(W) = \{ \phi, W, \{q\}, \{r\}, \{s\}, \{q, r\}, \{q, s\}, \{r, s\}, \{q, r, s\} \}$. An operation $q : \delta P_s O(W) \rightarrow P(W)$ is defined as follows, for each $H \in \delta P_s O(W)$

$$H^q = \begin{cases} H, & \text{if } q \in H \\ \{p, r\}, & \text{if } \{p, r\} = H; \{p, s\} \text{ if } \{p, s\} = H; \{r, s\} \text{ if } \{r, s\} = H \\ W, & \text{Otherwise} \end{cases}$$

Hence $q O(W) = \{ \phi, W, \{q\}, \{q, r\}, \{q, s\}, \{r, s\}, \{q, r, s\} \}$ and q -closed sets denoted by

$q C(W) = \{ \phi, W, \{p\}, \{p, q\}, \{p, r\}, \{p, s\}, \{p, r, s\} \}$. Here $\{q, s\}$ and $\{r, s\}$ are q -open sets, but $\{q, s\} \cap \{r, s\} = \{s\}$ is not a q -open set. Also, $\{p, q\}$ and $\{p, s\}$ are q -closed sets, but $\{p, q\} \cup \{p, s\} = \{p, q, s\}$ is not q -closed set. Thus, the collection of each q -open sets of any topological space (W, τ) is not a topology on W in general.

Definition 3.12: An operation $\gamma_{\delta p}$ on $\delta PO(W)$ is a mapping $\gamma_{\delta p} : \delta PO(W) \rightarrow P(W)$ satisfying that, $\cup U \subseteq U^{\gamma_{\delta p}}$ for each $U \in \delta PO(W)$, where $U^{\gamma_{\delta p}}$ denotes the value of U under $\gamma_{\delta p}$. A nonempty set S of W is called **$\gamma_{\delta p}$ -open** if for each $p \in S$, there will be a δ -preopen set U satisfying that, $p \in U$ and $U^{\gamma_{\delta p}} \subseteq S$.

Theorem 3.13: The properties below are true:

(a) If (W, τ) is semi- T_1 , then the operations q on $\delta P_s O(W)$ and $\gamma_{\delta p}$ on $\delta PO(W)$ are the same and hence q -open sets and $\gamma_{\delta p}$ -open sets coincide.

(b) In a locally indiscrete space (W, τ) the operations q on $\delta P_s O(W)$ and γ on τ are the same and hence q -open sets and γ -open sets coincide.

Proof:

(a) By theorem 2.8(ii), in a semi T_1 space δP_s -open sets coincide with δ -preopen sets. If the operations q on $\delta P_s O(W)$ and $\gamma_{\delta p}$ on $\delta PO(W)$ are defined the same then the q -open sets coincide with $\gamma_{\delta p}$ -open sets in (W, τ) .

(b) By theorem 2.8(i), in a locally indiscrete space δP_s -open sets coincide with open sets. If the operations q on $\delta P_s O(W)$ and γ on τ defined the same then the q -open sets coincide with γ -open sets in (W, τ) .

Definition 3.14: Let (W, τ) be any topological space. An operation q on $\delta P_s O(W)$ is considered to will be **δP_s -regular** if for each $p \in W$ and for each pair of δP_s -open sets H_1 and H_2 such that both having p , there will be a δP_s -open set F having p satisfying that, $F^q \subseteq H_1^q \cap H_2^q$.

Exemplar 3.15: Consider the space $W = \{p, q, r, s\}$ and $\tau = \{ \phi, W, \{r, s\} \}$

$\delta P_s O(W) = \{ \phi, W, \{r\}, \{s\}, \{r, s\} \}$. An operation $q : \delta P_s O(W) \rightarrow P(W)$ is defined as follows, for each $H \in \delta P_s O(W)$

$$H^q = \begin{cases} H, & \text{if } r \in H \\ \{r, s\}, & \text{if } r \notin H \end{cases}$$

Then q is δP_s -regular.

Proposition 3.16: The finite intersection of q -open sets is a q -open set if q is a δP_s -regular operation on $\delta P_s O(W)$ for a topological space (W, τ) .

Proof: Consider $S, T \subseteq W$ such that S and T are q -open sets and q is a δP_s -regular operation on $\delta P_s O(W)$. Let $p \in S \cap T$ then by definition 3.3, there are δP_s -open sets H_1 and H_2 satisfying H_1 contains p and H_1^q contained in S and H_2 contains p and H_2^q contained in T . Now q is δP_s -regular operation yielding for a δP_s -open set F having p satisfying that, $F^q \subseteq H_1^q \cap H_2^q \subseteq S \cap T$. Hence, $S \cap T$ is q -open set in (W, τ) .





Shanmugapriya et al.,

Remark 3.17: From proposition 3.10 (a) and proposition 3.16 " $\varrho O(W)$ forms a topology on W , for any δP_s - regular operation ϱ on $\delta P_s O(W)$.

Definition 3.18: A topological space (W, τ) with an operation ϱ on $\delta P_s O(W)$ is called **ϱ -regular** if for given $p \in W$ and for each δP_s -open set H having p , there will be a δP_s -open set F having p satisfying that $F^{\varrho} \subseteq H$.

Exemplar 3.19: Consider the space $W = \{p, q, r\}$ and $\tau = \{ \phi, W, \{p\}, \{q\}, \{p, q\}, \{p, r\} \}$
 $\delta P_s O(W) = \{ \phi, W, \{q\}, \{r\}, \{p, r\}, \{q, r\} \}$. An operation $\varrho : \delta P_s O(W) \rightarrow P(W)$ is defined as follows, for each $H \in \delta P_s O(W)$

$$H^{\varrho} = \begin{cases} clH, & \text{if } q \in H \\ H, & \text{if } q \notin H \end{cases}$$

Then (W, τ) is ϱ -regular space.

Theorem 3.20: Let (W, τ) be a topological space and $\varrho : \delta P_s O(W) \rightarrow P(W)$ be an operation on $\delta P_s O(W)$. Then the conditions below are identical:

- (a) $\delta P_s O(W) = \varrho O(W)$.
- (b) (W, τ) is a ϱ -regular space.
- (c) For given $p \in W$ and for each δP_s -open set H of (W, τ) having p , there will be a ϱ -open set V of (W, τ) satisfying that, $p \in V$ and $V \subseteq H$.

Proof: (a) \rightarrow (b) It is given that δP_s -open sets and ϱ -open sets are equivalent. Consider $p \in W$, where H is a δP_s -open set having p . By the criteria H is ϱ -open set, then by definition 3.3 there will be a δP_s -open set H_1 satisfying that $p \in H_1$ and $H_1^{\varrho} \subseteq H$. Thus (W, τ) is ϱ -regular, from definition 3.18.

(b) \rightarrow (c) It is given that (W, τ) is a ϱ -regular space and consider $p \in W$ and a δP_s -open set H having p , by definition 3.18 there will be a δP_s -open set V having p satisfying that $V^{\varrho} \subseteq H$. By definition 3.3, V itself is a ϱ -open set and we know that $V \subseteq V^{\varrho}$ in general.

Thus for $p \in W$ and a δP_s -open set H having p , there will be a ϱ -open set V having p satisfying that, $V \subseteq H$.

(c) \rightarrow (a) Consider a δP_s -open set $H, p \in H$. Then by (c), there will be a ϱ -open set V_p satisfying that, $p \in V_p \subseteq H$. Then $H = \cup_{p \in H} \{p\} \subseteq \cup V_p \subseteq \cup V_p^{\varrho} \subseteq H$, which implies

$H = \cup V_p$ is ϱ -open set, from proposition 3.10 (a).

Thus $\delta P_s O(W) \subseteq \varrho O(W)$.

Every ϱ -open set is δP_s -open set, by proposition 3.4, owing that $\varrho O(W) \subseteq \delta P_s O(W)$.

Thus, $\delta P_s O(W) = \varrho O(W)$.

Topological Properties of ϱ -Open Sets

Definition 4.1: Let S be any subset of a topological space (W, τ) and ϱ be an operation on $\delta P_s O(W)$. A point $p \in W$ is called **ϱ -limit point** of S if for each ϱ -open set G having p , $G \cap (S - \{p\}) \neq \phi$. The set of each ϱ -limit points of S is known as a **ϱ -derived set** of S and it is meant by $\varrho D(S)$.

Exemplar 4.2: Consider the space $W = \{p, q, r\}$ and $\tau = \{ \phi, W, \{p\}, \{q\}, \{p, q\} \} = \delta P_s O(W)$ and $\varrho C(W) = \{ \phi, W, \{r\}, \{p, r\}, \{q, r\} \}$. An operation $\varrho : \delta P_s O(W) \rightarrow P(W)$ is defined as follows, for each $H \in \delta P_s O(W)$

$$H^{\varrho} = \begin{cases} p \cup H, & \text{if } q \notin H \\ H, & \text{if } q \in H \end{cases}$$

Implies $\varrho O(W) = \{ \phi, W, \{q\}, \{p, q\} \}$.

Hence for a subset $A = \{p, q\}$ the ϱ -limit points of $\{p, q\}$ are p and r therefore, $\varrho D(\{p, q\}) = \{p, r\}$. Some properties of ϱ -derived set are mentioned in the theorem below:

Theorem 4.3: The following properties hold for any sets U and V in a topological space (W, τ) with an operation ϱ on $\delta P_s O(W)$.

- a. $\varrho D(\phi) = \phi$.





b. If $U \subseteq V$, then $qD(U) \subseteq qD(V)$.

c. $qD(U \cap V) \subseteq qD(U) \cap qD(V)$.

d. $qD(U \cup V) \supseteq qD(U) \cup qD(V)$.

e. $q(qD(U)) - U \subseteq qD(U)$.

f. $qD(U \cup qD(U)) \subseteq U \cup qD(U)$.

Proof: Proof of **(a)** is obvious.

(b) We have $U \subseteq V, U - \{p\} \subseteq V - \{p\} \Rightarrow G \cap (U - \{p\}) \subseteq G \cap (V - \{p\})$. Then

$G \cap (U - \{p\}) \neq \emptyset \Rightarrow G \cap (V - \{p\}) \neq \emptyset$. Hence $p \in qD(U) \Rightarrow p \in qD(V)$.

Thus $qD(U) \subseteq qD(V)$.

(c) We know that $U \cap V \subseteq U$ and $U \cap V \subseteq V$, then by (b) $qD(U \cap V) \subseteq qD(U) \cap qD(V)$.

(d) We know that $U \cup V \supseteq U$ or $U \cup V \supseteq V$, then by (b) $qD(U \cup V) \supseteq qD(U) \cup qD(V)$.

(e) Consider p in $q(qD(U)) - U$ then $p \in q(qD(U))$ and $p \notin U$. Now G is a q -open set having p , then $G \cap (qD(U)) - \{p\} \neq \emptyset$. Let $q \in (qD(U))$ and G is a q -open set having q , then $G \cap (U - \{q\}) \neq \emptyset \Rightarrow$ there is $r \in G \cap (U - \{q\})$, then $r \in U$. Now $p \notin U$, therefore $r \neq p$.

Thus $r \in G \cap (U - \{p\})$, this imply that $p \in qD(U)$. Therefore $q(qD(U)) - U \subseteq qD(U)$.

(f) Consider p in $qD(U \cup qD(U))$ and G is a q -open set having p , then

$G \cap ((U \cup qD(U)) - \{p\}) \neq \emptyset$. Thus $G \cap (U - \{p\}) \neq \emptyset$ or $G \cap (qD(U) - \{p\}) \neq \emptyset$.

Case (i) : $G \cap (U - \{p\}) \neq \emptyset$, In this case by definition 4.1 $p \in qD(U)$.

Case (ii) : $G \cap (qD(U) - \{p\}) \neq \emptyset$. Then $G \cap (qD(U)) \neq \emptyset$, then by (e) $p \in qD(U)$.

Therefore $qD(U \cup qD(U)) \subseteq qD(U)$.

Definition 4.4: Let S be any subset of a topological space (W, τ) and q be an operation on $\delta P_s O(W)$. The **q -closure** of S is explained as the intersection of each q -closed sets of W having S and it is meant by $qCl(S)$. $qCl(S) = \cap \{ E : A \subseteq E; W - E \text{ is } q\text{-open set in } W \}$.

Exemplar 4.5: Consider Exemplar 4.2,

Let $S = \{p\}$ then $qCl(S) = \{p, r\}$.

Here $qD(S) = qCl(S)$.

Some important properties of q -closure operator are given below :

Theorem 4.6.a: $qCl(\emptyset) = \emptyset$ and $qCl(W) = W$.

b. $qCl(S)$ is the smallest q -closed set having S .

c. $qCl(S)$ is a q -closed set in W .

d. $S \subseteq \delta P_s Cl(S) \subseteq qCl(S)$.

e. S is q -closed set iff $qCl(S) = S$.

f. If $qCl(S) \cap qCl(T) = \emptyset$, then $S \cap T = \emptyset$.

g. If $S \subseteq T$, then $qCl(S) \subseteq qCl(T)$.

h. $qCl(S \cap T) \subseteq qCl(S) \cap qCl(T)$.

i. $qCl(S) \cup qCl(T) \subseteq qCl(S \cup T)$.

j. $qCl(qCl(S)) = qCl(S)$.

Proof: **(a)** is obvious.

(b) The proof follows from the definition 4.4.

(c) The proof follows from (b)

(d) We know, Every q -open set is a " δP_s -open set" by proposition 3.4. Now, for a subset S of W , $qO(S) \subseteq \delta P_s O(S) \Rightarrow \delta P_s Cl(S) \subseteq qCl(S) \Rightarrow S \subseteq \delta P_s Cl(S) \subseteq qCl(S)$.

(e) If S is q -closed set then $qCl(S) = S$ [by (c)]

To prove converse, that is to prove $qCl(S)$ is q -closed set.

It is enough to prove that $(qCl(S))'$ is q -open set.

Now $(qCl(S))' = [\cap \{ E / S \subseteq E \text{ and } W - E \text{ is } q\text{-open set} \}]'$





Shanmugapriya et al.,

$$= \cup \{ W - E / S \subseteq E \} = \cup \{ \rho \text{-open set having } S \}$$

$$= \rho \text{-open. [by proposition 3.10 (a)]}$$

Thus, $\rho \text{Cl}(S)$ is ρ -closed set.

(f) Consider $\rho \text{Cl}(S) \cap \rho \text{Cl}(T) = \phi$. Suppose $S \cap T \neq \phi$ then $r \in S \cap T$ imply $r \in S$ and $r \in T$. Then by (d) $r \in \rho \text{Cl}(S)$ and $r \in \rho \text{Cl}(T)$, contradicting our criteria. Hence $S \cap T = \phi$.

(g) Let $S \subseteq T$, $\rho \text{Cl}(S) = \cap \{ \text{Each } \rho\text{-closed sets having } S \} = \cap \mathcal{S}$, where \mathcal{S} is the collection of each ρ -closed sets having S . As same, $\rho \text{Cl}(T) = \cap \{ \text{Each } \rho\text{-closed sets having } T \}$

$$= \cap \mathcal{T}, \text{ where } \mathcal{T} \text{ is the group of each } \rho\text{-closed sets having } T.$$

$$\mathcal{T} \subseteq \mathcal{S} \Rightarrow \cap \mathcal{S} \subseteq \cap \mathcal{T}, \text{ Therefore } \rho \text{Cl}(S) \subseteq \rho \text{Cl}(T).$$

(h) Now $S \cap T \subseteq S$ and $S \cap T \subseteq T$. Hence by (g) $\rho \text{Cl}(S \cap T) \subseteq \rho \text{Cl}(S)$ and $\rho \text{Cl}(S \cap T) \subseteq \rho \text{Cl}(T)$. Therefore, $\rho \text{Cl}(S \cap T) \subseteq \rho \text{Cl}(S) \cap \rho \text{Cl}(T)$.

(i) Now $S \subseteq S \cup T$ and $T \subseteq S \cup T$. Hence "by (g) $\rho \text{Cl}(S) \subseteq \rho \text{Cl}(S \cup T)$ and $\rho \text{Cl}(T) \subseteq \rho \text{Cl}(S \cup T)$. Therefore, $\rho \text{Cl}(S) \cup \rho \text{Cl}(T) \subseteq \rho \text{Cl}(S \cup T)$.

(j) From (c) $\rho \text{Cl}(S)$ is ρ -closed set and from (e), $\rho \text{Cl}(\rho \text{Cl}(S)) = \rho \text{Cl}(S)$.

Proposition 4.7: Let S be any subset of a topological space (W, τ) and ρ be an operation on $\delta P_s O(W)$. Then $p \in \rho \text{Cl}(S)$ if $f S \cap M \neq \phi$, for each ρ -open set M of W having p .

Proof: Consider, $p \in \rho \text{Cl}(S)$ and suppose $S \cap M = \phi$. For each ρ -open set M of W having p . Then $S \subseteq W - M$ and $W - M$ is a ρ -closed set in W . Then $\rho \text{Cl}(S) \subseteq W - M$, by definition 4.4.

Thus, $p \in (W - M)$, this is a contradiction. Hence $S \cap M \neq \phi$ for each ρ -open set M of W having p .

To prove the converse, if $p \notin \rho \text{Cl}(S)$ then there will be a ρ -closed set E satisfying that $S \subseteq E$ and $p \notin S$ so $p \notin E$. Then $W - E$ is ρ -open set satisfying that $p \in (W - E)$ and $S \cap (W - E) = \phi$ contradicting our hypothesis. Thus, $p \in \rho \text{Cl}(S)$.

From Definition 4.1 and Proposition 4.7, we have the corollary will below:

Corollary 4.8: Let S be any subset of a topological space (W, τ) and ρ be an operation on $\delta P_s O(W)$. Then $\rho D(S) \subseteq \rho \text{Cl}(S)$.

Proposition 4.9: Let S be any subset of a topological space (W, τ) and ρ be an operation on $\delta P_s O(W)$. Then S is ρ -closed iff S holds the set of its ρ -limit points.

Proof: If S is a ρ -closed subset of a space (W, τ) and let $p \notin S$, then $p \in W - S$ and $W - S$ is ρ -open set in W so $S \cap (W - S) = \phi$ which implies $p \notin \rho D(S)$, from proposition 4.7

Hence $\rho D(S) \subseteq S$.

To prove the converse, let $S \supseteq \rho D(S)$ Now to prove S is a ρ -closed set in W . It is enough to prove that $\rho \text{Cl}(S) \subseteq S$. Let $p \notin S \Rightarrow p \notin \rho D(S)$ [by assumption]

$\Rightarrow p$ is not a limit point of S

\Rightarrow there will be a ρ -open set U having p satisfying that $U \cap S = \phi$ since $p \notin S$

$\Rightarrow U \subseteq W - S$.

$\Rightarrow p \notin \rho \text{Cl}(S)$. Therefore S is ρ -closed if $f S$ holds the set of its ρ -limit points.

Proposition 4.10: Let (W, τ) will be a topological space and ρ will be an operation on $\delta P_s O(W)$. Then $S \cup \rho D(S)$ is ρ -closed in W for any subset S of a space W .

Proof: Consider $p \notin S \cup \rho D(S)$, implies $p \notin S$ and $p \notin \rho D(S)$, so there will be a ρ -open set G which holds no point of S other than p , but $p \notin S$. Hence no point of G is in $\rho D(S)$, implies that $G \subseteq W - \rho D(S) \subseteq W - (S \cup \rho D(S)) \Rightarrow S \cup \rho D(S)$ is ρ -closed in W .

Theorem 4.11: Let (W, τ) will be a topological space and ρ will be an operation on $\delta P_s O(W)$. Then $\rho \text{Cl}(S) = S \cup \rho D(S)$ for any subset S of a space W .





Proof: Now, $S \subseteq S \cup \varrho D(S)$ and $S \subseteq \varrho Cl(S)$ in general and by Corollary 4.8, $\varrho D(S) \subseteq \varrho Cl(S)$ hence $S \cup \varrho D(S) \subseteq \varrho Cl(S)$.

Let $q \in \varrho Cl(S)$ to show that $q \in S \cup \varrho D(S)$. If $q \in S$ then it is trivial that $q \in S \cup \varrho D(S)$. If $q \notin S$ and $q \in \varrho Cl(S)$, we know that each ϱ -open set G containing q is $G \cap S \neq \emptyset$, by proposition 4.7. Now $q \notin S$, $G \cap (S - \{q\}) \neq \emptyset$. Then by definition 4.1 $q \in \varrho D(S)$, hence $q \in S \cup \varrho D(S)$. Thus, $\varrho Cl(S) = S \cup \varrho D(S)$.

Theorem 4.12: For any subsets S, T of a topological space (W, τ) . If ϱ is a δP_s -regular operation on $\delta P_s O(W)$, then $\varrho Cl(S) \cup \varrho Cl(T) = \varrho Cl(S \cup T)$.

Proof: From properties 4.6 (i) $\varrho Cl(S) \cup \varrho Cl(T) \subseteq \varrho Cl(S \cup T)$ so it is enough to obtain that $\varrho Cl(S \cup T) \subseteq \varrho Cl(S) \cup \varrho Cl(T)$. Consider $p \notin \varrho Cl(A) \cup \varrho Cl(B)$, Then there will be two ϱ -open sets G_1 and G_2 having p such that $A \cap G_1 = \emptyset$ and $B \cap G_2 = \emptyset$. Since ϱ is a δP_s -regular operation on $\delta P_s O(W)$ then by proposition 3.16 $G_1 \cap G_2$ is a ϱ -open set in W so $(S \cup T) \cap G_1 \cap G_2 = \emptyset$. Therefore $p \notin \varrho Cl(S \cup T)$, thus $\varrho Cl(S \cup T) \subseteq \varrho Cl(S) \cup \varrho Cl(T)$.

Theorem 4.13: If ϱ is a δP_s -regular operation on $\delta P_s O(W)$, then $\varrho Cl(S) \cap U \subseteq \varrho Cl(S \cap U)$, for each ϱ -open set U and every subset S of W .

Proof: Consider $p \in \varrho Cl(S) \cap U$, for each ϱ -open set U . So $p \in \varrho Cl(A)$ and $p \in U$, Suppose V will be any ϱ -open set having p . Then by proposition 3.16, $U \cap V$ is a ϱ -open set having p . We have $p \in \varrho Cl(S)$, by proposition 4.7, $S \cap (U \cap V) \neq \emptyset \Rightarrow (S \cap U) \cap V \neq \emptyset$.

Hence $p \in \varrho Cl(S \cap U)$.

Thus, $\varrho Cl(S) \cap U \subseteq \varrho Cl(S \cap U)$.

Definition 4.14: Let S be any subset of a topological space (W, τ) and ϱ be an operation on $\delta P_s O(W)$. A point $p \in W$ is called closure ϱ point of the set S if for each δP_s -open set H having p , $H^\varrho \cap S \neq \emptyset$. The set of each closure ϱ point of S is known as **closure ϱ** of S and is meant by $Cl_\varrho(S)$.

Exemplar 4.15: Consider the space $W = \{p, q, r, s\}$ and $\tau = \{ \emptyset, W, \{p, q, r\} \}$

$\delta P_s O(W) = \{ \emptyset, W, \{s\} \}$. An operation $\varrho : \delta P_s O(W) \rightarrow P(W)$ is defined as follows, for each $H \in \delta P_s O(W)$

$$H^\varrho = \begin{cases} ClH, & \text{if } s \in H \\ H, & \text{if } s \notin H \end{cases}$$

For a subset $S = \{p, q, r\}$, $Cl_\varrho(S) = \{p, q, r\}$.

Theorem 4.16: Let S be any subset of a topological space (W, τ) and ϱ be an operation on $\delta P_s O(W)$. Then $\delta P_s Cl(S) \subseteq Cl_\varrho(S)$.

Proof: Consider $p \in \delta P_s Cl(S)$, then by definition 2.12, $S \cap H \neq \emptyset$, for each δP_s -open set H having p . Always $H \subseteq H^\varrho$, Which implies $S \cap H \neq \emptyset \subseteq S \cap H^\varrho \neq \emptyset$. By definition 4.14, $p \in Cl_\varrho(S)$.

Thus $\delta P_s Cl(S) \subseteq Cl_\varrho(S)$.

Remark 4.17: The Converse of above theorem is not true, which can be from the exemplar below:

Consider the space $W = \{a, b, c, d\}$ and $\tau = \{ \emptyset, W, \{p, q\} \}$, $\delta P_s O(X) = \{ \emptyset, W, \{r\}, \{s\}, \{r, s\} \}$.

An operation $\varrho : \delta P_s O(W) \rightarrow P(W)$ is defined as follows, for each

$H \in \delta P_s O(W)$

$$H^\varrho = \begin{cases} ClH, & \text{if } r \in H \\ H, & \text{if } r \notin H \end{cases}$$

For a subset $S = \{p, s\}$, $Cl_\varrho(S) = W$ and $\delta P_s Cl(S) = \{p, q, s\}$. Thus, $Cl_\varrho(S) \not\subseteq \delta P_s Cl(S)$.

Proposition 4.18: a. $Cl_\varrho(\emptyset) = \emptyset$, $Cl_\varrho(W) = W$ and $S \subseteq Cl_\varrho(S)$.

b. $S \subseteq Cl_\varrho(S) \subseteq \varrho Cl(S)$.

c. S is ϱ -closed set if and only if $Cl_\varrho(S) = S$.





Shanmugapriya et al.,

d. $Cl_q(S)$ is a δP_s -closed set in W .

e. If $S \subseteq T$, then $Cl_q(S) \subseteq Cl_q(T)$.

f. $Cl_q(S \cap T) \subseteq Cl_q(S) \cap Cl_q(T)$.

g. $Cl_q(S) \cup Cl_q(T) \subseteq Cl_q(S \cup T)$.

Proof: (a) The proof is clear.

(b) It follows from the definition that $S \subseteq Cl_q(S)$. To prove $Cl_q(S) \subseteq Cl(S)$.

Consider $x \notin Cl(S)$ then, for each q -open set U having x , $U \cap S = \phi$. Since U is a q -open set then for each $x \in U$, there will be a δP_s -open set H satisfying that, $x \in H$ and $H^q \subseteq U$, by definition 3.3. Thus, $H^q \cap S = \phi$. Thus, $x \notin Cl_q(S)$. Hence $Cl_q(S) \subseteq Cl(S)$.

(c) If S is q -closed set then $Cl(S) = S$, from theorem 4.6 (e).

From (b) $S \subseteq Cl_q(S) \subseteq Cl(S) = S$. Hence $S \subseteq Cl_q(S) \subseteq Cl(S) = S$.

Thus $Cl_q(S) = S$.

To prove the converse, assume $Cl_q(S) = S$. To prove S is q -closed set it is enough to prove that $W - S$ is q -open set, that is to prove there will be a δP_s -open set H satisfying that, $x \in H$ and $H^q \subseteq W - S$.

Now if $x \in S$ then $x \in Cl_q(S)$, so for each δP_s -open set H having x , $H^q \cap S \neq \phi$.

Take $y \in X - S$, implies $y \notin S$ and so $y \notin Cl_q(S)$ hence there will be a δP_s -open set H having x , satisfying that, $H^q \cap S = \phi \Rightarrow H^q \subseteq X - S$. Hence $X - S$ is a q -open set.

Thus, S is a q -closed set.

(d) To show, $Cl_q(S)$ is a δP_s -closed set in W .

It is enough to prove, $\delta P_s Cl(Cl_q(S)) = Cl_q(S)$.

Consider $x \in \delta P_s Cl(Cl_q(S))$, then for each δP_s -open set U having x , $Cl_q(S) \cap U \neq \phi$, by definition 2.12. Since $U \subseteq U^q$, we get $Cl_q(S) \cap U^q \neq \phi$, which gives $x \in Cl_q(S)$.

Hence $\delta P_s Cl(Cl_q(S)) \subseteq Cl_q(S)$.

On other hand, $Cl_q(S) \subseteq \delta P_s Cl(Cl_q(S))$ is always true.

Thus, $Cl_q(S)$ is a δP_s -closed set in W .

(e) Consider $x \notin Cl_q(T)$, by definition 4.14, there will be a δP_s -open set H having x , $H^q \cap T = \phi$ now $S \subseteq T$, implies for each δP_s -open set H having x ,

$H^q \cap S = \phi \Rightarrow x \notin Cl_q(S)$. Thus $Cl_q(S) \subseteq Cl_q(T)$.

(f) Now $S \cap T \subseteq S$ and $S \cap T \subseteq T$. Hence by (e) $Cl_q(S \cap T) \subseteq Cl_q(S)$ and

$Cl_q(S \cap T) \subseteq Cl_q(T)$. Thus, $Cl_q(S \cap T) \subseteq Cl_q(S) \cap Cl_q(T)$.

(g) Now $S \subseteq S \cup T$ and $T \subseteq S \cup T$. Hence by (e) $Cl_q(S) \subseteq Cl_q(S \cup T)$ and

$Cl_q(T) \subseteq Cl_q(S \cup T)$. Therefore, $Cl_q(S) \cup Cl_q(T) \subseteq Cl_q(S \cup T)$.

Theorem 4.19: If q is a δP_s -regular operation on $\delta P_s O(W)$, then $Cl_q(S) \cup Cl_q(T) = Cl_q(S \cup T)$.

Proof: From Proposition 4.18 (g) we have, $Cl_q(S) \cup Cl_q(T) \subseteq Cl_q(S \cup T)$.

On the other side, Consider $x \notin Cl_q(S) \cup Cl_q(T)$, there will be a pair of δP_s -open sets H_1 and H_2 satisfying that both having x , $H_1^q \cap S = \phi$ and $H_2^q \cap T = \phi$. Now q is a δP_s -regular operation on $\delta P_s O(W)$ then for each $x \in W$ and there will be a δP_s -open set F having x satisfying that, $F^q \subseteq H_1^q \cap H_2^q$.

So, $(S \cup T) \cap F^q \subseteq (S \cup T) \cap H_1^q \cap H_2^q \Rightarrow (S \cup T) \cap F^q = \phi$, but

$(S \cup T) \cap H_1^q \cap H_2^q = [(S \cup T) \cap H_1^q] \cap H_2^q = \phi \cap H_2^q = \phi$. Owing that $x \notin Cl_q(S \cup T)$.

Hence $Cl_q(S \cup T) \subseteq Cl_q(S) \cup Cl_q(T)$.

Thus, $Cl_q(S) \cup Cl_q(T) = Cl_q(S \cup T)$.

Definition 4.20: An operation q on $\delta P_s O(W)$ is called **open- q -operation** if for each δP_s -open set H having x , there will be a q -open set G having x satisfying that, $G \subseteq H^q$.

Exemplar 4.21: Consider the space $W = \{p, q, r, s\}$ and





Shanmugapriya et al.,

$\tau = \{ \phi, W, \{r\}, \{p,q\}, \{p,q,r\} \} = \delta P_s O(W)$. An operation $q : \delta P_s O(W) \rightarrow P(W)$ is defined as follows, for each $H \in \delta P_s O(W)$

$$H^q = \begin{cases} ClH, & \text{if } r \in H \\ H, & \text{if } r \notin H \end{cases}$$

$qO(W) = \{ \phi, X, \{p,q\} \}$

Here operation q is an open- q -operation.

Theorem 4.22: If S be any subset of a topological space (W, τ) and q is an open- q -operation on $\delta P_s O(W)$, then

- a. $Cl_q(S) = qCl(S)$.
- b. $Cl_q(Cl_q(S)) = Cl_q(S)$.
- c. $Cl_q(S)$ is q -closed set.

Proof: (a) From proposition 4.18 (b), $Cl_q(S) \subseteq qCl(S)$. Need to show that $qCl(S) \subseteq Cl_q(S)$, Consider $x \notin Cl_q(S)$, by definition 4.14, there will be a δP_s -open set H having x satisfying that $H^q \cap S = \phi$. Now here q is an open- q -operation, then there will be a q -open set G having x satisfying that $G \subseteq H^q$, which gives $G \cap S = \phi$. Hence by proposition 4.7 $x \notin qCl(S)$. Thus, $qCl(S) \subseteq Cl_q(S)$.

Hence $Cl_q(S) = qCl(S)$.

(b) Now from theorem 4.6 (j) we have $qCl(qCl(S)) = qCl(S)$ and by (a) we have

$Cl_q(S) = qCl(S)$.

Thus, $Cl_q(Cl_q(A)) = Cl_q(A)$.

(c) Now from theorem 4.6 (c) and (a) of this theorem " $Cl_q(S)$ is a q -closed set.

Remark 4.23: If an operation q is not an open- q -operation then $Cl_q(S) \neq qCl(S)$. Consider the space $W = \{p,q,r,s\}$ and $\tau = \{ \phi, W, \{p,q\}, \delta P_s O(X) = \{ \phi, W, \{r\}, \{s\}, \{r,s\} \}$. $\delta C(W) = \{ \phi, W \}$. An operation $q : \delta P_s O(W) \rightarrow P(W)$ is defined as follows, for each

$H \in \delta P_s O(W)$

$$H^q = \begin{cases} \delta ClH, & \text{if } s \in H \\ H, & \text{if } s \notin H \end{cases}$$

$qO(W) = \{ \phi, W, \{r\} \}$

$qC(W) = \{ \phi, W, \{p,q,s\} \}$. Here operation q is not an open- q -operation. For a subset $S = \{p,s\}$, $Cl_q(S) = W$ and $qCl(S) = \{p,q,s\}$. Thus, $Cl_q(S) \neq qCl(S)$.

CONCLUSION

In this paper, we introduced q operation on δP_s -open sets. We analysed q -open sets, q -regular spaces, and some topological properties of q -open sets especially q -limit points, q -closure and Cl_q .

REFERENCES

1. Alias B. Khalaf, and Baravan A. Asaad, "P_s-open sets and P_s-Continuity in Topological spaces," J. Duhok Univ., 12(2)(2009), 183-192.
2. [An T.V., Cuong D.X. and Maki H., "On operation preopen sets in topological spaces, Scientiae Mathematicae Japonicae Online," 681, 11-30, (e-2008), 241-260.
3. Baravan A. Asaad, "Operation Approaches On P_s-Open Sets and Its Separation Axioms," Journal of University of Zakhw, Vol. 4(A), No.2, (2016), Pp 236-243 .
4. Baravan A. Asaad, Zanyar A. Ameen, "Some properties of an operation on α -open sets, "New Trends in Mathematical Sciences, 7, No .2, (2019), 150-158.
5. Dontchev J., "Survey on preopen sets," The Proceedings of the Yatsushiro Topological Conference, (1998), 1-18.
6. Hayao Ogata, "Operations on topological spaces and associated topology, "Math. Japonica, 36 (1) (1991), 175-184.





Shanmugapriya et al.,

7. Jayashree, R. and Sivakamasundari, K., "Operation approaches on δ -open sets, International Journal of Mathematics Trends and Technology," Special issue, 2018, 73-78.
8. Kasahara S, "Operation compact spaces, "Math. Japonica, 241. (1979), 97-105.
9. Levine N., "Semi-open sets and semi-continuity in topological spaces", Amer. Math. Monthly, 70(1) (1963), 36-41.
10. Maheshwari S. N. and Prasad R., "Some new separation axioms," Ann. Soc. Sci. Bruxelles, Ser. I., 89(1975), 395-402.
11. Masshour A. S., El-Monsef M. E. A., and El-Deeb S.N., "On pre continuous and weak pre continuous mappings," Proc. Math. Phys. Soc., Egypt, 53(1982), 47-53.
12. Raychaudhuri S. and Mukherjee M. N., "On δ -almost continuity and δ -preopen sets, "Bull. Inst. Math. Acad. Sinica, 21 (1993), 357-366.
13. Vidhyapriya P, Shanmugapriya H and Sivakamasundari K, " δ Ps-Open Sets in Topological Spaces", Advances in Applicable Mathematics - ICAAM2020 AIP Conference Proceedings 2261(2020) 030103-1–030103-8.
14. Velicko N. V., "H-closed Topological spaces," Amer. Math. Soc. Transl., 78(2)(1968),103-118.





IOT Based Vehicular Emergency Communication and Location Tracking System

S. Sugumaran¹, P.Vimala^{2*}, A. Jegadish¹ and E. Vinothkumar¹

¹UG Student, Department of Electronics and Communication Engineering, Faculty of Engineering and Technology, Annamalai University, Annamalainagar, Chidambaram, Tamil Nadu, India.

²Assistant Professor, Department of Electronics and Communication Engineering, Faculty of Engineering and Technology, Annamalai University, Annamalainagar, Chidambaram, Tamil Nadu, India.

Received: 24 Feb 2021

Revised: 04 Mar 2021

Accepted: 10 Mar 2021

*Address for Correspondence

P. Vimala

Assistant Professor,
Department of Electronics and Communication Engineering,
Faculty of Engineering and Technology,
Annamalai University, Annamalainagar,
Chidambaram, Tamil Nadu, India.
Email: vimalakathirau@gmail.com



This is an Open Access Journal / article distributed under the terms of the **Creative Commons Attribution License** (CC BY-NC-ND 3.0) which permits unrestricted use, distribution, and reproduction in any medium, provided the original work is properly cited. All rights reserved.

ABSTRACT

A vehicle tracking system has been designed for rescue in case of the accident using Internet of Things (IoT). The IoT is a promising technology having the ability to change human life. A vehicle tracking system is one such system that enables communication and location tracking in an emergency to a remote vehicle. It has a Raspberry Pi embedded system for control, Global Positioning System (GPS) for tracking and Global System for Mobile communication (GSM) for positioning (Latitude and Longitude) of remote vehicle. The message is conveyed to the control room on an emergency of the in real time. The performance of the proposed system is verified by the prototype model designed with Raspberry Pi Model B+ and Wi Fi.

Keywords: Internet of Things, Location Tracking, Vehicular Emergency Communication.

INTRODUCTION

Now the world is moving towards the smart city in which every device can communicate 24×7 to each other regardless of their hardware and software structures. Internet of Things (IoT) basically describes the interlinking of embedded devices with the internet and that they communicate each other. The embedded devices also have sensors, actuators, motors etc. to communicate with the physical environment. So, it makes the human life smarter. [1-4]. In this connection, the current work presents life saver system for a vehicle when emergency situation



**Sugumaran et al.,**

occurred. Most of life saving can't be done during an accidents due to communication delay [5]. A GPS based partially automated location tracking system proposed in [6] collects information of location and send through SMS. A system is designed to for continuous monitoring of the vehicle by including GPS to determine the position of the vehicle and GSM modules to deliver the information [7]. Detection of an accident by smart sensors e.g. accelerometer sensor etc. and uses the phone with its 3G connection to transmit information about the accident in [8]. Intelligent Transportation System is proposed for future intelligent vehicles in [9]. Most of these kinds of systems does n't have provision to directly contact nearest control room for emergencies to avoid delay in rescue. Google's Geolocation [10] service used to get the location (latitude, longitude) in a real time basis.

Proposed System

A vehicle tracking system is designed for an emergency communication and location tracking of a vehicle in emergency. When a vehicle meets an accident the system starts automatically and tracks its location. It also takes photos with the preinstalled cameras and sends them immediately to the emergency control room. The GPS and GSM enable tracking of the vehicle and communicate. For the prototype design, the vehicle needs to be equipped with hardware for location tracking and communication. They includes Raspberry Pi Model B + that is used as main development board for the vehicle, Wi-Fi for communication internet, GPS is used to track the location of the vehicle, an Raspberry pi camera is also used to capture images of the inner parts of the vehicle. It detects the accident by gyroscope sensor. The location of the accident, time and GPS coordinates are sent to the specified mobile and computer. The block diagram of proposed system is shown in fig. 1.

Hardware Description

The Raspberry Pi Model B+ is a small and powerful lightweight ARM1176 based computer which integrates number of features like improved power consumption, increased connectivity and greater IO [11]. The Raspberry Pi Model B has two USB2.0 ports. The ARM1176 processor is deployed. The gyroscope sensor interfaced to the raspberry pi is used to detect the accidents by providing signals directly to the intended receiver. A gyroscope is a spinning wheel or disk whose axle device based on the principles of angular momentum for measuring orientation. It is free to take any orientation. This orientation changes is less in response to a given external torque and can be minimized by mounting the device in gimbals. Regardless of any motion of the platform on which it is mounted, the orientation remains nearly fixed. When an accident occurs alarm gives an audible warning in the vehicle when the gyroscope provides the signal and message generated and sent to the control room. GPS receiver [12] helps to navigate back to a starting point or other predetermined locations without the use of maps or any other equipment for message. Thus it allows collecting of location information. The location of the vehicle is shown in map in control room. The system uses Raspberry Pi camera module to take the snap shot of the accident location and mailed to the control room. It can be used to take high definition video, as well as photographs. It also has aids to fix the camera in the desired position and camera board protection. A 1200mA power supply will provide power to run Raspberry Pi. The maximum power that can be used by the Raspberry Pi is 1000mA. Typically, the model B uses power supply between 700-1000mA depending on peripherals that are connected. The HDMI port and the camera module require 50mA and 250mA respectively. The system uses 1200mA power supply.

Software Description

Raspberry Pi single board computers are running with Debian based operating system and Python is an interpreted, object oriented, high level programming language with dynamic semantics. It is very attractive for fast application development because of its built in high level data structures with dynamic typing and dynamic binding. It has easy syntax for learning and supports modules and packages. It encourages program modularity and code reuse. The standard library and interpreter of Python are available in binary form without charge. It offers increased productivity, no compilation step, incredibly fast edit-test-debug cycle and. easy debugging. It will never cause a segmentation fault instead, when an error is discovered by the interpreter, it raises an exception. When the program is not able to catch the exception, a stack trace is printed by the interpreter. A source level debugger allows check up



**Sugumaran et al.,**

of local and global variables, arbitrary expressions evaluation, breakpoints set, at a time step through the code a line and so on. A proposed system is controlled by Python program and the pseudo code of the same is given below.

```
import serial      #import serial pacakge
from time import sleep
import webbrowser   #import package for opening link in browser
import sys         #import system package
from picamera import PiCamera
import RPi.GPIO as GPIO
from gpiozero import LED
from gpiozero import Button
import smtplib
from gpiozero import MCP3008
import email
from email.mime.multipart import MIMEMultipart
from email.mime.text import MIMEText
from email.mime.base import MIMEBase
from email import encoders
import requests
gpgga_info = "$GPGGA,"
ser = serial.Serial ("/dev/ttyS0") #Open port with baud rate
GPGGA_buffer = 0
NMEA_buff = 0
lat_in_degrees = 0
long_in_degrees = 0
sender = 'rasp@iotclouddata.com'
password = 'Rasp1234$'
receiver = 'edvinoth03@gmail.com'
DIR = './Database/'
FILE_PREFIX = 'image'
camera = PiCamera()
camera.resolution = (320, 240)
buzzer = LED(18)
switch = Button(23)
```





Sugumaran et al.,

```
buzzer.off()
def send_mail():
    print ('Sending E-Mail')
    # Save image to file
    filename = 'speed.jpg'
    # Capture the face
    camera.rotation = 180
    camera.start_preview()
    sleep(1)
    camera.capture(filename)
    camera.stop_preview()
    # Sending mail
    msg = MIMEMultipart()
    msg['From'] = sender
    msg['To'] = receiver
    msg['Subject'] = 'Accident Detected'
    body = 'Picture is Attached.'
    msg.attach(MIMEText(body, 'plain'))
    attachment = open(filename, 'rb')
    part = MIMEBase('application', 'octet-stream')
    part.set_payload((attachment).read())
    encoders.encode_base64(part)
    part.add_header('Content-Disposition', 'attachment; filename= %s' % filename)
    msg.attach(part)
    server = smtplib.SMTP('smtpout.asia.secureserver.net', 3535)
    server.starttls()
    server.login(sender, password)
    text = msg.as_string()
    server.sendmail(sender, receiver, text)
    server.quit()
def GPS_Info():
```





```

global NMEA_buff
global lat_in_degrees
global long_in_degrees
nmea_time = []
nmea_latitude = []
nmea_longitude = []
nmea_time = NMEA_buff[0]           #extract time from GPGGA string
nmea_latitude = NMEA_buff[1]       #extract latitude from GPGGA string
nmea_longitude = NMEA_buff[3]      #extract longitude from GPGGA string
    print("NMEA Time: ", nmea_time,'\n')
    print ("NMEA Latitude:", nmea_latitude,"NMEA Longitude:", nmea_longitude,'\n')
lat = float(nmea_latitude)         #convert string into float for calculation
longi = float(nmea_longitude)      #convert string into float for calculation
lat_in_degrees = convert_to_degrees(lat) #get latitude in degree decimal format
long_in_degrees = convert_to_degrees(longi) #get longitude in degree decimal format
#convert raw NMEA string into degree decimal format
def convert_to_degrees(raw_value):
decimal_value = raw_value/100.00
    degrees = int(decimal_value)
mm_mmmm = (decimal_value - int(decimal_value))/0.6
    position = degrees + mm_mmmm
    position = "%.4f" %(position)
    return position
received_data = (str)(ser.readline()) #read NMEA string received
GPGGA_data_available = received_data.find(gpgga_info) #check for NMEA GPGGA string
if (GPGGA_data_available>0):
GPGGA_buffer = received_data.split("$GPGGA,")[1] #store data coming after "$GPGGA,"
string
NMEA_buff = (GPGGA_buffer.split(',')) #store comma separated data in buffer
GPS_Info() #get time, latitude, longitude
    print("lat in degrees:", lat_in_degrees," long in degree: ", long_in_degrees, '\n')

```





Sugumaran et al.,

```

map_link = 'http://maps.google.com/?q=' + lat_in_degrees + ',' + long_in_degrees #create link
to plot location on Google map
received_data = (str)(ser.readline()) #read NMEA string received
GPGGA_data_available = received_data.find(gpgga_info) #check for NMEA GPGGA string
if (GPGGA_data_available>0):
GPGGA_buffer = received_data.split("$GPGGA,",1)[1] #store data coming after "$GPGGA,"
string
NMEA_buff = (GPGGA_buffer.split(',')) #store comma separated data in buffer
GPS_Info() #get time, latitude, longitude
print("lat in degrees:", lat_in_degrees," long in degree: ", long_in_degrees, "\n")
map_link = 'http://maps.google.com/?q=' + lat_in_degrees + ',' + long_in_degrees #create link
to plot location on Google map
received_data = (str)(ser.readline()) #read NMEA string received
GPGGA_data_available = received_data.find(gpgga_info) #check for NMEA GPGGA string
if (GPGGA_data_available>0):
GPGGA_buffer = received_data.split("$GPGGA,",1)[1] #store data coming after "$GPGGA,"
string
NMEA_buff = (GPGGA_buffer.split(',')) #store comma separated data in buffer
GPS_Info() #get time, latitude, longitude
print("lat in degrees:", lat_in_degrees," long in degree: ", long_in_degrees, "\n")
map_link = 'http://maps.google.com/?q=' + lat_in_degrees + ',' + long_in_degrees #create link
to plot location on Google map
received_data = (str)(ser.readline()) #read NMEA string received
GPGGA_data_available = received_data.find(gpgga_info) #check for NMEA GPGGA string
if (GPGGA_data_available>0):
GPGGA_buffer = received_data.split("$GPGGA,",1)[1] #store data coming after "$GPGGA,"
string
NMEA_buff = (GPGGA_buffer.split(',')) #store comma separated data in buffer
GPS_Info() #get time, latitude, longitude
print("lat in degrees:", lat_in_degrees," long in degree: ", long_in_degrees, "\n")

```



**Sugumaran et al.,**

```
map_link = 'http://maps.google.com/?q=' + lat_in_degrees + ',' + long_in_degrees #create link
to plot location on Google map
received_data = (str)(ser.readline()) #read NMEA string received
GPGGA_data_available = received_data.find(gpgga_info) #check for NMEA GPGGA string
sleep(1)
while True:
    x = MCP3008(0)
    print('Accelerometer=' + str(x.value))
prox_state=GPIO.input(23)
    print(prox_state)
    if prox_state== 0:
buzzer.on()
        print('Emergency')
send_mail()
        r =requests.get('http://www.iotclouddata.com/20log/map001/iot20.php?A=' +
lat_in_degrees + '_' + long_in_degrees)
        else:
buzzer.off()
        x = MCP3008(0)
        print('Accelerometer=' + str(x.value))
        if x.value>0.4:
buzzer.on()
            print('Detected')
send_mail()
            r =requests.get('http://www.iotclouddata.com/20log/map001/iot20.php?A=' +
lat_in_degrees + '_' + long_in_degrees)
            else:
buzzer.off()
```

IMPLEMENTATION AND RESULTS

A vehicular emergency communication is necessary for proper safety and livelihood. The proposed system's prototype model is designed and shown in fig.2. Other very important feature of the system is the emergency camera in a vehicle. To store all necessary information on vehicle it needs databases. The information on the message generated in the on board of the vehicle and communicated to control room is given in fig.3. After generating the emergency message the system delivers the message to the emergency control room. The proposed system is able to

30546



**Sugumaran et al.,**

send automatic message to the control room with all relevant information of an emergency. The message gives emergency location to the control room that helps for the earliest reach to the location. The following screenshot fig. 4 shows the execution of the python programming during the emergency situation. The fig.5 shows the message received at the control room. The snapshots of the situation is received through Mail in the control room shown in the fig. 6

CONCLUSION

An emergency communication and location tracking system for a vehicular on road is proposed in this work with Raspberry pi model B+ processor and Wi Fi. The prototype model may also be used with existing infrastructure in the vehicle by providing Wi Fi. This proposed system is able to send emergency message with image and location map from a vehicle to the nearby control room. The system helps in minimizing emergency delays.

REFERENCES

1. L. Atzori, A. Iera, and G. Morabito, "The Internet of Things: A Survey", *Computer Networks*, vol. 54, no. 15, pp. 2787–2805, 2010.
2. J. Gubbi, R. Buyya, S. Marusic, and M. Palaniswami, "Internet of Things (IoT): A Vision, Architectural Elements and Future Directions", *Future Generation Computer Systems*, vol. 29, no. 7, pp. 1645–1660, 2013.
3. A. Zanella, N. Bui, A. Castellani, L. Vangelista, and M. Zorzi, "Internet of Things for Smart Cities," *Internet of Things Journal*, IEEE, vol.1, no. 1, pp. 22–32, 2014.
4. M. Chen, "Towards Smart City: M2M Communications with Software Agent Intelligence", *Multimedia Tools and Applications*, vol. 67, no. 1, pp. 167–178, 2013.
5. NCRB, "Accidental Deaths and Suicides in India 2014," New Delhi: National Crime Records Bureau, Ministry of Home Affairs, Tech. Rep., 2015.
6. J. Maleki, E. Foroutan, and M. Rajabi, "Intelligent Alarm System for Road Collision", *Journal of Earth Science and Engineering*, vol. 1, no. 3, 2011.
7. Albert Alexe, R. Ezhilarasie, "Cloud Computing Based Vehicle Tracking Information Systems", ISSN: 2229 - 4333 (Print), ISSN: 0976 - 8491 (Online) *IJCST* vol. 2, no. 1, March 2011.
8. B. Thompson, J. White, B. Dougherty, A. Albright, and D. C. Schmidt, "Using Smart Phones and Wireless Mobile Sensor Networks to Detect Car Accidents and Provide Situational Awareness to Emergency Responders", in *ICST Conf.*, June, 2010.
9. F. J. Martinez, C.K.Toth, J.C. Cano, C. T. Calafate, and P. Manzoni, "Emergency Services in Future Intelligent Transportation Systems Based on Vehicular Communication Networks", *Intelligent Transportation Systems Magazine*, IEEE, vol. 2, no. 2, pp. 6–20, 2010.
10. P. J. Zehler, "Method for Setting the Geolocation of a Non-GPS Enabled Device", US Patent 8,467,990, 2013.
11. S. Monk, *Raspberry Pi cookbook: Software and Hardware Problems and Solutions*, O'Reilly Media, Inc., ISBN: 9781491939109, June 2016.
12. A. Mounika, Anitha Chepuru, "IOT Based Vehicle Tracking and Monitoring System Using GPS and GSM", *International Journal of Recent Technology and Engineering (IJRTE)*, ISSN: 2277-3878, vol. 8, no. 2S11, September 2019.





Sugumaran et al.,

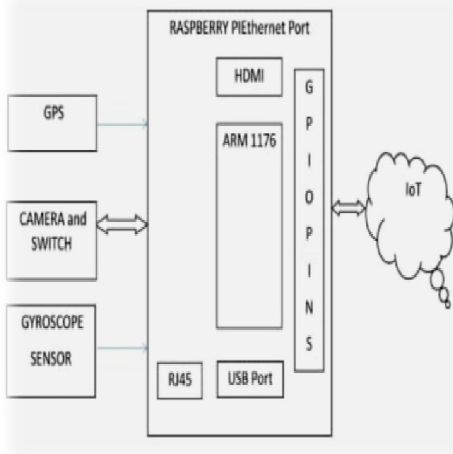


Fig. 1 Block Diagram of the Proposed System



Fig. 2 Experimental Kit

Emergency Message

Time	Location (Latitude, Longitude)	Image
------	-----------------------------------	-------

Fig.3. Message Structure

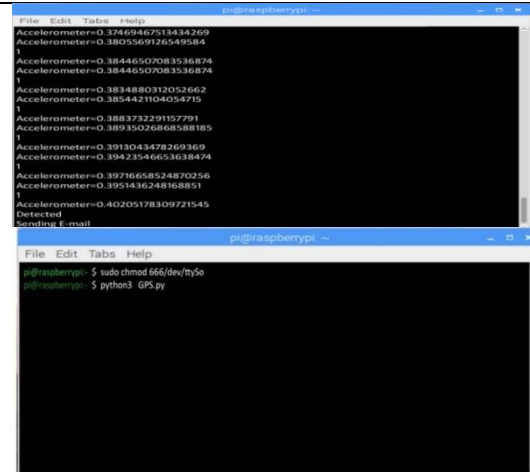


Fig. 4 Execution of Python during Emergency

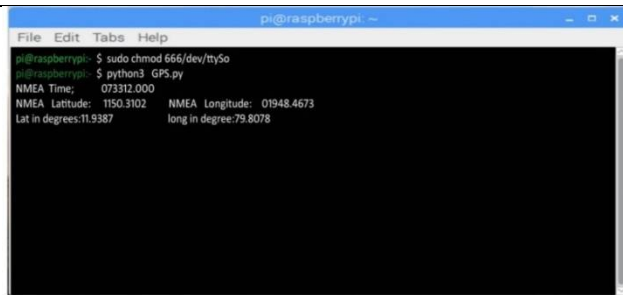


Fig. 5 Control Room Message

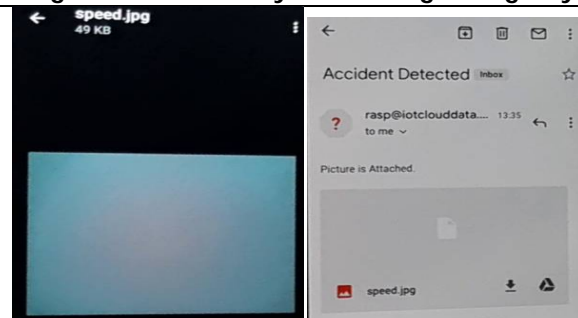


Fig. 6 Mail Received at the Control Room





Review on Ethnomedicine, Phytochemistry of Some Medicinal Plants and Trends to Improve Medicinal Efficacy

Suniti Yadav^{1*}, Ramesh Kumar¹ and Ritu Singh Rajput²

¹Bundelkhand University, Kanpur Road, Jhansi, Uttar Pradesh 284128, India.

²Jayoti Vidyapeeth women's University Jaipur, Rajasthan, India.

Received: 14 Mar 2021

Revised: 17 Mar 2021

Accepted: 20 Mar 2021

*Address for Correspondence

Suniti Yadav

Bundelkhand University,

Kanpur Road, Jhansi, Uttar Pradesh 284128, India.

Email: yadav.suniti@gmail.com



This is an Open Access Journal / article distributed under the terms of the **Creative Commons Attribution License** (CC BY-NC-ND 3.0) which permits unrestricted use, distribution, and reproduction in any medium, provided the original work is properly cited. All rights reserved.

ABSTRACT

Medicinal plants used in the traditional system are acquiring global attention in combination with modern techniques, forming a part of the overall global healthcare system. These medicinal plants are like hidden gems of nature that provide us with a stockpile of assorted chemicals having huge therapeutic potential for drug discovery. This review focuses on pharmaceutical applications and bioactive compounds present in *Carissa carandas*, *Chlorophyllum borivilianum*, *Tinospora cordifolia*, *Swertia chirata* and explained modern techniques that can boost efficacy. A web-based literature review was conducted using scientific databases such as Pub Med, Science Direct, Web of Science, and Google Scholar, with ethnobotanical and ethnomedicinal survey articles listed as inclusion criteria. This review highlights the advancements made in the assessment of biochemical profiles. We also briefly summarize studies on the phytochemistry, pharmacology and technical aspect. Biologically active molecules present in these plants interact with the biological system and displayed significant therapeutic values. Adverse effects of antibiotics can be mitigated by using medicinal plants and thus guarding the cause of green pharmacy. Likewise, these medicinally important plants show future healthcare aspect which is also a need of the hour in today's global scenario.

Keywords: Traditional plants, Green Pharmacy, Bioactive compounds, Modern Techniques

INTRODUCTION

Medicinal practices using traditional plants have survived and thrived since time immemorial in various forms and has been put to use effectively in different cultures and religions. Given the current situation wherein the entire world is heading towards an antibiotic-resistant era and confronting new disease, there is an indispensable need for developing medicines, WHO, and many health organizations are looking forward to therapies from alternate



**Suniti Yadav et al.,**

medicines. Most of the medicines are derived from Natural or semi-synthetic natural derivatives. The medicinal system of the United States of America relies on about 25% of plant constituents as well as developing countries like India and China reckon on 80% of plant drugs [1]. India is a rich repository of medicinal plants codified around 8000 herbal remedies. This includes approximately 7,000 plants being used in Ayurveda, 600 in Siddha, 700 in Unani, and 30 in modern medicine. As a result, this makes India one of the 12 mega biodiverse countries of the world [2].

People have turned to herbal medicine and complementary therapy when they feel that conventional medicine has a shortfall. An extract from the Chinese plant *Artimisia annua* is used to treat malaria. Taxol is used as cancer chemotherapy, which is derived from the Pacific yew tree, and natural aspirin, extracted from the willow tree likewise there is many examples [3]. Although widely accepted, herbal plants suffer some limitations due to the complexities of separation, identification and quantification of plant extracts. Accordingly, several separation techniques and detectors are developed to improve selectivity, sensitivity and speed during extract separation. In this study, we reviewed some Indian medicinal plants that possess effective pharmaceutical activities and are multipurpose plants that contain beneficial bioactive compounds that possess activity against various diseases and help in improving livelihood and justify their use as traditional medicine.

Carissa carandas, *Chlorophytum borivillianum*, *Tinospora cordifolia* and *Swertia chirata* have demonstrated pharmaceutical applications, bioactive compounds, and have made advancements in the assessment of biochemical profiles, especially using bioactive compounds. The importance of analytical methods in providing correct and reliable information about the biochemicals of medicinal plants whose chemistry is still poorly known or described is also emphasised. Techniques such as thin layer chromatography (TLC), high performance thin layer chromatography (HPTLC), high-performance liquid chromatography (HPLC), gas chromatography (GC), spectrophotometry, near-infrared spectroscopy (NIRS), nuclear magnetic resonance spectroscopy (NMR), fluorimetry and phosphorimetry, electrochemical, kinetic analysis, electrophoretic evaluation, flow injection and sequential injection analysis Chromatographic approaches, particularly liquid chromatography (LC), are the preferred methods for bio-analytical monitoring of drugs in biological materials. Continuous development of other hyphenated techniques such as ultra-high-performance LC (UHPLC), ion mobility (MS), etc are relevant and efficient, with the application of hyphenated techniques.

Therapeutic potential of *Carissa carandas*, *Chlorophytum borivillianum*, *Tinospora cordifolia*, *Swertia chirata* present status and perspectives

Bioactive compounds isolated from four commercially available medicinal plants

Bioactive compounds identification and isolation over the years has been an important research area for study, that assist the discovery of novel chemicals. Bioactive compounds of the four medicinal plants of interest mentioned based on available ethnobotanical literature.

Carissa carandas

The earlier report on *Carissa carandas* revealed several bioactive compounds including Lanostane triterpenoid, naringin, stigmasterol, lupeol, oleanolic, carrissone, scopoletin, triterpene carandinol isolated using different chromatographic techniques. As a follow up to the established reports, researchers have developed and validated different systems for quantification of these compounds including chromatography and spectroscopy approaches. In these studies, lupeol, stigmasterol, and b-sitosterol were estimated from the fruit of *Carissa carandas* by the HPLC-DAD method with a PDA detector. Furthermore, lanostane triterpenoid showing adaptogenic activity was isolated from fruit and characterized by combinational spectroscopic (UV, IR, ¹H, ¹³C NMR and MS) methods [17]. Cyanidin-3-O-glucoside is an anthocyanin compound identified in the fruit of *Carissa carandas* was characterized in coupling with HPLC and HRMS [18]. In addition to the aforementioned bioactive compounds GC method coupled with high-resolution mass spectroscopy and FT-IR is used to reveal steroid derivative 20-hydroxypregnan 18-oic acid which



**Suniti Yadav et al.,**

was found to show potent scavenging activity [19]. Comprehensive UPLC-MS/MS is used to chemo profiled leaf of *Carissa carandas* and to isolate naringin (NG) from different chromatography techniques that show anti-inflammatory activities [20]. In some more study UV, IR, Mass, ¹H-NMR, ¹³C-NMR, HMQC and HMBC are used to characterized des-Nmethylnoracronycine, an acridone alkaloid, carissone, carindone, lupeol besides stigmaterol, ursolic acid and its methyl ester from roots of *Carissa carandas* [21].

Tinospora cordifolia

Earlier research outlined seven compounds 11-hydroxymustakone, N-methyl-2-pyrrolidone, N-formylannonain, cordifolioside A, magnoflorine, tinocordiside, syringin obtained by *Tinospora cordifolia* stem, validated by nuclear magnetic resonance (NMR) and mass spectrometry (MS), whereas cordifolioside A and syringin have been reported to possess immunomodulatory activity [22]. In another study cordifolide A, a novel unprecedented sulfur-containing clerodane diterpene glycoside, along with two new diterpene glycosides, cordifolides B and C, and four known analogues, were purified by RP-18 column and confirmed by NMR and single-crystal X-ray crystallographic analysis [23]. Normal phase chromatography purification led to the isolation of N-formylannonain, magnoflorine, jatrorrhizine, palmatine, 11-hydroxymustakone, cordifolioside A, tinocordiside, yangambin and characterized based on NMR and mass spectroscopic techniques that show anticancer activity against KB and CHOK-1 [24]. Berberine a compound present in *Tinospora cordifolia* was analysed and quantified through LCMS-QTOF further its presence was confirmed by ESI-MS spectra [25]. On the contrary, combining direct analysis in real-time (DART) ion source coupled to high-resolution time-of-flight (TOF) mass spectrometer (MS) along with multivariate analysis was developed and applied for metabolic fingerprinting and screening of the major phytochemicals of *Tinospora cordifolia* [26].

Swertia chirata

The chemical profile of *Swertia chirata* shows xanthone and its nine-derivative isolated from roots and aerial parts was established by spectral evidence (UV, IR proton magnetic resonance, and mass spectrometry). High-performance liquid chromatography/electrospray ionization tandem mass spectrometry (LC/ESI-MS/MS) (Liquid chromatography/tandem mass spectrometric is used to isolate xanthone and secoiridoid glycosides contain mangiferin, amarogentin, amaroswerin, sweroside and swertiamarin [27]. However, *Swertia chirata* individually and in combination with other plants was evaluated using in vitro antioxidant assays and analyzed by HPLC-PDA for herbal formulation. The resultant data were analysed by principal component analysis (PCA) and chromatographic separation was performed using reversed-phase HPLC [28].

Chlorophytum borivilianum

Saponin considered as an active phytoconstituent of *Chlorophytum borivilianum*. Research on the isolation and characterization of saponin has been ongoing. Spirostane-type saponins named borivilianosides E-H (1-4) from *Chlorophytum borivilianum* were isolated together with two known steroid saponins (5 and 6), structures of 1-4 were elucidated using mainly 2D NMR spectroscopic techniques and mass spectrometry [29]. Conversely Infra-Red, Nuclear Mass Resonance, Mass spectroscopy and GC-MS analysis saponin named as Chlorophytoside-I (3 β , 5 α , 22R, 25R)- 26-(β -D-glucopyranosyloxy)- 22-hydroxy-furostan- 12-one-3yIO- β -Dgalactopyranosyl (1-4) glucopyranoside [30]. Quantitative analysis of 1'-acetoxychavicol acetate (ACA) isolated from *Chlorophytum borivilianum* was performed by photodiode array and, the structure of ACA was elucidated based on the spectral data of ¹H NMR, ¹³C NMR, DEPT, COSY, HMBC, HMQC [31]. Correspondingly Saponin- enriched fraction was confirmed by foam test and its composition was observed by ultra-high-performance liquid chromatography coupled with electrospray ionization quadrupole time-of-flight mass spectrometry (UPLC-ESI-Q-TOF-MS/MS) [32]. Another promising results of AgNPs of *Chlorophytum borivilianum*, callus was characterized by UV-visible spectrophotometry, X-ray Diffraction (XRD), Atomic Force Microscopy (AFM), and Fourier Transform Infrared Spectroscopy [33].



**Suniti Yadav et al.,**

Changing Approach to improve medicinal plant research

Sample Preparation

Sample preparation is the pivotal step to extract chemical constituents embedded in the matrix of plants, so for their extraction solvent extraction, distillation method, pressing and sublimation are some extraction method based on their principle. Constituents are present in very small amount, some are thermo labile, that losses at high temperature so there is an imperative need to adopt an advanced effective extraction method, such that we get greater extraction yield having a high solvent to solid ratio. A study shows that the Soxhlet extraction technique integrates the advantages of reflux extraction and percolation, with the concept of reflux and siphoning to extract the herb with fresh solvent continuously. Researchers use the Soxhlet method for extraction of *Carissa carandas* because of high extraction efficiency and consumption of less solvent as compared to maceration or percolation [34]. Likewise, Soxhlet is used in the extraction of *Tinospora cordifolia*, *Swertia chirata*, *Chlorophytum borivillianum*. In another study ultrasonic bath and sonicate is used to extract polyphenolic constituents from *Carissa carandas*, creating cavitation and accelerating the dissolution and diffusion of the solute as well as the heat transfer, that increase the efficiency of extraction, and are applicable for thermo labile and unstable compounds

[35].Alternatively, a high-efficiency homogenizer is used for *Carissa carandas* anticancer analysis [36]. The high temperature and long extraction time in the extraction from Soxhlet would increase the possibilities of thermal degradation, successful results are shown by maceration of *Tinospora cordifolia* [37], Percolation is more efficient than maceration because it is a continuous process in which the saturated solvent is constantly being replaced by fresh solvent researchers used this method in the extraction of *Tinospora cordifolia* [38],Correspondingly use percolation in the extraction of *Swertia chirata*. Microwave-assisted extraction generates heat through ionic conduction and dipole rotation mechanisms, heat transfer and mass transfer are in the same direction that enhances extraction yield resulting in decrease thermal degradation, extraction of *Swertia chirata* shows microwaves assisted extraction was found to be higher than aqueous extraction [39]. Although these studies have some limitations thermo labile and volatile compounds get degraded due to the high temperature, because of which a lot of solvents get wasted, resulting in an improper yield, consuming lots of time [40]. Herein, modern techniques come into play which is designed such that they could potentially overcome the pitfalls and obstacles which have been observed while using older techniques like Ultrasound-assisted extraction, microwave-assisted, pulse electric field, enzyme assisted extraction, supercritical fluid extraction (SFC), pressurized liquid extraction (PLE), hydro distillation and steam distillation consume moderate solvent and possess high selectivity and conquer temperature issue.

Isolation and Purification of Compounds

Natural compounds are the mixture of bio-diversified compounds, isolation and recovery of these compounds are strenuous processes. The first step in this process is a selection of an ideal technique to yield a target compound. Based on physicochemical properties various chromatography techniques designed for isolation of secondary metabolites, based on acid-base properties, solubility, stability, charge and molecular size. Separation techniques like Low-pressure column chromatography, Ion- exchange chromatography, thin- layer chromatography, high-performance thin-layer chromatography, high-speed counter-current chromatography, and high-performance liquid chromatography are in use. In a study of steroid fraction isolated from *Carissa carandas* using silica 60-120, mesh size column chromatography possesses potent antioxidant activity with an EC₅₀ value of (546.4µg/ml) [41].Likewise, naringin isolated from *Carissa carandas* using hydrophobic interaction chromatography on Dianion HP- 20 resin shows anti-inflammatory activity. Similarly, column chromatography on Dianion HP-20 was used in the separation of *Tinospora cordifolia* fractions. Priority is to work on modern isolation techniques that can resolve hindrance in the isolation process and prove to be more efficient. With this aim, Molecular distillation separates thermo sensitive and high-molecular-weight compounds, Gas chromatography is a fast and efficient method ideal for the separation of volatile compounds. Supercritical fluid chromatography (SFC) is a combination of GC and liquid chromatography (LC) that have high dissolving capability, high diffusivity and low viscosity, which enhance the separation efficiency. An attracted molecular imprinted technology has a unique feature that possesses high selectivity, low cost and easy





Suniti Yadav et al.,

preparation and is used widely in the separation of natural. Simulated moving bed (SMB) chromatography uses multiple columns with stationary phases (bed) is a continuous separation method and a powerful tool for the large-scale separation of natural products with the advantage of lower solvent consumption over a shorter period. Multi-dimensional separation based on the solid-phase extraction and coupling of multiple columns with different stationary phases greatly improves the separation efficiency having multiple dimensional separation equipment becoming more rapid, efficient and automated.

Analytical Techniques

Recent trends in combination with analytical chemistry, biochemistry, bioinformatics that improve the detection and identification of 50-1500Da size metabolites from a biological sample and study their target site. Widespread use of these instruments like GC-MS, NMR, and LC-MS are highly sophisticated instruments that can read very sensitive signal and reproduce the data. HPLC is a separation technique coupled with a diverse detector that has substantial applications. HPLC hyphenated with UV-photodiode array detection and mass spectrometry is a breakthrough in raw plant extract analysis. A significant innovation of high-resolution mass spectrometers using Orbit rap or hybrid quadrupole- time-flight (Q-TOF) mass spectrometers, enabling the direct identification of the molecular formula of the secondary metabolites. The full phytochemical characterization of complex extracts, as well as the determination of the structure of secondary metabolites, can be further enhanced by the use of relatively novel and advanced hyphenated techniques such as LC-NMR, LC-NMR-MS, LC-SPE-NMR, LC-DAD / MS-SPE-NMR and finally LC-HRMS-SPE-NMR. Hyphenated techniques are extremely useful in the process of dereplication, aimed at detection [42]. Metabolomics study of these identified compounds.

Synergism and Polyherbal Formulations

Individual constituents present in crude extract some time show inadequate therapeutic efficiency. Synergism and Polyherbal formulation is a concept that ameliorates therapeutic efficiency. The additive effect in combination with herbs enhanced pharmaceutical property and decrease toxicity as compared to an individual. Polyherbal formulation from *Tinospora cordifolia* shows the effective treatment of various diseases, its product Entox, Septilin possesses anti-inflammatory activity, Diasulin, Hyponid as an antidiabetic activity, Himolin as a hepatoprotective activity, Immu - 21 as an immunomodulatory activity. Furthermore, Diabegon is a polyherbal product that constituent *Swertia chirata* used for the treatment of diabetic [43]. Along with the study, *Chlorophytum borivillianum* shows synergistic evidence on spermatogenic effect for the treatment of oligospermia leading to infertility [44,45]. In this way, the polyherbal formulation provides a holistic approach for the treatment of various diseases.

Modifications and Optimisation of Lead Compounds

Secondary metabolites present in a natural product have an enormous lead compound that could show pharmaceutical properties, but the presence of multi scaffolds structure hampers, encounter to target binding site that can invoke physicochemical, pharmacokinetic and biopharmaceutical properties. Therefore, molecular modification of these structures could be a better strategy for increasing efficiency and led to drug discovery. The main aspect of the design of active compounds that have full medicinal, toxicological and druggable properties, for these modifications, work has been performed to increase strength and selectivity, enhance solubility and partitioning properties, increase metabolic and chemical stability, modulate pharmacokinetic parameters, remove or minimize toxicity and adverse reactions, and become novel. The key aspect to design an active compound that full fill pharmaceutical, toxicological, and druggable properties, for this modification performed activity to raise novelty and intellectual property [46].

CONCLUSION AND DISCUSSION

Investigation of Traditional medicinal plants for repurpose to use for the ailment of diseases by using modern technologies. This review summarised reassessment of some traditional medicinal plants, *Carissa carandas*,





Suniti Yadav et al.,

Chlorophytum borivilium, *Tinospora cordifolia*, *Swertia chirata* that confirmed the pharmaceutical, phytochemical and nutritional value of these plants. These plants have shown potential antimicrobial, antioxidant, antidiabetic, anticancer, anti-inflammatory etc. A lot of papers have reported on the knowledge of *Carissa carandas* is largely reported on crude extract to have very limited data on purified compounds, although research has been restricted only to terpenoids, so there is a need to shed light on other compounds to perpetuate traditional plants usage. Saponins and their derivative isolated from roots of *Chlorophytum borivilium* are notably important compounds, bioassay-guided isolated compounds using advance techniques might help to identify more lead compounds. Looking way forward attention should be given to advancement for exploring more traditional medicinal plants by using phylogenetic analysis, using tools of bioinformatics, and searching for new lead compounds.

ACKNOWLEDGEMENTS

The authors are thankful to the Department of Biochemistry and Central library of Bundelkhand University for providing the necessary facilities.

The authors declare no conflict of interest

REFERENCES

1. Khan, M.A., 2016. Introduction and importance of medicinal plants and herbs. *National Health Portal (NHP)*.
2. World Health Organization. *WHO Country Cooperation Strategy 2006-2011 India: Supplement on Traditional Medicine*. 2007.
3. Balunas, Marcy J., and A. Douglas Kinghorn. "Drug discovery from medicinal plants." *Life sciences* 78.5 (2005): 431-441.
4. Galipalli, S., Patel, N. K., Prasanna, K., & Bhutani, K. K. (2015). Activity-guided investigation of *Carissa carandas* (L.) roots for anti-inflammatory constituents. *Natural product research*, 29(17), 1670-1672.
5. Begum, Sabira, et al. "Carandinol: First isohopane triterpene from the leaves of *Carissa carandas* L. and its cytotoxicity against cancer cell lines." *Phytochemistry Letters* 6.1 (2013): 91-95.
6. Antonisamy, Paulrayer, et al. "Gastroprotective effect of epoxy clerodane diterpene isolated from *Tinospora cordifolia* Miens (Guduchi) on indomethacin-induced gastric ulcer in rats." *Phytomedicine* 21.7 (2014): 966-969.
7. Jain, Aastha, et al. "Comparative study of phytochemical screening and antibacterial activity of four medicinal plants." *Journal of Medicinal Plants* 7.4 (2019): 81-89.
8. Aranha, Ivan, Fatima Clement, and Yeldur P. Venkatesh. "Immunostimulatory properties of the major protein from the stem of the Ayurvedic medicinal herb, guduchi (*Tinospora cordifolia*)." *Journal of ethnopharmacology* 139.2 (2012): 366-372.
9. Sharma, Upendra, et al. "Immunomodulatory active compounds from *Tinospora cordifolia*." *Journal of ethnopharmacology* 141.3 (2012): 918-926.
10. Bala, Manju, et al. "Validation of ethnomedicinal potential of *Tinospora cordifolia* for anticancer and immunomodulatory activities and quantification of bioactive molecules by HPTLC." *Journal of ethnopharmacology* 175 (2015): 131-137.
11. Sharma, Neha, et al. "A new clerodane furano diterpene glycoside from *Tinospora cordifolia* triggers autophagy and apoptosis in HCT-116 colon cancer cells." *Journal of ethnopharmacology* 211 (2018): 295-310.
12. Ahmad, Syed Rehan, Abul Kalam, and Kishan Pal. "Phytochemical Analysis and antimicrobial activity of *Chlorophytum borivilium* against bacterial pathogen causing disease in Humans." *International Journal of Applied Science and Engineering* 2.2 (2014): 83.
13. Khanam, Zakia, et al. "Safed musli (*Chlorophytum borivilium*): A review of its botany, ethnopharmacology and phytochemistry." *Journal of ethnopharmacology* 150.2 (2013): 421-441.
14. Acharya, Debabrata, et al. "Cytotoxic spirostane-type saponins from the roots of *Chlorophytum borivilium*." *Journal of natural products* 72.1 (2009): 177-181.





Suniti Yadav et al.,

15. Sayyed, M., et al. "Pharmacognostical and phytochemical investigations of the whole plant of *Swertia chirata* and *Hemidesmus indicus*." *Journal of Pharmaceutical and Biosciences* 4 (2013): 141-145.
16. Banerjee, Shivaji, et al. "Assessment of the anti-inflammatory effects of *Swertia chirata* in acute and chronic experimental models in male albino rats." *Indian Journal of Pharmacology* 32.1 (2000): 21-24.
17. Arif, Muhammad, et al. "Adaptogenic activity of lanostane triterpenoid isolated from *Carissa carandas* fruit against physically and chemically challenged experimental mice." *Pharmacognosy Journal* 5.5 (2013): 216-220.
18. Sarkar, Rohan, et al. "Anthocyanin composition and potential bioactivity of karonda (*Carissa carandas* L.) fruit: An Indian source of biocolorant." *LWT* 93 (2018): 673-678.
19. Bhadane, Bhushan S., and Ravindra H. Patil. "Isolation, purification and characterization of antioxidative steroid derivative from methanolic extract of *Carissa carandas* (L.) Leaves." *Biocatalysis and agricultural biotechnology* 10 (2017): 216-223.
20. El-Desoky, Ahmed H., et al. "Anti-inflammatory and antioxidant activities of naringin isolated from *Carissa carandas* L.: In vitro and in vivo evidence." *Phytomedicine* 42 (2018): 126-134.
21. Ganapaty, S., Ch Bharath, and H. Laatsch. "Des-N-Methylnoracronycine from the roots of *Carissa conjesta* Wight." *International Journal of Green Pharmacy (IJGP)* 4.3 (2010).
22. Sharma, Upendra, et al. "Immunomodulatory active compounds from *Tinospora cordifolia*." *Journal of ethnopharmacology* 141.3 (2012): 918-926.
23. Pan, Li, et al. "Cordifolide A, a sulfur-containing clerodane diterpene glycoside from *Tinospora cordifolia*." *Organic letters* 14.8 (2012): 2118-2121.
24. Bala, Manju, et al. "Validation of ethnomedicinal potential of *Tinospora cordifolia* for anticancer and immunomodulatory activities and quantification of bioactive molecules by HPTLC." *Journal of ethnopharmacology* 175 (2015): 131-137.
25. Mittal, Jitendra, and Madan Mohan Sharma. "Enhanced production of berberine in *In vitro* regenerated cell of *Tinospora cordifolia* and its analysis through LCMS QToF." *3 Biotech* 7.1 (2017): 25.
26. Bajpai, Vikas, et al. "Metabolic fingerprinting of dioecious *Tinospora cordifolia* (Thunb) Miers stem using DART TOF MS and differential pharmacological efficacy of its male and female plants." *Industrial Crops and Products* 101 (2017): 46-53.
27. Suryawanshi, Satyendra, et al. "Liquid chromatography/tandem mass spectrometric study and analysis of xanthone and secoiridoid glycoside composition of *Swertia chirata*, a potent antidiabetic." *Rapid Communications in Mass Spectrometry: An International Journal Devoted to the Rapid Dissemination of Up-to-the-Minute Research in Mass Spectrometry* 20.24 (2006): 3761-3768.
28. Kaur, Pardeep, et al. "Development of aqueous-based multi-herbal combination using principal component analysis and its functional significance in HepG2 cells." *BMC complementary and alternative medicine* 19.1 (2019): 1-17.
29. Acharya, Debabrata, et al. "Cytotoxic spirostane-type saponins from the roots of *Chlorophytum borivilianum*." *Journal of natural products* 72.1 (2009): 177-181.
30. Deore, Sharada L., and Somshekhar S. Khadabadi. "Isolation and characterization of phytoconstituents from *Chlorophytum borivilianum*." *Pharmacognosy research* 2.6 (2010): 343.
31. Chua, B., et al. "Isolation, structure elucidation, identification and quantitative analysis of 1'-acetoxychavicol (ACA) from the roots of *chlorophytum borivilianum* (SAFED MUSLI)." *J Eng Sci Technol* 12.1 (2017): 198-213.
32. Singh, Rahul, et al. "A comparative analysis of saponin-enriched fraction from *Silene vulgaris* (Moench) Garcke, *Sapindus mukorossi* (Gaertn) and *Chlorophytum borivilianum* (Santapau and Fernandes): an in vitro hemolytic and cytotoxicity evaluation." *Animal Biotechnology* (2020): 1-7.
33. Huang, Fengchang, et al. "Safed Musli (*Chlorophytum borivilianum* L.) Callus - mediated biosynthesis of silver nanoparticles and evaluation of their antimicrobial activity and cytotoxicity against human colon cancer cells." *Journal of Nanomaterials* 2019 (2019).
34. Patil, Sandip, et al. "Steroidal fraction of *Carissa carandas* L. inhibits microbial hyaluronidase activity by mixed inhibition mechanism." *Preparative Biochemistry and Biotechnology* 49.3 (2019): 298-306.





Suniti Yadav et al.,

35. Siddiqi, Rahmanullah, et al. "Antimicrobial activity of the polyphenolic fractions derived from *Grewia asiatica*, *Eugenia jambolana* and *Carissa carandas*." *International journal of food science & technology* 46.2 (2011): 250-256.
36. Gupta, Priti, et al. "In-vitro cancer cell cytotoxicity and alpha amylase inhibition effect of seven tropical fruit residues." *Asian Pacific Journal of Tropical Biomedicine* 4 (2014): S665-S671.
37. Kumar, Vijay, et al. "Phytochemical, antioxidant, antimicrobial, and protein binding qualities of hydro-ethanolic extract of *Tinospora cordifolia*." *Journal of Biologically Active Products from Nature* 8.3 (2018): 192-200.
38. Sengupta, Subhabrata, et al. "Hypoglycemic activity of the antioxidant saponarin, characterized as α -glucosidase inhibitor present in *Tinospora cordifolia*." *Journal of enzyme inhibition and medicinal chemistry* 24.3 (2009): 684-690.
39. Kekuda, TR Prashith, et al. "Influence of extraction time on antifungal activity of *Hemidesmus indicus* and *Swertia chirata*." (2009).
40. Zhang, Qing-Wen, Li-Gen Lin, and Wen-Cai Ye. "Techniques for extraction and isolation of natural products: A comprehensive review." *Chinese medicine* 13.1 (2018): 1-26.
41. Bhadane, Bhushan S., and Ravindra H. Patil. "Isolation, purification and characterization of antioxidative steroid derivative from methanolic extract of *Carissa carandas* (L.) leaves." *Biocatalysis and agricultural biotechnology* 10 (2017): 216-223.
42. Cieřla, Łukasz, and Ruin Moaddel. "Comparison of analytical techniques for the identification of bioactive compounds from natural products." *Natural product reports* 33.10 (2016): 1131-1145.
43. Karole, Sarita, et al. "Polyherbal formulation concept for synergic action: a review." *Journal of Drug Delivery and Therapeutics* 9.1-s (2019): 453-466.
44. Hussain, Syed Ammar, et al. "Evaluation of the spermatogenic activity of polyherbal formulation in oligospermic males." *BioMed research international* 2018 (2018).
45. Balkrishna, Acharya, et al. "Anti-Acetyl cholinesterase activities of mono-herbal extracts and exhibited synergistic effects of the phytoconstituents: a biochemical and computational study." *Molecules* 24.22 (2019): 4175.
46. Guo, Zongru. "The modification of natural products for medical use." *Acta Pharmaceutica Sinica B* 7.2 (2017): 119-136.

Plant	Pharmacological activity	Active constituents	Analytical Technique	References
<i>Carissa Carandas</i>	Antimicrobial activity, cytotoxic activity, Antidiabetic activity, anti-inflammatory activity, antineoplastic activity	Lanostane triterpenoid, Naringin, Stigmasterol, lupeol, oleanolic, carrisone, scopoletin, triterpene carandinol.	UV, IR, 1H, 13C NMR and MS, High Resolution Mass Spectrometry, HPLC, FT-IR and GC-HRMS, UPLC-MS/MS, UV, IR, Mass, 1H-NMR, 13C-NMR, HMOC and HMBC.	4,5
<i>Tinospora cordifolia</i>	Antimicrobial, anti-inflammatory, anti-cancer, anti-oxidant, hepatoprotective activity	cordifolioside A and syringing, jatrorrhizine, palmatine, and magnoflorine, Bis(2-ethyl hexyl) 1H-pyrrole-3,4-dicarboxylate, N-formylannonain, magnoflorine, jatrorrhizine,	HPLC, normal phase chromatography, NMR and mass spectroscopic techniques, HPTLC, X-ray crystallographic analysis	6,7,8,9,10,11





Suniti Yadav et al.,

		palmatine, 11-hydroxymustakone, cordifolioside A, tinocordiside and yangambin, palmatine and berberine.		
<i>Chlorophytum borivilianum</i>	Antimicrobial activity, Anti-inflammatory activity, aphrodisiac activity, Cytotoxic activity	saponins, sapogenins, spirostane glycosides, furostane, Saponin stigmasterol, Spirostane-type saponins and borivilianosides E-H (1-4), 31% inulin-type fructans and 25% acetylated mannans.	2D NMR spectroscopic techniques and mass spectrometry,	12,13,14
<i>Swertia chirata</i>	Antimicrobial, antidiabetic, anti-oxidant, anti-hepatotoxicity, anticancer activity, Antiviral activity	Xanthone, Triterpenoids, oleanolic acid and 12-hydroxyoleanolic lactone.	UV, IR. proton magnetic resonance, and mass spectrometry, highperformance liquidchromatography/electrospray ionization tandem mass spectrometry (LC/ESIMS/MS)	15,16

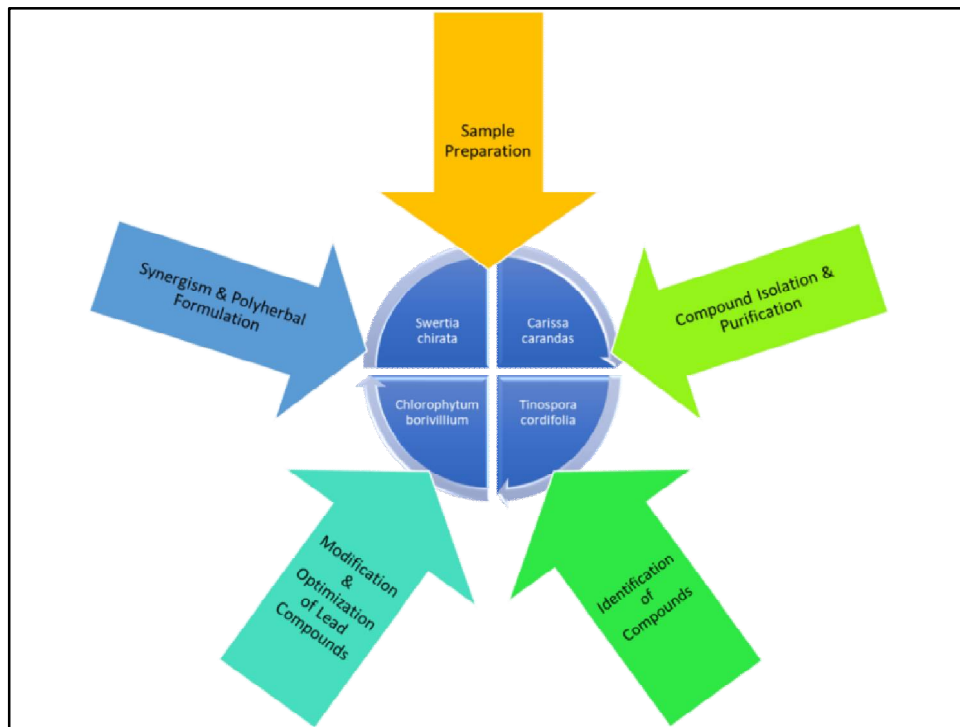


Figure 1: Diagrammatic representation of Medicinal plants with their prospect to increase efficiency.





Some Upper Bounds for the Divisor Degree Energy of Graphs and Divisor Degree Hyper Energy of Graphs

Kanniga Devi Sundaraperumal and Nagarajan. K*

Research Scholar, P.G and Research Department of Mathematics, Sri S. Ramasamy Naidu Memorial College, Sattur, Tamil Nadu, India.

Received: 19 Feb 2021

Revised: 03 Mar 2021

Accepted: 08 Mar 2021

*Address for Correspondence

Nagarajan. K

P.G and Research Department of Mathematics,
Sri S. Ramasamy Naidu Memorial College,
Sattur, Tamil Nadu, India.

Email: k_nagarajan_srnmc@yahoo.co.in



This is an Open Access Journal / article distributed under the terms of the **Creative Commons Attribution License** (CC BY-NC-ND 3.0) which permits unrestricted use, distribution, and reproduction in any medium, provided the original work is properly cited. All rights reserved.

ABSTRACT

The sum of the absolute values of eigen values of an adjacency matrix gives the energy of a graph G . With the motivation of energy of a graph, we newly defined divisor degree energy of graph G . In this paper, we acquire the upper bounds for the divisor degree energy of certain graph such as friendship graph, windmill graph, lollipop graph, tadpole graph and p -barbell graph. Also, we define the divisor degree hyper energy of graphs.

Keywords: Bounds, Energy, Divisor degree energy, Divisor degree matrix, Divisor degree hyper energy

INTRODUCTION

In this article, we are using a simple graph G with n vertices and m edges. Among n - vertex graph, its degree, maximum degree and minimum degree are denoted by d_i , Δ and δ respectively. The energy of a graph [1] was first initiated by Ivan Gutman in 1978. This concept was appeared from Mathematical chemistry. The energy of a graph is got from the adjacency matrix, is defined as follows:

An adjacency matrix of G [1], denoted by $A = A(G) = [a_{ij}]$ is a square matrix of order of n where

$$a_{ij} = \begin{cases} 1, & \text{if } v_i \text{ is adjacent to } v_j \\ 0, & \text{otherwise} \end{cases}$$





Kanniga Devi Sundaraperumal and Nagarajan

The eigen values of A , which are the zeros of $|\lambda I - A|$ are the eigen values of G . Since the adjacency matrix is a real symmetric matrix, all its eigen values are real and hence the eigen values are in non-increasing order. Then, the energy of G , denoted by $E(G)$ is defined as

$$E(G) = \sum_{i=1}^n |\lambda_i|.$$

Also, Ivan Gutman hypothesized that among n -vertex graph G , the complete graph K_n has the maximum energy. But, this was contradicted by Waliker *et al* [2]. He clarified the concept of hyper energetic graphs that a graph with n vertices satisfies $E(G) > E(K_n)$. With this idea, we introduced a new energy of a graph called divisor degree energy [3]. For that, we newly defined a following matrix:

A real symmetric matrix with n vertices gives divisor degree matrix $DD(G)$ [3] of a graph G as

$$dd_{ik} = \begin{cases} \left[\frac{d_i}{d_k} \right] + \left[\frac{d_k}{d_i} \right] & \text{if } v_i, v_k \text{ are adjacent and } d_i \neq d_k \\ 1 & \text{if } v_i, v_k \text{ are adjacent and } d_i = d_k \\ 0 & \text{otherwise} \end{cases}$$

where $[x]$ denotes integral part of real number x and its eigen values are in non-increasing order. The divisor degree energy (DDE) is defined as

$$E_{DD}(G) = \sum_{i=1}^n |\gamma_i|.$$

We noticed that $A(G)$ and $DD(G)$ of regular graphs would have same eigen values of a graph G .

SOME KNOWN RESULTS

The following known results are required for the later part of this paper to find the upper bounds for the divisor degree energy of graph G .

Theorem 2.1.[4] For a star $K_{1,n-1}$ $E_{DD}(K_{1,n-1}) = 2(n-1)\sqrt{n-1}$.

Theorem 2.2.[4] If G is a r -regular graph with triangle free and $n = 2r$ then $E_{DD}(G) = n$.

Proposition 2.3.[5] If A is an $m \times n$ matrix and B is a $p \times q$ matrix, then the Kronecker product $A \otimes B$ is the $mp \times nq$ block matrix:

$$A \otimes B = \begin{bmatrix} a_{11}B & \cdots & a_{1n}B \\ \vdots & \ddots & \vdots \\ a_{m1}B & \cdots & a_{mn}B \end{bmatrix}$$





Kanniga Devi Sundaraperumal and Nagarajan. K

Proposition 2.4.[5] Let A and B be square matrices of order n and m . Let $\lambda_i (i = 1, 2, \dots, n)$ and $\mu_j (j = 1, 2, \dots, m)$ be the eigen values of A and B respectively. Then $\lambda_i \mu_j$ is the eigen values of $A \otimes B$.

Proposition 2.5.[6,7] Let the adjacency matrices of G_1, G_2 and G_3 satisfy the condition $A(G_1) + A(G_2) = A(G_3)$. Then $E(G_1) + E(G_2) \geq E(G_3)$.

Remark 2.6.[3,8]

$$E(K_n) = E_{DD}(K_n) = 2(n-1).$$

$$E(K_{p,q}) = n, \text{ where } n = p + q.$$

MAIN RESULTS

In this portion, we acquire some upper bounds for the divisor degree energy of graphs and also define the divisor degree hyper energy of graphs.

Theorem 3.1. For a friendship graph $F_3^{(p)}$ with $2p+1$ vertices, then $tr(DD(F_3^{(p)}))^2 = 2p(2p^2 + 1)$ and $E_{DD}(F_3^{(p)}) < \sqrt{n(np - p + 1)(n - 1)}$.

Proof. The divisor degree matrix of $F_3^{(p)}$ is given by

$$DD(F_3^{(p)}) = \begin{bmatrix} 0 & 1 & 0 & 0 & \dots & 0 & 0 & n \\ 1 & 0 & 0 & 0 & \dots & 0 & 0 & n \\ 0 & 0 & 0 & 1 & \dots & 0 & 0 & n \\ 0 & 0 & 1 & 0 & \dots & 0 & 0 & n \\ \vdots & & & \ddots & & & & \vdots \\ 0 & 0 & 0 & 0 & \dots & 0 & 1 & n \\ 0 & 0 & 0 & 0 & \dots & 1 & 0 & n \\ n & n & n & n & \dots & n & n & 0 \end{bmatrix}$$

$$tr(DD(F_3^{(p)}))^2 = (p^2 + 1)2p + 2p^2 \times p = 2p(2p^2 + 1).$$

Then by using Cauchy-Schwarz inequality,

$$\sum_{i=1}^n \gamma_i < \sqrt{2np(2p^2 + 1)}$$

Therefore, $E_{DD}(F_3^{(p)}) < \sqrt{n(np - p + 1)(n - 1)}$

Theorem 3.2. For a windmill graph $K_n^{(n)}$ with $N = n(n - 1) + 1, (n \geq 3)$ vertices, then $tr(DD(K_n^{(n)}))^2 = N(n^2 + n - 2)$ and $E_{DD}(K_n^{(n)}) < \sqrt{n(n^4 - 2n^2 + 3n - 2)}$.

Proof. The divisor degree matrix of $K_n^{(n)}$ is given by





Kanniga Devi Sundaraperumal and Nagarajan. K

$$DD(K_n^{(n)}) = \begin{bmatrix} 0 & 1 & \dots & 1 & 1 & \dots & 0 & 0 & \dots & 0 & 0 & \frac{N-1}{n-1} \\ 1 & 0 & \dots & 1 & 1 & \dots & 0 & 0 & \dots & 0 & 0 & \frac{N-1}{n-1} \\ \vdots & & \ddots & & \vdots & \vdots & \vdots & & \ddots & & \vdots & \frac{N-1}{n-1} \\ 1 & 1 & \dots & 0 & 1 & \dots & 0 & 0 & \dots & 0 & 0 & \frac{N-1}{n-1} \\ 1 & 1 & \dots & 1 & 0 & \dots & 0 & 0 & \dots & 0 & 0 & \frac{N-1}{n-1} \\ \vdots & \vdots & \dots & \vdots & \vdots & \dots & \vdots & \vdots & \dots & \vdots & \vdots & \frac{N-1}{n-1} \\ 0 & 0 & \dots & 0 & 0 & \dots & 0 & 1 & \dots & 1 & 1 & \frac{N-1}{n-1} \\ 0 & 0 & \dots & 0 & 0 & \dots & 1 & 0 & \dots & 1 & 1 & \frac{N-1}{n-1} \\ \vdots & & \ddots & & \vdots & \vdots & \vdots & & \ddots & & \vdots & \frac{N-1}{n-1} \\ 0 & 0 & \dots & 0 & 0 & \dots & 1 & 1 & \dots & 0 & 1 & \frac{N-1}{n-1} \\ 0 & 0 & \dots & 0 & 0 & \dots & 1 & 1 & \dots & 1 & 0 & \frac{N-1}{n-1} \\ \frac{N-1}{n-1} & \frac{N-1}{n-1} & \dots & \frac{N-1}{n-1} & \frac{N-1}{n-1} & \dots & \frac{N-1}{n-1} & \frac{N-1}{n-1} & \dots & \frac{N-1}{n-1} & \frac{N-1}{n-1} & 0 \end{bmatrix}$$

$$tr(DD(K_n^{(n)}))^2 = \left(\frac{N-1}{n-1} + (n-2)\right)N = N(n^2 + n - 2)$$

Then by using Cauchy-Schwarz inequality,

$$\sum_{i=1}^N \gamma_i < \sqrt{Nn(n^2 + n - 2)}$$

Therefore, $E_{DD}(K_n^{(n)}) < \sqrt{n(n^4 - 2n^2 + 3n - 2)}, (n \geq 3)$.

Theorem 3.3. Let $L_{p,q}$ be lollipop graph of order $n = p + q (p > 2)$. Then

$$tr(DD(L_{p,q}))^2 = p(p-1) + 2\left[\frac{p}{2}\right]^2 + 2q + 4$$

and

$$E_{DD}(L_{p,q}) < \sqrt{(p+q)\left(p(p-1) + 2\left[\frac{p}{2}\right]^2 + 2q + 4\right)}$$

Proof. (i) The divisor degree matrix of $L_{p,q}$ is given by

$$DD(L_{p,q}) = \begin{bmatrix} 0 & 1 & \dots & 1 & 1 & 0 & 0 & 0 & \dots & 0 & 0 & 0 \\ 1 & 0 & \dots & 1 & 1 & 0 & 0 & 0 & \dots & 0 & 0 & 0 \\ \vdots & & \ddots & & \vdots & \vdots & & & \ddots & & \vdots & \\ 1 & 1 & \dots & 0 & 1 & 0 & 0 & 0 & \dots & 0 & 0 & 0 \\ 1 & 1 & \dots & 1 & 0 & \left[\frac{p}{2}\right] & 0 & 0 & \dots & 0 & 0 & 0 \\ 0 & 0 & \dots & 0 & \left[\frac{p}{2}\right] & 0 & 1 & 0 & \dots & 0 & 0 & 0 \\ 0 & 0 & \dots & 0 & 0 & 1 & 0 & 1 & \dots & 0 & 0 & 0 \\ 0 & 0 & \dots & 0 & 0 & 0 & 1 & 0 & \dots & 0 & 0 & 0 \\ \vdots & & \ddots & & \vdots & \vdots & & & \ddots & & \vdots & \\ 0 & 0 & \dots & 0 & 0 & 0 & 0 & 0 & \dots & 0 & 1 & 0 \\ 0 & 0 & \dots & 0 & 0 & 0 & 0 & 0 & \dots & 1 & 0 & 2 \\ 0 & 0 & \dots & 0 & 0 & 0 & 0 & 0 & \dots & 0 & 2 & 0 \end{bmatrix}$$





Kanniga Devi Sundaraperumal and Nagarajan. K

$$\begin{aligned} tr(DD(L_{p,q}))^2 &= (p-1)^2 + (p-1) + \left[\frac{p}{2}\right]^2 + \left[\frac{p}{2}\right]^2 + 1 + 2(q-3) + 5 + 4 \\ &= p(p-1) + 2\left[\frac{p}{2}\right]^2 + 2q + 4, (p > 2). \end{aligned}$$

Then by using Cauchy-Schwarz inequality,

$$\sum_{i=1}^{p+q} \gamma_i < \sqrt{(p+q) \left(p(p-1) + 2\left[\frac{p}{2}\right]^2 + 2q + 4 \right)}$$

Therefore, $E_{DD}(L_{p,q}) < \sqrt{(p+q) \left(p(p-1) + 2\left[\frac{p}{2}\right]^2 + 2q + 4 \right)}$.

Theorem 3.4. Let $T_{p,q}$ be Tadpole graph of order $n = p + q$. Then

$$tr(DD(T_{p,q}))^2 = 2(p+q+3) \text{ and}$$

$$E_{DD}(T_{p,q}) < \sqrt{2(p+q)(p+q+3)}.$$

Proof. (i) The divisor degree matrix of $T_{p,q}$ is given by

$$DD(T_{p,q}) = \begin{bmatrix} 0 & 1 & 0 & \dots & 0 & 0 & 1 & 0 & 0 & 0 & \dots & 0 & 0 & 0 \\ 1 & 0 & 1 & \dots & 0 & 0 & 0 & 0 & 0 & 0 & \dots & 0 & 0 & 0 \\ 0 & 1 & 0 & \dots & 0 & 0 & 0 & 0 & 0 & 0 & \dots & 0 & 0 & 0 \\ \vdots & & & \ddots & & & \vdots & \vdots & & & \ddots & & \vdots & \\ 0 & 0 & 0 & \dots & 0 & 1 & 0 & 0 & 0 & 0 & \dots & 0 & 0 & 0 \\ 0 & 0 & 0 & \dots & 1 & 0 & 1 & 0 & 0 & 0 & \dots & 0 & 0 & 0 \\ 1 & 0 & 0 & \dots & 0 & 1 & 0 & 1 & 0 & 0 & \dots & 0 & 0 & 0 \\ 0 & 0 & 0 & \dots & 0 & 0 & 1 & 0 & 1 & 0 & \dots & 0 & 0 & 0 \\ 0 & 0 & 0 & \dots & 0 & 0 & 0 & 1 & 0 & 1 & \dots & 0 & 0 & 0 \\ 0 & 0 & 0 & \dots & 0 & 0 & 0 & 0 & 1 & 0 & \dots & 0 & 0 & 0 \\ \vdots & & & \ddots & & & \vdots & \vdots & & & \ddots & & \vdots & \\ 0 & 0 & 0 & \dots & 0 & 0 & 0 & 0 & 0 & 0 & \dots & 0 & 1 & 0 \\ 0 & 0 & 0 & \dots & 0 & 0 & 0 & 0 & 0 & 0 & \dots & 1 & 0 & 2 \\ 0 & 0 & 0 & \dots & 0 & 0 & 0 & 0 & 0 & 0 & \dots & 0 & 2 & 0 \end{bmatrix}$$

$$\begin{aligned} tr(DD(T_{p,q}))^2 &= 2(p-1) + 3 + 2(q-2) + 5 + 4 \\ &= 2(p+q+3) \end{aligned}$$

(ii) Using Cauchy-Schwarz inequality,

$$\sum_{i=1}^{p+q} \gamma_i < \sqrt{2(p+q)(p+q+3)}$$

Therefore, $E_{DD}(T_{p,q}) < \sqrt{2(p+q)(p+q+3)}$.





Kanniga Devi Sundaraperumal and Nagarajan. K

Theorem 3.5. For p -barbell graph of order $n = 2p(p > 2)$, then

$$tr(DD(p\text{-barbell}))^2 = 2(p^2 - p + 1) \text{ and}$$

$$E_{DD}(p\text{-barbell}) < 2\sqrt{p(p^2 - p + 1)}..$$

Proof. (i) The divisor degree matrix of p -barbell is

$$\begin{bmatrix} 0 & 1 & 1 & \dots & 1 & 1 & 1 & 0 & 0 & 0 & \dots & 0 & 0 & 0 \\ 1 & 0 & 1 & \dots & 1 & 1 & 1 & 0 & 0 & 0 & \dots & 0 & 0 & 0 \\ 1 & 1 & 0 & \dots & 1 & 1 & 1 & 0 & 0 & 0 & \dots & 0 & 0 & 0 \\ \vdots & & \ddots & & & & & \vdots & \vdots & & \ddots & & & \vdots \\ 1 & 1 & 1 & \dots & 0 & 1 & 1 & 0 & 0 & 0 & \dots & 0 & 0 & 0 \\ 1 & 1 & 1 & \dots & 1 & 0 & 1 & 0 & 0 & 0 & \dots & 0 & 0 & 0 \\ 1 & 1 & 1 & \dots & 1 & 1 & 0 & 1 & 0 & 0 & \dots & 0 & 0 & 0 \\ 0 & 0 & 0 & \dots & 0 & 0 & 1 & 0 & 1 & 1 & \dots & 1 & 1 & 1 \\ 0 & 0 & 0 & \dots & 0 & 0 & 0 & 1 & 0 & 1 & \dots & 1 & 1 & 1 \\ 0 & 0 & 0 & \dots & 0 & 0 & 0 & 1 & 1 & 0 & \dots & 1 & 1 & 1 \\ \vdots & & \ddots & & & & & \vdots & \vdots & & \ddots & & & \vdots \\ 0 & 0 & 0 & \dots & 0 & 0 & 0 & 1 & 1 & 1 & \dots & 0 & 1 & 1 \\ 0 & 0 & 0 & \dots & 0 & 0 & 0 & 1 & 1 & 1 & \dots & 1 & 0 & 1 \\ 0 & 0 & 0 & \dots & 0 & 0 & 0 & 1 & 1 & 1 & \dots & 1 & 1 & 0 \end{bmatrix}$$

$$\begin{aligned} tr(DD(p\text{-barbell}))^2 &= (p-1)(2p-2) + 2p \\ &= 2(p^2 - p + 1), (p > 2). \end{aligned}$$

Then by using Cauchy-Schwarz inequality,

$$\sum_{i=1}^{2p} \gamma_i < \sqrt{4p(p^2 - p + 1)}$$

Therefore, $E_{DD}(p\text{-barbell}) < 2\sqrt{p(p^2 - p + 1)}$.

Observation 3.6. The following graph represents the relation between the number of vertices and divisor degree energy of some standard graphs.

Result 3.7. Let G be a simple graph of order n . Then $n \leq E_{DD}(G) \leq 2(n-1)\sqrt{n-1}$.

Theorem 3.8. Let G be a simple, connected and planar graph with n vertices

and m edges. Then $\frac{m+6}{3} \leq E_{DD}(G) \leq 2(3(n-2))\frac{3}{2}$.

Proof. By result 3.7, we have $n \leq E_{DD}(G) \leq 2m\sqrt{m}$.

If G is a planar graph, then $m \leq E_{DD}(G) \leq 3n - 6 (n \geq 3)$

Now, $E_{DD}(G) \leq 2m\sqrt{m} \Rightarrow E_{DD}(G) \leq 2(3(n-2))\frac{3}{2}$.





Kanniga Devi Sundaraperumal and Nagarajan. K

Also $E_{DD}(G) \geq n \Rightarrow E_{DD}(G) \geq \frac{m+6}{3}$

Therefore, $\frac{m+6}{3} \leq E_{DD}(G) \leq 2(3(n-2)) \frac{3}{2}$.

Corollary 3.9. Let G be a simple, connected and planar graph with n vertices

and m edges having no cycle of length 3. Then $\frac{m+4}{2} \leq E_{DD}(G) \leq 2(2(n-2)) \frac{3}{2}$.

Theorem 3.10. Let the adjacency matrices G_1, G_2 and G_3 satisfy the condition $DD(G_1) + DD(G_2) = DD(G_3)$. Then $E_{DD}(G_1) + E_{DD}(G_2) \geq E_{DD}(G_3)$.

Proof. Clearly, $E_{DD}(G) \geq E_{DD}(K_n)$ and by using proposition 2.3, we get $E_{DD}(G_1) + E_{DD}(G_2) \geq E_{DD}(G_3)$.

Definition 3.11. A graph G on n vertices is said to be divisor degree hyper energy if $E_{DD}(G) > 2(n-1)\sqrt{n-1}$.

Theorem 3.12. If $\overline{S_n}$ is the complement of star graph S_n , then

$$E_{DD}(\overline{S_n}) = 2(n-2)$$

$S_n + \overline{S_n}$ is a divisor degree hyper energy matrix.

Proof. (i) The divisor degree matrix of $\overline{S_n}$ is

$$DD(\overline{S_n}) = \begin{bmatrix} 0 & 1 & 1 & \dots & 1 & 0 \\ 1 & 0 & 1 & \dots & 1 & 0 \\ 1 & 1 & 1 & \dots & 1 & 0 \\ \vdots & & & \ddots & & \vdots \\ 1 & 1 & 1 & \dots & 0 & 0 \\ 0 & 0 & 0 & \dots & 0 & 0 \end{bmatrix} = \begin{bmatrix} DD(K_{n-1}) & O \\ O & O \end{bmatrix}$$

By proposition 2.3 and 2.4, we have $DD(\overline{S_n}) = \begin{bmatrix} 1 & 0 \\ 0 & 0 \end{bmatrix} \otimes DD(K_{n-1})$

$Spec(\overline{S_n}) = (0, -\gamma_i)$, where $\gamma_i (i=1,2,\dots,n-1)$ are the eigen values of K_{n-1} ,

in which 0,-1 are the eigen values of $\begin{bmatrix} 1 & 0 \\ 0 & 0 \end{bmatrix}$.

Hence, $E_{DD}(\overline{S_n}) = \sum_{i=1}^{n-1} |-\lambda_i| = \sum_{i=1}^{n-1} |\lambda_i| = E_{DD}(K_{n-1}) = 2(n-2)$.

(ii) We have,

$$\begin{aligned} E_{DD}(S_n) + E_{DD}(\overline{S_n}) &= 2(n-1)\sqrt{n-1} + 2(n-2) \\ &= 2((n-2) + (n-1)\sqrt{n-1}) \end{aligned}$$





Kanniga Devi Sundaraperumal and Nagarajan. K

Using result 3.7., we get

$$E_{DD}(S_n + \overline{S_n}) \leq 2((n-2) + (n-1)\sqrt{n-1})$$

Therefore, $S_n + \overline{S_n}$ is a divisor degree hyper energy matrix.

CONCLUSION

With the motivation of energy and hyper energy of graph, we defined new indices named divisor degree energy and found out its hyper energy called divisor degree hyper energy of graph.

REFERENCES

1. Gutman I, The Energy of a Graph, Ber. Math. Stat. Sect. Forschungszent Graz, 1978;103:1-22.
2. Walikar H. B, Ramane H. S, and Hampiholi P, On the energy of a graph, in: Balakrishnan R, Mulder H. M, Vijayakumar A, (Eds.), Graph Connections, Allied Publishers, New Delhi 1999;120-123.
3. Kanniga Devi S.P, and Nagarajan K, Divisor Degree Energy of Graphs, International Journal of Mathematical. Archive 2017;8:29-35.
4. Kanniga Devi S.P, and Nagarajan K, Divisor Degree Index of Graphs, International Journal of Mathematics and its Application 2018;6(3):27-30.
5. Horn R.A, Johnson, C.R., Matrix Analysis, Cambridge Univ. Press, New York; 1990.
6. Fan K, Maximum properties and inequalities for the eigen values of completely continuous operators, Proceedings of the National Academy of Sciences of the United States of America 1951; 37:760-766.
7. Wasin So, Maria Robbiano, Nair Maria Maia de Abreu, Ivan Gutman, Application of a theorem of Ky Fan in the theory of graph energy, Linear Algebra and its Application 2010; 432: 2163-2169.
8. Owen Jones, Spectra of Simple Graphs, whitman college, May 13, 2013.

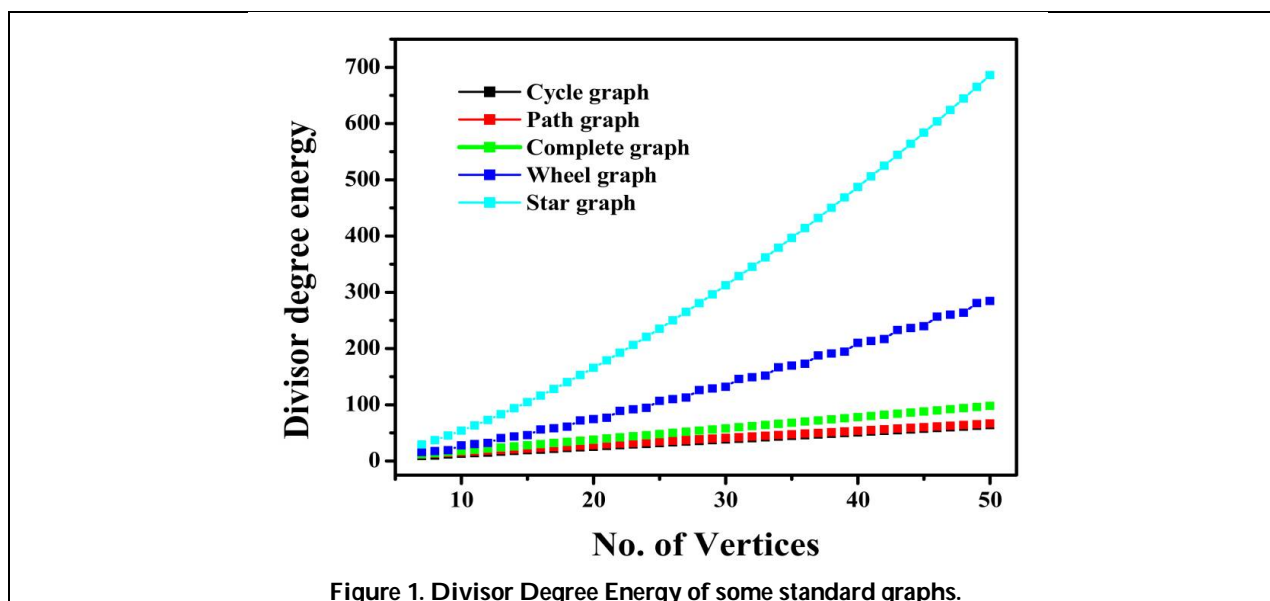


Figure 1. Divisor Degree Energy of some standard graphs.





Vertex Domination in Intuitionistic Fuzzy Graphs

R.Vinitha^{1*} and B.Sreeja²

¹Assistant Professor, Department of Mathematics, KG College of Arts and Science, Coimbatore, Tamil Nadu, India.

²II M.Sc.Mathematics, Department of Mathematics, KG College of Arts and Science, Coimbatore, Tamil Nadu, India.

Received: 19 Feb 2021

Revised: 04 Mar 2021

Accepted: 08 Mar 2021

*Address for Correspondence

R. Vinitha

Assistant Professor,
Department of Mathematics,
KG College of Arts and Science,
Coimbatore, Tamil Nadu, India.
Email: vinitha.r@kcgcas.com



This is an Open Access Journal / article distributed under the terms of the **Creative Commons Attribution License** (CC BY-NC-ND 3.0) which permits unrestricted use, distribution, and reproduction in any medium, provided the original work is properly cited. All rights reserved.

ABSTRACT

Let G be an intuitionistic fuzzy graph. A vertex domination of IFG is a set of vertices such that every strong edge of the intuitionistic fuzzy graph is incident to at least one vertex of the set. In this paper we introduce the concept of intuitionistic fuzzy vertex domination and obtain some interesting results on vertex domination in intuitionistic fuzzy graphs.

Keywords: Intuitionistic, Fuzzy, IFG, Vertex, graph.

INTRODUCTION

The initial definition of fuzzy graphs was proposed by Kafmann from the fuzzy relations introduced by Zadeh. Even though Rosenfeld introduce another elaborated definition, including fuzzy vertex and fuzzy edges, and several fuzzy analogs of graph theoretic concepts such as paths, cycles, connectedness and etc. The theory of domination in fuzzy graphs was investigated by S. Somasundaram and A. Somasundaram [8] at hand the concepts of independent domination, total domination, connected domination of fuzzy graphs [9]. C. Natarajan and S.K. Ayyaswamy introduce the strong (weak) domination in fuzzy graph [3]. The first definition of intuitionistic fuzzy graphs was planned by Atanassov [2]. The idea of domination in intuitionistic fuzzy graphs was investigated by R.Parvathi and G.Thamizhendhi. In this paper weexp and the concept of vertex domination and obtain some interesting results in intuitionistic fuzzy graph [7].





Vinitha and Sreeja

Preliminaries

Graph 2.1

A graph consists of a pair of (V, E) where V is a non empty finite set whose elements are called vertices and E is a set of unordered pairs of distinct elements of V called edges.

Dominating Set 2.2

In graph theory, a dominating set for a graph $G = (V, E)$ is a subset D of V such that each vertex not in D is adjacent to at least one member of D .

Domination Number 2.3

The fuzzy domination number is the minimum cardinality in use over all minimal fuzzy dominating set of G .

Perfect Dominating Set 2.4

A dominating set D of a fuzzy graph G is assumed to be a perfect dominating set if for each vertex v not in D , v is adjacent to exactly one vertex of D . A perfect dominating set D of a fuzzy graph G is assumed to be a minimal perfect dominating set if for each one vertex v in D , $D - \{v\}$ is not a dominating set. A perfect dominating set with smallest cardinality is call a minimum perfect dominating set. It is denoted by γ_{pf} set of G . The cardinality of a minimum perfect dominating set is known the perfect domination number of the fuzzy graph G . It is denoted by $\gamma_{pf}(G)$.

Strength of the Path 2.5

If v_i, v_j are vertices in $G = (V, E)$ and if they are connected using a path then the strength of that path is defined as $(\min_{i,j} \mu_{2ij}, \max_{i,j} \gamma_{2ij})$ where $\min_{i,j} \mu_{2ij}$ is the μ -strength of the weakest arc and $\max_{i,j} \gamma_{2ij}$ is the γ -strength of the strongest arc.

Isolated Vertex 2.6

A vertex $u \in V$ of an Intuitionistic Fuzzy Graph $G = (V, E)$ is said to be an isolated vertex if $\gamma_2(u, v) = 0$ and $\mu_2(u, v) = 0$ for all $v \in V$. (i.e.), $N(u) = \phi$. Since the definition, we came to know that an isolated vertex was never dominating any other vertex in G .

Dominating Edge 2.7

Let $G = (V, E)$ be an intuitionistic fuzzy graph. Let e_i and e_j be two edges of G . We say that e_i dominates e_j , if e_i is a strong arc in G and adjacent to e_j .

Edge Dominating Set 2.8

D be a minimum dominating set of intuitionistic fuzzy graph G . If for every $e_j \in (G) - D$, there exists $e_i \in D$ such that e_i dominates e_j , then D is called an edge dominating set of G . The minimum intuitionistic fuzzy cardinality of all edge dominating set of intuitionistic fuzzy graph G is identified as edge domination number and it is denoted by $\gamma_e(G)$.

Intuitionistic Fuzzy Graph 2.9

An intuitionistic fuzzy graph is of the form $G = (V, E)$, where $V = \{v_1, v_2, \dots, v_n\}$ such that $\mu_1: V \rightarrow [0,1]$, $\gamma_1: V \rightarrow [0,1]$ denote the degree of membership and non membership of the element $v_i \in V$ respectively and $0 \leq \mu_1(v_i) + \gamma_1(v_i) \leq 1$ for every $v_i \in V$, ($i = 1, 2, \dots, n$). $E \subseteq V \times V$ where $\mu_2: V \times V \rightarrow [0,1]$ and $\gamma_2: V \times V \rightarrow [0,1]$ are such that $\mu_2(v_i, v_j) \leq \mu_1(v_i) \wedge \mu_1(v_j)$, $\gamma_2(v_i, v_j) \leq \gamma_1(v_i) \vee \gamma_1(v_j)$, and $0 \leq \mu_2(v_i, v_j) + \gamma_2(v_i, v_j) \leq 1$. An arc of an IFG G is known an strong arc if $\mu_2(v_i, v_j) = \mu_1(v_i) \wedge \mu_1(v_j)$, $\gamma_2(v_i, v_j) = \gamma_1(v_i) \wedge \mu_1(v_j)$.

Vertex Domination

Let $G = (V, E)$ be a graph with order $n = |V(G)|$ and $m = |E(G)|$. Then open neighborhood of a vertex v is $N(v) = \{u | uv \in E(G)\}$, and the closed neighborhood of a vertex v is $N[v] = N(v) \cup \{v\}$. The open neighborhood of a set $S \subseteq V(G)$ is $N(S) = \cup_{v \in S} N(v)$, and the closed neighborhood of a set S is $N[S] = \cup_{v \in S} N[v]$. A vertex v is a private





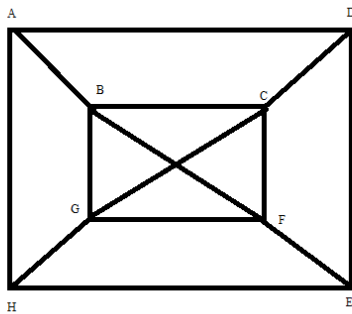
Vinitha and Sreeja

neighbor of a vertex u in asset $S \subseteq V(G)$ if $N[v] \cap S = \{u\}$. The private neighbor set of u with respect to S is defined as $pn[u, S] = \{v | N[v] \cap S = \{u\}\}$.

A vertex $u \in V(G)$ ve-dominates an edge $vw \in E(G)$ if

1. $u = v$ or $u = w$ (u is incident to vw)
2. uv or uw is an edge in G (u is incident to an edge that is adjacent to vw).

In other words, a vertex u ve-dominates the edges incident to vertices in $N[u]$. A set $S \subseteq V(G)$ is a vertex edge dominating set (or simply a ve-dominating set) if for all edges $e \in E(G)$, there exists a vertex $v \in S$ that ve-dominates e . The minimum cardinality of a ve-dominating set of G is called the vertex edge domination number.



In this graph of 8 vertices and 14 edges, the vertices $\{B, C, D, F, H\}$ are adjacent to at least one vertices of the set $\{A, G, E\}$. Hence the vertices $\{A, G, E\}$ dominates the vertices $\{B, C, D, F, H\}$.

Theorem 3.1

Every vertex dominating set D of an Intuitionistic Fuzzy Graph G contains atleast one dominating set D' in G .

Proof

Let D be a vertex dominating set of Intuitionistic Fuzzy Graph G . Let us assume that the vertex dominating set D of the Intuitionistic Fuzzy Graph G contains no dominating set D' in G . This implies that any two vertices of D are independent and non adjacent.

Hence all v_i 's are not strong in D .

Therefore for every $v_i \in V - D$, there exists no v_j in D

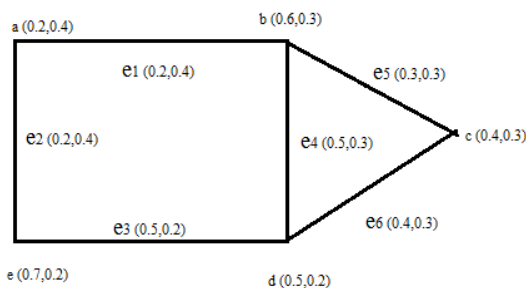
Such that v_i will not dominate v_j .

That contradicts to D .

Therefore D must contain at least one dominating set D' in G .

Example 3.2

Consider a figure





Vinitha and Sreeja

1. The vertex a is dominated by the vertices b and e.
2. The vertex b is dominated by the vertices a, c and d.
3. The vertex d is dominated by the vertices b, c and e.
4. The vertex e is dominated by the vertices a and d.

Let $D' = \{a, c\}$ all the vertices $\{b, d, e\}$ which are not in D' is dominated by at least one of the vertices in D' .

Hence D' is a dominating set.

The vertices a and c represent a minimum dominating set for G .

Hence the domination number is 2.

Let $D' = \{a, e\}$ then $V - D' = \{b, c, d\}$ which implies that D' is a dominating set.

Theorem 3.3

Let D be a cycle non-split vertex dominating set then $(V - D)$ vertex cover includes all the vertices of G .

Proof

We know that D is a cycle non-split vertex dominating set of G . Assume that the vertex cover of $(V - D)$ does not include all the vertices of G . Then $(V - D)$ may be connected or disconnected

Case(i)

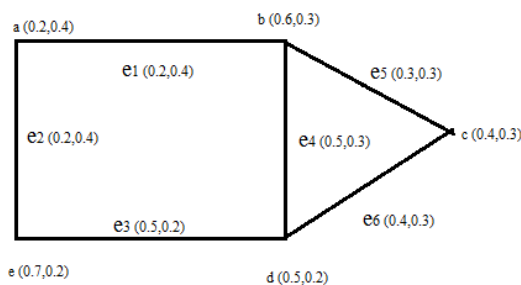
If $(V - D)$ is connected then any two vertices of vertex dominating set D contains no common vertex and is disconnected. This implies D is a non-split edge dominating set. That contradicts the assumption that D is a cycle non-split dominating set.

Case(ii)

If $(V - D)$ is disconnected then any two vertices of vertex dominating set D are non-adjacent and there exists independent vertices in D . Also at least one edge of end node occurs in D . This implies vertex dominating set D is a split dominating set. That is contradiction to our assumption.

Therefore from the above two cases, we conclude that the vertex cover of $(V - D)$ must contain all the vertices of G .

Example 3.4



Let $D = \{a, c\}$ and $V - D = \{b, d, e\}$
 Therefore D is a cycle that includes all the vertices of G .
 Hence we obtained the results.

Theorem 3.5

If D is a vertex dominating set of the Intuitionistic Fuzzy Graph G , then at least one vertex dominating set D is a vertex independent set.





Vinitha and Sreeja

Proof

Let G be an Intuitionistic Fuzzy Graph and D a vertex dominating set in G .

Case(i)

Let D contain an isolated vertex v_1 in G , by the definition of an intuitionistic fuzzy vertex independent set every v_i is a vertex independent set in G . Obviously D is a vertex independent set.

Case(ii)

Suppose D is not an intuitionistic fuzzy vertex independent set. Then each vertex v_i in G will be strong. Thus we get G that must an intuitionistic fuzzy graph with only strong arcs, this gives a contradiction to our assumption. Therefore at least one vertex dominating set must be a vertex independent set.

Theorem 3.6

Let D_1 and D_2 be a vertex dominating set of Intuitionistic Fuzzy Graph G_1 and G_2 respectively. Then $D_1 \times D_2$ is not a vertex dominating set of $G_1 \times G_2$.

Proof

Let D_1 and D_2 be a vertex dominating set of Intuitionistic Fuzzy Graph G_1 and G_2 respectively. Then $D_1 \times D_2$ is the connected Intuitionistic Fuzzy Graph. Most of the vertices in $D_1 \times D_2$ are strong vertices. Since the connected graph $D_1 \times D_2$ is the part of the graph $G_1 \times G_2$, many of the vertices of $G_1 \times G_2$ are non adjacent to this connected graph $D_1 \times D_2$. Also some vertices of $D_1 \times D_2$ has common edge with the vertices of $G_1 \times G_2$. This implies for each $v_j \in V - \{D_1 \times D_2\}$ there exist $v_i \in \{D_1 \times D_2\}$ such that v_i dominates v_j . This is not true for all $v_j \in V - \{D_1 \times D_2\}$. And then this leads to a contradiction. Therefore $D_1 \times D_2$ cannot become a vertex dominating set of $G_1 \times G_2$.

CONCLUSION

In this paper we categorized the vertex domination number of given Intuitionistic fuzzy graph. And also we have investigated the relationship between the vertex domination set, vertex cover and independent vertex dominating set. Then we proved results relating to these domination parameters.

REFERENCES

1. Anthony Shannon and Krassimir Atanassov. On a Generalization of Intuitionistic Fuzzy Graphs, NIFS Vol. 12 (2006), 1, 24-29.
2. K. Atanassov, Intuitionistic Fuzzy sets: Theory and Applications, Physica- verlag, Newyork (1999)
3. Ayyaswamy.S and Natarajan .C, strong (weak) dominance in fuzzy graphs, International Journal of Computational and mathematical Sciences (2010).
4. A.Bozhenyuka, M.Knyazevab and I.Rozenbergc. Algorithm for Finding Domination Set in Intuitionistic Fuzzy Graph (2019)
5. J.Johnstephan, N.Vinothkumar, P.Gajendran & Dr. A muthaiyan. Vertex Edge Domination in Intuitionistic Fuzzy Graph(2019).
6. Mohammadesmail Nikfar. Vertex Domination in Fuzzy Graphs (2019)
7. R.Parvathi and G.Thamizhendhi, Dominance in Intuitionistic Fuzzy Graphs, Fourteenth Int. Conf. On IFSS, Sofia 15-16 May (2010).
8. Somasundaram A, Somasundaram S (1998) Domination in Fuzzy Graphs-I, Pattern Recognition letters, 19, pp. 787-791.
9. Somasundaram A (2004) Domination in Fuzzy Graphs-II, Journal of Fuzzy Mathematics.





A Model for Optimal Reserve Inventories between Three Machines with Reference to Repair Time Distribution

T. Vivekanandan^{1*} and S. Sachithanatham²

¹Research Scholar, Department of Statistics, Bharathiar University, Coimbatore, Tamil Nadu 621 212, India.

²Department of Statistics, Arignar Anna Government Arts College, Villupuram, Tamil Nadu 605 602, India.

Received: 23 Feb 2021

Revised: 03 Mar 2021

Accepted: 06 Mar 2021

*Address for Correspondence

T. Vivekanandan

Research Scholar, a

Department of Statistics,

Bharathiar University, Coimbatore, Tamil Nadu 621 212, India.

Email: mtvivek2017@gmail.com



This is an Open Access Journal / article distributed under the terms of the **Creative Commons Attribution License** (CC BY-NC-ND 3.0) which permits unrestricted use, distribution, and reproduction in any medium, provided the original work is properly cited. All rights reserved.

ABSTRACT

A System comprises three machines M_1 , M_2 and M_3 in series is considered and the output of machine M_1 is input to the machine M_2 and the output of machine M_2 is input to the machine M_3 . When the machine M_1 in repair state, it leads to make the machines M_2 and M_3 to be halted and hence the entire system is forced to be in idle state. This lead to the loss in the production and this can be overcome by maintaining the reserve inventory S_1 and S_2 between machines M_1 and M_2 and between the machines M_2 and M_3 respectively. Considering the related holding cost and idle time cost the optimal reserve inventories \hat{S}_1 and \hat{S}_2 are obtained under the assumption that the machine M_1 only under the repair state and the repair time is a random variable which is followed as exponential distribution.

Keywords: Optimal Reserves inventory, repair time, truncation point, SCBZ property and Leibnitz rule.

INTRODUCTION

In inventory control theory, determining the optimal reserve inventory between two machines is an important model and these models have been studied by many researchers. The base model for optimal reserve between two machines has been initially studied by Hanssman.F *et al.*,(1962).Determining the optimal reserves between more than two machines in series is also an inevitable method in the inventory control theory. Rajagopal and sathiyamoorthy *et al.*,(2003) have studied the three machine problem and the authors have obtained the expression for optimal reserves between machines.

Selvamurugan (2018) have discussed the three machines model with the assumption that the repair time of machine M_1 is a random variable, which follows exponential distribution and satisfies the setting the clock back to zero

30571





Vivekanandan and Sachithanatham

property. The authors also assumed that the truncation point itself a random variable and it is followed as uniform distribution and with these assumptions the expression for optimal reserves have been obtained.

Notations

- S₁ : Reserve inventory between M₁ and M₂.
- S₂ : Reserve inventory between M₂ and M₃.
- h₁ : Cost per unit time of holding per unit of reserve inventory S₁.
- h₂ : Cost per unit time of holding per unit of reserve inventory S₂.
- d₁ : Cost per unit time of idle time of machine M₂.
- d₂ : Cost per unit time of idle time of machine M₃.
- μ : Mean time interval between successive breakdowns of machine M₁, assuming exponential distributions of inter-arrival times.
- t : Continuous random variable denoting the repair time of M₁ with probability density function g(.) and CDF G(.).
- r₁ : Constant consumption rate per unit time of machine M₂.
- r₂ : Constant consumption rate per unit time of machine M₃.
- T : Random variable denoting the idle time of M₂ and M₃.

Model I

In this model, the same three machines problem is taken up with the novel concept, the so called SCBZ properly is applied to the probability function of the repair time of Machine M₁. In doing so, the probability function of the repair time of machine M₁ is assumed to follow exponential distribution and which takes a parametric change (SCBZ) after the truncation point. It is also assumed that the truncation point itself a random variable, which follows uniform distribution. Thus the pdf of the repair time is

$$g(t, \theta) = \begin{cases} \theta e^{-\theta t}, & \text{if } t > t_0 \\ \theta^* e^{-\theta^* t} e^{t_0(\theta^* - \theta)}, & \text{if } t < t_0 \end{cases}$$

Where t₀ is a random variable denoting that truncation point, which follows uniform distribution (a, b). Hence the p.d.f of repair time can be stated as

$$g(t) = g(t, \theta)P(t \leq t_0) + g(t, \theta^*)P(t > t_0)$$

$$g(t) = \theta e^{-\theta t} \left(\frac{1}{b-a} \right) (b-t) + \theta^* e^{-\theta^* t} e^{t_0(\theta^* - \theta)} \left(\int_t^b \frac{1}{b-a} dt_0 \right)$$

The expected cost is given by

$$E(C) = h_1 S_1 + h_2 S_2 + \frac{d_1}{\mu_1} \int_{\frac{S_1}{r_1}}^{\infty} \left(t - \frac{S_1}{r_1} \right) g(t) dt + \frac{d_2}{\mu_2} \int_{\frac{S_1+S_2}{r_1+r_2}}^{\infty} \left(t - \frac{S_1}{r_1} - \frac{S_2}{r_2} \right) g(t) dt$$

$$\frac{\partial E(C)}{\partial S_1} = 0 \Rightarrow$$

$$h_1 - \frac{d_1}{\mu_1 r_1 (b-a)} \left[\left\{ b - \frac{S_1}{r_1} - \frac{1}{\theta} \right\} e^{-\frac{S_1}{r_1} \theta} + \frac{\theta^*}{(\theta^* - \theta) \theta} \left\{ e^{-\frac{S_1}{r_1} \theta} - e^{a(\theta^* - \theta) - \frac{S_1}{r_1} \theta^*} \right\} \right] - \frac{d_2}{\mu_2 r_1 (b-a)} \left[\left\{ b - \left(\frac{S_1}{r_1} + \frac{S_2}{r_2} \right) - \frac{1}{\theta} \right\} e^{-\left(\frac{S_1}{r_1} + \frac{S_2}{r_2} \right) \theta} + \frac{\theta^*}{(\theta^* - \theta) \theta} \left\{ e^{-\left(\frac{S_1}{r_1} + \frac{S_2}{r_2} \right) \theta} - e^{a(\theta^* - \theta) - \left(\frac{S_1}{r_1} + \frac{S_2}{r_2} \right) \theta^*} \right\} \right] = 0$$

$$\frac{\partial E(C)}{\partial S_2} = 0 \Rightarrow$$

$$h_2 - \frac{d_2}{\mu_2 r_2 (b-a)} \left[\left\{ b - \left(\frac{S_1}{r_1} + \frac{S_2}{r_2} \right) - \frac{1}{\theta} \right\} e^{-\left(\frac{S_1}{r_1} + \frac{S_2}{r_2} \right) \theta} + \frac{\theta^*}{(\theta^* - \theta) \theta} \left\{ e^{-\left(\frac{S_1}{r_1} + \frac{S_2}{r_2} \right) \theta} - e^{a(\theta^* - \theta) - \left(\frac{S_1}{r_1} + \frac{S_2}{r_2} \right) \theta^*} \right\} \right] = 0$$

This model has been discussed by Selvamurugan.C (2018).





Vivekanandan and Sachithanatham

RESULTS

In this Model, it is assumed that the repair time of machine M_1 is a random variable and it undergoes parametric change of distribution in the sense that the repair time changes its probability distribution after a certain change point (truncation point). In doing so before the truncation point the repair time distribution is exponential and it changes to Erlang (2) after the truncation point.

Hence,

$$g(t) = \begin{cases} \theta e^{-\theta t} & , t \leq t_0 \\ \theta^* e^{-\theta^* t} e^{t_0(\theta^* - \theta)} & , t > t_0 \end{cases}$$

If t_0 is a random variable denoting that truncation point and it is assumed to be followed as exponential with parameter λ , then the probability density function of the repair time can be written as

$$g(t) = g(t, \theta)p(t \leq t_0) + g(t, \theta^*)p(t > t_0)$$

$$= \theta e^{-\theta t} \int_t^\infty \lambda e^{-\lambda t_0} dt_0 + \theta^* e^{-\theta^* t} e^{t_0(\theta^* - \theta)} \int_0^t \lambda e^{-\lambda t_0} dt_0$$

$$g(t) = \theta e^{-t(\lambda + \theta)} + \lambda \theta^* \frac{e^{-\theta^* t}}{(\lambda + \theta - \theta^*)} [1 - e^{-t(\lambda + \theta - \theta^*)}]$$

$$E(C) = h_1 S_1 + h_2 S_2 + \frac{d_1}{\mu} E(T_{M_2}) + \frac{d_2}{\mu} E(T_{M_3}) \tag{1}$$

$$E(T_{M_2}) = \int_{\frac{S_1}{r_1}}^\infty \left(t - \frac{S_1}{r_1} \right) g(t) dt$$

$$= \int_{\frac{S_1}{r_1}}^\infty \left(t - \frac{S_1}{r_1} \right) \left\{ \theta e^{-t(\lambda + \theta)} + \lambda \theta^* \frac{e^{-\theta^* t}}{(\lambda + \theta - \theta^*)} [1 - e^{-t(\lambda + \theta - \theta^*)}] \right\} dt$$

$$E(T_{M_2}) = \theta \int_{\frac{S_1}{r_1}}^\infty \left(t - \frac{S_1}{r_1} \right) e^{-t(\lambda + \theta)} dt + \frac{\lambda \theta^*}{(\lambda + \theta - \theta^*)} \int_{\frac{S_1}{r_1}}^\infty \left(t - \frac{S_1}{r_1} \right) e^{-\theta^* t} dt - \frac{\lambda \theta^*}{(\lambda + \theta - \theta^*)} \int_{\frac{S_1}{r_1}}^\infty \left(t - \frac{S_1}{r_1} \right) e^{-t(\lambda + \theta)} dt$$

$$E(T_{M_2}) = I_1 + I_2 - I_3$$

$$\frac{dE(T_{M_2})}{dS_1} = \frac{dI_1}{dS_1} + \frac{dI_2}{dS_1} - \frac{dI_3}{dS_1}$$

$$\frac{dI_1}{dS_1} = \frac{d}{dS_1} \theta \int_{\frac{S_1}{r_1}}^\infty \left(t - \frac{S_1}{r_1} \right) e^{-t(\lambda + \theta)} dt$$

$$\frac{dI_1}{dS_1} = -\frac{\theta e^{-\frac{S_1}{r_1}(\lambda + \theta)}}{r_1(\lambda + \theta)}$$

$$\frac{dI_2}{dS_1} = \frac{d}{dS_1} \left(\frac{\lambda \theta^*}{(\lambda + \theta - \theta^*)} \int_{\frac{S_1}{r_1}}^\infty \left(t - \frac{S_1}{r_1} \right) e^{-\theta^* t} dt \right)$$

$$\frac{dI_2}{dS_1} = \frac{-\lambda}{r_1(\lambda + \theta - \theta^*)} e^{-\theta^* \frac{S_1}{r_1}}$$





Vivekanandan and Sachithanatham

$$\frac{dI_3}{dS_1} = \frac{d}{dS_1} \left(\frac{\lambda\theta^*}{(\lambda+\theta-\theta^*)} \int_{\frac{S_1}{r_1}}^{\infty} \left(t - \frac{S_1}{r_1} \right) e^{-t(\lambda+\theta)} dt \right)$$

$$\frac{dI_3}{dS_1} = - \frac{\lambda\theta^* e^{-\frac{S_1}{r_1}(\lambda+\theta)}}{r_1(\lambda+\theta-\theta^*)(\lambda+\theta)}$$

$$\frac{dE(T_{m_2})}{dS_1} = 0 \Rightarrow$$

$$-\frac{\theta e^{-\frac{S_1}{r_1}(\lambda+\theta)}}{r_1(\lambda+\theta)} - \frac{\lambda e^{-\theta^* \frac{S_1}{r_1}}}{r_1(\lambda+\theta-\theta^*)} + \frac{\lambda\theta^* e^{-\frac{S_1}{r_1}(\lambda+\theta)}}{r_1(\lambda+\theta-\theta^*)(\lambda+\theta)} = 0 \tag{2}$$

$$\frac{dE(T_{m_2})}{dS_2} = \frac{dI_1}{dS_2} + \frac{dI_2}{dS_2} - \frac{dI_3}{dS_2}$$

$$\frac{dE(T_{m_2})}{dS_2} = 0 \tag{3}$$

$$E(T_{m_3}) = \int_{\frac{S_1}{r_1} + \frac{S_2}{r_2}}^{\infty} \left(t - \frac{S_1}{r_1} - \frac{S_2}{r_2} \right) g(t) dt$$

$$= \int_{\frac{S_1}{r_1} + \frac{S_2}{r_2}}^{\infty} \left(t - \frac{S_1}{r_1} - \frac{S_2}{r_2} \right) \left\{ \theta e^{-t(\lambda+\theta)} + \frac{\lambda\theta^* e^{-\theta^* t}}{(\lambda+\theta-\theta^*)} [1 - e^{-t(\lambda+\theta-\theta^*)}] \right\} dt$$

$$E(T_{m_3}) = \theta \int_{\frac{S_1}{r_1} + \frac{S_2}{r_2}}^{\infty} \left(t - \frac{S_1}{r_1} - \frac{S_2}{r_2} \right) e^{-t(\lambda+\theta)} dt + \frac{\lambda\theta^*}{(\lambda+\theta-\theta^*)} \int_{\frac{S_1}{r_1} + \frac{S_2}{r_2}}^{\infty} \left(t - \frac{S_1}{r_1} - \frac{S_2}{r_2} \right) e^{-\theta^* t} dt - \frac{\lambda\theta^*}{(\lambda+\theta-\theta^*)} \int_{\frac{S_1}{r_1} + \frac{S_2}{r_2}}^{\infty} \left(t - \frac{S_1}{r_1} - \frac{S_2}{r_2} \right) e^{-t(\lambda+\theta)} dt$$

$$E(T_{m_3}) = I_4 + I_5 - I_6$$

$$\frac{dE(T_{m_3})}{dS_1} = \frac{dI_4}{dS_1} + \frac{dI_5}{dS_1} - \frac{dI_6}{dS_1}$$

$$\frac{dI_4}{dS_1} = \frac{d}{dS_1} \left(\theta \int_{\frac{S_1}{r_1} + \frac{S_2}{r_2}}^{\infty} \left(t - \frac{S_1}{r_1} - \frac{S_2}{r_2} \right) e^{-t(\lambda+\theta)} dt \right)$$

$$\frac{dI_4}{dS_1} = \frac{-\theta e^{-\left(\frac{S_1}{r_1} + \frac{S_2}{r_2}\right)(\lambda+\theta)}}{-r_1(\lambda+\theta)}$$

$$\frac{dI_5}{dS_1} = \frac{d}{dS_1} \left(\frac{-\lambda\theta^*}{(\lambda+\theta-\theta^*)} \int_{\frac{S_1}{r_1} + \frac{S_2}{r_2}}^{\infty} \left(t - \frac{S_1}{r_1} - \frac{S_2}{r_2} \right) e^{-\theta^* t} dt \right)$$

$$\frac{dI_5}{dS_1} = \frac{-\lambda e^{-\left(\frac{S_1}{r_1} + \frac{S_2}{r_2}\right)\theta^*}}{r_1(\lambda+\theta-\theta^*)}$$

$$\frac{dI_6}{dS_1} = \frac{d}{dS_1} \left(\frac{-\lambda\theta^*}{(\lambda+\theta-\theta^*)} \int_{\frac{S_1}{r_1} + \frac{S_2}{r_2}}^{\infty} \left(t - \frac{S_1}{r_1} - \frac{S_2}{r_2} \right) e^{-t(\lambda+\theta)} dt \right)$$





Vivekanandan and Sachithanatham

$$\frac{dI_6}{dS_1} = \frac{-\lambda\theta^* e^{-\left(\frac{S_1+S_2}{r_1+r_2}\right)(\lambda+\theta)}}{r_1(\lambda+\theta-\theta^*)(\lambda+\theta)}$$

$$\frac{dE(T_{m_3})}{dS_1} = 0 \Rightarrow$$

$$-\frac{\theta e^{-\left(\frac{S_1+S_2}{r_1+r_2}\right)(\lambda+\theta)}}{r_1(\lambda+\theta)} - \frac{\lambda e^{-\left(\frac{S_1+S_2}{r_1+r_2}\right)\theta^*}}{r_1(\lambda+\theta-\theta^*)} + \frac{\lambda\theta^* e^{-\left(\frac{S_1+S_2}{r_1+r_2}\right)(\lambda+\theta)}}{r_1(\lambda+\theta-\theta^*)(\lambda+\theta)} = 0 \tag{4}$$

$$\frac{dE(T_{m_3})}{dS_2} = \frac{dI_4}{dS_2} + \frac{dI_5}{dS_2} - \frac{dI_6}{dS_2}$$

$$\frac{dI_4}{dS_2} = \frac{d}{dS_2} \left(\theta \int_{\frac{S_1+S_2}{r_1+r_2}}^{\infty} \left(t - \frac{S_1}{r_1} - \frac{S_2}{r_2} \right) e^{-t(\lambda+\theta)} dt \right)$$

$$\frac{dI_4}{dS_2} = \frac{-\theta e^{-\left(\frac{S_1+S_2}{r_1+r_2}\right)(\lambda+\theta)}}{-r_2(\lambda+\theta)}$$

$$\frac{dI_5}{dS_2} = \frac{d}{dS_2} \left(\frac{-\lambda\theta^*}{(\lambda+\theta-\theta^*)} \int_{\frac{S_1+S_2}{r_1+r_2}}^{\infty} \left(t - \frac{S_1}{r_1} - \frac{S_2}{r_2} \right) e^{-\theta^*t} dt \right)$$

$$\frac{dI_5}{dS_2} = \frac{-\lambda e^{-\left(\frac{S_1+S_2}{r_1+r_2}\right)\theta^*}}{r_2(\lambda+\theta-\theta^*)}$$

$$\frac{dI_6}{dS_2} = \frac{d}{dS_2} \left(\frac{-\lambda\theta^*}{(\lambda+\theta-\theta^*)} \int_{\frac{S_1+S_2}{r_1+r_2}}^{\infty} \left(t - \frac{S_1}{r_1} - \frac{S_2}{r_2} \right) e^{-t(\lambda+\theta)} dt \right)$$

$$\frac{dI_6}{dS_2} = \frac{-\lambda\theta^* e^{-\left(\frac{S_1+S_2}{r_1+r_2}\right)(\lambda+\theta)}}{r_2(\lambda+\theta-\theta^*)(\lambda+\theta)}$$

$$\frac{dE(T_{m_3})}{dS_2} = 0 \Rightarrow$$

$$-\frac{\theta e^{-\left(\frac{S_1+S_2}{r_1+r_2}\right)(\lambda+\theta)}}{r_2(\lambda+\theta)} - \frac{\lambda e^{-\left(\frac{S_1+S_2}{r_1+r_2}\right)\theta^*}}{r_2(\lambda+\theta-\theta^*)} + \frac{\lambda\theta^* e^{-\left(\frac{S_1+S_2}{r_1+r_2}\right)(\lambda+\theta)}}{r_2(\lambda+\theta-\theta^*)(\lambda+\theta)} = 0 \tag{5}$$

$$\frac{dE(C)}{dS_1} = 0 \Rightarrow$$

$$h_1 + \frac{d_1}{\mu} \left\{ \frac{dE(T_{m_2})}{dS_1} \right\} + \frac{d_2}{\mu} \left\{ \frac{dE(T_{m_3})}{dS_1} \right\} = 0$$

From (2) and (4), we get

$$\frac{dE(C)}{dS_1} = 0 \Rightarrow h_1 + \frac{d_1}{\mu} \left\{ -\frac{\theta e^{-\frac{S_1}{r_1}(\lambda+\theta)}}{r_1(\lambda+\theta)} - \frac{\lambda e^{-\theta^*\frac{S_1}{r_1}}}{r_1(\lambda+\theta-\theta^*)} + \frac{\lambda\theta^* e^{-\frac{S_1}{r_1}(\lambda+\theta)}}{r_1(\lambda+\theta-\theta^*)(\lambda+\theta)} \right\}$$

$$+ \frac{d_2}{\mu} \left\{ -\frac{\theta e^{-\left(\frac{S_1+S_2}{r_1+r_2}\right)(\lambda+\theta)}}{-r_1(\lambda+\theta)} - \frac{\lambda e^{-\left(\frac{S_1+S_2}{r_1+r_2}\right)\theta^*}}{r_1(\lambda+\theta-\theta^*)} + \frac{\lambda\theta^* e^{-\left(\frac{S_1+S_2}{r_1+r_2}\right)(\lambda+\theta)}}{r_1(\lambda+\theta-\theta^*)(\lambda+\theta)} \right\} = 0 \tag{6}$$

$$\frac{dE(C)}{dS_2} = 0 \Rightarrow$$





Vivekanandan and Sachithanatham

$$h_2 + \frac{d_1}{\mu} \left\{ \frac{dE(T_{m_2})}{dS_2} \right\} + \frac{d_2}{\mu} \left\{ \frac{dE(T_{m_3})}{dS_2} \right\} = 0$$

From (3) and (5), we get

$$\frac{dE(C)}{dS_2} = 0 \Rightarrow$$

$$h_2 + \frac{d_1}{\mu} \{0\} + \frac{d_2}{\mu} \left\{ -\frac{\theta e^{-\left(\frac{S_1+S_2}{r_1+r_2}\right)(\lambda+\theta)}}{r_2(\lambda+\theta)} - \frac{\lambda e^{-\left(\frac{S_1+S_2}{r_1+r_2}\right)\theta^*}}{r_2(\lambda+\theta-\theta^*)} + \frac{\lambda\theta^* e^{-\left(\frac{S_1+S_2}{r_1+r_2}\right)(\lambda+\theta)}}{r_2(\lambda+\theta-\theta^*)(\lambda+\theta)} \right\} = 0 \tag{7}$$

Solving the equation (6) and(7), we get

$$h_1 r_1 - h_2 r_2 + \frac{d_1}{\mu} \left\{ -\frac{\theta e^{-\frac{S_1(\lambda+\theta)}{r_1}}}{(\lambda+\theta)} - \frac{\lambda e^{-\theta^* \frac{S_1}{r_1}}}{(\lambda+\theta-\theta^*)} + \frac{\lambda\theta^* e^{-\frac{S_1(\lambda+\theta)}{r_1}}}{(\lambda+\theta-\theta^*)(\lambda+\theta)} \right\} = 0 \tag{8}$$

Solving the equations (7) and (8) numerically by taking fixed value for $h_1, h_2, r_1, r_2, d_1, d_2, \mu, \lambda, \theta$ & θ^* the optimal value of \hat{S}_1 & \hat{S}_2 can be obtained.

Numerical Illustrations

The variations in the values of \hat{S}_1 & \hat{S}_2 consequent to the changes in the parameter $h_1, h_2, r_1, r_2, d_1, d_2, \mu, \lambda, \theta$ and θ^* have been studied by taking the numerical illustrations. The tables and the corresponding curves are given.

Case (i) For the fixed values of $h_1 = 30, h_2 = 10, d_1 = 50, d_2 = 60, r_1 = 2, r_2 = 2, \theta = 1.2, \theta^* = 1.2, \mu = 1.0, \lambda = 1$. The variations in the values of the optimal reserve inventory \hat{S}_1 & \hat{S}_2 for various values of h_1 is shown in the table.

Case(ii) For the fixed values of $h_1 = 30, h_2 = 10, d_1 = 50, d_2 = 60, r_1 = 2, r_2 = 2, \theta = 1.2, \theta^* = 1.2, \mu = 1.0, \lambda = 1$. The variations in the values of the optimal reserve inventory \hat{S}_1 & \hat{S}_2 for various values of h_2 is shown in the table.

Case(iii) For the fixed values of $h_1 = 30, h_2 = 10, d_1 = 50, d_2 = 60, r_1 = 2, r_2 = 2, \theta = 1.2, \theta^* = 1.2, \mu = 1.0, \lambda = 1$. The variations in the values of the optimal reserve inventory \hat{S}_1 & \hat{S}_2 for various values of d_1 is shown in the table.

Case (iv) For the fixed values of $h_1 = 30, h_2 = 10, d_1 = 50, d_2 = 60, r_1 = 2, r_2 = 2, \theta = 1.2, \theta^* = 1.2, \mu = 1.0, \lambda = 1$. The variations in the values of the optimal reserve inventory \hat{S}_1 & \hat{S}_2 for various values of d_2 is shown in the table.

Case(v) For the fixed values of $h_1 = 30, h_2 = 10, d_1 = 50, d_2 = 60, r_1 = 2, r_2 = 2, \theta = 1.2, \theta^* = 1.2, \mu = 1.0, \lambda = 1$. The variations in the values of the optimal reserve inventory \hat{S}_1 & \hat{S}_2 for various values of μ is shown in the table.

CONCLUSIONS

From the tables and graphs, it is observed that i. As the inventory holding cost h_1 increases, the value of \hat{S}_1 decreases suggesting a smaller stock level. At the same time \hat{S}_2 increases suggesting a higher inventory. ii. If inventory holding cost h_2 increases then a higher value of \hat{S}_1 is suggested. At the same time the value of \hat{S}_2 decreases suggesting a smaller stock level. iii If d_1 the shortage cost of inventory increases, a higher level of \hat{S}_1 is suggested. But a smaller inventory \hat{S}_2 is suggested. iv. As d_2 , the shortage cost of inventory increases a larger inventory \hat{S}_2 is suggested. v. As The parameter μ , mean inter-arrival time between successive breakdowns is exponentially distributed and if μ is in increase then the optimal reserve inventory increase. A smaller inventory \hat{S}_1 is suggested. And also smaller inventory \hat{S}_2 is suggested.





Vivekanandan and Sachithanatham

REFERENCES

1. Hanssman.F. Operations Research in Production and Inventory Control, *John Wiley and sons, Inc. New York, (1962).*
2. Ramachandran .V and Sathiyamoorthy.R. Optimal Reserve for two machines, *IEEE Trans. On Reliability, Vol.R-30, No.4, 397- 397, (1981).*
3. RajaRao.B and Talwalker. S. Setting the Clock Back to Zero Property of a Family of life Distributions, *Journal of Statistical Planning and Inference, Vol. 24, 347-352. (1990).*
4. Stangl.D.K, Exponential change point model, *Statistics in Medicine, Vol.14,pp.2173- 2190.(1995).*
5. Rajagopal and Sathiyamoorthi.S. An Extension to the Optimal Reserve Inventory level between Machines Model-*Proceedings of the second National Conference on Mathematical and Computational Models-PSG College of Engg.,Dec.11-12(2003)*
6. Sachithanatham, S. Ganesan.V and Sathyamoorthy.R. Optimal Reserve between two Machines with repair time having SCBZ Property , *Bulletin of pure and Applied Sciences Vol.25E (No.2) , 487-497, (2006).*
7. Sachithanatham.S, Ganesan. V and Sathiyamoorthi. R, A Model for optimal Reserve inventory between two Machines in Series, *The Journal of Indian Academy of Mathematics, Vol.29, No.1, 59-70. (2007)*
8. Ramerthilagam.S, Hentry.L and Sachithanatham.S, A Model for optimal reserve inventory between two machine in series with repair time undergoes a parametric Change, *Ultra Scientist Vol.26(3)B, 227-237, (2014).*
9. Venketesan .T, Muthu. C and Sathiyamoorthy .R, Determination of optimal Reserves between three Machines in series, *International journal of advanced research in Mathematics and applications, , Vol .1, ISSN 2350-028X. (2016).*
10. Govindhan.M, Elangovan.R and Sathyamoorthi.R. Determination of Optimal Reserve Inventory between one Machine in First Stage and Two at Second Stage, *International Journal of Operations Research and Optimization. Vol.7,No.1,PP.21-34(2018).*
11. T.Vivekanandan and S.Sachithanatham. Determination of Optimal Reserve between Two Machines in Series with the Repair Time has Change of Distribution after the Truncation Point.*GIS Business Vol-14-Issue-6-November-December-2019.*

Table 1.The optimal reserve inventory for varying h₁

h ₁	29	30	31	32
S ₁	0.4659	0.3776	0.2941	0.2149
S ₂	1.4869	1.5752	1.6587	1.7379

Table 2.The optimal reserve inventory for varying h₂

h ₂	9	10	11	12
S ₁	0.2941	0.3776	0.4659	0.5596
S ₂	1.8564	1.5752	1.3094	1.0547

Table 3.The optimal reserve inventory for varying d₁

d ₁	50	60	70	80
S ₁	0.3776	0.694	0.9669	1.2067
S ₂	1.5752	1.2588	0.9859	0.7461

Table 4.The optimal reserve inventory for varying d₂

d ₂	60	70	80	90
S ₂	1.5752	1.8648	2.1179	2.3426

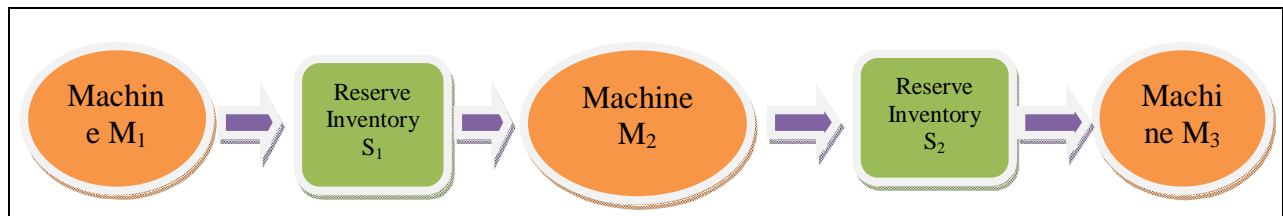




Vivekanandan and Sachithanatham

Table 5. The optimal reserve inventory for varying μ

μ	0.9	1.0	1.1	1.2
S_1	0.5596	0.3776	0.2149	0.0682
S_2	1.5909	1.5752	1.5604	1.5461



The picture of the system of the current studying model can be depicted as under

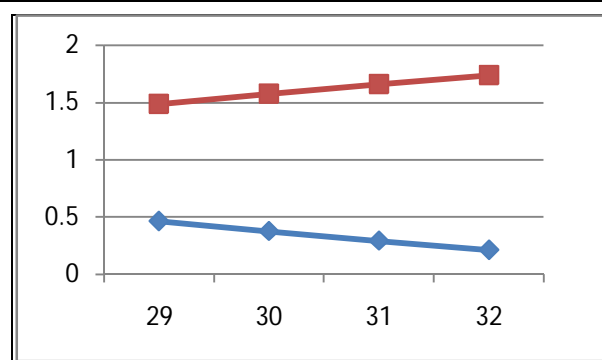


Fig.1. The optimal reserve inventory for varying h_1

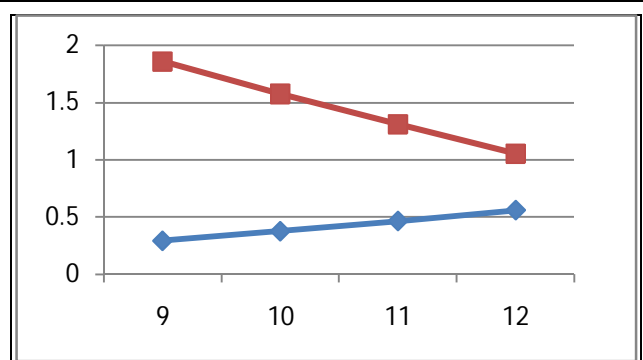


Fig.2. The optimal reserve inventory for varying h_2

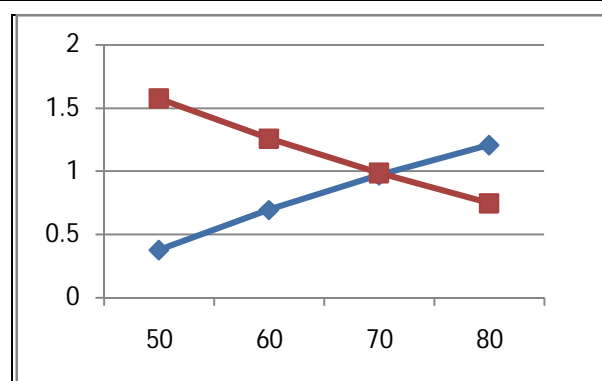


Fig.3. The optimal reserve inventory for varying d_1

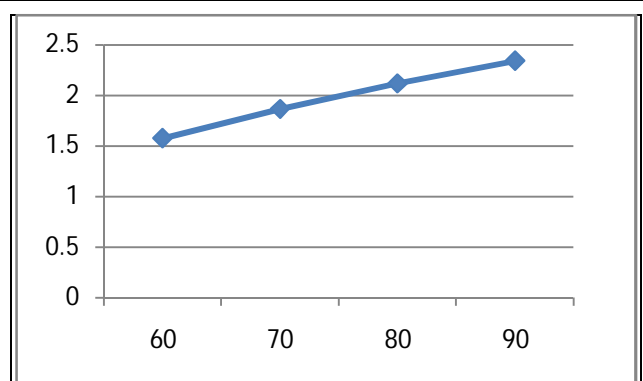


Fig.4. The optimal reserve inventory for varying d_2





Vivekanandan and Sachithanantham

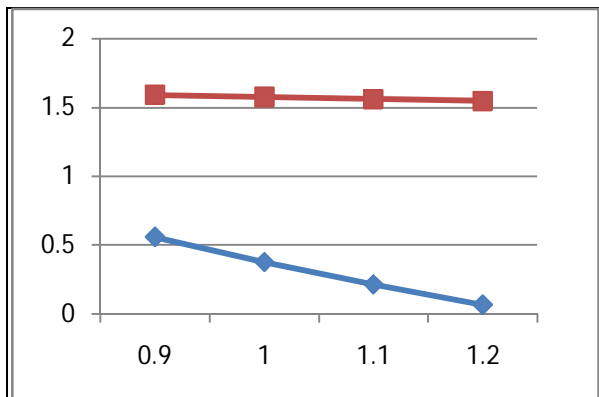


Fig.5.The optimal reserve inventory for varying μ





An Empirical Analysis of Manpower and Equipment Productivity in Major Construction Projects

N. Raja^{1*}, B. Yasodha Jagadeeswari² and P.N. Ragunath³

¹Research scholar, Department of Civil and Structural Engineering, Annamalai University, Annamalai Nagar, Tamil Nadu, India.

²Assistant Professor, PG and Research Department of Economics, Holy Cross College (Autonomous), Tiruchirappalli, Tamil Nadu, India.

³Professor and Head, Department of Civil and Structural Engineering, Annamalai University, Annamalai Nagar, Tamil Nadu, India.

Received: 25 Feb 2021

Revised: 10 Mar 2021

Accepted: 15 Mar 2021

*Address for Correspondence

N. Raja

Research scholar,
Department of Civil and Structural Engineering,
Annamalai University,
Annamalai Nagar, Tamil Nadu, India.
Email: ernnraja@gmail.com



This is an Open Access Journal / article distributed under the terms of the **Creative Commons Attribution License** (CC BY-NC-ND 3.0) which permits unrestricted use, distribution, and reproduction in any medium, provided the original work is properly cited. All rights reserved.

ABSTRACT

The construction sector has a strategic role in all developing and developed countries. At the present stage of economic development, one of the main components of successful industrial organizations is planning productivity. Increased productivity reduces the cost of work on the production unit or an increase in output. During the last two decades, the growth in Construction Industry is phenomenal. Construction projects involve huge input of resources which are primarily materials, manpower and machinery. The productivity level of construction industry is mostly depending upon three factors they are Manpower, machinery and materials. The concept of Residential Buildings has undergone a sea change with individual houses paving way for multi storied apartments. The important aspect of construction is that the duration of the projects has also reduced significantly. A project is a unique endeavor with a definite start and finish. Project is a specific activity on which money is spent (in form of resources i.e., men, materials and equipment) in the expectation of returns. The need for raw materials, cement etc. has led to the construction of factories. Manpower and Equipment being the other input account up to 30% of the project outlay. Better productivity management will produce significant improvement in meeting the predetermined targets of the project. Productivity Management has to be followed in every level with push from the top level of the project. Productivity hence is a driving force in a construction project. The Data required for the study have been collected from both the primary and secondary sources. This paper aims at measurement, study and analysis of Productivity of Manpower and Equipment in Major

30580



**Raja et al.,**

Construction Projects and Quantification in financial terms the impact due to variance in Manpower and Equipment Productivity on Project Profitability.

Keywords: Workers productivity, Labor, Material management, Construction, Resource, Environmental factors, Motivation.

INTRODUCTION

During the last few decades, the growth in Construction Industry is phenomenal. The Government is concentrating in the development of Infrastructure by constructing roads, airports, sea ports and power plants such as Hydro-Electric plants, Thermal Plants and Nuclear Plants. The growth rate sustained by the Government in the last decade has also enhanced the quality of life of the individual and thereby shopping malls, Educational institutions with modern teaching gadgets and Hospitals to accommodate sophisticated medical equipment are also being constructed across our country. The concept of Residential Buildings has undergone a sea change with individual houses paving way for multi storied apartments. The need for raw materials, cement etc. has led to the construction of multi-dimensional factories. The other important aspect of construction is that the duration of the projects has also reduced significantly. It is possible to construct one of the world's largest Airports in a record time of three years with a capital outlay of Rs.9000 crores. Dams which took almost a decade for construction are being constructed in 30 months. It is possible to complete many kilometers of roads and railways in one month. The above construction adds to the Gross National Product (GNP) as capital assets and at the same time increase the productivity of other sectors of economy as well. Major construction projects involve two critical resources of manpower and equipment. A project in general, is bounded by the limitations of a definite scope of work and a time of completion giving certain pre-determined benefits to the user on completion of the project. Each activity of the project is allotted time required for its completion and resources like manpower, materials, know how etc. Most of the modern construction projects are multi-disciplinary and complex in nature, both in Technical and managerial point of view. Such projects require expert knowledge in various fields and require more attention to the construction process. In addition, timely completion of the construction project is very important so as to get social benefits in time as well as starting of return on investment, as delay in implementation of the project adds to the interest burden on the capital investment. Hence Construction Management which is a large system having several subsystems like contract management, human resource management, finance management, productivity management, finance management for ensuring project completion in time as well as budgeted cost is absolute essential. Rising construction costs and labor shortages persist, challenging the industry to innovate competitive new ideas, while stricter regulations contribute to a reduced margin for error and waste. This year, the COVID-19 pandemic changed how the construction industry does business, from scheduling projects to hiring workers to meeting with clients. Looking forward, many industry trends will be affected by the fallout from the pandemic. New technology continues to change the construction site, improve the ability to win projects, and increase profit margins. Trends and movements are changing the roles of industry professionals and frontline workers. As the industry becomes more competitive and the market shifts, harnessing these construction trends will prove valuable for any construction firm.

REVIEW OF LITERATURE

A few studies on manpower and equipment productivity for major construction projects which have direct relevance to the current study are discussed in this section.

Durdyev, S.; Ismail, S.; Kandymov, N (2018) found that Construction Labor Productivity deeply affected by various internal and external factors including social culture, environmental and legal constraints, inappropriate management actions, extreme weather, excessive overtime, and transportation conditions.



**Raja et al.**

David Ngwoke M bazor and Sunday Okuoma Okoh (2015) observed that Productivity is a complex phenomenon at all levels be it individual, organised private sector or government the world over and in all spheres of human endeavour particularly in construction project delivery. Low productivity in the construction industry is as a result of diverse identifiable reasons such as; high reduction in skill level of construction workers, shift work, shortages of materials and equipment, change orders, labour shortages, weathers, low level of monitoring and control of projects etc. key factors that leads to productivity improvement in construction project delivery were analysed. These comprise of project planning, productivity measurement, avoidance of construction site congestion, motivation of workforce and good communication among others. It was therefore recommended that time management, application of project management tools like pert master, precedence diagram, research and development, provision of new equipment, plant and machinery.

Wen yi& Albert P.C.Chan, (2014) studied that Labour productivity is also one of the performance indicators to assess the success of the construction project. Because construction is a labour intensive industry, it can be argued that the work force is the dominant productive resource. Thus, construction productivity is primarily dependent on human effort and performance. Labour productivity is important index because of concentration of labour needed to complete specific work.

Gupta and Kansal (2014) examined the factors affecting labour productivity in construction sites in India. They invited professionals such as project managers, project engineers, site engineers, architects, assistance project managers, assistance project engineers and others who worked on the project, from management to execution level, to participate in a questionnaire survey. The questionnaire had four primary groups of factors, i.e. management, technological, human/labour and external. They found that ten factors of clarification in technical specifications (labour supervision, method of construction, delay in payment, labour fatigue, lack of construction managers' leadership, extent of variations/change in order during execution, late arrival, early quitting and frequent unscheduled breaks, labour skill, and availability of experienced labour) affected construction labour productivity in the Chambal Region.

Enshassi (2007) has listed component affecting the fluctuation of productivity into 10 factors. These factors include working labour force, governance, factors associated with work, inspiration factor with regards of time, materials resources and machinery, inadequate supervision, project related specifications, protection, quality of the worked achieved and other factors of the project.

Jaideep Motwani (1995) research has outlined that productivity, especially in the construction industry, has always been very difficult to measure and control. All estimating professionals would agree that the quantity of work to be performed and the cost per hour for labour to perform that work can be established with considerable accuracy. However, it is the identifying and evaluating of the critical factors which influence productivity that provides a challenge. Every error in productivity estimation causes an inverse effect in the actual cost of labour to perform a scope of work.

Productivity Definitions and Concepts

The fundamental concept underlying all productivity measures is a comparison of the output of a production process, an enterprise, an industry, or an economy with the corresponding factors of production (inputs) required to generate that output. Productivity can be defined in many ways. In construction, productivity is usually taken to mean labor productivity, that is, units of work placed or produced per man-hour. The inverse of labor productivity, man-hours per unit (unit rate), is also commonly used

Productivity issues can be divided into macro and micro level. At the macro level, one deals with contracting methods, labour legislation, and labour organization; at the micro-level, with the management and operation of a project, mainly at the job site.





Raja et al.,

The two most important measures of labour productivity are:

- The effectiveness with which labour is used in the construction process;
- The relative efficiency of labour doing what it is required to do at a given time and place.

Construction Labor Productivity Measurement

Different measures of productivity serve different purposes. It is important to choose a measure that is appropriate to the purpose. Productivity is generally ratio of output to input. In form of equation, it can be shown as follows:

$$\text{Productivity} = \frac{\text{Output}}{\text{Input}}$$

$$= \frac{\text{Total output}}{\text{Total work hour}}$$

Productivity is expressed as units of output per dollar or work-hour. At the project site, contractors are often interested in labor productivity. It can be defined in one of the following ways (Thomas and Mathews, 1985 cited in Thomas et al., 1990:

a) Economic Model: Total Factor Productivity (TFP)

$$\text{(TFP)} = \frac{\text{Total Output}}{\text{Labour} + \text{Material} + \text{Equipment} + \text{Energy} + \text{Capital}}$$

b) Project Specific Model:

$$\text{Productivity} = \frac{\text{Output}}{\text{Labour} + \text{Material} + \text{Equipment}}$$

c) Activity Oriented Model:

$$\text{Labour Productivity} = \frac{\text{Output}}{\text{Labour cost}}$$

(Or)

$$\text{Labour Productivity} = \frac{\text{Output}}{\text{Work hour}}$$

Scope of the Study

In this study, the task level productivity of Manpower and Equipment for 12 activities of civil works and Architectural finishes is arrived at by collecting data of manpower engaged and quantity of work done from major construction projects. The 12 activities are the core activities in any project which include Concreting, Reinforcement, Shuttering, Piling, Excavation, Brick work / Block work, Plastering, Painting, Flooring, Structural Steel Work, Back Filling and Waterproofing.

Objectives of the Study

The objectives of this research are:

- To study the productivity of manpower and equipment in 12 activities of civil works and architectural finishes in major construction projects.
- To record and analyze the variances in Productivity with respective to above.
- To identify the causes and factors leading to the variances in productivity
- To quantify in financial terms the impact of productivity in terms of percentages of Contract value.
- To examine and classify the factors affecting productivity of manpower and equipment in major construction projects.

Limitations of the Study

Study is conducted in major construction projects indifferent locations of Puducherry region. Results may not be useful for other projects, projects being unique endeavors. After analyzing the factors leading to variance in productivity, it is necessary to implement the tasks eliminating these factors which may not be covered under the scope of this study. Time constraints limit the depth of penetration of study. The results of the study may pinpoint the



**Raja et al.,**

lack of control on part of the middle level management and hence there may be hesitation on their part to share the data.

RESEARCH METHODOLOGY

Data Source

The present study has been carried out on the basis of data and information generated from both primary and secondary sources.

Data Collection

Primary data: Data was collected from major construction projects in different locations for a consecutive period of 6 months for the twelve basic activities of construction: Concreting, Reinforcement, Shuttering, Piling, Excavation, Brick work / Block work, Plastering, Painting, Flooring, Structural Steel Work, Back Filling and Waterproofing. Productivity models based on the combined usage of manpower and equipment resources in construction for major construction projects in different locations of Puducherry region.

Secondary data: Secondary data for this study was collected from various published sources like standard textbooks, journals, magazines, web pages, periodicals and newspapers.

Sampling Technique and Size:

In this study, the task level productivity is estimated by collecting manpower data and the quantity of work done against the manpower deputed. This data is taken over a span period of time of 6 months in different projects for 12 activities.

Tools of Analysis

The data collected from different sources were processed according to the objectives laid down for the study. In this research work data were statistically analysed by SPSS software package. Appropriate statistical tools like percentage analysis, RS means, standard deviation, range and ANOVA-test were applied to analyse the data and to draw valid conclusions.

Analysis and Interpretation

The collected data is then analyzed in a systematic fashion project wise and activity wise using excels charts. The factors affecting productivity are also listed and analyzed. The financial impact on the project on account of productivity or lack of productivity is finally estimated.

Now the impact of Manpower and equipment productivity is statically tested by one way analysis of variance has been employed to test. Based on the ANOVA test from the above result, it is obvious that the calculated value of "F" is lesser than the critical "F" value, (0.8248>2.717). It is concluded that there is significant difference between Manpower and equipment productivity in major construction projects.

Manpower Productivity

The table 2 showing the actual manpower productivity calculated from the data collected from the project in comparison to the Budget productivity and the percentage of productivity activity wise is tabulated. It is observed that the manpower productivity is less the benchmark productivity in most of the activities in major construction projects. Only in arth work (Excavation and Backfilling), the productivity is marginally higher in the project. The table showing the productivity is also given below for easy reference.



**Raja et al.,**

Equipment Productivity

The table 3 shows the actual equipment productivity of the project in comparison to the Budget productivity and the percentage of productivity activity wise is tabulated. It is observed that the equipment productivity is considerably less the benchmark productivity in most of the activities in the major construction projects.

Impact on the Project Profitability Due To Lack of Productivity

The Financial impact on the project profitability due to lack of productivity is calculated to the projects. The summary of the same is presented below in form of a summary table.

The table 4 shows that the overall impact in these projects is to the extent of Rs.1005 Lacs (ie Rs.10.05.Cr) which is a very huge amount considering the economy of our country. All measures should be undertaken to arrest this lack of productivity

RESULT AND DISCUSSION

The construction of buildings is related to the execution of various types of tasks, which require different material expenditures and efforts from workers, who should possess a variety of skills. The type of construction work performed, and the characteristics of the manpower and equipment strongly influence the time spent on performing a particular task. Manpower and equipment resources are one of the main resources, so manpower and equipment productivity, as well as completeness and correctness of the executive project, plays a key role in predicting the time and cost of construction activities. Productivity study and analysis is a vital factor in every major construction project particularly for manpower and equipment which has many variables and factors affecting their efficiency. While new products and technologies are flooding the construction industry every day, improving the overall productivity of the project and the industry, the task level productivity still remains an area which needs individual attention by the project team to ensure that the predetermined objectives of the project are achieved. During this study, it has been observed that the project team is concerned about the task level productivity and want methods and tools to improve the efficiency and out turn from manpower and equipment resources. The novelty of the approach proposed by the authors is rooted in taking into account various factors that have the potential to influence the productivity of manpower and equipment resources. On the basis of an analysis of the literature, 12 factors having a fundamental impact on the productivity of manpower and equipment were selected and analyzed. This work was intended to study the task level productivity in major construction projects and focused to 12 particular activities which were the core activities of any major construction project. The impact on project profits due to productivity or lack of productivity of manpower and equipment resources was the cause of concern for the project team. Hence it was decided to study the task level productivity in 12 activities of major construction projects and estimate the impact of productivity on the project profitability in these projects. This study has been completed in major construction projects in different locations of Puducherry region and the conclusions from the study are summarized.

CONCLUSION

The construction industry is one of the most important and significant sectors that supports the economic development of a country. Productivity of manpower and equipment resources in construction projects is usually calculated using empirical methods, experience of personnel and in some cases the manufacturer's recommendation. Manpower and Equipment Productivity is in the decline all across the world particularly in Construction work. The main outcome from the literature is that there is no standard definition of productivity. This study provides a guide for necessary steps required to improve construction labor productivity and consequently, the project performance. It can help improve the overall performance of construction projects through the implementation of the concept of benchmarks. Also, it gives an up-to-date concept of loss of productivity measurement for construction productivity claims. The Study identifies ways to use manpower and equipment resources in construction projects increasing the



**Raja et al.,**

productivity in major construction projects. Task Level productivity in Construction projects has to be measured, analyzed and improved in every project. Better productivity management will produce significant improvement in meeting predetermined targets. This study also identifies the factors affecting manpower and equipment productivity, and also the intensity of their effect. The planning factors affect the productivity more than other factors and need to be addressed in construction projects, particularly in major construction projects. The findings conclude that there is gap in that research development in major construction project and it has not been explored in India. These findings motivate the researchers to go for further research in major construction project i.e., "framework for improving on-site construction productivity in Indian scenario". There is a need for exploring more efficient strategies for improving the productivity. The biggest differentiator for builders and developers this year is likely to be technology in construction specifically, the innovations that can enhance efficiency.

REFERENCES

Newspapers

1. Lior Zitzman (2021), "Top 10 Construction Industry Trends to Watch for in 2021", BIG RENTZ, 19 January, 2021.
2. PTI (2020), "NBCC bags order worth Rs 65 crore from BHEL", The Economic Times, 2 March 2020
3. Business Line Bureau (2020). "Standardise large infra projects for make in India to succeed", The Hindu Business Line, 11 January 2020
4. The Hindu Data Team (2020). "Budget 2020: what's hindering India's Infrastructure push?", The Hindu, 2 February 2020
5. Abhinaya Hari Govind (2019). "Major corporation projects in limbo", The Hindu, 1 December 2019

Books & Journals

6. Venkatesh M, Saravana Natarajan P.S (2019), "Improvement of Manpower and Equipment Productivity in Indian Construction Projects", International Journal of Applied Engineering Research, Volume 14, Number 2 (2019) pp. 404-409
7. M K Parthasarathy, R Murugasan, Ramya Vasan (2018). "Modelling manpower and equipment productivity in tall residential building projects in developing countries", Journal of the South African Institution of Civil Engineering, Vol 60, pp. 23-33
8. Durdyev, S.; Ismail, S.; Kandymov, N. (2018) Structural Equation Model of the Factors Affecting Construction Labor Productivity. J. Constr. Eng. Manag., 144, 11.
9. Shree Raja T.G. Gopal, k. Murali (2016) "Secondary Data Analysis on Factors Affecting Labour Productivity in Construction" International Journal of Scientific and Research Publications, Volume 6, Issue 5, pp. 401-405
10. Attar, A A, Gupta, A K & Desai, DB (2014). A study of various factors affecting labor productivity and methods to improve it. IOSR Journal of Mechanical and Civil Engineering, 14(1): 11-14.
11. William Ibbs (2005), 'Impact of Change's Timing on Labor Productivity', Journal of Construction Engineering and Management, ASCE, Vol. 131(11), pp. 1219-1223.

Websites Used

12. <http://www.ijaresm.net>
13. <http://www.see.eng.osakau.ac.jp>
14. <https://www.bigrentz.com/blog/construction-trends>.





Raja et al.,

Table 1 Data Collection in Major construction projects

SI.No	Activity Description	Unit	Observation Summary			
			No.of. Days	Quantity	Worker (Hrs)	Equipment (Hrs)
1	Concrete	Cum	41	12128	56010	2566
2	Reinforcement	MT	41	1956.02	289320	1517
3	Formwork	Sqm	41	46819	274800	1886
4	Piling	Rmt	21	8330	2520	840
5	Excavation	Cum	21	18300	10210	1560
6	Blockwork	Sqm	25	5955	37350	50
7	Plastering	Sqm	25	10885	28900	50
8	Painting	Sqm	20	2732	1710	16
9	Flooring	Sqm	20	353	4056	62
10	Structural Steel work	MT	20	16.49	7272	552
11	Back Filling	Cum	20	3500	5120	360
12	Waterproofing	Sqm	20	1458	1184	52

Source: Primary data from the field survey.

ANOVA

Source of Variation	SS	df	MS	F	P-value	F crit
Between Groups	6.15E+10	11	5.59E+09	0.824842	0.621664	2.717331
Within Groups	8.13E+10	12	6.77E+09			
Total	1.43E+11	23				

Source: Computed.

Table 2 Manpower Productivity in Major construction Projects

SI.No.	Activity of Work	Productivity			
		Unit	Standard	value	Percentage
1	Concreting	Cum / hr	0.30	0.20	66.67%
2	Reinforcement	Kgs / hr	8.33	6.59	79.11%
3	Formwork	Sqm / hr	0.24	0.16	66.67%
4	Excavation	Cum / hr	2.04	2.23	109.31%
5	Piling	Rmt / hr	6.67	3.31	49.63%
6	Blockwork	Sqm / hr	0.20	0.18	90.00%
7	Plastering	Sqm / hr	0.45	0.40	88.89%
8	Painting	Sqm / hr	2.00	1.56	78.00%
9	Flooring	Sqm / hr	0.10	0.09	90.00%
10	Structural Steel	Kgs / hr	3.00	2.42	80.67%
11	Back Filling	Cum / hr	0.70	0.73	104.29%
12	Waterproofing	Sqm / hr	2.00	1.18	59.00%

Source: Computed.





Raja et al.,

Table 3 Equipment Productivity in Major construction projects

Sl.No	Activity of work	Equipment	Productivity			
			Unit	Standard	Value	Percentage
1	Concreting	Concrete pump	Cum/hr	30.00	16.35	54.50%
2	Reinforcement	Tower crane	Kgs/hr	10000.00	7670.19	76.70%
3	Formwork	Tower crane	Sqm/hr	250.00	169.66	67.86%
4	Excavation	Excavator	Cum/hr	100.00	60.24	60.24%
5	Piling	Piling rigs	Rmt/hr	20.00	9.92	49.60%
6	Blockwork	Tower crane	Sqm/hr	200.00	132.40	66.20%
7	Plastering	Tower crane	Sqm/hr	400.00	295.60	73.90%
8	Painting	Tower crane	Sqm/hr	400.00	169.09	42.27%
9	Flooring	Tractor trailer	Sqm/hr	8.00	5.59	69.88%
10	Structural steel	Mobile crane	Kgs/hr	150.00	89.69	59.79%
11	Back filling	JCB	Cum/hr	30.00	13.33	44.43%
12	Water proofing	Tower crane	Sqm/hr	50.00	29.56	59.12%

Source: Computed.

Table 4 Impact of Productivity on Project Profitability

Sl.No	Description	Values (Rs. Lacs)	Remarks
1	Contract Value	58200.00	
2	Labour cost Planned in 12 activities	2844.00	
3	Actual Labour cost expected	3612.00	
4	Overrun due to less Productivity	768.00	(A)
5	% of Contract Value	1.32%	
6	% of Planned Labour Cost	27.00%	
7	Equipment cost Planned in 12 activities	317.00	
8	Actual Equipment cost expected	554.00	
9	Overrun due to less Productivity	237.00	(B)
10	% of Contract Value	0.41%	
11	% of Planned Equipment Cost	74.76%	
12	TOTAL OVER RUN (A+B)	1005.00	
	% of Contract Value	1.73%	

Source: Computed.





Millimeter Wave Generation for Radio over Fiber Applications

Karthika Pragadeeswari C^{1*} and Krishnamariselvi T²

¹Assistant Professor, Department of ECE, Alagappa Chettiar Government College of Engineering and Technology, Karaikudi, Tamil Nadu, India.

²PG Scholar, Department of ECE, Alagappa Chettiar Government College of Engineering and Technology, Karaikudi, Tamil Nadu, India.

Received: 01 Mar 2021

Revised: 05 Mar 2021

Accepted: 18 Mar 2021

*Address for Correspondence

Karthika Pragadeeswari

Assistant Professor,

Department of ECE, Alagappa Chettiar Government College of Engineering and Technology,

Karaikudi, Tamil Nadu, India.

Email: bk.karthika@accetedu.in



This is an Open Access Journal / article distributed under the terms of the **Creative Commons Attribution License** (CC BY-NC-ND 3.0) which permits unrestricted use, distribution, and reproduction in any medium, provided the original work is properly cited. All rights reserved.

ABSTRACT

The photonic age of the Millimeter Wave (MMW) signal in RoF transmission framework is an overwhelming interaction. In MMW-RoF, transformation of an optical sign to an incredibly high recurrence radio signal is by using photonic up-change plot. This outcome in getting the photonic age of Millimeter Wave. This wave is utilized for information transmission. Machzehnder modulator is utilized for dependable transmission to meet the presentation attributes. Reenactment is finished with the assistance of Opti framework programming. The presentation examination of is done to acquire results greatest Q-factor and less BER than the phase modulator.

Keywords: Millimeter-wave, High frequency Radio signal, Photonic generator, Radio-over-fiber.

INTRODUCTION

The remote advances have arisen with different innovations, for example,[1] Coordinated Multipoint (CoMP) Transmission, Distributed Antenna System (DAS), Millimeter - Wave (MMW), Software Defined Radio (SDR), Software Defined Network (SDN), Cognitive Radio (CR).Plan of telecom network is the for all intents and purposes attainable, less unpredictable, huge data transmission, low misfortunes and financially savvy organization. The RoF frameworks basically need to be planned with a diminished expense and lesser operational intricacies of which is CS, BS and ODN. The ideal plan of RoF ought to be to such an extent that the less difficult plan frameworks. The RoF plan for MM-Wave age is utilizing Mach Zehnder modulator and the reproduction results are high information rate, high Q-factor and low BER.





Karthika Pragadeeswari and Krishnamariselvi

METHODOLOGY

The Radio over Fiber (RoF) [7] transmission framework mostly comprises of three areas to be specific, Central Station (CS), Base Station (BS) and Optical Distribution Network (ODN) or Optical Fiber Network (OFN). The Millimeter Wave (MM-Wave) [11] comprises of a range of Extremely High Frequencies (EHF) going from recurrence groups of 30GHz to 300 GHz. MM waves can give high information rates up to 10 Gbps. The incredibly high radio recurrence transporter wave is optically created and is alluded to as the photonic age of Millimeter Wave. This optical transporter is used for optical information balance of the transmitter information. As demonstrated in Fig.1, the optically adjusted information is communicated through fiber-optic channel and the sign is identified at the collector end. The identified sign is changed over to electrical sign and the Millimeter Wave recurrence signal is communicated through the remote channel. Fig.1 shows the block diagram of of the Radio over Fiber using MZM.

RoF using Machzehnder Modulator

Fig.2 shows the circuit design of the RoF using MZM. The continuous wave laser is utilized to produce a frequency of a 193.1 THz transporter signal. In the focal office (CO), a 10Gb/s baseband signal for remote assistance is blended in with the 30 GHz transporter. The transporter signal is given to the plentifulness modulator. The blended sign is applied to one of the terminals of the double cathode MZM. Simulation parameters in Table:1. Also, a baseband signal for wired assistance is straightforwardly taken care of into the other anode of the double cathode MZM. The regulated light wave is enhanced by an erbium-doped fiber intensifier before it is sent over single mode fiber and scattering repaying fiber. An optical band pass sift is utilized to dismiss through band enhanced unconstrained outflow commotion. At the base station, a fiber grinding is used to isolate these two signs and each sign is communicated to the relating photograph indicator. FBG with a 3-dB data transmission of 0.1nm and a reflection proportion of 0.99 is utilized to isolate the MM-Wave sign and BB signal. The MM-Wave and the baseband signal are gotten by the photograph locators at the collector end.

Frequency Tupled MZ-Modulator Technique

Fig.3 shows the circuit design of frequency tupled MZM. Optical Millimeter Wave (MM-Wave) age with the most noteworthy recurrence duplication factor is perhaps the most encouraging methods which can wipe out the need of high recurrence nearby oscillator at the focal station. The transmission Performance of the produced MM-Waves is assessed by regulating 10Gbps information over a Single Mode Fiber (SMF) with the assistance of Optisystem recreation software. Simulation parameters in Table:2. A polarization controlled CW laser source with a focal recurrence of 193.1 THz with 10 MHz otherworldly width and the force of the CW laser source is set to 10 dBm. The MZM1 is driven by a 0° stage moved and the MZM 2 is driven by a 45° phase moved. The MZM 3 is driven by a 90° stage moved and the MZM 4 is driven by a 130° phase moved. The lessening co-productive of the SMF is 0.2 dB/km. An optical intensifier with 20 dB acquire with a commotion figure of 4 dB is utilized to remunerate the misfortunes over the connection. At the base station a PIN photograph indicator with 0.7 A/W responsivity and 10 nA dull current is utilized to identify the regulated sign.

RESULTS & DISCUSSION

Building up a basically doable, less unpredictable, huge limit, low force utilization, huge data transfer capacity, high yield force and financially savvy transmission framework. The input wave and output Millimeter Wave spectrum Fig.5 to 8. This framework would be configuration to high Q factor and least BER. It very well may be accomplished for up to 40 km fiber transmission distance. An eye design is appeared in the above Fig. 4. This example is otherwise called an eye graph. It is an oscilloscope show in which an advanced sign from a beneficiary is monotonously tested and applied to the vertical info, while the information rate is utilized to trigger the flat range. It is supposed on the grounds that, for a few sorts of coding, the example resembles a progression of eyes between a couple of rails. It is an





Karthika Pragadeeswari and Krishnamariselvi

apparatus for the assessment of the consolidated impacts of channel commotion and intersymbol impedance on the exhibition of a baseband beat transmission framework. It is the synchronized superposition of all potential acknowledge of the sign of interest saw inside a specific flagging stretch. From the reproduction results, it tends to be surmised that a MMW-RoF, with photonic age of MM-Wave Mach-Zehnder Modulator as optical modulator gives great execution with the deliberate boundaries, for example, Q factor and BER. An eye diagram is appeared in the above Fig.9. Spectrum

Q factor

Q factor measures the quality of an transmission signal in terms of its signal-to-noise ratio (SNR). Q factor is the difference between the mean values of the signal levels for a "1" and a "0" divided by the sum of the noise values at those two signal levels assuming Gaussian noise and the probability of a '1' and '0' transmission being equal ($P(1) = P(0) = \frac{1}{2}$). The greater that difference is, the higher the Q-Factor and the better the BER performance.

BER:

It is the number of bit errors per unit time. It is the number of bit errors divided by the total number of transferred bits during a studied time interval.

From the simulation results, it can be inferred that design using phase modulator got high bit error and low quality factor compared to MZ modulator. From the graph representation in Fig.11 and comparison between the existing and proposed techniques Table.3.

CONCLUSION

There are numerous troublesome assignments in the planning of MMW-RoF transmission framework. By and by, incorporated innovation is a promising innovation that can uphold high information rate and enormous transmission capacity. There are a few transmission media advancements utilized for wide band arrangement conspires that acts like a solid competitor for the Radio-over-Fiber Transmission Systems. It offers us a chance to build up a MMW-RoF, with photonic age of MMW utilizing MZ modulator as optical modulator. This framework would be intended to meet high Q factor and least BER. The research paper, we have present a novel 16 tupled MMW average strategy utilizing fell blend of four LN-MZMs and concurrent RoF transmission framework. The eighth request sidebands are distant from everyone else produced with no optical filters. An blunder free transmission of 10 Gbps information more than 50 km SMF is illustrated. The framework can be essentially actualized for the age of optical MM-Waves and transmission of future multi-Gbps administrations to the clients.

REFERENCES

1. Joaquin Beas "Millimeter-wave frequency radio over fiber system" *IEEE publications* March 2013.
2. Nael A. Al-Sharee, Syed I. S. Hassan, Fareq Malek, Razali Ngah, Sura A. Abbas, and Syed A. Aljunid, "A cost-effective method for high-quality 60 GHz optical Millimeter Wave signal generation based on frequency quadrupling" *Progress in Electromagnetics Research*, Vol. 137, 255-274, 2013.
3. Timothy P. McKenna, Jeffrey A. Nanzer, and Thomas R. Clark Jr. "Photonic Millimeter-Wave System for High-Capacity Wireless Communications" Johns Hopkins APL Technical Digest, Volume 33, Number 1, 2015.
4. Andreas Stöhr, Senior Member, *IEEE* "Millimeter-Wave Photonic Components for Broadband Wireless Systems" 2015.
5. Dalma Novak, Fellow, "Radio-over-Fiber Technologies for Emerging Wireless Systems" *IEEE J. Quantum Electronics*, vol. 52, issue 1, 2016.
6. Faris Mohammed Ali "Performance Analysis of Radio over Optical Fiber System with OFDM Using Multiplexing Techniques" *International Journal of Applied Engineering Research* ISSN0973-4562 Volume 13, Number 12, 2018.





Karthika Pragadeeswari and Krishnamariselvi

7. Guang Li 1,2, Zhihua Lin 1,3, Xuguang Huang 4 and Jianqing Li Article “A Radio over Fiber System with Simultaneous Wireless Multi-Mode Operation Based on ha Multi-Wavelength Optical Comb and Pulse-Shaped 4QAM-OFDM” *Electronics* 2019, 8, 1064.
8. Jiangnan Xiao, Chuang Zhao “Review on the Millimeter-Wave Generation Techniques Based on Photon Assisted for the RoF Network System” *Hindawi Advances in Condensed Matter Physics* Volume 2020.
9. Saifur Rahman, Farman Ali “Mitigation of Nonlinear Distortions for a 100 Gb/s Radio-Over-Fiber-Based WDM Network” www.mdpi.com/journal/electronics *Electronics* 2020.
10. Jeonghun Lee, Jiayuan He, Ke Wang “FPGA-based neural network accelerators for Millimeter-Wave radio-over-fiber systems *A Preprint* February 20, 2020.
11. Stefan Nilsson-Gustvik “Optical theory for communication networks” - second edition.
12. Prof. Igor Minin “Microwave and Millimeter Wave Technologies: from Photonic Bandgap Devices to Antenna and Applications”.

Table 1:Simulation Parameters

Components	Parameters	Value
CW Laser	Frequency	193.1THz
	Power	10 dBm
EDFA	Gain	10.8 dB
Single Mode Fiber	Length	40 km
Uniform fiber Grating	Frequency	193.1THz
	Bandwidth	0.15nm

Table 2:Simulation Parameters

Components	Parameters	Value
CW Laser	Frequency	193.1THz
	Power	10 dBm
Phase Shift	Azimuth Angle	0 degree
Phase Shift 1	Azimuth Angle	45 degree
Phase Shift 2	Azimuth Angle	90 degree
Phase Shift 3	Azimuth Angle	130 degree
Optical Fiber	Length	40 km

Table 3:Comparison between Existing and Proposed techniques

Parameters	Phase Modulator	Machzehnder Modulator
Q-Factor	8.55588	12.5731
BER	5.10553e-018	1.41365e-036





Karthika Pragadeeswari and Krishnamariselvi

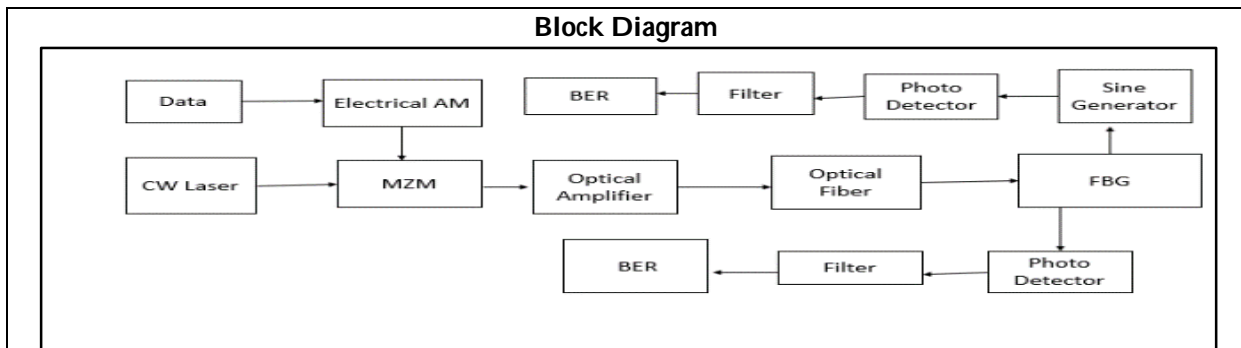


Fig.1 Block Diagram of the RoF using MZM

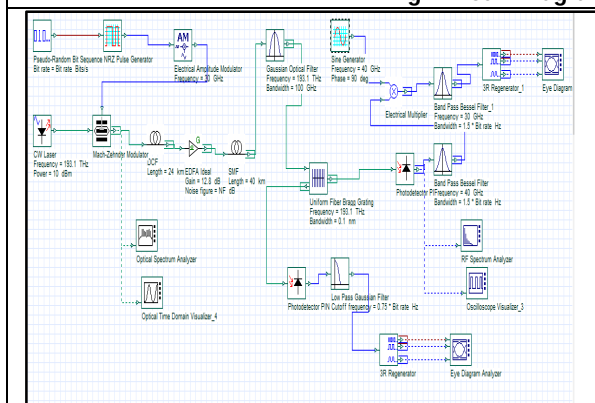


Fig.2 Circuit Design of the RoF using MZM

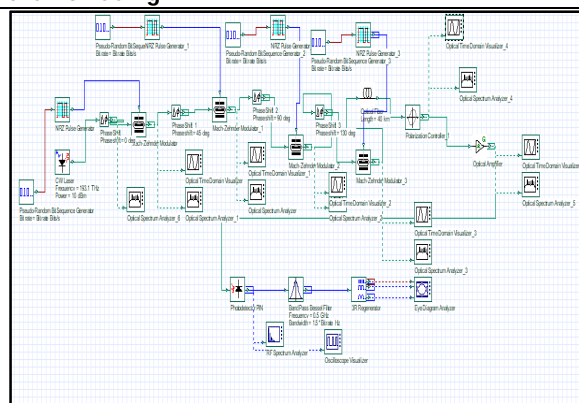


Fig.3 Circuit Design of Frequency Tuned MZM

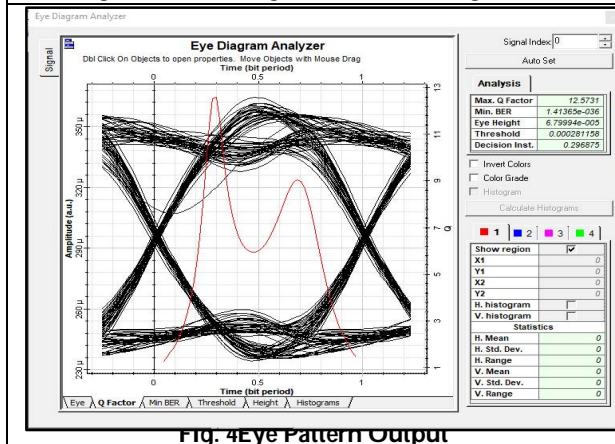


Fig. 4 Eye Pattern Output

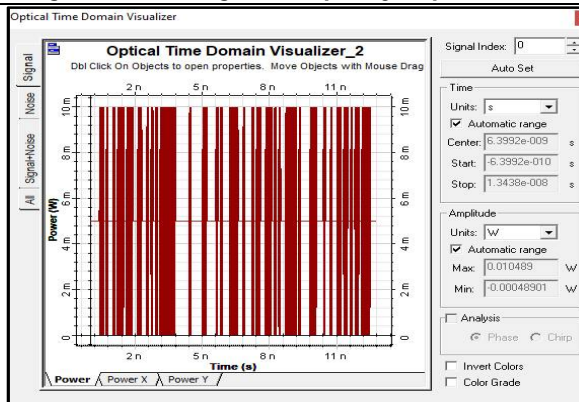


Fig. 5 Inputwave





Karthika Pragadeeswari and Krishnamariselvi

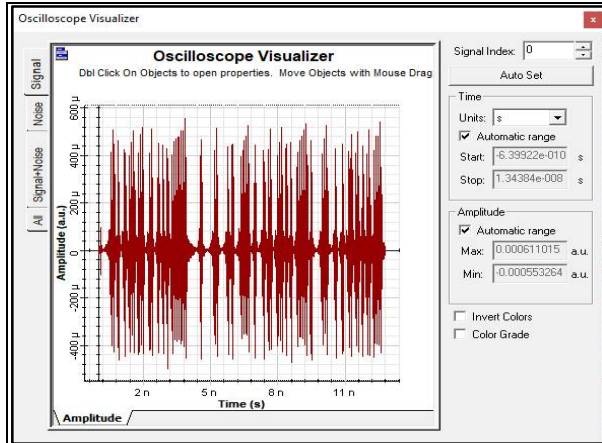


Fig.6 Output Millimeter Wave

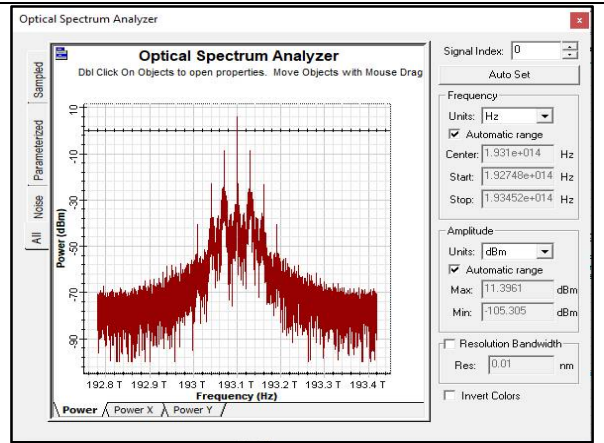


Fig.7 Input Spectrum

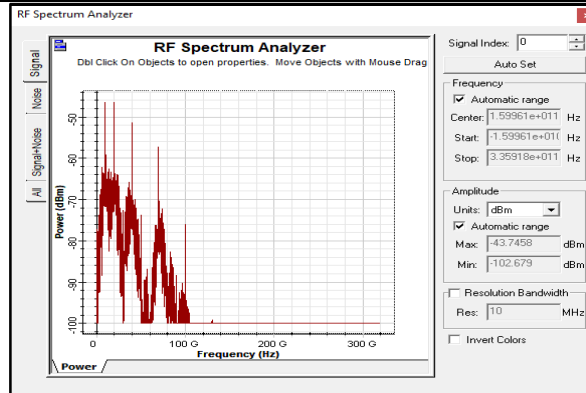


Fig.8 Output Millimeter Wave

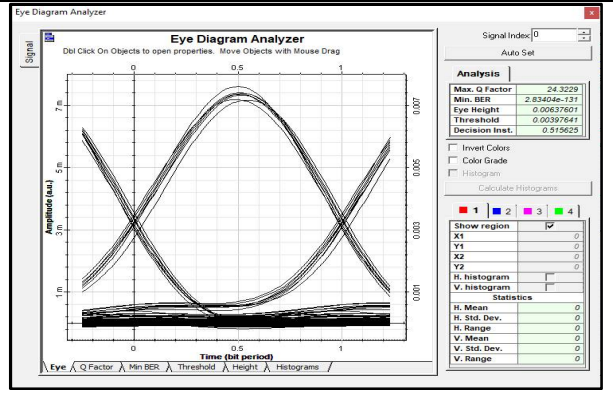


Fig.9 Eye Diagram

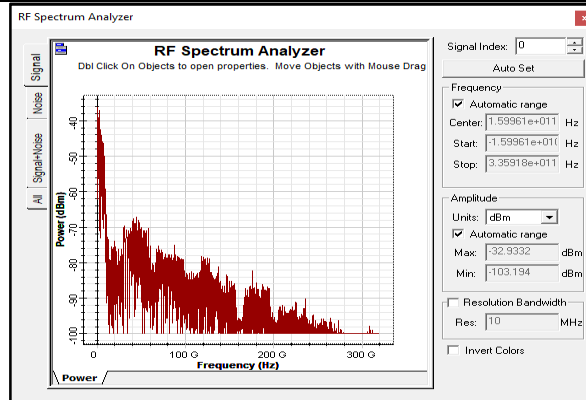


Fig.10 Output Millimeter Wave

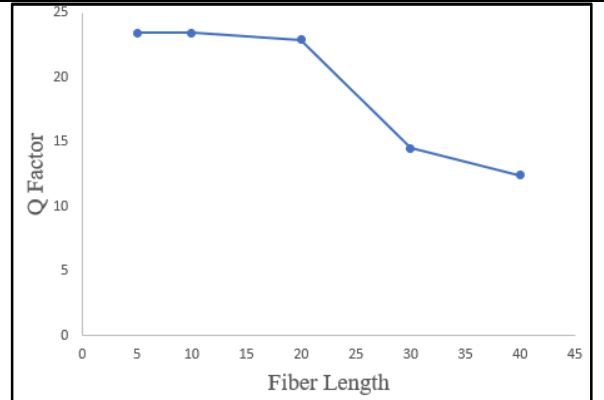


Fig.11 Fiber Length vs Q Factor





Builders of Sumeria: Simple Construction Terms and Mathematics used by them.

Purushothaman P¹, Suresh E.S.M² and Ramasamy, A.M.S³

¹Professor, Department of Civil Engineering, Agni College of Technology, Chennai, Tamil Nadu, India.

²Professor and Head of Department of Civil Engineering, NITTTR, Chennai, Tamil Nadu, India.

³Professor, Department of Mathematics, Pondicherry University, Pondicherry, Tamil Nadu, India.

Received: 05 Mar 2021

Revised: 11 Mar 2021

Accepted: 17 Mar 2021

*Address for Correspondence

Purushothaman P

Professor,
Department of Civil Engineering,
Agni College of Technology,
Chennai, Tamil Nadu, India.
Email: ellapura@gmail.com



This is an Open Access Journal / article distributed under the terms of the **Creative Commons Attribution License** (CC BY-NC-ND 3.0) which permits unrestricted use, distribution, and reproduction in any medium, provided the original work is properly cited. All rights reserved.

ABSTRACT

Sumerians built temples, buildings and canals. They used burnt bricks in buildings and used river water for irrigation. They had number systems. There were builders, architects, surveyors and mathematicians-experts. They taught mathematics and accounting in their schools. It will be interesting to understand how mathematics had played in civil engineering in those days. This paper attempts a preliminary investigation using present form of Tamil in this regard. The study suggests that mathematics offer better opportunities to recover the terms in present day language forms as context are well defined.

Keywords: Sumerians, buildings, architects, mathematicians, Tamil

INTRODUCTION

Kramer (1) introduces Sumerians of third millennium BC as endowed with unusually creative intellect and with unusual flair for technological inventions. He notes that Sumerians exploited the richness of river sediments overflow from the two major rivers for cultivation; they also used clay for brick making and plastering reed mats for buildings. Kramer (1) observes that any modern-day professional can identify his or her prototype in Sumerians such as poets, philosophers, architects, lawyers, accountants and so on. It seems that the need to keep accounting and to do business motivated Sumerians to invent numbers and further invented writing on clay tablets (1,2,3). Kramer notes research on Sumerians is incomplete and sees scope for further research. As it appears that we do not know who Sumerians were and where from they came and settled on the Southern parts of present Iraq. Nobody knew where they left and what language they spoke. The Sumerian language was discovered indirectly through other ancient languages not spoken now. It is also believed that nobody is speaking the Sumerian language anywhere in

30595





Purushothaman et al.,

the world (1,2). However, Pawaner, Sathasivam, Loganathan and others have seen some connection to Dravidian languages (4,5,6). Loganathan specifically claimed that Sumerian language was archaic form of Tamil and all Indian languages (6). Subsequent work by Purushothaman, Suresh, Menon showed the link as between Sumerian words and present form of Tamil words (7,8). Further, if we could consider cultural continuity as between Sumerians and Indians, we could find refinements over standard translations of Sumerian works (6,7,8,9).

Sumerian culture was temple based as similar to ours in Tamilnadu (1,6). They built temples. There were temple-city strong relations. Each city was having ruling deities. One of a very ancient type of temple was excavated by archaeologists at Eridu. The temple was of simple shape and of small size 12'x15'. There were two characteristics which remained constant: One a niche for god emblem or statute, another an offering table in front of it (1). Later periods, big temples called ziggurats were built by raising platforms (1,2). New temples have been built over the foundation of older temples, say as in Eridu (2). It is very interesting to note that both terms to count and builder have common root syllables in Sumerian literature: The Sumerian word "sid" means to count, likewise the word, "sidim" means builder (11,12). As people from Tamilnadu, we can easily identify these words as closely sounding as "chith" (relating to Siddhar) and "chithim" respectively (13). Whereas, "thimmi" in Tamil is an ancient type of foundation. Now also, we use the word or tools, "thimms" to compact earth. Like this, we could relate only few words as between Tamil words and Sumerian words as found in web resources ETCSL (11) and ePSD (12). This is also an area for further research. However, in this paper, an attempt is made as an exploratory, preliminary study on few instances of construction (survey, building) and application of basic mathematics through comparing standard translation and as recovered in present form of Tamil. This is expected to help us deepening our understanding of ancient construction methods and mathematics applications in those days.

RESEARCH METHOD OR APPROACH

Sathasivam (5) had compared Dravidian lexicon with Sumerian words matching first few letters and meanings. Whereas, Purushothaman, Suresh, Menon (7,8,9) have shown further elaboration that present form of Tamil words could be extracted from Sumerian literature as root words as forming words in the beginning, middle or at the end; or by combining or by expanding as may be required to match phonetic values and meanings, allowing some flexibility as trial and error approach. Similar approach is used here to recover terms, poems, instructions as relating to few specific instances of application of mathematics and survey settings in the field. The specific situations considered are, one a mathematical problem- solving procedure written in early Babylonian period (10); another, a passage in the temple construction (11). The standard translations are compared as recovered in present form of Tamil further translating it to English to enable comparison. In both cases, we have transliteration and translation of Sumerian work in English as standard work (10,11). These are used as data to recover in present form of Tamil and as translated in English for comparison. By doing this way, we only expect refinement over the standard translation works.

Case-1 Sumerian early Babylonian mathematical problem-procedure as outlined in reference (10): Let us take the Catalogue No. BM 13901, # 10 Obv. II

Going through the detailed working of the problem and explanation given by Jens Høyrup (10), we can restate the problem so that present day high school students can solve, as: Given two squares whose sides are in the proportion of 7:6. What would be the sizes of the sides of these squares, if total area of these two squares is 21.25 area units? The answers for this problem are 3.5 and 3.0 length units, respectively for each square.

Appendix-1 shows the transliteration and standard translation work of Jens Høyrup (10) and as recovered in present form of Tamil, it's transliteration and translation for comparison, in the same order, for each line of instructions for the problem, procedure and solution.

Case-2 The building of Ningîrsu's temple (Gudea, cylinders A and B) (c.2.1.7), lines c217.471 to 481 (reference-11).





Purushothaman et al.,

This set or passage was taken from ETCSL, particularly selected by searching the database for the key term, "IKU". The gloss table in its standard form is taken, the first three rows for each poem showing transliteration, key terms, it's gloss in English. To this two more rows are added to show as recovered in Tamil, it's English translation, so that standard and Tamil forms can be compared. The ETCSL as well gives for each table or set, a consolidated translation in English and to compare with this a consolidated translation of Tamil work is also provided.

Limitations: Whatever terms given in Tamil for the early Sumerian or Babylonian period are tentative.

RESULTS

Case -1 Catalogue No. BM 13901, #10 Obv. II

The standard translation work gives eight steps as shown below:

1. The surfaces of my two confrontations I have heaped: $21^{\circ}15'$.
2. Confrontation (compared) to confrontation, the seventh it has become smaller.
3. 7 and 6 you inscribe. 7 and 7 you make hold, 49.
4. 6 and 6 you make hold, 36 and 49 you heap:
5. $1^{\circ}25'$. IGI $1^{\circ}25'$ is not detached. What to $1^{\circ}25'$
6. May I posit which $21^{\circ}15'$ gives me? By $15'$, $30'$ is equal
7. $30'$ to 7 you raise: $3^{\circ}30'$ the first confrontation.
8. $30'$ to 6 you raise: 3 the second confrontation.

The eight steps as seen through Tamil but translated are as shown below:

1. To get 21.25 units of area bound by bunds by traditional methods:
2. Small piece of land and bunds/bounds are easy to form and handle.
3. (Consider two areas of sides or) bunds sides of 7 and 6 each; let us multiply 7 by 7 as 49.
4. Likewise multiply 6 by 6 as 36; add 49 to this, (we get 85, note this as $60+25$ as 1,25).
5. We don't get any reference to this value 1,25 in the tables; do you get any spark of idea?
6. Do you remember? We taught you, square of (0,30) is (0,15); (square of side $\frac{1}{2}$ is area $\frac{1}{4}$. Note area of 21.25 is $\frac{1}{4}$ times of 85.)
7. Multiplying 7 by $\frac{1}{2}$ we get 3.5 as length measure of one side of bund, (bound as a square area of 12.25)
8. Multiplying 6 by $\frac{1}{2}$ we get 3 as length measure of one side of bund as bound (as a square area of 9. Totalling $12.25+9$), we get the desired area of equal value [21.25 ie (21,15).]

Case – 2 The building of Ningîrsu's temple (Gudea, cylinders A and B) (c.2.1.7), line c217.471

Standard Translation:

Lines 471-481 paragraph t217.p60

Towards the house whose halo reaches to heaven, whose powers embrace heaven and earth, whose owner is a lord with a fierce stare, whose warrior Ningîrsu is expert at battle, towards E-ninnu-the-white-Anzud-bird, Gudea went from the south and admired it northwards. From the north he went towards it and admired it southwards. He measured out with rope exactly one iku. He drove in pegs at its sides and personally verified them. This made him extremely happy.

As recovered through Tamil for lines 271 to 281

The temple as arising to the sky is as equal to it

It is true delight as we reach sky high feeling like flying

The ruler eyes go red because of heat as close to sun but in style

The Sangam head is our deity Ningîrsu, a fact like the crown moon

As the temple stands with the sky as it's wings, it looks like a white bird in the open space

The head person of the town is set to draw the square on the ground





Praise our village which is on the river draining plains
 If the plot is set as a square that would be great
 The expert is here to set the limits and boundary
 The work is completed using the measuring sticks, driving pins or pegs
 People show their joy by raising traditional ululation, now the plot is marked.

DISCUSSION

Most of the written tablets were found in Sumerian – Mesopotamian schools called e-dub-ba-a and these tablets were used as education or teaching materials (1, 10, 14). The tablet what we have considered (BM 13901) is also one such teaching material to train students on solving mathematical problems (10). Going through the standard translation, it is very difficult to understand the steps as self reading material, however with peer support and instructor's support, learning to solve the intended problem is possible. Note, the problem itself is not well defined but required to be understood, as explained in detail (10). Purushothaman and Suresh (7) have brought out mathematics teaching situation in Sumerian e-dub-ba-a that the teacher would go round and help them, in addition to senior students helping juniors. The standard translation of this problem brings out the English terms such as confrontation, heap, raise and equal respectively as square area, adding, multiply and equal. This also brings out a technical term of the period, IGI referring to mathematics table (10).

When we look at the Tamil version, we have the advantage of going through the explanation and understanding of the problem as given by Jens Høyrup (10), so we can recover the instructions better. Further, we see few more tips, possibly, as the problem appears to be the one faced in forming agricultural fields for irrigation, not only forming suitable size plots but also to keep the bunds small and strong. We also find a teaching situation where students' attentions are drawn to a previously taught concept. We could also see a learning situation where, the teacher inquires the students for spark of ideas to solve the problem. We propose lots of Tamil words of which kunitham, idusi, edusi, samam respectively for multiplication, input, output (for squaring are of interest) and equal; these, we have to explore looking at more Babylonian mathematical problems to have better understanding. IGI as referred in standard form as to a mathematical table, we have taken that as akki in Tamil (this was proposed by Loganathan as eye). We can also consider these two Tamil words from Tamil lexicon (13): akkiyam meaning 14th of 15 divisions of a day and akkirachandani a register kept by Yama, both show some distant use of tables. Fowler and Robson (14) have mentioned lists of tables and an attempt was also made to see some special mathematics terms through present form of Tamil (as shown in appendix-3).

While we consider the second case: The building of Ninġirsu's temple (Gudea, cylinders A and B) (c.2.1.7), line c217.471.

We find the standard version is cohesive, although the gloss gives some clues to the situations; we could see that some intuition had been applied while consolidation. Taking cues, similarly, the Tamil version also gives a cohesive picture through intuition, however, we find few sections in the narrative: The first few lines are poetic as what the temple would look like, as could be like an architect's visualisation. Further some tips on the need for a square plot. Then how the plot was laid but with less details than what we would be wanting as engineers. Finally, the passage ends with people all around raising happy ululation. The last few lines would suggest that the poet was describing a layout marking ceremony. We have north south reference in standard version, but could not see it in the Tamil version. But, we see some reference to site location in a town in the lower plains of the river as we could see from the Tamil version. The critical search term in standard version remains as IKU a standard area measurement (that is about 0.36 hecter), but the details are missing of how that was fixed at site. Whereas, the Tamil version, the same term IKU as in the transliteration as iku was taken to mean Tamil word igal to mean to set limits or boundary and alternatively as root word of vaguththal (iguththal) in Tamil for dividing land or quantities. An attempt is also made to recover Tamil key words as labels have been used interpreting the architect plan of Gudea (Wikimedia commons:





Purushothaman et al.,

Eninnu), as shown in appendix-4. As we compare the standard translations and those recovered through Tamil, in both cases, we see refinements and we get more details. However, this is subjective and requires further studies.

In previous works particularly working through terms found in Sumerian dictionary (ePSD), we have noted internal consistency in the form of matching meaning and phonetic value not just with one term with one meaning, but for one term with many meanings(7,8,9). One such term, the root syllable is, “sa” with meanings of equal, tuning music, half, wages etc. We could readily identify the Tamil words like samam>>equal, half; sariga ma >> tuning; sathamkooli>> wages and so on. Such of these root words are special which increase the confidence level. As for civil engineers and architects, the recovery of the Sumerian literature which runs into more than 1000 poem lines, on Building of Ningirsu temple would be a treasure to work on. Likewise, working further on more problems of Sumerian and Babylonian mathematics would help us to motivate children to take more interest on mathematics. Further, recovering Sumerian – Babylonian mathematical problems would show us much more of terms still we use at present in the field. Some of the words common to inquest and mathematics are en, en.nam, an.na that these can be seen in Tamil as en>>number; en.nam>>thought, what; aanaal>>but, what if and so on. These remain now as proposals, however requiring further studies.

CONCLUSION

Sumerians could be considered the first ever innovators of human kind who not only wrote about their innovations and left their monuments standing as testimonials. We have considered two major case studies one involving teaching a mathematical problem another field setting of a temple plot. We found refined information as we compare standard translations as with recovered through Tamil. This indicates scope for further studies both in building and mathematics related literature of Sumerians. As situations or context relating to mathematics are clear, opportunities are better while recovering the terms in present forms.

REFERENCES

1. Kramer , S.N., 1971, The Sumerians, The University of Chicago Press
2. Postgate, J.N, 2004, Early Mesopotamia, Routledge, London & New York
3. Denise S B, 2006, How writing came about, University of Texas Press
4. Kandaiya Pillai N Si, Varalaru kaalaththirku murrpatta pazhanthamizh, Progressive Achchagam, 1948.
5. Sathasivam.A., Sumerian – A Dravidan Language, PhD thesis, Berkeley California – 1965.
6. Loganathan.K, Sumerian Tamil, Towered temple in Sumeria, Web based resources
7. P Purushothaman, ESM Suresh Reflecting On Pedagogical Issues Of e-dub-ba-a of Sumeria Linking To Our Present Times, 2014/6, NITTTR, Bhopal, ISSN: 0976-0121
8. Menon, R., Purushothaman, P. <https://www.academia.edu/s/cdf08cef37/sumerian-and-tamil-a-comparison-and-study-with-reference-to-a-transliterated-text-and-standard-translations?source=news>
9. Purushothaman, P.; Suresh, ESM, Collection of our papers in Tamil on Sumerians, draft https://drive.google.com/file/d/1WrHlmy6lg-i_-rInElafGrSYDjSURPH8/view?usp=drivesdk
10. Jens Høyrup, 2013, Algebra in Cuneiform Introduction to an Old Babylonian Geometrical Technique, pre-print, Max Planck Institute for the History of Science, Solved problems of Catalogue No. BM 13901, #10 Obv. II
11. ETCSL – Electronic Texts Collection of Sumerian Literature, web based resources <http://etcsl.orinst.ox.ac.uk/>
12. ePSD – Electronic Pennsylvania Sumerian Dictionary, web based resources <http://psd.museum.upenn.edu/epsd/nepsd-frame.html>
13. Madras University Lexicon<http://dsal.uchicago.edu/dictionaries/tamil-lex/>
14. Fowler, D., Robson, L., 1998, Square Root Approximations in Old Babylonian Mathematics: YBC 7289 in Context, HISTORIA MATHEMATICA 25 (1998), 366–378 ARTICLE NO. HM982209





Appendix-1 Comparing standard and Tamil versions in the context of tablet BM 13901 #10

Babylonian tablet BM 13901 #10, restatement of the problem in present form: Given two squares whose sides are in the proportion of 7:6. What would be the sizes of the sides of these squares, if total area of these two squares is 21.25 area units?

Line-11

- A: a.šāši-ta mi-it-ha-ra-ti-iaak-mur-ma 21,15
 B: The surfaces of my two confrontations I have heaped: $21^{\circ}15'$.
 C: அசல்சிட்டாமிகுதிகரைதீரம்அய்யாமுறைமைஆக (21,15)
 D: Acalciṭṭāmikutikaraitīramayyāmuraimaiāka (21,15)
 E: To get 21.25 units of area bound by bunds by traditional methods:

Line-12

- A: mi-it-har-tum a-na mi-it-har-timsi-bi-a-timim-ti
 B: Confrontation (compared) to confrontation, the seventh it has become smaller.
 C: மிகுந்தகரையாகும்மமாத்துவம்ஆனால்நிம்மதிமிகுந்தகரைதிம்மி; சிட்டாபிரித்தால்நிம்மதி.
 D: Mikuntakaraiyākumkam'māttuvamāḥnim'matimikuntakaraitim'mi; ciṭṭāpirittānim'mati.
 E: Small piece of land and bunds/bounds are easy to form and handle.

Line-13

- A: 7 ù 6 ta-la-pa-at 7 ù 7 tu-uš-ta-kal 49
 B: 7 and 6 you inscribe. 7 and 7 you make hold, 49.
 C: 7 உடன் 6 தலைபட்டு, 7 உடன் 7 அதுஉஸ்தாக்கல்பெருக்க 49.
 D: 7 Uḥa 6 talaipaḥu, 7 ḥa 7 atu us tākkalperukka 49
 E: Consider two areas of sides or bunds sides of 7 and 6 each; let us multiply 7 by 7 as 49.

Line-14

- A: 6 ù 6 tu-uš-ta-kal 36 ù 49 ta-ka-mar-ma
 B: 6 and 6 you make hold, 36 and 49 you heap:
 C: 6 உடன் 6 அதுஉஸ்தாக்கல்பெருக்க 36, அத்துடன் 49 ஐகமாரசுட்ட,
 D: 6 Uḥa 6 atu us tākkalperukka 36, attuḥa 49 aikamāraḥḥa,
 E: Likewise multiply 6 by 6 as 36; add 49 to this, (we get 85, note this as 60+25 as 1,25).

Line-15

- A: 1,25 igi 1,25 ú-la ip-pa-ta-ar mi-nam a-na 1,25
 B: 1`25. IGI 1`25 is not detached. What to 1`25 1,25 அக்கி 1,25
 C: அட்டவணையில்உள்ளில்லைகைப்படார்; மின்எண்ணம்என்னாம், ஆனமட்டும் 1,25.
 D: 1,25 Akki 1,25 aḥḥavaḥaiyituluḥaikaippār; miḥḥameḥam, āḥamaḥum 1,25.
 E: We don't get any reference to this value 1,25 in the tables; do you get any spark of idea?

Line-16

- A: Lu-uš-ku-un ša 21,15 i-na-di-nam 15.e 30 ḥb.si
 B: May I posit which $21^{\circ}15'$ gives me? By $15'$, $30'$ is equal
 C: அள்ளுஉள்ளுணுகுணிதம் (21,15) சமம், இன்னஓதினம் (0,30) இடுசி (0,15) எடுசி.
 D: Aḥḥuḥaḥukukuḥitam (21,15) camam, iḥḥaḥōḥitam (0,30) iḥḥuci (0,15) eḥuci.





Purushothaman et al.,

E: Do you remember? We taught you, square of (0,30) is (0,15); square of side $\frac{1}{2}$ is area $\frac{1}{4}$. Note area of 21.25 is $\frac{1}{4}$ times of 85.

Line-17

A: 30 a-na 7 ta-na-ši-ma 3,30 mi-it-har-tum iš-ti-a-at

B: 30 to 7 you raise: 3:30 the first confrontation.

C: 7 அதன் (0,30) அணைக்கநசிக்கமீதி (3,30) கரையாகும்இதுதீர்வுஆகும்

D: 7 Ata (0,30) aḷaiḷkanacikkamīti (3,30) karaiyākumitūtīrvuākum

E: Multiplying 7 by $\frac{1}{2}$ we get 3.5 as length measure of one side of bund, bound as a square area of 12.25

Line-18

A: 30 a-na 6 ta-na-ši-ma 3 mi-it-har-tum ša-ni-tum

B: 30 to 6 you raise: 3 the second confrontation.

C: 6 அதன் (0,30) அணைக்கநசிக்கமீதி (3,00) கரையாகும்சமன்இதும்

D: 6 Ata (0,30) aḷaiḷkanacikkamīti (3,00) karaiyākumcamālitum

E: Multiplying 6 by $\frac{1}{2}$ we get 3 as length measure of one side of bund as bound as a square area of 9. Totalling 12.25+9, we get the desired area equal value of 21.25 ie (21,15).

Appendix-2 Building of Ningirsu – Comparing standard and Tamil versions; ETCSL glossing

The building of Ningirsu's temple (Gudea, cylinders A and B) (c.2.1.7) lines 471-481

Translation of lines 471-481 paragraph t217.p60

Towards the house whose halo reaches to heaven, whose powers embrace heaven and earth, whose owner is a lord with a fierce stare, whose warrior Ningirsu is expert at battle, towards E-ninnu-the-white-Anzud-bird, Gudea went from the south and admired it northwards. From the north he went towards it and admired it southwards. He measured out with rope exactly one iku. He drove in pegs at its sides and personally verified them. This made him extremely happy.

Gloss-translation-in present form of Tamil-Tamil transliteration & translation

Note: Proposed Tamil terms are as trials to match meaning & phonetic value that would corresponding to Tamil in present form.

Link for line 471 <https://etcsl.orinst.ox.ac.uk/edition2/etcslgloss.php?lookup=c217.471&charenc=gcirc>

The building of Ningirsu's temple (Gudea, cylinders A and B) (c.2.1.7), line c217.471

e ₂	me-lem ₄ -bi	an-ne ₂	us ₂ -sa
e₂	me-lem₄	an	us₂
house(hold)	(awesome) radiance	heaven	to be adjacent
இல்லம்கோயில்	மேலெழும்பி	வான்றேர்	உசரசமம்
Temple	As arising	To the sky	Height equal

The building of Ningirsu's temple (Gudea, cylinders A and B) (c.2.1.7), line c217.472

me-bi	an	ki-da	gu ₂	la ₂ -a
me	an	ki	gu₂	la₂
essence	heaven	place	neck	to hang
மெய்பிரகாசம்	வான்	கிட்ட	குலாவ	துலாஉலா
True brightness	sky	As nearer	As we could catch	We feel flying





Purushothaman et al.,

The building of Ningirsu's temple (Gudea, cylinders A and B) (c.2.1.7), line c217.473

lugal-bi	en	igi	huš	il ₂ -il ₂
lugal	en	igi	huš	il₂
king	lord	eye	to be reddish	to raise
ஆளுகள்	அய்யன்	அக்கிகண்	உஷ்ணம்	அயில்ஓயில்
The ruler	The respected	eyes	Feeling heat	But so high, a good sight

The building of Ningirsu's temple (Gudea, cylinders A and B) (c.2.1.7), line c217.474

ur-saĝ	^a nin-ĝir ₂ -su	me ₃	gal-zu-bi
ur-saĝ	nin-ĝir ₂ -su	me₃	gal-zu
hero	Ningirsu (DN)	battle	skilful
ஊர்சங்கம்	தெய்வம்நின்கீரன் சூரன்	மெய்யே	சூரன்பிறை
Assembly head	Deity yours scribe skilled	A fact	A crown moon

The building of Ningirsu's temple (Gudea, cylinders A and B) (c.2.1.7), line c217.475

e ₂ -ninnu	anzud ₂ ^{mušen}	babbar ₂ -še ₃
e ₂ -ninnu	anzud	babbar
E-ninnu (TN)	Anzud (DN)	white
கோயில்நின்னு	வான்கூடிபறவைபோல	பப்பரவெளிபரப்புவெண்மைசேர
Temple as it stands	Sky spreading as wings	The outside brightness, look like a white large bird

The building of Ningirsu's temple (Gudea, cylinders A and B) (c.2.1.7), line c217.476

gu ₃ -de ₂ -a	sig-ta	ba-ši-ĝen
gu ₃ -de ₂ -a	sig	ĝen
Gudea (RN)	to be low	to go
குடிகளின்அய்யா	அந்தசிகில்ரதம்தர	படுசிவரையஆங்கென்
Respected Chief	To build the temple	Set to draw the square

The building of Ningirsu's temple (Gudea, cylinders A and B) (c.2.1.7), line c217.477

nim-še ₃	u ₅	bi ₂ -dug ₄
nim	u₅	dug₄
upper (land)	wonder	to say
நிம்சேரிஊர்	உத்தமம்	எனதுக்கிபேசங்கள்
Your village drain plains	Is very good	praise

The building of Ningirsu's temple (Gudea, cylinders A and B) (c.2.1.7), line c217.478

nim-ta	ba-ši-ĝen	sig-še ₃	u ₅	bi ₂ -dug ₄
nim	ĝen	sig	u₅	dug₄
upper (land)	to go	to be low	wonder	to say
நிம்தளம்	படுசிசதுரம் ஆங்கின்	சிகில்ரதம்செய்ய	உன்னதம்	தூக்கிபேச
Your land	As being laid	To make a temple	Appreciate	Praise





Purushothaman et al.,

The building of Ningirsu's temple (Gudea, cylinders A and B) (c.2.1.7), line c217.479

iku	zid-dam	eš ₂	i ₃ -ġar-ġar
iku	zid	eš₂	ġar
area measure	right	rope	to place
இகல்இகுத்தல்வகுத்தல்	சித்தம்	ஈஸ்வர்	அய்யங்கார்ஆங்கே
To set limits boundary	As prepared thought	The expert	Iyengar is there

The building of Ningirsu's temple (Gudea, cylinders A and B) (c.2.1.7), line c217.480

a ₂ -ba	ġi ₃ š	bi ₂ -ġar	ni ₂ -te-ni	mu-zu
a₂	ġi₃š	ġar	ni₂-te-a-ni	zu
arm	tree	to place	himself, herself	to know
அப்ப	கிஷ்குகிஷ்கா	பிரித்து ஆங்கே	நீட்டிஆணி	முளைஅடித்துதும்ந்து முழு
Then	Using measuring stick	Dividing	Using long nail pegs	Driving pins, work completed

The building of Ningirsu's temple (Gudea, cylinders A and B) (c.2.1.7), line c217.481

hul ₂ -la-gin ₇	im-ma-na-ni-ib ₂ -ġar
hul₂	ġar
to be happy	to place
குலவைகுரல்எழுப்பிஆகின்	இம்மனைஇப்பஆங்கே
Raising happy voice by all	Now, the plot is marked, there

The building of Ningirsu's temple (Gudea, cylinders A and B) (c.2.1.7), line c217.427

na	gal-gal-bi	lagab-ba	mi-ni-de ₆
na	gal	lagab	de₆
stone	to be big	slab	to carry
நாங்கள்	கல்தரம்பிரித்து	உழலைமரம்கப்பிகயிறுகட்டிபடகு	மின்னுதே
We	Sorted stone slabs	Prepared wooden rollers and boat to transport	A delightful sight!

Appendix-3, Special mathematics terms in present form of Tamil, (see Fowler and Robson (14))

Given in the order of Akkadian (Sumerian)>> English standard version >> Tamil >> English Tamil version

1. **Muttarrittum**>> "thing that always goes down;" >>முற்றம்தாழ்வாரம்>> court yard, corridor, ridges, valleys, hip
2. **tallum**>> "long transversal" >>தள்ளும்,தாழும்>> as pushing, lowering
3. **SAG.KAK-kums`asa-am-na-[tuna]-a`s-ha 26 15 i-[gi-gu-bu-s`u]** >> A triangle from which an eighth part is subtracted: 0;26 15 is its coefficient.>>சங்கசந்திக்கும்அசல்சாய்வுசமானாதூண்அஸ்கா 26 15 அக்கிக்குப்பகுணாயுச>> as equal slanting or meeting arms or pillar, take correct or area multiplying by 26 15!
4. **ta-al-li SAG.KAK-ki 52 30 i-[gi-gu-bu-s`u]** >> The long transversal of a triangle: 0;52 30 is its coefficient. >>தள்ளிசங்கசந்திக்கும்கை 52 30 அக்கிக்குப்பகுணாயுச>> the shifted arm, meeting, multiply by 26 15
5. **2 37 30 IGI.GUB s`a` SAG.6**>> 2;37 30, the coefficient of a hexagon >>2 37 30 அக்கிக்குப்பகுணாசமாசங்க 6 .. ஆறுசங்கமுனைகள்கொண்டதற்குபெருக்க 2 37 30 >> Multiply by 2 37 30 for hexagon
6. **3 41 IGI.GUB s`a` SAG.7** >> 3;41, the coefficient of a heptagon >>அக்கிக்குப்பகுணாசமாசங்க 7 ..ஏழுசங்கமுனைகள்கொண்டதற்குபெருக்க 3;41 >> multiply by 3;41 for heptagon





Purushothaman et al.,

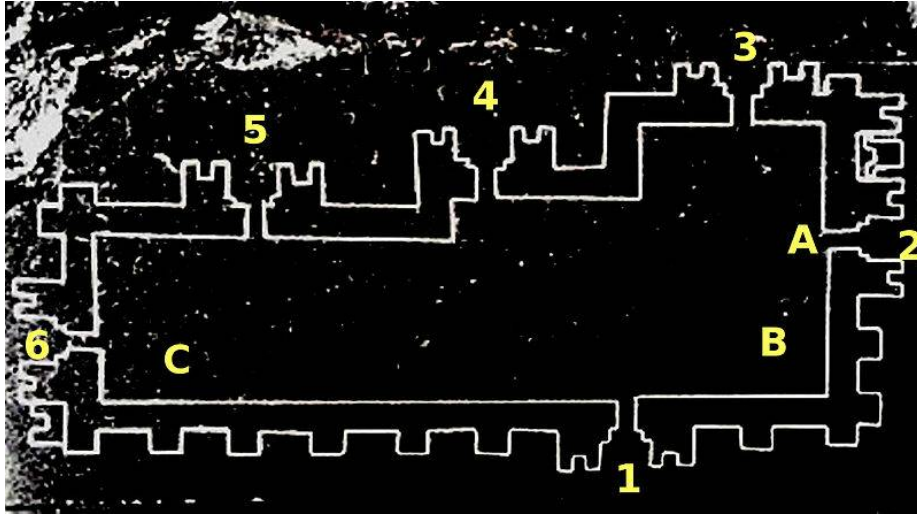
Appendix-4 Interpreting the architect plan of Gudea (Wikimedia commons: Eninnu)

Wikimedia commons: <https://it.m.wikibooks.org/wiki/File:Eninnu.jpg>

Translation from Italian

The legend was inserted by me deriving it from the reconstruction proposal elaborated by WolfgangHeimpel, in Journal of Cuneiform Studies 48 (1996), p. 21.

1. Gate in front of the city (igi-uruki-še) : ஊருக்குசேரும்கண்அக்கி- city view
 2. Carrying arms (a-gatukulá) : ஆநீர்தூக்குபள்ளம்- water source
 3. Shining door (šu-ga-lam): சுகம்களம்தோட்டம்- garden
 4. Door of wonders (ká-sur-ra): கவிதைசுரம்- music tuning
 5. Bring advice (tar-sír-sír): தார்சீர்மேளம்- drums
 6. Gate of Baba (a-ga dba-ba6): அகம்உள்பிரகாரம்அப்பாபாபா- prime deity
- A. Cedar portico (a-gaeren-na): அகம்ஏரிஏர்என்ன? – lake view
- B. House of the Eagle (é-anzu-muišen): இல்லம்வான்தழுகழுமுகுமுகுசின்- sky view
- C. House of councils (é-tar-sír-sír): இல்லம்தார்சீர்பாடல்- chorus team





Substantial and Fragile Domination in Bipolar Fuzzy Incidence Graphs

M. Rajeshwari^{1*}, R. Murugesan² and K. A. Venkatesh³

¹Assistant Professor in Mathematics, School of Engineering, Presidency University, Bangalore.

²Professor, Department of Mathematics, Reva University, Bangalore.

³Professor of Mathematics and Comp. Science, Myanmar Institute of Information Technology, Myanmar.

Received: 01 Mar 2021

Revised: 05 Mar 2021

Accepted: 10 Mar 2021

*Address for Correspondence

M. Rajeshwari

Assistant Professor in Mathematics,
School of Engineering, Presidency University,
Bangalore.
Email: rajeakila@gmail.com



This is an Open Access Journal / article distributed under the terms of the **Creative Commons Attribution License** (CC BY-NC-ND 3.0) which permits unrestricted use, distribution, and reproduction in any medium, provided the original work is properly cited. All rights reserved.

ABSTRACT

In this paper, we defined bipolar fuzzy incidence graph (BFIG), Complete bipolar fuzzy incidence graph (CBFIG), size, order, domination of bipolar fuzzy incidence graph, bipolar effective incidence pair (BEIP) and Bipolar fuzzy incidence dominating number (BFIDN). We also explore the relation between smallest incidence degree, topmost incidence degree size and order of BFIG and also the relation between the Substantial and fragile domination in bipolar fuzzy incidence graphs.

Keywords: Bipolar fuzzy graph, Fuzzy incidence graph, Fuzzy graph, domination number.

INTRODUCTION

A simple method to communicate data, including hookup between different companies is easily done by a graph. The companies are shown as vertices and connections among these vertices are characterized as an edges. The idea of fuzzy set was given by Zadeh's [8]. The introduction of fuzzy graph was given by Rosenfeld [5]. Prior to fluffy sets, the confusions in systems were for the most part worried about separation instead of the decrease in flow. In fast systems, for example, the web, the issue of decrease of quality is significant than the detachment. Fuzzy graph hypothesis played an important part in these regions and has a lot of employments in various fields. Bang and Yeh worked independently on FGs [19]. For a thorough report on FGs, we may allude to the peruser [2, 4]. Order and size in FGs were presented by Gani [3]. Akram presented bipolar FGs [1]. Somasundaram and Somasundaram have started Domination in FGs by utilizing effective edges (EEs) [6]. Domination of bipolar fuzzy graph was started by Karunambigai, Akram, Kasilingam and shanmugam [9]. Total strong (weak) domination in bipolar fuzzy graph was presented by Muthuraj and Kanimozhi [10].





CONNECTION AMONG ORDER AND SIZE OF BIPOLAR FUZZY INCIDENCE GRAPHS

Definition 2.1.

Consider the BFIG $G = (\varepsilon, \tau, \zeta)$ where ε and τ are BFS of vertex and edges respectively and ζ is the BFI of G with both positive and negative membership values.

$$\mu_{\zeta}^P(q, e) \leq \min(\mu_{\varepsilon}^P(q), \mu_{\tau}^P(e)) \text{ and } \mu_{\zeta}^N(q, e) \geq \max(\mu_{\varepsilon}^N(q), \mu_{\tau}^N(e)) \text{ for every } q \in V \text{ and } e \in E.$$

Note 2.2.

If $(\max(\mu_{\varepsilon}^P(q)), \min(\mu_{\varepsilon}^N(q))) > 0$, where $q \in V$ is said to be in the support of μ_{ε}^P and μ_{ε}^N , $(\max(\mu_{\tau}^P(qr)), \min(\mu_{\tau}^N(qr))) > 0$, where $qr \in E$ is said to be in the support of μ_{τ}^P and μ_{τ}^N and $(\max(\mu_{\zeta}^P(s, qr)), \min(\mu_{\zeta}^N(s, qr))) > 0$, where $(s, qr) \in V \times E$ is said to be in the support of μ_{ζ}^P and μ_{ζ}^N .

The supports of μ_{ε} , μ_{τ} and μ_{ζ} denoted as μ_{ε}^* , μ_{τ}^* and μ_{ζ}^* for positive and negative membership.

Definition 2.3.

A BFIG is said to be CBFIG if $\mu_{\zeta}^P(i, ij) = \min(\mu_{\varepsilon}^P(i), \mu_{\tau}^P(ij))$ and $\mu_{\zeta}^N(i, ij) = \max(\mu_{\varepsilon}^N(i), \mu_{\tau}^N(ij))$ for each $(\mu_{\zeta}^P(i, ij), \mu_{\zeta}^N(i, ij)) \in \mu_{\zeta}^*$. Also $\mu_{\zeta}^P(i, ij) = \mu_{\zeta}^P(j, ji)$ and $\mu_{\zeta}^N(i, ij) = \mu_{\zeta}^N(j, ji)$ for each $j, i \in \mu_{\zeta}^*$.

Definition 2.4.

Let G be a BFIG the incidence degree (d_i) of a node $q \in \mu_{\zeta}^*$ is defined as $d_i^P(q) = \sum_{q \neq r} \mu_{\zeta}^P(q, qr)$ and

$d_i^N(q) = \sum_{q \neq r} \mu_{\zeta}^N(q, qr)$. The smallest d_i of G is defined by $\Omega(G) = \{(\min d_i^P(q), \max d_i^N(q)) | q \in V\}$. The

topmost d_i of G is defined by $\Delta(G) = \{(\max d_i^P(q), \min d_i^N(q)) | q \in V\}$.

Definition 2.5.

Let $G = (\varepsilon, \tau, \zeta)$ be the BFIG. Then the order and size are defined as respectively

$$O(G) = \sum_{q \neq r, q, r \in V} (\mu_{\zeta}^P(q, qr), \mu_{\zeta}^N(q, qr)) \text{ and } S(G) = \sum_{e \in \tau} (\mu_{\tau}^P(e), \mu_{\tau}^N(e)).$$

Example 2.6.

Let $G = (\varepsilon, \tau, \zeta)$ be the BFIG having

$$\varepsilon = (u, v, w), \varepsilon(u) = (0.5, -0.4), \varepsilon(v) = (0.6, -0.5), \varepsilon(w) = (0.9, -0.6),$$

$$\tau(uv) = (0.5, -0.4), \tau(vw) = (0.5, -0.3), \tau(wu) = (0.4, -0.2), \zeta(u, uv) = (0.4, -0.3),$$

$$\zeta(u, uw) = (0.3, -0.2), \zeta(v, vu) = (0.3, -0.4), \zeta(v, vw) = (0.5, -0.1), \zeta(w, wu) = (0.4, -0.2),$$

$$\zeta(w, wv) = (0.4, -0.3). \text{ Then } O(G) = (2.3, -1.5) \text{ and } S(G) = (1.4, -0.9).$$

Proposition 2.7.

In a BFIG $S(G) \leq O(G)$ for the positive membership values.





Rajeshwari et al.,

Proof:

Let $G = (\varepsilon, \tau, \zeta)$ be a BFIG with one vertex. Then $S(G) = O(G) = 0$. i.e

(1) $S(G) = O(G)$.

It is a trifling case. Accept G two or more vertices. $O(G)$ is the whole of all incidence pairs of G. Since incidence pairs are multiple times of edges. Consequently, the all-out whole of all the positive enrollment estimations of the edges is below the all-out aggregate of all the positive enrollment estimations of the incidence pairs.

(2) $S(G) < O(G)$

From equations (1) and (2), we get $S(G) \leq O(G)$, only for positive membership value.

Proposition 2.8.

In a BFIG $S(G) \geq O(G)$ for the negative membership values.

Proof:

Let $G = (\varepsilon, \tau, \zeta)$ be a BFIG with one vertex. Then $S(G) = O(G) = 0$. i.e

(1) $S(G) = O(G)$.

It is a trifling case. Accept G two or more vertices. $O(G)$ is the whole of all incidence pairs of G. Since incidence pairs are multiple times of edges. Consequently, the all-out whole of all the negative enrollment estimations of the edges is greater the all-out aggregate of all the negative enrollment estimations of the incidence pairs.

(2) $S(G) > O(G)$

From equations (1) and (2), we get $S(G) \geq O(G)$, only for the negative membership values.

Proposition 2.9.

For any BFIG the inequality holds: $\Omega(G) \leq \Delta(G) \leq S(G) \leq O(G)$, for the positive membership values.

Proof. Assume $G = (\varepsilon, \tau, \zeta)$ is a BFIG with non-empty vertex set. Since $\Omega(G)$ represents

Smallest of d_i and $\Delta(G)$ denotes topmost d_i of G.

(1) $\Omega(G) \leq \Delta(G)$.

We know $O(G) = \sum_{q \neq r, q, r \in V} (\mu_\zeta^P(q, qr), \mu_\zeta^N(q, qr))$ and $S(G) = \sum_{e \in \tau} (\mu_\tau^P(e), \mu_\tau^N(e))$

By definition of size of G, $S(G) = \sum_{e \in \tau} (\mu_\tau^P(e), \mu_\tau^N(e)) \geq \{(\max d_i^P(q), \min d_i^N(q)) | q \in V\}$

i.e.

(2) $\Delta(G) \leq S(G)$

Also, in a BFIG, G by proposition 2.1

(3) $S(G) \leq O(G)$

From inequalities (1), (2) and (3), we obtained $\Omega(G) \leq \Delta(G) \leq S(G) \leq O(G)$.

Proposition 2.10.

For any BFIG the inequality holds: $O(G) \leq S(G) \leq \Omega(G) \leq \Delta(G)$, for the negative membership values.

Proof. Assume $G = (\varepsilon, \tau, \zeta)$ is a BFIG with non-empty vertex set. Since $\Omega(G)$ represents

Smallest of d_i and $\Delta(G)$ denotes topmost d_i of G.





(1) $\Omega(G) \leq \Delta(G).$

We know $O(G) = \sum_{q \neq r, q, r \in V} (\mu_{\zeta}^P(q, qr), \mu_{\zeta}^N(q, qr))$ and $S(G) = \sum_{e \in \tau} (\mu_{\tau}^P(e), \mu_{\tau}^N(e))$

By definition of size of G, $S(G) = \sum_{e \in \tau} (\mu_{\tau}^P(e), \mu_{\tau}^N(e)) \leq \{(\min d_i^P(q), \max d_i^N(q)) | q \in V\}.$

i.e.

(2) $S(G) \leq \Omega(G)$

Also, in a BFIG, G by proposition 2.2

(3) $O(G) \leq S(G)$

From inequalities (1), (2) and (3), we obtained $O(G) \leq S(G) \leq \Omega(G) \leq \Delta(G)$ for negative membership value.

Proposition 2.11.

The d_i sum of all vertices in a BFIG is equal to the twice the average sum of all the incidence pairs. i.e.

$$\sum_{j \in \mu_{\tau}^*} d_i(j) = 2 \sum_{j, k \in V} \left(\left(\frac{\mu_{\tau}^P(j, jk) + \mu_{\tau}^P(k, kj)}{2} \right), \left(\frac{\mu_{\tau}^N(j, jk) + \mu_{\tau}^N(k, kj)}{2} \right) \right)$$

Proof. Let $G = (\varepsilon, \tau, \zeta)$ is a BFIG, where V is the subset of ε , E is the subset of τ and $\zeta \subseteq V \times E$

Since $d_i(q) = (d_i^P(q), d_i^N(q))$, where $d_i^P(q) = \sum_{q \neq r} \mu_{\zeta}^P(q, qr)$ and $d_i^N(q) = \sum_{q \neq r} \mu_{\zeta}^N(q, qr)$.

$$d_i(q_1) = (\mu_{\zeta}^P(q_1, q_1q_2), \mu_{\zeta}^N(q_1, q_1q_2)) + (\mu_{\zeta}^P(q_1, q_1q_3), \mu_{\zeta}^N(q_1, q_1q_3)) + \dots + (\mu_{\zeta}^P(q_1, q_1q_n), \mu_{\zeta}^N(q_1, q_1q_n))$$

$$d_i(q_2) = (\mu_{\zeta}^P(q_2, q_2q_1), \mu_{\zeta}^N(q_2, q_2q_1)) + (\mu_{\zeta}^P(q_2, q_2q_3), \mu_{\zeta}^N(q_2, q_2q_3)) + \dots + (\mu_{\zeta}^P(q_2, q_2q_n), \mu_{\zeta}^N(q_2, q_2q_n))$$

⋮
⋮
⋮

$$d_i(q_n) = (\mu_{\zeta}^P(q_n, q_nq_1), \mu_{\zeta}^N(q_n, q_nq_1)) + (\mu_{\zeta}^P(q_n, q_nq_3), \mu_{\zeta}^N(q_n, q_nq_3)) + \dots + (\mu_{\zeta}^P(q_n, q_nq_{n-1}), \mu_{\zeta}^N(q_n, q_nq_{n-1}))$$

This implies,

$$\sum_{q \in V} d_i(q) = (\mu_{\zeta}^P(q_1, q_1q_2), \mu_{\zeta}^N(q_1, q_1q_2)) + (\mu_{\zeta}^P(q_1, q_1q_3), \mu_{\zeta}^N(q_1, q_1q_3)) + \dots + (\mu_{\zeta}^P(q_1, q_1q_n), \mu_{\zeta}^N(q_1, q_1q_n)) +$$

$$(\mu_{\zeta}^P(q_2, q_2q_1), \mu_{\zeta}^N(q_2, q_2q_1)) + (\mu_{\zeta}^P(q_2, q_2q_3), \mu_{\zeta}^N(q_2, q_2q_3)) + \dots + (\mu_{\zeta}^P(q_2, q_2q_n), \mu_{\zeta}^N(q_2, q_2q_n)) +$$

$$\dots + (\mu_{\zeta}^P(q_n, q_nq_1), \mu_{\zeta}^N(q_n, q_nq_1)) + (\mu_{\zeta}^P(q_n, q_nq_3), \mu_{\zeta}^N(q_n, q_nq_3)) + \dots +$$

$$(\mu_{\zeta}^P(q_n, q_nq_{n-1}), \mu_{\zeta}^N(q_n, q_nq_{n-1}))$$

$$\sum_{q \in V} d_i(q) = \frac{2}{2} \left[\begin{aligned} & (\mu_{\zeta}^P(q_1, q_1q_2), \mu_{\zeta}^N(q_1, q_1q_2)) + (\mu_{\zeta}^P(q_1, q_1q_3), \mu_{\zeta}^N(q_1, q_1q_3)) + \dots + (\mu_{\zeta}^P(q_1, q_1q_n), \mu_{\zeta}^N(q_1, q_1q_n)) + \\ & (\mu_{\zeta}^P(q_2, q_2q_1), \mu_{\zeta}^N(q_2, q_2q_1)) + (\mu_{\zeta}^P(q_2, q_2q_3), \mu_{\zeta}^N(q_2, q_2q_3)) + \dots + (\mu_{\zeta}^P(q_2, q_2q_n), \mu_{\zeta}^N(q_2, q_2q_n)) + \\ & \dots + (\mu_{\zeta}^P(q_n, q_nq_1), \mu_{\zeta}^N(q_n, q_nq_1)) + (\mu_{\zeta}^P(q_n, q_nq_3), \mu_{\zeta}^N(q_n, q_nq_3)) + \dots + \\ & (\mu_{\zeta}^P(q_n, q_nq_{n-1}), \mu_{\zeta}^N(q_n, q_nq_{n-1})) \end{aligned} \right]$$

by rearranging terms





$$\sum_{q \in V} d_i(q) = 2 \left\{ \begin{aligned} &\left(\frac{\mu_\zeta^P(q_1, q_1 q_2) + \mu_\zeta^P(q_2, q_2 q_1)}{2}, \frac{\mu_\zeta^N(q_1, q_1 q_2) + \mu_\zeta^N(q_2, q_2 q_1)}{2} \right) + \\ &\left(\frac{\mu_\zeta^P(q_1, q_1 q_3) + \mu_\zeta^P(q_3, q_3 q_1)}{2}, \frac{\mu_\zeta^N(q_1, q_1 q_3) + \mu_\zeta^N(q_3, q_3 q_1)}{2} \right) + \dots + \\ &\left(\frac{\mu_\zeta^P(q_1, q_1 q_n) + \mu_\zeta^P(q_n, q_n q_1)}{2}, \frac{\mu_\zeta^N(q_1, q_1 q_n) + \mu_\zeta^N(q_n, q_n q_1)}{2} \right) + \dots + \\ &\left(\frac{\mu_\zeta^P(q_2, q_2 q_3) + \mu_\zeta^P(q_3, q_3 q_2)}{2}, \frac{\mu_\zeta^N(q_2, q_2 q_3) + \mu_\zeta^N(q_3, q_3 q_2)}{2} \right) + \\ &\left(\frac{\mu_\zeta^P(q_2, q_2 q_4) + \mu_\zeta^P(q_4, q_4 q_2)}{2}, \frac{\mu_\zeta^N(q_2, q_2 q_4) + \mu_\zeta^N(q_4, q_4 q_2)}{2} \right) + \dots + \\ &\left(\frac{\mu_\zeta^P(q_2, q_2 q_n) + \mu_\zeta^P(q_n, q_n q_2)}{2}, \frac{\mu_\zeta^N(q_2, q_2 q_n) + \mu_\zeta^N(q_n, q_n q_2)}{2} \right) + \dots + \\ &\left(\frac{\mu_\zeta^P(q_n, q_n q_{n-1}) + \mu_\zeta^P(q_{n-1}, q_{n-1} q_n)}{2}, \frac{\mu_\zeta^N(q_n, q_n q_{n-1}) + \mu_\zeta^N(q_{n-1}, q_{n-1} q_n)}{2} \right) \end{aligned} \right\}$$

$$\sum_{q \in V} d_i(q) = 2 \sum_{q, r \in V} \left\{ \frac{\mu_\zeta^P(q, qr) + \mu_\zeta^P(r, rq)}{2}, \frac{\mu_\zeta^N(q, qr) + \mu_\zeta^N(r, rq)}{2} \right\}$$

Example 2.12.

Let $G = (\varepsilon, \tau, \zeta)$ be the BFIG having $\varepsilon = (u, v, w)$. $\sum_{q \in V} d_i(q) = (2.3, -1.5)$ and

$$\sum_{q, r \in V} \left\{ \frac{\mu_\zeta^P(q, qr) + \mu_\zeta^P(r, rq)}{2}, \frac{\mu_\zeta^N(q, qr) + \mu_\zeta^N(r, rq)}{2} \right\} = (1.15, -0.75). \quad \text{This implies}$$

$$\sum_{q \in V} d_i(q) = 2 \sum_{q, r \in V} \left\{ \frac{\mu_\zeta^P(q, qr) + \mu_\zeta^P(r, rq)}{2}, \frac{\mu_\zeta^N(q, qr) + \mu_\zeta^N(r, rq)}{2} \right\}.$$

DOMINATION IN BIPOLAR FUZZY INCIDENCE GRAPHS

Definition 3.1.

Let $G = (\varepsilon, \tau, \zeta)$ be the BFIG is also called as bipolar effective incidence pair (BEIP) if

$$\mu_\zeta^P(s, sr) = (\mu_\zeta^P(s, sr), \mu_\zeta^N(s, sr)), \quad \text{Where} \quad \mu_\zeta^P(s, sr) = \mu_\varepsilon^P(s) \wedge \mu_\tau^P(sr) \text{ and}$$

$$\mu_\zeta^N(s, sr) = \mu_\varepsilon^N(s) \vee \mu_\tau^N(sr).$$





Rajeshwari et al.,

Definition 3.2.

The node r of effective d_i is defined as $d_{BEIP}(r) = (\sum \mu_\zeta^P(r, rq), \sum \mu_\zeta^N(r, rq))$. The smallest effective d_i of G is defined by $\Omega_{d_{BEIP}}(G) = \{(\min d_{BEIP}^P(r), \max d_{BEIP}^N(r)) | r \in V\}$. The topmost effective d_i of G is defined by $\Delta_{d_{BEIP}}(G) = \{(\max d_{BEIP}^P(r), \min d_{BEIP}^N(r)) | r \in V\}$.

Definition 3.3.

A vertex s in a BFIG dominates to vertex r if $\mu_\zeta^P(s, sr) = \mu_\varepsilon^P(s) \wedge \mu_\tau^P(sr)$ and $\mu_\zeta^N(s, sr) = \mu_\varepsilon^N(s) \vee \mu_\tau^N(sr)$ and if a vertex r dominates to s if $\mu_\zeta^P(r, rs) = \mu_\varepsilon^P(r) \wedge \mu_\tau^P(rs)$ and $\mu_\zeta^N(r, rs) = \mu_\varepsilon^N(r) \vee \mu_\tau^N(rs)$. The set of these types of vertices is called a bipolar fuzzy incidence dominating set (BFIDS) of BFIG.

Definition 3.4.

The Bipolar fuzzy incidence dominating number (BFIDN) is the minimum bipolar fuzzy incidence cardinality (BFIC) of BFIDS among all BFIDSs in G . It is represented by η_{BFI} .

Example 3.5.

Let $G = (\varepsilon, \tau, \zeta)$ be the BFIG having BFIDS are $D_1 = \{q, s\}, D_2 = \{q, u\}$ and $D_3 = \{s\}$ with $\eta_{BFI} = (\mu_\varepsilon^P(s), \mu_\varepsilon^N(s)) = (0.5, -0.1)$

Definition 3.6.

The node s of BFIG is named as an isolated node if $\mu_\zeta(s, sr) = (\mu_\zeta^P(s, sr), \mu_\zeta^N(s, sr))$. Where $\mu_\zeta^P(s, sr) < \mu_\varepsilon^P(s) \wedge \mu_\tau^P(sr)$ and $\mu_\zeta^N(s, sr) > \mu_\varepsilon^N(s) \vee \mu_\tau^N(sr)$ for all $r \in V - \{s\}$. Consequently, the isolated node does not dominate any node in BFIG on the other hand an isolated node dominates to itself.

Definition 3.7.

Let $G = (\varepsilon, \tau, \zeta)$ be the BFIG the complement of G is indicated by $\overline{G} = (\mu_\zeta^P(s, sq), \mu_\zeta^N(s, sq))$ where $\mu_\zeta^P(s, sq) = \min(\max(\mu_\varepsilon^P(s), \mu_\tau^P(sq) - \mu_\zeta^P(s, sq)), \mu_\varepsilon^P(s) \wedge \mu_\tau^P(r) - \mu_\zeta^P(s, sq))$ and $\mu_\zeta^N(s, sq) = \max(\min(\mu_\varepsilon^N(s), \mu_\tau^N(sq) - \mu_\zeta^N(s, sq)), \mu_\varepsilon^N(s) \wedge \mu_\tau^N(r) - \mu_\zeta^N(s, sq))$. The vertex value will be same as G in \overline{G} .

Example 3.8.

Let $G = (\varepsilon, \tau, \zeta)$ be the BFIG the complement of G is indicated as \overline{G} .

SUBSTANTIAL AND FRAGILE DOMINATION IN BIPOLAR FUZZY INCIDENCE GRAPHS

Definition 4.1.

Let $G = (\varepsilon, \tau, \zeta)$ be the BFIG and $\varepsilon = (q, r, s)$ in G . If s is Substantial dominates r or r fragile dominates s then the following condition satisfies, $(\mu_\zeta^P(s, sr), \mu_\zeta^N(s, sr)) \geq (\mu_\zeta^P(r, rs), \mu_\zeta^N(r, rs))$ and if a vertex r Substantial dominates s or s fragile dominates r then $(\mu_\zeta^P(s, sr), \mu_\zeta^N(s, sr)) \leq (\mu_\zeta^P(r, rs), \mu_\zeta^N(r, rs))$ where





Rajeshwari et al.,

$$\mu_{\zeta}^P(s, sr) = \mu_{\varepsilon}^P(s) \wedge \mu_{\tau}^P(sr) \quad , \mu_{\zeta}^N(s, sr) = \mu_{\varepsilon}^N(s) \vee \mu_{\tau}^N(sr) \quad , \mu_{\zeta}^P(r, rs) = \mu_{\varepsilon}^P(r) \wedge \mu_{\tau}^P(rs) \quad \text{and} \\ \mu_{\zeta}^N(r, rs) = \mu_{\varepsilon}^N(r) \vee \mu_{\tau}^N(rs).$$

Definition 4.2.

Let R alone be the subset of V is a substantial BFIDS if every vertex in V - R is substantial fuzzy incidence dominated by partly one vertex in R. In comparable manner, R is known as a fragile BFIDS if every vertex in V - R is fragile fuzzy incidence dominated by partly one vertex in R.

Definition 4.3.

The most minimal BFIC of a substantial BFIDS is expressed as the substantial BFIDN and it is characterized as SBFI(G) or SBFI and the most minimal BFIC of a fragile BFIDS is named as the fragile BFIDN and it is characterized as FBFI(G) or FBFI .

Theorem 4.4.

For any CBFIG $\mu_{\zeta}^P(s, sr) = \mu_{\varepsilon}^P(s) \wedge \mu_{\tau}^P(sr)$ with for all $s \in V, sr \in E$ the inequality given below is always holds $\mu_{FBFI}^P \leq \mu_{SBFI}^P$.

Proof. Assume $\mu_{\varepsilon}^P(s)$ for all $s \in V$ is same then $\mu_{\tau}^P(sr) = \mu_{\tau}^P(s) \wedge \mu_{\tau}^P(r)$ for all $s, r \in V$ and $sr \in E$. Since $G = (\varepsilon, \tau, \zeta)$ be the CBFIG with $\mu_{\zeta}^P(s, sr) = \mu_{\varepsilon}^P(s) \wedge \mu_{\tau}^P(sr)$ for all $s \in V$ and $sr \in E$. Thus every $s \in V$ is substantial as well as fragile BFIDS is

$$(1) \mu_{FBFI}^P = \mu_{SBFI}^P$$

Assume $\mu_{\varepsilon}^P(s)$ for all $s \in V$ is not same. Then CBFIG any one of the vertex substantial on other vertex $(\mu_{\zeta}^P(s, sr), \mu_{\zeta}^N(s, sr)) \geq (\mu_{\zeta}^P(r, rs), \mu_{\zeta}^N(r, rs))$ in the event that it is smallest among all the vertex then the BFIDS with that vertex is called fragile BFIDN that is $\mu_{FBFI}^P = \mu_{\zeta}^P(s)$ with $(\mu_{\zeta}^P(s, sr), \mu_{\zeta}^N(s, sr)) \leq (\mu_{\zeta}^P(r, rs), \mu_{\zeta}^N(r, rs))$. Certainly, the substantial BFIDS has a vertex set other than the that vertex set. This means

$$(2) \mu_{FBFI}^P < \mu_{SBFI}^P$$

From equations (1) and (2), we get $\mu_{FBFI}^P \leq \mu_{SBFI}^P$.

Theorem 4.5.

For any CBFIG $\mu_{\zeta}^N(s, sr) = \mu_{\varepsilon}^N(s) \wedge \mu_{\tau}^N(sr)$ with for all $s \in V, sr \in E$ the inequality given below is always holds $\mu_{FBFI}^N \geq \mu_{SBFI}^N$.

Proof. Assume $\mu_{\varepsilon}^N(s)$ for all $s \in V$ is same then $\mu_{\tau}^N(sr) = \mu_{\tau}^N(s) \wedge \mu_{\tau}^N(r)$ for all $s, r \in V$ and $sr \in E$. Since $G = (\varepsilon, \tau, \zeta)$ be the CBFIG with $\mu_{\zeta}^N(s, sr) = \mu_{\varepsilon}^N(s) \wedge \mu_{\tau}^N(sr)$ for all $s \in V$ and $sr \in E$. Thus every $s \in V$ is fragile as well as substantial BFIDS is

$$(1) \mu_{FBFI}^N = \mu_{SBFI}^N$$

Assume $\mu_{\varepsilon}^N(s)$ for all $s \in V$ is not same. Then CBFIG $(\mu_{\zeta}^P(s, sr), \mu_{\zeta}^N(s, sr)) \leq (\mu_{\zeta}^P(r, rs), \mu_{\zeta}^N(r, rs))$ from all the vertex one of the vertex fragile on other vertex in the event that it is largest among all the vertex then the BFIDS with that vertex is called substantial BFIDN that is $\mu_{SBFI}^N = \mu_{\zeta}^N(s)$ with





Rajeshwari et al.,

$(\mu_{\zeta}^P(s, sr), \mu_{\zeta}^N(s, sr)) \geq (\mu_{\zeta}^P(r, rs), \mu_{\zeta}^N(r, rs))$. Certainly, the fragile BFIDS has a vertex set other than the that vertex set. This means

$$(2) \quad \mu_{FBFI}^N > \mu_{SBFI}^N$$

From equations (1) and (2), we get $\mu_{FBFI}^N \geq \mu_{SBFI}^N$

Theorem 4.6.

For a CFG the inequalities given below is true $\mu_{BFI} \leq \mu_{FBFI} \leq \mu_{SBFI} \leq O(G) - \Delta_{d_{BFI}}(G) \leq O(G) - \Omega_{d_{BFI}}(G)$

Proof. From definition 4.1,4.2 and 4.3 we have the weight of BFIG is less than or equal to fragile BFIG because the vertices of fragile FIDS F, it weakly dominates any one of the Vertices and fragile BFI is less than or equal to substantial BFI

$$(1) \quad \mu_{BFI} \leq \mu_{FBFI} \leq \mu_{SBFI}$$

We know that O(G) is the sum of BFIG and also,

$$(2) \quad O(G) - \Delta_{d_{BFI}}(G) \leq O(G) - \Omega_{d_{BFI}}(G), \text{Where}$$

$$\Delta_{d_{BFI}}(G) = \{(\max d_{BFI}^P(r), \min d_{BFI}^N(r)) | r \in V\} \text{ and}$$

$$\Omega_{d_{BFI}}(G) = \{(\min d_{BFI}^P(r), \max d_{BFI}^N(r)) | r \in V\}.$$

From (1) and (2) we have

$$\mu_{BFI} \leq \mu_{FBFI} \leq \mu_{SBFI} \leq O(G) - \Delta_{d_{BFI}}(G) \leq O(G) - \Omega_{d_{BFI}}(G)$$

Example 4.7.

Let $G = (\varepsilon, \tau, \zeta)$ be the BFIG having $\varepsilon = (u, v, w)$.

$$d(s)=(1,-1.4), \quad d(q)=(1,-1.5), \quad d(r)=(0.6,-1.5), \quad O(G)=(2.6,-2), \quad \mu_{FBFI} = (0.3,-0.9), \quad \mu_{SBFI} = (0.8,-0.7),$$

$$\mu_{BFI} = (0.3,-0.9), \quad \Delta_{d_{BFI}}(G) = (1,-1.4) \text{ and } \Omega_{d_{BFI}}(G) = (0.6,-1.5)$$

We know that $\mu_{BFI} \leq \mu_{FBFI} \leq \mu_{SBFI} \leq O(G) - \Delta_{d_{BFI}}(G) \leq O(G) - \Omega_{d_{BFI}}(G)$.

$$\therefore (0.3,-0.9) \leq (0.3,-0.9) \leq (0.8,-0.7) \leq (1.6,-0.6) \leq (2,-0.5).$$

APPLICATION OF BFID IN TEXTILE

Assume there are five textile company are working in a city for directing new brands. In BFIGs, the vertices show the company and edges show the agreement conditions among the company to share the brand material. The incidence pair show the moving of consumer in that city from one company to other in search of brands. BFIDS (Fig. 05) of the diagram is the set of company's which marketing the new brands. From this way we can save the time of the consumer by giving the better company brands.

Let $G = (\varepsilon, \tau, \zeta)$ be the BFIG having

$$\varepsilon = \{a, b, c, d, e\}, \varepsilon(a) = (0.2,-0.9), \varepsilon(b) = (0.3,-0.8), \varepsilon(c) = (0.4,-0.7), \varepsilon(d) = (0.5,-0.6),$$

$$\varepsilon(e) = (0.6,-0.7), \tau(ab) = (0.2,-0.8), \tau(ac) = (0.2,-0.7), \tau(bc) = (0.3,-0.7), \tau(ce) = (0.4,-0.7),$$

$$\tau(cd) = (0.4,-0.6), \tau(de) = (0.5,-0.6), \zeta(a, ab) = (0.2,-0.3), \zeta(b, ba) = (0.1,-0.3), \zeta(b, bc) = (0.3,-0.1),$$

$$\zeta(c, cb) = (0.2,-0.1), \zeta(c, cd) = (0.4,-0.5), \zeta(d, dc) = (0.3,-0.1), \zeta(d, de) = (0.5,-0.5),$$

$$\zeta(e, ed) = (0.4,-0.1), \zeta(a, ac) = (0.1,-0.1), \zeta(c, ca) = (0.1,-0.1), \zeta(c, ce) = (0.4,-0.1), \zeta(e, ec) = (0.4,-0.5).$$





Rajeshwari et al.,

BFIDS = {a, b, c, e} and $\mu_{BFI} = (0.2, -0.9)$. The consumer can visit any of the company in the set to have their benefits.

CONCLUSION

In this paper, the possibility of bipolar fuzzy incidence, Substantial and fragile domination in bipolar fuzzy incidence graphs are examined. The outcomes review in this paper may be utilized to contemplate disparate BFIGs invariants.

ACKNOWLEDGEMENTS

The authors are thankful to the referees for their valuable comments and suggestions.

REFERENCES

1. M. Akram, Bipolar fuzzy graphs, Informaion Sciences 181(2011) 5548 - 5564.
2. P. Bhattacharya, Some remarks on fuzzy graphs, Pattern Recognit. Lett. 6(1987) 297 - 302.
3. M. Ahamed and A. Gani, Order and size in fuzzy graph, Bulletin of Pure and Applied Sciences.22E (1)(2003) 145 - 148.
4. S. Mathew, J. N. Mordeson and D. Malik, Fuzzy Graph Theory, Springer, 2018.
5. A. Rosenfeld, Fuzzy graphs, in: L. A. Zadeh, K. S. Fu, M. Shimura (Eds.), Fuzzy sets and their applications, Academic Press, New York, (1975) 77 - 95.
6. A. Somasundaram and S. Somasundaram, Domination in fuzzy graphs, Pattern Recognit. Lett. 19(1998) 787 - 791.
7. R. T. Yeh and S. Y. Bang, Fuzzy relations, fuzzy graphs and their applications to clustering analysis, in: L. A. Zadeh, K. S. Fu, M. Shimura(Eds.), Fuzzy sets and their Applications, Academic Press, (1975) 125 - 149.
8. L. A. Zadeh, Fuzzy sets, Inf. Control 8(1965) 338 - 353.
9. Karunambigai M. G., Akram. M., Palanivel. K., & Sivasankar. S Domination in bipolar fuzzy graphs. 2013 IEEE International Conference on Fuzzy Systems (FUZZ-IEEE), (2013). doi:10.1109/fuzz-ieee.2013.6622326
10. R. Muthuraj and Kanimozhi, Total strong (weak) domination in bipolar fuzzy graph, International Journal of Computational and Applied Mathematics ,Volume 12, Number 1 (2017) .

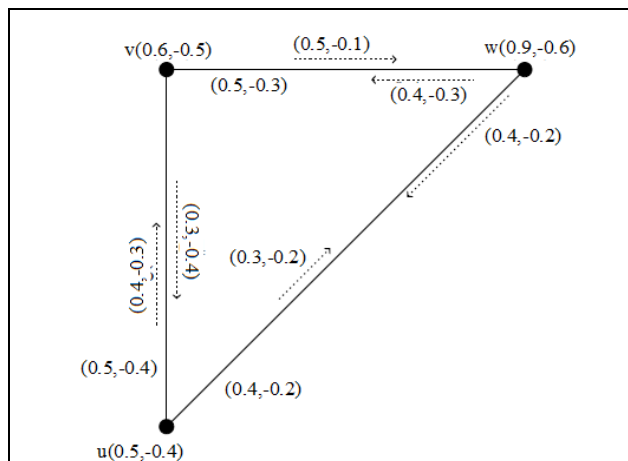


Figure 1. Bipolar fuzzy incidence graph

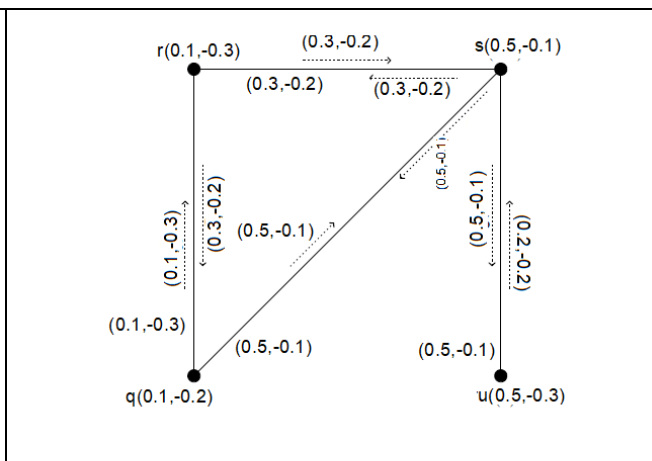


Figure 2. Bipolar fuzzy incidence graphs

$\eta_{BFI} = (0.5, -0.1)$





Rajeshwari et al.,

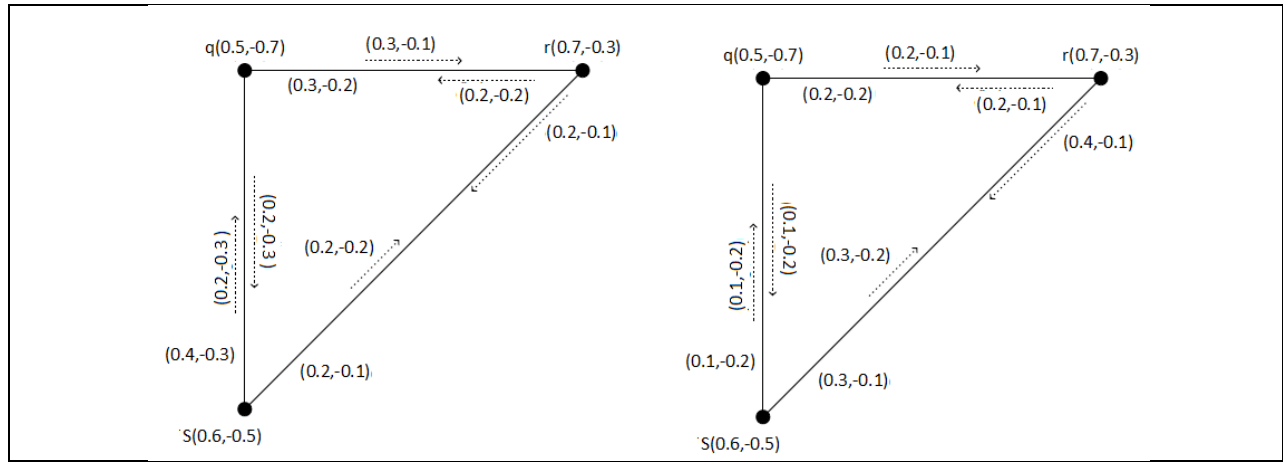


Figure 3. Bipolar fuzzy graph G is complement of bipolar fuzzy graph \bar{G}

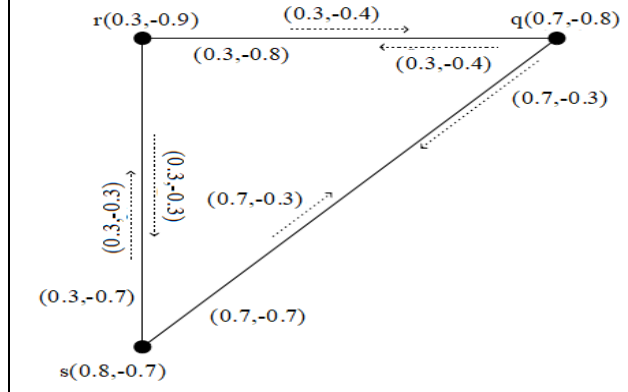


Figure 4. G having $\mu_{FBFI} \leq \mu_{SBFI}$

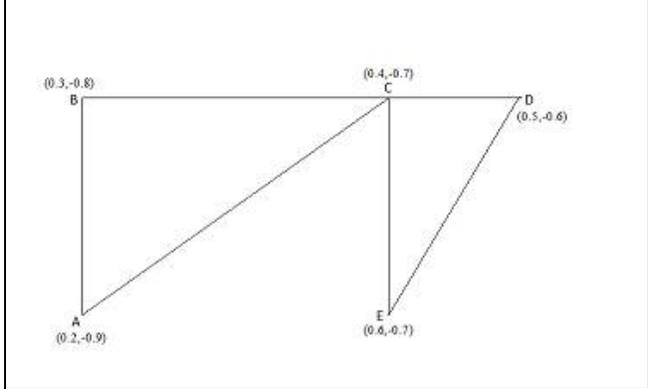


Figure 5. BFI with $\mu_{BFI} = (0.2, -0.9)$





The Impact of Recycled Concrete Aggregate on Water Permeability with Rice Husk Ash

Bandana Jethy^{1*}, Sriparna Paul² and Bidyutprava Behera³

¹Assistant Professor, Department of Civil Engineering, Gandhi Institute for Technological Advancement, Biju Patnaik University of Technology, Rourkela, Odisha.

²Assistant Professor, Department of Civil Engineering, Bhubaneswar Institute of Technology, Biju Patnaik University of Technology, Rourkela, Odisha.

³Research Scholar, PhD, National Institute of Technology (NIT), Rourkela, Odisha.

Received: 01 Mar 2021

Revised: 05 Mar 2021

Accepted: 10 Mar 2021

*Address for Correspondence

Bandana Jethy

Assistant Professor,
Department of Civil Engineering,
Gandhi Institute for Technological Advancement,
Biju Patnaik University of Technology, Rourkela, Odisha.
Email: bandanajethy28@gmail.com



This is an Open Access Journal / article distributed under the terms of the **Creative Commons Attribution License** (CC BY-NC-ND 3.0) which permits unrestricted use, distribution, and reproduction in any medium, provided the original work is properly cited. All rights reserved.

ABSTRACT

The destruction of building and structures has become an important part of construction industry due to which researchers having a keen interest on analyzing construction and demolition waste material, especially recycled concrete aggregates. The utilization of recycled concrete aggregate provides an environment friendly alternative solution to the construction industry. Recycled concrete aggregates are found to be more porous structure compared to virgin aggregate, materials rich in SiO₂, have therefore been used to improve the strength properties of concrete. Therefore, rice husk ash (RHA) from agricultural wastes, are considered. From the patterns of the X-ray diffraction (XRD) of the source materials (Nuaklong et al.), observed that the traces of crystalline products, including quartz (SiO₂), anhydrite (CaSO₄), calcium oxide (CaO), and magnesioferrite (MgFe₂O₄) were detected by the sharp peak feature in the XRD pattern due to the occurrence of highly amorphous silica in the material which is supposed to have positive effects on the geopolymer gel structure. The decreased Rice Husk Ash (RHA) particle size shows better effect on permeability behavior of hardened concrete. The permeability of water increases with the percentage of replacement of volume the finer natural aggregate with finer recycled aggregate (RA). In this paper, the effect of water permeability behavior of recycled aggregate concrete with RHA is reviewed thoroughly from experiments carried out by different authors. The absorption capacity of water in submerged concrete samples tend to decrease with rising days of concrete formation: 7, 21, and 90 days. The absorption capacity observed for 7 days of curing for U series relative to other series was decreasing, but the water absorption increased in the M series compared to the Co series at 7, 28 days of curing may be due to the existence of hygroscopic RHA particles (*Givi et al.*)

30615





Keywords: Rice Husk Ash, Water Permeability, Recycled Concrete Aggregate, XRD

INTRODUCTION

Now a day's destruction of building and structures has become an important part of construction industry due to which researchers having a keen interest on analyzing construction and demolition waste material, especially recycled concrete aggregates. Rattanachu et al. (2020) observed that the utilization of high amount of RCA is considered to replace natural aggregate, which resulted in lower compressive strength. Lower resistance to corrosion and chloride penetration as compared to conventional concrete. Knuckling et al. (2020) has attempted to use rice husk ash (RHA) for the improved the permeability effect of recycled aggregate concrete and resulted that permeability test performed at 28 days, percentage of water absorption reduced to 50%. Givi et al. (2010) prepared 3 series of concrete mixtures of RHA i.e., 95-micron meter and 5-micron meter particle size respectively, replacing 5 percent to 20 percent of cement with RHA, resulting in a reduction in permeability with prolonged curing, increasing ages of wet curing and percentages of rice husk ash. In this paper, the effect of water permeability behavior of recycled a concrete aggregate with rice husk ash (RHA) reviewed thoroughly from experiments carried out by different authors.

MATERIALS AND METHODS

Nuaklong et al. (2020) used 10-M NaOH (sodium hydroxide) and Na_2SiO_3 (sodium silicate) as alkaline activators. The patterns of X ray diffraction (XRD) of the source material is shown Fig 1. It can be observed that the traces of crystalline products, including quartz (SiO_2), anhydrite (CaSO_4), calcium oxide (CaO), and magnesioferrite (MgFe_2O_4) were detected by the sharp peak feature in the XRD pattern due to the occurrence of highly amorphous silica in the material which is supposed to have positive effects on the geopolymer gel structure. The XRD finding, unlike nS, shows that the RHA consists of amorphous silica with cristobalite and quartz crystal. There have been similar results published by He et al. (2013).

In a laboratory concrete drum mixer, Givi et al. (2010) prepared mixtures of the series M and U by compounding the fine material, coarse material and the powder materials (Cement and RHA). In order to test the workability following the mixing process, slumps obtained from fresh concrete were immediately determined. The cubes were prepared in the size of 100 mm edge and compacted on a vibrating table into two layers, The layers were vibrated for 10seconds each. The molds were then covered with sheets of polyethylene, humidified for 24 h. Then the specimens were taken out of the mold to be cured temperature of 20°C in water till the test days. After 7, 28 and 90 days, compressive strength and water absorption of the concrete samples were tested. The findings stated are the complex of three studies.

Rattanachu et al. (2020) used three dissimilar quantity fractions (20, 35 and 50 percent wt of cemented materials) of GRHA (Ground Rice Husk Ash) to partly replace OPC for casting the concrete. The concrete specimens were cured in water after casting for 1 day and divided into 3 groups: I traditional concrete (CT concrete) is concrete composed of natural aggregates (crushed limestone and river sand), (ii) RA concrete is concrete composed of river sand, and R-CA, like GBA, was used to replace OPC with 20 to 50 percent watts of binder (RA20, RA35, and RA50 concrete) and (ii) (RB20, RB35, and RB50 concretes).

RESULTS AND DISCUSSION

Experiment performed by Rattanachu et. al (2020) showed that water absorption of RCA was resulted in higher mixing of water as compared to natural concrete, which caused weakening the strength of concrete mix. Nuaklang et al. (2020) noted that the microstructure of the samples became more orderly. The use of recycled concrete in the



**Bandana Jethy et al.,**

geopolymer composite as coarse aggregates causes a decrease in strength and an increase in permeability. It also improves the workability of fresh concrete at the same time. In addition, compared with standard concrete made from recycled concrete aggregates, they demonstrated higher compressive strength at all ages. The rise in the content of silica also decreased the porosity and thus the absorption of water. Givi et al. (2010) commented that there is a decrease sorption rate in concrete samples submerged in water, the impact of rising days of concrete formation: 7, 21, and 90 days was also observed. The water absorption was decreasing at 7 days of curing for U series relative to other series, but there was an increase in percentage of water absorption in the M series compared to the Coseries at 7 and 28 days of curing due to the existence of hygroscopic RHA particles. It was suggested that increasing ages and percentages of RHA in both series lead to a decrease in permeability with prolonged curing period. This may be due to the RHA pozzolanic effect and filler effect given by both RHA series, although better results have been shown by the U series.

CONCLUSION

1. The decrease of RHA particle size shows better effect on permeability behavior of hardened concrete.
2. The permeability of water increases with the percentage of replacement of volume of fine natural aggregate with fine recycled aggregate.
3. Water absorption co-efficient is taken as a measure of permeability of water. When RHA percentage increases up to 10% for 7 days, it affects more.

REFERENCES

1. Cook, J.D. (1986) Rice husk ash. In: Swamy RN, editor. Concrete technology and design, cement replacement materials, vol. 3. London: Surrey University Press; 171–95.
2. Givi, A. N., Rashid, S. A., Aziz, F. N. A., & Salleh, M. A. M. (2010). Assessment of the effects of rice husk ash particle size on strength, water permeability and workability of binary blended concrete. *Construction and Building Materials*, 24(11), 2145–2150.
3. He, J., Jie, Y., Zhang, J., Yu, Y., & Zhang, G. (2013). Synthesis and characterization of red mud and rice husk ash-based geopolymer composites. *Cement and Concrete Composites*, 37, 108-118.
4. Nuaklong, P., Jongvivatsakul, P., Pothisiri, T., Sata, V., & Chindaprasirt, P. (2020). Influence of rice husk ash on mechanical properties and fire resistance of recycled aggregate high-calcium fly ash geopolymer concrete. *Journal of Cleaner Production*, 252, 119797.
5. Rattanachu, P., Toolkasikorn, P., Tangchirapat, W., Chindaprasirt, P., & Jaturapitakkul, C. (2020). Performance of recycled aggregate concrete with rice husk ash as cement binder. *Cement and Concrete Composites*, 108(January), 103533.
6. W. Tangchirapat, R. Buranasing, C. Jaturapitakkul, P. Chindaprasirt,(2008). Influence of rice husk-bark ash on mechanical properties of concrete containing high amount of recycled aggregates, *Construct. Build. Mater.* 22 (8), 1812–1819.





Bandana Jethy et al.,

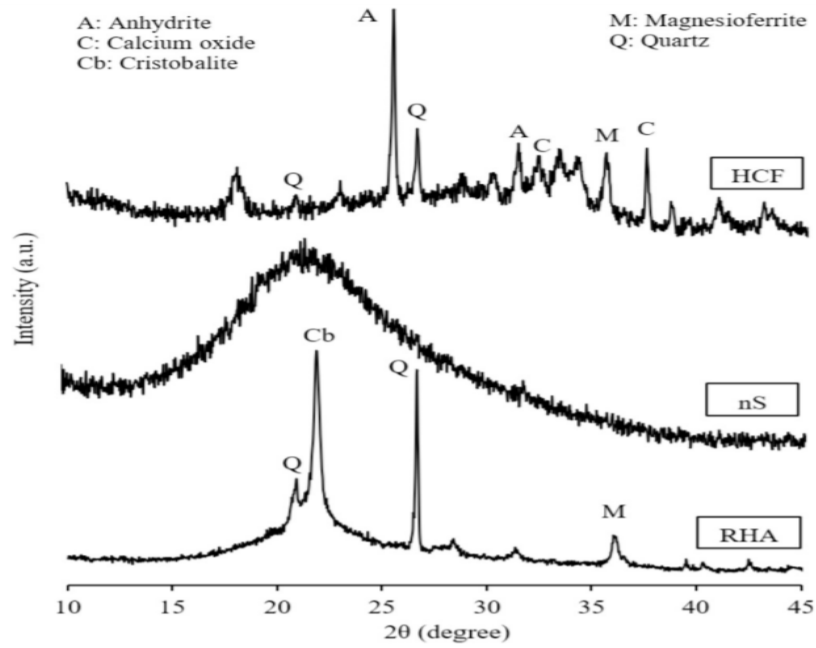


Fig 1. XRD results of HCF, nS and RHA (Source: Nuaklong et al. (2020))





Effect of Four Weeks Small Sided Games on Acceleration Speed of Junior Soccer Players

Ravi Shankar Bhagat¹, Rina Poonia², Pradeep Singh Chahar³

¹ Research Scholar, Department of Arts (Physical Education), Manipal University Jaipur, India.

² Associate Professor, Department of Arts (Physical Education), Manipal University Jaipur, India.

³ Assistant Professor, Department of Physical Education, Banaras Hindu University, Varanasi, India.

Received: 25 Feb 2021

Revised: 02 Mar 2021

Accepted: 06 Mar 2021

*Address for Correspondence

Ravi Shankar Bhagat

Research Scholar,

Department of Arts (Physical Education),

Manipal University Jaipur, India,

Email: raviorey24@gmail.com



This is an Open Access Journal / article distributed under the terms of the **Creative Commons Attribution License** (CC BY-NC-ND 3.0) which permits unrestricted use, distribution, and reproduction in any medium, provided the original work is properly cited. All rights reserved.

ABSTRACT

The goal of the study was to analyze the impact of small sided games (SSG) for four weeks on the acceleration speed of junior soccer players. Pre test - Post test Random Design was used to assign 40 (n=40) junior soccer players from Kendriya Vidyalaya, Churachandpur, Manipur, India as subjects were divided into two equal group and provided four weeks small sided games (soccer) to the experimental group, The control group did not undergo any training, however. Dependent variables selected: Acceleration Speed was measured using the 30 mts Sprint Test. For data normality, the Shapiro-Wilk Test was used. Standard deviation and standard error of means were determined as the mean for Descriptive Statistics. In addition, One-Way Co-Variance Analysis (ANCOVA) was applied and the level of significance was set at 0.05. IBM SPSS program was used to compute all statistical analyses; version: 25. The outcome showed that small-sided soccer games have a significant effect ($p < 0.05$) on the speed of acceleration ($p < 0.05$) of junior soccer players.

Keywords: Small-sided games, Acceleration Speed, Soccer players

INTRODUCTION

In most of the world, the soccer game called football is considered to be the most popular sport in the world. Two teams of eleven players are involved in soccer on a large grass field, soccer is played with a goal on both end. The purpose of the game is to get the soccer ball into the goal of the opposing team. The concept to soccer is that players do not touch the ball with their hands, with the exception of the goalkeeper, only kick, dribble or head the ball to advance it or score a goal. From small baby's leagues to professional and international teams, soccer is play at all



**Ravi Shankar Bhagat et al.**

levels around the globe. Perhaps the most famous soccer tournament is the World Cup (Soccer: Learn all about the sport of Soccer n.d.), football | History, Rules, & Significant Players | Britannica n.d.). Soccer is such a game which demands almost all physical fitness components like speed, strength, agility, coordination, endurance, balance, perception, reaction time, power, aerobic and anaerobic capacity too.

Small-sided games (SSG) are modified games played on reduced fields, often using adapted rules and limited number of players than standard football games, referred to as skill-based conditioning games or game-based training. Small-sided games allow for the integrated training of young soccer players in the technical and tactical aspects of basic development. During SSGs, the variability in movement leads to the development of a more generalized motor program to deal with a number of related but distinct situations. In addition, their structure and organisation allows them to be freely used on any surface or space of play by any category of young people (e.g., street football), favouring the development of skills suitable for long-term development. However, above all, they allow for engagement in activities deliberately designed to improve football performance. Evidence suggests that deliberate practice is more likely to lead to elite status when compared with more generic football-related activities and SSGs contribute to this specific area of talent development (Sarmiento et al. 2018, Ford, Hodges, and Williams 2009). Keeping all such things in mind the investigator thus has design the present study as: A study on effect of small sided soccer games on acceleration speed of junior soccer players.

PURPOSE OF THE STUDY

The purpose of the study was to investigate the effect of four weeks small sided games (SSG) on acceleration speed of junior soccer players.

DESIGN OF THE STUDY**Selection of Subjects**

Pre test - Post test Random Design was used by which 40 (n=40) soccer players were selected as subjects from KVS, Churachandpur, Manipur, India and equally divided into two groups, namely Experimental Group (EG) Control Group (CG) The experimental group was trained with small sided games (soccer) for four weeks in five days per week.

Training Protocol

There were three parts of the training protocol: Warm-Up Part, Main Part and Cooling down Part. The control group was not given any training; this group was involved with only warming-up part. Details of training protocol has been given in table no. 01

Assessments

For the collection of data the selected dependent variable: Acceleration Speed was assessed by 30 mts Sprint Test before and after the completion of four weeks Small sided soccer games. The unit of acceleration speed was seconds.

Statistical Procedure

For normality of the data Shapiro-Wilk Test was applied. In Shapiro-Wilk Test P-value of Pre-Test and Post-Test Data of acceleration speed were 0.472 and 0.165 ($p>0.05$), that's mean the data are approximately normal distribution. As Descriptive Statistics mean, standard deviation and standard error of means were calculated. Further, One-Way Analysis of Co-Variance (ANCOVA) was applied (Verma and Ghufraan 2012); (Verma 2009). The significance level was set at 0.05. Lastly, all statistical analyses were computed on IBM SPSS software; Version: 25 (IBM SPSS Statistics 25 Free Download 2017).



**Ravi Shankar Bhagat et al.**

In the above table : 03 it has been found that means \pm standard deviations of experimental group and control group in pre test are 5.057 ± 0.222 and 5.011 ± 0.153 seconds on acceleration speed, whereas in case of post test it is 4.535 ± 0.210 and 4.858 ± 0.162 seconds respectively. On the other hand standard error in pre test is 0.043 second in both groups respectively and in post test it is 0.042 seconds on acceleration speed in both groups.

In the above table : 04 (ANCOVA) it is evident that 'F' value and 'P' value are .599 and .444 in pre-test respectively, where 'P' value (.444) is greater than 0.05 level of significance ($p > 0.05$). That's mean there is no significant difference between experimental group and control group on acceleration speed in pre-test phase. On the other hand 'F' values and 'P' values in post-test and adjusted post-test are 29.833, 51.947 and .000, .000 respectively, where 'P' values (.000 & .000) are less than 0.05 level of significance ($p < 0.05$). That's mean there is significant difference between experimental group and control group on acceleration speed in post-test and adjusted post-test phase respectively.

DISCUSSION AND FINDINGS

The aim of the study was to investigate the impact of small sided games (SSG) on acceleration speed of junior soccer players during various SSG formats (1 vs 1, 2 vs 2, 3 vs 3, 4 vs 4, 5 vs 5 and 7 vs 7) and different small-sided dimensions of the field (5 x 5 mts, 5 x 8 mts, 6 x 6 mts, 8 x 8 mts, 15 x 15 mts, 16 x 16 mts, 15 x 10 mts, 25 x 20 mts, 30 x 25 mts, 40 x 40 mts etc) (5 x 5 mts, 5 x 8 mts, 6 x 6 mts, 8 x 8 mts, 15 x 15 mts, 16 x 16 mts, 15 x 10 mts, 25 x 20 mts, 30 x 25 mts, 40 x 40 mts etc). From the results it has been found that there is a statistically significant difference between experimental group and control group. More specifically is to be said that there is substantial impact of small sided soccer games on acceleration speed of junior soccer players. The explanation behind significant impact could be the proper implementation of four weeks small sided soccer game on experimental group.

In the present study the investigator increased the players with the progression of small-sided games (Training). Not only that with the increased players, dimensions of the play-field also had been modified. The investigator altered the dimensions of the field by increasing and decreasing the dimensions such as 5 x 5 mts, 5 x 8 mts, 6 x 6 mts, 8 x 8 mts, 15 x 15 mts, 16 x 16 mts etc. and often several circles of different radius were made for the purpose of passing, attacking and defending the ball inside the stipulated circles or rectangle or square. Due to small-sided games (SSG) with altering the numbers of players, one has to move quickly and take direction for sprint quickly. In small-sided games (SSG) usually one has to sprint or run even more due to a smaller number of players than the real games (11 sided games). In the present study the investigator also applied the same thing, that's why the acceleration speed of the soccer players have been significantly increased after four weeks small-sided games (Training). Many studies which directly or indirectly support the present studies like Katis and Kellis 2009, Los Arcos et al. 2015, G. Rajasekar et al. 2014, Dellal et al. 2011, Owen et al. 2011 etc.

CONCLUSIONS

It is concluded that there is a positive effect of four weeks small-sided games on acceleration speed of junior soccer players.

REFERENCES

1. Dellal, A., Hill-Haas, S., Lago-Penas, C., & Chamari, K. (2011). Small-sided games in soccer: amateur vs. professional players' physiological responses, physical, and technical activities. *The Journal of Strength & Conditioning Research*, 25(9), 2371-2381.
2. Ford, P. R., Ward, P., Hodges, N. J., & Williams, A. M. (2009). The role of deliberate practice and play in career progression in sport: the early engagement hypothesis. *High ability studies*, 20(1), 65-75.





Ravi Shankar Bhagat et al.

3. G, Rajsekhar et al., (2014). Impact of small sided games on acceleration speed and dribbling ability of inter collegiate level of soccer players. *Indian journal of research*, 7(3) 2250-1991.
4. Katis, A., & Kellis, E. (2009). Effects of small-sided games on physical conditioning and performance in young soccer players. *Journal of sports science & medicine*, 8(3), 374.
5. Los Arcos, A., Vázquez, J. S., Martín, J., Lerga, J., Sánchez, F., Villagra, F., & Zulueta, J. J. (2015). Effects of small-sided games vs. interval training in aerobic fitness and physical enjoyment in young elite soccer players. *PLoS one*, 10(9), e0137224.
6. Owen, A. L., Wong, D. P., McKenna, M., & Dellal, A. (2011). Heart rate responses and technical comparison between small-vs. large-sided games in elite professional soccer. *The journal of strength & conditioning research*, 25(8), 2104-2110.
7. Sarmento, H., Clemente, F. M., Harper, L. D., Costa, I. T. D., Owen, A., & Figueiredo, A. J. (2018). Small sided games in soccer—a systematic review. *International journal of performance analysis in sport*, 18(5), 693-749.
8. Hill-Haas, S. V., Dawson, B., Impellizzeri, F. M., & Coutts, A. J. (2011). Physiology of small-sided games training in football. *Sports medicine*, 41(3), 199-220.
9. Aguiar, M., Botelho, G., Lago, C., Maças, V., & Sampaio, J. (2012). A review on the effects of soccer small-sided games. *Journal of human kinetics*, 33(2012), 103-113.
10. Halouani, J., Chtourou, H., Gabbett, T., Chaouachi, A., & Chamari, K. (2014). Small-sided games in team sports training: a brief review. *The journal of strength & conditioning research*, 28(12), 3594-3618.
11. Rampinini, E., Impellizzeri, F. M., Castagna, C., Abt, G., Chamari, K., Sassi, A., & Marcora, S. M. (2007). Factors influencing physiological responses to small-sided soccer games. *Journal of sports sciences*, 25(6), 659-666.
12. Owen, A., Twist, C., & Ford, P. (2004). Small-sided games: the physiological and technical effect of altering pitch size and player numbers. *Insight*, 7(2), 50-53.
13. Katis, A., & Kellis, E. (2009). Effects of small-sided games on physical conditioning and performance in young soccer players. *Journal of sports science & medicine*, 8(3), 374.

Table: 01

Training Protocol on Small Sided Games, Total Duration: 72 Minutes						
Warm-Up Part	Main Part, Duration: 50 Min.					Cooling Down Part
10 Min.	Week-1					12 Min.
	Day-1	Day-2	Day-3	Day-4	Day-5	
	1 v/s 1 (With Goalpost), Area: 5 x 5 Mts.	2 v/s 2 (With Goalpost), Passing & Supporting Area: 5 x 8 Mts.	3 v/s 3 (With Goalpost), Passing, Supporting & Defending Area: 8 x 8 Mts.	4 +1GK v/s 4 +1GK Passing, Supporting, Defending & Depth	Match Day (Small Sided)	
Warm-Up Part	Main Part, Duration: 50 Min.					Cooling Down Part
	Week-2					
	Day-1	Day-2	Day-3	Day-4	Day-5	





Ravi Shankar Bhagat et al.

10 Min	4 v/s 4 + 4 Supporter Outside the Square Area: 15 x 15 Mts.	4 v/s 4+1 Common (Common will play / Join the team who having the ball), Area: 16 x 16 Mts. .	3 v/s 1 (4 Markers will be placed in a square formation 3 players will play against 1 defender and attackers will help to each other in four markers), Area: 6 x 6 Mts.	4 v/s 4+2 Common (Box play = Ground will be divided into 6 boxes: 2+2+2, Middle 2 boxes for common players and only 2 defenders can go to the box), Area: 15 x 10 Mts.	Match Day (Small Sided)	12 Min.
Warm-Up Part	Main Part, Duration: 50 Min.					Cooling Down Part
10 Min	Week-3					12 Min.
	Day-1	Day-2	Day-3	Day-4	Day-5	
	5 v/s 5 (4 Goal Posts = 2 in each end line) Area: 25 x 20 Mts.	7 v/s 7 (Double rondo) Two circles will be made in which 5 players will stand outside the circle with two opponents inside the circle, Area: 5 mts radius 2 circles in 10 mts distance.	2+2+1 common v/s 2 (In a circle), Area: 5 mts radius circle	5 Defenders v/s 3+1 common (Common will only support attackers during counter attack in attacking third), Hi pressing by attackers Area: 30 x 25 Mts.	Match Day (Small Sided)	
Warm-Up Part	Main Part, Duration: 50 Min.					Cooling Down Part
	Week-4					
	Day-1	Day-2	Day-3	Day-4	Day-5	
	4 v/s 4 (Passing & Supporting = 2 squares will be made and 4,4 players will	7 v/s 7 (Player can't pass back to the same player with whom he got the ball), Area: 30 x 25	1 v/s 1 (Use only weak foot), Area: 5 x 5 mts.	4 = 1GK V/S 5 (Ball supply by coach to free player, quick marking by defenders if not than	Match Day (Small Sided)	





Ravi Shankar Bhagat et al.

10 Min	be divided into 2 squares, ball will be played in one square and only 2 v/s players can go to other square area) Area: 15 x 7 Mts.			shooting by attackers) Area: 40 x 40 Mts.		12 Min.
--------	---	--	--	--	--	---------

Table: 02

Normality Test of Data of Soccer Players			
Shapiro-Wilk Test			
		df	P-value (Sig.)
Acceleration Speed	Pre-Test	40	0.472*
	Post-Test	40	0.165*

*Not Significant at $p \leq 0.05$

Table: 03 : Descriptive Statistics

Mean, SD and Standard Error of Experimental and Control Group in Pre-Post Test on Acceleration Speed of Soccer Players						
Variable	Group	N	Pre-Test		Post-Test	
			Mean \pm SD	Std. Error	Mean \pm SD	Std. Error
AccelerationSpeed (Unit: Second)	Experimental	20	5.057 \pm 0.222	0.043	4.535 \pm 0.210	0.042
	Control	20	5.011 \pm 0.153	0.043	4.858 \pm 0.162	0.042

Table: 04

One Way Analysis of Co-Variance (ANCOVA) Between Experimental Group & Control Group in Pre - Post Test on Acceleration Speed of Soccer Players							
Variable			Sum of Squares	df	Mean Sum of Square	F- ratio	p-value (Sig.)
Acceleration Speed Unit: Second	Pre-Test	B	.022	1	.022	5.99	.444
		W	1.387	38	.037		
	Post-Test	B	1.047	1	1.047	29.833*	.000*
		W	1.333	38	.035		
Adjusted Post-Test	B	1.211	1	1.211	51.947*	.000*	
	W	.863	37	.023			

*Significant at 0.05 level, $F_{0.05}(1, 38) = 4.10$, $F_{0.05}(1, 37) = 4.11$ or $p \leq 0.05$





Ravi Shankar Bhagat et al.

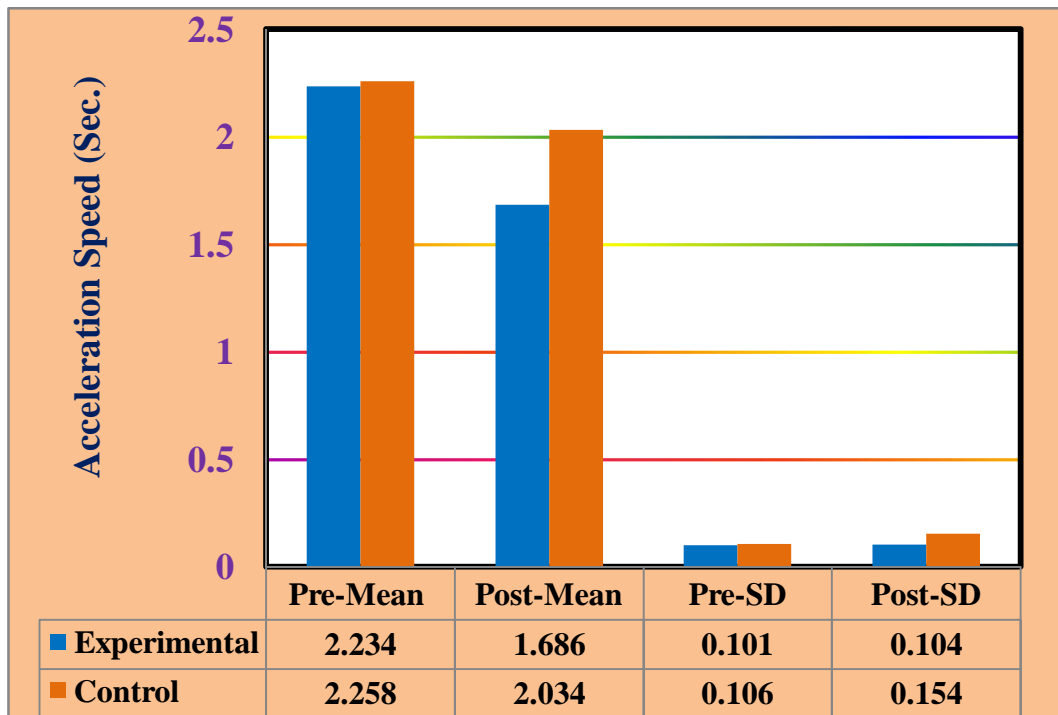


Figure: 01 Comparing Means & SD in Pre-Post Test of Experimental Group & Control Group in Respect of Acceleration Speed of Soccer Players





RESEARCH ARTICLE

Acaricidal Activity of Crude Ethanolic Extract of Aerial Parts of *Leucas lavandulifolia* Sm. against *Rhipicephalus (Boophilus) annulatus*

Prashant Somalingappa Kurbet^{1*}, Birur Mallappa Amrutha¹, Karapparambu Gopalan Ajith Kumar¹, Ashwathappa Nandini¹, Christophe Angeline Felicia Bora¹, Lanchalung Malangmei¹, Gatchanda Shravan Kumar¹, Prabodh Kumar Hembram¹, Kavya Marulappa², Krupa Theranya Lokesh², Shijin Mudikkunnath Sivadasan³, Anju Varghese¹, Chundiylil Kalarickal Deepa¹, Sanis Juliet³ and Reghu Ravindran¹

¹Department of Veterinary Parasitology, Kerala Veterinary and Animal Sciences University, Pookode, Wayanad, Kerala, India.

²Department of Veterinary Pathology, Kerala Veterinary and Animal Sciences University, Pookode, Wayanad, Kerala, India.

³Department of Veterinary Pharmacology and Toxicology College of Veterinary and Animal Sciences, Kerala Veterinary and Animal Sciences University, Pookode, Wayanad, Kerala, India.

Received: 21 Jan 2021

Revised: 01 Feb 2021

Accepted: 24 Feb 2021

*Address for Correspondence

Prashant Somalingappa Kurbet

Department of Veterinary Parasitology,
Kerala Veterinary and Animal Sciences University,
Pookode, Wayanad, Kerala, India.



This is an Open Access Journal / article distributed under the terms of the **Creative Commons Attribution License** (CC BY-NC-ND 3.0) which permits unrestricted use, distribution, and reproduction in any medium, provided the original work is properly cited. All rights reserved.

ABSTRACT

The acaricidal effects of crude ethanolic extract of the aerial parts of *Leucas lavandulifolia* Sm. against *Rhipicephalus (Boophilus) annulatus* was studied. Different dilutions of the extract such as 2.5, 5, 10, 15 and 20 per cent were tested against *R. (B.) annulatus* by using adult immersion test (AIT). The crude ethanolic extract of *L. lavandulifolia* caused a significant dose-dependent increase in adult tick mortality with maximum mortality of 95.83 per cent at the highest concentration tested. Though the inhibition of fecundity at 20 per cent concentration was 97.6 per cent, hatching of eggs was not affected by any of the concentration studied. The LC₅₀ value of the extract against *R. (B.) annulatus* was 2.87 per cent.

Keywords: *Leucas lavandulifolia*., *Rhipicephalus (Boophilus) annulatus*, Acaricidal

INTRODUCTION

Ticks are voracious blood suckers responsible for heavy blood loss, low-quality hides (Jongejan and Uilenberg, 1994), secondary bacterial infections (Ambrose *et al.*, 1999), lowered productivity in terms of weight gain (Pegram and Oosterwig, 1990), milk yield (Sajid *et al.*, 2007) and heavy mortality (Niyonzema and Kiltz, 1986). It has been estimated





Prashant Somalingappa Kurbet *et al.*,

that 80 per cent of the world's cattle population is exposed to tick infestation (FAO, 1984). The annual cost of management of ticks and tick-borne diseases (TTBDs) in India has been estimated to the tune of US\$ 498.7 million (Minjauw and Mcleod, 2003). The acaricides used for the control of ticks are synthetic pyrethroids, organophosphates, phenylpyrazoles, macrocyclic lactones and formamidines. The continuous application and indiscriminate usage of these chemical acaricides resulted in acaricidal resistance, environmental pollution, residues in food and toxicity to man (Shakya *et al.*, 2020). There is an urgent need for an alternative safe method for tick control. Acaricides of plant origin / herbal acaricides / botanical acaricides are one such alternative. Several herbal extracts were analyzed for their acaricidal effects in different laboratories of the world (Kumar *et al.*, 2011; Ravindran *et al.*, 2011; 2012; Juliet *et al.*, 2012; Zaman *et al.*, 2012; Nithy *et al.*, 2013; Sunil *et al.*, 2013; Divya *et al.*, 2014). The activities of plant extracts such as preventing blood-feeding, moulting, fecundity, and hatching of eggs were reported in the literature. Besides, these herbal acaricides have many advantages over synthetic acaricides since they are ecofriendly and cheaper and are with minimum environmental and mammalian toxicity (Rates, 2001; Habeeb, 2010). *Leucas lavandulifolia* is a common weed seen on wastelands and roadsides all over India (Fig. 1). Ravindran *et al.* (2011) reported that ethanolic extract of *L. aspera* at very low concentrations inhibited the hatching of eggs laid by the treated *R. (B.)annulatu* sticks. The present study was done to evaluate the effect of crude ethanolic extract of *L. lavandulifolia* Sm for their acaricidal activity against *R. (B.) annulatu* stick.

MATERIALS AND METHODS

Plant Material

Aerial parts of *Leucas lavandulifolia* Sm. were collected from Lakkidi, Wayanad, Kerala, India during December 2017 to January 2018.

Crude Ethanolic Extract

The collected plant leaves were cleaned by washing in running water. The aerial parts were dried at room temperature for 30 days. The dried leaves (100 g) were powdered in a plant sample grinder at controlled temperature and extracted using methanol in a Soxhlet extraction apparatus attached with a rotary vacuum evaporator (M/s Buchi, Switzerland). Solvents were removed using rotary vacuum evaporator at 175 mbar at a temperature ranging from 40°C to 60°C.

Ticks

Fully engorged adult female *R. (B.) annulatus* were collected from the naturally infested calves with a history of no prior exposure to any conventional acaricides. They were washed with distilled water, dried on an absorbent paper.

Adult Immersion Test (AIT)

Adult immersion test was performed based on Drummond *et al.* (1973). The different concentrations of extract ranging from 2.5 per cent to 20 per cent were prepared in absolute methanol. For AIT, four replicates, each with six ticks, were used for each concentration. Ticks were immersed for two minutes in the respective concentration in a tube containing 10 mL extract. Ticks were recovered from the solution, dried using absorbent paper, and placed in a separate plastic specimen tube (25 mm × 50 mm). The tubes were incubated at 28 ±2°C temperature and 80% relative humidity in a biological oxygen demand (BOD) incubator. The adult tick mortality was observed up to 15th day post-treatment. After oviposition, the eggs laid by the female ticks were collected and weighed. The eggs were kept under the same incubation conditions in a BOD incubator for the next 30 days.

The index of egg-laying (IE) and per cent inhibition of fecundity (IF) were calculated (FAO 2004) as follows:

Index of egg laying (IE) = weight of eggs laid (mg) / weight of females (mg)

Per cent inhibition of fecundity (IF) = [IE (control group)-IE (treated group)] × 100 / IE (control group).

The hatching of eggs was observed visually.





Prashant Somalingappa Kurbet et al.,

Statistical Analysis

The analysis of data was performed (Snedecor & Cochran, 1994). The groups were compared using one-way analysis of variance (ANOVA) for repeated measurements using statistical package for the social science (SPSS) software. Duncan's test was used for post hoc analysis to understand significance levels for the difference between the groups of means. A value of < 0.05 was considered significant.

Probit Analysis

Dose-response data were analysed by the probit method (Finney, 1952). The median lethal concentration (LC_{50}) value of crude ethanolic extract of aerial parts of *L. lavandulifolia* Sm. against *R. (B.) annulatus* was determined by applying regression equation analysis to the probit transformed data of mortality.

RESULTS

The results of the acaricidal efficacy of crude ethanolic extract of *L. lavandulifolia* against *R. (B.) annulatus* are summarised in Table 1. The mortality of engorged female ticks and inhibition of fecundity were dose-dependent. The per cent adult tick mortality varied from 41.67 to 95.83% when tested at concentrations ranging from 2.5 to 20%. Peak mortality was observed after day five of treatment. No mortality was recorded in the control group. Before death, ticks were swollen and black and they did not lay eggs. The inhibition of fecundity ranged from 19.00 to 98.775% on the treated ticks, with a maximum inhibition at 15% concentration. All the eggs laid by ticks treated in different concentration (2.5% to 20%) hatched. Dose-response curve by probit analysis is shown in Figure 1. The LC_{50} value of the extract against *R.(B.) annulatus* was 2.87 per cent.

DISCUSSION

Plant extracts possess various secondary metabolites such as phenolics, terpenoids, coumarins and alkaloids (Harbone, 1993 and Ahn et al., 1998) which may possess insecticidal, larvicidal, pupicidal, growth inhibitory, anti-moulting, insect repellent activities, antimicrobial, anti-tumour, antibacterial and growth inhibitory properties (Ghosh et al., 2007a; Suresh et al., 2011; Ravindran et al., 2011; Darsana, 2014; Divya et al., 2014; Thirumangalath et al., 2019). Different plant preparations including the leaf extracts of *L. aspera* revealed significant larvicidal activity against first, second, third and fourth instar larvae of *Culex quinquefasciatus* (Muthukrishnan et al., 1997). Maheswaran et al. (2008) and Bagavan et al. (2008) reported the larvicidal activity of hexane extract of *L. aspera* against *Culex quinquefasciatus* Say. and *Aedes aegypti* L. Extracts of leaf, flower and seeds of *L. aspera* showed larvicidal potential against two mosquito species viz., *Anopheles subpictus* Grassi and *Culex tritaeniorhynchus* Giles (Kamaraj et al., 2009).

As per the earlier reports, catechin identified from the hexane fraction of *Leucas aspera* showed 100 % mortality against fourth instars of the mosquito species against *Ae. aegypti*, and *An. stephensi*, and *C. quinquefasciatus* tested at 20 ppm (Elumalai et al., 2015). The activity of methyl-p-hydroxybenzoate, a phenolic derivative isolated from the leaves of *Vitex trifolia* also resulted in 100 % mortality against *C. quinquefasciatus*, *An. stephensi*, and *Ae. aegypti* at 20 ppm (Kannathan et al. 2011). It is clear from the above reports that the adult tick mortality may be due to the presence of catechin in the *Leucas* spp. plant.

In the present study, the crude ethanolic extract of *L. lavandulifolia* produced adult tick mortality and inhibition of fecundity in treated ticks. The effect on mortality was found to be concentration-dependent. The per cent adult tick mortality produced by the ethanolic extract of *L. lavandulifolia* was 4.16 to 54.16 per cent in a dose-dependent manner when examined at lower concentrations ranging from 1.56 to 100 mg/mL (Ravindran et al., 2011). Similarly, in the present study, there was a dose-dependent increase in mortality from 41.67 ± 8.33 % to 95.83 ± 4.167 % when tested at higher concentrations. However Ravindran et al. (2011) reported the complete enclosin blocking of eggs laid by ticks treated with ethanolic extract of *L. aspera*. In the present study this feature was not evident even though the extract of





Prashant Somalingappa Kurbet et al.,

L. lavandulifolia caused high inhibition of fecundity. This reveal as inhibitory effect on the reproductive system of ticks due to the unidentified molecules in the *Leucas* spp. This variation in the bioactivity may be due to the difference in the species of the *Leucas* used for the studies or the season of collection of the plant materials which can affect the concentration and composition of secondary metabolites in the plant species.

CONCLUSION

It is evident from the present study that the acaricidal activity of *L. lavandulifolia* from crude ethanolic extract caused significant adult tick mortality and inhibition of fecundity at 20 per cent concentration. It could be used as a herbal acaricide in the control of ticks as this plant is available as a weed in the roadside and wasteland of Wayanad, district of Kerala. So further studies are needed to isolate the active biomolecule present in the *L. lavandulifolia*.

REFERENCES

1. Ambrose, N., Lloyd, D. and Maillard, J.C., 1999. Immune responses to *Dermatophilus congolensis* infections. *Parasitol. Today*. **15**: 295-300.
2. Adehan, S.B., Biguezoton, A., Adakal, H., Assogba, M.N., Zoungrana, S.E., Gbaguidi, A.M., Tonouhewa, A., Kandé, S., Achi, L., Kagone, H. and Adehan, R., 2016. Acaricide resistance of *R. microplus* ticks in Benin. *African Indian J. Agric. Res.***11**: 1199–1208
3. Ahn, Y.J., Lee, S.B., Lee, H.S. & Kim, G.H.(1998). Insecticidal and acaricidal activity of carvarol and β -thujaplicine derived from *Thujopsis dolabrata* var. *Hondai*Sawdust. *J. Chem. Ecol.***24**: 81-90.
4. Bagavan, A., Rahuman, A.A., Kamara, C. & Geetha, K. (2008). Larvicidal activity of saponin from *Achyranthesaspera* against *Aedesegypti* and *Culex quinquefasciatus* (Diptera: Culicidae). *Parasitol. Res.***103**: 223-229.
5. Castro-Janer, E., Martins, J. R., Mendes, M. C., Namindome, A., Klafke, G. M. and Schumaker, T. T. S. 2010. Diagnoses of fipronil resistance in Brazilian cattle ticks (*Rhipicephalus (Boophilus) microplus*) using in vitro larval bioassays. *Vet. Parasitol.***173**: 300-306.
6. Chopra, R.N., Nayar, S.L. & Chopra, I.C. (2002). Glossary of Indian Medicinal Plants. NISCAIR, CSIR, New Delhi. pp. 153.
7. Crosby, D.G. & Jacobson, M. (1971a). *Naturally Occurring Insecticides* (1stEd). Marcel Dekker, Inc: New York. pp. 198- 205.
8. Crosby, D.G. & Jacobson, M. (1971b). *Naturally Occurring Insecticides* (1stEd). Marcel Dekker Inc: New York. pp.186-198.
9. Darsana, U. 2014. Acaricidal activity of extracts and fractions of *Atrémisia nilagirica* (Clarke) Pamp. and *Clerodendrum philippinum* Schauer. against *Rhipicephalus (Boophilus) annulatus*.
10. M.V.Sc thesis, Kerala Veterinary and Animal Sciences University, Pookode, 129p.
11. Divya, T.M., Soorya, V.C., Amithamol, K.K., Juliet, S., Ravindran, R., Nair, S.N. and Ajithkumar, K.G., 2014. Acaricidal activity of alkaloid fractions of *Leucas indica* Spreng against *Rhipicephalus (Boophilus) annulatus* tick. *Trop. Med.***31**: 46-53.
12. Dutta, S., Godara, R., Katoch, R.,Yadav, A., Katoch, M. and Singh, N.K.,2017. Detection of amitraz and malathion resistance in field populations of *Rhipicephalus (Boophilus) microplus* (Acari: Ixodidae) in Jammu region of India. *Exp. Appl. Acarol.***71**: 291–301.
13. Drummond, R., Ernst, S.E., Trevino, J.L., Gladney, W.J. & Graham, O.H. (1973). *Boophilus annulatus* and *Boophilus microplus*: laboratory tests for insecticides. *J. Econ. Entomol.***66**: 130-133.
14. FAO. 1984. Ticks and ticks borne disease control. A practical field manual. Volume 1. Tick control. Rome.
15. Finney, D.J., 1952. *Probit analysis: a statistical treatment of the sigmoid response curve*. Cambridge university press, cambridge.





Prashant Somalingappa Kurbet et al.,

16. Ghosh, S., Azhahianambi, P. and Yadav, M.P., 2007. Upcoming and future strategies of tick control: a review. *J. Vector Borne Dis.***44**: 79.
17. Ghosh, S., Kumar, R., Nagar, G., Kumar, S., Sharma, A.K., Srivastava, A., Kumar, S., Kumar, K.A. and Saravanan, B.C., 2015. Survey of acaricides resistance status of *Rhipicephalus (Boophilus) microplus* collected from selected places of Bihar, an eastern state of India.
18. *Ticks Tick Borne Dis.* **6**:668–675.
19. Habeeb, S.M., 2010. Ethno-veterinary and medical knowledge of crude plant extracts and its methods of application (traditional and modern) for tick control. *World Appl. Sci. J.***11**: 1047-1054.
20. Harbone, J.B. (1991). *Phytochemical methods: Guide to modern techniques of plant analysis* (2nd Ed). Chapman and Hall, India. pp.653.
21. Harborne, J.B. (1993). *Introduction to Ecological Biochemistry* (4th Ed).Academic Press, New York. pp. 81-131.
22. Jongejan, F. and Uilenberg, G., 1994. Ticks and control methods. *Revue Scientifique et Technique-Office International des epizooties*, **13**: 1201-1201.
23. Juliet, R. Ravindran, S. A. Ramankutty et al., "Jatropha curcas (Linn) leaf extract -a possible alternative for population control of *Rhipicephalus (Boophilus) annulatus*," *Asian Pac. J. Trop. Dis.* vol. 2, no. **3**: 225–229, 2012.
24. Jyothimol, G., Ravindran, R., Juliet, S., Ajith Kumar, K.G., Suresh, N.N., Vimalkumar, M.B., Lenka, D.R., arghese, S. and Ghosh, S. 2014. Low level deltamethrin resistance in ticks from cattle of Kerala, a south Indian state. *Vet. Parasitol.* **204**: 433–438.
25. Kamaraj, C., Bagavan, A., Rahuman, A.A., Zahir, A.A., Elango, G. & Pandiyan, G. (2009).
26. Larvicidal potential of medicinal plant extracts against *Anopheles subpictus* Grassi and *Culex tritaeniorhynchus* Giles (Diptera: Culicidae). *Parasitol. Res.***104**: 1163-1171.
27. Kayaa, G.P. (2000). The potential for anti-tick plants as components of an integrated tick control strategy. *Ann. N. Y. Acad. Sci.***916**: 576-582.
28. Kirtikar, K.R. & Basu, B.D. (1990). *Indian Medicinal Plants*. In: Blatter, E., Caius J.F. and Mhaskar, K.S. (eds.), Periodical Experts Book Company. pp. 2019.
29. Kumar, A., Singh, S., Mahour, K. and Vihan, V.S., 2011. In vitro and in vivo acaricidal activity of some indigenous plants under organized and farmer flock. *Pharmacol.***3**: 361-369.
30. Lenka, D.R., Ravindran, R., Jyothimol, G., Udaykumar, M., Reddy, P.M.T., Sathish, N., Palla, I., Chandramohan, B., Ajithkumar, K.G., Nair, S.N. and Chandrasekhar, L., 2016. Deltamethrin resistance in south Indian isolates of *Rhipicephalus (Boophilus) microplus*. *Vet.Parasitol.* (Amst), **5**: 37–41
31. Lee, C.H., Lee, S.G. & Lee, H.S. (2010). Acaricidal effects of *Thymus vulgaris* leaf-derived materials and monoterpene alcohols against *Dermatophagoides* spp. *J. Korean Soc. Appl. Biol. Chem.***53**: 170-174.
32. Mangathayar, K., Thirumurugan, D., Patel, P.S., Pratap, D.V.V., David, V.J. & Karthikeyan, J. (2006). Isolation and identification of nicotine from *Leucasaspera* (Willd). *Indian J. Pharm. Sci.***68**: 88-90.
33. Mansour, F., Azaizeh, H., Saad, B., Tadmor, Y., Abo-Moch, F. & Said, O. (2004). The potential of Middle Eastern flora as source of new safe bio-acaricides to control *Tetranychus cinnabarinus*, the Carmine Spider Mite. *Phytoparasitica***32**: 66-72.
34. Maheswaran, R., Sathish, S. & Ignacimuthu, S. (2008). Larvicidal activity of *Leucasaspera* (Willd) against the larvae of *Culex quinquefasciatus* Say. and *Aedes aegypti* L. *Int. J. Integr. Biol.***2**: 214-217.
35. Minjauw, B. and McLeod, A. 2003. In: Tick-borne diseases and poverty: the impact of ticks and tick-borne diseases on the livelihoods of small-scale and marginal livestock owners in India and eastern and southern Africa.
36. Muthukrishnan, J., Puphlantha, H. & Kasthuribhai, K. (1997). Biological effects of four plant extracts on *Culex quinquefasciatus* Say. Larval stages. *Insect Sci. Appl.***17**:389-394.
37. Muhammad, S., Fatima, A. & Yahaya, M.M.(2012). The phytochemical components of *Leucas martinicensis* that cause repellence of adult mosquito. *Int. J. Mod.Botany* **2**: 1-5.





Prashant Somalingappa Kurbet et al.,

38. Nandi, A., Sagar, S.V., Chigure, G., Fular, A., Sharma, A.K., Nagar, G., Kumar, S., Saravanan, B.C. and Ghosh, S., 2018. Determination and validation of discriminating concentration of ivermectin against *Rhipicephalus microplus*. *Vet. Parasitol.* **250**:30-34.
39. Nithya, V., Kamalam, M. and Umakanthan, T., 2015. Screening of indigenous medicinal plants for their acaricidal activity against cattle ticks under in vivo condition. *Int. J. Pharm. Sci. Res.* **6**: 3049.
40. Niyonzema, A. and Kiltz, H. H. 1986. Control of ticks and tick-borne diseases in Burundi. *ACIAR Proc.* **17**: 16–17.
41. Park, B.S., Lee, S.E., Choi, W.S., Jeong, C.Y., Song, C. & Cho, K.Y. (2002). Insecticidal and acaricidal activity of piperonaline and piperocetadecalidine derived from dried fruits of *Piper longum* L. *Crop. Prot.* **21**: 249-251.
42. Pegram, R. G. and Oosterwijk, K. 1990. The effect of *Amblyomma variegatum* on live weight of cattle in Zambia. *Med.Vet.Entomol.* **4**:327-330.
43. Reddy, K.M., Viswanathan, S., Thirugnanasambantham, D., Santa, R. & Lalitha, K.(1993). Analgesic activity of *Leucasaspera*. *Fitoterapia* **64**: 151-154.
44. Rates, S.M.K., 2001. Plants as source of drugs. *Toxicon*, **39**:603-613.
45. Ravindran, R., Juliet, S., Sunil, A.R., Kumar, K.G.A., Nair, S.N., Amithamol, K.K., Bandyopadhyay, A., Rawat, A.K.S. and Ghosh, S., 2012. Acaricidal activity of *Cassia alata* against *Rhipicephalus (Boophilus) annulatus*. *Exp. Appl. Acarol.* **56**: 69-74.
46. Ravindran, R., Juliet, S., Sunil, A.R., AjithKumar, K.G., Nair, S.N., Amithamol, K.K., Shynu, M., Rawat, A.K.S. & Ghosh, S. (2011). Ecllosion blocking effect of extract of *Leucasaspera* (Lamiaceae) on *Rhipicephalus (Boophilus) annulatus*. *Vet.Parasitol.* **179**: 287-290.
47. Sajid, M. S., Iqbal Z, Khan, M. N., Muhammad, G. and Iqbal, M. U. 2007. Effect of Hyalomma ticks (*Acari:Ixodidae*) on milk production of dairy buffaloes (*Bos Bubalus Bubalis*) of Punjab (Pakistan). *Italian J. Anim. Sci.* **6**: 939-941.
48. Shakya, M., Kumar, S., Fular, A., Upadhaya, D., Sharma, A.K., Bisht, N., Nandi, A. and Ghosh, S., 2020. Emergence of fipronil resistant *Rhipicephalus microplus* populations in Indian states. *Experimental and Applied Acarology*, pp.1-12.
49. Sunil, A.R., Amithamol, K.K., Juliet, S., Nair, S.N., Ajithkumar, K.G., Soorya, V.C., Divya, T.M., Jyothymol, G., Ghosh, S. and Ravindran, R., 2013. Acaricidal effect of *Cassia fistula* Linn. leaf ethanolic extract against *Rhipicephalus (Boophilus) annulatus*. *Trop Biomed.* **30**: 231-237.
50. Snedecor, G.W. & Cochran, W.G. (1994). *Statistical Methods* (8th Ed). Iowa State University Press, Ames, Iowa. pp. 491.
51. Vudriko, P., Okwee-Acai, J., Tayebwa, D.S., Byaruhanga, J., Kakooza, S., Wampande, E. and Suzuki, H., 2016. Emergence of multi acaricide resistant *Rhipicephalus* ticks and its implication on chemical tick control in Uganda. *Parasit. Vectors.* **9**: 4
52. Zaman, M.A., Iqbal, Z., Abbas, R.Z., Khan, M.N., Muhammad, G., Younus, M. and Ahmed, S., 2012. *In vitro* and *in vivo* acaricidal activity of an herbal extract. *Vet.Parasitol.* **186**: 431-436.

Table: 1 Effects of different concentrations of crude ethanolic extract of *Leucas lavandulifolia* against *R. (B.) annulatus*

SI no.	Concentration (%)	Mean tick weight per \pm SEM	Mean % of adult mortality within 15 \pm SEM days	Mean eggs mass per \pm SEM	Index of fecundity \pm SEM	Inhibition of fecundity (%)	Hatching % (visual)
1	Control	1.026 \pm 0.090	0	0.400 \pm 0.020	0.396 \pm 0.031 ^a	0.00 ^c	100
2	20	1.072 \pm 0.011	95.83 \pm 4.167	0.011 \pm 0.011	0.010 \pm 0.010 ^{bc}	97.59 ^{ab}	100
3	15	0.919 \pm 0.019	91.67 \pm 4.811	0.005 \pm 0.003	0.005 \pm 0.003 ^{ab}	98.77 ^{bc}	100
4	10	0.873 \pm 0.038	83.33 \pm 6.804	0.025 \pm 0.008	0.039 \pm 0.017 ^{bc}	90.20 ^{ab}	100
5	5	0.857 \pm 0.042	75.00 \pm 4.81	0.047 \pm 0.012	0.055 \pm 0.016 ^{ab}	72.64 ^{bc}	100
6	2.5	0.873 \pm 0.024	41.67 \pm 8.33	0.188 \pm 0.028	0.218 \pm 0.037 ^{ab}	44.97 ^{bc}	100

n= 4, values are Mean \pm SEM means bearing different superscripts a, b or c (P 0.05), indicates significant difference when compared with control.





Prashant Somalingappa Kurbet et al.,

Fig 2 Dose-response curve of crude ethanolic extract of *Leucas lavandulifolia* against adult *R. (B) annulatus*

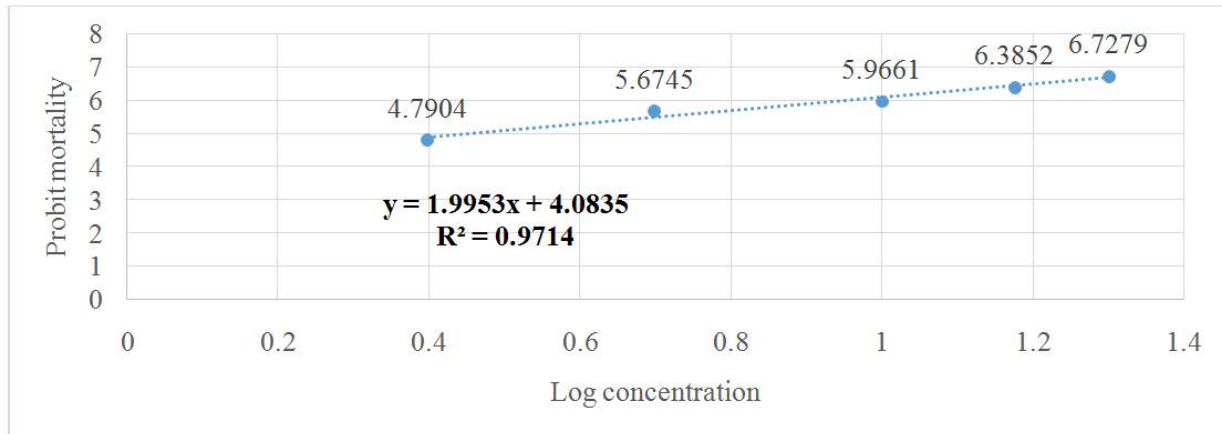


Figure legend: Figure 1: *Leucas lavandulifolia* Sm.





Sustainable Development of Business through Green Marketing – A Conceptual Perspective

Lavanya D¹, Parveen Roja M^{2*} and Geethanjali N²

¹Assistant Professor, Department of Management Studies, PSNA College of Engineering and Technology, Dindigul, Tamil Nadu, India.

²Associate Professor, Department of Management Studies, PSNA College of Engineering and Technology, Dindigul, Tamil Nadu, India.

Received: 07 Feb 2021

Revised: 18 Feb 2021

Accepted: 05 Mar 2021

*Address for Correspondence

Parveen Roja M
Associate Professor,
Department of Management Studies,
PSNA College of Engineering and Technology,
Dindigul, Tamil Nadu, India.



This is an Open Access Journal / article distributed under the terms of the **Creative Commons Attribution License** (CC BY-NC-ND 3.0) which permits unrestricted use, distribution, and reproduction in any medium, provided the original work is properly cited. All rights reserved.

ABSTRACT

One of the principal problems in recent years of globalization is to retain the ecosystem environment friendly in addition to creating a sustainable business. Green marketing focuses on inculcating ozone-friendly approaches to the various sectors of society. In pursuance of building a socially responsible and sustainable business, the companies should follow eco-friendly principles which act as a competitive advantage that attracts new customers and also retain the existing ones. It also raises the question of whether a business can be profitable while being socially responsible and environmentally safe. This paper examines the benefits and challenges of green marketing and its influence in achieving a sustainable business.

Keywords: Green marketing, environmental marketing, socially responsible, Sustainable development.

INTRODUCTION

Today Green Marketing also known as ecological marketing or environmental marketing came into the limelight in the late 1980s and 1990s. Green Marketing includes a variety of things such as developing environment-friendly products, non-polluting packaging, adopting sustainable business practices and concentrating on communicating the product's eco-friendly benefits. Green marketing deals with the operations of selling goods and services based on their ecological benefits. These products may be manufactured or packaged in an environmental friendly manner. Green marketing primarily focus on assuring that the marketing activities of a business are equipped to be responsible to minimize environmental threats. The firms are recognizing the importance of cementing their





Lavanya et al.,

relationship with the customers who this who are also showing a greater eagerness to preserve the environment. Firms have realized the importance of green marketing in satisfying the customer needs albeit valuing its importance to the development and sustainability of a business. Green marketing reflects the dramatic shift in their strategies in the way the firms are hold out and connect with their customers. Firms nowadays carry out a number of green marketing strategies to create a sustainable development in the business.

METHODOLOGY

The paper reviews the relationship between green marketing and organizational sustainability, benefits, challenges, and the green marketing strategies for a successful business. This is a review based focused on Literature review, journals, newspapers, books, websites, and other reliable sources.

Green Marketing - Evolution

Over the years the Green Marketing has evolved. According to Peattie (2001), the evolution of green marketing can be classified into three phases. Phase one was termed as “Ecological” green marketing, throughout this period almost all the marketing activities were focused on helping the environmental problems and providing solutions to these environmental problems. Phase two was “Environmental” green marketing and there was a shift in the focus to clean technology which involves innovative design on new products. Phase three was “Sustainable” green marketing. It came into the limelight in the late 1900 and early 2000. Its focuses on developing products that meet the standards of quality, pricing, performance, and ease of use in an environmentally friendly way. (Neringa Vilkaite-Vaitone et al., 2019)

Green Product

Green products are the products that are manufactured without wasting the natural resources, do not pollute the environment and has the attribute to recycle it easily. Green products help to save natural resources, reduces toxins, pollution and waste.

Green Price

The most important element of the marketing mix is the Green Price. Many customers are willing to pay a premium price if there is an assumption of the added value to the products. This value can enhance design, performance, aesthetics, taste, and features. The eco-friendly benefit will be an added attraction but mostly will be the ultimate deciding factor that will be the competitive advantage for the companies over their competitors.

Green Place

A distribution logistics is a significant factor in green marketing. The ultimate decision of making the product available in an appropriate location has a significant influence in attracting customers. It can be achieved within store promotions and using recycled materials to showcase the significance of the environment.

Green Promotion

Promoting products and services in target markets involving direct marketing, sales promotion, onsite promotions, advertising, public relations, and advertising. Sustainable marketing and various communication tools can be used by green marketers to strengthen environmental credibility. Credibility is the key to a successful green marketing mix. Green marketing strategy can be executed through the process called the Greening of Marketing Mix, including External Green 7P, Internal Green 7P, and Green 4S for Success.





Lavanya et al.,

Green Marketing – Benefits

- Green marketing reign to bring commercial, environmental, and social benefits. Some of the benefits of green marketing include the following
- Establish a strong relationship with the customers. Green marketing is used to develop a close relationship with the customers, which is developed based on trust.
- Profit maximization. Increased profitability can be achieved through green marketing.
- Organizational goal achievement. Organizations believe that green marketing is essential to accomplish the organizational goals and objectives.
- Foster competitive advantage. Green marketing helps the companies to gain the core competitive advantage over their competitors.
- Overall cost reduction. Though green marketing may look like a cost-demanding initiative, in the beginning, it surely is going to be favorable, economical, and essential in the long run. Organizational behavior change in the disposal of wastages and increased efficiency in raw materials consumption will save money in the long run.
- Strengthening of brand reputation. Because of the initiatives of the organizations green marketing increases the brand reputation. A strong relationship with customers will retain them within the organization and also paves the way to new markets.

Researchers of green marketing are more focused on commercial benefits rather than environmental benefits. Social benefits are unexpected in researches of green marketing. The advantages of green marketing ensue in sustainability of development in business, enhancement of the ecosystem, and increased wellbeing. Therefore, marketers are advised to embrace green marketing strategies.

CONCLUSION

New age marketers need to realize the significant impact of green marketing. Customers are showing their growing concern for the safe environment and are ready to pay a premium price for green products. Green marketing and green product development will be used by firms to increase competitive advantages and can satisfy the customers better than their competitors. By finding an opportunity to improve the product's performance and increasing the number of loyal customers' organizations can achieve a sustainable development in the business. In the future researches can be carried out to find the level of influence of commercial, environmental and social benefits of green marketing have on various industries

REFERENCES

1. Andrew Crane (2000) Facing the backlash: green marketing and strategic reorientation in the 1990s, *Journal of Strategic marketing*, 8:3, 277-296,
2. Domazet, Ivana and Kovačević, Milica (2018), The role of green marketing in achieving sustainable development. In: *Sustainable growth and development in small open economies*. Institute of World Economics; Centre for Economic and Regional Studies of the Hungarian Academy of Sciences, Budapest, pp. 57-72. ISBN 978-963-301-663-3
3. Margareta Nadanyiova * , Lubica Gajanova and Jana Majerova Green Marketing as a Part of the Socially Responsible Brand's Communication from the Aspect of Generational Stratification , *Sustainability* 2020, 12, 7118
4. R. Shrikanth*, D.Surya Narayana Raju Contemporary Green Marketing - Brief Reference to Indian Scenario *International Journal of Social Sciences & Interdisciplinary Research*, Vol.1, No. 1, January 2012, ISSN 2277 3630
5. Dr. C. Vijai, P. Anitha, The Importance Of Green Marketing, *International Journal of Future Generation Communication and Networking*, *International Journal of Future Generation Communication and Networking* Vol. 13, No. 3, (2020), pp. 4137–4142 Vol. 13, No. 3, (2020), pp. 4137–4142





Lavanya et al.,

6. Zuzana Dvořáková Lišková*, Eva Cudlínová, Petra Pártlová, Dvořák Petr Importance of Green Marketing and Its Potential Visegrad Journal on Bioeconomy and Sustainable Development Vol. 5, No.2,(2016)
7. Neringa Vilkaite-Vaitone*, Ilona Skackauskiene, Green marketing orientation: evolution, conceptualization and potential benefits Open Economics 2019; 2: 53–62
8. Dinuk Arseculeratne & Rashad Yazdanifard How Green Marketing Can Create a Sustainable Competitive Advantage for a Business International Business Research Vol. 7, No. 1; 2014
9. Parul Yadav, Ankit Singh, Introduction to Green Marketing, Irjmsst Vol 5 Issue 10 [Year 2014] Issn 2250 – 1959 (Online) 2348 – 9367 (Print)
11. Aparna Choudhary, Samir Gokarn, GREEN MARKETING: A MEANS FOR SUSTAINABLE DEVELOPMENT, International Refereed Research Journal, Vol.–IV, Issue–3(3), July 2013 [26]
12. B.Chitra, A Study on Evolution of Green Products and Green Marketing, Quest Journals Journal of Research in Business and Management Volume 3 - Issue 5(2015) pp: 35-38 ISSN (Online): 2347-3002
13. RavinderKaur, Green Marketing in India –An Overview, Biz and Bytes (Vol. 8. Issue: 1, 2017) E-ISSN: 0976 0458, Print ISSN: 2320 897X
14. Peattie, K., 1995, "Environmental Marketing Management," London: Pitman
15. Peattie, K., 2001, "Towards Sustainability: The Third Age of Green Marketing," Marketing Review, 2(2), 129-147.
16. Rennyta Yusiana, Arry Widodo, Agus Maolana Hidayat, Green Marketing: Perspective of 4P's, Advances in Economics, Business and Management Research, Series volume number 141
17. Shruti Garg, Vandana Sharma, Green Marketing: An Emerging Approach to Sustainable Development, International Journal of Applied Agricultural Research ISSN 0973-2683 Volume 12, Number 2 (2017) pp. 177-184
18. Kavita Kumara, Green Marketing In India: A Review of Literature, Biz and Bytes (Vol. 8. Issue: 1, 2017) E-ISSN: 0976 0458, Print ISSN: 2320 897X
19. <https://www.esg.adec-innovations.com/resources/newsletters/july-2016-effective-green-marketing-strategies/5-effective-green-marketing-strategies/>
20. https://blogs.siliconindia.com/nayan/marketing_mix_of_green_marketing-bid-uQo5nC9M98069957.html
21. https://en.wikipedia.org/wiki/Green_marketing
22. <https://www.ipl.org/essay/Competitive-Advantages-Of-Green-Marketing-F3P3SKKRCED6>
23. http://www.marketingpower.com/_layouts/dictionary.aspx
24. <https://www.ipl.org/essay/The-Importance-Of-Green-Marketing-PJY9PZ5YNR>

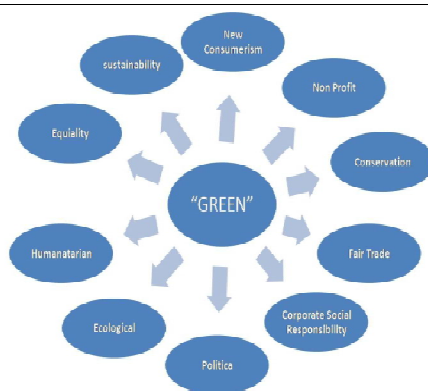


Fig :1 Meaning of green (Source: Peattie, 2001)





Lavanya et al.,

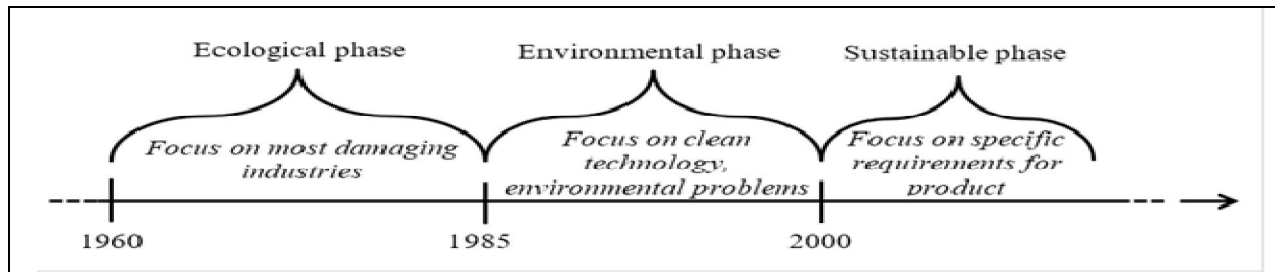


Fig :2 Green Marketing Mix

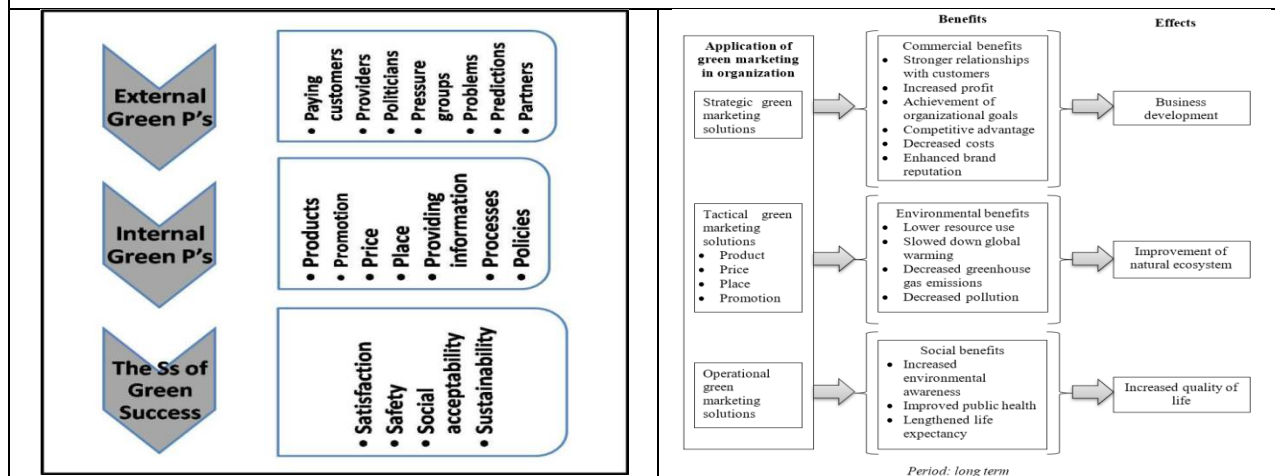


Fig : 3 Green Marketing Process (Source: Peattie, 2001

Fig : 4 : Commercial, environmental and social benefits of green marketing and their effects





RESEARCH ARTICLE

A Study on Biodiversity and Variation in Population Listed of Algal sp. from Dravyavati River in a Different Season from 3 Industrial Sites

Ritu Singh Rajput ^{1*}, Sonali Pandey ² and Seema Bhadauria ³

¹Jayoti Vidyapeeth Women's University, Vedant Gyan Valley, Mahla-Jobner Link Road, Ajmer-Jaipur Expy, Jharna, Rajasthan, India.

²Department of Botany, JECRC University, Ramchandrapura, Sitapura Industrial Area, Jaipur, Rajasthan, India.

³Department of Botany, University of Rajasthan, Jaipur, India.

Received: 05 Dec 2020

Revised: 20 Dec 2020

Accepted: 22 Dec 2020

*Address for Correspondence

Dr. Ritu Singh Rajput

Jayoti Vidyapeeth Women's University,

Vedant Gyan Valley,

Mahla-Jobner Link Road,

Ajmer-Jaipur Expy,

Jharna, Rajasthan, India.

Email: ritusingh71213@gmail.com



This is an Open Access Journal / article distributed under the terms of the **Creative Commons Attribution License** (CC BY-NC-ND 3.0) which permits unrestricted use, distribution, and reproduction in any medium, provided the original work is properly cited. All rights reserved.

ABSTRACT

The Dravyavati River (Amanishah Nala) – “the life line of Jaipur” – is the most polluted waterway in Jaipur. The diversity of the algal population is an indication of the true sanitary and ecological condition of the river. It also indicates its potential for self-purification. We relied on algal bio-indicators to determine pollution levels in the various seasons – rainy, winter and summer – to arrive at an estimate of the self-purification probability of the river system. Commonly used animal indicators of ecosystem health are less useful and unique than bio-indicators provided by algae. The algae allow us to recognize signals in ecosystem changes that identify acceptable – as opposed to unacceptable – environmental situations. In addition, algae are the most cost-effective monitoring tool in our arsenal.

Keywords: Biodiversity; Algae; Industries, water pollution

INTRODUCTION

Water is an important resource because all living organisms require it to survive. Polluted water poisons flora and fauna, and has a direct impact on humans. The main causes of water pollution are sewage, industrial wastes, oil spills and utilization of pesticides in agriculture. When untreated sewage merges into rivers, it causes water borne diseases. Grey water like sewerage water needs to be recharged after proper treatment. Dravyavati River and other

30638



**Ritu Singh Rajput et al.,**

recharge areas should be taken care of pollution & encroachment. Wastewater environment is an ideal media for a wide range of microorganisms specially bacteria, viruses, protozoa and algae. The majority is harmless and can be used in biological sewage treatment (Palmer, 1969). Serious interests in natural methods for wastewater treatment have reemerged. The intensive growth and consequent harvesting of the algal biomass as a method for removing wastewater borne nutrients was first suggested (Abdel-Raouf *et al* , 2012). Algae are significant markers of environment conditions since they react rapidly both in species synthesis and densities to an extensive variety of water conditions because of changes in water science (Rajput *et al*, 2017). For example, increases in water acidity due to acid-forming chemicals that influence lake pH levels, as well as heavy metals discharged from industrial areas, affect the composition of genera that are able to tolerate these conditions (Bellinger and David, 2010). Algae have gotten to be noteworthy living beings for natural cleaning of wastewater since they can aggregate plant supplements, substantial metals, pesticides, natural and inorganic harmful substances and radioactive matters in their cells/bodies (Jothinayagi *et.al*, 2009).

MATERIAL AND METHOD

Study Area

Dravyavati River is considered the lifeline of Jaipur. **Dravyavati River** flows in the central part of the Jaipur. In 1844 a dam was built across **Dravyavati River**, but it was breached in 1853. At the opportunity of the dam construction, **Dravyavati River** was a perennial nala. However, after some years, the inflow of water into the **Dravyavati River** became low in summer seasons. Heavy silting of the dam also contributed to reduction in the size of **Dravyavati River**.

Sampling Procedure

The water samples were collected from three selected Industrial sites of - **Dravyavati River**, one meter away from both the banks for each sampling station. The samples were collected from a depth of 10 to 15 cm from surface. The time of the sampling ranged between 8 to 11 a.m. throughout the study period. Nine samples were collected from **Dravyavati River**, in different seasons (summer, winter and rainy). The water samples were collected in the sterilized glass bottles. These sample bottles were rinsed three times with source water to minimize the risk of external contamination before sampling. Samples for the investigation of phytoplankton were collected randomly from the site. Algae was identified and counted microscopically. 100 ml water sample was collected from the selected locations. Fifteen ml samples were taken and centrifuged at 3000 rpm at room temperature. The concentrated ~20 μ l of the sample was taken on to a glass slide, counted and enumerated under a light microscope (40 X). Representative images were taken at 100 X magnification. The identification of algal species was carried out based on the morphological features, unicellular, filamentous, color, motility, and reproductive structures (Prescot, 1956).

RESULTS

Algal Diversity observed from Sitapura, Sanganer and Mansarovar Industrial area (Palmer, 1969)

The comparative algal sp. diversity and the population density was studied from all three sites (Sitapura, Sanganer and Mansarovar industrial area) and in all three season (summer, winter and rainy) at a time interval of 15 days .It was followed palmer index method for identified the diversity of algal sp.

The summary statistics of the diverse generic population of algae in the wastewater are given in Table 1.The population study from Sitapura industrial area site collected water samples showed which were identified in 1-15 days interval. The highest occurrences of algal sp. were *Oscillatoria limosa* (2 ± 1.33), *Navicula radiosa* (3 ± 0.5), *Nostoc spongiforme* (4 ± 1.11), *Anabaena variabilis* (4 ± 1.02) and *Chlorella variabilis* (2 ± 0.31). *Polytoma uvella*, *Spirogyra hyaline Cleve*, *Spirulina subrhynchiformis*, *Synedra acus*, *Chlamydomonas reinhardtii*, and *Pandorina morum* occurrences were low.



**Ritu Singh Rajput et al.,**

The summary statistics of the diverse generic population of algae in the wastewater are given in Table 2. The population study from Sanganer industrial area site collected water samples showed which were identified in 1-15 days interval. The highest occurrences of algal sp. were *Oscillatoria limosa* (6 ± 1.77), *Navicula radiosa* (8 ± 3.34), *Nostoc spongiforme* (10 ± 3.65), *Anabaena variabilis* (9 ± 2.68) and *Chlorella variabilis* (11 ± 3.43). *Polytoma uvella*, *Spirogyra hyaline Cleve*, *Spirulina subrhynchiformis*, *Synedra acus*, *Chlamydomonas reinhardtii*, and *Pandorina morum* occurrences were low.

The summary statistics of the diverse generic population of algae in the wastewater are given in Table 3. The population study from Mansarovar industrial area site collected water samples showed which were identified in 1-15 days interval. The highest occurrences of algal sp. were *Oscillatoria limosa* (8 ± 1.9), *Navicula radiosa* (14 ± 2.38), *Nostoc spongiforme* (2 ± 0.84), *Anabaena variabilis* (2 ± 1.14) and *Chlorella variabilis* (10 ± 2.74). *Polytoma uvella*, *Spirogyra hyaline Cleve*, *Spirulina subrhynchiformis*, *Synedra acus*, *Chlamydomonas reinhardtii*, and *Pandorina morum* occurrences were low.

The summary statistics of the diverse generic population of algae in the wastewater are given in Table 4. The population study from Sitapura industrial area site collected water samples showed which were identified in 1-15 days interval. The highest occurrences of algal sp. were *Oscillatoria limosa* (2 ± 0.67), *Navicula radiosa* (3 ± 0.82), *Nostoc spongiforme* (4 ± 1.14), *Anabaena variabilis* (3 ± 1.51) and *Chlorella variabilis* (3 ± 0.87). *Polytoma uvella*, *Spirogyra hyaline Cleve*, *Spirulina subrhynchiformis*, *Synedra acus*, *Chlamydomonas reinhardtii*, and *Pandorina morum* occurrences were low.

The summary statistics of the diverse generic population of algae in the wastewater are given in Table 5. The population study from Sanganer industrial area site collected water samples showed which were identified in 1-15 days interval. The highest occurrences of algal sp. were *Oscillatoria limosa* (7 ± 2.26), *Navicula radiosa* (10 ± 3.93), *Nostoc spongiforme* (3 ± 1.76), *Anabaena variabilis* (7 ± 1.93) and *Chlorella variabilis* (7 ± 2.58). *Polytoma uvella*, *Spirogyra hyaline Cleve*, *Spirulina subrhynchiformis*, *Synedra acus*, *Chlamydomonas reinhardtii*, and *Pandorina morum* occurrences were low.

The summary statistics of the diverse generic population of algae in the wastewater are given in Table 6. The population study from Mansarovar industrial area site collected water samples showed which were identified in 1-15 days interval. The highest occurrences of algal sp. were *Oscillatoria limosa* (6 ± 2.46), *Navicula radiosa* (7 ± 2.68), *Nostoc spongiforme* (2 ± 0.22), *Anabaena variabilis* (6 ± 1.97) and *Chlorella variabilis* (6 ± 2.5). *Polytoma uvella*, *Spirogyra hyaline Cleve*, *Spirulina subrhynchiformis*, *Synedra acus*, *Chlamydomonas reinhardtii*, and *Pandorina morum* occurrences were low.

The summary statistics of the diverse generic population of algae in the wastewater are given in Table 7. The population study from Sitapura industrial area site collected water samples showed which were identified in 1-15 days interval. The highest occurrences of algal sp. were *Oscillatoria limosa* (6 ± 2.47), *Navicula radiosa* (11 ± 3.04), *Nostoc spongiforme* (5 ± 1.47), *Anabaena variabilis* (8 ± 1.47) and *Chlorella variabilis* (8 ± 2.55). *Polytoma uvella*, *Spirogyra hyaline Cleve*, *Spirulina subrhynchiformis*, *Synedra acus*, *Chlamydomonas reinhardtii*, and *Pandorina morum* occurrences were low.

The summary statistics of the diverse generic population of algae in the wastewater are given in Table 8. The population study from Sanganer industrial area site collected water samples showed which were identified in 1-15 days interval. The highest occurrences of algal sp. were *Oscillatoria limosa* (8 ± 3.16), *Navicula radiosa* (8 ± 2.17), *Nostoc spongiforme* (9 ± 2.85), *Anabaena variabilis* (3 ± 1.63) and *Chlorella variabilis* (9 ± 1.92). *Polytoma uvella*, *Spirogyra hyaline Cleve*, *Spirulina subrhynchiformis*, *Synedra acus*, *Chlamydomonas reinhardtii*, and *Pandorina morum* occurrences were low.

The summary statistics of the diverse generic population of algae in the wastewater are given in Table 9. The population study from Mansarovar industrial area site collected water samples showed which were identified in 1-15 days interval. The highest occurrences of algal sp. were *Oscillatoria limosa* (4 ± 1.09), *Navicula radiosa* (3 ± 0.75), *Nostoc spongiforme* (5 ± 1.78), *Anabaena variabilis* (4 ± 1.08) and *Chlorella variabilis* (6 ± 2.38). *Polytoma uvella*, *Spirogyra hyaline Cleve*, *Spirulina subrhynchiformis*, *Synedra acus*, *Chlamydomonas reinhardtii*, and *Pandorina morum* occurrences were low.

Identified Algae sp. from Dravyavati River

Representative images were taken at 100X magnification. Morphological features – cell character, motility, color, physical and reproductive structures – were used to identify algal species. It had identified 11 algal sp. from





Ritu Singh Rajput et al.,

Dravyavati River. Which were present in all 3 different seasons (summer, winter, rainy). Bellinger and Sige 2015, key followed for the Identification of algal sp.

1. *Oscillatoria limosa*: - *Oscillatoria* is a genus of filamentous cyanobacteria. It has more than 100 species. It is named for the oscillation in its movement. Filaments in the colonies can slide back and forth against each other. Thus the whole mass is reoriented to its light source. It is very common in moist places rich in decay organic matter. It is commonly found in watering-troughs waters like streams, roadside ditches, drains and sewers. It is mainly blue-green or brown-green. It forms a thin blue green mucilaginous coating on the surface of flowing water.

2. *Navicula radiosa*: - *Navicula* is a genus of boat-shaped algae primarily aquatic, eukaryotic, photosynthetic organisms, ranging in size from a single cell. *Navicula* is a diatom. Mostly found in polluted water. Cells are boat-shaped, motile, and solitary. Cells are rectangular in girdle view, and widely lanceolate in valve view. Both valves have a central longitudinal raphe with a nodule (bump) in the middle. Valve surface is covered in transverse striations that are crossed by finer longitudinal striations.

3. *Spirogyra hyaline* Cleve:- *Spirogyra* is a green algae belonging to the class Chlorophyceae. They are commonly found floating in fresh water resources like ponds, lake, ditches etc. and some are also found in slow running stream or river. The vegetative structure or plant body is known as thallus. Thallus is unbranched multicellular filamentous structure formed by arrangement of cylindrical cells head to head in a single row. *Spirogyra*, one of the commonest green filamentous algae is named because of the helical or spiral arrangement of the chloroplasts. There are more than 400 species of *Spirogyra* in the world.

4. *Chlamydomonas reinhardtii*:- *Chlamydomonas* is a genus of unicellular green algae (Chlorophyceae). These algae are found all over the world, in soil, fresh water, oceans, and even in snow on mountaintops. Algae in this genus have a cell wall, a chloroplast, an "eye" that perceives light and two anterior flagella with which they can swim using a breast-stroke type motion.

5. *Nostoc spongiforme*:- *Nostoc* is a diverse genus of cyanobacteria. They are found in gelatinous colonies, composed of filaments called "Trichome" surrounded by a thin sheath. They are common in both aquatic and terrestrial habitats. These organisms are known for their unusual ability to lie dormant for long periods of time and abruptly recover metabolic activity when rehydrated with liquid water. *Nostoc*s are photosynthesizers which use cytoplasmic photosynthetic pigments rather than chloroplasts in their metabolic process *Nostoc*'s genetics are worth studying because of the genus' unique adaptations which allow them to survive and even thrive in extreme environments.

6. *Pandorina morum*:- *Pandorina* is a genus of green algae composed of 8, 16, or sometimes 32 cells, held together at their bases to form a sack globular colony surrounded by mucilage. The cells are ovoid or slightly narrowed at one end to appear keystone- or pear-shaped. It forms a thick greenish growth in dirty, polluted water. Chloroplast so present has at least one pyrenoid. Basically it inhabits a very wide variety of habitat including ponds, streams, pools, and lakes. *Pandorina* is considered a Bioindicator. It is used as an indicator of organically polluted waters.

7. *Polytoma uvella*: - *Polytoma* is a genus of green algae, specifically of the Chlamydomonadaceae. *Polytoma* is one of the most primitive, free swimming, nucleated organisms. *Polytoma* is a genus of colorless, free-living Chlorophytes similar in form to *Chlamydomonas* but lacking chlorophyll. *Polytoma* species are entirely saprotrophic, obtaining nutrients from decaying organic matter.

8. *Chlorella variabilis*:- *Chlorella* is a member of Chlorophyceae class. They are unicellular, non motile green algae. The small cells are non motile, round or oval, usually found solitary; sometimes in a group. The cell protoplast is enclosed in a membrane. The pyrenoids are usually absent. The stigma and contractile vacuoles are lacking. The





Ritu Singh Rajput et al.,

growth of this alga is therefore encouraged in sewage disposal plants where it crowds out by its rapid rate of multiplication and suppresses harmful bacteria.

9. *Spirulina subrhynchiformis*:- *Spirulina* is a fresh water blue green algae. *Spirulina* is a spiral-shaped microalgae that grows naturally in the wild in warm, fresh water lakes. *Spirulina* provides the highest concentration of protein in the world, all in the form of essential amino acids for muscle, health and cellular growth.

10. *Synedra acus* - *Synedra* is a diatom that has long needle shaped cells. Diatoms are small phytoplankton that lives in a shell made of silica which sinks to the bottom when the organism dies. The silica plays a role in global cycling through the aquatic food web. The shells are currently used in pool filters, kitty litter, and water treatment. Diatoms are commonly found in oceans, lakes, slow flowing rivers, and streams. When diatoms become too thick they can cause harmful growth by developing an odor in drinking water and block water treatment filters.

11. *Anabaena variabilis*:- *Anabaena* is a genus of filamentous cyanobacteria, or blue-green algae. It found as plankton. It is known for its nitrogen fixing abilities. *Anabaena* is found in all types of water. Blooms or massive growths can occur in waters with a lot of nutrients. It has filamentous structure. Its filament resembles the filament of *Nostoc*. Sometimes it becomes difficult to differentiate between trichomes of *Nostoc* and *Anabaena*. There is only one difference. The filaments of *Nostoc* are covered by mucilage and form a colony. It is absent in *Anabaena*. The filament of *Anabaena* consists of string of beaded cells (Bellinger and Sige 2015).

DISCUSSION

The comparative algal sp. diversity was studied from the three sites (Sitapura, Sanganer and Mansarovar industrial area) in the summer Rainy and Winter season at a time interval of 15 days respectively (15th April to 30th June 2017, 15th July to 30th September 2017, and 15 December to 28 February 2017). *Navicula radiosa* (Sitapura, Sanganer and Mansarovar industrial area) were reported dominant sp. in all three sites in summer season. *Navicula radiosa*, *Chlorella variabilis* and *Anabaena variabilis* (Sitapura, Sanganer and Mansarovar industrial area) was reported dominant sp. in all three site in Rainy and Winter season. *Oscillatoria limosa* was observed dominate sp. in 2 sites (Sanganer and Mansarovar industrial area) in the summer and Rainy season. Similarly *Nostoc spongiforme* was reported dominate sp. at Site 2(Sanganer industrial area) in Winter Season.

REFERENCES

1. Abdel-Raouf N., Al-Homaidan A.A. and Ibraheem I.B.M. (2012). Microalgae and wastewater treatment. *Saudi Journal of Biological Sciences*, 19(3), 257-275.
2. Bellinger, E.G. and Sige, D.C., 2015. *Freshwater algae: identification and use as Bioindicators*. John Wiley & Sons.
3. Edward, G.B. and David, C.S., 2010. *Freshwater algae identification and use as Bioindicators*. A John Wiley & Sons, Ltd, 101.
4. Jothinayagi, N. and Anbazhagan, C., 2009. Effect of seaweed liquid fertilizer of *Sargassum wightii* on the growth and biochemical characteristics of *Abelmoschus esculentus* (L.) Medikus. *Recent Research in Science and Technology*, 1(4).
5. Palmer C.M. (1969). A Composite Rating of Algae Tolerating Organic Pollution. *Journal of Phycology*, 5(1), 78-82.
6. Palmer, C.M., 1969. A Composite Rating of Algae Tolerating Organic Pollution 2. *Journal of Phycology*, 5(1), pp.78-82.
7. Prescott G.W. (1956). A guide to the literature on ecology and life histories of the algae. *The Botanical Review*, 22 (3), 167-240.
8. Rajput R.S., Pandey S. and Bhadauria S. (2017). Status of water pollution in relation to industrialization in Rajasthan. *Reviews on Environmental Health*, 32(1), 1-8.





Ritu Singh Rajput et al.,

Table 1:- Algal sp. Isolated from Sitapura industrial area in the Summer Season (15th April to 30 June , 2017)

Sr. no	Algae	15 th April	30 th April	15 th May	1 June	15 th June	30 June	M±SE
1	<i>Oscillatoria limosa</i>	0	0	1	0	4	8	2 ± 1.33
2	<i>Polytoma uvella</i>	0	0	0	0	0	0	0 ± 0
3	<i>Navicula radiosa</i>	1	1	3	3	3	4	3 ± 0.5
4	<i>Chlorella variabilis</i>	1	1	2	2	2	3	2 ± 0.31
5	<i>Spirogyra hyaline Cleve</i>	0	0	0	0	0	0	0 ± 0
6	<i>Spirulina subrhynchiformis</i>	0	0	0	0	0	0	0 ± 0
7	<i>Chlamydomonas reinhardtii</i>	0	0	0	0	0	0	0 ± 0
8	<i>Synedra acus</i>	0	0	0	0	0	0	0 ± 0
9	<i>Nostoc spongiforme</i>	1	0	4	6	6	6	4 ± 1.11
10	<i>Anabaena variabilis</i>	1	0	5	5	6	5	4 ± 1.02
11	<i>Pandorina morum</i>	0	0	0	0	0	0	0 ± 0

Table 2:- Algae Identification isolated from Sanganer industrial area in the Summer season (15th April to 30 June , 2017)

Sr. no	Algae	15 th April	30 th April	15 th May	1 June	15 th June	30 June	M±SE
1	<i>Oscillatoria limosa</i>	1	0	5	7	10	10	6 ± 1.77
2	<i>Polytoma uvella</i>	0	0	0	0	0	0	0 ± 0
3	<i>Navicula radiosa</i>	1	1	3	7	12	22	8 ± 3.34
4	<i>Chlorella variabilis</i>	1	1	12	12	14	23	11 ± 3.43
5	<i>Spirogyra hyaline Cleve</i>	0	0	0	0	0	0	0 ± 0
6	<i>Spirulina subrhynchiformis</i>	0	0	0	0	0	0	0 ± 0
7	<i>Chlamydomonas reinhardtii</i>	0	0	0	0	0	0	0 ± 0
8	<i>Synedra acus</i>	0	0	0	0	0	0	0 ± 0
9	<i>Nostoc spongiforme</i>	0	0	10	10	20	20	10 ± 3.65
10	<i>Anabaena variabilis</i>	0	5	8	10	15	18	9 ± 2.68
11	<i>Pandorina morum</i>	0	0	0	0	0	0	0 ± 0

Table 3:- Algae Identification in isolated from Mansarovar industrial area in the Summer season (15th April to 30 June , 2017)

Sr. no	Algae	15 th April	30 th April	15 th May	1 June	15 th June	30 June	M±SE
1	<i>Oscillatoria limosa</i>	2	2	13	10	10	10	8 ± 1.9
2	<i>Polytoma uvella</i>	0	0	0	0	0	0	0 ± 0
3	<i>Navicula radiosa</i>	12	14	4	15	18	21	14 ± 2.38
4	<i>Chlorella variabilis</i>	2	1	12	14	16	15	10 ± 2.74
5	<i>Spirogyra hyaline Cleve</i>	0	0	0	0	0	0	0 ± 0





Ritu Singh Rajput et al.,

6	<i>Spirulina subrhynchiformis</i>	0	0	0	0	0	0	0 ± 0
7	<i>Chlamydomonas reinhardtii</i>	0	0	0	0	0	0	0 ± 0
8	<i>Synedra acus</i>	0	0	0	0	0	0	0 ± 0
9	<i>Nostoc spongiforme</i>	0	0	0	3	2	5	2 ± 0.84
10	<i>Anabaena variabilis</i>	0	0	0	3	3	7	2 ± 1.14
11	<i>Pandorina morum</i>	0	0	0	0	0	0	0 ± 0

Table 4:- Algae Identification isolated from Sitapura industrial area in the Rainy Season (15th July to 30 September, 2017)

Sr. no	Algae	15 th July	30 th July	15 th Aug	1st Sep	15 th Sep	30 Sep	M±SE
1	<i>Oscillatoria limosa</i>	0	1	2	3	4	4	2 ± 0.67
2	<i>Polytoma uvella</i>	0	0	0	0	0	0	0 ± 0
3	<i>Navicula radiosa</i>	0	2	2	5	4	5	3 ± 0.82
4	<i>Chlorella variabilis</i>	1	2	4	2	3	7	3 ± 0.87
5	<i>Spirogyra hyaline Cleve</i>	0	1	1	2	3	3	2 ± 0.49
6	<i>Spirulina subrhynchiformis</i>	0	0	0	0	1	1	0 ± 0.21
7	<i>Chlamydomonas reinhardtii</i>	0	0	0	0	2	2	1 ± 0.42
8	<i>Synedra acus</i>	0	0	0	0	0	0	0 ± 0
9	<i>Nostoc spongiforme</i>	1	1	3	4	6	8	4 ± 1.14
10	<i>Anabaena variabilis</i>	0	0	0	4	8	7	3 ± 1.51
11	<i>Pandorina morum</i>	0	0	0	0	0	0	0 ± 0

Table 5:-Algae Identification isolated from Sanganer in the Rainy season (15th July to 30 September, 2017)

Sr. no	Algae	15 th July	30 th July	15 th Aug	1st Sep	15 th Sep	30 Sep	M±SE
1	<i>Oscillatoria limosa</i>	1	0	6	10	10	14	7 ± 2.26
2	<i>Polytoma uvella</i>	0	0	0	0	0	0	0 ± 0
3	<i>Navicula radiosa</i>	2	1	3	13	18	24	10 ± 3.93
4	<i>Chlorella variabilis</i>	2	1	2	12	12	15	7 ± 2.58
5	<i>Spirogyra hyaline Cleve</i>	0	0	0	0	0	0	0 ± 0
6	<i>Spirulina subrhynchiformis</i>	0	0	0	0	0	0	0 ± 0
7	<i>Chlamydomonas reinhardtii</i>	0	0	0	0	0	0	0 ± 0
8	<i>Synedra acus</i>	0	0	0	0	0	0	0 ± 0
9	<i>Nostoc spongiforme</i>	0	0	0	2	7	10	3 ± 1.76
10	<i>Anabaena variabilis</i>	0	2	6	9	10	12	7 ± 1.93
11	<i>Pandorina morum</i>	0	0	0	0	0	0	0 ± 0





Ritu Singh Rajput et al.,

Table 6: Algae Identification isolated from Mansarovar in the Rainy season(15th July to 30 September , 2017)

Sr. no	Algae	15 th July	30 th July	15 th Aug	1st Sep	15 th Sep	30 Sep	M±SE
1	<i>Oscillatoria limosa</i>	0	1	2	8	12	14	6 ± 2.46
2	<i>Polytoma uvella</i>	2	2	2	4	4	6	3 ± 0.67
3	<i>Navicula radiosa</i>	1	1	3	7	15	15	7 ± 2.68
4	<i>Chlorella variabilis</i>	1	1	3	4	11	16	6 ± 2.5
5	<i>Spirogyra hyaline Cleve</i>	0	0	0	0	0	0	0 ± 0
6	<i>Spirulina subrhynchiformis</i>	0	0	0	0	1	2	1 ± 0.34
7	<i>Chlamydomonas reinhardtii</i>	0	0	0	0	1	3	1 ± 0.49
8	<i>Synedra acus</i>	0	0	1	0	0	2	1 ± 0.34
9	<i>Nostoc spongiforme</i>	2	1	1	1	2	2	2 ± 0.22
10	<i>Anabaena variabilis</i>	0	0	6	8	11	10	6 ± 1.97
11	<i>Pandorina morum</i>	1	0	3	4	2	5	3 ± 0.76

Table 7:-Algae Identification isolated from Sitapura in the winter season(15th December to 30 February , 2017)

Sr. no	Algae	15 th Dec	30 th Dec	15 th Jan	1st Feb	15 th Feb	28 th Feb	M±SE
1	<i>Oscillatoria limosa</i>	0	1	1	11	12	12	6 ± 2.47
2	<i>Polytoma uvella</i>	0	0	0	0	0	0	0 ± 0
3	<i>Navicula radiosa</i>	0	10	11	8	16	22	11 ± 3.04
4	<i>Chlorella variabilis</i>	0	2	8	12	12	16	8 ± 2.55
5	<i>Spirogyra hyaline Cleve</i>	0	0	0	0	0	0	0 ± 0
6	<i>Spirulina subrhynchiformis</i>	0	0	0	0	0	0	0 ± 0
7	<i>Chlamydomonas reinhardtii</i>	0	0	0	0	0	0	0 ± 0
8	<i>Synedra acus</i>	0	0	0	0	0	0	0 ± 0
9	<i>Nostoc spongiforme</i>	1	1	6	5	9	9	5 ± 1.47
10	<i>Anabaena variabilis</i>	3	4	8	10	10	12	8 ± 1.47
11	<i>Pandorina morum</i>	0	0	0	0	0	0	0 ± 0

Table 8:- Algae Identification isolated from Sanganer in the Winter Season(15th December to 30 February , 2017)

Sr. no	Algae	15 th Dec	30 th Dec	15 th Jan	1st Feb	15 th Feb	28 th Feb	M±SE
1	<i>Oscillatoria limosa</i>	1	2	3	6	16	19	8 ± 3.16
2	<i>Polytoma uvella</i>	0	0	0	0	0	0	0 ± 0
3	<i>Navicula radiosa</i>	1	1	8	10	12	13	8 ± 2.17
4	<i>Chlorella variabilis</i>	1	6	12	12	11	13	9 ± 1.92
5	<i>Spirogyra hyaline Cleve</i>	0	0	0	0	0	0	0 ± 0
6	<i>Spirulina subrhynchiformis</i>	0	0	0	0	0	0	0 ± 0
7	<i>Chlamydomonas reinhardtii</i>	0	0	0	0	0	0	0 ± 0





Ritu Singh Rajput et al.,

8	<i>Synedra acus</i>	0	0	0	0	0	0	0 ± 0
9	<i>Nostoc spongiforme</i>	0	5	5	8	16	18	9 ± 2.85
10	<i>Anabaena variabilis</i>	0	0	0	4	7	9	3 ± 1.63
11	<i>Pandorina morum</i>	0	0	0	0	0	0	0 ± 0

Table 9:- Algae Identification isolated from Mansarovar in the winter season (15th December to 30 February, 2017)

Sr. no	Algae	15 th Dec	30 th Dec	15 th Jan	1st Feb	15 th Feb	28 th Feb	M±SE
1	<i>Oscillatoria limosa</i>	2	2	2	6	6	8	4 ± 1.09
2	<i>Polytoma uvella</i>	0	0	2	2	4	3	2 ± 0.65
3	<i>Navicula radiosa</i>	1	1	3	4	5	5	3 ± 0.75
4	<i>Chlorella variabilis</i>	1	1	2	8	12	14	6 ± 2.38
5	<i>Spirogyra hyaline Cleve</i>	0	0	0	1	2	2	1 ± 0.4
6	<i>Spirulina subrhynchiformis</i>	0	0	1	1	1	2	1 ± 0.31
7	<i>Chlamydomonas reinhardtii</i>	0	0	0	0	0	0	0 ± 0
8	<i>Synedra acus</i>	0	0	0	0	0	0	0 ± 0
9	<i>Nostoc spongiforme</i>	1	0	4	10	7	10	5 ± 1.78
10	<i>Anabaena variabilis</i>	2	0	6	5	5	7	4 ± 1.08
11	<i>Pandorina morum</i>	0	0	0	0	0	0	0 ± 0

Sample Collection Sites



Fig 1(A)Sitapura Industrial area Site



Fig 1(B)Mansarovar Industrial area Site

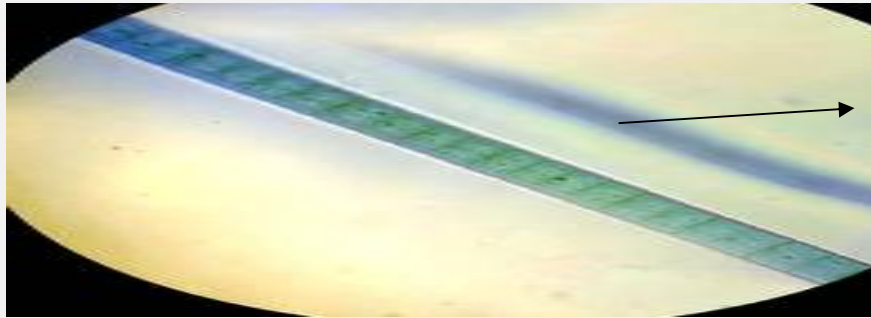




Ritu Singh Rajput et al.,



Fig 1(C)Sanganer Industrial area Site



Vegetative

A



20 μ m



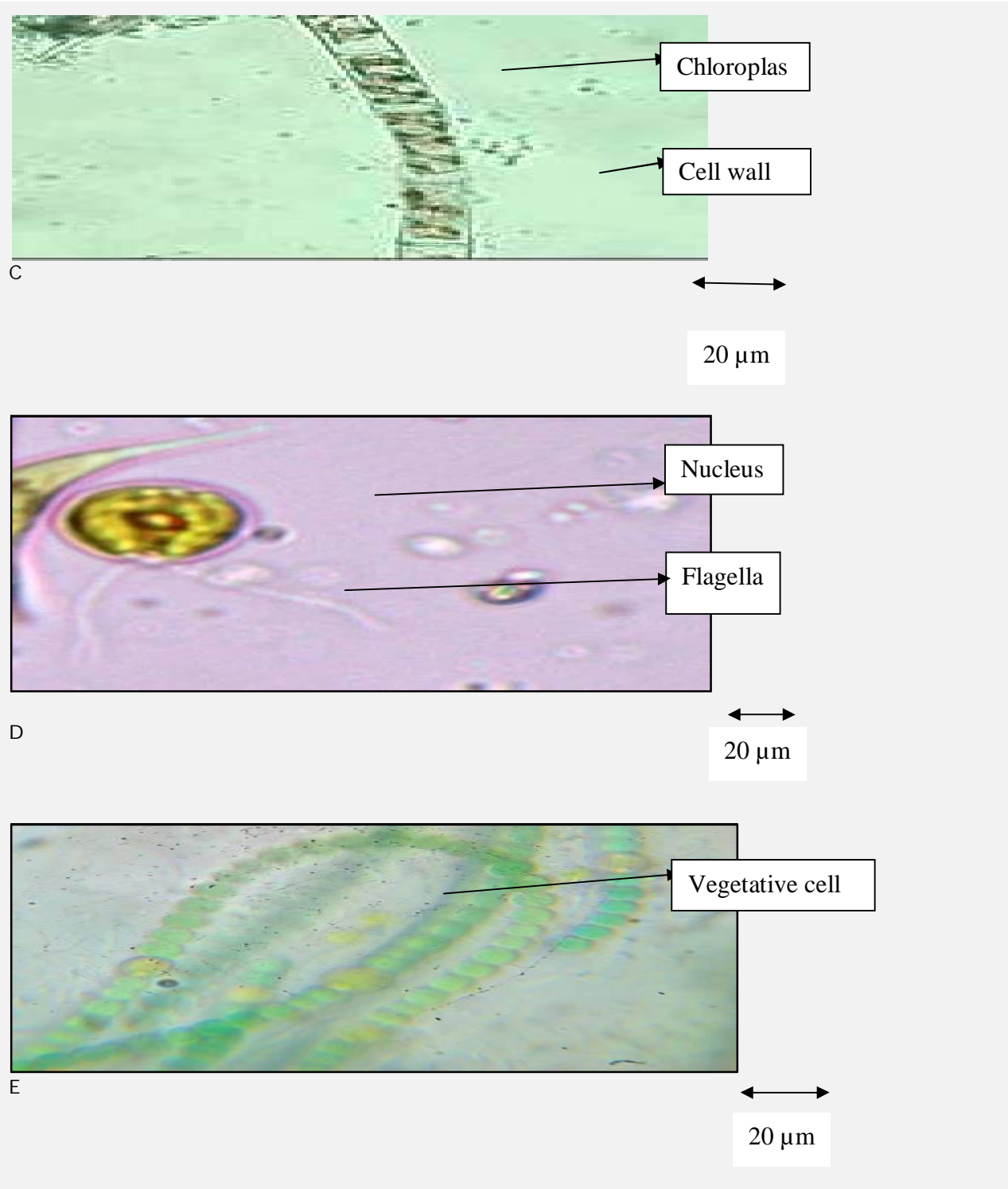
Chloropla

B



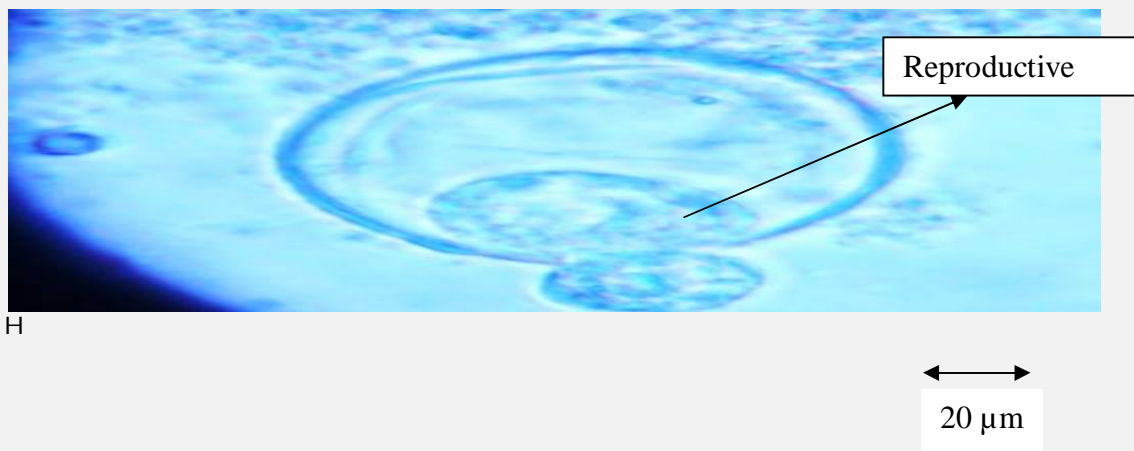
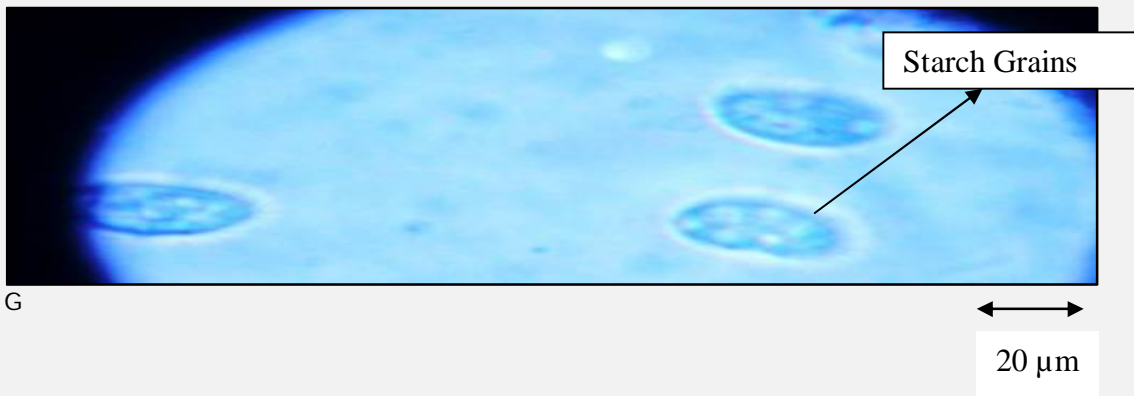
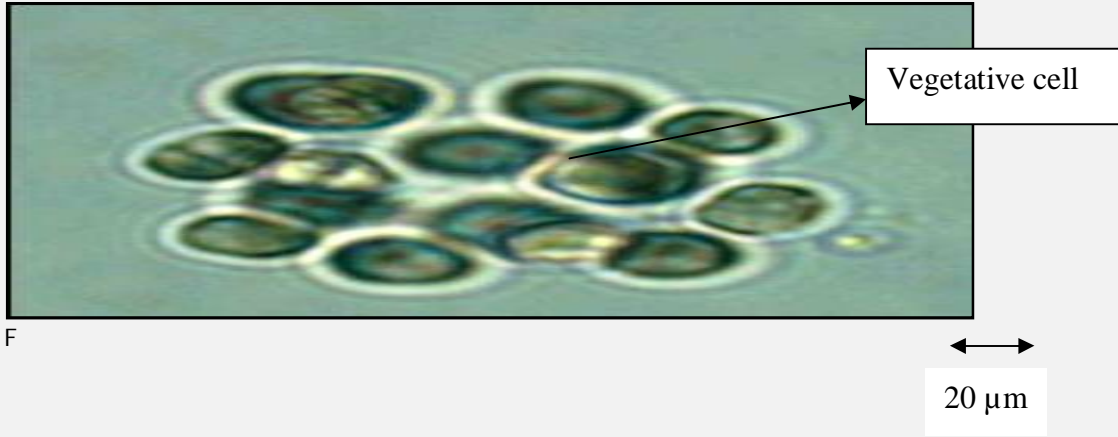


Ritu Singh Rajput et al.,



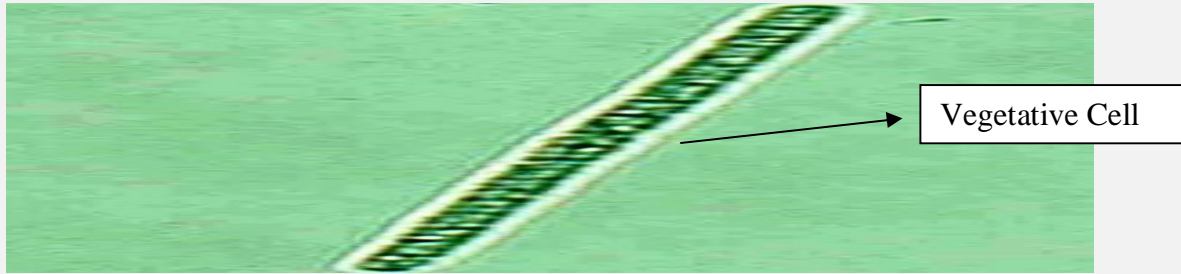


Ritu Singh Rajput et al.,

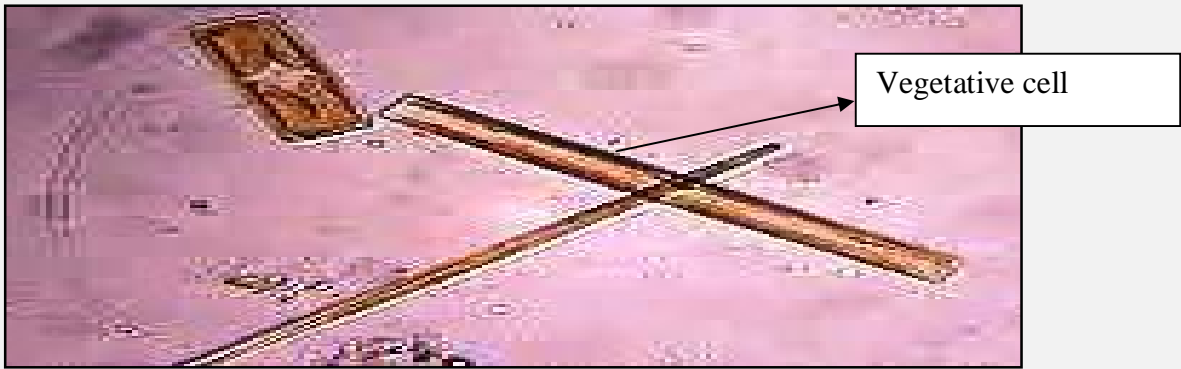




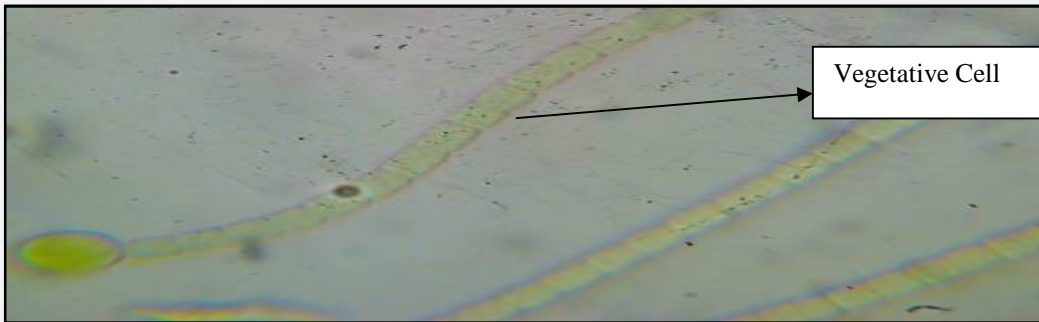
Ritu Singh Rajput et al.,



I



J



K





RESEARCH ARTICLE

Development of Arduino-Based Trainer in Electronics Teaching Laboratory

Michael P. Yujoco^{1*}, Ronita E. Talingting¹ and Edilmar P. Masuhay²

¹Surigao State College of Technology, Surigao City, Philippines

²Surigao State College of Technology-Mainit Campus, Surigao del Norte, Philippines

Received: 05 Feb 2021

Revised: 15 Feb 2021

Accepted: 25 Feb 2021

*Address for Correspondence

Michael P. Yujoco

Surigao State College of Technology,
Surigao City, Philippines



This is an Open Access Journal / article distributed under the terms of the **Creative Commons Attribution License** (CC BY-NC-ND 3.0) which permits unrestricted use, distribution, and reproduction in any medium, provided the original work is properly cited. All rights reserved.

ABSTRACT

The paper assessed the feasibility in the development of Arduino Based Trainer in Electronics Teaching Laboratory. Combined Qualitative and Quantitative designs specifically developmental, inferential and descriptive were utilized in the study employing the Frequency count and percent, mean and ordinal rank, Kruskal-Wallis ANOVA and Friedman test and Wilcoxon test with Bonferroni correction in analysing the data. Findings revealed that the 3 groups of respondent unanimously evaluated as “Agree” the Trainer as financially feasible and “Strongly Agree” that it is feasible in terms of technical, management, marketing, and educational and socio-economic factors. There was no significant difference on the feasibility of the proposed device to the type of respondents. Likewise, no significant difference on the feasibility of the proposed device among the five factors. The study concluded that the Arduino – Based Trainer is affordable, attractive, handy, easy to operate and maintain, low voltage and easy to market and it is very feasible to be used in electronics teaching laboratory.

Keywords: Arduino, Trainer; Electronics Laboratory; Technical Management and Marketing; Educational Socio-Economic Feasibility.

INTRODUCTION

The use of Instructional materials in teaching is considerably significant in the learning process of the students. Its importance cannot be underestimated by using textbooks, charts, models, graphics, real objects as well as improvised materials as they complement in the efficiency and effectiveness in the delivery of instructions by the teacher. Ajoke (2017) disclosed that the instructional materials help improve students' academic performance in school as it provides the much needed sensory experiences for an effective and meaningful behavioral change. The performance of the students on the intended learning outcomes offers the validation – twist on the success of the interaction and instruction in the classroom.





Michael P. Yujoco et al.,

Reforms in teaching Electronics subject in school are the concern of every teacher for the students to reflect the technological changes and objectives of education in the twenty-first century. One of the objectives is to foster student’s broad competencies in designing, in problem solving, in creative thinking and teamwork conventional to electronics hardware instruction, and to programmable devices considering that teaching electronics is placing greater emphasis on project-based learning. The development of Arduino Based Trainer in teaching electronics laboratory is considered one of the effective devices to be utilized as a teaching strategy that would capture the learning interest of the students. Aside from being affordable, it reduces the work load of the teacher and provides convenience on the part of the students. (“Arduino Technology Architecture and Its Applications,” 2021).

This study assessed the development of Arduino Based Trainer in Teaching Electronics Laboratory more probably the technical design and financial developed by the trainer was determined. The feasibility of the trainer device in regards to technical, financial, marketing, management, educational and socio-economic feasibility was also assessed. Significant difference of respondents as to the feasibility levels of the Arduino-Based trainer in electronics teaching laboratory and significant difference among the factors of feasibility of the trainer in electronics teaching laboratory were also determined. This paper also ascertained the technology management philosophy which was derived from the interplay of the variables in the study.

METHODS

Research Design

This study made use of the combined qualitative and quantitative designs specifically, developmental, inferential and descriptive. These designs were considered appropriate because the study assessed the feasibility in the development of electronics teaching laboratory in terms of technical, management, financial and marketing aspects (Adamson, 2005);

The Technical Designs in the Development of Arduino Trainer

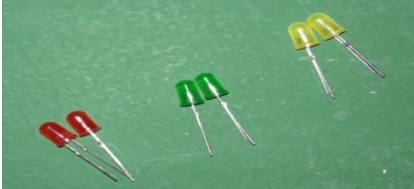
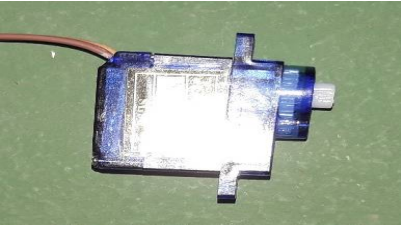
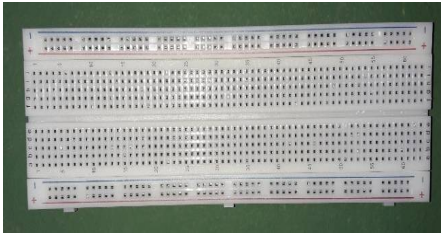
Materials

Parts of Arduino-Based Trainer and Function	Picture
<p>Aluminum Box with Glass and Lock – A box made of aluminum which is a lightweight metal with glass on the top portion and lock for safety to transport.</p>	
<p>Arduino Uno Board - is an open-source microcontroller board based on the Microchip ATmega328P microcontroller and developed by Arduino. The board is equipped with sets of digital and analog input/output (I/O) pins that may be interfaced to various expansion boards (shields) and other circuits.</p>	





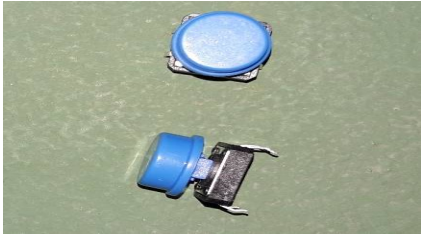
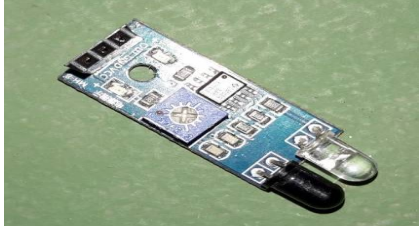
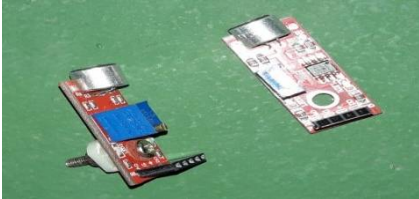
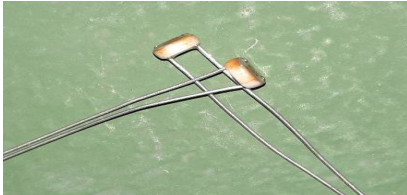
Michael P. Yujoco et al.,

<p>Arduino Uno Transparent Case - is a two-piece injection-moulded ABS enclosure that snaps together around the Arduino Uno. Holds the Arduino Uno firmly in place. It provides tough protection for the Arduino Uno while providing access to all Arduino Uno's connectors. Includes reset key for use with the board's reset button.</p>	
<p>LCD 1602 - A kind of dot matrix module to show letters, numbers, and characters and so on. It's composed of 5x7 or 5x11 dot matrix positions; each position can display one character. There's a dot pitch between two characters and a space between lines, thus separating characters and lines.</p>	
<p>8X8 LED Dot Matrix Display - is an 8x8 matrix which has 8 columns and 8 rows, contains a total of 64 LEDs. The MAX7219 chip makes it easier to control the dot matrix, by just using 3 digital pins of the Arduino board.</p>	
<p>Light Emitting Diode (LED) - is an electronic device that emits light when an electrical current is passed through it.</p>	
<p>Micro Servo Mini SG90 - Tiny and lightweight with high output power. Servo can rotate approximately 180 degrees (90 in each direction).</p>	
<p>MB102 Bread Board - Is a construction base for prototyping of electronics. Originally the word referred to a literal bread board, a polished piece of wood used for slicing bread. In the 1970s the solder less breadboard (a.k.a. plug board, a terminal array board) became available and nowadays the term "breadboard" is commonly used to refer to these.</p>	





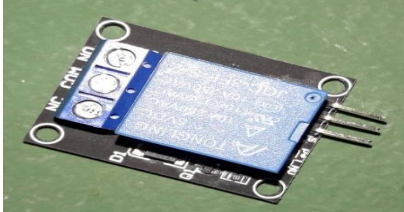
Michael P. Yujoco et al.,

<p>10k Potentiometer - is a three-terminal resistor with a sliding or rotating contact that forms an adjustable voltage divider. If only two terminals are used, one end and the wiper, it acts as a variable resistor or rheostat.</p>	
<p>Momentary push button switch with Caps - A type of switch usually in the form of a push button that is only engaged while it is being depressed, as opposed to a typical "on/off" switch, which latches in its set position.</p>	
<p>Switch Rocker 2 pin - is an on/off switch that rocks (rather than trips) when pressed, which means one side of the switch is raised while the other side is depressed much like a rocking horse rocks back and forth.</p>	
<p>IR Infrared Obstacle Avoidance - Is a multipurpose infrared sensor which can be used for obstacle sensing, color detection, fire detection, line sensing, etc. and also as an encoder sensor.</p>	
<p>Sound Detection Sensor Module - Is a small board that combines a microphone and some processing circuitry, it has the ability to detect different sizes of sound.</p>	
<p>Photo Resistor (LDR) - Is an active component that decreases resistance with respect to receiving luminosity on the component's sensitive surface.</p>	





Michael P. Yujoco et al.,

<p>IR Receiver Module - is hardware that sends information from an infrared remote control to another device by receiving and decoding signals.</p>	
<p>5V Piezo Buzzer Component - Is an audio signaling device, which may be mechanical, electromechanical, or piezoelectric (piezo for short).</p>	
<p>1 Channel Relay Module - is a separate hardware device used for remote device switching.</p>	

Financial

No of Item	Quantity	Description	Unit Price	Total Price
1	Box	Aluminum Box with Glass and Lock	P 1,800.00	P 1,800.00
1	Pc.	Arduino Uno Board	340.00	340.00
1	Pc.	Arduino Uno Transparent Case	150.00	150.00
1	Pc.	LCD 1602 with IIC	280.00	280.00
1	Pc.	LED Dot Matrix Display	478.00	478.00
6	Pcs.	Light Emitting Diode	8.00	48.00
1	Pc.	Micro Servo Mini SG90	228.00	228.00
1	Pc.	MB102 Bread Board	140.00	140.00
2	Pcs.	10k Potentiometer	120.00	240.00
2	Pcs.	Switches with Cap	30.00	60.00
2	Pcs.	Switch Rocker 2 pin	20.00	40.00
1	Pc.	IR Infrared Obstacle Avoidance	280.00	280.00
2	Pcs.	Sound Detector Sensor Module	90.00	180.00
2	Pcs.	Photo Resistor (LDR)	15.00	30.00
2	Pcs.	IR Receiver Modules	95.00	190.00
2	Pcs.	5V Piezo Buzzer Component	15.00	30.00
1	Pc.	1 Channel Relay Module	150.00	150.00
		Labor Cost(40% from the sub-total cost)		1,865.60
		TOTAL		Php 6,529.60

The Process Flow in the Development of Arduino Based Trainer

There are 10 steps in the development of Arduino Based Trainer in Electronics laboratory teaching





Michael P. Yujoco et al.,

Step 1. Planning and Designing.

- Create a working drawing with the materials needed for the Assembling of the box.
- Select proper sections and views where to make holes for the attachment of the Arduino parts.
- Procure all the materials needed for the assembly of the device.

List of Materials

- Aluminum Open Box
- Glass
- PVC Plastic sheet
- Soldering Lead
- Mighty Bond
- Air Box Buckle Lock

- Prepare all the hand tools and power tools needed for the fabrication including electrical testing instruments.

List of Hand Tools

- Screw Drivers (Phillips and Standard Tip)
- Electrical Pliers
- Jewelry Screw Drivers
- Utility Cutter
- Hack Saw
- Edge Cutters
- Desoldering Tool
- Soldering Iron

List of Power Tools

- Portable Electric Drill + Drill bit

Electrical Testing Instrument

- DC Voltmeter
- Ohmmeter

Step 2. Testing of Arduino Parts

All the Arduino Uno parts used for the fabrication of the device is tested for defects. It is necessary to test all the parts before it is connected to the circuit so that it is easy to troubleshoot if ever the circuit will mal-function.

Step 3. Assembling the Parts of Arduino Based Trainer

- Insert all parts to its proper location.
- Connect the parts of the fabricated device.
- Check for proper placements.

Step 4: Download Arduino Software

Download Arduino Integrated Development Environment (IDE) for the appropriate computer operating system. (www.Arduino.Cc/En/Main/Software for the Appropriate Computer Operating System. - Search Results, n.d.)

Step 5: Arduino Based Installation

This set up can be installed on the Laptop/PC





Michael P. Yujoco et al.,

Step 6: Connect Arduino USB Cable Port to Laptop

Step 7: Open the Arduino Software on the Laptop/PC.

Open the Arduino IDE software on the computer. And get to know the interface and identify the icons. This step is to set the IDE to identify the Arduino Uno being used in this work. Take note of the four most important commands; Open, Verify, Upload, Serial monitor.

Step 8: Selecting the Board

Select the board following the trend: Tools > Board>Arduino

Step 9: Select the Serial Device

Select the serial device using: Tools> Serial Port> COM 'port number'. With the Windows OS used in this work, select the COM number for the serial device of the Arduino board from the Tools/Serial Port menu.

Step 10: Final Testing of the Device

The device should be tested for its functionality. Testing whether the device will work on all the tasks to be performed. It will be tested one task to the other whether it functions as expected.

Research Environment

The study was conducted at Surigao State College of Technology, Surigao City Campus. The only State College in the province of Surigao del Norte. SSCT is mandated to provide higher vocational, professional and technological instruction and training in the fields of agriculture, fisheries, engineering and sciences, as well as short-term technical courses. Moreover, the College provides primary consideration to the integration of research/studies for the development of the Province of Surigao del Norte ((*Surigao State College of Technology*, n.d.)).

Respondents

The respondents of the study were the 4 electronics experts, 8 instructors and students from Bachelor in Electronics Technology (23), Bachelor of Science in Electronics Communication Engineering (19) and Bachelor of Science in Industrial Technology (30) of Surigao State College of Technology, Surigao City Campus.

Research Instrument

Data were gathered through a researcher-made questionnaire. The four-point Likert-type scale was used. Respondents rated each item as Strongly Agree/ Very Feasible, Agree/ Feasible, Disagree/ Less Feasible, and Strongly Agree/ Not Feasible and coded as 4(4.51-4.00), 3 (3.51-4.50), 2(2.51-3.50) and 1(1.00-2.50) respectively (Asún, Rdz-Navarro & Alvarado, 2016).

RESULTS AND DISCUSSION

The Table 1 shows that the respondents strongly agree that the Arduino- Based Trainer in Electronics Teaching Laboratory is technically feasible. This is based on the obtained average value of 3.63. It got the highest technical feasibility mean value of 3.85 in item 5 "The device is portable" and followed by the mean value of 3.76 in item 6 "It is user-friendly". Both items are described as 'strongly agree'. They also strongly agree on the rest of the items on technical feasibility except on item 4 "The device can tolerate shock if it falls from a table" which got the lowest mean value of 3.35 and item 3 "The device no unnecessary parts" with a mean value of 3.42. Although these items got the lowest mean values, the respondents agree that the trainer is technically feasible.

The Table 2 shows that the respondents agree on the financial feasibility of the Arduino- Based Trainer in Electronics Teaching Laboratory. This is based on the obtained average value of 3.45. It got the highest mean value of 3.57 in

30657





Michael P. Yujoco et al.,

item 3 “The Alduino-Based Trainer has available free software on the net”. The respondents strongly agree on this financial feasibility of the trainer. Moreover, the respondents agree on the rest of the items of financial feasibility including the statement on item 2 “has a student-friendly price” which got the lowest mean value of 3.36.

Shown in the Table 3 is an average value of 3.59 which indicates that the respondents strongly agree that the trainer has a management feasibility. It got the highest management mean feasibility value of 3.6 in item 6 “has aluminum case for its current”. This is followed by the mean value of 3.64 at item 1 “is easy to upkeep and maintain”. The respondents strongly agree on these two items. They also strongly agree on the rest of the management feasibility items including item 5 ‘is non-toxic’ which got the lowest mean value of 3.50.

Gleaned from the Table 4 is an average value of 3.59 which indicates that respondents strongly agree that the trainer is feasible inasmuch as marketing is concerned. It got the highest mean value of 3.64 in item 1 “The Alduino-Based Trainer device is saleable” and followed by a mean value of 3.61 on item 4 “response to needs of the community”. The respondents strongly agree on these items. In fact they strongly agree on the rest of the marketing feasibility statements including in item 5 “easy to market” which got the lowest mean value of 3.50.

Shown in the Table 5 is an average value of 3.80 which entails that the respondents strongly agree that the trainer has educational and socio-economic feasibility. The highest mean value of 3.88 is obtained in item 1 “It can effectively help in teaching electronics laboratory classes” and followed by the mean value of 3.87 in item 3 “It is an effective learning tool”. The respondents strongly agree on both statements. They also strongly agree in all the rest of the statements concerning educational and socio-economic feasibility of the trainer including in item 5 “It alleviates financial burden of students when making technical projects” which got the lowest mean value of 3.66.

Table 6: Shown are mean values of 3.80 for educational and socio-economic feasibility, 3.63 for technical feasibility, 3.59 for both management and marketing feasibility, and 3.45 for financial capability. The respondents strongly agree on the feasibility of the trainer in all factors except in financial feasibility to which they just agree but not much. The overall average of 3.61 indicates that the respondents strongly agree that the trainer is indeed feasible.

The Table 7 shows that the obtained Chi-Square values are 2.02 for technical, 5.42 for financial, 2.76 for management, 2.81 for marketing, and 4.34 for educational and socio-economic feasibility. These values are less than the critical Chi-square value of 5.99 at 2 degrees of freedom. With these, the null hypotheses are not rejected which entails that there is no significant difference on the evaluations of the three groups of respondents.

The Table shows that when the six factors of feasibility are compared, the obtained Chi-squared value is 80.77. This is greater than the critical chi-squared value of 9.49 at 4 degrees of freedom. This then brought the rejection of the null hypotheses which entail that there is a significant difference among the six feasibility factors.

Table 9 shows that financial feasibility obtained a Z-value of -4.62 when compared with technical feasibility, $Z=-4.23$ when compared with management feasibility, and $Z=-3.41$ when compared with marketing feasibility. Since these z-values are less than the adjusted critical z-value of -2.82, their respective null hypotheses are rejected. Similarly, educational and socio-economic feasibility obtained $Z=-5.64$ when compared with technical feasibility, $Z=-6.36$ when compared with financial feasibility, $Z=-5.85$ when compared with management feasibility, and $Z=-5.40$ when compared with marketing feasibility. The null hypotheses are also rejected.

These results entail that there is a significant difference between these pairs. Based on their mean values, educational and socio-economic feasibility turned out to have the highest mean value of 3.80 while financial feasibility turned out to have the lowest mean value of 3.45. It can be deduced then that financial feasibility is relatively the weakest and educational and socio-economic feasibility is the strongest.





Michael P. Yujoco et al.,

Technology Management Philosophy

Based from the results of the study, the Instructional Electric Device Inverted Feasibility Tendency model is hereby proposed. The model posits that the measure of feasibility of a developed educational device specifically an electronic one depicts an inverted pyramidal pattern from requirements to management and end-goal. The very purpose of developing an electronic device for instructional purposes is to aid teaching and improve learning at a minimal cost possible. This is the target. The realization of this goal starts with actual development of the device. The most basic requirement of device development is its financial feasibility. Marketing, technical and management aspects come next while educational and socio-economic feasibility takes the topmost concern. However, the achievement of feasibility of these device development aspects tend have an inverse pattern.

The model shows that financial feasibility is at the bottom indicating that it is the very first concern in realizing the desired electronic device. Without financial resources, one cannot develop a reliable electronic device. However, the area of the polygon is narrow which indicates relatively lower measure of feasibility as compared to others. This implies that this is a challenging feasibility to achieve despite its foundational importance to the entire development process because materials needed in the development of the device might be costly. Once financial constraints are overcome, other necessary aspects are considered. These are technical, management and marketability feasibility. These aspects are contained within the higher level after to financial feasibility to indicate hierarchy of the development process. The area of the polygon containing these three aspects is relatively higher than that financial of financial feasibility. This indicates that these factors have higher feasibility measure. These are less challenging to achieve as compared to financial feasibility because developers are assumed to have technical experts before deciding to develop an electronic device which are required for technical and management concerns. The target clients of a specialized electronic device are also identified at the outset of the development process.

Finally, the educational and socio-economic feasibility is placed at the topmost part of the pyramid to indicate that this is the very goal of instructional device development. The rest of the feasibility concerns are useless if this feasibility is not met. The area of its polygon is relatively the largest of the three. This entails that it has the highest measure of feasibility and the easiest to achieve since the developed device is specialized for instructional purposes.

CONCLUSION

The Arduino – Based Trainer is handy, affordable, attractive, easy to operate and maintain, low voltage and easy to market. It is very feasible to use as an aid for instruction. There is consistency on the evaluations of feasibility of the Arduino-Based Trainer in Electronics Teaching Laboratory by the students, teachers and experts. Financial feasibility is relatively the weak factor of Arduino-Based Trainer in Electronics Teaching Laboratory while the educational and socio-economic benefits are its strongest factor.

REFERENCES

1. Adamson, J. (2005). Combined qualitative and quantitative designs. *Handbook of health research methods Investigation, measurement and analysis*, 230-245;
2. Ajoke, A. R. (2017). The Importance of instructional materials in teaching English as a Second Language. *International Journal of Humanities and Social Science Invention*, 6(9), 36-44;
3. Arduino Technology Architecture and its Applications. (2021, January 8). *WatElectronics.Com*. <https://www.watelectronics.com/arduino-technology-architecture-and-applications/>;
4. Asún, R. A., Rdz-Navarro, K., & Alvarado, J. M. (2016). Developing multidimensional Likert scales using item factor analysis: The case of four-point items. *Sociological Methods & Research*, 45(1), 109-133.
5. *Surigao State College of Technology*. (n.d.). Retrieved February 5, 2021, from <https://www2.ssct.edu.ph/>;

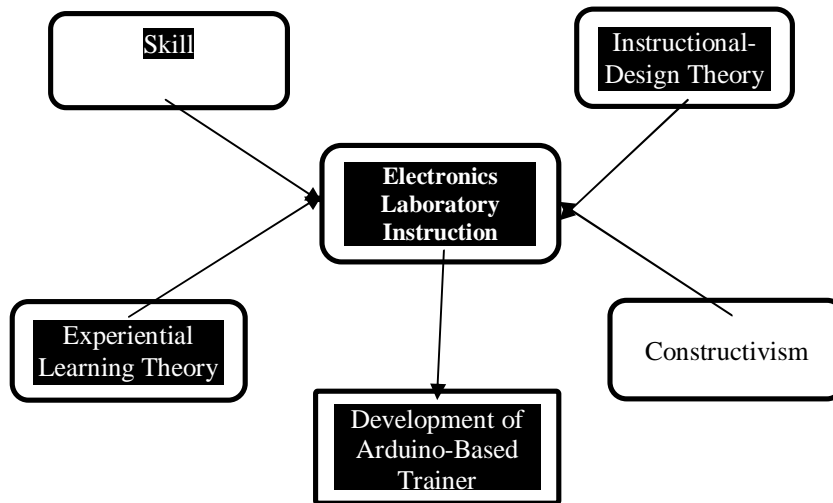




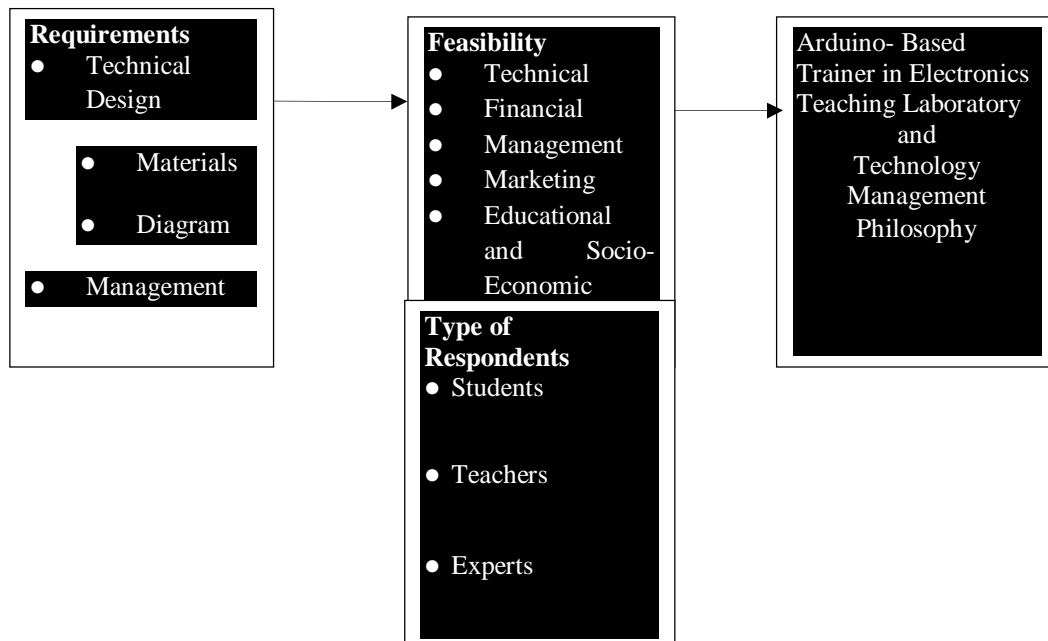
Michael P. Yujoco et al.,

6. www. Arduino.cc/en/Main/Software for the appropriate computer operating system. - Search results. (n.d.). Retrieved February 5, 2021, from https://s3arch.page/results.php?q=www.%20Arduino.cc/en/Main/Software%20for%20the%20appropriate%20computer%20operating%20system.

The Theoretical Framework of the Study



The Conceptual Framework of the Study





Michael P. Yujoco et al.,

Table 1. Respondents Evaluation Result in terms of Technical Feasibility

Statement	Mean	Rank	Description
1. Its color combination is appealing.	3.71	3.5	Strongly Agree
2. The sequencing of parts is attractive.	3.71	3.5	Strongly Agree
3. The device has no unnecessary parts.	3.42	9	Agree
4. The device can tolerate shock if it falls from a table to the ground.	3.35	10	Agree
5. The device is portable.	3.85	1	Strongly Agree
6. It is user-friendly.	3.76	2	Strongly Agree
7. It is easy to operate.	3.66	6	Strongly Agree
8. It effectively blends with available softwares.	3.53	8	Strongly Agree
9. It can test electronic circuits.	3.70	5	Strongly Agree
10. It can troubleshoot circuit problems.	3.61	7	Strongly Agree
Average	3.63		Strongly Agree

Table 2. Respondents Evaluation Result in terms of Financial Feasibility

Statement	Mean	Rank	Description
<i>The Arduino-Based Trainer device...</i>			
1. is less expensive.	3.37	4	Agree
2. has a student-friendly price.	3.36	5	Agree
3. has available free software on the net.	3.57	1	Strongly Agree
4. does not cost much to develop.	3.49	2	Agree
5. does not cost much to maintain.	3.48	3	Agree
Average	3.45		Agree

Table 3. Respondents Evaluation Result in terms of Management Feasibility

Statement	Mean	Rank	Description
<i>The Arduino-Based Trainer device...</i>			
is easy to upkeep and maintain.	3.64	2	Strongly Agree
2. has maintenance procedures.	3.55	7	Strongly Agree
3. has available tools for maintenance.	3.60	4.5	Strongly Agree
4. has available supplies and materials for maintenance.	3.57	6	Strongly Agree
5. is non-toxic	3.50	8	Strongly Agree
6. has aluminum casing for its current.	3.67	1	Strongly Agree
7. has low current or voltage.	3.60	4.5	Strongly Agree
8. It won't damage other parts in case of short-circuit.	3.63	3	Strongly Agree
Average	3.59		Strongly Agree

Table 4. Respondents Evaluation Result in terms of Marketing Feasibility

Statement	Mean	Rank	Description
<i>The Arduino-Based Trainer device is ...</i>			
1. saleable.	3.64	1	Strongly Agree
2. affordable if sold.	3.54	4	Strongly Agree
3. necessary for technical works.	3.63	2	Strongly Agree
4. responsive to needs of the community.	3.61	3	Strongly Agree
5. easy to market.	3.50	5	Strongly Agree
Average	3.59		Strongly Agree





Michael P. Yujoco et al.,

Table 5. Respondents Evaluation Result in terms of Economic Feasibility

Statement	Mean	Rank	Description
1. It can effectively help in teaching electronics laboratory classes.	3.88	1	Strongly Agree
2. It addresses economic concerns of schools.	3.74	4	Strongly Agree
3. It is an effective learning tool.	3.87	2	Strongly Agree
4. It can motivate students to learn.	3.86	3	Strongly Agree
5. It alleviates financial burden of students when making technical projects.	3.66	5	Strongly Agree
Average	3.80		Strongly Agree

Table 6. Summary on Feasibility of Arduino- Based Trainer in Electronics Teaching Laboratory

Factor	Mean	Rank	Description
Technical	3.63	2	Strongly Agree
Financial	3.45	5	Agree
Management	3.59	3.5	Strongly Agree
Marketing	3.59	3.5	Strongly Agree
Educ'l & Socio-Economic	3.80	1	Strongly Agree
Overall Average	3.61		Strongly Agree

Table 7. Difference on Feasibility of Arduino- Based Trainer in Electronics Teaching Laboratory by Profile

Factor	df	χ^2	$\chi^2_{0.05}$	Decision on Ho
Technical	2	2.02	5.99	Not Rejected
Financial	2	5.42	5.99	Not Rejected
Management	2	2.76	5.99	Not Rejected
Marketing	2	2.81	5.99	Not Rejected
Educ'l & Socio-Economic	2	4.34	5.99	Not Rejected

Table 8. Difference on Feasibility of Arduino- Based Trainer in Electronics Teaching Laboratory among Factors

df	χ^2	$\chi^2_{0.05}$	Decision on Ho
4	80.77	9.49	Rejected

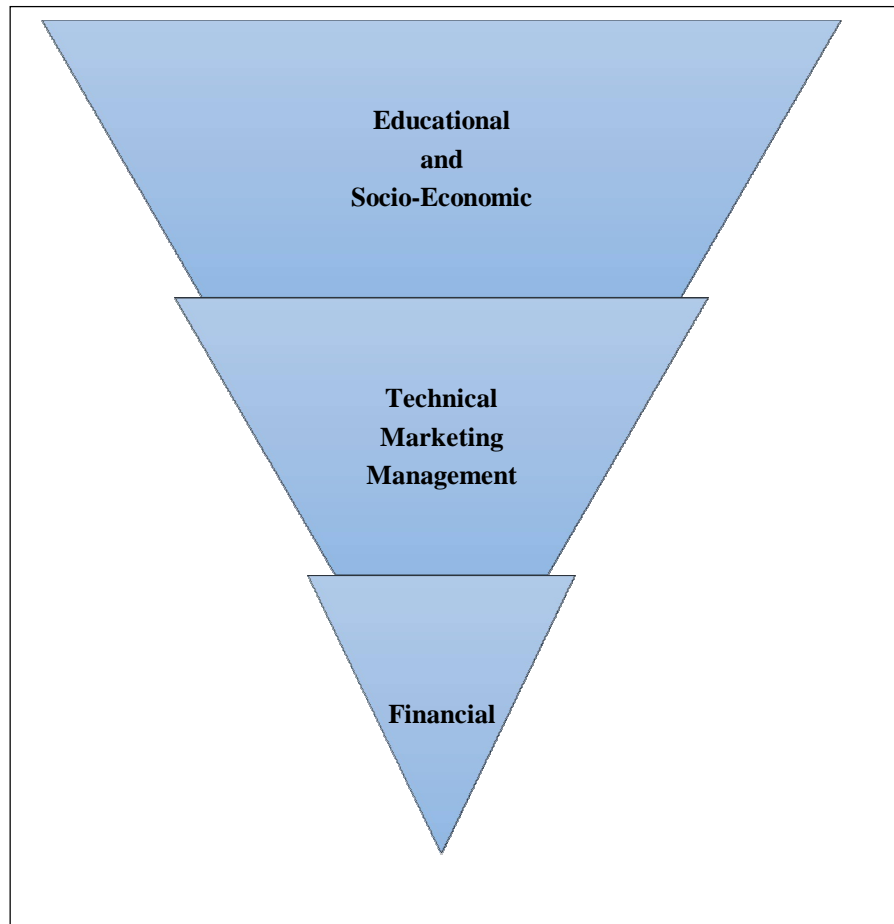
Table 9. Post Hoc Test for Difference on Feasibility of Arduino- Based Trainer in Electronics Teaching Laboratory by Profile

Factor	Z	Z _{0.05}	Adj Z _{0.005}	Decision on Ho
Technical (M=3.63) Financial (M=3.45)	-4.62	±1.96	±2.82	Rejected
Technical (M=3.63) Management (M=3.59)	-1.08	±1.96	±2.82	Not Rejected
Technical (M=3.63) Marketing (M=3.59)	-1.47	±1.96	±2.82	Not Rejected
Technical (M=3.63) Educ'l & SE (M=3.80)	-5.64	±1.96	±2.82	Rejected
Financial (M=3.45) Management (M=3.59)	-4.23	±1.96	±2.82	Rejected
Financial (M=3.45) Marketing (M=3.59)	-3.41	±1.96	±2.82	Rejected
Financial (M=3.45) Educ'l & SE (M=3.80)	-6.36	±1.96	±2.82	Rejected
Management (M=3.59) Marketing (M=3.59)	-1.05	±1.96	±2.82	Not Rejected
Management (M=3.59) Educ'l & SE (M=3.80)	-5.85	±1.96	±2.82	Rejected
Marketing (M=3.59) Educ'l & SE (M=3.80)	-5.40	±1.96	±2.82	Rejected





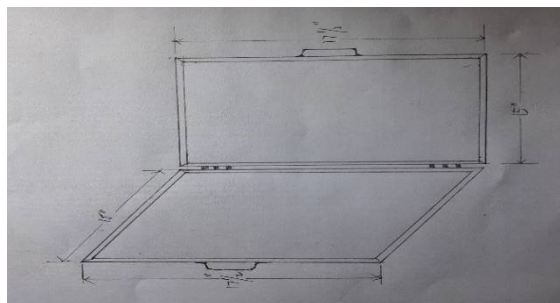
Michael P. Yujoco et al.,



**Instructional Electronic Device's
Inverted Feasibility Tendency Model**

APPENDICES

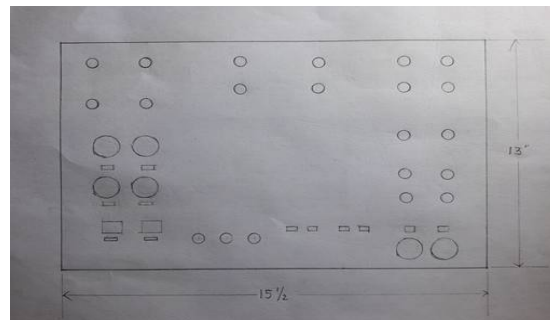
Create a working drawing with the materials needed for the Assembling of the box.





Michael P. Yujoco et al.,

Select proper sections and views where to make holes for the attachment of the Arduino parts.



Testing of Arduino Parts

All the Arduino Uno parts used for the fabrication of the device is tested for defects. It is necessary to test all the parts before it is connected to the circuit so that it is easy to troubleshoot if ever the circuit will mal-function.



Assembling the Parts of Arduino Based Trainer

- Insert all parts to its proper location



- Connect the parts of the fabricated device.





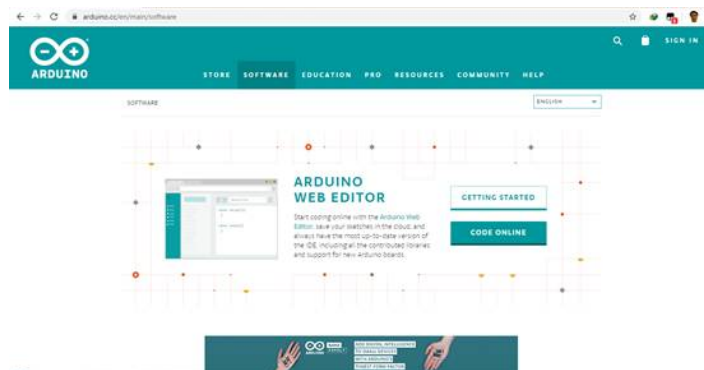
Michael P. Yujoco et al.,

- Check for proper placements.



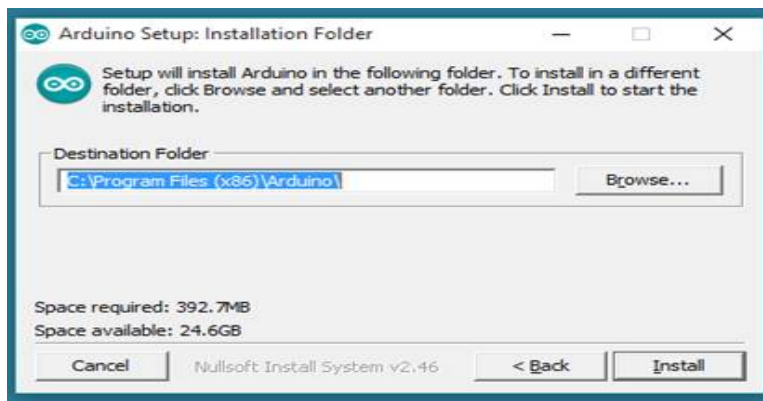
Download Arduino Software

Download Arduino Integrated Development Environment (IDE) from [www. Arduino.cc/en/Main/Software](http://www.Arduino.cc/en/Main/Software) for the appropriate computer operating system.



Arduino Based Installation

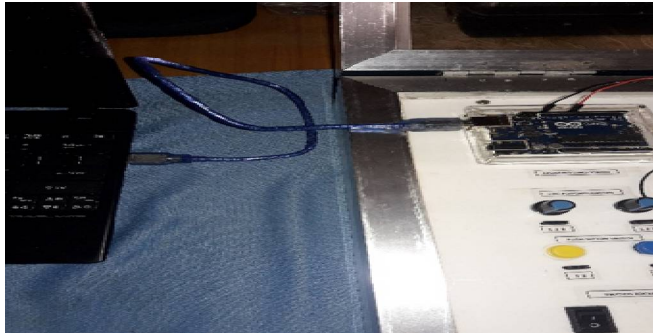
This set up can be installed on the Laptop/PC





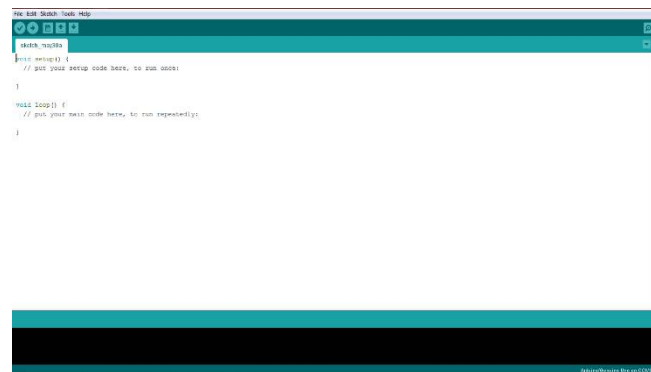
Michael P. Yujoco et al.,

Connect Arduino USB Cable Port to Laptop



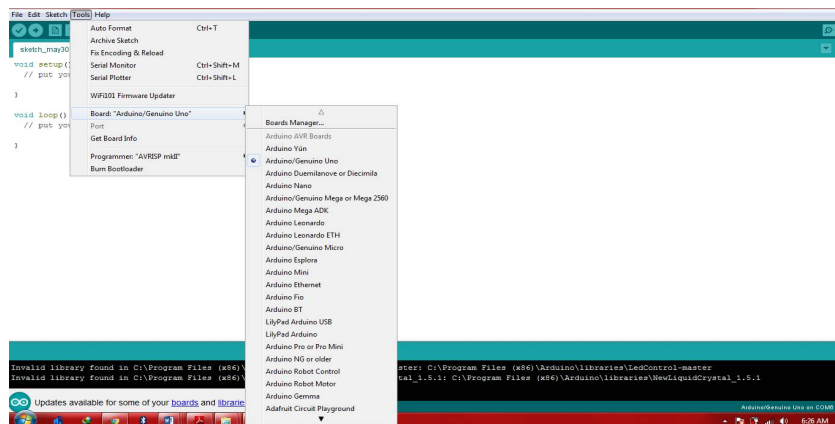
Open the Arduino Software on the Laptop/PC.

Open the Arduino IDE software on the computer. And get to know the interface and identify the icons. This step is to set the IDE to identify the Arduino Uno being used in this work. Take note of the four most important commands; Open, Verify, Upload, Serial monitor.



Selecting the Board

Select the board following the trend: Tools > Board>Arduino

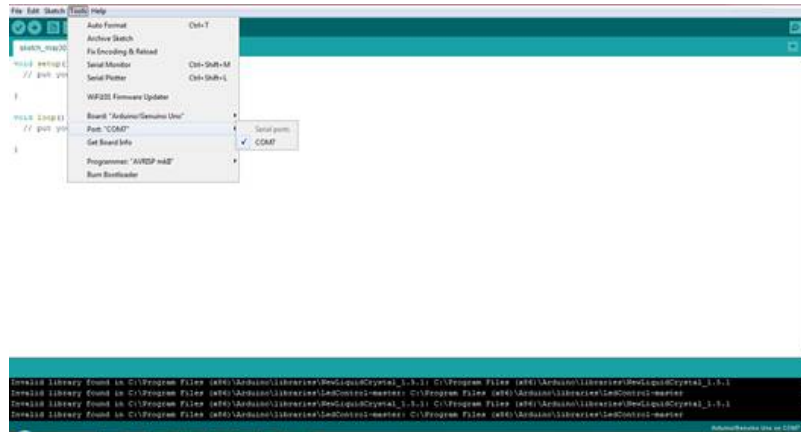




Michael P. Yujoco et al.,

Select the Serial Device

Select the serial device using: Tools> Serial Port> COM 'port number'. With the Windows OS used in this work, select the COM number for the serial device of the Arduino board from the Tools/Serial Port menu.



Final Testing of the Device

The device should be tested for its functionality. Testing whether the device will work on all the tasks to be performed. It will be tested one task to the other whether it functions as expected.





RESEARCH ARTICLE

***In-silico* Screening of a Core Scaffold Pyrazolone Fused Heterocyclic Analogues as Potent Biological Agent**

Sumathy Arunachalam^{1*}, Suresh Ramalingam², Gowrishankar Narayanasamy Lachmanan¹ and Srinivasan Nagarajan²

¹Department of Pharmaceutical Chemistry, Prime College of Pharmacy, Palakkad, Kerala, India.

²Department of Pharmacy, Faculty of Engineering and Technology, Annamalai University, Chidambaram, Tamil Nadu, India.

Received: 09 Feb 2021

Revised: 20 Feb 2021

Accepted: 26 Feb 2021

***Address for Correspondence**

Sumathy Arunachalam,

Associate Professor,

Department of Pharmaceutical Chemistry,

Prime College of Pharmacy, Palakkad, Kerala, India.

Email: sumathy512@gmail.com



This is an Open Access Journal / article distributed under the terms of the **Creative Commons Attribution License** (CC BY-NC-ND 3.0) which permits unrestricted use, distribution, and reproduction in any medium, provided the original work is properly cited. All rights reserved.

ABSTRACT

Globally, there were 1.2 million new cases of prostate cancer registered which representing 7.1% of all cancers in men. Prostate cancer incidence rates are highly variable worldwide. Even though, several drugs available for the treatment of prostate cancer, its side effects by damaging the other cells are huge due to its anti-cytotoxic activity, hence a study was aimed to perform a docking and *In-silico* screening of core scaffold pyrazolone fused heterocyclic analogues as potent therapeutic agent for prostate cancer. Molecular docking was performed on a diverse set of substituted pyrazolone fused derivatives as potent anti-prostate cancer agents by targeting on Androgen Receptor (AR). The compounds are characterized by melting point, TLC, FTIR, H¹NMR and mass spectroscopy. Pyrazolone was used as an intermediate for synthesizing the study compounds. Among the designed analogues the significant binding energy and inhibitory constant were compared with standard drug, Enzalutamide. The speculated results have been compared with the laboratory screening in ongoing research methods adopted. Primary five moieties synthesized were docked by using software IGEM DOCK. The studies on structure activity relationship showed the presence of electron withdrawing substitution in pyrazolone derivatives which significantly improves the binding with protein. The compound T2 (-49.3984) shown lowest and the compound T5 (-70.2138) shown highest binding energies, whereas compound T3 (-60.1253) and T4 (-61.1289) shown moderate binding energy compared to the standard drug Enzalutamide. Result of pharmacokinetics prediction revealed most of these compounds tested has *in-silico* drug likeliness. The Schiff Base substituted pyrazolone derivatives was found to possess a moderate cytotoxicity effects. Even though the synthesised compounds shown moderate to high binding energy compared to standard drug,





Sumathy Arunachalam et al.,

extensive studies need to be carried out to find out compounds with highest binding energy. Studies at receptor level are warranted to target the prostate cancer cells even at the initial stage of cancer.

Keywords: *In-silico*, Pyrazolone, IGEM DOCK, Anticancer, Enzalutamide, 1Z8Lprotein

INTRODUCTION

Prostate cancer (PCa) is the second and most common malignant form of cancer among men worldwide. Drugs acting as antagonists or partial agonists of hormone receptors against the prostate tissue are mainly used as maintenance therapy in PCa [1-3]. This research focus has led to the development of novel analogues (pyrazolone fused heterocyclic moieties) which do not show any cytotoxic activity and have significant inhibition on androgen receptor (AR). In drug designing, the protein-ligand interactions play a major role which is commonly studied using molecular docking [4-7]. Molecular docking as a problem of "lock-and-key", in which one wants to find the correct relative orientation of the "key" which will open up the "lock" (where on the surface of the lock is the key hole, which direction to turn the key after it is inserted, etc.). Here, the protein can be thought of as the "lock" and the ligand can be thought of as a "key". Molecular docking may be defined as an optimization problem, which would describe the "best-fit" orientation of a ligand that binds to a particular protein of interest. However, since both the ligand and the protein are flexible, a "hand-in-glove" analogy is more appropriate than "lock-and-key". During the course of the docking process, the ligand and the protein adjust their conformation to achieve an overall "best-fit" and this kind of conformational adjustment resulting in the overall binding is referred to as "induced-fit".

Molecular docking research focuses on computationally simulating the recognition process. It aims to achieve an optimized conformation for both the protein and ligand and relative orientation between protein and ligand such that the free energy of the overall system is minimized. Pyrazolone, a heterocyclic compound that is commonly used as an intermediate for synthesizing numerous pharmaceutical compounds. Pyrazolone molecules has been shown to possess a wide spectrum of biological activities such as tranquillizing, psychoanaleptic, antihypertensive, and antitumour. Pyrazolone fused heterocyclic were screened for *in-silico* drug likeliness properties based on the pharmacokinetics such as absorption, distribution, metabolism, and excretion prediction. The current study was aimed to screen the designed analogues and investigate its binding affinity against AR.

MATERIALS AND METHODS

In the present study, molecular docking was performed using IGEM DOCK. The construction and energy minimization were also done using Chemdraw ultra 12.0, IGEM DOCK was used to create a ligand based computer modelling algorithm for the binding energy prediction and inhibition constants calculation of the designed anticancer scaffolds with the 1Z8Lprotein [13,14]. The protein sequence retrieval system NCBI and Microbial Genome Database were also used to retrieve the study materials.

Preparation of the Protein Structure

The required protein structures were acquired from Protein Data Bank (PDB ID: 1Z8L). The proteins were prepared using the Protein Preparation Wizard [15-17]. The Protein was optimized prior docking using MOE software. Pre-processed bond orders were assigned, water molecules were deleted, hydrogens were added, and metals were treated. Energy was reduced using RMSD 0.30°A. By using the site score and site's hydrophilic or hydrophobic areas with better cavity, the best binding pockets were selected.





Sumathy Arunachalam et al.,

Preparation of Ligand

The ligand molecules for the process of docking are mostly metal complex compounds [18,19]. Chemdraw software was used to draw the ligand structures. Prior to docking, the structures were optimized using MOE software. The commonly used iGEMDOCK software normally accepts SYBYL MOL2, MDL MOL, and PDB format for ligand files [20]. Hence, the ligand files were transformed into PDB format using Chemdraw 3D. Later, the ligand was docked using accurate docking function with their binding sites of each PDB files (Standard docking). Finally, the compounds are ranked using the post analysis tool visualization and screened by combining the pharmacological interactions and energy-based scoring function.

Docking Methodology

Docking Module

Protein with the drug and the standard compounds were docked using iGEM docking software. iGEMDOCK, provides an integrated virtual screening environment from preparations through the post-screening analysis and pharmacological interactions [20-22]. This software delivers interactive interfaces that ease the preparation of both binding site of the target protein and also the screening compound library. Each compound present in the library is later docked with the binding site using in-house docking tool iGEMDOCK. The protein-compound interaction profiles of hydrogen-bonding (H), electrostatic (E), and the Van der Waal's (V) interactions were studied with iGEMDOCK [23]. Based on these resulted profiles and compound structures, iGEMDOCK gathers the compounds' pharmacological interactions and groups the screening compounds for post-screening analysis. Lastly, it ranks and visualizes the compounds by linking its pharmacological interactions and the energy-based scoring function in iGEMDOCK. The three-dimensional (3D) structures of AR was obtained from the Protein Data Bank, and docked using 3D Pubchem structures IGEM DOCK. Molecular docking and drug likeness of compounds are carried out using absorption, distribution, metabolism, excretion and toxicity (ADMET) properties while Lipinski's rule of five has been performed for planned analogues to evaluate its anti-prostate cancer activity [8,9]. The finding showed that the speculated analogues exhibits best binding affinity with AR. The speculation was done by inhibiting AR signaling pathways [10-12] and compared with the standard drug Enzalutamide which is a potent androgen receptor antagonist [11-13].

RESULTS AND DISCUSSION

Docking results of 1Z8L protein with ligands (T1-T5) were observed using Igemdock software docking scores (Total energy). The data are presented in Table 1. The protein-ligand (drug) interactions binding energies are very important to define how exactly the drug binds to the target macromolecule(s). The binding energy between ligand and protein 1Z8L is calculated using iGEMDOCK [21-23]. The dock possess are analysed and their docking interaction are listed above in table 1. The 5 compounds were docked at the active site of the protein and by analysing it we can calculate the compounds that have maximum binding energy compare with standard (Enzalutamide). From those results we found that the compound T2 (-49.3984) shows lowest and the compound T5 (-70.2138) shows highest binding energies. In this result shows T2 (-49.3984) have minimum binding energy, then T3 (-60.1253) and T4 (-61.1289) shows moderate binding energy and T1 (-68.1081) and T5 (-70.2138) shows maximum binding energy when compared to standard drug Enzalutamide.

CONCLUSION

Pyrazolones are a nitrogenous compounds containing five membered lactumring with one ketone group in its structure. It has divergent activities like antimicrobial, antibacterial, antimycobacterial, anti-inflammatory, including anticancer activities. In this study, an attempt has been made to combine the pyrazolone compounds with Schiff base and various aromatic amines. It could maintain the anticancer properties of the novel scaffolds derivatives; however, their mode of action varies from that of standard drug. The molecular stimulation studies of the intended



**Sumathy Arunachalam et al.,**

compounds shown a light to the newer areas for the synthesis and also the experimental evaluation, which evident the anticancer activity of the compounds compared to the standard. The *in-silico* study reveals that the designed pyrazolone fused heterocyclic analogues have antiprostata cancer effect by targeting the androgen receptor. The designed analogues are focused to show significant cytotoxicity against human prostate cancer cell line androgen dependent (LNCaP) as well as antiandrogenic activity. The Schiff Base substituted pyrazolone derivatives was found to possess a moderate cytotoxicity effect by literature, which will be extensively studies in future by incorporating few heterocyclic nuclei such as thiazolidionone, oxadiazole and azetidinone. The current research focus using the standard drug (Enzalutamide) for prostate cancer is being done due to the heterocyclic moiety, which is similar to the pyrazolone analogue with a difference of nitrogen positions. Future speculations need to be carried out at receptor levels in extended ongoing research activity.

REFERENCES

1. Morgan TM, Koreckij TD, Corey E. Targeted therapy for advanced prostate cancer: inhibition of the PI3K/Akt/mTOR pathway. *Current Cancer Drug Targets*. 2009;9(2):237-49. DOI: 10.2174/156800909787580999.
2. Andrea PM, Lewis CC. Targeting a common collaborator in cancer development. *Science Translational Medicine*. 2010;2(48):45-48. DOI: 10.1126/scitranslmed.3001251.
3. Liu H, Zhang L, Zhang X, Cui Z. PI3K/AKT/mTOR pathway promotes progesterin resistance in endometrial cancer cells by inhibition of autophagy. *Onco Targets and Therapy*. 2017;10:2865-71. DOI: 10.2147/OTT.S95267.
4. Saidachary G, Veera Prasad K, Divya D, Ashita S, Ramesh U, Sridhar B, China Raju B. Convenient one-pot synthesis, antimycobacterial and anticancer activities of novel benzoxepinoisoxazolones and pyrazolones. 2014;76:460-469. *European Journal of Medicinal Chemistry*. 2014;76:460-9. DOI: 10.1016/j.ejmech.2014.02.042.
5. Parmar N, Shashikant T, Rikin P, Barad H, Jajda H, Thakkar V. Synthesis, antimicrobial and antioxidant activities of some 5-pyrazolone based schiff bases. *Journal of Saudi Chemical Society*, 2015;19(1):36-41. <https://doi.org/10.1016/j.jscs.2011.12.014>.
6. Ramajayam R, Tan KP, Liu HG, Liang PH. Synthesis and evaluation of pyrazolone compounds as SARS-coronavirus 3C-like protease inhibitors. *Bioorganic & Medicinal Chemistry*. 2010;18:7849-54. Available from: <https://dokumen.tips/documents/synthesis-and-evaluation-of-pyrazolone-compounds-as-sars-coronavirus-3c-like.html>.
7. GunizKuçukguze S, Rollas S, Erdeniz H, Kiraz M, Cevdet Ekinci A, Vidin A. Synthesis, characterization and pharmacological properties of some 4-arylhydrazono-2-pyrazoline-5-one derivatives obtained from heterocyclic amines. *European Journal of Medicinal Chemistry*. 2000;35(7-8):761-71. DOI: 10.1016/s0223-5234(00)90179-x.
8. Andrew D, Simon EW. *The Handbook of Medicinal Chemistry: Principles and Practice*. Royal Society of Chemistry, Cambridge, UK. 2015. Available from: http://www.pharma2z.com/wp-content/uploads/2019/03/Andrew-Davis-Simon-E-Ward-eds.-The-handbook-of-medicinal-chemistry-_-principles-and-practice.pdf.
9. Balbas MD, Evans MJ, Hosfield DJ, Wongvipat J, Arora VK, Watson PA, et al. Overcoming mutation based resistance to antiandrogens with rational drug design. *Elife*. 2013;2:e00499. DOI: 10.7554/eLife.00499.
10. Beer TM, Armstrong AJ, Rathkopf DE, Loriot Y, Sternberg CN, Higano CS, et al. Enzalutamide in metastatic prostate cancer before chemotherapy. *New England Journal of Medicine*. 2014;371(5):424-33. DOI: 10.1056/NEJMoa1405095.
11. Scher HI, Fizazi K, Saad F, Taplin ME, Sternberg CN, Miller K, et al. Increased survival with enzalutamide in prostate cancer after chemotherapy. *New England Journal of Medicine*. 2012;367(13):1187-97. DOI: 10.1056/NEJMoa1207506.
12. Rubina B, Dharam PP, Asif H, Garima K, Ravi K. A review on recent development of pyrazoline as a pharmacologically active molecule. *International Journal of Pharmaceutical Sciences and Research*. 2015;6(10):4113-28. DOI: 10.13040/IJPSR.0975-8232.6(10).4113-28.





Sumathy Arunachalam et al.,

13. Thirunarayanan G, Sekar KG. SiO₂-H₂SO₄ catalysed, microwave-assisted cyclization cum acetylation of 2-propenones under solvent-free condition: Synthesis and spectral correlations of some 1-acetyl pyrazolines. *Journal of Taibah University for Science*. 2014;8:124-36. <https://doi.org/10.1016/j.jtusci.2013.11.003>.
14. Vijayvergiya D, Kothari S, Verma BL. Synthesis and biological activity of some new 3,5-diaryl-1-phenyl/isonicotinoyl-2-pyrazolines and 3,5-diaryl-6-carbomethoxy cyclohexenone derivatives. *Indian Journal of Heterocyclic Chemistry*. 2003;13(2):105-10.
15. Gurubasavaraj VP, Synesh C, Madhusudan NP, Srinivasalu N, Udupi RH. Synthesis, anticonvulsant and antibacterial activities of some novel pyrazolines derived from benzoxazole and benzimidazole. *Indian Journal of Heterocyclic Chemistry*. 2008;17(4):387-8.
16. Sampson PB, Picard C, Handerson S, McGrath TE, Domagala M, Andrew Leeson, et al. Spiro-naphthyridinonepiperidines as inhibitors of *S. aureus* and *E. coli* enoyl-ACP reductase (FabI). *Bioorganic & Medicinal Chemistry Letters*. 2009;19(18):5355-8. DOI: 10.1016/j.bmcl.2009.07.129.
17. Reddy GV, Maitraie D, Narshiah B, Rambabu Y, Rao PS. Microwave assisted Knoevenagel condensation: a facile method for the synthesis of chalcones. *Synthetic Communications*. 2001;31(18):2881-4. <https://doi.org/10.1081/SCC-100105339>.
18. Mark AS, William HM, Kenneth AN, Walter JB, David JP, Stephen FR, et al. Inhibitors of bacterial enoyl acyl carrier protein reductase (FabI): 2,9-disubstituted 1,2,3,4-tetrahydropyrido[3,4-b]indoles as potential antibacterial agents. *Bioorganic & Medicinal Chemistry Letters*. 2001;11(17):2241-4. [https://doi.org/10.1016/S0960-894X\(01\)00405-X](https://doi.org/10.1016/S0960-894X(01)00405-X).
19. Mohamad Y, Payal J. Synthesis and biological studies of pyrazolines and related heterocyclic compounds. *Arabian Journal of Chemistry*. 2014;7(5):553-96. <https://doi.org/10.1016/j.arabjc.2011.09.013>.
20. Babu VH, Sridevi CH, Joseph A, Srinivasan KK. Synthesis and biological evaluation of some novel pyrazolines. *Indian Journal of Pharmaceutical Sciences*. 2007;69(3):470-3. DOI: 10.4103/0250-474X.34569.
21. Yang JM. Development and evaluation of a generic evolutionary method for protein-ligand docking. *Journal of Computational Chemistry*. 2004;25(6):843-57. DOI: 10.1002/jcc.20013.
22. Jinn-Moon Y, Tsai-Wei S. A pharmacophore-based evolutionary approach for screening selective estrogen receptor modulators. *Proteins*. 2005;59(2):205-20. <https://doi.org/10.1002/prot.20387>.
23. Macke TJ, Ecker DJ, Gutell RR, Gautheret D, Case DA, Sampath R. RNAMotif, an RNA secondary structure definition and search algorithm. *Nucleic Acids Research*. 2001;29(22):4724-35. DOI: 10.1093/nar/29.22.4724.

Table 1. The interaction energies (kcal mol⁻¹) of 1Z8L and ligands

S.No	Lead Compound	Total energy	VDW	H-bond	Aver Con Pair
1	T1	-68.1081	-62.1081	-6	16.3667
2	T2	-49.3984	-49.3984	0	14.3667
3	T3	-60.1253	-43.8403	-16.285	13.5484
4	T4	-61.1289	-50.5629	-10.566	13.2581
5	T5	-70.2138	-52.5808	-17.6331	13.9375
6	Standard	-74.4023	-37.978	-36.4243	17.8485

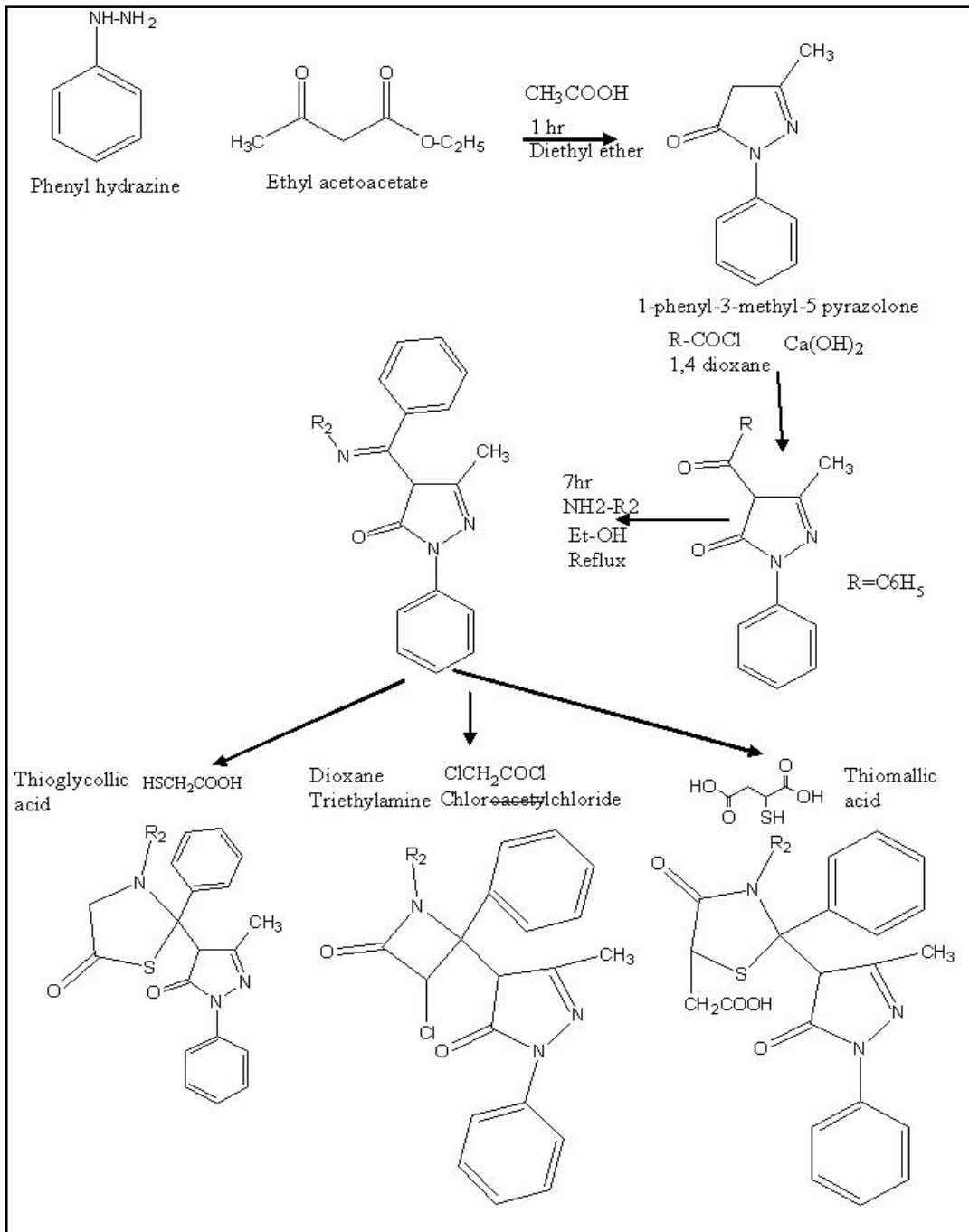




Sumathy Arunachalam et al.,

Design of the Pyrazolone Fused Heterocyclic Analogues as 1Z8L Antagonist

General Scheme for the Synthesis





Sumathy Arunachalam et al.,

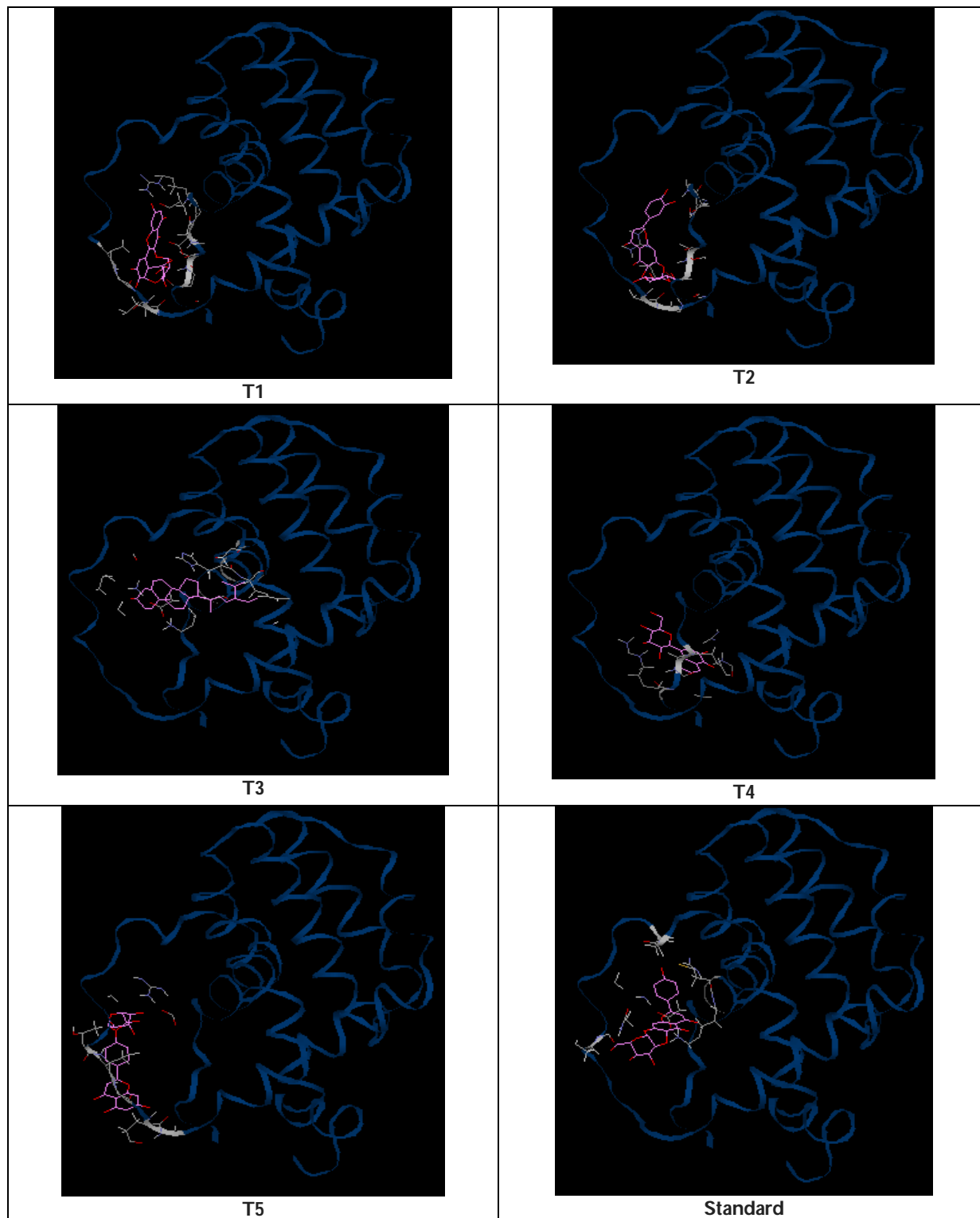


Fig 1. BINDING interaction of 1Z8L WITH LIGAND (T1-T5)





A Critical Insight Alkaloids as an Influenza H1N1 Pandemic Survivor

Shivangi Maurya, Anjali Shukla and Nainesh Modi*

Department of Botany, Bioinformatics and Climate Change Impacts Management, School of Science, Gujarat University, Ahmedabad, Gujarat, India.

Received: 10 Mar 2021

Revised: 20 Mar 2021

Accepted: 27 Mar 2021

*Address for Correspondence

Nainesh Modi

Department of Botany,
Bioinformatics and Climate Change Impacts Management,
School of Science, Gujarat University,
Ahmedabad, Gujarat, India.
Email: nrmodi@gujaratuniversity.ac.in



This is an Open Access Journal / article distributed under the terms of the **Creative Commons Attribution License** (CC BY-NC-ND 3.0) which permits unrestricted use, distribution, and reproduction in any medium, provided the original work is properly cited. All rights reserved.

ABSTRACT

Influenza A viruses (IAV -H1N1) are responsible for the respiratory tract, lung infection and cause a high mortality rate. Neuraminidase (NA) and hemagglutinin (HA) are the major surface glycoprotein and main targeted protein responsible for viral inhibition. There are various therapeutic drugs like zanamivir, oseltamivir and baloxavir for H1N1 in the market. This review explains the effect of plant-based secondary metabolites (Alkaloids) on IAV. Major alkaloids such as Theacrine from Kucha tea inhibit NS1 protein, TA from *Alstoniascholaris* *Peganum harmala* seed extract inhibits viral infection, TA from *Peganum harmala* seed extract inhibits RNA polymerase, Emerimidine B & Homonojirimycin inhibit the virus, Quinazoline alkaloids inhibit H1N1 stimulation and MCP-1 production, Isoquinolone & quinolizidine inhibit NA, Berberine inhibit post translation of virus. Indirubin decreases the rate of mortality in mice.

Keywords: Alkaloids, Hemagglutinin, Influenza A virus H1N1, Inhibitors, Neuraminidase

INTRODUCTION

Pandemic outbreaks have been known to occur on and off since time immemorial, causing not only social and economic harm to population but also high death tolls. The influenza virus is one of the most common strains that has been related to epidemics and pandemics [1]. During April 2009 a novel swine flu virus H1N1 was recognized in California and also detected as major outbreak of respiratory disease in Mexico [2]. Which was the combination of the pig, birds and humans influenza virus strains [3]. On the basis of antigenic composition influenza A is classified into two major surface antigens hemagglutinin (HA) and neuraminidase (NA), HA is further classified into 18 types and NA into 11 different types, it is a member of Orthomyxoviridae family [4]. H1N1 is the sub type of the swine influenza viruses this H1N1 virus called as 'classical swine' [5]. The association of the origins with the Mexican pig farming region raised suspect that porcine influenza was involved in this infection. According to World health



**Shivangi Maurya et al.,**

organization H1N1 was outbreak of pandemic character [2]. According to Smith *et al.* [6] a phylogenetic estimation shows the multiple genetic ancestry of swine origin influenza virus (S-OIV) is not an artificial origin. During the pandemic of 1918-1919 50 million people was killed worldwide, the mortality rate of 'Spanish' influenza (H1N1) was high in young adults [7]. Based on several data pregnant women are at high risk of infections due to immunological and physiological changes which affect respiratory, cardiovascular and other organs [8]. The US Centers for Disease Control and Prevention (CDC) reported the first S-OIV from a patient's specimen on April 15, 2009. The CDC discovered a second case of S-OIV infection on April 17, 2009. On April 23, 2009, the CDC held its first press conference and told the public about the outbreak. The World Health Organization (WHO) declared a global pandemic on April 26, 2009 [9]. During only in two months it became the first pandemic of 21st century and spread out among 170 countries [10]. According to a research [11] it was proven that H1N1 is a transmitted disease, they took ferret as a model because after infection their lungs and pathology behave like humans, in trachea, bronchi and bronchioles viruses were replicated and affected the upper and lower respiratory tract, virus was transmitted through aerosol or respiratory droplets [12, 13].

Influenza A viruses has single standard negative sense RNA and eight segmented genome. Size of virions are 80-120 nm in diameter and size of genome is 13.5 kb approximately, there are 8 different regions of segmented and encode 11 different types of proteins. HA and NA are envelope proteins also known as surface glycoprotein. PB2, PB1, PB1-F2, PA and PB are the viral RNA polymerase, M1 and M2 are the matrix proteins, NS1 and NS2 are nonstructural proteins and these are necessary for efficient pathogenesis and replication of viral. HA make red blood cells to cluster together which attaches the virus to the infected cells and with the help of NA virus particles moves through the infected cell helps in budding from host cells. H1N1 swine influenza viruses cause infections in humans due to changes in antigenic characters [3,14,15]. According to a retrospective analysis Fever, headache, cough, muscular pain and rhinorrhoea were the main symptoms of H1N1 infection in humans and severity of disease was not associated with Sex [16].

The modern medical system is based on medical paradigm that primarily provides symptomatic care and places a greater emphasis on therapy. It stresses substance use, mechanical testing, invasive procedures such as surgery, and a patient-centered approach [17]. While therapeutic options for viral infections have improved over the last decade, many approved drugs are toxic and costly [18]. Many drugs are available in the market for the treatment of H1N1 among which Oseltamivir and zanamivir are the NA inhibitors they blocking sialic acid cleavage on host cells and Amantadine and rimantadine M2 channel inhibitors [19-22]. Alternative and complementary drugs have been used to treat human illness for several years in different parts of the world, Ayurveda is the ancient Indian system of medicine, Traditional Chinese medicine (TCM), Unani, Siddha, Japanese traditional medicine (Kampo) and other complementary and alternative medicines fall under this group [17].

Due to opting for swine flu alternative medicines Ayurveda and swine flu got more popularity. Sahoo *et al.* discussed about plant extract of garlic, ginger, kalmegh, ajwain, green tea, turmeric, tulsi, mentha. Which are traditionally used for the treatment of influenza virus. Jyotsana [23] discussed Ayurvedic formula in her article which keep away swine flu and build immune response. Ayurveda recommends ingesting or decocting herbs that contain a particular metabolic compound that protects against swine flu [24]. The majority of antiviral drugs have side effects, necessitating the study and production of natural phytochemical-based antiviral drugs. Secondary metabolites are found in plants, and alkaloids are one of them. Generally alkaloids found in higher plants and containing nitrogenous base pair in their structure. Alkaloids possesses therapeutic activity like anticancer, antibacterial and antiasthma [25]. Alkaloids considered potentially as an anti-influenza virus agent due to effects on inhibition of IAV replication, with chemical modification they may be more effective as IAV controller [26]. The objective of this review is to compile plant-based alkaloids for their therapeutic usage and to discover other phyto-related compounds that could be used to treat various forms of harmful viruses.





Shivangi Maurya et al.,

INHIBITION OF H1N1

IAV has 100nm in diameter, it is made up of lipid bilayer and derived from host plasma membrane, there are eight negative sense single-stranded RNA (ssRNA) with polymerase proteins (PB1, PB2, and PA) and nucleoprotein (NP). There are 12 viral proteins which are encoded by eight ssRNA. HA and NA inserted into bilayer lipid as spikes beneath the lipid layer M1 matrix protein is present which is involved in nuclear export. M2 ion channel helps in pH maintenance and embedded in the lipid bilayer. Polymerase acidic protein (PA) and polymerase basic protein form RNA-dependent RNA polymerase [28]. Oseltamivir and zanamivir are the anti-flu drugs which is targeted on neuraminidase (neuraminidase inhibitors NAIs), hydrophobic residue Try347 in H1N1-NA match with the hydrophilic carboxyl group of oseltamivir [29]. Amantadine and rimantadine anti-flu drugs are the target on M2 proton channel [30]. Oseltamivir is the most widely used drug for seasonal H1N1 [22].

ALKALOIDS ACT AS INHIBITORS

Total alkaloid from *Alstonia scholaris*

Alstonia scholaris is an evergreen tree (Apocynacy family) native to Southeast Asian countries and the Indian subcontinent. Plant has been used in traditional medicines like Ayurvedic, Unani Siddha, etc. *In vivo* assays showed anti-inflammatory and analgesic effects [31]. Zohu et al. 2020 [32] described the importance of total alkaloid in their research paper by their experiment. Their experiment was on Madin-Darby canine kidney (MDCK) and A549 cells and U937-derived macrophages which were infected with influenza H1N1. In the presence of total alkaloid replication of viral was inhibited in A549 cells and derived macrophages. At the mRNA and protein levels production of cytokine and chemokine was reduced. In cell, A549 total alkaloid blocked the activation of pattern recognition receptor (PRR) and IFN activated signal transduction. Total alkaloid reduced the viral infection and increased the rate of survival, in a mouse model total alkaloid improved the lung pathology.

Total alkaloid of *Peganum harmala* seed extract

Peganum harmala is a perennial glabrous plant (Nitrariaceae family) that was initially found in central Asia but now also grows in the southwest of America, Australia, and north of Africa [33]. *Peganum harmala* has the most important alkaloid constituents like harmalol, harmaline, and harmine. *Peganum harmala* showed antiviral activity *in vitro* study. Ethyl alcohol extraction of *Peganum harmala* seeds and their total alkaloids experimented on MDCK (Madin-Darby canine kidney) cells against Influenza A virus (H1N1) After introducing the extract with viral infection it's total alkaloid showed inhibitory effect against influenza A virus and inhibit RNA replication and viral polymerase activity which resulted in that seed extract and alkaloid content of *Peganum harmala* responsible for the inhibition of viral RNA transcription and decreased the titer of virus [34].

Theacrine

Theacrine (1,3,7,9- tetramethyluric acid) is one of the major purine alkaloid present in buds and young leaves of Kucha tea, which is a Chinese tea (*Camellia assamica* var. kucha) [35]. According to a research [36] theacrine alkaloid act as anti-influenza activity and no or low cytotoxicity was observed. Theacrine inhibited the NS1 protein of the viral. They made a plaque assay which shows the viral progeny reduced by theacrine, expression of NS1 in the presence of theacrine was reduced at the concentration of 50 μ M at 12 hpi.

Emerimidine B

Many plant species have Endophytes, they are living with host cells and some of the endophytic fungi producing the compounds which are helpful in several diseases [37]. Mangroove plant *Aegiceras corniculatum* possesses endophytic fungus *Emericella* sp. Which has nitrogen-containing secondary metabolites Emerimidine. Different research suggested that this alkaloid is a major anti-viral compound and used as an anti-viral for different types of viral



**Shivangi Maurya et al.,**

strains. By using CPE inhibition assay antiviral activity against influenza A virus was evaluated which gave the positive result at 50% inhibition concentration (IC₅₀), cytoprotection against viral infection was 50% [38].

Homonojirimycin

Homonojirimycin (HNJ) is an alkaloid that is present in *Commelina communis* commonly known as day flower. Total alkaloid of *C. communis* showed the antiviral effect Zhang *et al.* 2013 [39] researched on 96 well-cultured plates cell line was MDCK, they prepared the solution by using total alkaloid with 0.1% DMSO and more than 95% of compounds, the antiviral activity of the alkaloids was determined by cytopathic effect (CEP) reduction method. After their experiment, they concluded that Homonojirimycin inhibited the growth of the influenza A virus.

Quinazoline alkaloids

Quinazoline are major alkaloids present in *Evodia rutaecarpa* which is used as an anti-inflammatory herbal remedy, in Research [40] took quinazoline alkaloids dehydroevodiamine (DeHE), rutaecarpine (Rut) and evodiamine (Evo) with ethanolic extract of *Evodia rutaecarpa* and studied inhibitory effects against H1N1. Induced chemokines production was observed in A549 lung epithelial cells and their results showed that *E. rutaecarpa* was an inhibitor of RANTES which is a protein and secreted by H1N1 in inoculated cells (A549). Evo was the most potent and inhibited H1N1 induced RANTES production. They concluded as these three major alkaloids showed different potentials for the inhibition of the cell migration and inhibited chemokines secretion and induced the production of RANTES and MCP-1 production in epithelial cells of human lungs.

Isoquinoline alkaloids

Isoquinoline alkaloids present in rhizomes of *Coptis chinensis* which includes six alkaloids which are palmatine, jatrorrhizine, berberine, epiberberine, columbamine, and coptisine. Literature showed that it has the potential to treat influenza A. It inhibit the neuraminidase (NA). Le *et al.* 2020 [41] describe Protein-Ligand Interaction Profiler (PLIP) for demonstration of the bond formed between the binding pocket of the receptor of interest and ligand. Isoquinoline alkaloids showed higher affinity compare to oseltamivir, zanamivir, and natural binding ligand sialic acid they explained the results via a 2D picture. They took the 3D structure of NA protein as the receptor and bioactive compound as ligand and utilized molecular docking. On NA-1 and NA-2 it showed good inhibitor action with higher binding affinity to all receptors of interest.

Cytisine

Cytisine is a quinolizidine alkaloid that is reported for anti-influenza activity. 9-carboxamides of methylcytosine worked against Influenza A virus. The reason behind this is their interactions with 4R7B active site of NA [42].

Berberine

Berberine is an isoquinoline alkaloid found in many plants, used in India and China for a very long time as antimicrobial [43]. In RAW 264.7 macrophage-like cells, A549 human lung epithelial-derived cells, and murine bone marrow-derived macrophages, influenza A strains PR/8/34 or WS/33 showed strong inhibition in their growth. Berberine inhibits the virus protein maturation by inhibiting the post-translation which causes the inhibition on the growth of the virus. Berberine inhibits the production of TNF- α and PGE₂ from A/pr/8/34 infected-RAW 264.7 cells. In A549 human lung epithelial cells growth of IAV inhibits by berberine and it also blocked the growth of strain A/PR8/34 (98% inhibition at 48 hours) [44].

Indirubin

Indirubin is a bisindole alkaloid which is present in *Isatis indigotica* one research [45] suggested that it is useful for the reduced susceptibility of H1N1. The research was designated on mice, indirubin causes the lower mortality rate and reduces lung damage. Indirubin also protects against pneumonia which caused by H1N1 in stressed mice and promotes INF- β generation through MAVS antiviral signaling.



**Shivangi Maurya et al.,**

CONCLUSION

Swine flu sparked a pandemic in the twentieth century, and its deadly effects resulted in death. Many antiviral drugs and vaccines are now affordable, but they come with their own set of side effects. Every country has its own traditional way of treating any disease. Many plants have anti-viral and anti-fungal activity, secondary metabolites are formed by plants for their own protection; literature review revealed that many plants have secondary metabolites that cure a variety of diseases, as seen in the preceding review alkaloid has a lot of potential as a viral inhibitor. Alkaloids can be a better alternative to antiviral drugs and can also help to prevent pandemics and above review proved that alkaloid stand out to be most important/ promising secondary metabolite for influenza treatment.

ACKNOWLEDGEMENT

The authors are thankful to the authorities of Gujarat University, Ahmedabad, Gujarat, India.

REFERENCES

1. Dhiman R, Rakheja V, Saxena R. An Ophthalmologist's Insight Into The Viral Pandemics. *Journal of Optometry*. 2021 Jan 6.
2. Schnitzler SU, Schnitzler P. An update on swine-origin influenza virus A/H1N1: a review. *Virus genes*. 2009 Dec 1;39(3):279-92.
3. Jilani TN, Jamil RT, Siddiqui AH. H1N1 influenza (swine flu). *StatPearls [Internet]*. 2020 Jun 29.
4. Sebastian MR, Lodha R, Kabra SK. Swine origin influenza (swine flu). *The Indian Journal of Pediatrics*. 2009 Aug;76(8):833-41.
5. Novel Swine-Origin Influenza A (H1N1) Virus Investigation Team. Emergence of a novel swine-origin influenza A (H1N1) virus in humans. *New England journal of medicine*. 2009 Jun 18;360(25):2605-15.
6. Smith GJ, Vijaykrishna D, Bahl J, Lycett SJ, Worobey M, Pybus OG, Ma SK, Cheung CL, Raghvani J, Bhatt S, Peiris JM. Origins and evolutionary genomics of the 2009 swine-origin H1N1 influenza A epidemic. *Nature*. 2009 Jun;459(7250):1122-5.
7. Dalal A, Mohan H, Prasad M, Pundir CS. Detection methods for influenza A H1N1 virus with special reference to biosensors: a review. *Bioscience reports*. 2020 Feb;40(2):BSR20193852.
8. Rasmussen SA, Jamieson DJ, Uyeki TM. Effects of influenza on pregnant women and infants. *American journal of obstetrics and gynecology*. 2012 Sep 1;207(3):S3-8.
9. Neumann G, Noda T, Kawaoka Y. Emergence and pandemic potential of swine-origin H1N1 influenza virus. *Nature*. 2009 Jun;459(7249):931-9.
10. Garten RJ, Davis CT, Russell CA, Shu B, Lindstrom S, Balish A, Sessions WM, Xu X, Skepner E, Deyde V, Okomo-Adhiambo M. Antigenic and genetic characteristics of swine-origin 2009 A (H1N1) influenza viruses circulating in humans. *science*. 2009 Jul 10;325(5937):197-201.
11. Munster VJ, de Wit E, van den Brand JM, Herfst S, Schrauwen EJ, Bestebroer TM, van de Vijver D, Boucher CA, Koopmans M, Rimmelzwaan GF, Kuiken T. Pathogenesis and transmission of swine-origin 2009 A (H1N1) influenza virus in ferrets. *Science*. 2009 Jul 24;325(5939):481-3.
12. Maines TR, Jayaraman A, Belser JA, Wadford DA, Pappas C, Zeng H, Gustin KM, Pearce MB, Viswanathan K, Shriver ZH, Raman R. Transmission and pathogenesis of swine-origin 2009 A (H1N1) influenza viruses in ferrets and mice. *Science*. 2009 Jul 24;325(5939):484-7.
13. Cauchemez S, Donnelly CA, Reed C, Ghani AC, Fraser C, Kent CK, Finelli L, Ferguson NM. Household transmission of 2009 pandemic influenza A (H1N1) virus in the United States. *New England Journal of Medicine*. 2009 Dec 31;361(27):2619-27.



**Shivangi Maurya et al.,**

14. Jones S, Nelson-Sathi S, Wang Y, Prasad R, Rayen S, Nandel V, Hu Y, Zhang W, Nair R, Dharmaseelan S, Chirundodh DV. Evolutionary, genetic, structural characterization and its functional implications for the influenza A (H1N1) infection outbreak in India from 2009 to 2017. *Scientific reports*. 2019 Oct 11;9(1):1-0.
15. Chauhan N, Narang J, Pundir S, Singh S, Pundir CS. Laboratory diagnosis of swine flu: a review. *Artificial cells, nanomedicine, and biotechnology*. 2013 Jun 1;41(3):189-95.
16. Echevarría-Zuno S, Mejía-Aranguré JM, Mar-Obeso AJ, Grajales-Muñiz C, Robles-Pérez E, González-León M, Ortega-Alvarez MC, Gonzalez-Bonilla C, Rascón-Pacheco RA, Borja-Aburto VH. Infection and death from influenza A H1N1 virus in Mexico: a retrospective analysis. *The Lancet*. 2009 Dec 19;374(9707):2072-9.
17. Arora R, Chawla R, Marwah R, Arora P, Sharma RK, Kaushik V, Goel R, Kaur A, Silambarasan M, Tripathi RP, Bhardwaj JR. Potential of complementary and alternative medicine in preventive management of novel H1N1 flu (Swine flu) pandemic: thwarting potential disasters in the bud. *Evidence-Based complementary and alternative medicine*. 2010;2011.
18. Balasubramanian P, Jayalakshmi K, Vidhya N, Prasad R, Sheriff AK, Kathiravan G, Rajagopal K, Sureban SM. Antiviral activity of ancient system of ayurvedic medicinal plant *Cissus quadrangularis* L.(Vitaceae). *Journal of basic and clinical pharmacy*. 2010 Feb 15;1(1).
19. Sahoo M, Jena L, Rath SN, Kumar S. Identification of suitable natural inhibitor against influenza A (H1N1) neuraminidase protein by molecular docking. *Genomics & informatics*. 2016 Sep;14(3):96.
20. Eiland LS, Eiland EH. Zanamivir for the prevention of influenza in adults and children age 5 years and older. *Therapeutics and clinical risk management*. 2007 Jun;3(3):461.
21. Heinonen S, Silvennoinen H, Lehtinen P, Vainionpää R, Vahlberg T, Ziegler T, Ikonen N, Puhakka T, Heikkinen T. Early oseltamivir treatment of influenza in children 1–3 years of age: a randomized controlled trial. *Clinical infectious diseases*. 2010 Oct 15;51(8):887-94.
22. Nguyen HT, Sheu TG, Mishin VP, Klimov AI, Gubareva LV. Assessment of pandemic and seasonal influenza A (H1N1) virus susceptibility to neuraminidase inhibitors in three enzyme activity inhibition assays. *Antimicrobial agents and chemotherapy*. 2010 Sep 1;54(9):3671-7.
23. Dr. Jyoti Jyotsna. Study of anti swine flu prospects of medicinal plants. *Pharma Innovation* 2020;9(10):429-435.
24. Shah A, Krishnamurthy R. Swine flu and its herbal remedies. *Int J Eng Sci*. 2013;2(5):68-78.
25. Ghildiyal R, Prakash V, Chaudhary VK, Gupta V, Gabrani R. Phytochemicals as antiviral agents: recent updates. *InPlant-derived bioactives 2020* (pp. 279-295). Springer, Singapore.
26. Moradi MT, Karimi A, Lorigooini Z. Alkaloids as the natural anti-influenza virus agents: a systematic review. *toxin reviews*. 2018 Jan 2;37(1):11-8.
27. Tao YJ, Zheng W. Visualizing the Influenza genome. *Science*. 2012 Dec 21;338(6114):1545-6.
28. Sriwilaijaroen N, Suzuki Y. Molecular basis of the structure and function of H1 hemagglutinin of influenza virus. *Proceedings of the Japan Academy, Series B*. 2012 Jun 11;88(6):226-49.
29. Wang SQ, Du QS, Huang RB, Zhang DW, Chou KC. Insights from investigating the interaction of oseltamivir (Tamiflu) with neuraminidase of the 2009 H1N1 swine flu virus. *Biochemical and Biophysical Research Communications*. 2009 Aug 28;386(3):432-6.
30. Melén K, Kinnunen L, Fagerlund R, Ikonen N, Twu KY, Krug RM, Julkunen I. Nuclear and nucleolar targeting of influenza A virus NS1 protein: striking differences between different virus subtypes. *Journal of virology*. 2007 Jun 1;81(11):5995-6006.
31. Shang JH, Cai XH, Feng T, Zhao YL, Wang JK, Zhang LY, Yan M, Luo XD. Pharmacological evaluation of *Alstonia scholaris*: Anti-inflammatory and analgesic effects. *Journal of ethnopharmacology*. 2010 May 27;129(2):174-81.
32. Zhou HX, Li RF, Wang YF, Shen LH, Cai LH, Weng YC, Zhang HR, Chen XX, Wu X, Chen RF, Jiang HM. Total alkaloids from *Alstonia scholaris* inhibit influenza a virus replication and lung immunopathology by regulating the innate immune response. *Phytomedicine*. 2020 Oct 1;77:153272.
33. Niroumand MC, Farzaei MH, Amin G. Medicinal properties of *Peganum harmala* L. in traditional Iranian medicine and modern phytotherapy: a review. *Journal of Traditional Chinese Medicine*. 2015 Feb 15;35(1):104-9.



**Shivangi Maurya et al.,**

34. Moradi MT, Karimi A, Rafieian-Kopaei M, Fotouhi F. In vitro antiviral effects of Peganum harmala seed extract and its total alkaloids against Influenza virus. *Microbial pathogenesis*. 2017 Sep 1;110:42-9.
35. Zheng XQ, Ye CX, Kato M, Crozier A, Ashihara H. Theacrine (1, 3, 7, 9-tetramethyluric acid) synthesis in leaves of a Chinese tea, kucha (*Camellia assamica* var. kucha). *Phytochemistry*. 2002 May 1;60(2):129-34.
36. Lin PR, Kuo PC, Li YC, Jhuo CF, Hsu WL, Tzen JT. Theacrine and strictinin, two major ingredients for the anti-influenza activity of Yunnan Kucha tea. *Journal of Ethnopharmacology*. 2020 Nov 15;262:113190.
37. Rashmi M, Kushveer JS, Sarma VV. Secondary metabolites produced by endophytic fungi from marine environments. *Endophytes and secondary metabolites. Reference series in phytochemistry*. Springer, Cham. 2019:491-526.
38. Zhang G, Sun S, Zhu T, Lin Z, Gu J, Li D, Gu Q. Antiviral isoindolone derivatives from an endophytic fungus *Emericella* sp. associated with *Aegiceras corniculatum*. *Phytochemistry*. 2011 Aug 1;72(11-12):1436-42.
39. Zhang G, Zhang B, Zhang X, Bing F. Homonojirimycin, an alkaloid from dayflower inhibits the growth of influenza A virus in vitro. *Acta Virol*. 2013 Jan 1;57(1):85-6.
40. Chiou WF, Ko HC, Wei BL. *Evodia rutaecarpa* and three major alkaloids abrogate influenza A virus (H1N1)-induced chemokines production and cell migration. *Evidence-Based Complementary and Alternative Medicine*. 2011 Jan 1;2011.
41. Le K, Tran D, Nguyen A, Le L. A Screening of Neuraminidase Inhibition Activities of Isoquinolone Alkaloids in *Coptis chinensis* Using Molecular Docking and Pharmacophore Analysis. *ACS omega*. 2020 Nov 11;5(46):30315-22.
42. Fedorova VA, Kadyrova RA, Slita AV, Muryleva AA, Petrova PR, Kovalskaya AV, Lobov AN, Zileeva ZR, Tsypyshev DO, Borisevich SS, Tsypysheva IP. Antiviral activity of amides and carboxamides of quinolizidine alkaloid (-)-cytisine against human influenza virus A (H1N1) and parainfluenza virus type 3. *Natural product research*. 2020 Jan 21:1-9.
43. Kulkarni SK, Dhir A. Berberine: a plant alkaloid with therapeutic potential for central nervous system disorders. *Phytotherapy Research: An International Journal Devoted to Pharmacological and Toxicological Evaluation of Natural Product Derivatives*. 2010 Mar;24(3):317-24.
44. Cecil CE, Davis JM, Cech NB, Laster SM. Inhibition of H1N1 influenza A virus growth and induction of inflammatory mediators by the isoquinoline alkaloid berberine and extracts of goldenseal (*Hydrastis canadensis*). *International immunopharmacology*. 2011 Nov 1;11(11):1706-14.
45. Jie C, Luo Z, Chen H, Wang M, Yan C, Mao ZF, Xiao GK, Kurihara H, Li YF, He RR. Indirubin, a bisindole alkaloid from *Isatis indigotica*, reduces H1N1 susceptibility in stressed mice by regulating MAVS signaling. *Oncotarget*. 2017 Dec 1;8(62):105615.
46. National Center for Biotechnology Information. PubChem Compound Summary for CID 75324, 1,3,7,9-Tetramethyluric acid. https://pubchem.ncbi.nlm.nih.gov/compound/1_3_7_9-Tetramethyluric-acid. Accessed Mar. 29, 2021.
47. National Center for Biotechnology Information. PubChem Compound Summary for CID 53363662, Emerimidine B. <https://pubchem.ncbi.nlm.nih.gov/compound/Emerimidine-B>. Accessed Mar. 29, 2021.
48. National Center for Biotechnology Information. PubChem Compound Summary for CID 159496. <https://pubchem.ncbi.nlm.nih.gov/compound/alpha-Homonojirimycin>. Accessed Mar. 29, 2021.
49. National Center for Biotechnology Information. PubChem Compound Summary for CID 9817839, Dehydroevodiamine. <https://pubchem.ncbi.nlm.nih.gov/compound/Dehydroevodiamine>. Accessed Mar. 29, 2021.
50. National Center for Biotechnology Information. PubChem Compound Summary for CID 65752, Rutaecarpine. <https://pubchem.ncbi.nlm.nih.gov/compound/Rutaecarpine>. Accessed Mar. 29, 2021.
51. National Center for Biotechnology Information. PubChem Compound Summary for CID 442088, Evodiamine. <https://pubchem.ncbi.nlm.nih.gov/compound/Evodiamine>. Accessed Mar. 29, 2021.
52. National Center for Biotechnology Information. PubChem Compound Summary for CID 10177, Indirubin. <https://pubchem.ncbi.nlm.nih.gov/compound/Indirubin>. Accessed Mar. 29, 2021.
53. National Center for Biotechnology Information. PubChem Compound Summary for CID 2353, Berberine. <https://pubchem.ncbi.nlm.nih.gov/compound/Berberine>. Accessed Mar. 29, 2021.





Shivangi Maurya et al.,

54. National Center for Biotechnology Information. PubChem Compound Summary for CID 10235, Cytisine. <https://pubchem.ncbi.nlm.nih.gov/compound/Cytisine>. Accessed Mar. 29, 2021.
55. Narayanan MM, Nair CB, Sanjeeva SK, Rao PS, Pullela PK, Barrow CJ. Design of multiligand inhibitors for the swine flu H1N1 neuraminidase binding site. *Advances and applications in bioinformatics and chemistry: AABC*. 2013;6:47.
56. Lin CH, Chang TT, Sun MF, Chen HY, Tsai FJ, Chang KL, Fisher M, Chen CY. Potent inhibitor design against H1N1 swine influenza: structure-based and molecular dynamics analysis for M2 inhibitors from traditional Chinese medicine database. *Journal of Biomolecular Structure and Dynamics*. 2011 Feb 1;28(4):471-82.
57. Alhazmi MI. Molecular docking of selected phytochemicals with H1N1 Proteins. *Bioinformation*. 2015;11(4):196.

Table 1: Docking with natural compound

Inhibition On	Source/Compound	Reference
NA	Garlic, Ginger, Kalmegh, Scutellaria galericulata, Ajwain, Green tea, Lico rice, Turmeric, Mentha, Tulsi, Green tea, Giloy Methyl salicylate, Menthol, camphor	[19] [55]
M2 Channels	Quinic acid, genipin, syringic acid, cucurbitine, fagarine and methyl isoferulate (Traditional Chinese medicine)	[56]
NA and HA	Tulsi	[57]

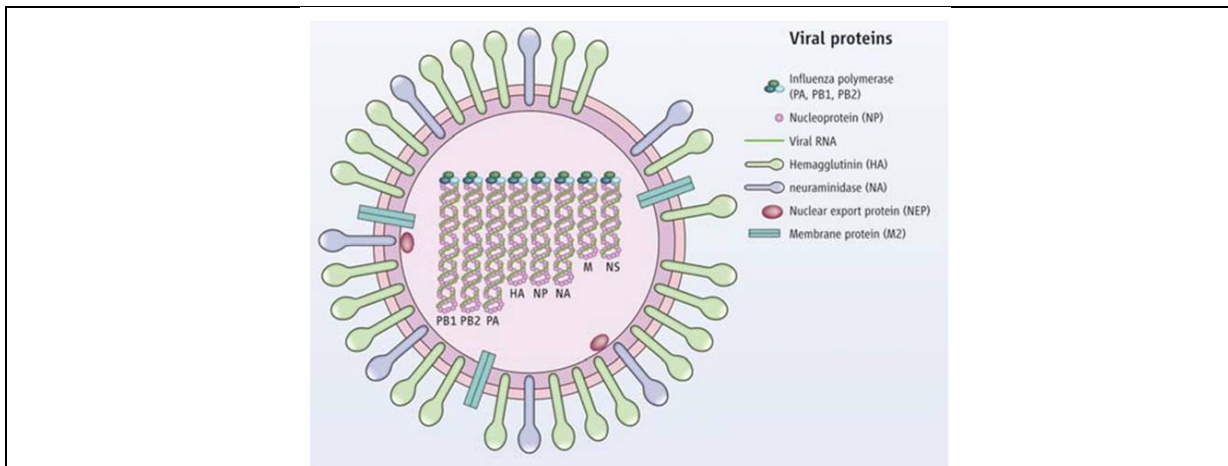
Table 2: The effects of various forms of alkaloids on H1N1 are seen

Alkaloid	Studied on	Inhibition factor/ viral resistance	Reference
TA of Alstonia scholaris	MDCK (Madin-Darby canine kidney)	Inhibit viral replication	[32]
TA of Peganum harmala seed	MDCK	Inhibit RNA replication and Polymerase activity	[34]
Theacrine (50 µM conc)	MDCK	NS1 protein inhibit	[36]
Emerimidine	MDCK	Inhibit Virus	[38]
Homonojirimycin	MDCK	Inhibit virus replication	[39]
Quinazoline (DeHE, Rut, Evo)	A549 cells	Induced RANTE and MCP-1	[40]
Isoquinoline alkaloids	Molecular docking	Inhibit NA-1, NA-2	[41]
Cytisine	MDCK	Inhibit NA	[42]
Berberine	264.7 macrophage-like cells, A549 human lung epithelial	Inhibit post- translation and also inhibit TNF-α and PGE2 in 264.7	[44]
Indirubin	Mice	Decrease mortality	[45]

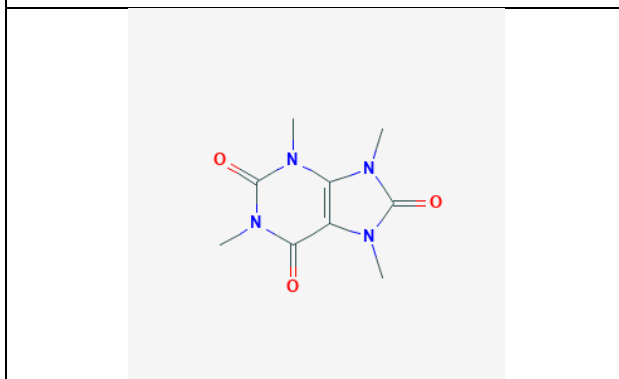
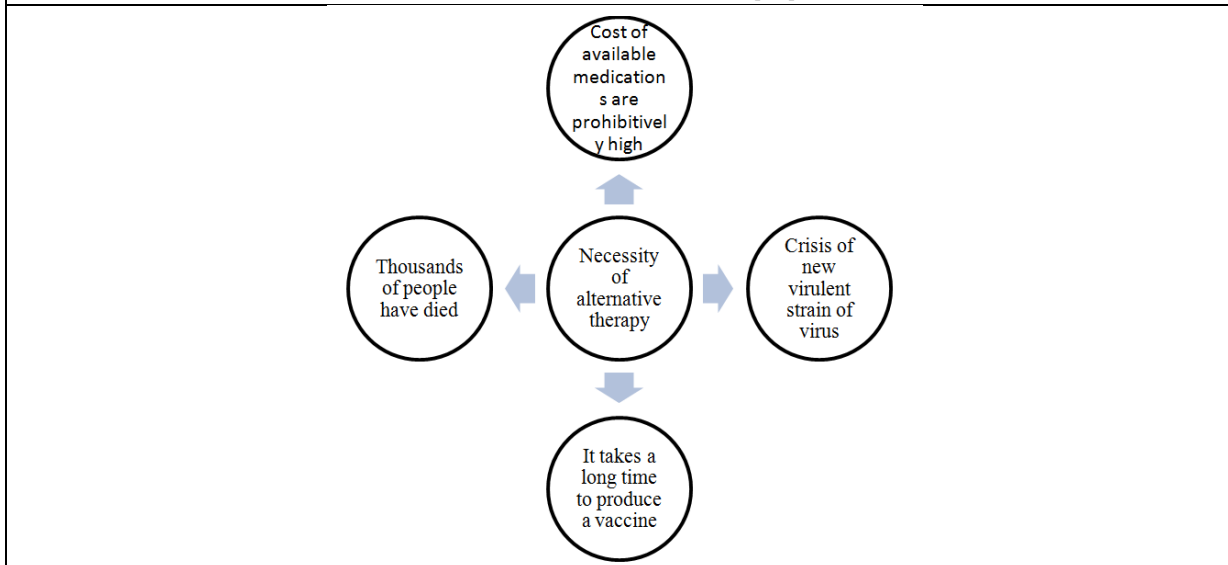




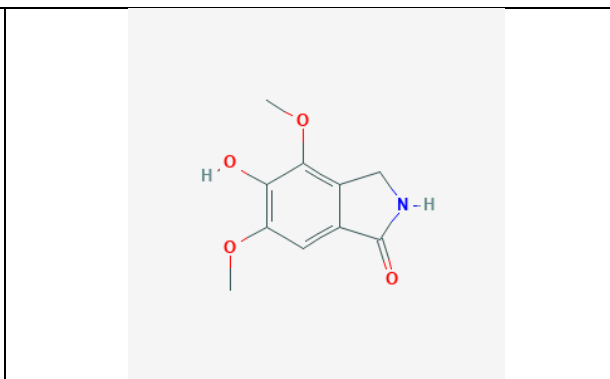
Shivangi Maurya et al.,



Structure of H1N1 Virus [27]



Theacrine [46]

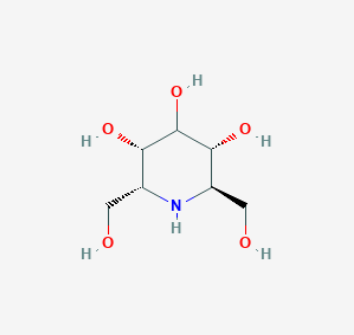
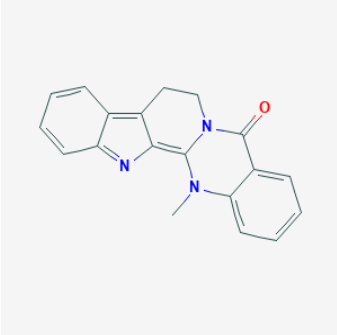
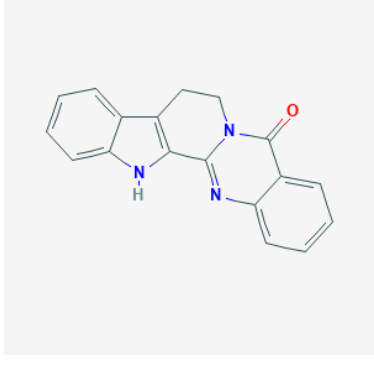
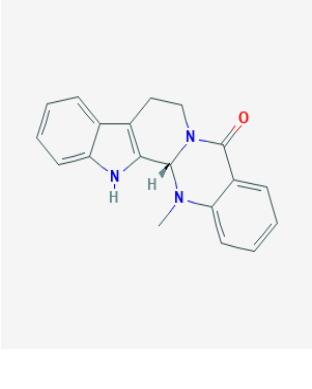
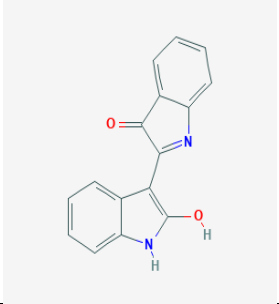
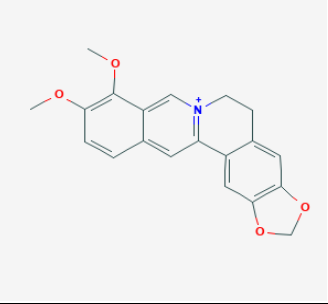
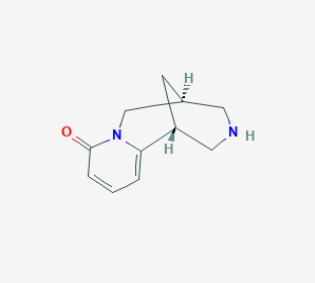


Emerimidine B [47]





Shivangi Maurya et al.,

	
<p>Homonojirimycin [48]</p>	<p>Dehydroevodiamine [49]</p>
	
<p>Rutaecarpine [50]</p>	<p>Evodiamine [51]</p>
	
<p>Indirubin [52]</p>	<p>Berberine [53]</p>
	
<p>Cytisine [54]</p>	
<p>Structure of Alkaloids</p>	





Homomorphism- A Study on Intuitionistic Fuzzy Subgroups

Sheena.K.P¹ and K .Umadevi²

¹Research Scholar, Noorul Islam Centre for Higher Education, Tamil Nadu, India.
(Asst. Professor, Mahatma Gandhi Govt. Arts College, Mahe, U.T of Puducherry, India).

²Asst. Professor, Noorul Islam Centre for Higher Education, Tamil Nadu, India.

Received: 26 Feb 2021

Revised: 12 Mar 2021

Accepted: 18 Mar 2021

*Address for Correspondence

Sheena K P

Assistant Professor,
Mahatma Gandhi Govt. Arts College, Mahe,
P.O. New Mahe-673311, U.T. of Puducherry, India.
Email: sheenasneham@yahoo.com



This is an Open Access Journal / article distributed under the terms of the **Creative Commons Attribution License** (CC BY-NC-ND 3.0) which permits unrestricted use, distribution, and reproduction in any medium, provided the original work is properly cited. All rights reserved.

ABSTRACT

Fuzzy Set was presented by [1] L.A.Zadeh in 1965. In a Fuzzy set, the characteristic function assigns a range of membership values for the elements, while in a crisp set, the characteristic function assigns only two values 1 and 0. In crisp set every member in the universe is assigned a membership value either zero or one. Zadeh extended this range $\{0,1\}$ to the closed interval $[0,1]$ and introduced Fuzzy set. The concept of Fuzzy Set was generalized to Intuitionistic Fuzzy Set by [2] Atanassov by taking into the consideration of the grade of membership and non-membership value for every element in the universe. In this paper some of the aspects of the Fuzzy Homomorphism on Intuitionistic Fuzzy Subgroups have been investigated.

Keywords: Intuitionistic Fuzzy Sets, Intuitionistic Fuzzy Subgroups, Intuitionistic Fuzzy Points, Fuzzy Homomorphism.

INTRODUCTION

More generalizations of the ideas for fuzzy Sets have been made in various areas. In this paper some of the results related to Fuzzy sets and Fuzzy subgroups are generalized for the Intuitionistic Fuzzy sets and Intuitionistic Fuzzy Subgroups with the main focus is in the area of Fuzzy Homomorphism.

Preliminaries

1) [2] For a nonempty set X , an Intuitionistic Fuzzy Set (I.F.S) A of X is defined as an object of the form, $A = \{(x, \mu_A(x), \nu_A(x)) / x \in X\}$. Here $\mu_A: X \rightarrow [0,1]$ indicates the degree of membership and $\nu_A: X \rightarrow [0,1]$ indicates the degree of non-membership of the element $x \in X$ and for every element $x \in X, 0 \leq \mu_A(x) + \nu_A(x) \leq 1$.





Sheena and Umadevi

2) An I.F.S, A on X which takes the values α and β as Membership value and Non Membership value at some point $x \in X$ where $0 \leq \alpha \leq 1, 0 \leq \beta \leq 1, 0 < \alpha + \beta \leq 1$ and takes the values 0 and 1 as Membership value and Non Membership value at all other points $y \in X, y \neq x$ is called an Intuitionistic Fuzzy point and is denoted by $x_{\alpha,\beta}$

3) [3] An I.F. Set A is said to be an I.F Subgroup of G if, a) $\mu_A(xy) \geq \mu_A(x) \wedge \mu_A(y); \mu_A(x^{-1}) = \mu_A(x)$, and b) $\nu_A(xy) \leq \nu_A(x) \vee \nu_A(y); \nu_A(x^{-1}) = \nu_A(x)$ for all $x, y \in G$

4) A and B are I.F. Subgroups of a Group G . Zadeh’s extension principle defines $A \circ B$ and A^{-1} as follows.

$$(A \circ B)(x) = (\mu_{A \circ B}(x), \nu_{A \circ B}(x)), \text{ where } \mu_{A \circ B}(x) = \sup_{st=x} \min(\mu_A(s), \mu_B(t))$$

$$= 0, \text{ if } x \text{ can not be expressed as } x = st, \text{ and}$$

$$\nu_{A \circ B}(x) = \inf_{st=x} \max(\nu_A(s), \nu_B(t))$$

$$= 1, \text{ if } x \text{ can not be expressed as } x = st$$

$$A^{-1}(x) = (\mu_{A^{-1}}(x), \nu_{A^{-1}}(x)) \text{ where } \mu_{A^{-1}}(x) = \mu_A(x^{-1}), \nu_{A^{-1}}(x) = \nu_A(x^{-1})$$

Proposition 1: If G is a group and $x_{\alpha,\beta}, y_{\gamma,\delta}$ are I.F points, then

$$a) x_{\alpha,\beta} \cdot y_{\gamma,\delta} = (x, y)_{\alpha \wedge \gamma, \beta \vee \delta} \quad \text{and} \quad ((x_{\alpha,\beta})^{-1}) = (x^{-1})_{\alpha,\beta}$$

Proof: $x_{\alpha,\beta}(t) = (\alpha, \beta)$, if $t = x$, where $0 < \alpha + \beta \leq 1$
 $= (0,1)$, if $t \neq x$
 $(x_{\alpha,\beta} \cdot y_{\gamma,\delta})(t) = (\sup_{a,b=t} \min(\mu_{x_{\alpha,\beta}}(a), \mu_{y_{\gamma,\delta}}(b)), \inf_{a,b=t} \max(\nu_{x_{\alpha,\beta}}(a), \nu_{y_{\gamma,\delta}}(b)))$
 $= (0,1)$, otherwise

$$= \begin{cases} (\min(\alpha, \gamma), \max(\beta, \delta)), & \text{if } x = a \text{ and } y = b \\ (0,1), & \text{otherwise} \end{cases}$$

$$= \begin{cases} (\min(\alpha, \gamma), \max(\beta, \delta)), & \text{if } x \cdot y = a \cdot b = t \\ (0,1), & \text{otherwise} \end{cases}$$

$$= (x, y)_{\alpha \wedge \gamma, \beta \vee \delta}$$

Since $A^{-1}(x) = (\mu_{A^{-1}}(x), \nu_{A^{-1}}(x))$, where $\mu_{A^{-1}}(x) = \mu_A(x^{-1}), \nu_{A^{-1}}(x) = \nu_A(x^{-1})$,
 $((x_{\alpha,\beta})^{-1})(t) = (x_{\alpha,\beta})(t^{-1})$
 $= (\alpha, \beta)$ if $t^{-1} = x$, that is if $t = x^{-1}$
 $= (0,1)$ otherwise
 $= ((x^{-1})_{\alpha,\beta})(t)$

Proposition 2: For an I.F Subgroup A of a Group G , define,

$\tilde{A} = \{x_{\alpha,\beta} / \mu_A(x) \geq \alpha, \nu_A(x) \leq \beta, x \in G\}$ where $\alpha \in [0, \mu_A(e)], \beta \in [\nu_A(e), 1]$. Then under the operation defined by, $x_{\alpha,\beta} \cdot y_{\gamma,\delta} = (x, y)_{\alpha \wedge \gamma, \beta \vee \delta}$, \tilde{A} is a monoid
 In particular the set $\tilde{A}_e = \{x_{\mu_A(e), \nu_A(e)} / x \in G\}$ is a group

Proof: Let $x_{\alpha,\beta}, y_{\gamma,\delta} \in \tilde{A}$

$$x_{\alpha,\beta} \cdot y_{\gamma,\delta} = (x, y)_{\alpha \wedge \gamma, \beta \vee \delta}$$

$$\mu_A(x) \geq \alpha \text{ and } \mu_A(y) \geq \gamma$$

$$\Rightarrow \mu_A(xy) \geq \min(\mu_A(x), \mu_A(y))$$

$$\geq \min(\alpha, \gamma) = \alpha \wedge \gamma$$

$$\nu_A(x) \leq \beta \text{ and } \nu_A(y) \leq \delta$$

$$\Rightarrow \nu_A(xy) \leq \max(\nu_A(x), \nu_A(y))$$

$$\leq \max(\beta, \delta) = \beta \vee \delta$$

$$\Rightarrow x_{\alpha,\beta} \cdot y_{\gamma,\delta} \in \tilde{A}$$





Sheena and Umadevi

Clearly associative law holds good.

Here $e_{\mu_A(e), \nu_A(e)} \in \tilde{A}$

Also $x_{\alpha, \beta} \cdot e_{\mu_A(e), \nu_A(e)} = (x \cdot e)_{\alpha \wedge \mu_A(e), \beta \vee \nu_A(e)} = x_{\alpha, \beta} = e_{\mu_A(e), \nu_A(e)} \cdot x_{\alpha, \beta}$

$\Rightarrow e_{\mu_A(e), \nu_A(e)}$ is the identity element.

\tilde{A} is a monoid.

Proposition 3: If A is an I.F.Sub group of a group G and $\alpha \in [0, \mu_A(e))$, $\beta \in (\nu_A(e), 1]$, then the set , $\sigma_{\alpha, \beta}(A) = \{x \in G / \mu_A(x) > \alpha, \nu_A(x) < \beta\}$ is a subgroup of G .

Proof: Let $x, y \in \sigma_{\alpha, \beta}(A)$

$\Rightarrow \mu_A(x) > \alpha \Rightarrow \mu_A(y) > \alpha$ and $\nu_A(x) < \beta; \nu_A(y) < \beta$

$\Rightarrow \mu_A(xy) \geq \min(\mu_A(x), \mu_A(y)) > \alpha$ and $\nu_A(xy) \leq \max(\nu_A(x), \nu_A(y)) < \beta$

$\Rightarrow x \cdot y \in \sigma_{\alpha, \beta}(A)$

$\Rightarrow \mu_A(x^{-1}) = \mu_A(x) > \alpha$ and $\nu_A(x^{-1}) = \nu_A(x) < \beta$

$\Rightarrow x^{-1} \in \sigma_{\alpha, \beta}(A)$

Since $\mu_A(e) > \alpha$ and $\nu_A(e) < \beta$, $e \in \sigma_{\alpha, \beta}(A)$

$\sigma_{\alpha, \beta}(A) = \{x \in G / \mu_A(x) > \alpha, \nu_A(x) < \beta\}$ is a subgroup of G .

Definition: [4] Let A and B be I.F.S.Gs of the Groups G and G' separately. A mapping, $\tilde{f}: \tilde{A} \rightarrow \tilde{B}$ is said to be a Fuzzy Homomorphism if it preserves the group operation.

That is if $\tilde{f}(x_{\alpha, \beta} \cdot y_{\gamma, \delta}) = \tilde{f}(x_{\alpha, \beta}) \tilde{f}(y_{\gamma, \delta})$, for all $x_{\alpha, \beta}, y_{\gamma, \delta} \in \tilde{A}$

A fuzzy Homomorphism $\tilde{f}: \tilde{A} \rightarrow \tilde{B}$ is said to be a Fuzzy Isomorphism, if it is a bijection.

The following results are the generalizations of the corresponding results in Fuzzy Subgroups given by Fang Jin-xuan[4]

Proposition4: A and B are I.F.S.Gs of G, G' respectively and $\tilde{f}: \tilde{A} \rightarrow \tilde{B}$ is a Fuzzy Homomorphism. Then a) $\text{supp } \tilde{f}(e_{\alpha, \beta}) = e'$ and $\text{supp } \tilde{f}(x_{\alpha, \beta}) = \text{supp } \tilde{f}(x_{\gamma, \delta})$ for all $\alpha \in [0, \mu_A(e)], \beta \in [\nu_A(e), 1]$

Therefore corresponding to the fuzzy Homomorphism, $\tilde{f}: \tilde{A} \rightarrow \tilde{B}$, there exists a function $f: G \rightarrow G'$ and the restriction functions, $\phi_x: [0, \mu_A(e)] \rightarrow [0, \mu_{B'}(e')]$ and $\psi_x: [\nu_A(e), 1] \rightarrow [\nu_{B'}(e'), 1]$, such that $\tilde{f}(x_{\alpha, \beta}) = (f(x))_{\phi_x(\alpha), \psi_x(\beta)}$, for all $x_{\alpha, \beta} \in \tilde{A}$

Proof: $\tilde{A} = \{x_{\alpha, \beta} / \mu_A(x) \geq \alpha, \nu_A(x) \leq \beta, x \in G\}$ where $\alpha \in [0, \mu_A(e)], \beta \in [\nu_A(e), 1]$

Let $\tilde{f}(e_{\alpha, \beta}) = y_{\lambda, \mu}$, where $y_{\lambda, \mu} \in \tilde{B}$

$\Rightarrow \text{supp } \tilde{f}(e_{\alpha, \beta}) = y$

$\tilde{f}(e_{\alpha, \beta}) \cdot \tilde{f}(e_{\alpha, \beta}) = \tilde{f}(e_{\alpha, \beta} \cdot e_{\alpha, \beta})$

$\Rightarrow y_{\lambda, \mu} \cdot y_{\lambda, \mu} = \tilde{f}(e \cdot e)_{\alpha, \beta}$

$\Rightarrow (y \cdot y)_{\lambda, \mu} = \tilde{f}(e_{\alpha, \beta}) = y_{\lambda, \mu}$

$\Rightarrow y \cdot y = y$

$\Rightarrow y = e'$

$\Rightarrow \text{supp } \tilde{f}(e_{\alpha, \beta}) = e'$

Let $\tilde{f}(x_{\alpha, \beta}) = y'_{\alpha', \beta'}$ and $\tilde{f}(x_{\gamma, \delta}) = z'_{\gamma', \delta'}$

$x_{\alpha \wedge \gamma, \beta \vee \delta} = (x \cdot e)_{\alpha \wedge \gamma, \beta \vee \delta} = x_{\alpha, \beta} \cdot e_{\gamma, \delta}$

$\tilde{f}(x_{\alpha \wedge \gamma, \beta \vee \delta}) = \tilde{f}(x_{\alpha, \beta} \cdot e_{\gamma, \delta}) = \tilde{f}(x_{\alpha, \beta}) \cdot \tilde{f}(e_{\gamma, \delta}) = (y'_{\alpha', \beta'}) \cdot (e'_{h, k})$

$= (y' \cdot e')_{\alpha' \wedge h, \beta' \vee k} = (y')_{\alpha' \wedge h, \beta' \vee k}$

Also $\tilde{f}(x_{\alpha \wedge \gamma, \beta \vee \delta}) = \tilde{f}(x_{\gamma, \delta} \cdot e_{\alpha, \beta}) = \tilde{f}(x_{\gamma, \delta}) \cdot \tilde{f}(e_{\alpha, \beta}) = z'_{\gamma', \delta'} \cdot e'_{s, t} = z'_{\gamma' \wedge s, \delta' \vee t}$

$\Rightarrow \text{supp } \tilde{f}(x_{\alpha, \beta}) = \text{supp } \tilde{f}(x_{\gamma, \delta})$

Proposition 5: If A and B are I F Subgroups of G, G' respectively and $\tilde{f}: \tilde{A} \rightarrow \tilde{B}$ is a fuzzy homomorphism, then $\phi_x(\alpha) \leq \phi_e(\alpha)$ and $\psi_e(\beta) \leq \psi_x(\beta)$

Proof: $\tilde{f}(x_{\alpha, \beta}) = \tilde{f}((x \cdot e)_{\alpha, \beta}) = \tilde{f}(x_{\alpha, \beta} \cdot e_{\alpha, \beta}) = \tilde{f}(x_{\alpha, \beta}) \cdot \tilde{f}(e_{\alpha, \beta})$





Sheena and Umadevi

$$\begin{aligned} \Rightarrow (f(x))_{\phi_x(\alpha), \psi_x(\beta)} &= (f(x))_{\phi_x(\alpha), \psi_x(\beta)} \cdot (f(e))_{\phi_e(\alpha), \psi_e(\beta)} \\ &= (f(x))_{\phi_x(\alpha), \psi_x(\beta)} \cdot e'_{\phi_e(\alpha), \psi_e(\beta)} \\ \Rightarrow (f(x))_{\phi_x(\alpha), \psi_x(\beta)} &= (f(x))_{\phi_x(\alpha) \wedge \phi_e(\alpha), \psi_x(\beta) \vee \psi_e(\beta)} \\ \Rightarrow \phi_x(\alpha) &= \phi_x(\alpha) \wedge \phi_e(\alpha) \text{ and } \psi_x(\beta) = \psi_x(\beta) \vee \psi_e(\beta) \\ \Rightarrow \phi_x(\alpha) \leq \phi_e(\alpha) \text{ and } \psi_e(\beta) &\leq \psi_x(\beta) \end{aligned}$$

Proposition 6: If A and B are I F Subgroups of G, G' respectively and $\tilde{f}: \tilde{A} \rightarrow \tilde{B}$ be a fuzzy homomorphism, then $x_{\alpha, \beta} \leq x_{\gamma, \delta}$ implies that $\tilde{f}(x_{\alpha, \beta}) \leq \tilde{f}(x_{\gamma, \delta})$. That is \tilde{f} is order preserving.

Proof: $x_{\alpha, \beta} \leq x_{\gamma, \delta} \Rightarrow \alpha \leq \gamma$ and $\delta \leq \beta$
 $\Rightarrow \alpha \wedge \gamma = \alpha$ and $\beta \vee \delta = \beta$
 $\Rightarrow x_{\alpha, \beta} = x_{\alpha \wedge \gamma, \beta \vee \delta} = x_{\gamma, \delta} \cdot e_{\alpha, \beta}$
 $\Rightarrow \tilde{f}(x_{\alpha, \beta}) = \tilde{f}(x_{\gamma, \delta} \cdot e_{\alpha, \beta}) = \tilde{f}(x_{\gamma, \delta}) \cdot \tilde{f}(e_{\alpha, \beta})$
 $\Rightarrow (f(x))_{\phi_x(\alpha), \psi_x(\beta)} = (f(x))_{\phi_x(\gamma), \psi_x(\delta)} \cdot e'_{\phi_e(\alpha), \psi_e(\beta)}$
 $\Rightarrow (f(x))_{\phi_x(\alpha), \psi_x(\beta)} = (f(x))_{\phi_x(\gamma) \wedge \phi_e(\alpha), \psi_x(\delta) \vee \psi_e(\beta)}$
 $\Rightarrow \phi_x(\alpha) = \phi_x(\gamma) \wedge \phi_e(\alpha)$ and $\psi_x(\beta) = \psi_x(\delta) \vee \psi_e(\beta)$
 $\Rightarrow \phi_x(\alpha) \leq \phi_x(\gamma)$ and $\psi_x(\delta) \leq \psi_x(\beta)$
 $\Rightarrow (f(x))_{\phi_x(\alpha), \psi_x(\beta)} \leq (f(x))_{\phi_x(\gamma), \psi_x(\delta)}$
 $\Rightarrow \tilde{f}(x_{\alpha, \beta}) \leq \tilde{f}(x_{\gamma, \delta})$.
 $\Rightarrow \tilde{f}$ is order preserving.

CONCLUSION

Relative to I.F.Sets and I.F Subgroups, some of the aspects of the Fuzzy homomorphism has been investigated . More indications of the aspects of Fuzzy Homomorphism in the context of fuzzy Subgroups can be applied for I.F subgroups also.

REFERENCES

1. L.A Zadeh, "Fuzzy sets", Information and Control 8,(1965),338-353
2. K.T. Atanassov, "Intuitionistic fuzzy sets", Fuzzy Sets and Systems 20(1986),NO-1,87-96
3. Sharma.P.K (2011), "Intuitionistic fuzzy Groups", International Journal of Data Ware housing & Mining (IJDWMM),Vol.1,Issue 1,86-94
4. Fang Jin-xuan, "Fuzzy homomorphism and fuzzy isomorphism", Fuzzy Sets and systems 63 (1994) 237-242
5. P.K. Sharma, "Homomorphism of intuitionistic Fuzzy Groups", International Mathematical Forum,Vol.6,2011,no.64,3169-3178





Diabetic Ketoacidosis Management: A Review

Kirti Joshi*, Sakshi Pandey, Manisha Singh and Krutika Shenmare

Assistant Professor, Department of Food and Biotechnology, JVW University, Jaipur.

Received: 07 Dec 2021

Revised: 15 Dec 2021

Accepted: 22 Dec 2021

*Address for Correspondence

Kirti Joshi

Assistant Professor,
Department of Food and Biotechnology,
JVW University, Jaipur.



This is an Open Access Journal / article distributed under the terms of the **Creative Commons Attribution License** (CC BY-NC-ND 3.0) which permits unrestricted use, distribution, and reproduction in any medium, provided the original work is properly cited. All rights reserved.

ABSTRACT

Diabetic ketoacidosis (DKA) is a medical emergency caused by insulin deficiency. It is characterized by hyperglycemia, metabolic acidosis, and ketoacidosis. DKA arises from lack of insulin, with or without a precipitating event that leads to a cascade of pathophysiological changes. Diabetic ketoacidosis (DKA) is an acute, major, life-threatening complication of diabetes that requires immediate treatment. Diabetic ketoacidosis (DKA) remains a significant complication of diabetes around the world and also associated with high rates of hospitalization. Therefore, it becomes important to manage the hyperglycemic calamity associated with diabetes by the healthcare professional. Additionally, with expanding medical services costs and a changing medical care framework, avoidance of diabetic ketoacidosis stays fundamental. The goals of DKA treatment are to normalize volume status, hyperglycemia, electrolytes, and ketoacidosis. Pharmacists in community or ambulatory-care settings can assist in preventing DKA, while inpatient pharmacists play a role in management of DKA. Allergic reaction to insulin is rare, especially when using recombinant human insulin. Generally, DKA may be characterized by significant hyperglycemia, metabolic acidosis, and ketoacidosis. However, DKA may present in various ways, from euglycemia to severe hyperglycemia with or without dehydration and coma.³⁻⁵ The treatment approach for each patient is highly individualized based on a patient's clinical factors.⁵ This review discusses the treatment of DKA, with emphasis on the controversial aspect of initial fluid replacement therapy.

Keywords: Diabetic ketoacidosis, hyperglycemia, gluconeogenesis, metabolic acidosis

INTRODUCTION

Diabetic ketoacidosis and the hyperosmotic hyperglycemic state are the two major hyperglycemic crises associated with diabetes. Diabetic ketoacidosis primarily results from hyperglycemic hyperosmolar state (HHS) and insulin deficiency from severe insulin resistance [1]. Both of the crises result in consequent glucagon and counter-regulatory hormone overload from lack of restraint from insulin [2]. Normally, with raised blood glucose, as occurs after a digested meal, there are production and release of insulin by the beta cells in the islets of Langerhans. Diabetic

30689



**Kirti Joshi et al.,**

ketoacidosis (DKA) is characterized by the triad of hyperglycemia, ketosis, and metabolic acidosis [3]. This results from a relative or absolute deficiency of insulin and an excess of counter-regulatory hormones including glucagon, cortisol, catecholamines, and growth hormones leading to hyperglycemia, glycosuria, dehydration, and hyperosmolarity of varying severity. Dehydration and hyperglycemia results in hyper tonicity and an efflux of water from the intracellular space to the hypertonic extracellular space. There is also a potassium efflux from the intracellular space, aggravated by acidosis, lack of effective insulin action, and breakdown of intracellular proteins [4].

Pathophysiology

DKA results from insulin inadequacy from new-beginning diabetes, insulin resistance, remedy or illegal medication use and expanded insulin need due to disease [4]. This insulin deficiency stimulates the elevation of the counter regulatory hormones (glucagon, catecholamines, cortisol, and growth hormone). Simply put, DKA is caused by too little insulin and a response from the endocrine system that causes an increase in catecholamines, cortisol, glucagon, and growth hormone.[5] The lack of insulin or other precipitating conditions stimulates the release of the regulatory hormones leading to hyperglycemia. The lack of glucose utilization and increase in gluconeogenesis and glycogenolysis causes hyperglycemia. Hyperglycemia further causes diuresis, leading to dehydration, electrolyte abnormalities, and kidney dysfunction [3,4]. Because the body is unable to use glucose, lipase breaks down adipose tissue for energy, some of which is broken down into ketones, thereby leading to ketoacidosis [6]. In DKA, decreased efficacious insulin concentrations and increased concentrations of counter regulatory hormones (catecholamines, cortisol, glucagon, and growth hormone) lead to hyperglycemia and ketosis. Hyperglycemia occurs as a result of three actions

1. Increased gluconeogenesis (generation of glucose from certain non-carbohydrate carbon substrates)
2. Accelerated glycogenolysis (breakdown of the molecule glycogen into glucose)
3. Impaired glucose utilization by peripheral tissues [7-8].

This is boost by transient insulin resistance due to the imbalance of hormone itself as well as the elevated free fatty acid concentrations. The blend of insulin deficiency and increased counter regulatory hormones in DKA moreover leads to the release of free fatty acids into the circulation from adipose tissue (lipolysis) and to uncontrolled hepatic fatty acid oxidation in the liver to ketone bodies (β -hydroxybutyrate and acetoacetate) [9], with resulting ketonemia and metabolic acidosis.

Diagnosis

Typical Clinical Presentation

The management of Diabetic ketoacidosis (DKA) varies with severity and concurrent situation. Polyuria with polydipsia is the most common symptom and was found in 98 percent of persons in one study of childhood type 1 diabetes. Other common symptoms included weight loss (81 percent), fatigue (62 percent), dyspnea (57 percent), vomiting (46 percent), preceding febrile illness (40 percent), abdominal pain (32 percent), and polyphagia (23 percent) [10]. Dehydration causes tachycardia, poor skin turgor, dry mucous membranes, and orthostatic hypotension. The metabolic acidosis may lead to compensatory deep (Kussmaul) respirations, whereas increased acetone can be sensed as a fruity smell on the patient's breath. Mental status can vary from somnolence to lethargy and coma. A detailed evaluation may reveal precipitating factors, especially no adherence to medical regimens and infection, which are common causes of DKA.

Differential diagnosis

Not all patients suffering from ketoacidosis have Diabetic ketoacidosis (DKA). Ketosis and alcoholic ketoacidosis due to starvation are differentiated by clinical history and by plasma glucose concentrations that range from mildly



**Kirti Joshi et al.,**

raised (rarely >200 mg/dl) to hypoglycemia (11). In addition, although alcoholic ketoacidosis can result in profound acidosis, the serum bicarbonate concentration in starvation ketosis is usually not less than 18 mEq/l. Diabetic ketoacidosis must also be distinguished from other causes of high-anion gap metabolic acidosis, including lactic acidosis; ingestion of drugs such as salicylate, methanol, ethylene glycol, and paraldehyde; and acute chronic renal failure (12). Since lactic acidosis is more normal in patients with diabetes than in non-diabetic people because elevated lactic acid levels may occur in severely volume-contracted patients, plasma lactate should be measured on admission. A clinical history of past medication misuse ought to be looked for. Estimation of serum salicylate and blood methanol level might be useful. Ethylene glycol (antifreeze) is recommended by the presence of calcium oxalate and hippurate crystals in the urine. Ingestion of Paraldehyde is designated by its characteristic strong odor on the breath. Because these intoxicants are low-molecular weight organic compounds, they can produce an osmolar gap in addition to the anion gap acidosis (13). A recent report states that active cocaine use is an independent risk factor for recurrent DKA (14).

Diagnostic Testing

The initial laboratory evaluation of patients consist of determination of plasma glucose, creatinine, blood urea nitrogen, electrolytes (with calculated anion gap), osmolality, serum and urinary ketones, and urinalysis, as well as initial arterial blood gases and a complete blood count with a differential. An electrocardiogram (ECG), chest X-ray, and urine, sputum or blood cultures should also be obtained. The diagnosis of DKA is based on an elevated serum glucose level (greater than 250 mg per dL [13.88 mmol per L]), an elevated serum ketone level, a pH less than 7.3, and a serum bicarbonate level less than 18 mEq per L (18 mmol per L).[15] Although arterial blood gas measurement remains the most widely recommended test for determining pH, measurement of venous blood gas has gained acceptance.

In DKA the key diagnostic feature is the elevation in circulating total blood ketone concentration. Assessment of increased ketonemia is usually performed by the nitroprusside reaction, which provides a semiquantitative estimation of acetoacetate and acetone levels. Although the nitroprusside test (both in urine and in serum) is highly sensitive, it can underestimate the severity of ketoacidosis because this assay does not recognize the presence of β -hydroxybutyrate, the main metabolic product in ketoacidosis [16,17]. If available, measurement of serum β -hydroxybutyrate may be useful for diagnosis [18]. Accumulation of ketoacids results in an increased anion gap metabolic acidosis. The anion gap is calculated by subtracting the sum of chloride and bicarbonate concentration from the sodium concentration: $[Na - (Cl + HCO_3)]$. A normal anion gap is between 7 and 9 mEq/l and an anion gap >10–12 mEq/l indicate the presence of increased anion gap metabolic acidosis [19].

Hyperamylasemia has been reported in 21–79% of patients with DKA; however, there is slight association between the degree, presence, or isoenzyme type of hyperamylasemia and the presence of gastrointestinal symptoms (abdominal pain, nausea and vomiting) or pancreatic imaging studies. A serum lipase assurance might be advantageous in the differential analysis of pancreatitis; however, lipase could as well be raised in DKA without pancreatitis [20]. Further initial laboratory studies should comprise measurement of electrolytes, phosphate, blood urea nitrogen, and creatinine; urinalysis; complete blood count with differential; and electrocardiography. [21] Potassium level is normal or low in persons with DKA, despite renal losses caused by the acidic environment. An initial potassium level less than 3.3 mEq per L (3.3 mmol per L) indicates profound hypokalemia. Amylase and lipase levels may be increased in persons with DKA, even in those without associated pancreatitis; however, 10 to 15 percent of persons with DKA do have concomitant pancreatitis [22-20].

Treatment

Successful treatment of DKA requires correction of dehydration, hyperglycemia, and electrolyte imbalances; identification of comorbid precipitating events; and above all, frequent patient monitoring. Protocols for the management of patients with DKA and HHS are summarized in Figure below [23].



**Kirti Joshi et al.,****Fluid Replacement**

After determining the level of dehydration, intravenous fluid replacement should be started. In most persons, saline 0.9 percent is started at 15 to 20 ml/kg per hour or 1 L per hour initially. Fluid status, urine output, blood pressure, cardiac status and electrolyte level should be monitored. As the patient stabilizes, fluids can be lowered to 4 to 14 ml/kg per hour, or 250 to 500 ml per hour. Once the corrected sodium concentration is normal or high (greater than 135 mEq per L [135 mmol/l]), the solution can be changed to saline 0.45%. Dextrose is added when the glucose level decreases to 200 mg per dl (11.10 mmol/l) [24]. During treatment of DKA, hyperglycemia is recovered faster than ketoacidosis. The mean duration of treatment until blood glucose is <250 mg/dl and ketoacidosis (pH >7.30; bicarbonate >18 mmol/l) is corrected is 6 and 12 h, respectively [25-26]. Once the plasma glucose is ~ 200 mg/dl, 5 percent dextrose should be added to replacement fluids to allow nonstop insulin administration until ketonemia is controlled while at the same point avoiding hypoglycemia.

Insulin Therapy

The basis in the treatment of DKA requires the administration of regular insulin through continuous intravenous infusion or by recurrent subcutaneous or intramuscular injections. Randomized controlled studies in patients with DKA have shown that insulin therapy is effective regardless of the route of administration. The administration of continuous intravenous infusion of regular insulin is the preferred route because of its short half-life and easy titration and the delayed onset of action and prolonged half-life of subcutaneous regular insulin [27-28-29].

To further correct hyperglycemia, insulin should be added to intravenous fluids one to two hours after fluids are initiated. An initial bolus of 0.1 units per kg should be given with an infusion of 0.1 units per kg per hour.[30] Some believe this bolus is unnecessary as long as an adequate infusion of insulin is maintained.[31] An infusion of 0.14 units per kg per hour is recommended in the absence of a bolus. Glucose level should decrease by about 50 to 70 mg per dl (2.77 to 3.89 mmol/l) per hour, and the insulin infusion should be adjusted to achieve this goal.[30] Once the glucose level decreases to 200 mg per dl, the insulin infusion rate should be decreased to 0.05 to 0.1 units per kg per hour, and dextrose should be added to the intravenous fluids to maintain a glucose level between 150 and 200 mg per dl (8.32 and 11.10 mmol/l).[30] Subcutaneous insulin is an effective alternative to intravenous insulin in persons with uncomplicated DKA.

Treatment with subcutaneous rapid-acting insulin analogs (lispro and aspart) has been shown to be an effective alternative to the use of intravenous regular insulin in the treatment of DKA. Treatment of patients with mild and moderate DKA with subcutaneous rapid-acting insulin analogs every 1 or 2 h in non-intensive care unit (ICU) settings has been shown to be as safe and effective as the treatment with intravenous regular insulin in the ICU [32-33]. The rate of decline of blood glucose concentration and the mean duration of treatment until correction of ketoacidosis were similar among patients treated with subcutaneous insulin analogs every 1 or 2 h or with intravenous regular insulin. However, until these studies are confirmed outside the research arena, patients with severe DKA, hypotension, anasarca, or associated severe critical illness should be managed with intravenous regular insulin in the ICU.

Potassium

Despite total-body potassium depletion, mild-to-moderate hyperkalemia is common in patients with hyperglycemic complications. Correction in Insulin therapy of acidosis and volume expansion decrease serum potassium concentration. To prevent hypokalemia, potassium replacement is initiated after serum levels fall below the upper level of normal (5.0–5.2 mEq/l). The treatment goal is to maintain serum potassium levels within the normal range of 4–5 mEq/l. Generally, 20–30 mEq potassium in each liter of infusion fluid is sufficient to maintain a serum potassium concentration within the normal range. Rarely, DKA patients may present with significant hypokalemia. In such cases, potassium replacement should begin with fluid therapy, and insulin treatment should be delayed until potassium concentration is restored to >3.3 mEq/l to avoid life-threatening arrhythmias and respiratory muscle



**Kirti Joshi et al.,**

weakness [34-35]. Some guidelines recommend potassium replacement with potassium chloride, whereas others recommend combining it with potassium phosphate or potassium acetate. Clinical trials are lacking to determine which is best, although in the face of phosphate depletion, potassium phosphate is used.

Bicarbonate

Bicarbonate therapy in persons with DKA is somewhat controversial. Proponents believe that severe acidosis will cause cardiac and neurologic complications. However, studies have not demonstrated improved clinical outcomes with bicarbonate therapy, and treatment has been associated with hypokalemia. In one retrospective quasi-experimental study of 39 persons with DKA and a pH between 6.9 and 7.1, there was no difference in outcomes between those who received bicarbonate therapy and those who did not.[36] A second study of 106 adolescents with DKA showed no difference in outcomes in patients treated with and without sodium bicarbonate, but few had a pH below 7 and only one had a pH below 6.9.[37]

Phosphate and Magnesium

Phosphate levels may be normal to elevated on presentation, but decline with treatment as the phosphate enters the intracellular space. Studies have not shown a benefit from phosphate replacement, and it can be associated with hypocalcemia and hypomagnesemia. However, because phosphate deficiency is linked with muscle fatigue, rhabdomyolysis, hemolysis, respiratory failure, and cardiac arrhythmia, replacement is recommended when the phosphate level falls below 1.0 mg per dL (0.32 mmol per L) or when these complications occur. Persons with anemia or respiratory problems and congestive heart failure may benefit from phosphate. This can be achieved by adding 20 to 30 mEq of potassium phosphate to the intravenous fluid [6]. DKA can cause a drop in magnesium, which can result in paresthesia, tremor, muscle spasm, seizures, and cardiac arrhythmia. It should be replaced if it falls below 1.2 mg per dL or if symptoms of hypomagnesemia develop [38].

Complication

Hypoglycemia and hypokalemia are two common complications with overzealous treatment of DKA with insulin and bicarbonate, respectively, but these complications have occurred less often with the low-dose insulin therapy. Hyperchloremic non-anion gap acidosis, which is seen during the recovery phase of DKA, is self-limited with few clinical consequences [39]. This may be caused by loss of ketoanions, which are metabolized to bicarbonate during the evolution of DKA and excess fluid infusion of chloride containing fluids during treatment [4]. Cerebral edema is the most severe complication of DKA. It occurs in 0.5 to 1 percent of all DKA cases, and carries a mortality rate of 21 to 24 percent. Survivors are at risk of residual neurologic problems.[40] Cerebral edema predominantly occurs in children, although it has been reported in adults.

Prevention

Many cases of DKA can be prevented by better access to medical care, proper patient education, and effective communication with a health care provider during an intercurrent illness. Paramount in this effort is improved education regarding sick day management, which includes the following:

1. Early contact with the health care provider.
2. Emphasizing the importance of insulin during an illness and the reasons never to discontinue without contacting the health care team.
3. Review of blood glucose goals and the use of supplemental short- or rapid-acting insulin.
4. Having medications available to suppress a fever and treat an infection.
5. Initiation of an easily digestible liquid diet containing carbohydrates and salt when nauseated.
6. Education of family members on sick day management and record keeping including assessing and documenting temperature, blood glucose, and urine/blood ketone testing; insulin administration; oral intake; and weight. Similarly, adequate supervision and staff education in long-term facilities may prevent many of the admissions for HHS due to dehydration among elderly individuals who are unable to recognize or treat this evolving condition. [41]



**Kirti Joshi et al.,**

Physicians should recognize signs of diabetes in all age groups, and should educate patients and caregivers on how to recognize them as well. In one study, persons with DKA had symptoms of diabetes for 24.5 days before developing DKA. 17 Persons with diabetes and their caregivers should be familiar with adjusting insulin during times of illness. More accessible home measurement of serum ketones with a commercial glucometer may allow for earlier detection of DKA and decreased hospital visits. [42] Persons with an insulin pump need to know their pump settings, and should maintain a prescription for basal insulin in case of pump failure.

REFERENCES

1. Chaithongdi N, Subauste J, Koch C, Geraci S. Diagnosis and management of hyperglycemic emergencies. *Hormones*. 2011;10(4):250–60.
2. Chiasson JL, Aris-Jilwan N, Bélanger R, et al. Diagnosis and treatment of diabetic ketoacidosis and the hyperglycemic hyperosmolar state. *Can Med Assoc J*. 2003;168:859–66.
3. Nyenwe EA, Kitabchi AE. Evidence-based management of hyperglycemic emergencies in diabetes mellitus. *Diabetes Res Clin Pract* (2011) 94(3):340–51. 10.1016/j.diabres.2011.09.012
4. Kitabchi AE, Umpierrez GE, Miles JM, Fisher JN. Hyperglycemic crisis in adult patients with diabetes. *Diabetes Care*. 2009;32(7):1335–1343.
5. Tran TTT, Pease A, Wood A, et al. Review of evidence for adult diabetic ketoacidosis management protocols. *Front Endocrinol (Lausanne)*. 2017;8:106.
6. Kitabchi AE, Umpierrez GE, Murphy MB, Kreisberg RA. Hyperglycemic crises in adult patients with diabetes. *Diabetes Care* 2006; 29: 2739– 2748
7. Kahn CR, Weir GCKitabchi AE, Fisher JN, Murphy MB, Rumbak MJ. Diabetic ketoacidosis and the hyperglycemic hyperosmolar nonketotic state. In *Joslin's Diabetes Mellitus*. 13th ed. Kahn CR, Weir GC Eds. Philadelphia, Lea & Febiger, 1994, p. 738– 770
8. Felig P, Sherwin RS, Soman V, Wahren J, Hendler R, Sacca L, Eigler N, Goldberg D, Walesky M . Hormonal interactions in the regulation of blood glucose. *Recent Prog Horm Res* 1979; 35: 501– 532
9. Miles JM, Haymond MW, Nissen S, Gerich JE . Effects of free fatty acid availability, glucagon excess and insulin deficiency on ketone body production in postabsorptive man. *J Clin Invest* 1983; 71: 1554– 1561
10. Xin Y, Yang M, Chen XJ, Tong YJ, Zhang LH. Clinical features at the onset of childhood type 1 diabetes mellitus in Shenyang, China. *J Paediatr Child Health*. 2010;46(4):171–17
11. Umpierrez GE, DiGirolamo M, Tuvlin JA, Isaacs SD, Bhoola SM, Kokko JP. Differences in metabolic and hormonal milieu in diabetic- and alcohol-induced ketoacidosis. *J Crit Care* 2000; 15: 52– 59
12. Kitabchi AE, Umpierrez GE, Murphy MB, Barrett EJ, Kreisberg RA, Malone JI, Wall BM . Management of hyperglycemic crises in patients with diabetes. *Diabetes Care* 2001; 24: 131– 153
13. DeFronzo RA, Matzuda M, Barret E. Diabetic ketoacidosis: a combined metabolic-nephrologic approach to therapy. *Diabetes Rev* 1994; 2: 209– 238
14. Nyenwe E, Loganathan R, Blüm S, Ezuteh D, Erani D, Wan J, Palace MR, Kitabchi AE . Active use of cocaine: an independent risk factor for recurrent diabetic ketoacidosis in a city hospital. *Endocr Pract* 2007; 13: 22– 29
15. Kitabchi AE, Umpierrez GE, Miles JM, Fisher JN. Hyperglycemic crisis in adult patients with diabetes. *Diabetes Care*. 2009;32(7):1335–1343.
16. Kitabchi AE, Umpierrez GE, Murphy MB, Barrett EJ, Kreisberg RA, Malone JI, Wall BM . Management of hyperglycemic crises in patients with diabetes. *Diabetes Care* 2001; 24: 131– 153
17. Kahn CR, Weir GCKitabchi AE, Fisher JN, Murphy MB, Rumbak MJ. Diabetic ketoacidosis and the





Kirti Joshi et al.,

- hyperglycemic hyperosmolar nonketotic state. In Joslin's Diabetes Mellitus. 13th ed. Kahn CR, Weir GC Eds. Philadelphia, Lea & Febiger, 1994, p. 738– 770
18. Sheikh-Ali M, Karon BS, Basu A, Kudva YC, Muller LA, Xu J, Schwenk WF, Miles JM . Can serum β -hydroxybutyrate be used to diagnose diabetic ketoacidosis? Diabetes Care 2008; 31: 643– 647
 19. Kitabchi AE, Umpierrez GE, Murphy MB, Barrett EJ, Kreisberg RA, Malone JI, Wall BM . Management of hyperglycemic crises in patients with diabetes. Diabetes Care 2001; 24: 131– 153
 20. Yadav D, Nair S, Norkus EP, Pitchumoni CS. Nonspecific hyperamylasemia and hyperlipasemia in diabetic ketoacidosis: incidence and correlation with biochemical abnormalities. Am J Gastroenterol 2000; 95: 3123– 3128
 21. Wilson JF. In clinic. Diabetic ketoacidosis Ann Intern Med. 2010;152(1):ITC1-1-ITC1-15.
 22. Nair S, Yadav D, Pitchumoni CS. Association of diabetic ketoacidosis and acute pancreatitis: observations in 100 consecutive episodes of DKA. Am J Gastroenterol. 2000;95(10):2795–2800.
 23. Kuzuya T, Matsuda A, Sakemoto Y, Yamamoto K, Saito T, Yoshida S . A case of pituitary gigantism who had two episodes of diabetic ketoacidosis followed by complete recovery of diabetes. Endocrinol Jpn 1983; 30: 323– 334
 24. Kitabchi AE, Umpierrez GE, Miles JM, Fisher JN. Hyperglycemic crisis in adult patients with diabetes. Diabetes Care. 2009;32(7):1335–1343.
 25. Umpierrez GE, Kelly JP, Navarrete JE, Casals MM, Kitabchi AE. Hyperglycemic crises in urban blacks. Arch Intern Med 1997; 157: 669– 675
 26. Umpierrez GE, Jones S, Smiley D, Mulligan P, Keyler T, Temponi A, Semakula C, Umpierrez D, Peng L, Cerón M, Robalino G . Insulin analogs versus human insulin in the treatment of patients with diabetic ketoacidosis: a randomized controlled trial. Diabetes Care 2009; 32: 1164– 1169
 27. Alberti KGGM, Hockaday TDR, Turner RC. Small doses of intramuscular insulin in the treatment of diabetic 'coma.' Lancet 1973; 5: 515– 522
 28. Fisher JN, Shahshahani MN, Kitabchi AE. Diabetic ketoacidosis: low-dose insulin therapy by various routes. N Engl J Med 1977; 297: 238– 241
 29. Kitabchi AE, Umpierrez GE, Fisher JN, Murphy MB, Stentz FB. Thirty years of personal experience in hyperglycemic crises: diabetic ketoacidosis and hyperglycemic hyperosmolar state. J Clin Endocrinol Metab 2008; 93: 1541– 1552
 30. Kitabchi AE, Umpierrez GE, Miles JM, Fisher JN. Hyperglycemic crisis in adult patients with diabetes. Diabetes Care. 2009;32(7):1335–1343.
 31. Kitabchi AE, Murphy MB, Spencer J, Matteri R, Karas J. Is a priming dose of insulin necessary in a low-dose insulin protocol for the treatment of diabetic ketoacidosis? Diabetes Care. 2008;31(11):2081–2085.
 32. Umpierrez GE, Latif K, Stoeber J, Cuervo R, Park L, Freire AX, Kitabchi AE . Efficacy of subcutaneous insulin lispro versus continuous intravenous regular insulin for the treatment of diabetic ketoacidosis. Am J Med 2004; 117: 291– 296
 33. Umpierrez GE, Latif KA, Cuervo R, Karabell A, Freire AX, Kitabchi AE . Treatment of diabetic ketoacidosis with subcutaneous insulin aspart. Diabetes Care 2004; 27: 1873– 1878
 34. Kitabchi AE, Umpierrez GE, Murphy MB, Barrett EJ, Kreisberg RA, Malone JI, Wall BM . Management of hyperglycemic crises in patients with diabetes. Diabetes Care 2001; 24: 131– 153
 35. Kitabchi AE, Umpierrez GE, Murphy MB, Kreisberg RA. Hyperglycemic crises in adult patients with diabetes. Diabetes Care 2006; 29: 2739– 2748
 36. Viallon A, Zeni F, Lafond P, et al. Does bicarbonate therapy improve the management of severe diabetic ketoacidosis? Crit Care Med. 1999;27(12):2690–2693.

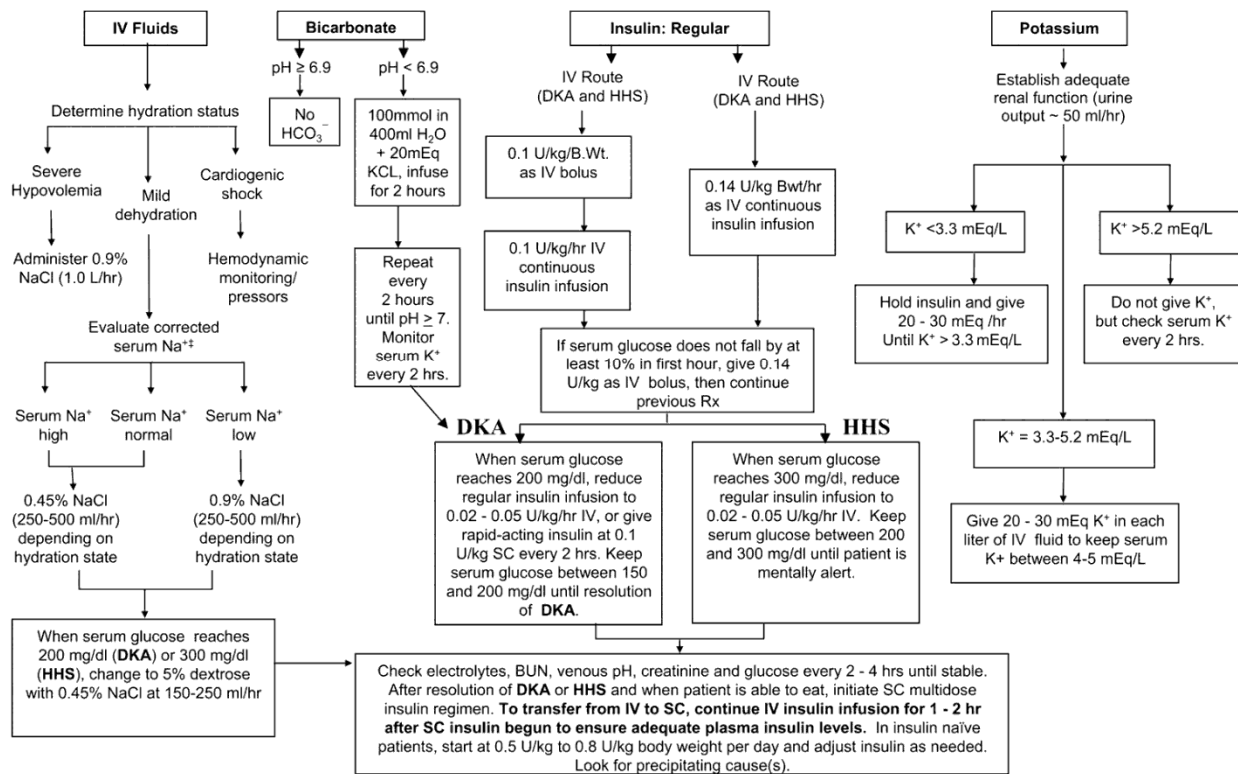




Kirti Joshi et al.,

37. Green SM, Rothrock SG, Ho JD, et al. Failure of adjunctive bicarbonate to improve outcome in severe pediatric diabetic ketoacidosis. *Ann Emerg Med.* 1998;31(1):41–48.
38. Chansky M, Haddad G. Acute diabetic emergencies, hypoglycemia, and glycemic control. In: Parrillo JE, Dellinger RP, eds. *Critical Care Medicine: Principles of Diagnosis and Management in the Adult.* 3rd ed. Philadelphia, Pa.: Mosby Elsevier; 2008:1245–1257.
39. Adrogue HJ, Wilson H, Boyd AE, 3rd, Suki WN, Eknoyan G. Plasma acid-base patterns in diabetic ketoacidosis. *N Engl J Med* 1982; 307: 1603– 1610
40. Dunger DB, Sperling MA, Acerini CL, et al. ESPE/LWPES consensus statement on diabetic ketoacidosis in children and adolescents. *Arch Dis Child.* 2004;89(2):188–194.
41. Sheikh-Ali M, Karon BS, Basu A, Kudva YC, Muller LA, Xu J, Schwenk WF, Miles JM. Can serum β -hydroxybutyrate be used to diagnose diabetic ketoacidosis? *Diabetes Care* 2008; 31: 643– 6
42. Laffel LM, Wentzell K, Loughlin C, Tovar A, Moltz K, Brink S. Sick day management using blood 3-hydroxybutyrate (3-OHB) compared with urine ketone monitoring reduces hospital visits in young people with T1DM: a randomized clinical trial. *Diabet Med.* 2006;23(3):278–284.

Complete initial evaluation. Check capillary glucose and serum/urine ketones to confirm hyperglycemia and ketonemia/ketonuria. Obtain blood for metabolic profile. Start IV fluids: 1.0 L of 0.9% NaCl per hour.†





Dominating Safe Sets in Graphs

D.Yokesh¹, R.Sundareswaran^{2*} and V. Swaminathan³

¹Department of Mathematics, Kirirom Institute of Technology, Cambodia.

²Department of Mathematics, Sri Sivasubramaniya Nadar College of Engineering, Chennai, Tamil Nadu, India.

³Department of Mathematics, Ramanujan Research Centre in Mathematics, S.N College, Madurai, Tamil Nadu, India.

Received: 09 Mar 2021

Revised: 15 Mar 2021

Accepted: 18 Mar 2021

*Address for Correspondence

R.Sundareswaran

Department of Mathematics,
Sri Sivasubramaniya Nadar College of Engineering,
Chennai, Tamil Nadu, India.
Email: sundareswaranr@ssn.edu.in



This is an Open Access Journal / article distributed under the terms of the **Creative Commons Attribution License** (CC BY-NC-ND 3.0) which permits unrestricted use, distribution, and reproduction in any medium, provided the original work is properly cited. All rights reserved.

ABSTRACT

Shinya Fujitha et al. introduced the concept of safe set of a graph, to optimize facility location problems. A non empty subset S is said to be a safe set, for every connected component C of $G[S]$ and every component D of $V - S$, we have $|C| \geq |D|$, whenever there exists an edge of G between C and D . If $G[S]$ is dominating, then S is called adominating safe set. In this paper, we discuss the properties and bounds of the dominating safe set.

Keywords: Safe set, Dominating set, Dominating safe set, Facility Location Problem.

2010 Mathematics subject classification: 05C69, 05C90.

INTRODUCTION

All graphs considered here finite, undirected, without loops or multiple edges. The sub graph of a graph G induced by $S \subseteq V(G)$ is denoted by $G[S]$. Let $\delta(G)$, $\Delta(G)$ be the minimum and maximum degree of G . A component of G is a connected induced sub graphs. A set is independent (or stable) if no two vertices in it are adjacent. An independent dominating set of G is a set that is both dominating and independent in G . The independent domination number of G , denoted by $i(G)$, is the minimum size of an independent dominating set. The independence number of G , denoted $\alpha(G)$, is the maximum size of an independent set in G . To address the problem of maximize the amount of business space in such a way that the temporary refuges be effectively located, a safe set of a graph was introduced. A non-empty subset $S \subseteq V(G)$ is a safe set if, for every component C of $G[S]$ and every component D of $G - S$, we have $|C| \geq |D|$. Whenever $E(C, D) \neq \emptyset$. The minimum cardinality of a safe set is called the safe set number of G , denoted by $s(G)$. The concept of connected safe set of G is also studied by them. If $G[S]$ is connected, then S is called a connected





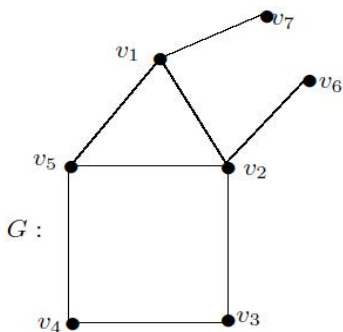
Yokesh et al.,

safe set. In this model, the graph G describes the topology of the building. The safe set of G corresponding to the vertices for location of the temporary refuges in the building. In a administrative set up, decisions are taken by a small group who have effective communication links with other members of the organization. Domination in graphs provides a model for such a concept. A subset D of $V(G)$ of a graph is a dominating set if for every $u \in V - D$, there exists a $v \in D$ such that $uv \in E(G)$. The minimum cardinality of a dominating set is called dominating number $\gamma(G)$ of G . Suppose, there are terrorists (or enemies). Then, there should be a person in the defense for every person in the enemy camp to retaliate his attack. Also, if there is a group of terrorists who work together and if at least one person in a group of defenders is in contact with this group of terrorists, then the strength of the group of defenders should be at least that of offenders. To address this problem, we propose a mathematical model, namely, a dominating safe set of a graph.

Basic Results on Dominating Safe Set Number

Definition 2.1. Let $G = (V, E)$ be a simple graph. The dominating safe set of G is defined as $\min_{S \subseteq V(G)} \{ |S| : S \text{ is a dominating set as well as a safe set of } G \}$. The minimum cardinality of a dominating safe set is called dominating safe set number and denoted by $ds(G)$. Clearly, for any graph G , $\max\{\gamma(G), s(G)\} \leq ds(G)$.

Example 2.2.



$S = \{v_2, v_5\}$ is a safe set of G and hence $s(G) = 2$. Clearly, $\gamma(G) = 3$. So $S \cup \{v_1\}$ is a minimum dominating safe set of G . Thus, $ds(G) = 3$.

Proposition 2.3. For connected graph G of order $n \geq 2$ has a dominating safe set of size at most $\lceil \frac{n}{2} \rceil$.

Proof:

Let $G = (V, E)$ be a simple graph with a maximal independent set S . Since every maximal independent set is a minimal dominating set, $G - S$ is dominating set of G and also is a safe set of G . Hence $G - S$ is a dominating safe set. Hence $|V(G - S)| < \lceil \frac{n}{2} \rceil$.

Proposition 2.4. For any connected graph G ; $\delta(G) \leq ds(G) \leq \alpha(G)$.

Proof:

Clearly every dominating safe set is a safe set and every vertex cover S of G is a minimal dominating set of G and $V - S$ is an independent set.

Proposition 2.5. For any connected graph G , $\gamma(G) \leq ds(G)$.

Proof:

Any dominating safe set is a dominating set of G . Hence $\gamma(G) \leq ds(G)$.

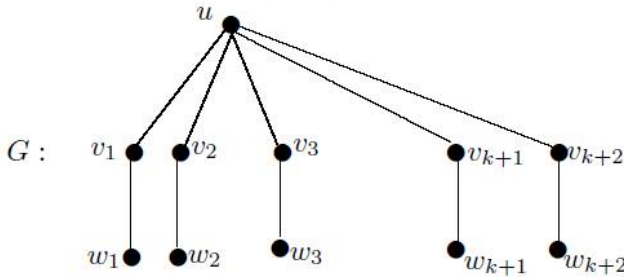




Yokesh et al.,

Proposition 2.6.

Given any two positive integers n and k such that there exists a graph of order n and $ds(G) - s(G) = k$



$\{u, v_1\}$ is a safe set and $s(G) = 2 \cdot ds(G) = k + 2$ ($\{u, v_1, v_2, v_3, \dots, v_{k+1}, v_{k+2}\}$ is a dominating safe set).

Proposition 2.7. For the Complete graph $K_n, n \geq 2, ds(K_n) = \lfloor \frac{n}{2} \rfloor$.

Proof:

By the structure of K_n , every vertex $v \in V(K_n)$ is connected with the remaining $n - 1$ vertices in K_n . The removal of a set S of $\lfloor \frac{n}{2} \rfloor$ vertices from K_n only produces a component of order $\lfloor \frac{n}{2} \rfloor$ in $V - S$. Clearly, S is a dominating set as well as a safe set of K_n .

Proposition 2.8. For the Complete bipartite graph $K_{m,n}, m, n \geq 2, ds(K_{m,n}) = \min\{m, n\}$.

Proof:

Since $K_{m,n}$ is a complete bipartite graph with bi-partition of the vertex set into two partite sets of cardinality m and n . Consider $k = \min\{m, n\}$. The removal of a set S of k vertices from $K_{m,n}$ only produces a totally independent set with cardinality $(m + n) - k$ in $V - S$. Clearly, S is a dominating set as well as a safe set of $K_{m,n}$.

Corollary 2.9. For the Star graph $K_{1,n-1}, n \geq 4, ds(K_{1,n-1}) = 1$.

Observation 2.10. For the Double star graph $S_{m,n}, ds(S_{m,n}) = 2$.

Proposition 2.11. For the Path $P_n, n \geq 2, ds(P_n) = \begin{cases} \lfloor \frac{n}{2} \rfloor, & n \text{ is even} \\ \lfloor \frac{n}{2} \rfloor - 1, & n \text{ is odd} \end{cases}$

Proposition 2.12. For the Cycle $C_n, n \geq 3, ds(C_n) = \lfloor \frac{n}{2} \rfloor$.

Proposition 2.13. Safe set property is neither super hereditary nor hereditary. But the property of dominating safe sets is super hereditary.

Proof:

Let D be a dominating safe set of G . Let $u \in V - D$. Then there exists $v \in D$ such that u and v are adjacent. Let v belong to a component C of $\langle D \rangle$ and u belong to a component F of $\langle V - D \rangle$. Then $|C| \geq |F|$. When u is added to D then $u \in C$ and hence $D \cup \{u\}$ is a safe set. Clearly $D \cup \{u\}$ is a dominating set of G . Hence, the property of safe dominating set is super hereditary. Hence a dominating safe set is minimal if and only if it is 1-minimal.

Characterization of minimal dominating safe set

Proposition 3.1. Let $G = (V, E)$ be a simple graph. Let D be a dominating safe set of G . Then D is minimal if and only if the following holds

- (i) Let $u \in D$. Then either u is an isolate of D or u has a private neighbor in $V - D$.





Yokesh et al.,

(ii) There exists a component say C in $\langle D - \{u\} \rangle$ and a component F in $\langle (V - D) \cup \{u\} \rangle$ such that $E(C, F) \neq \emptyset$ and $|C| < |F|$.

Definition 3.2. A subset D of $V(G)$ satisfying (i) and (ii) is called an irredundant dominating safe set.

Proposition 3.3. Any minimal dominating safe set is an irredundant safe set. The property of irredundant safe set of G is hereditary.

Proof:

Let D be an irredundant safe set of G . Let S be a subset of G . Then any u in S is an element of D and hence it is an isolate of D or has a private neighbour in $V - D$. Clearly, $V - S$ contains $V - D$. Therefore, u is either an isolate of S or has a private neighbour in $V - S$. Let C be a component of $\langle D - \{u\} \rangle$ and F is a component of $\langle (V - D) \cup \{u\} \rangle$ such that $|C| < |F|$, $E(C, F) \neq \emptyset$. Let $C_1 = S \cap C$. $S - \{u\}$ is a subset of $D - \{u\}$. Therefore, C_1 is a component of $S - \{u\}$. Let $F_1 = F \cap \langle V - S \rangle \cup \{u\}$. F_1 is a component of $\langle V - S \rangle \cup \{u\}$. Also, $E(C_1, F_1) \neq \emptyset$. Hence the result.

Complexity of Dominating Safe set (DS) Problem

For a given graph $G = (V, E)$ and input an integer k , the dominating set problem concerns testing whether $\gamma(G) \leq k$; it is a classical NP-complete decision problem in computational complexity theory (Garey & Johnson 1979 [7]). Clearly, there may be no efficient algorithm that finds a smallest dominating set for all graphs, although there are efficient approximation algorithms, as well as both efficient and exact algorithms for certain graph classes.

The Decision problem DS is defined as follows:

INSTANCE: A graph $G = (V, E)$ and an integer k .

QUESTION: Does there exist a dominating safe set $S \subseteq V(G)$ with $1 \leq |S| \leq k$?

The complexity of the problem is determined by using the following construction:

Let $G = (V, E)$ be a connected graph with $V(G) = \{v_1, v_2, \dots, v_n\}$. Let H be a graph constructed from G by adding two new vertices v_{n+1}, v_{n+2} , and $n + 1$ vertex-disjoint paths $P_i = p_{i1}p_{i2}\dots p_{in-k}$, $1 \leq i \leq n + 1$, each of order $n - k$, by joining v_{n+1} to each of v_1, v_2, \dots, v_n and then joining v_i and p_{i1} for $i = 1, 2, \dots, n + 1$. After that, joining v_{n+2} to all the vertices of each path P_i ; $1 \leq i \leq n + 1$. Clearly the new graph H is a connected graph of order $(n + 1)(n - k + 1) + 1$, and

Proposition 4.1. Let G be a connected graph with $\alpha(G) \geq k$ if and only if H has a dominating safe set of size $n - k + 2$.

Proof:

Let S be an independent set of size k in G , and let $S = (V(G) - X) \cup \{v_{n+1}, v_{n+2}\}$. Thus, $|S| = n - k + 2$, is a connected and dominating set of H . Since every component of $H - S$ has size at most $n - k + 1$, the set S forms a dominating safe set of size $n - k + 2$ which is also connected. Conversely, let S_1 be a dominating safe set of H with size $n - k + 2$. Note that $v_{n+1}, v_{n+2} \in S_1$ since otherwise $H - S_1$ contains a component of size greater than $n - k + 1$. The set $S_1 \cap V(G)$ contains at most $n - k$ vertices of G . Note that every vertex of $G - S_1$ belongs to a component of $H - S_1$ of size at least $n - k + 1$. Since S_1 is a dominating safe set of H , each component of $H - S_1$ contains at most one vertex of G . Consequently, the vertices of $G - S_1$ are an independent set of size at least k .

Hence DOMINATING SAFE SET is NP-complete.

REFERENCES

1. Raquel Gueda, Nathann Cohen, Shinya Fujita, Sylvain Legay, Yannis Manoussakis, Yasuko Matsui, Leandro Montero, Reza Naserasr, Hirotaka Ono, Yota Otachi, Tadashi Sakuma, Zsolt Tuza, Renyu Xu, Safe sets in graphs:





Yokesh et al.,

- Graph classes and structural parameters, International Conference on Combinatorial Optimization and Applications, COCOA : Combinatorial Optimization and Applications, 241 - 253(2016)
2. Shinya Fujita, Tommy Jensen, Boram Park, Tadashi Sakuma, On Weighted Safe Set Problem on Path and Cycles, preprint. arXiv:1802.03579.
 3. Fujita S, Mac Gillivray G, Sakuma T, Safe set problem on graphs, Discrete Appl Math 215:106 -111(2016).
 4. Ravindra B. Bapat, Shinya Fujita, Sylvain Legay, Yannis Manoussakis, Yasuko Matsui, Tadashi Sakuma, Zsolt Tuza, Safe sets, network majority on weighted trees, Networks, 71:81 - 92(2018).
 5. C. Berge, Graphs and Hypergraphs, North-Holland, Amsterdam, (1973).
 6. S. Ehard and D. Rautenbach, Approximating connected safe sets in weighted trees, preprint. arXiv:1711.11412
 7. Garey, Michael R.; Johnson, David S. , Computers and Intractability: A Guide to the Theory of NP-Completeness, W. H. Freeman, ISBN 0-7167-1045-5, p. 190, problemGT2(1979).

